EU Horizon 2020 Research & Innovation Program
Digital transformation in Health and Care
SC1-DTH-06-2020
Grant Agreement No. 101016496

SimCardioTest - Simulation of Cardiac Devices & Drugs for in-silico Testing and Certification

SIM CARDIO TEST

Technical Report

D 6.2: Validation of the model predictions for the use cases of WP2-4

Work Package 6 (WP6)

Verification, validation, uncertainty quantification & certification

Task Lead: MPC, France
WP Lead: MPC, France

PUBLIC

DELIVERABLE INFORMATION

Deliverable number	D6.2
Deliverable title	Validation of the model predictions for the use cases of WP2-4
Description	Implementation of Validation on a selection of Models developed for the Use Cases of WP2-4
Lead authors	Romano SETZU (MPC)
Contributors	For UC1 (WP2): Yves COUDIERE (UBx) For UC2 (WP3): Jordi MILL, Andy L OLIVARES, Carlos ALBORS, Oscar CAMARA (UPF) For UC3 (WP4): Beatriz TRENOR (UPV), Maria Teresa MORA (UPV)
Due date	M30
Submission date	30/06/2023 And 25/09/2025
Comments	This version, updated on 24 September 2025, includes **ANNEX A** (WP6 complement of D6.1 and D6.2) & **ANNEX C** (WP6 UC3 PK Validation), which cover the additional work carried out between M30 and M54.

Document history			
Date	**Version**	**Author(s)**	**Comments**
22/05/2023	V1	R. SETZU	First Draft
22/06/2023	V2	R. SETZU M. LEGUEBE, D. FEUERSTEIN, G. FAURE, G. RAVON, Y. COUDIERE A. OLIVARES, J. MILL, C. ALBORS, O. CAMARA M. T. MORA, J. LLOPIS, S. BAROUDI, K. KOLOSKOFF, H. AREVALO, B. TRENOR	First consolidated draft including contributions from UC1/2/3
29/06/2023	V3	H. AREVALO	Quality Review
30/06/2023	V4	R. SETZU	Final Version
01/07/2024	V5	R. SETZU M. BARBIER	Format editing
24/09/2025	VF	M. BARBIER	Addition of **Annexes A** (WP6 complement of D6.1 and D6.2) & **C** (WP6 UC3 PK Validation)

TABLE OF CONTENTS

EXECUTIVE SUMMARY

This report and its annexes constitute the SimCardioTest WP6 deliverable D6.2 due in June 2023 (M30). It describes all validation activities engaged for assessing the credibility of computational models developed in the frame of Use Cases 1 to 3 (cf. WP2, 3, and 4 respectively). This report is closely linked to SCT deliverable D6.1 which reports the verification activities also supporting the credibility of these same models.

Validation is conducted on one specific model per each Use Case, corresponding to a pre-selected Question of Interest (QI). All validation activities are conducted according to ASME VV40 standard guidelines. In addition, this document describes the uncertainty analysis conducted on the uncertainty sources coming from the validation activities. Finally, it includes a discussion on the Applicability of the validated models.

A series of attachments complete the main document, reporting detailed technical description of some validation work. These attachments are included in the annex of the main document.

Some of the engaged validation activities are still ongoing at the date of this publication, and will be documented at later time once completed.

Acronyms

Table 1: List of Acronyms.

Acronym	Meaning
AF	Atrial Fibrillation
ASME	The American Society of Mechanical Engineers
BC	Boundary Conditions
CEPS	Cardiac electrophysiology solver (cf. Use Case 1)
CFD	Computational Fluid Dynamics
CiPA	Comprehensive in-vitro Proarrhythmia Assay (cf. Use Case 3)
COU	Context of Use
CT	Computed Tomography
dCT	Dynamic CT
DE	Discretization Error (in Verification)
DM	Dynamic Mesh
DRT	Device-Related Thrombosis
ECAP	Endothelial Cell Activation Potential
EP-0D	0D Electrophysiology Model (cf. Use Case 3)
EP-3D	3D Electrophysiology Model (cf. Use Case 3)
EXC	ExactCure
FDA	US Food and Drug Administration
IST	INSILICOTRIALS TECHNOLOGIES SRL Also referring to the Cloud service hosting the models
LA	Left Atrium
LAAO	Left Atrial Appendage Occluders
MOTS	Modified Off-the-Shelf Software
MPC	MICROPORT CRM - SORIN CRM SAS
MRI	Magnetic Resonance Imaging
MV	Mitral Valve
N.A. / n.a.	Not Applicable
NCV	Numerical Code Verification

NSE	Numerical Solver Error (in Verification)
OTS	Off-the-Shelf Software
PK	Pharmacokinetics Model (cf. Use Case 3)
PR	Pulmonary Ridge
PV	Pulmonary Vein
QI	**Question** of Interest
QoI	**Quantity** of Interest
RSPV	Right Superior Pulmonary Vein
SCT	SimCardioTest
SQA	Software Quality Assurance (in Verification)
SRL	SIMULA RESEARCH LABORATORY AS
TC	Test Condition (in Validation)
TdP	Torsade de Pointe
TS	Test Sample (in Validation)
UB / U.B.	Uncertainty Budget
UBx	Université de Bordeaux
UC	Use Case
UD	User Developed (Software)
UE	Use Error (in Verification)
UI	Ultrasound Imaging
UPF	UNIVERSIDAD POMPEU FABRA
UPV	UNIVERSITAT POLITECNICA DE VALENCIA
V&V, VV	Verification & Validation
VVUQ	Verification, Validation, and Uncertainty Quantification
WP	Work Package

Table 2 : Verification Credibility Factors (cf. ASME VV40).

Background Cell Colour-Code
"Light Green" for Verification Items
"Salmon" for Validation Items
"Light Blue" for Applicability Items

1. Introduction

This report and its annexes constitute the SimCardioTest WP6 deliverable D6.2 due in June 2023 (M30). It describes all validation activities engaged for assessing the credibility of computational models developed in the frame of Use Cases 1 to 3 (cf. WP2, 3, and 4 respectively). This report is closely linked to SCT deliverable D6.1 which reports the verification activities also supporting the credibility of these same models.

1.1 Normative Background

Until recently, medical device and drugs manufacturers have been lacking a harmonized framework for supporting the use of computational modeling in their regulatory submissions. For this reason the American Society of Mechanical Engineers (ASME) together with the US Food and Drug Administration (FDA) and key industry stakeholders have developed a risk-supported credibility assessment framework. The result of this joint effort is the ASME VV40 standard which has been published in 2019 [1].

ASME VV40 organizes the V&V activities in three distinct phases:

- Model Verification
- Model Validation
- Model Applicability

Model Verification comprises those activities meant to demonstrate that the numerical model accurately represents the underlying mathematical model. Model Validation comprises those activities meant to show how well the numerical model represents reality. Finally Model Applicability comprises those activities meant to show the relevance of validation activities to support the use of the numerical model in the selected context of use.

Each V&V activity listed in ASME VV40 addresses a specific credibility factor. All credibility factors contribute to the overall credibility of the numerical model. How well a credibility factor must be investigated depends on the model risk, intended as the result on the importance that the numerical model supposedly has in taking clinical decisions and the severity of clinical consequences in case the model leads to wrong decisions.

Up to this date VV40 remains to our knowledge the most appropriate document for addressing verification and validation of numerical models. Nor are we aware of other international standards addressing this topic on the process of being written.

WP6 recognizes that currently this document is the most complete and sound approach for conducting V&V activities meant to support the credibility of the computational models developed in the frame of the SimCardioTest project.

1.2 Global V&V Strategy

Running full Validation and Verification according to ASME VV40 guidance in the frame of WP6 activities has a double objective. On one hand it allows to gain credibility on the selected numerical models, and to show how a file should be built for presenting numerical models as part of official regulatory submissions of new drugs and medical devices. On the other hand it allows to benchmark the feasibility and the usability of the ASME VV40 standard itself in a real case scenario, this document being relatively young and still lacking relevant feedback from the industry on its applicability.

Due to the significant amount of work and complexity for running a complete V&V on a given numerical model according to ASME VV40 guidelines, only one model per Use Case will be addressed in the frame of WP6 activities.

The selected models will address these specific aspects:

- For Use Case 1 (WP2): Pacing leads electrical performance
- For Use Case 2 (WP3): Left Atrial Appendage Occluders (LAAO) safety
- For Use Case 3 (WP4): Drugs safety

Even if only one numerical model will be directly addressed, the V&V framework consolidated at the end of this work will be directly applicable to other numerical models. In addition, we expect that much of the V&V results are also applicable to other models in the frame of SimCardioTest project (for instance models sharing the same algorithms or relying on the same physical comparators for validation).

The following sub-sections present the V&V activities undertaken by each Use Case on the selected models.

1.2.1 Model Description

Before running any V&V activity, it is important to clarify the perimeter of the model. According to ASME VV40 guidelines, for each Use Case and for the selected numerical model the following key concepts are clarified:

- **Device/Drug Description**: the device or drug for which the numerical model is developed
- **Question of Interest**: the question concerning the device/drug safety/efficacy addressed by the selected numerical model
- **Context of Use**: the context in which the numerical model is used in the device/drug life cycle (e.g. device/drug design, validation, clinical use)
- **Model Risk**: the risk related to using the numerical model in the defined context of use

1.2.2 Model Verification

The purpose of Model Verification as intended by ASME VV40 is to demonstrate that the computational model numerical implementation is a robust and accurate representation of the mathematical model describing the phenomenon that the model aims to replicate.

Verification Credibility factors are grouped in two main areas:

- Code Verification
- Calculation Verification

Code Verification credibility factors are intended to demonstrate that the numerical model is developed and runs using robust software and hardware, and correctly implements the underlying mathematical equations which describe the model.

Calculation Verification credibility factors are intended to assess the numerical error associated with the numerical discretization of the mathematical problem, as well as with the implemented numerical solver strategy. In addition, this phase addresses how user errors are handled and possibly mitigated in both model inputs and outputs management.

Table 3 summarizes the Credibility Factors to be addressed in the frame of the computational model validation activities according to ASME VV40.

Table 3 : Verification Credibility Factors (cf. ASME VV40).

Activity	Credibility Factor	VV40§	Guidance
Code Verification	Software Quality Assurance Software functions correctly and gives repeatable results in a specified Hardware/Software environment. (OTS / MOTS / UD)	5.1.1.1	Consider following steps: - Provide evidence that software works correctly (software validation, or software quality development assurance) - Installation Qualification of Hardware and Software prior running simulations - Maintenance activity vs software releases, and analysis of impact of new bugs on model prior running simulations
Code Verification	Numerical Code Verification - NCV Demonstrate correct implementation and functioning of algorithms. Compare to analytical solutions.	5.1.1.2	List key algorithms which need verification. For key algorithms: + Compare solution to analytical benchmarks OR to solution from another verified code. ++ Run grid convergence analysis vs exact solution.
Calculation Verification	Discretization Error Run spatial/temporal grid sensitivity analysis	5.1.2.1	Run grid convergence analysis and estimate discretization error.
Calculation Verification	Numerical Solver Error Run solver parameters sensitivity analysis	5.1.2.2	Example: Run Sensitivity on Simulation Convergence.
Calculation Verification	Use Error [Verify I/O controls in place]	5.1.2.3	How is it verified that simulation practitioner does not introduce errors when running the model? (key inputs and outputs verification).

1.2.3 Model Validation

The purpose of Model Validation as intended by ASME VV40 is to demonstrate that the computational model provides reliable information about the real-life phenomena it wants to represent.

Validation Credibility factors are grouped in three main areas:

- Computational Model
- Comparator
- Assessment

Computational Model credibility factors are intended to fully describe and quantify the model ability to address its question of interest. Its form, properties and conditions are addressed, as well as its inputs. The investigation includes both sensitivity analysis and uncertainty analysis of these quantities (when applicable) meant to assess the model accuracy.

Comparator credibility factors are intended to fully describe and quantify the comparator(s) used for validating the computational model. Comparators may be of different nature depending on the nature of the numerical model: pre-existing clinical literature data, in-vitro comparators, pre-clinical (animal) or clinical data. There may be one or more comparators addressing different aspects of the numerical model under investigation. Comparator uncertainties are also investigated.

Assessment credibility factors are relative to the actual comparison of the numerical model with the selected comparator. Both inputs and outputs to the comparison are taken into account in this analysis.

Table 4 summarizes the Credibility Factors to be addressed in the frame of the computational model validation activities according to ASME VV40.

NOTE: when multiple items are given for a specific credibility factor, not all of them may be applicable to the numerical model under consideration. Each Use Case will select and justify the credibility factor items to be addressed.

Table 4 : Validation Credibility Factors (cf. ASME VV40).

Activity	Credibility Factor	VV40§	Guidance
Computational Model	Model Form: • Conceptual Formulation of Numerical Model • Mathematical formulation of Numerical Model Address 4 items: • Governing Equations (governing modeled phenomena) • System Configuration (Geometry of device/environment)	5.2.1.1	Evaluate Influence of Model Form Assumptions on Model Output Examples: • Scale Analysis • Sensitivity Analysis • PIRT (Phenomena Identification and Ranking Table)

Activity	Credibility Factor	VV40§	Guidance
	• System proprieties (Bio. Chem. Phys. Properties) • System conditions (boundary & initial cond.)	5.2.1.1	
Computational Model	Model Inputs Address 4 items: • Governing Equations Parameters (governing modeled phenomena) • System Configuration (Geometry of device/environment) • System proprieties (Bio. Chem. Phys. Properties) • System conditions (boundary & initial cond.)	5.2.1.2	Evaluate Model Input Sensitivities and Uncertainties
	Quantification of Sensitivities		Evaluate Sensitivities of selected inputs
	Quantification of Uncertainties		Evaluate Uncertainties of selected inputs
Comparator	Test Samples (TS) Address 4 items:	5.2.2.1	Describe Comparator (for information)
	• Quantity of TS		Covering number of samples used in comparator: • Single; few; statistically relevant
	• Range of Characteristics of TS		Covering range of each characteristic of interest across samples • Single Value; Nominal Range; Extreme Range; Full Range
	• Measurements of TS		Covering: • Characterization of Comparator Inputs • Characterization of Comparator Outputs
	• Uncertainty of TS measurements		Covering Uncertainty of tools/methods used to get measurements of test samples
Comparator	Test Conditions (TC) Address 4 items:	5.2.2.2	
	• Quantity of TC		Covering number of test conditions in comparator study: • Single; few; many
	• Range of TC		Covering range of values of test conditions: • Single Value; Nominal Range; Extreme Range; Full Range
	• Measurements of TC		Rigor in characterizing test conditions
	• Uncertainty of TC measurements		Covering Uncertainty of tools/methods used to get measurements of test conditions

Activity	Credibility Factor	VV40§	Guidance
Assessment	Equivalency of Input Parameters between Numerical Model and Comparator	5.2.3.1	Evaluate type and range of all inputs
Assessment	Output Comparison Address 4 items: • Quantity • Equivalency of Output Parameters • Rigor of Output Comparison • Agreement of Output Comparison	5.2.3.2	 How many outputs are compared: single vs multiple Type of outputs observed How the outputs are compared: visual; arithmetic difference; comparison vs. Uncertainty Evaluate the level of agreement, and state if it is satisfactory

1.2.4 Model Applicability

The ultimate purpose of verifying and validating the numerical model is to gain confidence that the model outputs can be used to make predictions on the represented medical device/drug. However, the validation space (*in primis* the comparator selected for model validation) is a limited representation of the reality which the model aims to replicate.

ASME VV40 predicates an additional analysis, referred to as applicability, meant to assess the relevance of the engaged validation activities to support the use of the numerical model for the selected context of use.

Table 5 summarizes the Credibility Factors to be addressed in the frame of the computational model applicability assessment according to ASME VV40.

Table 5 : Model Applicability (cf. ASME VV40).

Activity	Credibility Factor	VV40§	Guidance
Applicability	Relevance of the Quantities of Interest QoI of Validation may be surrogate to the QoIs of COU	5.3.1	Compare QoIs of Validation vs COU: related, identical
Applicability	Relevance of the Validation Activities to the COU Proximity of Validation Points to COU	5.3.2	Compare range of Validation points vs. range of COU

1.2.5 Credibility Factors Coverage Level

According to ASME VV40, the model risk is the result of the combination of two factors:

- The ***Decision Consequence***: the clinical consequence of making a wrong decision based on a false prediction of the model
- The ***Model Influence***: the importance of the contribution of the model outcome in making clinical decisions, weighted amongst all other available inputs, such as available literature, design, in-vitro, pre-clinical and clinical information

Decision Consequence can be weighted as:

- **low**: an incorrect decision would not adversely affect patient safety or health, but might result in a nuisance to the physician or have other minor impacts
- **medium**: an incorrect decision could result in minor patient injury or the need for physician intervention, or have other moderate impacts
- **high**: an incorrect decision could result in severe patient injury or death, or have other significant impacts

Model Influence can be weighted as:

- **low**: simulation outputs from the computational model are a minor factor in the decision
- **medium**: simulation outputs from the computational model are a moderate factor in the decision
- **high**: simulation outputs from the computational model are a significant factor in the decision

Figure 1 gives a graphical representation of the Model Risk resulting from the combination of Decision Consequence and Model Influence.

Model influence	**high**	**3**	**4**	**5**
	medium	**2**	**3**	**4**
	low	**1**	**2**	**3**
		low	**medium**	**high**
		Decision consequence		

Figure 1: *Model Risk Matrix (cf. ASME VV40).*

Each of the credibility factors previously described may be investigated in several ways, each with a different level of investigation. The selected way of investigating each credibility factor may depend on several variables, such as complexity, available knowledge, or available means in the timeframe of this project.

ASME VV40 gives guidance on how to evaluate whether the credibility factors have been sufficiently investigated. For each credibility factor, a score varying from 1 to 5 is given to indicate how deeply the item has been investigated, where 1 means none or little investigation, and 5 means a thorough investigation. The scores are then compared to the model risk level as defined. Whenever a credibility factor coverage level does not match the risk level, a justification is given. This evaluation is summarized in a matrix as shown in Table 6.

Table 6 : Credibility Factors Coverage Level (cf. ASME VV40). The model risk level is set to Medium (3) in this table for illustration purposes. The coverage level of the credibility factors is given an arbitrary score on a 1-to-5 scale for illustration purposes.

Model Risk					x		
Credibility Factor Coverage Level		1	2	3	4	5	
Code Verification: Software Quality Assurance	I			x			
Code Verification: Numerical Code Verification - NCV	I			x			
Calculation Verification - Discretization Error	II			x			
Calculation Verification - Numerical Solver Error	II			x			
Calculation Verification - Use Error	III			x			
Validation - Model [Form]	III			x			
Validation - Model [Inputs]	III			x			
Validation - Comparator [Test Samples]	IV			x			
Validation - Comparator [Test Conditions]	IV			x			
Validation - Assessment [Input Parameters]	IV			x			
Validation - Assessment [Output Comparison]	V			x			
Applicability: Relevance of the Quantities of Interest	V			x			
Applicability: Relevance of the Validation Activities to the COU	V			x			

1.3 Deliverables Organization

The V&V activities conducted in the frame of WP6 are summarized in two official deliverables:

- Deliverable D6.1 - Verification & uncertainty quantification for the use cases of WP2-5
- Deliverable D6.2 - Validation of the model predictions for the use cases of WP2-5

V&V activities described below are split between the two official deliverable documents as follows:

- Model Verification activities are reported in deliverable D6.1
- Model Validation activities and resulting Uncertainty Analysis are reported in deliverable D6.2
- Model Applicability is reported in deliverable D6.2

NOTE: As stated in the SimCardioTest Statement of Work, the official D6.2 deliverable title is: “Validation of the model predictions for the use cases of WP2-5”. The following deviations in the deliverable content with respect of this title are made:

1. Only Work Packages 2, 3, 4 develop numerical models needing V&V activities. These correspond to Use Case 1, 2 and 3 respectively. WP5 corresponds to the in-silico trial activities which will be carried out based on these numerical models.
2. Uncertainty Quantification activities are carried out according to ASME VV40 guidelines. As such, for sake of consistency with VV40, they are reported in SCT deliverable D6.2, rather than in deliverable D6.1.

For sake of clarity, the general introduction addresses both Verification and Validation activities and is identical for both deliverables. In addition, for each Use Case the Model Summary section describing the numerical model undergoing V&V is identical in both deliverables.

NOTE: Each deliverable may contain several attachments detailing the technical work necessary to address specific credibility factors. The list of attachments is presented in the 7 Appendices section.

2. Use Case 1

2.1 UC1 Model Summary

NOTE: This section is identical for both deliverables D6.1 and D6.2. Refer to section 0 for document organization.

2.1.1 Background

The role of a cardiac pacing lead is to effectively stimulate the heart when it is deficient. Current pacemakers offer a wide range of stimulation pulse amplitudes and pulse durations to ensure that the therapy is effectively delivered. However, the higher the stimulation amplitude (and duration), the more energy is drained from the pacemaker battery, which can have an impact on the device longevity. When developing new leads, it is therefore important that the stimulation threshold remains in normal range.

2.1.2 Device Description

Medical devices addressed by the model are cardiac pacing leads. More precisely, their electrical behaviour, and interaction with the cardiac tissue is addressed.

2.1.3 Question of Interest

The Question of Interest addressed by the model is the following:

- What are the stimulation pulse characteristics (voltage amplitude in V and pulse duration in ms) required for a bradycardia lead in bipolar (tip/ring) mode to capture (stimulate) healthy cardiac tissue?

2.1.4 Context of Use

The computational model can be used to help pacing lead manufacturers when developing new products, providing information on the energy levels (pulse amplitudes and durations) required to successfully trigger action potentials and stimulate cardiac tissue.

2.1.5 Model Risk

The following considerations support the assessment of the risk associated with the numerical model.

- Decision Consequence: Low

An error in the model prediction may result in either an underestimation or an overestimation of the energy required to stimulate the cardiac tissue for a given pacing lead design. The clinician will adjust the energy in order to stimulate correctly. An overestimation of the energy by the model has no negative clinical influence on the delivered therapy, as it would result in an increase of the device battery life, which would actually be an unexpected benefit. An underestimation of the energy would have a minor clinical influence, as it would require the physician to increase the programmed therapy energy in order to achieve cardiac stimulation, resulting in a decrease of the expected battery life.

- Model Influence: Medium

Results of simulations with a new design will be systematically compared to those of previous well-established designs. In addition, pre-clinical and clinical data collected during the validation of the new lead design would contribute to corroborate the data provided by the models.

- Model Risk: 2/5 (Low-Medium)

Model Risk is based on Decision Consequence and Model Influence stated above, according to Risk Matrix in Figure 2 (cf. section 1.2.5).

Model	**high**	**3**	**4**	**5**
influence	**medium**	**2 COU**	**3**	**4**
	low	**1**	**2**	**3**
		low	**medium**	**high**
		Decision	**consequence**	

Figure 2: *Model Risk Matrix (cf. ASME VV40) evaluating the COU included in UC1.*

2.1.6 Model Description

The model aims to reproduce capture threshold detection measurements that are performed ex vivo on a healthy ventricular wedge.

The model includes the tissue and the surrounding electrolyte, the pacing circuit of the device, and the contact between the device and the tissue. Given a pulse duration and amplitude, it computes the transmembrane voltage in the cardiac tissue, the electric potential in the tissue and electrolyte, as well as the voltage drops at the tip and ring electrodes.

Simulations are parametrized by:

- Contact properties between the leads and the tissue/electrolyte (modelled by parallel RC-circuits)
- The geometry of both the lead and computational domain
- Micro-structural description of the tissue and its electrical properties
- A model that describes ionic exchanges at the cell membranes

The contact properties are characterized by bench experiments. The geometry and microstructure of the tissue are obtained from 9.4T MR imaging. The shape of the lead is chosen among a family of designs, with the possibility of modifying several parameters (such as inter electrode distance, or radius). The ionic model is chosen from the standardized “cellML” database [2], with parameters adjusted from optical mapping data.

To compute an approximate solution of the model, we need a geometrical mesh of the domain, a spatial discretization scheme (e.g. P1 Lagrange Finite Elements), a time stepping method and an algorithm to solve large linear systems.

In **Erreur ! Source du renvoi introuvable.** we show the computation of the electric field created by t he pacemaker in a slab of passive tissue, which will be the shape of the excitation of the cardiac tissue at the beginning of pacing.

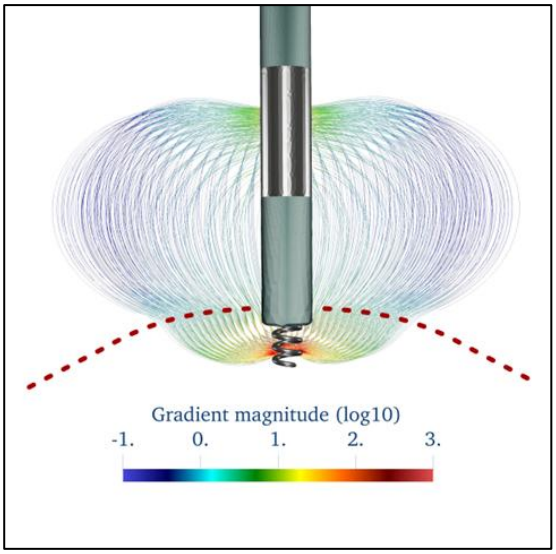

Figure 3: *Electric field generated by a pacemaker lead, computed in a computational domain representing blood and a passive tissue, above and below the dotted line, respectively.*

Computing the solution for various amplitudes and durations of stimulation allows to locate the so-called Lapicque curve, which is the threshold between capturing and non-capturing stimulations in the amplitude/duration plane (see Figure 4).

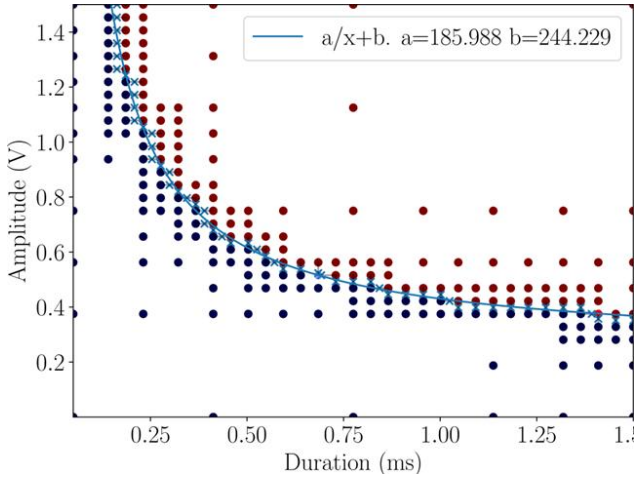

Figure 4: *Lapicque Curve obtained from the solutions of an exploratory 0D model. For each blue/red point of the diagram, ie for each pair of amplitude and duration of stimulation, the model computes the response to 5 stimulations, and evaluates whether or not an action potential was triggered after each stimulation. Blue dots are for 0 out of 5 captures, red dots are for 5 out 5 captures.*

2.2 UC1 Model Validation

2.2.1 Computational Model Form

The mathematical model combines the standard bidomain equations for the cardiac and electrolyte electrical activities to a simple pacemaker model. The alternative, simpler, monodomain equations cannot be used because the bidomain equations constitute the only available model to represent extracellular stimulation, and also the only model that describes the electrical field associated to an excitable tissue in an electrolyte bath, hence being necessary. These two sets of equations are coupled by a model of the contact between the leads and the tissue. The model gathers:

1. Partial differential equations (PDE) describing two electrical potential fields;
2. Ordinary differential equations modelling ionic currents through the cell membranes;
3. Ordinary differential equation modelling the electrical function of the pacemaker, resulting from a 0D lumped parameter model;
4. Boundary conditions on the PDE that couples equations 1. and 2. for the tissue to the equations 3. for the device.

The contact model has been calibrated against bench tests data at MicroPort CRM (result presented at the 11th FIMH conference in 2023 [3]). The complete model has been proven to be well-posed (article to be submitted by Dec. 2023).

To answer the question of interest, we need to output from computations the Lapicque curve, namely the threshold curve between capture and no capture regions in the duration - voltage domain. In order to define the Lapicque threshold, we need to monitor the transmembrane voltage near the surface of the tissue: we consider that capture is successful if all the tissue has been depolarized. Hence each simulation of the model corresponds to one point in the duration - voltage domain. We assume that capture is a local phenomenon, that can be studied only in the vicinity of the implanted lead (specified below).

In addition, we may monitor also:

- The distribution of the total energy in the system, especially the ratio between the energy dissipated by the contacts and the energy that is really delivered to the tissue
- The apparent conduction velocity on the cardiac surface

All these quantities of interest can be extracted from the outputs of the computational model. Voltage and velocities are not directly measurable, but are derived from optical measurements. However, the distribution of energy cannot be obtained from the experiments, and is additional information provided by the model.

2.2.2 Computational Model Inputs

Model Parameters

Once the equations are set (see above), the model is defined by the items below, that cover the inputs listed in the ASME VV40 guideline as “System Configuration”, “System Properties”, and “System Conditions”.

They are:

- The geometry of the computational PDE domain, which includes:
    - The geometry of the tissue and its bath, including some real boundaries (metal of the electrodes, non-conductive material of the lead or the experimental box), and artificial ones (artificial cut through the tissue)
    - The geometry of the pacemaker lead, which defines the corresponding boundaries of the domain
- The data of an ionic model, taken from the Cell ML database of cardiac models [2]; currently we use the Beeler Reuter (BR) model [4]
- The values of some ionic conductance from the ionic model (see below), which may be spatially distributed
- The spatial distribution of the conductivity coefficients which appear in partial differential equations on the electric potentials (point 1. above)
- Some scalar coefficients defining the Robin boundary conditions that are set for the PDEs on the artificial boundaries
- The initial conditions to be set on the electrical fields and the ionic variables

Although they are considered computational input parameters, the previous inputs are in reality model parameters, that describe the system properties and conditions, and are not inputs directly related to the QI to be addressed.

The parameters of the contact model have been fixed after some bench experiments done at MicroPort CRM, in a passive saline solution. The computational domain is a simplified and truncated cardiac geometry: our hypothesis is that we can use a subdomain because only a small activated volume of cells is necessary to trigger an action potential on the whole ventricle. Additionally, the electric field generated by the pacemaker in bipolar mode is localized in a small neighbourhood of the lead. The size of this subdomain, as well as the coefficient of the Robin boundary condition will be fixed through numerical experimentation (by sensitivity analysis). The initial conditions are given by the ionic models, as they maintain the steady state of the system. Depending on the test conditions, the initial conditions may be chosen as the steady state, or the resting state associated to the intrinsic frequency of the study.

The experiments already completed, and the ones planned, at UBx, will be used to calibrate the other biophysical parameters of the model. During an experiment, optical signals are recorded by a 2D camera during the stimulation tests. After the experiment, the tissue sample is imaged in a 9.4T MR machine.

We plan to:

- Calibrate the ionic conductance parameters based on the action potential obtained from the optical mapping measurements
- Obtain the spatial distribution of the electrical conductivity coefficients by combining velocity information from optical maps and high-resolution images (that are directly connected to the micro-structure of the tissue)

The calibration method is not completely determined yet for the conductivity coefficients. Up to now, an optimization algorithm was developed in order to retrieve ionic model parameters from optical mapping signals. It fits action potentials computed with the Beeler-Reuter model to measured optical signals, considered as normalized and scaled transmembrane voltages (see example in Figure 5).

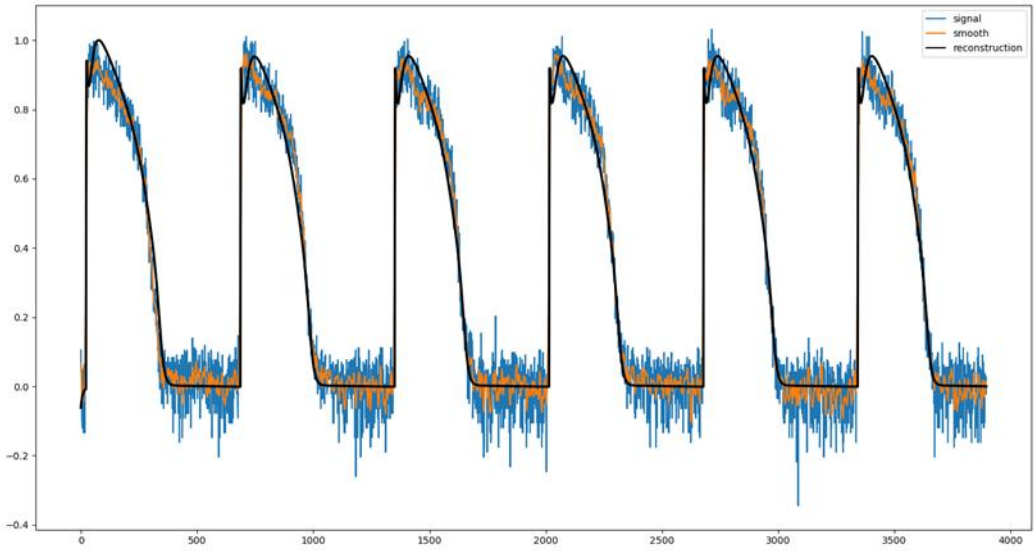

Figure 5: *Example of optimization result from one animal experiments with a commercial pacemaker. The solid line is the model simulation, the blue line is obtained from raw data, and the orange line is smoothed data. The calibration is done from the smoothed data.*

Inputs related to the QI

We expect the model to output a valid answer assuming that the tissue, the electrodes and the contact are well characterized, so that the real inputs of the model in view of the question of interest are twofold:

- The geometrical design parameters and the associated bio-electrical contact impedance values, for each lead to be tested
- The pacing duration and amplitude to be evaluated by each model simulation

In addition, we may consider also the angle of the lead with respect to the surface of the heart, or the depth of the insertion, if these parameters can be retrieved from experiments.

2.2.3 Comparator Description

Two comparators with experimental data are being set up.

2.2.3.1 Comparator 1 - Lapicque Curve

A Lapicque curve can be constructed from the computational model with a high resolution (typically with increment of 0.04 V and 0.05 ms). The experiments consist in labelling a few points as being above or below the Lapicque curve. The experiments hence define a region in which the Lapicque curve is assumed to belong. The comparator evaluates to what extent this is true. The answer may be of type PASS / FAIL, with criteria that have to be specified (see below, comparator uncertainty).

2.2.3.2 Comparator 2 - Optical Map

During the experiments, an optical fluorescence system records the apparent electrical activity near the surface of the cardiac tissue. Activation maps (i.e. maps of the time of arrival of the cardiac depolarization) are obtained by this experimental process. The activation map is defined in the computational model also, using the first time of arrival of the depolarization. The second comparator will quantify the discrepancies between the computational and experimental activation maps, for one or several points in the voltage - duration domain. From a quantitative point of view, several solutions are possible, for instance a dice coefficient may be used. It is possible also to compare the total surface (or volume) activated after a fixed duration, or equivalently the delay to observe the activation breakthrough on each surface (endo and epi).

NOTE: Both Comparator 1 and 2 are preliminary ideas on the comparators, which may be adapted during the realization of the validation activities. As explained above (section 0), the model parameters will be first calibrated using optical mapping data, and high resolution MR images. Afterward, we will run comparisons, and iterate between calibration and comparison as necessary. The comparators may be adapted during this process, to best match our needs and validation capacities.

2.2.4 Comparator - Test Samples

Four sets of bradycardia leads and pacemaker have already been used for the calibration of the contact parameters in a saline solution. Two different models of lead will be tested in animal experiments. A lead coupled to a pacemaker is a test sample. They will each have bio-electrical interface characterized by previous bench experiments, and be chosen so as to have different capture behaviour, in order to challenge the computational model. The contact parameters range from 24 to 28 Ω, and 1.8 to 2.5 µF, respectively for the resistance, and capacitance of the ring electrode. For the tip electrode, the range is 2.5 to 5.5 kΩ for the resistance, and 8 to 12 µF for the capacitance.

Series of tests are realized with various test conditions (see below).

2.2.4.1 Comparator 1 - Lapicque Curve

An experiment consists in a test with one of these test samples, and it aims at localizing as precisely as possible the Lapicque curve in the voltage - duration plane. This is done by decreasing the voltage of pulse duration and for each voltage allowed by the pacemaker, for a sequence of 5 pulses at 1.5 Hz. The durations and voltages allowed by the pacemaker range from 0.12 to 1 ms by uneven steps longer than 0.1 ms, and from 0.25 to 5 V (the useful range is only up to 1 V) by steps of 0.25 V. Hence, the main output of a test is a region that is supposed to contain the experimental Lapicque curve.

2.2.4.2 Comparator 2 - Optical Map

During the experiment, a fluorescent dye is used to evaluate the transmembrane voltage in a thin surface layer of the wedge, yielding optical signals recorded by a 2D camera. The optical activation maps are obtained by processing these signals. They measure the cardiac activation. Additionally, voltage measurement on the connectors of the electrodes monitor the voltage along time.

2.2.5 Comparator - Test Conditions

Both Lapicque and optical maps are acquired during the same tests, all carried out on wedges of sheep's hearts placed in a bath. The wedges include the right ventricle, the septum, and a portion of the left ventricle. A test condition is given by the nature of the cardiac tissue for a given sheep, healthy or infarcted, and the position of the lead in the wedge.

For instance, in a healthy ventricular wedge, we recorded data at three locations, apex, septum, and base, for two animals. Up to now, it constitutes six test conditions. In an infarct heart, we plan to record data at a few different sites, at variable distance from the infarct: in the core, in the border zone, in the surviving myocardium.

A minimum of 3 different test conditions is expected for each type of animal: three locations in a healthy heart, and three locations in an infarcted heart. Our initial plan is to complete experiments with 4 different healthy animals (i.e. 4x3 test conditions), and 4 different infarct animals (i.e. 4x3 test conditions). Up to now 2 healthy animals have been done.

In parallel to the capture, we record optical maps, showing the activation near the surface of the heart as explained above. We also take pictures on which anatomical structures are visible. On infarct heart, the scar is visible because of the change of tissue coloration. After the experiment, high-resolution images (resolution of 250 µm on average) of the tissue sample are done, using various MRI acquisition sequences. They inform us on the microstructure of the tissue wedge, and in particular on the location of the heterogeneities (fibrosis, infarct, fibre direction) in the tissue.

2.2.6 Equivalence of Input Parameters

All experimental inputs are also explicit inputs of the computational model.

In the experiments:

- Pacing voltage are set from 0.25 V to 5 V by steps of 0.25 V
- Pacing duration are set from 0.12 ms to 1 ms by uneven steps of more than 0.1ms
- Five consecutive pulses are used
- The frequency used for the test is 1.5 Hz

In the computational model, we also use 5 pulses at 1.5 Hz, and can vary continuously the voltage and duration, including the values used during the experiments.

The input parameters are as follows:

- For existing leads the CAD model is used to produce the computational mesh;
- The electrical properties of the contact are calibrated in a preliminary step, based on bench experiments, as explained above;

Some model parameters have more influence on one comparator, for instance the lead geometry (spatial distribution of the associated electrical field) on optical maps, although we expect most of them to have influence on both comparators. This is to be refined by a precise sensitivity analysis.

2.2.7 Output Comparison

The output of the experiments are:

1. Low and high boundaries for the Lapicque curve obtained by the threshold test
2. Optical signals, and derived activation maps. The latency of activation after stimulation can be extracted from these maps, and the apparent surface of depolarized tissue can be estimated at a certain time instant post-stimulation

The output considered from the computational model are:

1. Lapicque curve, possibly with uncertainty associated to uncertainty on the contact impedance parameters
2. Activation maps, latency, and apparent surface of depolarized tissue at the same time instant after each pulse

2.2.7.1 Comparator 1 - Lapicque Curve

For each amplitude and duration of stimulation, the computer model simulation yields the number of stimulations out of five, that trigger an AP, as done during the threshold tests in the experiments. The model can then place a Lapicque curve in the Lapicque plane, as the 50%-level contour line of capture percentage. For validation, we will then check if the experimental points are located on the correct side of the curve.

Lapicque curves are acceptable if the computed Lapicque curve lies in the experimental region with a tolerance to be defined. Computational Lapicque curve may refer to: a high density set of threshold points obtained by dichotomy, or the chronaxie and rheobase numbers, that parameterize the standard Lapicque curve model.

2.2.7.2 Comparator 2 - Optical Map

The optical system measures the fluorescence of a dye, activated by transmembrane voltage, whereas the simulation directly outputs the voltage. However, it is known that the maximum derivative of fluorescence coincide with the maximum derivative of the potential. This maximum derivative precisely characterizes the cardiac activation. Consequently, the activation maps from optical signals can be used for direct comparison with activation maps from the computational model. We foresee three possible levels of validation for activation maps:

1. Visual comparison (qualitative only)

2. Measure of time needed to completely activate the whole tissue (can be quantified, but may be vague)

3. Apparent activated surface of tissue at a given time, which may be quantified with some dice coefficient (from image segmentation)

2.3 UC1 Validation Uncertainty

2.3.1 Model Uncertainty

The equations used in the computational models are well known and recognized as a reference for representing the contact impedance, and the triggering and propagation of an action potential in a cardiac domain immersed in an electrolyte. They are based on a representation of the cardiac tissue as a continuum, which implicitly assumes that the tissue is homogeneous at a medium scale (around 0.1 - 1 mm). This is consistent with the resolution of the structural imaging techniques used (250 µm for the MRI). As a consequence, rather than the partial differential equations themselves, uncertainties concern the choice of the ionic model, from the CellML database, and overall the parameterization of the equations (ionic conductance values, electrical conductivity coefficients).

The electrode geometry is fixed by design with very good accuracy, while the contact model is uncertain, and may be a critical part. We choose to fix the contact model, because it represents very accurately the distribution of energy in typical pulse sequences in our bench experiments [3]. Since contact impedance is a complex nonlinear phenomena, this is a limitation, but we don't plan to study the effect of a change of contact model during the project. Instead, we will pay special attention to uncertainties on the contact model's parameters, which we expect to be an important source of uncertainty. Indeed, they were calibrated on bench experiments, with electrodes entirely immersed in a (passive) saline bath, while the tip (anodal) electrode is part in the (active) tissue, and part in the (passive) blood pool in reality.

We also assume that the electrical components of the pacemaker circuit are known very accurately by the manufacturer. The uncertainty on these parameters is negligible with respect to the one on other parameters.

2.3.2 Comparator Uncertainty

Limitation of the device allowing only a few points in the Lapicque plane: commercial pacemakers do not provide a continuous range of duration and voltages, and are usually restricted to only a few points in the voltage - duration plane. Hence, we can plot the lowest capturing, and highest non capturing points obtained with a commercial lead. This process provides only coarse bounds on the location of the Lapicque curve.

Activation signals are obtained by an optical process. It really measures the fluorescence from the interaction between light and a chemical voltage-sensitive dye attached to the cell membrane, in a layer of a few millimetres below the tissue surface. This process is well known, but may anyway lead to uncertainty when comparing optical maps, especially if the activation wave-front becomes parallel to the surface. The uncertainty is minimal for wave-front perpendicular to the tissue surface.

2.3.3 Sources of Uncertainty

The sources of uncertainty related to the model and the comparator have been discussed above. It remains sources related to the animal experiments themselves. For instance, we observed during the first experiment changes in the optical signals associated to the natural evolution of the tissue sample along time during the experiment. There might be variability also between animals, although we expect the discrepancies between location within the same animal to be larger than the ones between animals (in the same conditions).

In order to study these uncertainties, it may be possible to quantify uncertainty on the model parameters as soon as we have enough experiments completed. For instance, we already have a good idea of the possible statistical distribution of the contact parameters from the bench experiments. It will be much more difficult, and may be not possible during the time line of this project to understand the effect of these uncertainties on the output of the model, and on the comparisons.

In a first step, we may study the sensitivity of the output (Lapicque curve or activation map) to the parameter of interest of the computational model, for instance the contact parameters. This can be done with local methods, like variational analysis, or with global methods, for instance using Sobol indices. Anyway, global methods may require very large amount of computational time. In a second step, we would ideally propagate the uncertainty in the model, in order to obtain uncertainty on the output. This can be done with MC or MCMC methods, also requiring very large amount of computations, or with intrusive method, which require mathematical work, and to change the core of the computational model. These additional changes may not be consistent with numerical calculation verification. Note also that the Lapicque curve is calculated from several runs of the computational models, in order to cover the input parameter plane. Propagation of uncertainty in this context may not be straightforward. The influence of other modelling parameters, ionic channel conductance values, electrical conductivity, geometry, may be studied afterwards, although additional complexity and difficulties are expected since they may be spatially distributed parameters.

All these ideas will be explored as much as possible along the SimCardioTest project.

2.4 UC1 Model Applicability

The model and the experiments are designed precisely to address the specified Question of Interest. Due to practical limitations, the validation is only performed on a small number of pacing amplitudes and durations, which may not allow to give a complete answer to the QI (finding the threshold in both amplitude and duration to achieve capture) and may negatively affect model's applicability to the QI. The computational model aims at mimicking threshold detection tests like they are completed on an animal model. As a consequence, validation has to be considered with respect to the animal model identified, specifically healthy and infarcted sheep.

Concerning the applicability to human, the sheep model that was chosen is well known to be adapted to translation to human, having similar anatomical structures, size, distribution of fibers, see [5], and electrical conduction properties, see [6]. In addition, we have a well-defined model of myocardial infarction with a reproducible scar formation and electrical remodeling, similar to the model reported in [6], that has been accepted by the FDA. A well-defined animal model is also needed for reproducibility. It represents a typical case of infarct scar, and not the complete diversity of conditions encountered for human patients. Four samples (animals) in each case (with and without scars) combined with three lead locations are expected to be sufficient for reproducibility concerns, since we target only typical characteristics of a sheep heart.

In addition, applicability to human is not part of our COU (which concerns threshold detection in an animal model), but the model may anyway be extrapolated to fit human data. This extrapolation can

be completed by modifying the model parameters in order to fit the human behavior. We foresee three possibilities for that: human values for conductivity coefficients and ionic conductances from the literature can be used, optical data and 9.4T MR images of human samples, available at Liryc, may be used, though they were obtained in a different context, or we may have opportunities to realize the experiment on human samples (possible within a research program from IHU Liryc).

2.5 UC1 Discussion and Future Work

In this document, we have specified as much as possible technical, and quantified, information that define the mathematical model, identified the input and output parameters related to the QI. We also have explained the COU of the model, and how bench and animal experiments have been setup to obtain both calibration and validation data in the context of use of the model. We finally fixed two comparators that allow to evaluate the use of the computational model to answer the QI, namely comparing Lapicque curves, and comparing activation maps. Preliminary ideas on uncertainty quantification have been given.

This document results from initial discussions on possible questions of interest for UC1, “pacing leads & catheters”. Questions related to the electrical and mechanical behaviour of a pacemaker have been listed. Among 4 QoI concerning the electrical capture or sensing, the question discussed in this document was chosen in particular because it was easier (than for the other QoI) to design animal experiments directly related to the QoI. In parallel, the model has been established during the first year of the project, and its implantation in the CEPS solver is still an active task.

Table 7 below summarizes our draft evaluation of the credibility factors, based on the content of this document.

Table 7 : Validation and Applicability Credibility Factors Coverage Level for Use Case 1 (cf. ASME VV40); * indicates validation activities not yet completed; N/A indicates activities which requires completion to be evaluated.

Model Risk				x			
Credibility Factor Coverage Level			1	2	3	4	5
Validation - Model [Form]	III			x			
Validation - Model [Inputs] *	III			x			
Validation - Comparator [Test Samples] *	IV			x			
Validation - Comparator [Test Conditions] *	II			x			
Validation - Assessment [Input Parameters] *	III			x			
Validation - Assessment [Output Comparison]	N.A.			x			
Applicability: Relevance of the Quantities of Interest *	V			x			
Applicability: Relevance of the Validation Activities to the COU *	V			x			

Model Form is ranked (**3**) because the are some strong argument for the credibility of the model, balanced by some weaknesses. The governing equations are very well known, and currently there is a scientific consensus on their credibility for the COU (bath-loading, extracellular electrical stimulation), while we made a strong assumption on the geometry (using only a subset of the

complete experimental geometry). In addition, we do not plan to study the sensitivity of the model to the choice of the ionic model.

Model Input is ranked (**3**) for similar reasons. The parameters of the governing equations are uncertain, some of this uncertainty is to be studied (uncertainty on the contact parameters), the translation from bench to tissue of the contact parameters is also a limitation, but the main input parameters (duration and voltage of the pulses) are very well known and represented in the model in a very consistent manner.

The test sample properties (pacemaker and animal ventricular wedge) are well identified: the pacemaker is well characterized (geometry, contact parameters), and the uncertainty on its characteristics is known. The cardiac wedge is characterized by extensive measurements (optical signals, high-resolution MRI, electrical measurements). Anyway, living tissues are very complex systems, which cannot be completely characterized, we don't have a fine knowledge of the corresponding model parameters, and their uncertainty has not yet been studied. We ranked (**4**) the characterization of Comparator test samples in view of comparisons. In our COU, the nature of the tissue is expected to impact the answer to the QI, because it is a key factor of its excitability. Hence the corresponding key factor (on Comparator Test Conditions) is ranked (**2**).

Equivalence of the Input Parameter is well established, as explained in section 0. Anyway the model parameters are calibrated from data obtained during the same experiments, which may impair the credibility of the model. The coverage of this credibility factor is then ranked (**3**).

Quantities of Interest have not been explicitly defined in the previous sections, but are the quantities used in the comparators: Lapicque curve, and activation maps. Lapicque curves are exactly the numbers looked for in the QI. For this reason, they are the more important Quantities of Interest, and their relevance can clearly be ranked (**5**).

The COU and the experiments have been designed simultaneously, so that the planned validation activities are clearly relevant to the COU (the COU is precisely the use of the device in the ex-vivo experiment), and therefore the Applicability is ranked (**5**).

Validation results will be obtained once the model run in a verified manner (see SimCardioTest deliverable D6.1), experiments have been completed and there data fully exploited. The technical pipeline to exploit the data is now under construction. Some procedures have been already established to calibrate the model's parameters, like the calibration of the contact parameters, or of the ionic maximal conductance values of interest. We are now working on identifying model's parameters from the MR images of the cardiac microstructure (cardiac fibres, electrical conductivity coefficients). The comparators will also require that optical signals are registered to the MR images, which requires us to redesign the experiments using physical landmarks. We expect this ongoing work, complete calibration of the model and possible comparison (using the 2 comparators) to be finished at the end of the project. Conducting the sensitivity and uncertainty analysis can be based approaches, techniques or methods listed above, but anyway requires additional resources, which may not be available.

3 Use Case 2

3.1 UC2 Model Summary

NOTE: This section is identical for both deliverables D6.1 and D6.2. Refer to section 0 for document organization.

3.1.1 Background

Atrial fibrillation (AF) is considered the most common of human arrhythmias. AF is currently seen as a marker of an increased risk of stroke since it favours thrombus formation inside the left atrium (LA). Around 99% of thrombi in non-valvular AF are formed in the left atrial appendage (LAA) [7]. LAA shapes are complex and have a high degree of anatomical variability among the population [8]. Percutaneous left atrial appendage occlusion (LAAO) can be an efficient strategy to prevent cardioembolic events in selected non-valvular AF patients, as an alternative to life-long oral anticoagulation (OAC) [9], as shown in large clinical trials (ACP Multicentre [10], EWOLUTION [11]), where LAAO procedures demonstrated non-inferiority. However, a successful implantation of LAAO devices remains a challenge in some cases, due to the complexity of LA geometry. Sub-optimal LAAO settings can lead to device-related thrombosis (DRT), i.e., a thrombus formed at the device, becoming a major concern [12] since it can lead to stroke. Based on the Virchow's triad, three factors are thought to contribute to thrombus formation: hypercoagulability, endothelial injury (replaced by a nitinol surface after LAAO) and blood stasis [13]. Related to the latter, key hemodynamic factors with demonstrated influence in thrombus formation in LAAO include (see Figure 6):

1. Occluder design and position: The geometry and characteristics of the occluder device can impact the flow patterns in the left atrium. Different occluder designs, such as shape, size, and surface properties, can influence the likelihood of thrombus formation. The position and alignment of the occluder within the left atrium can affect the flow patterns and the likelihood of thrombus formation. For instance, covering the pulmonary ridge (see Figure 7) may have a protective effect regarding DRT. Studying different occluder positions can help determining the optimal placement to minimize the DRT risk.

2. Blood flow velocity: Areas with low flow velocity or regions of recirculation may be prone to stasis and clot formation.

3. Blood viscosity: Altering the viscosity can provide insights into how changes in blood composition or conditions, such as hematocrit or temperature, affect thrombus formation. Parameters related to blood coagulation, such as platelet activation or coagulation cascade dynamics, can be simulated to understand their impact on thrombus formation.

4. Wall shear stress: Wall shear stress is the frictional force exerted by the flowing blood on the atrial wall. Low wall shear stress regions can be associated to thrombus formation. Evaluating different wall shear stress levels can help identify critical areas. Wall injuries due to abnormal stresses can also be caused by the device deployment.

To avoid blood stasis, it is crucial to properly choose the type of device and the position where the device is going to be deployed. Thus, different planning tools has emerged to find the optimal device

configuration for each patient such as the commercial products from FEOPS [14] and Pie Medical [15], or the VIDAA platform [16], developed by UPF. However, none of these solutions include functional information on blood stasis, which is key for assessing the risk of DRT. In-silico computational fluid dynamic (CFD) can help to describe and relate patient-specific LA/LAA morphology and complex hemodynamics to understand the mechanism behind thrombus formation. Moreover, computational models of the blood flow can be used to predict the effectiveness of LAAO devices, to evaluate new device designs, and to better understand clinical outcomes such as DRT.

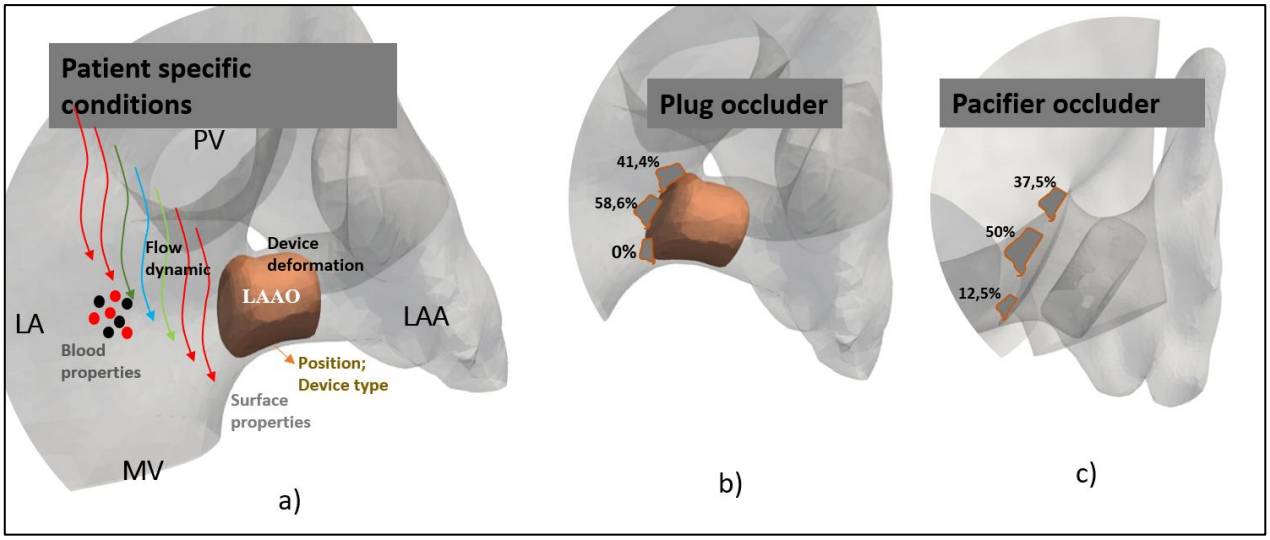

Figure 6: *a) Principal factors associated to thrombus formation, including blood properties, device type and positioning. b,c) Percentages of device-related thrombus (DRT) in different parts of the device, reported in Sedaghat et al.* ***[12]*** *for the plug- and pacifier-type of occluder devices (b and c, respectively). LAAO: left atrial appendage occluder. MV: mitral valve. PV: pulmonary veins.*

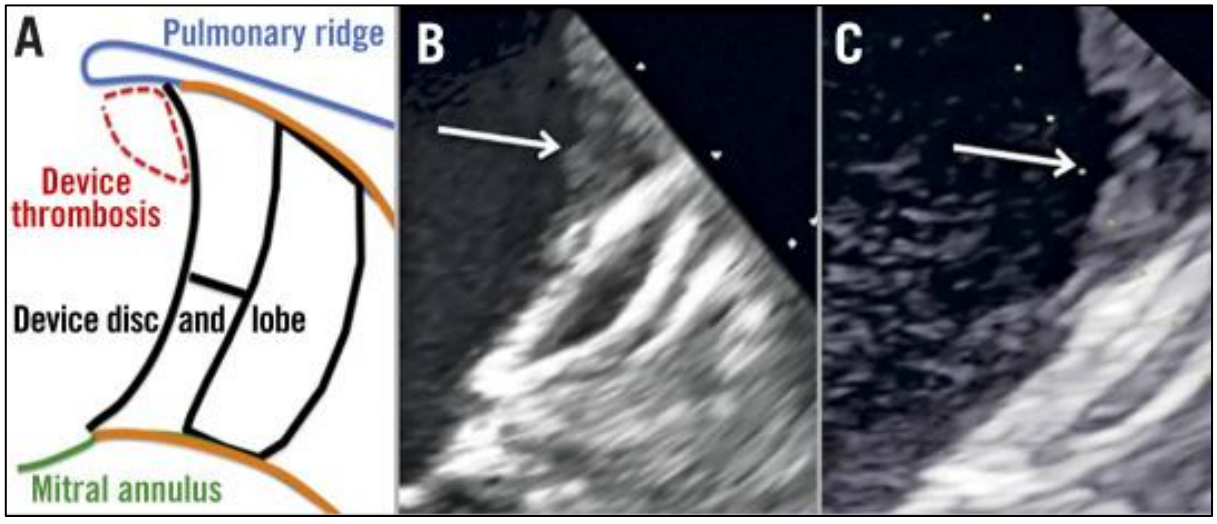

Figure 7: *Influence of covering the pulmonary ridge (PR) for avoiding device-related thrombosis, from Freixa et al.* ***[17]****. The arrows point to uncovered PR where thrombus is found after left atrial appendage occluder implantation.*

3.1.2 Device Description

Left atrial appendage closure devices (see Figure 8) are used to reduce the risk of stroke in patients with atrial fibrillation by occluding or sealing off the left atrial appendage, which is a small pouch-like structure in the heart where blood clots can form. Here are two commonly used device types:

1. Plug-Type Devices
   - Plug-type left atrial appendage occluders are designed to completely seal off the left atrial appendage (LAA). These devices typically consist of a self-expanding frame or mesh structure that fills and completely occludes the LAA, preventing blood flow into the appendage. The frame or mesh is often covered with a fabric or membrane material to enhance closure.
   - The Watchman device is an example of a plug-type occluder. It is developed by Boston Scientific, and it is a fabric-covered, self-expanding nitinol frame with fixation barbs. It is delivered through a minimally invasive procedure and placed in the left atrial appendage to block blood flow, thereby preventing blood clots from forming and potentially causing a stroke.

2. Pacifier-Type Devices
   - Pacifier-type left atrial appendage occluders, as the name suggests, partially occlude the LAA while allowing some blood flow to continue. These devices have a central channel or opening that allows limited blood flow through the LAA while reducing the risk of blood clot formation. This design is intended to maintain some physiological flow patterns and potentially reduce the risk of complications associated with complete occlusion.
   - The Amplatzer Amulet device is an example of a pacifier-type occluder. It is manufactured by Abbott and it consists of a self-expanding nitinol frame covered with a permeable polyester fabric. Similar to the Watchman, it is implanted in the left atrial appendage to close it off and reduce the risk of stroke.

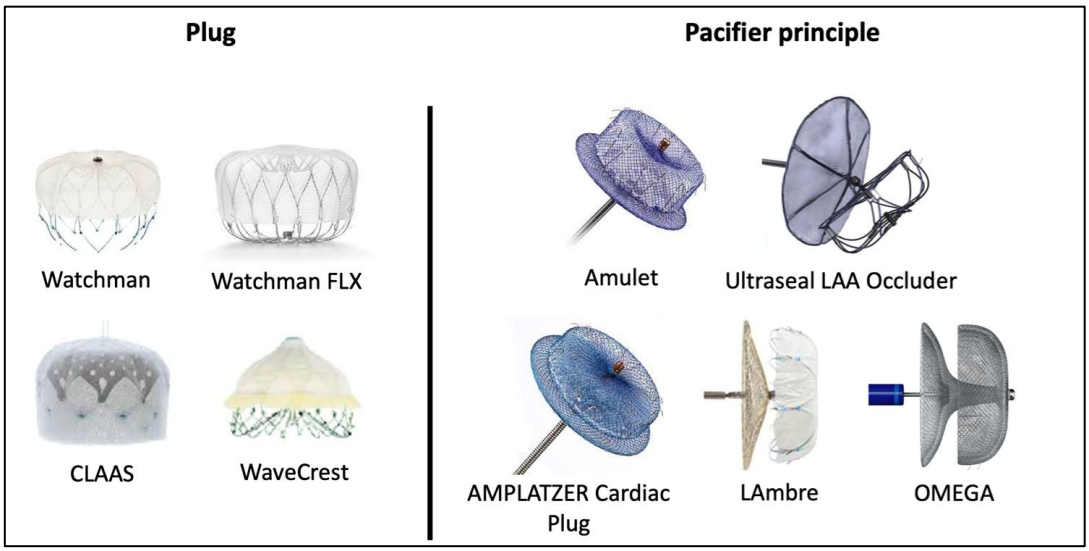

Figure 8: *Types of left atrial appendage devices, classified as plug or pacifier types. The most used devices are the Watchman and Watchman FLX (plug-type), developed by Boston Scientific (left), and the Amplatzer Amulet device (pacifier-type), manufactured by Abbott (right).*

3.1.3 Question of Interest

Several relevant questions of interest (QI) can be answered by computational fluid simulations applied to left atrial appendage occluder devices, encompassing different aspects of the device design and applicability. The different stakeholders involved in SimCardioTest, including device manufacturers, clinicians and academic partners defined multiple QIs during the project, which were ranked based on the most critical aspects to study in relation to possible adverse events during the implantation, especially regarding DRT.

The QI that had the maximum level of priority and feasibility, being selected to guide the V&V exercise of Use Case 2 according to ASME VV40 guidelines, is the following:

- Does covering of the pulmonary ridge with a LAAO device (plug or pacifier) relate with the likelihood of low blood flow velocities around the device and induce the device-related thrombus (DRT)?

The QI above follows the formulation found in pioneering V&V works on cardiac devices [18] and studies the influence of device settings (type and position) in relation to DRT by measuring low blood flow velocities.

3.1.4 Context of Use

From the selected QI, two different Contexts of Use (COU), assessing the device performance, were defined. These COUs have different level of influence on the decision of whether the covering of the pulmonary ridge (PR) with the LAAO device is equivalent to or better than placing it deeper into the LAA (i.e., with an uncovered PR). In both cases, the computational model is used to assess blood flow velocities near the device. The performed evaluations are based on two different cohorts, depending on the COU. In the first COU, pre-operative and follow-up imaging data from twenty patients who underwent LAAO has been used, half of them suffering DRT. The second COU is based on a set of two patient-specific geometries obtained from clinical cases: one suffers from AF, and the other acts as a control case.

- **COU1** - Performance evaluation with computational fluid simulations only. Computational modelling is used to identify low blood flow velocities near the device, placed in a proximal or distal position (e.g., covering or not the PR) with both device types (i.e., plug and pacifier). There is no supporting data from in-vitro testing available for assessing the performance of the occluder devices.

- **COU2** - Performance evaluation with computational fluid simulations and in-vitro data. In addition to in-silico experiments, in-vitro testing is conducted to create additional evidence on whether the covering of the PR is critical for DRT with both types of device.

3.1.5 Model Risk

The following considerations support the assessment of the risk associated with the numerical model.

- Decision Consequence: Medium

Based on VV40 guidelines, both COUs have a Medium consequence since the intended users are engineers from manufacturers, using computational fluid simulations and in-vitro testing experiments to optimize the design of next-generation occluder devices and provide better implantation guidelines to prevent DRT. If simulations and experiments are incorrect (i.e., under- or over-estimating the risk of DRT), they could lead to sub-optimal design of new devices and recommendations, potentially increasing abnormal events after implantation such as device embolization, DRT or peri-device leaks.

- Model Influence for COU 1: High
- Model Influence for COU 2: Medium

Based on VV40 guidelines, COU1 has a High influence because the computational model results are the only ones informing the decision. COU2 has a Medium influence because supporting data from in-vitro testing complement the computational modelling studies.

- Model Risk for COU 1: 4/5 (Medium-High)
- Model Risk for COU 2: 3/5 (Medium-Medium)

Model Risk is based on Decision Consequence and Model Influence stated above, according to Risk Matrix in Figure 9 (cf. section 1.2.5).

Model influence	**high**	**3**	**4 COU1**	**5**
	medium	**2**	**3 COU2**	**4**
	low	**1**	**2**	**3**
		low	**medium**	**high**
		Decision consequence		

Figure 9: *Model Risk Matrix (cf. ASME VV40) evaluating the COU1 and COU2 included in UC2.*

3.1.6 Model Description

Simulating blood flow in the left atrium with an implanted occluder device can indeed facilitate the identification of the parameters that may contribute to thrombus formation. By conducting blood flow simulations with the occluder device in place, researchers can explore the impact of various factors, such as the shape or position of the device, on flow characteristics and the potential for thrombus formation. The initial step involves processing patient-specific medical images to extract a three-dimensional model, followed by the building of an appropriate 3D volumetric mesh. In COU1, for each left atrial geometry, the two studied device positions (covering and uncovering the pulmonary ridge) have been previously defined. In COU2, fluid simulations from two patients are compared with an in-vitro setup. The blood flow magnitude and directions will serve as the primary parameters evaluated in the current V&V study, for detecting blood stagnation zones around the LAAO device.

As a previously required step for VV40 analysis of flow simulations with LAAO devices, verification and validation experiments to assess the credibility of blood flow simulations in the left atria without a device are also required. In SimCardioTest, we performed the largest VV40 study available in literature for such type of simulations, testing several numerical parameters in mesh and time-step convergence analysis, as reported in SCT deliverables D3.2 and D6.1, and recently published [19]. This study contributed to identify most of the numerical parameters to be used in fluid simulations of the left atria. The rest of the document will mainly focus on the complementary VV40 experiments performed on simulations including LAAO devices.

3.2 UC2 Model Validation

3.2.1 Computational Model Form

The commercial ANSYS Fluent solver, which was selected to run the fluid simulations in the left atria with occluder devices, specifically solves the equations of conservation of mass and momentum, as well as the stress tensor of the fluid using the finite volume method. In our use case, blood was finally considered as an incompressible Newtonian fluid in a laminar regime, so additional equations considering transport, turbulence effects, heat transfer, compressibility, species mixing and reactions were not used. Therefore, in computational fluid dynamics (CFD) simulations, the mass conservation equation reads as follows:

$$\frac{\partial \rho}{\partial t} + \nabla \cdot (\rho \mathbf{u}) = S_m,$$

where ρ is the fluid density, u is the fluid velocity field, and S_m is a source term that represents the addition of mass to the continuous phase from another second phase or any user-defined source. In our case, Sm is set to 0. On the other hand, the conservation of momentum equation reads as follows:

$$\rho \frac{\partial \mathbf{u}}{\partial t} + \rho \mathbf{u} \nabla \cdot \mathbf{u} = -\nabla p + \nabla \cdot \bar{\bar{\tau}} + \rho \mathbf{g} + \mathbf{F},$$

where p is the pressure field, ρg and F are the gravitational and external forces that act on the fluid, respectively, and $\bar{\bar{\tau}}$, is the stress tensor, defined by:

$$\bar{\bar{\tau}} = \mu \left[\left(\nabla \mathbf{u} + \nabla \mathbf{u}^T \right) - \frac{2}{3} \nabla \cdot \mathbf{u} I \right],$$

In addition, two different rheological scenarios were tested: (i) assuming the blood as an homogeneous and incompressible Newtonian fluid [20] [21] with constant density (1060 kg/m^3) and 0.0035 Pa/s viscosity; and (ii) assuming a Carreau´s model [22] to define a non-Newtonian approach [23], where the viscosity is a function dependent on the shear rate (γ). The dynamic viscosity in a Carreau's model is described by the following equation:

$$\eta = \eta_\infty + (\eta_0 - \eta_\infty)[1 + \gamma^2 \lambda^2]^{(n-1)/2}$$

where λ as time constant, n the power-law index, η_0 the zero shear viscosity and η, the infinite shear one. The values, (η_0\) = 0.056 Pa-s, η = 0.0035 Pa-s, λ= 1.902 s, n = 0.3568, were implemented from

[23] to model the blood conditions. The observed differences in blood flow velocity around the device, one of the chosen quantities of interest (QOI), were not significant (see Figure 10) and did not impact the conclusions or outcomes of our study.

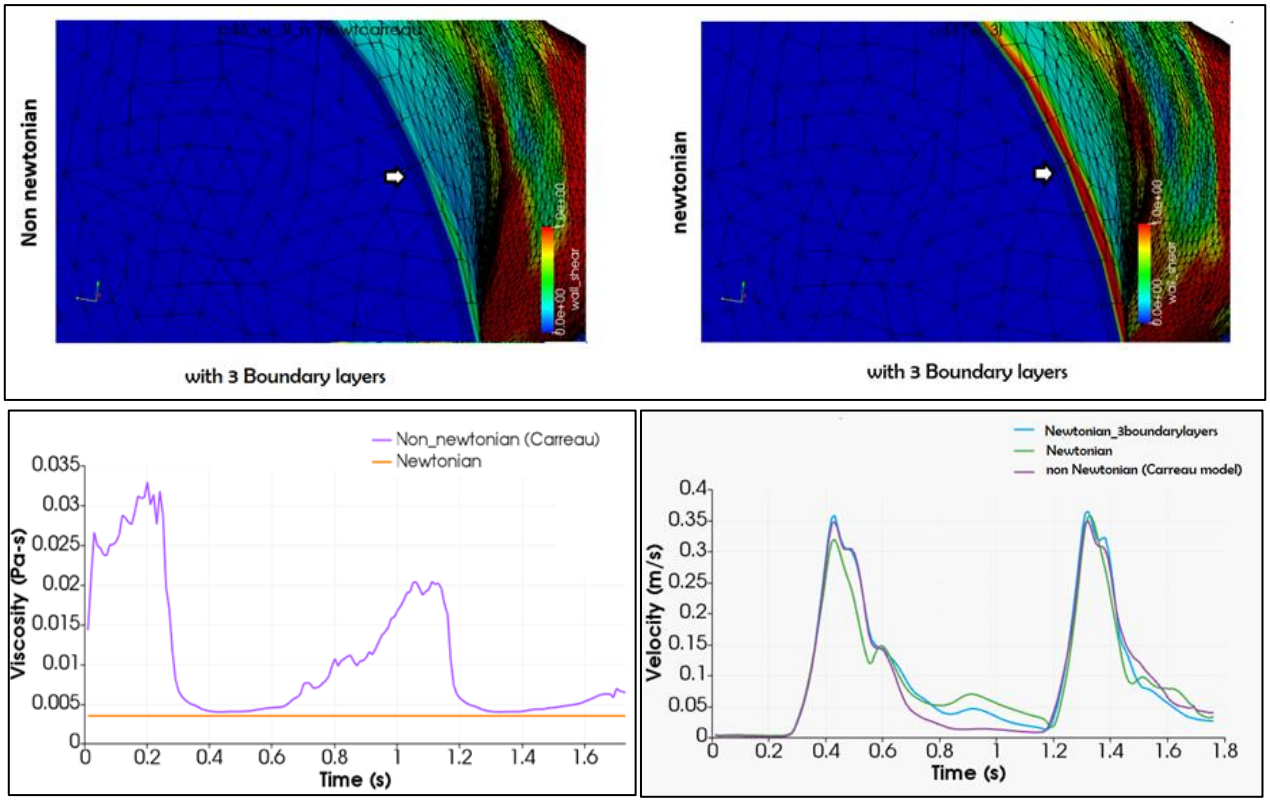

Figure 10: *Comparison of non-Newtonian and Newtonian flow models. Top: wall shear stress map. Bottom: variation of blood viscosity (left) and average velocity around the occluder device (right).*

In addition, in the large cohort of fluid simulations included in COU1, generic left atrial wall movement was assumed since personalized deformation data from dynamic computed tomography (CT) scans was not available for every analysed case. This assumption was evaluated in two cases where dynamic CT was available, to study the impact on the final simulation results [24].

For COU2, patient-specific dynamic CT data was available for the cases used to build the in-vitro testing experiments. Specialized actuators (see Figure 11), designed and manufactured by the group of Ellen Roche at MIT, collaborators of UPF in Use Case 2, were carefully devised and fixed to the LA wall of a 3D printed model [25], to apply the left atrial wall deformation extracted from the dynamic CT scans in the two processed cases. Given the dimensions of the actuators, certain assumptions had to be made. The three regions exhibiting the greatest magnitude of motion were identified and designated as the optimal placements for these actuators, since it was not possible to reach the node-precision of the image-derived information.

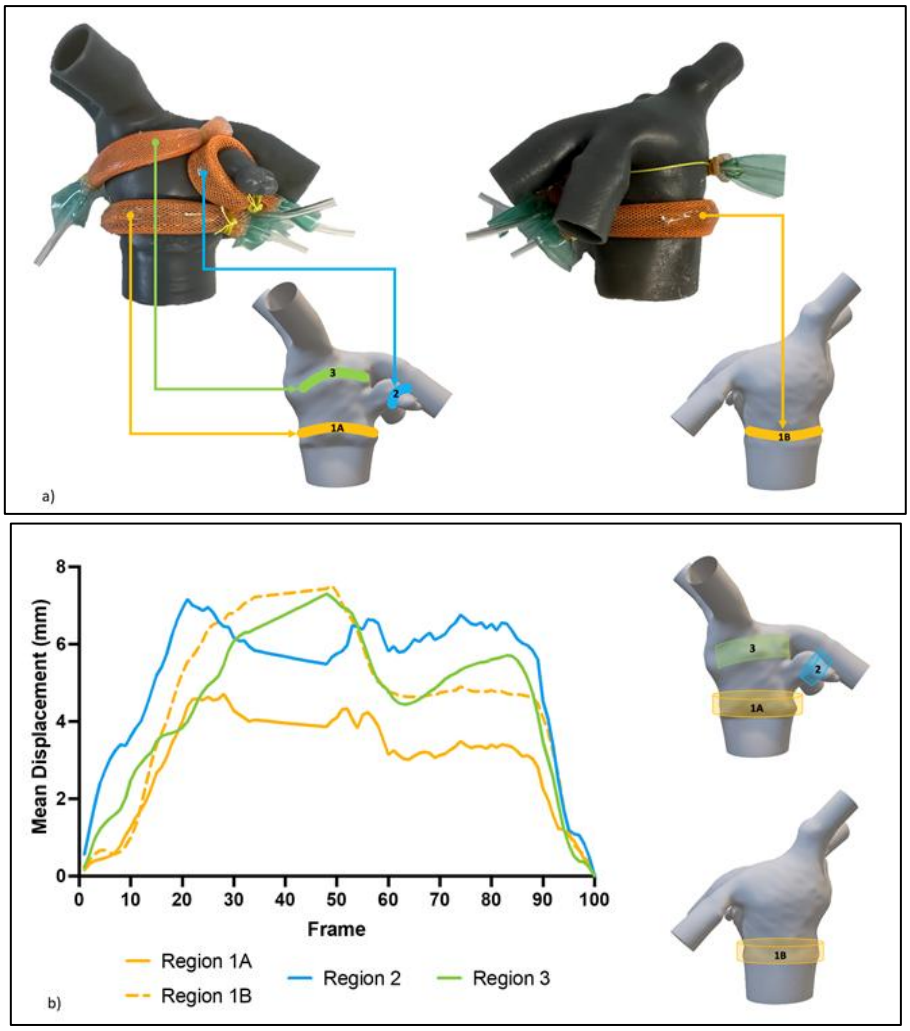

Figure 11: *Left atrial (LA) phantom data for the in-vitro test. a) Actuators and measurement zone (1A, 1B, 2 and 3) in the 3D printing LA model. b) Measured displacements in the zones using the actuators.*

The following is the gradation of activities, listed from lowest to highest credibility, that reflects the extent to which model form assumptions can be evaluated.

A) Influence of model form assumptions was not explored
B) Influence of expected key model form was explored
C) Comprehensive evaluation of model form assumption was conducted

The level of rigor of the credibility factor is currently (**B**), since the designed uncertainty plan has not been executed yet.

3.2.2 Computational Model Inputs

The gradation of activities, listed from lowest to highest credibility, related to the computational model inputs is the following:

A) Sensitivity analysis was not performed
B) Sensitivity analysis on expected key parameters was performed
C) Comprehensive sensitivity analysis was performed

The inputs and outputs of the Navier-Stokes equations can be either velocities or pressure values. The definition of which ones act as an input or output is often determined according to the accessibility to data where the boundary conditions (BC) are defined (i.e., pulmonary veins and mitral valve in our case). The inputs and outputs are the same for both COUs, so sensitivity analyses were performed to set the best configuration to increase the credibility of the validation. The first one, published in Mill et al. [20], studied four scenarios (Figure 12 and Figure 13), depending on the inlet and outlet BC, as well as the behaviour of the left atrial wall. Scenario 3, provided the more robust simulation results, highlighting the importance of personalized conditions. In Use Case 2, patient-specific mitral valve velocity profiles derived from Doppler echocardiography, are included as outlet BCs, while a generic pressure wave is imposed at the PV inlets. As for LA wall motion, a dynamic mesh approach guided by the displacement of the mitral valve annulus ring provided better simulation results than assuming rigid walls.

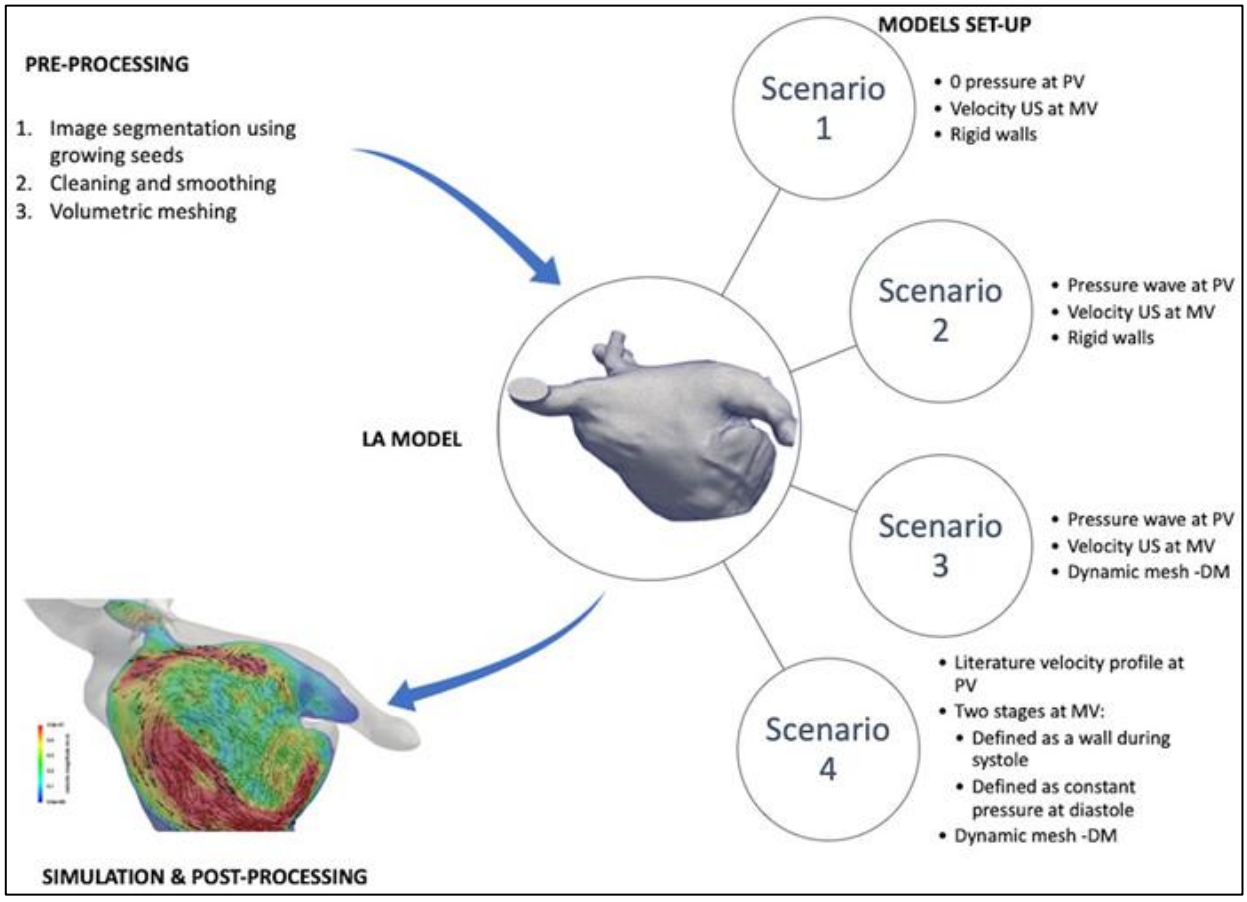

Figure 12: *Fluid modeling pipeline* ***[20]*** *including pre-processing steps to build patient-specific left atrial (LA) meshes and four different boundary conditions scenarios. PV: pulmonary veins; MV: mitral valve; US: ultrasound imaging; DM: dynamic mesh.*

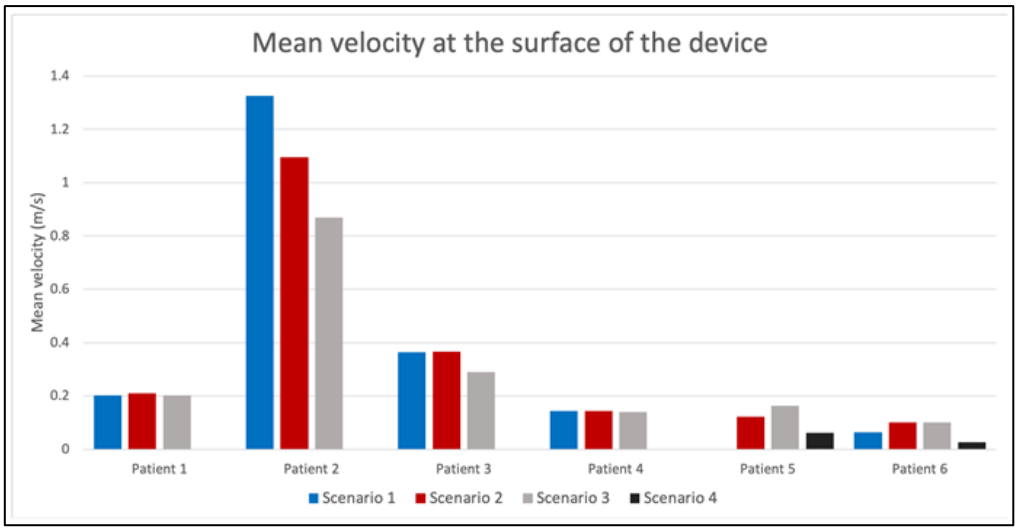

Figure 13: *Average blood flow velocities near the device surface for the different simulated scenarios in all analyzed patients, without and with device-related thrombus (Patients 1 – 3 and Patients 4 – 6, respectively). Missing bars in some patients indicate simulation divergence.*

The second study included two boundary condition settings of the inlets/outlets (pulmonary veins/mitral valve), which were tested in each of the analysed LA geometrical models [23]. First, a patient-specific velocity profile at the pulmonary veins (PV) was estimated from the derivative of left atrial and left ventricular volume changes measured from the dynamic CT (dCT) segmented images. In the first BC scenario (Configuration 1), the mitral valve was modelled as a wall during ventricular systole, representing its closing, and a constant pressure value (7 and 8 mmHg for healthy and AF cases, respectively, following [26]) at ventricular diastole, simulating its opening. In the second BC configuration (Configuration 2), a generic pressure curve was defined at the PV (in sinus rhythm and with AF for the healthy and diseased cases, respectively). A patient-specific velocity profile was defined at the mitral valve, also derived from dCT-derived volume changes of the LA and LV. To define the passive motion of the mitral annulus in the DM-SB scheme, a displacement function from literature [27] was imposed in the MV annulus plane, describing the longitudinal excursion of the MV. Then, a spring-based dynamic solution of the CFD solver was employed to ensure motion diffusion through the LA wall geometry.

The obtained results (see Figure 14) demonstrated that the ideal situation is to use LA wall motion derived from patient-specific dCT images, while using a dynamic mesh approach or rigid walls tend to provide lower blood flow velocities, thus over-estimating the risk of thrombus formation. Unfortunately, dCT images are rarely available for patients undergoing LAAO interventions; using a dynamic mesh approach was finally selected since it estimated more similar blood flow velocity patterns to the dCT ones compared to a rigid wall assumption.

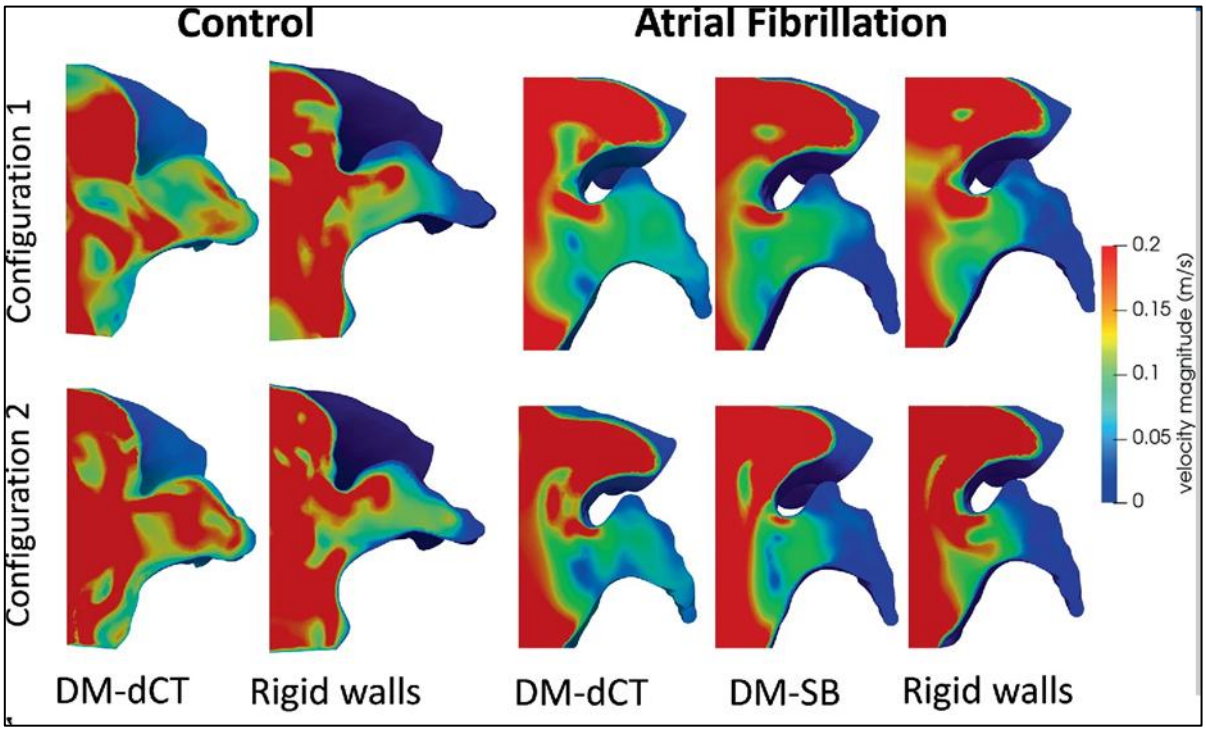

Figure 14: *Blood velocity patterns in the left atria (LA) during early diastole (t = 0.6 s) in a control and an atrial fibrillation (AF) patient with the different evaluated boundary conditions (BC) and left atrial wall motion approaches. BC configuration 1: velocity profile at the pulmonary veins (PV) inlet and constant pressure values at the mitral valve (MV) outlet. BC configuration 2: pressure at the PV inlet and velocities at the MV outlet. DM-dCT and DM-SB: left atrial wall movement approach guided by dynamic computed tomography images and spring-based method, respectively.*

The level of rigor of the "Computational Model Inputs" credibility factor is (**B**). Despite performing several sensitivity analysis involving different set of boundary conditions, more exhaustive experiments (e.g., including more LA geometries) could be designed to improve this credibility level. However, we positively identified the configuration of the key modelling parameters providing the more realistic simulations in terms of inlets/outlets and the LA wall motion behaviour.

Quantification of Uncertainties

The gradation of activities, listed from lowest to highest credibility, related to the quantification of uncertainties is the following:

A) Uncertainties were not identified
B) Uncertainties on expected key inputs were identified
C) Uncertainties were identified and quantified, but were not propagated to quantitatively assess the effect on the simulation results
D) Uncertainties on all the inputs were identified and quantified, and were propagated to quantitatively assess the effect on the simulation results

Velocity, pressure, wall motion, and fluid properties are indeed important factors in creating a model for studying fluid dynamics. Personalized data can help address uncertainties and improve the accuracy of the model by incorporating individual-specific information:

1. Velocities in mitral valve or in pulmonary veins using Doppler data
2. Pressure in mitral valve or in pulmonary veins using Doppler data
3. Displacement of the LA wall using dCT
4. Blood properties (e.g., hematocrit level) from standard clinical analysis

Moreover, even if personalized data is available, we need to consider variability in the measured parameters due to possible changes in each patient (e.g., during the day). As for the BC used in Use Case 2, pressure waves in the PV inlets and LA wall motion dynamics are difficult to obtain in a personalized manner, thus a range of generic profiles should be used. Finally, another source of uncertainty could be related to possible image acquisition and segmentation errors, which would lead to LA geometries not completely faithful to the real anatomy of the patient.

The credibility level of this factor is (**B**), since the main sources of uncertainty have been identified. However, they were not properly quantified or studied their effect on the simulation results.

3.2.3 Comparator Description

3.2.3.1 Comparator 1 - COU1

As the blood flow velocities were imposed at the MV in the designed modelling pipeline, it was deemed illogical from a physical standpoint to measure the velocity derived from the simulations at the same location where they were defined. Additionally, obtaining accurate velocity measurements at the LA poses several challenges. In fact, the MV area is considered the most favourable for acquiring measurements, as it is the easiest region to access with the transducer. On the other hand, capturing the flow accurately in other areas, such as the PV, can be challenging due to the ribs obstructing the ultrasound signal. One potential alternative is utilizing 4D flow magnetic resonance imaging (MRI), which would enable a thorough study of LA hemodynamics as well. However, we lacked access to ultrasound data at the PV or 4D flow MRI data. Therefore, in the case of COU1, we will rely on literature as a reference.

3.2.3.2 Comparator 2 - COU2

The bench-top circulatory model employed for COU2 is a sophisticated in-vitro flow model created by the Ellen Roche Lab at MIT. The schematic representation of this design is illustrated in Figure 15. The benchmark set-up includes connection to a flow pump to fill the system with liquid, soft actuators, and pressure sensors. It allows to test different patient-specific LA geometries represented as 3D printed models (i.e., silicon casting), which are incorporated into the cardiac simulator [25].

Following post-processing, smoothing, and shelling of the patient-specific meshes derived from dCT images, each LA geometry was 3D printed (Object Connex 500) and used to make a silicone casting (Ecoflex00-20) that was integrated into the cardiac simulator. Pneumatic artificial muscles (PAMs), a type of soft-robotic actuator, were used to make the LA contract cyclically. Pressure was measured

inside the LA/LAA while the actuation regime of the PAMs was varied (input pressure: 5-15 pounds per square (psi), [27]). Echocardiographic images were acquired during the experiment, as shown in Figure 16, to further analyse blood flow velocities in the LA.

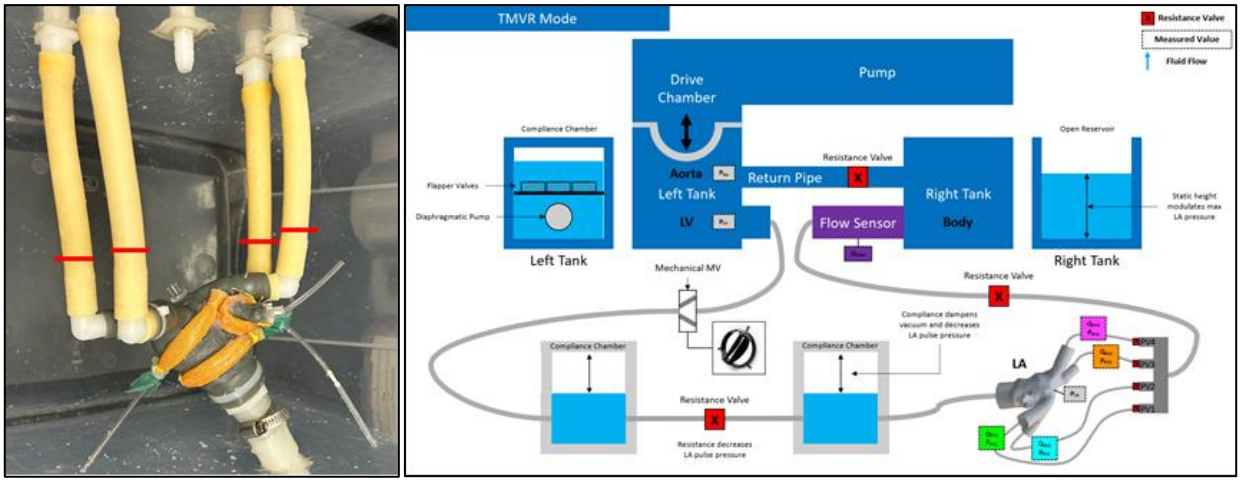

Figure 15: *Picture of 3D-printed left atria and the connections with the flow system (left). Schematic representation of whole setup system installed in MIT (right).*

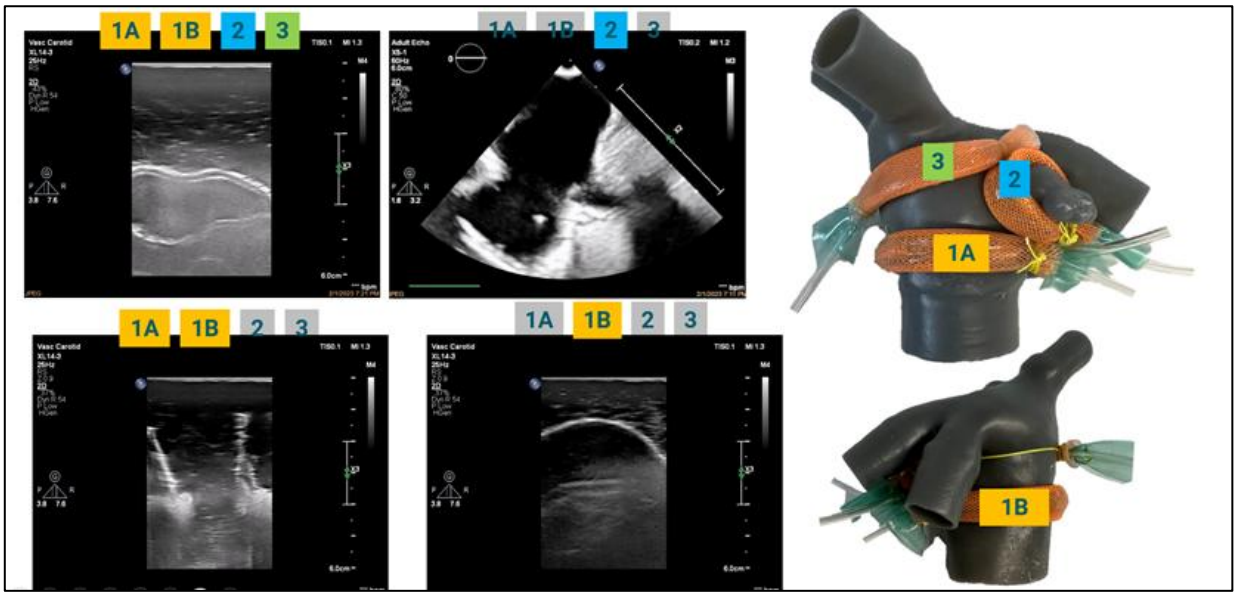

Figure 16: *Echocardiographic images acquired during the in-vitro test and the identification of the actuators zone.*

3.2.4 Comparator - Test Samples

The following is our gradation of activities, listed from lowest to highest credibility, that reflects the rigor of the quantity of samples used in the comparator study:

A) A single sample was used
B) Multiple samples were used, but the statistical distributions and the uncertainties are unknown
C) A statistically relevant number of samples were used

For both COUs, the assessment of the modelling pipeline performance is based on a set of patient-specific geometries obtained from clinical cases. For COU1, CT images of 20 non-valvular AF were provided by Hôpital Haut-Lévêque (Bordeaux, France) after the approval of the ethical committee and informed consent of the patients. The protocol of acquisition can be found in SCT deliverable 6.1 (Model Verification).

The selected QI aims at evaluating the occluder device parameters having an influence on covering or not the pulmonary ridge (PR), in relation to the risk of device-related thrombus. Therefore, for the clinical cases where the PR was uncovered, a new device position/configuration was virtually created to cover the PR with the device. A total of 33 different device configurations were then evaluated in COU1. Although this represents the largest in-silico study ever performed with fluid simulations incorporating occluder devices, there is a larger number of device positions and PR morphologies that were not analysed in the experiments, preventing a complete study of uncertainties and statistical distribution. Therefore, the credibility level of this factor was set to (**B**).

The COU2 comprises clinical cases in which patients underwent dynamic CT (dCT). This imaging modality enables the extraction of LA wall movement; however, it is not routinely included in the hospital's protocols, making it challenging to gather substantial cohorts. As a result, a single case was utilized for this particular COU2 study. Initial experiments are currently being conducted without the presence of the device in order to calibrate the flow loop. Once calibration is completed, a device will be introduced into the flow model. The planning, selection, and positioning of the device are carried out by an interventional cardiologist. Thus, for COU2, the credibility level is designated as (**A**). Nonetheless, the model risk for this COU is also lower.

3.2.5 Comparator - Test Conditions

The gradation of activities of this credibility factor include the analysis of the number and range of test conditions, as following:

Number of test conditions

A) A single test condition was examined (COU1)
B) Multiple (two to four) test conditions were examined (COU2)
C) More than four test conditions were examined

Range of test conditions

A) A single test condition was examined (COU1)
B) More than one test condition was examined (COU2)
C) Test conditions representing a range of conditions near nominal were examined
D) Test conditions representing the expected extreme conditions were examined
E) Test conditions representing the entire range of conditions were examined

In COU1, a single test was specified, involving pressure at the inlet, and Doppler-based velocity measurements at the mitral valve. The same boundary conditions were imposed to all samples. For COU2, the inputs in the computational system, such as velocities or pressure, differed from those in the bench-top 3D printed model. Hence, in order to enhance the credibility of our model, various test

conditions were examined to determine whether the simulations could consistently yield similar outcomes to those of the bench-top model.

From the computational model perspective, two distinct configurations of boundary conditions (BC) were tested, following the sensitivity analysis conducted in the preceding sections. This adjustment did not impact the bench-top model, where the inputs were the cardiac output and beats per minute. On the other hand, different beats per minute were assessed (100 and 60) to explore their effects on the flow within the left atrium (LA) and the 0.20 m/s threshold on blood flow velocities near the device. This input adjustment influenced and modified the configuration of both the computational model and the bench-top model.

Hence, when considering the number of test conditions, COU1 was assigned grade level (**A**), while COU2 was designated grade level (**B**). In terms of the range of test conditions, COU1 received the lowest grade (**A**) as it involved only a single test condition. Conversely, COU2 obtained a grade of (**B**), due to the examination of various values for cardiac output (CO) and beats per minute (bpm).

Another aspect of this credibility factor involves the measurements of test conditions, being associated with the following gradation of activities:

A) Test conditions were qualitatively measured and/or characterized
B) One or more key characteristics of the test conditions were measured
C) All key characteristics of the test conditions were measured (COU1 and COU2)

In both COUs, the primary test condition focused on measuring blood flow velocities. For COU1, beyond velocities, a range of in-silico indices were also computed from the simulation results to characterize the hemodynamic variations across the 33 device configurations. Specifically, the measurement area extended from the fold of the left superior pulmonary vein to the surface of the device, which constituted a vulnerable zone for low flow velocities (i.e. < 0.2 m/s) and complex fluid dynamics. Qualitative assessment of the blood flow was conducted using streamlines computed from the fluid simulations, while the quantitative evaluation involved calculating the average velocity within the volume encompassing this area. The analysis was performed during critical cardiac cycle phases (late-systole, and early/late-diastole) in the second cardiac beat to minimize convergence issues. The resulting simulation data underwent post-processing, visualization, and analysis using ParaView version 5.7.0 (https://www.paraview.org/). Consequently, COU1 was assigned the highest grade, (**C**), in this aspect of the credibility factor.

In COU2, the same hemodynamic indices were derived from the fluid simulations. When it comes to comparing the in-vitro experiment with the simulation results, the initial test was performed without the device, to evaluate the feasibility of the 3D printed model. However, the plan is to utilize the same measurement points as in COU1 with a device placed on the phantom model. Under this circumstance, only velocities and pressures can be obtained from the phantom model, restricting the possibility of analysing more detailed indices for comparison. Nevertheless, the key parameter, blood flow velocities, can be measured. For this reason, grade (**C**) was also given to COU2.

The last point of this credibility factor involves the uncertainty of test conditions measurements, which is graded as follows:

A) Test conditions were not characterized or were characterized with gross observations; measurement uncertainty was not addressed
B) Uncertainty analysis incorporated instrument accuracy only
C) Uncertainty analysis incorporated instrument accuracy and repeatability (i.e., statistical treatment of repeated measurements)
D) Uncertainty analysis incorporated a comprehensive uncertainty quantification, which included instrument accuracy, repeatability, and other conditions affecting the measurements

For COU1, the sensitivity analysis involved comparing differences among various results. However, since the context of use could not be compared with other imaging data or phantoms, no additional uncertainty measurements were conducted. Conversely, in the case of COU2, instrument accuracy is going to be analysed, including instrument repeatability and a more comprehensive uncertainty quantification once the calibration and construction of the 3D flow loop are completed, leading to a level (**C**) in this credibility factor.

3.2.6 Equivalency of Input Parameters

3.2.6.1 COU1

The inputs for the various simulation samples are consistent, and the ranges are equivalent as well. The velocity curve remains unchanged, with variations occurring solely based on the location within the mitral valve area.

3.2.6.2 COU2

The flow-loop circuit's inputs consist of the patient's cardiac output. As mentioned in the preceding sections, one of the test we are conducting is changing the inlet conditions in the simulations to determine which one aligns better with the aforementioned flow-loop inputs.

In the first test condition, pressure at the pulmonary valve (PV) and velocity at the outlet (i.e., mitral valve, MV) were applied to the computational model. The 3D flow-loop model is calibrated to ensure that the achieved pressure matches the measurements obtained from the cathlab, which serve as boundary conditions for the simulations. Therefore, pressure is not directly introduced into the 3D printed system, but through the calibration process, the pressure at the PV during measurements is made equivalent to that in the simulations.

In the second test, velocity at the PV and pressure at the MV were employed. The flow entering the left atrium (LA) is converted to velocity until the magnitude passing through the PV is identical in both simulations and the bench-top model (i.e., the inlet conditions are consistent for both systems).

In contrast to COU1, the patients involved in COU2 exhibit patient-specific velocity curves derived from the movement observed in dCT scans. Consequently, the inputs for the two tested scenarios

(i.e., healthy and atrial fibrillation) possess distinct shapes and values, albeit falling within the same magnitude range.

3.2.7 Output Comparison

The gradation of activities of this credibility factor has the two following components:

Quantity

A) A single output was compared
B) Multiple outputs were compared (COU2, COU1)

Equivalency of Output Parameters

A) Types of outputs were dissimilar
B) Types of outputs were similar
C) Types of outputs were equivalent (COU1)
D) Types of outputs were equivalent and case specific (COU2)

3.2.7.1 Comparator 1 (COU1)

To attain the credibility required for COU1, we are currently quantifying flow and velocity changes on a dataset comprising over 90 echocardiographic images at the mitral valve (MV). Consequently, the types of output are expected to be comparable. However, since both the input and the utilized database in COU1 are not patient-specific with the samples studied, there may exist minor differences, although not significant. The range should remain consistent.

Additional outputs, including pressure, particle attachment, and the endothelial cell activation potential (ECAP), have been computed to provide additional insights for our models. However, it is important to note that, apart from pressure, these outputs cannot be validated using either medical imaging or in-vitro models. Nonetheless, recent studies have suggested a potential association between these parameters and device-related thrombus (DRT), making them of interest for computation and comparison with follow-up CT scans of the patients. However, it is crucial to be cautious when interpreting the relationship between ECAP and other hemodynamic indices with DRT, as they have not been directly validated or compared with the outputs. Moreover, it is essential to acknowledge that non-hemodynamic factors may also contribute to this phenomenon. Nevertheless, in our experiments the primary output of interest, velocity, is directly linked to our Quantity of Interest (QoI).

3.2.7.2 Comparator 2 (COU2)

This sub-section presents the initial findings obtained from comparing fluid simulation results with the bench-top flow in-vitro experiment. As previously mentioned, various test conditions were evaluated, specifically by altering the heart rate (either 60 or 100 bpm) or interchanging the boundary conditions with velocity at the pulmonary vein (PV) and pressure at the mitral valve (MV), and vice-versa, to determine which configuration better aligns with the bench-top model. In the following, we showcase the healthy case with a heart rate of 60 bpm and the atrial fibrillation (AF) case with a heart rate of 100 bpm as a preliminary result.

Results obtained from the 3D-printed benchtop model under various test conditions

Healthy case (60 bpm) - Configuration: Pressure at the PV and velocity at the MV (Figure 17)

The outcomes derived from the 3D printed-base in-vitro setting require further refinement but show good preliminary results. The in-vitro experiment successfully replicated the four pressure waves observed in PV physiology (A, V, Y, X as depicted in Figure 17). However, the Y wave still exhibits insufficient magnitude. Similarly, when it comes to velocity, the simulation accurately captures the E (atrium emptying) and A (atrial kick) waves, albeit with velocities lower than the desired levels. Adjusting this discrepancy does not involve a mathematical formula but rather relies heavily on the configuration of the bench-top model. Manual adjustments of compliance chambers and valves are necessary until the desired reference values are achieved.

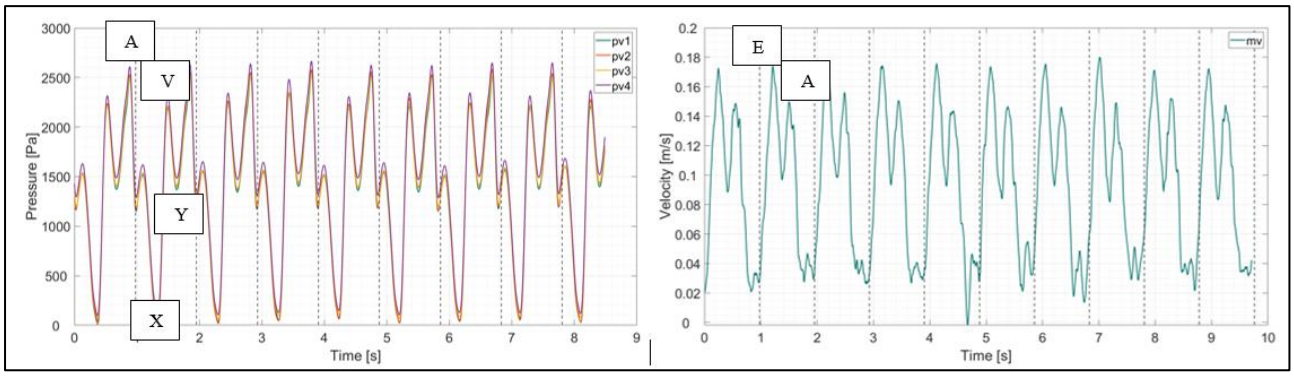

Figure 17: *Pressure data at the pulmonary veins and velocity measurements at the mitral valve were obtained from the phantom model using catheter-based measurements in the control scenario.*

Healthy case (60 bpm) - Configuration: Velocity at the PV and Pressure at the MV (Figure 18)

The alteration of boundary conditions demonstrates that there is minimal variation in the pressure within the left atrium between the pulmonary vein and mitral valve. The significant pressure difference occurs between the left atrium and left ventricle. On the other hand, the velocity results show promise, but further refinement is necessary with this configuration. The systolic and diastolic curves are generated, although the regurgitation wave, commonly referred to as A in the literature, is not observed. This discrepancy may be attributed to the simplification of the contraction using the soft actuators, which may not contract with sufficient strength. Additionally, the systolic curve is not entirely smooth and exhibits sub-peaks that are not observed in the medical imaging derived from patient data.

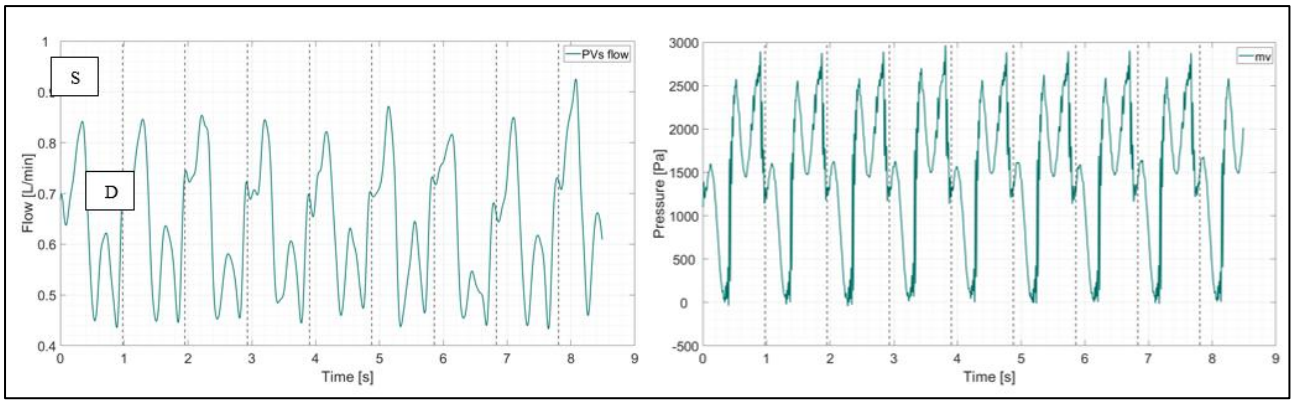

Figure 18: *Blood flow data from the pulmonary veins and pressure measurements at the mitral valve were obtained by extracting data from the phantom model using catheter measurements in the control case. It is assumed that the flow through all the pulmonary veins is equivalent, as the measurement was taken from only one of them.*

Atrial fibrillation case (100 bpm) - Configuration: Pressure at the PV and velocity at the MV (Figure 19)

As the heart rate increases, the various phases of the cardiac cycle are shortened. However, the issues with low velocities and the weak Y wave persist. This indicates that the problem lies in the calibration of the compliance and resistance of the system, rather than being dependent on the heart rate set by the pump.

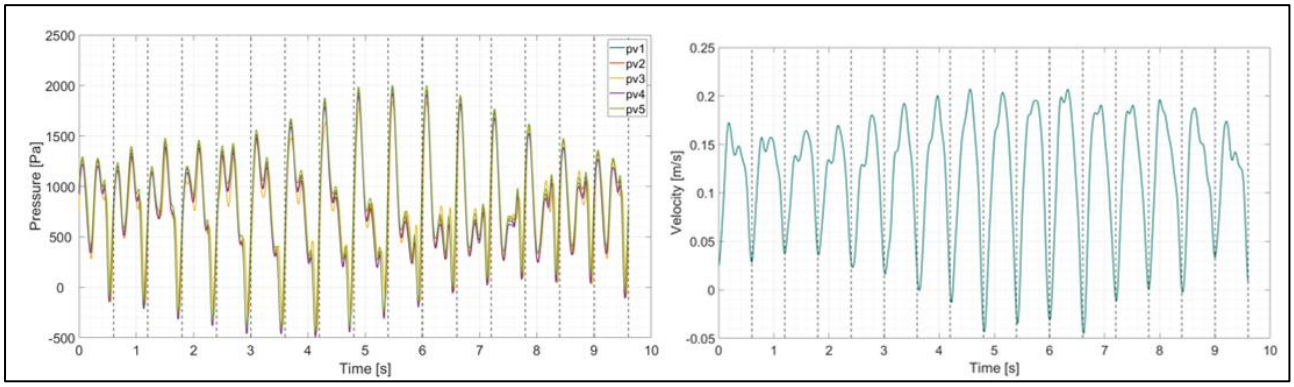

Figure 19: *The pressure data at the pulmonary veins and the velocity at the mitral valve were obtained by extracting them from the phantom model using catheter measurements in the case of atrial fibrillation.*

Atrial fibrillation case (100 bpm)- Configuration: Velocity at the PV and pressure at the PV (Figure 20)

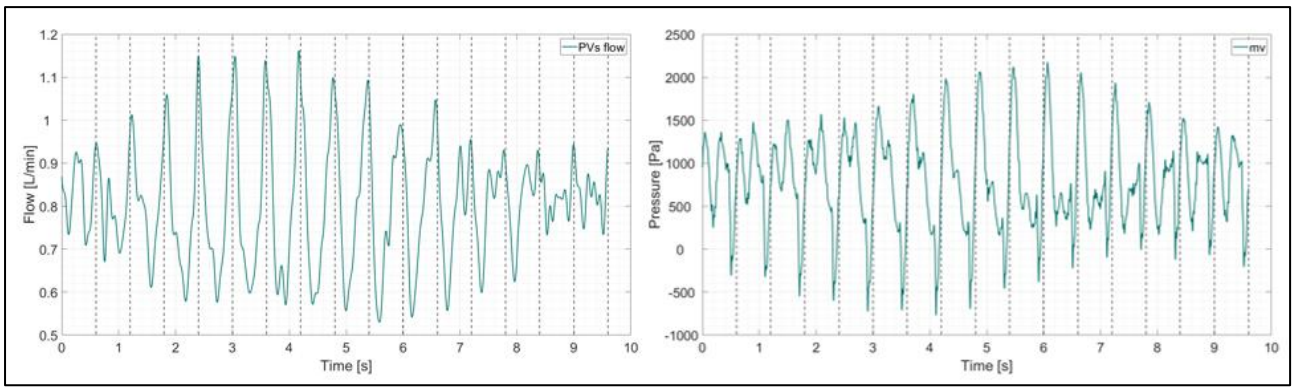

Figure 20: *Flow data at the pulmonary veins and pressure at the mitral valve extracted from the phantom model via catheter measurements in the atrial fibrillation case.*

Verification of boundary conditions from the phantom model in the simulation setup

Healthy case (60 bpm) - Configuration: Pressure at the PV and velocity at the MV

As depicted in Figure 21, the velocity curve derived from the bench-top model has been accurately aligned with our simulation model, along with the corresponding pressure values.

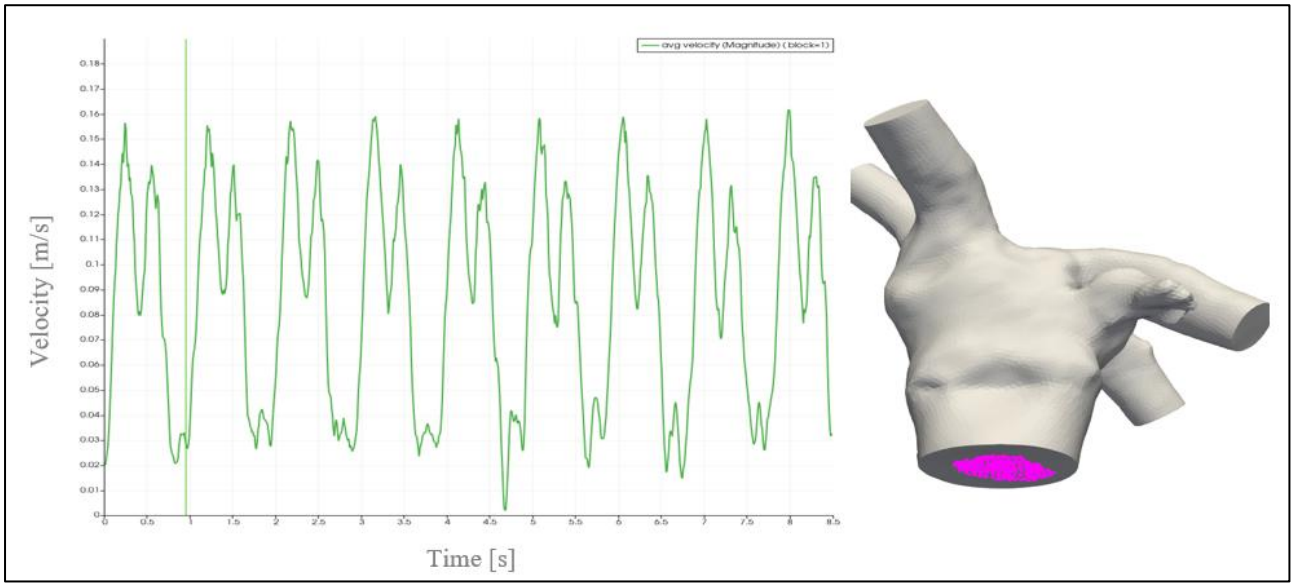

Figure 21: *Validation of the mitral valve velocity outlet was conducted based on the extracted data from the simulation results. The graph on the left illustrates the velocity profile observed over the course of nine simulated cardiac cycles. On the right, the measurement point is highlighted in pink for reference.*

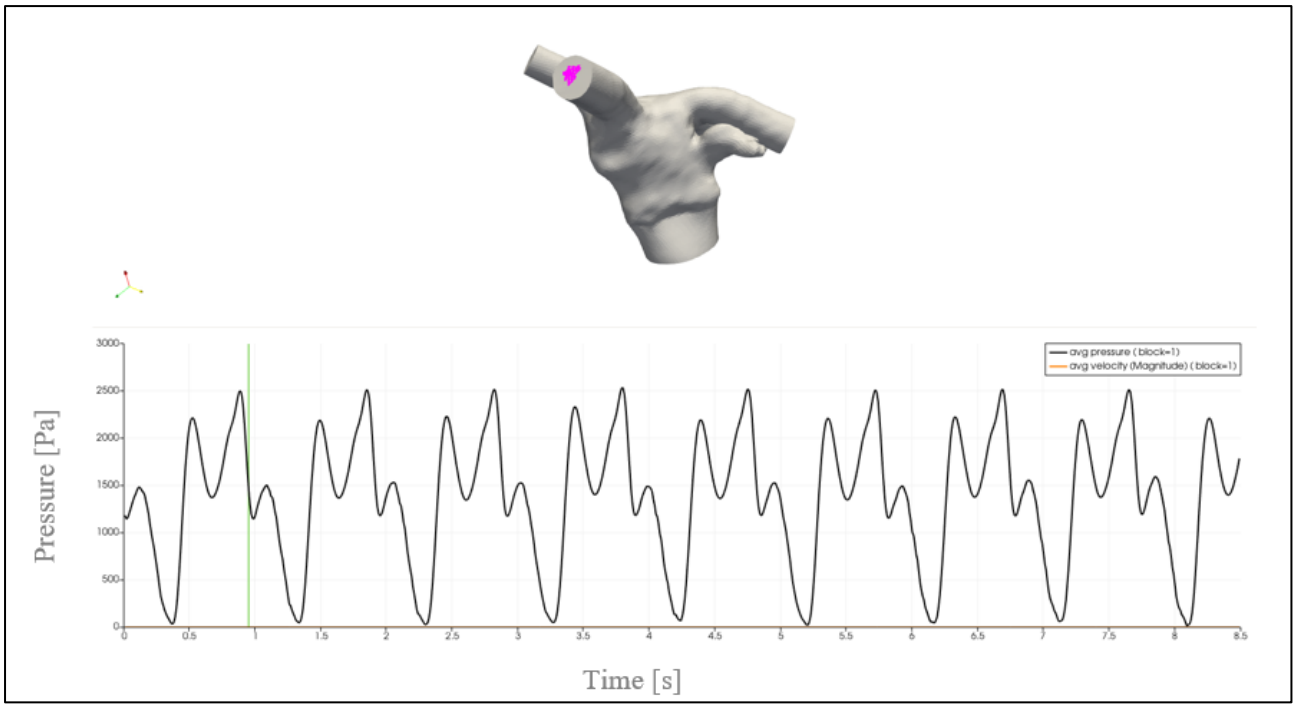

Figure 22: *The validation of the pressure inlet from the pulmonary veins was performed using the data extracted from the simulation results. The graph at the bottom displays the pressure profile throughout the nine simulated cardiac cycles. Positioned at the top is the measurement point highlighted in pink, specifically located at the right superior pulmonary vein (RSPV).*

Comparison between the 3D benchtop model and the flow simulations

As showed earlier, we have initiated the data collection process and conducted experiments using the bench-top flow model, excluding the device component. This crucial step is necessary because there are still adjustments required to accurately replicate the physiological behaviour of the circulatory system.

Subsequently, the gathered data must be incorporated into the 3D computational models, and simulations need to be executed with the defined characteristics and settings determined through verification and sensitivity analysis conducted in previous stages. It should be noted that these simulations can last for several days, and this ongoing work continues to progress. Nevertheless, within this deliverable, we present the initial comparison between the healthy case at 60 bpm, where pressure is measured at the pulmonary veins and velocity is measured at the mitral valve.

Healthy case (60 bpm) - Configuration: Pressure at the PV and velocity at the MV

The findings presented, as previously indicated, reveal that despite identical conditions, the velocity observed in the 3D printed model is lower than anticipated. In fact, when compared with Doppler data from patients, the simulation results align more closely with reality. We hypothesize that this disparity mainly arises from the imperfect replication of natural movement in the 3D printed model, even though contraction is simulated through soft robotics. Simulations, with their superior spatial resolution, are better equipped to replicate such scenarios. Additionally, another contributing factor to this variation could be the relatively brief duration of ventricular systole in the 3D printed model.

Consequently, the flow has more time to exit the atrium, resulting in a slower velocity. Another intriguing observation pertains to the discrepancy in the inflow of pulmonary vein (PV) flow within the simulations. This phenomenon has been documented in scientific literature [28]. However, in our 3D bench-top model, the sensor remains fixed in a single pulmonary vein, limiting our ability to assess whether this occurs in our setup as well. Furthermore, a notable distinction is evident in Figure 23, where each of the four pulmonary veins features additional tubes connected to the flow circuit. These tubes are arranged in parallel to one another. This configuration potentially establishes an analogy to a parallel circuit, thereby validating the assumption that the flow in each pulmonary vein remains consistent.

In conclusion, from a physiological perspective, the simulations at the pulmonary vein (PV) exhibit the presence of three distinct peaks. The two prominent peaks correspond to the S and D waves, while the third peak represents the A wave. The A wave displays an opposite direction, indicative of regurgitant flow. It is worth noting that the positive depiction of all three peaks in our visualization is attributed to plotting the magnitude of velocity, thus disregarding the directional information.

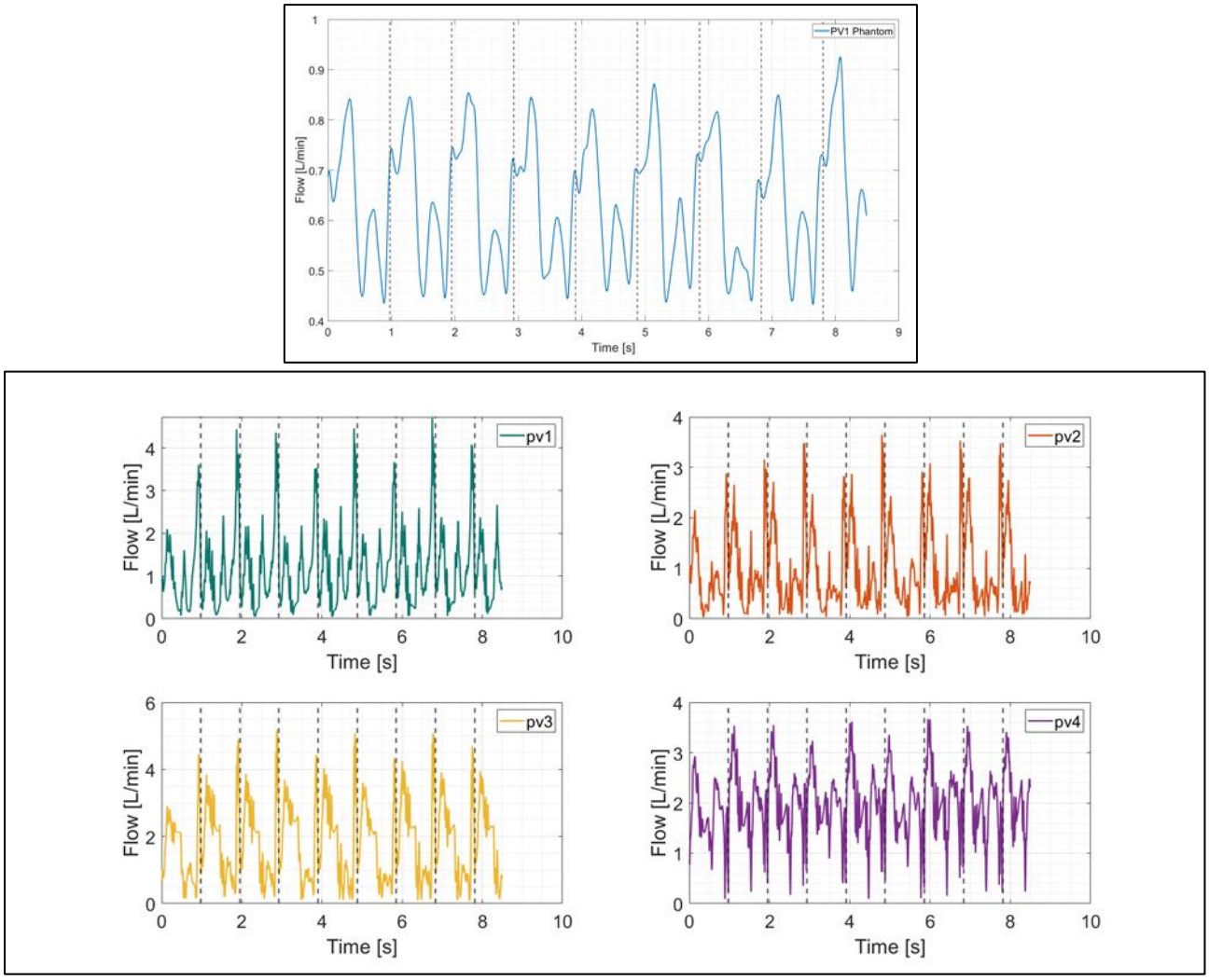

Figure 23: *The flow results obtained from the simulation outputs depict the measurements taken from each pulmonary vein (pv1 - pv4) in the model over the course of nine cardiac cycles.*

3.3 UC2 Validation Uncertainty

3.3.1 Model Uncertainty

Discussion on Model Uncertainty can be found in above sections 0 and 0.

3.3.2 Comparator Uncertainty

Discussion on Comparator Uncertainty for both COU1 and COU2 can be found in above sections 0 and 0.

3.3.3 Sources of Uncertainty

See sections above.

3.4 UC2 Model Applicability

Relevance of the QI

A) The QoIs from the validation activities were related, though not identical, to those for the COU
B) Subset of the QoIs from the validation activities were identical to those for the COU
C) The QoIs from the validation activities were identical to those for the COU (COU1 and maybe COU2)

In our study, we have successfully aligned the Quantities of Interest (QoIs) from the validation study, specifically the velocities near the Left Atrial Appendage Occlusion (LAAO) device, with the specifications outlined for Context of Use 1 (COU1), thus obtaining the (**C**) level. Additionally, in COU2, we have the opportunity to examine the velocities near the device using simulations. However, it remains to be seen whether we can gather data on the phantom model in that specific area using ultrasound imaging.

We were able to achieve alignment between the QoIs of the validation study and the COUs due to multiple iterations following the VV40 guidelines and implementing the suggested workflow (as shown in Figure 24). Initially, our variable of interest in the QoI was device-related thrombus. However, we realized that this had a significant impact on the validation process, leading to discrepancies not only in the comparator but also in the QoIs themselves, such as velocities and pressures, which differed from the QoIs of the COUs, specifically Device-Related Thrombus (DRT). As a result, the credibility of the simulations was compromised.

In the ongoing iterative process, we made the decision to focus on (low) blood flow velocities, which are correlated with DRT in non-valvular atrial fibrillation (AFib) patients [29]. Consequently, the variables of interest remained consistent between the COUs and the validation process, leading to better alignment and comparability.

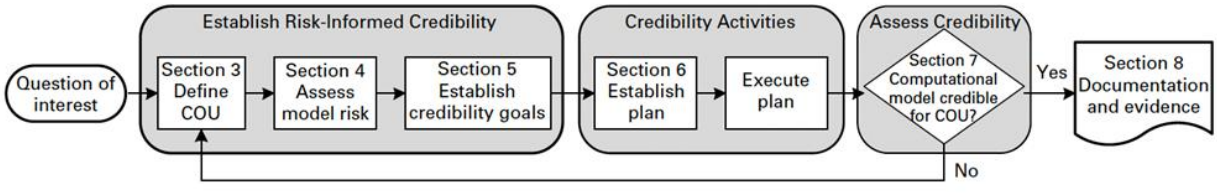

Figure 24: *Model Credibility Assessment workflow according to ASME VV40* ***[1]****.*

Relevance of the Validation Activities to the COU

A) There was no overlap between the ranges of the validation points and the COU
B) There was partial overlap between the ranges of the validation points and the COU
C) The COU encompassed some of the validation points COU
D) The COU encompassed all validation points
E) The validation points spanned the entire COU space

The validation points were situated within the defined space of the Context of Use (COU), thus obtaining a (**D**) level in this credibility factor. However, the inherent variability in the shapes of the left atrium (LA), particularly the orientation of the pulmonary veins (PV), as well as the shapes of the Left Atrial Appendage (LAA), can have an impact not only on the positioning of the device but also on the hemodynamics in the vicinity of the device.

To address this, it was decided to utilize two different contexts of use, enabling the use of two distinct datasets. In the first dataset, there was insufficient available information to generate a phantom model and patient-specific simulations, leading to certain assumptions, particularly regarding the behaviour of the LA wall. However, the sample size (N) for this dataset was large, resulting in a better representation of the overall population. Nonetheless, it is possible that the sample size in COU1 may still be inadequate. Consequently, in collaboration with the "Hospital de la Santa Creu i Sant Pau", we conducted an initial study to determine the necessary number of patients to enrol in a clinical trial focusing on studying device-related thrombus (DRT) using simulations. Considering the incidence of DRT and other relevant factors, a sample size of 200 patients was determined.

In COU2, the data is specific to individual patients, resulting in a simulation model and subsequent validation that are of higher quality. However, the cohort size is naturally smaller, rendering it less representative of the overall population and making the model more sensitive to cases that may exhibit significant differences.

3.5 UC2 Discussion and Future Work

The validation of computational fluid simulations including left atrial appendage occluder devices is even more complex than its verification (cf. SCT deliverable D6.1), due to the difficulty to obtain reliable data for comparison of the simulations. Fortunately, within SimCardioTest, we had access to a large clinical dataset of patients that underwent LAAO intervention, as well as some cases with available dynamic CT images. Additionally, we have collaborated with MIT researchers to develop an in-vitro experimental set-up based on 3D printed LA geometries connected to soft actuators to mimic the LA wall motion dynamics.

In this deliverable, we have analysed the different factors relevant for the model validation, uncertainty quantification and applicability. Overall, we have tested several model options (e.g., Newtonian vs non-Newtonian), identifying the necessary boundary conditions (e.g., inlets/outlets, LA wall motion behaviour) to answer the selected QI. However, additional uncertainty quantification studies (e.g., different pressure waves as inlets, analysing segmentation error influence, various heart rates) could be beneficial to increase the credibility level of some analysed factors. Furthermore, running simulations on a larger dataset of patient-specific LA geometries, currently in

progress, would increase the confidence on the chosen modelling pipeline configurations. For instance, dynamic CT images have been available only on two cases due to the issues for acquiring this type of data in every patient. We are currently working a larger dataset of dCT scans to derive statistical atlases of LA wall motion behaviour, which could be applied when patient-specific information on the LA wall motion is not available. Still, dCT scans including LAAO devices are not available yet.

The initial comparisons between fluid simulation and in-vitro experimental results are very promising, validating the use of the actuators to impose a LA wall motion behaviour obtained from the dCT scans. However, including a LAAO device in the bench-top set-up has been a challenge due to the complexity of the printing process that the time needed to tune every analysed scenario. Moreover, blood flow velocities obtained in the in-vitro set-up are lower than expected, thus further calibration is required to obtain more physiological values.

It is important to emphasize the alignment between the QI/COU and the quantities of interest (QoI) that are possible to measure through experiments. A detailed analysis of the available data is necessary before initiating any validation task, giving priority to have a reliable comparison rather than selecting more interesting but challenging to measure quantities of interest. If not enough data can be acquired, the influence of the model needs to be reduced (cf. ASME VV40 guidelines [1]).

Table 8 and

Table 9 summarize the validation credibility factor coverage in the model risk analysis for the COU1 and COU2 respectively. Coverage level determined in section 0 was converted in a 1-to-5 scale for consistency with section 1.2.5.

Table 8 : Validation and Applicability Credibility Factors Coverage Level for Use Case 2 - COU1 (cf. ASME VV40); * indicates validation activities not yet completed.

Model Risk						x	
Credibility Factor Coverage Level			1	2	3	4	5
Validation - Model [Form]	III					x	
Validation - Model [Inputs]	III					x	
Validation - Comparator [Test Samples]	III					x	
Validation - Comparator [Test Conditions]	I					x	
Validation - Assessment [Input Parameters]	III					x	
Validation - Assessment [Output Comparison] *	IV					x	
Applicability: Relevance of the Quantities of Interest	V					x	
Applicability: Relevance of the Validation Activities to the COU	IV					x	

Table 9 : Validation and Applicability Credibility Factors Coverage Level for Use Case 2 - COU2 (cf. ASME VV40); * indicates validation activities not yet completed.

Model Risk					x		
Credibility Factor Coverage Level			1	2	3	4	5
Validation - Model [Form]	III				x		
Validation - Model [Inputs]	III				x		
Validation - Comparator [Test Samples] *	I				x		
Validation - Comparator [Test Conditions]	III				x		
Validation - Assessment [Input Parameters]	V				x		
Validation - Assessment [Output Comparison] *	V				x		
Applicability: Relevance of the Quantities of Interest	V				x		
Applicability: Relevance of the Validation Activities to the COU *	IV				x		

The lowest score for COU1 involves the "Test Conditions" credibility factor since only one set of boundary conditions was applied to all cases, based on sensitivity analyses previously performed (see SimCardioTest deliverable 6.1). However, this does not affect the outcome of the validation task nor the ability of the computational model to answer the QI, i.e., identifying low blood flow velocities near the occluder device depending on device settings and coverage of the pulmonary ridge. As for COU2, the lowest score is related to the "Test Samples" credibility factor, due to having tested the in-vitro experimental set-up only on one patient-specific left atrial geometry. Testing more LA geometries would be relatively easy with the calibrated experimental set-up, but with only one geometry and different boundary conditions (heart rate, inlet/outlet configuration), it can already be demonstrated the match between simulation results and experimental measurements in different conditions to increase the credibility of the developed modelling pipeline.

Ongoing and future work on validation activities to improve the credibility level of VV40 factors include the use of 4D flow MRI data for a complementary QI, using the whole set of available clinical data from Bordeaux' s hospital involved in SimCardioTest (> 230 LAAO cases), employing ultrasound images for validation of the blood flow velocities. As for the in-vitro experiment, further calibration is required to have more physiological ranges of velocities and pressures, and first tests adding a LAAO device and more advanced measurement techniques (e.g., fluorescent particles for particle image velocimetry).

In any case, the performed validation on fluid simulations with LAAO devices is unique due to the data available in SimCardioTest, including a large database of clinical data, in-vitro phantoms, and advanced imaging scans. We have identified the required experiments and quantities of interest to perform reliable comparisons in the defined QI and COU, also establishing the credibility level of all

important factors in the VV40 guidelines. Additional uncertainty studies could be beneficial for increasing some credibility levels, but it will not be critical for the work in SimCardioTest due to the defined model risk.

4 Use Case 3

4.1 UC3 Model Summary

NOTE: This section is identical for both deliverables D6.1 and D6.2. Refer to section 0 for document organization.

4.1.1 Background

Safety pharmacology studies evaluate cardiac risks induced by drugs. Since Torsade de Pointe (TdP), a well-known malignant arrhythmia, was related to pharmacological effects, regulatory guidelines have looked for biomarkers able to identify arrhythmogenic effects of drugs in order to withdraw them from the development process. Consequently, research efforts to ensure the safety of new molecules have become time-consuming and expensive for drug developers, delaying the release of new medicines into the market. Besides, initial tests focused on hERG (human ether-à-go-go related gene) activity and in vitro repolarization assays limited the development of potentially beneficial compounds, and the increasing attrition rate urged the design of new strategies.

The first initiative to include in-silico models was the Comprehensive in-vitro Proarrhythmia Assay (CiPA), which proposed integrating drug effects obtained in-vitro into a cardiomyocyte model to predict TdP risk. Furthermore, the continuous development of new models opens the possibility to personalize computer simulations to optimize drug therapy.

4.1.2 Drug Description

Drugs are chemical compounds that exert a therapeutic action by modulating physiology. Besides the therapeutic effects, undesirable secondary effects can alter the normal functioning of different organs, including the heart.

Some molecules can modulate cardiac function by interacting with cellular mechanisms. Specifically, molecules that induce critical changes in ion channel permeability alter myocyte electrical activity, causing changes in heart rhythm with potentially fatal consequences. For this reason, drug developers need to perform safety pharmacology tests to evaluate drug candidates.

Before reaching cardiac tissue, drugs undergo a series of processes inside the body from its administration, including a distribution phase. Pharmacokinetics describes all these steps inside a living organism until the complete elimination of the substance, but interactions between each chemical compound and each organism differ. Pharmacokinetic processes are influenced by many external variables such as gender, age, weight, and previous pathologies, and the analysis of all the contributors is needed to determine the better therapeutic dose and route of administration.

Integrating pharmacokinetics and electrophysiology studies in drug assessment allows a more complete and personalized evaluation of the proarrhythmic risk by including the dosage and specific characteristics of the patient.

4.1.3 Question of Interest

The Question of Interest addressed by the model is the following:

- What is the maximum concentration/dose regimen of a drug to assure TdP-related safety in a population of healthy subjects?

4.1.4 Context of Use

A human electrophysiological (EP) model with pharmacokinetics (PK) can be used at early phases of drug development to obtain biomarkers that guide in selecting drugs and doses without TdP-risk for each subpopulation (male/ female/ age). This computational model is not intended to replace in vitro or animal experiments but to enrich and complement them by predicting additional outcomes. The goal of the in-silico trials is to help in designing clinical trials, to reduce the number of participants and protect them from suffering malignant arrhythmogenic events.

TdP-risk index is a metric obtained from a single or a set of electrophysiological biomarkers. By using appropriate threshold values, it performs a binary classification (safe/unsafe).

Quantities of Interest (QoI)

To obtain TdP-risk index, we considered action potential duration (APD90) and QT interval as the main indicators. Secondary biomarkers were calculated to improve predictions.

4.1.5 Model Risk

The following considerations support the assessment of the risk associated with the numerical model.

- Decision Consequence: Medium

An incorrect prediction with the computational model can have a risk on the development of the clinical trial if torsadogenic concentrations were administered. Low concentrations, on the other hand, do not have negative electrophysiological consequences.

- Model Influence: Medium

The model will complement preclinical and non-clinical (animal) experimental data and will help to design and refine the inclusion criteria and dosage in posterior clinical trials. In vitro and in vivo tests will still be required, but the number of participants in clinical trials as well as malignant arrhythmogenic events can be reduced. Therefore, the model will act as a complementary approach in determining safe drug concentrations.

- Model Risk: 3/5 (Medium-Medium)

Model Risk is based on Decision Consequence and Model Influence stated above, according to Risk Matrix in Figure 25 (cf. section 1.2.5).

Model influence	**high**	**3**	**4**	**5**
	medium	**2**	**3 COU**	**4**
	low	**1**	**2**	**3**
		low	**medium**	**high**
		Decision consequence		

Figure 25: *Model Risk Matrix (cf. ASME VV40) evaluating the COU included in UC3.*

4.1.6 Model Description

The computational model for proarrhythmic risk prediction integrates the following steps:

- Pharmacokinetics
- Heart electrophysiology
- Cardiac mechanics

One particular aspect of this in-silico strategy we propose for drug assessment is the inclusion of patient characteristics to optimize predictions.

The model pipeline initiates with drug pharmacokinetics, which consists of obtaining the plasmatic concentration following a specific compound dosage. This concentration is used as the input of the cellular model to simulate the drug effect on myocyte electrophysiology based on the interaction of the pharmacological molecule with ion channels. The last step of the computational model is to simulate and predict the electrophysiological activity in the whole heart.

Verification activities were evaluated separately in each computational model because the tools were developed independently.

4.2 UC3 Model Validation

4.2.1 Computational Model Form

4.2.1.1 PK Model

Models form were evaluated according to the structure of the models, which may be in the form of population models, or models built from non-compartmental data. A score is attributed to each model according to its structure.

See details in annex A6.2-UC3-PK (UC3 PK Validation Annex), Model Form section.

4.2.1.2 EP-0D Model

Model form was evaluated by a sensitivity analysis (Figure 26) to identify the important contributors to model uncertainty. The influence of key model parameters, i.e. maximum conductivities and fluxes, that can impact predictions within the COU was explored and the strategy proposed to address model uncertainty was a population of cellular models.

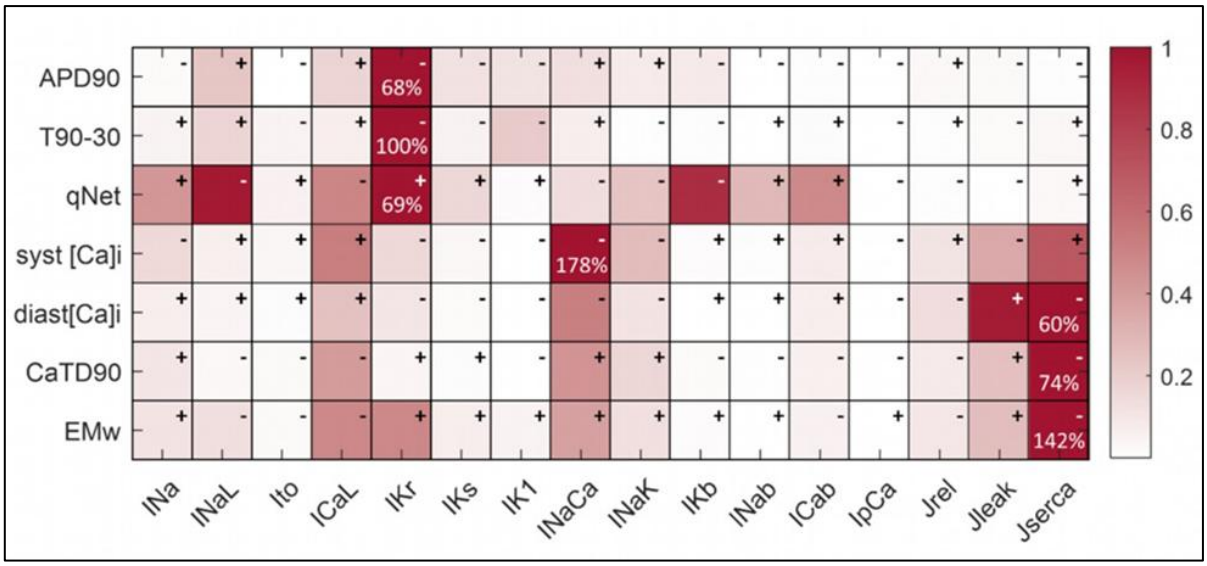

Figure 26: *Sensitivity analysis in the cellular model. Relative sensitivities for each marker (rows) represented by the color code, being dark red the maximum value and percentages indicate the maximum absolute value. Signs indicate whether the dependency is direct (+) or inverse (-).*

See details in annex A6.2-UC3-0D (UC3 0D Validation Annex), Model Form section.

4.2.1.3 EP-3D Model

Model forms were evaluated with respect to the effects of different input parameters to the accuracy of predictions within the COU. We looked at the effects of the different ion channel populations as well as the effects of geometry. See details in annex A6.2-UC3-3D (UC3 3D Validation Annex), Model Form section.

4.2.2 Computational Model Inputs

4.2.2.1 PK Model

Models inputs are evaluated according to the type of data (i.e., NC data or popPK data) and the variability described around the parameters. A score is attributed for each model according to model robustness criteria. See details in annex A6.2-UC3-PK (UC3 PK Validation Annex), Model Inputs section.

4.2.2.2 EP-0D Model

We assessed model inputs by exploring key parameters modulated by drugs and quantifying uncertainty propagation on quantities of interest. First, a sensitivity analysis identified the contribution of each ion channel and then uncertainty in the main IC50 parameter was propagated to APD90. We also examined the influence of inter-individual variability depending on the subpopulation under study by generating new populations of models adapted to patient sex, and by propagating these uncertainties to simulation results. See details in annex A6.2-UC3-0D (UC3 0D Validation Annex), Model Inputs section.

4.2.2.3 EP-3D Model

The main tissue parameters that will be explored in the validation strategy is the conductivity parameter and the effects of the geometry. We will use a benchmark study to ensure that conductivity parameters used in the simulations reflect realistic conduction velocities. Additionally, since simplified geometries will be used in the platform, we will also investigate how simulation results using a realistic 3D torso model differs from using the simplified tissue slab. See details in annex A6.2-UC3-3D (UC3 3D Validation Annex), Model Inputs section.

4.2.3 Comparator Description

4.2.3.1 PK Model

In PK, there are several types of comparator to confirm the accuracy of predictions. The most robust comparators are observed databases derived from patient blood samples. In practice, these databases are difficult to access, both because they are restrictive and because they are not often disclosed by hospitals. Other comparators exist, and are derived directly from the analysis of these databases. These are non-compartmental endpoints (area under the curve, half-life of elimination, etc.). There are also therapeutic thresholds, used in practice to monitor the plasma concentration of molecules for which it is imperative to do so in order to optimize drug efficacy and safety. We therefore assessed the comparators according to all these criteria. See details in annex A6.2-UC3-PK (UC3 PK Validation Annex), Comparator section.

4.2.3.2 EP-0D Model

The comparator consisted of historical experimental data, taken from literature. We carried out an extensive research on electrophysiological cellular data obtained from in-vitro repolarisation assays and/or in-vivo studies with drugs. We analysed and selected data according to experimental settings such as type of sample, drug exposure, and other physiological conditions that can influence results, but the final comparator used as validation reference was limited by data availability and experimental quality.

A second comparator based on the gold standard classification of drugs as safe or unsafe (made by the CiPA initiative [30]) was used to validate the classification predicted by simulations.

See details in annex A6.2-UC3-0D (UC3 0D Validation Annex), Comparator section.

4.2.3.3 EP-3D Model

Similar to the EP-0D model, the comparator used will be historical data on the effects of the drug on the pseudo-ECG signal. We will use data available for drugs with known effects on different ECG markers and evaluate how closely our simulations can predict these changes. See details in annex A6.2-UC3-3D (UC3 3D Validation Annex), Comparator section.

4.2.4 Comparator - Test Samples

4.2.4.1 PK Model

Several types of data are available for model validation. These test samples are evaluated according to their robustness. See details in annex A6.2-UC3-PK (UC3 PK Validation Annex), Comparator section.

4.2.4.2 EP-0D Model

Selected experimental data sets for the validation defined the quantity, range and uncertainty of samples. The better controlled credibility factor was input characteristics, as we particularised the comparator for each drug. As an example, clarithromycin experimental observations extracted from literature are shown in Figure 27.

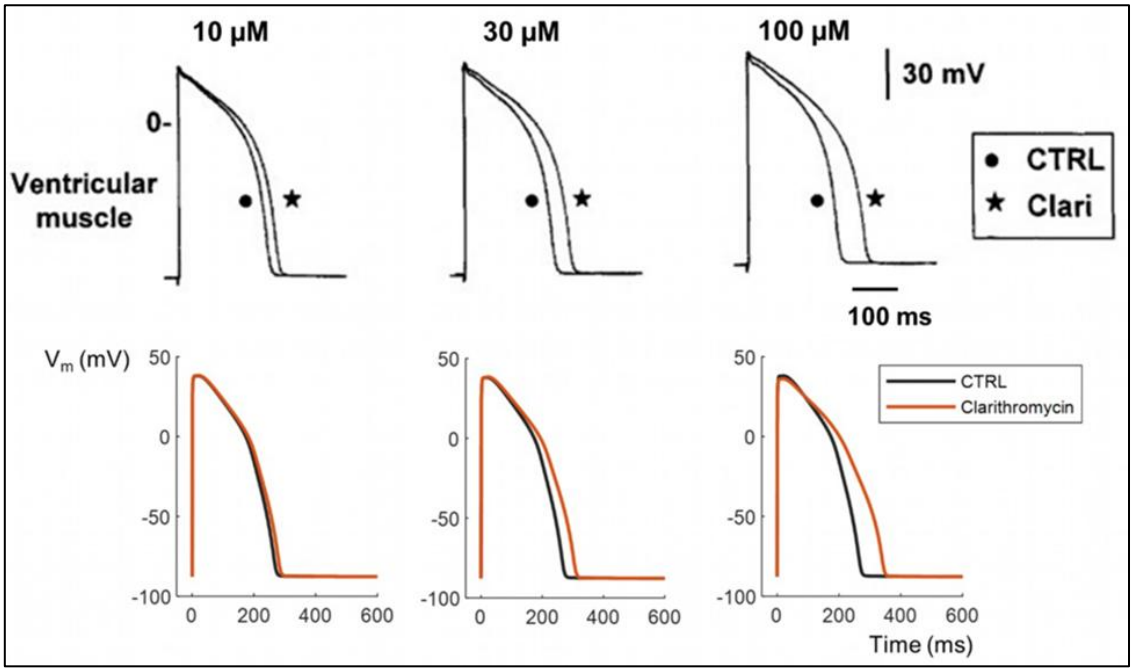

Figure 27: *Action potential prolonging effects of different concentrations of clarithromycin. Simulated results (lower panels) compared to experimental observations extracted from Gluais et al. (upper panels).*

See details in annex A6.2-UC3-0D (UC3 0D Validation Annex), Comparator section.

4.2.4.3 EP-3D Model

We will use the most recent clinical data that we have available for effects of drugs on different populations. The same challenges outlined in EP-0D Model will be present in the test samples for the EP-3D validation. See details in annex A6.2-UC3-3D (UC3 3D Validation Annex), Comparator section.

4.2.5 Comparator - Test Conditions

4.2.5.1 PK Model

The test conditions must reflect all possible configurations in which the model can be used. Thus, test conditions are rated according to their ability to reproduce all necessary test scenarios, the model's ability to be specific for the sub-populations covered by the drug, and the ability of official dose recommendations to cover all patients whose specificities will vary the PK of the drug. See details in annex A6.2-UC3-PK (UC3 PK Validation Annex), Comparator section.

4.5.2.2 EP-0D Model

Existing experimental studies determined the conditions of the comparator, which means they were not specifically chosen to fit the QI, but basic conditions were assured thanks to standardised protocols used to experimentally assess the effect of drugs. We performed a screening of experimental data sets to exclude unsuitable settings from the validation. See details in annex A6.2-UC3-0D (UC3 0D Validation Annex), Comparator section.

4.2.2.3 EP-3D Model

Due to computational limitations, the test conditions that will be simulated will not completely match the comparator experiments. Individualized simulations of entire populations is not currently feasible and these properties are not available in the experimental or clinical comparator data. Thus, we will use simplified models that will account for the most important factors needed to predict arrhythmic risk. See details in annex A6.2-UC3-3D (UC3 3D Validation Annex), Comparator section.

4.2.6 Equivalency of Input Parameters

4.2.6.1 PK Model

The equivalency of input parameters reflects the fact that if for a given patient and dosage we want to use a PK model, then this model must be able to cover this patient and dosage and therefore it must be as exhaustive as possible. This capacity depends on the completeness of the training dataset, and on the risk associated with extrapolation, which may be low in some cases. A score has been assigned to each model according to its coverage capacity. See details in annex A6.2-UC3-PK (UC3 PK Validation Annex), Assessment section.

4.2.6.2 EP-0D Model

The use of specific data for each drug assured that input parameters were equivalent, and we applied the same concentration range in the model to reproduce experimental results. However, studies did not provide specific information that separated samples according to sex category, so this input could not be explored. See details in annex A6.2-UC3-0D (UC3 0D Validation Annex), Assessment section.

4.2.6.3 EP-3D Model

Due to the lack of geometry data or patient-specific EP profile, we are unable to develop individualized models. But since the goal of the study is to look into population level response to drugs, we incorporate a reasonable variability in the population of ionic models incorporated in the model. This represents the largest variability in the tissue simulations. All other aspects will be held

constant across simulations to facilitate comparison of drug response. See details in annex A6.2-UC3-3D (UC3 3D Validation Annex), Assessment section.

4.2.7 Output Comparison

4.2.7.1 PK Model

The comparison of outputs was evaluated on the basis of correspondence with the comparators described above in the "test samples" section. Figure 28 shows an example of how simulated outputs were evaluated.

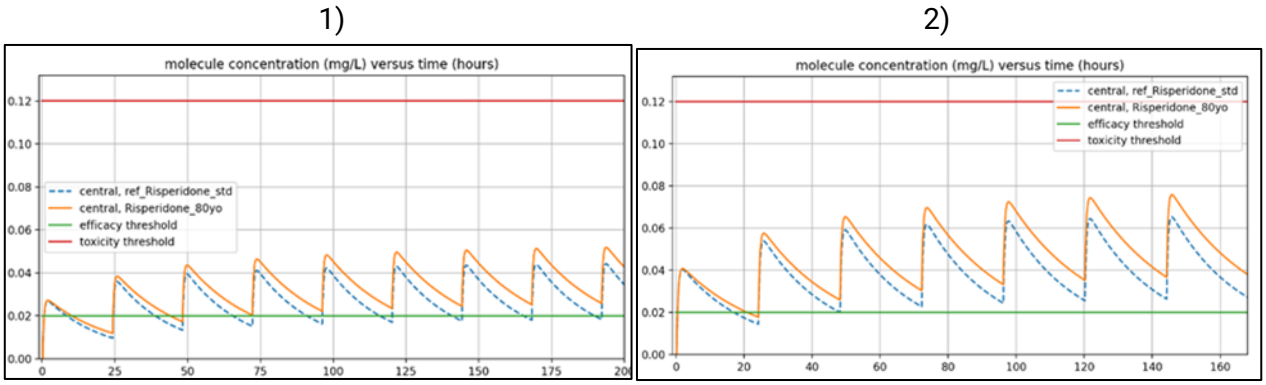

Figure 28: *Agreement of risperidone model outputs when using 1) usual and 2) maximal posology with the therapeutic thresholds used in routine clinical therapeutic drug monitoring.*

See details in annex A6.2-UC3-PK (UC3 PK Validation Annex), Assessment section.

4.2.7.2 EP-0D Model

Several outputs were used for the comparison, although only one (APD90) was equivalent to the marker measured in experiments. The rest of biomarkers were used to calculate the torsadogenic indices to create the binary TdP-risk classifier for 22 CiPA drugs, a safe/unsafe classification that was compared with the ground truth.

The difference between computational and experimental results was compared visually (inside a reasonable error area), qualitatively (predicted category), and numerically (accuracy), and the level of agreement of the output comparison was satisfactory in general, with some discrepancies found for some evaluated drugs.

See details in annex A6.2-UC3-0D (UC3 0D Validation Annex), Assessment section.

4.2.7.2 EP-3D Model

For validation of the 3D results, we will use the same Assessment criteria presented in the EP-0D model. We will measure the simulator’ s accuracy in predicting ECG changes with and without known drugs. We will quantify how closely these biomarkers match the clinical data as well as the effectiveness of the simulator in identifying which drugs can possible cause arrhythmia.

Figure 29 shows that electrophysiological simulation of sotalol reproduces experimental ECG prolongation, after agreeing with APD prolongation observations at the cellular level and being classified in the correct risk group by the binary classifier.

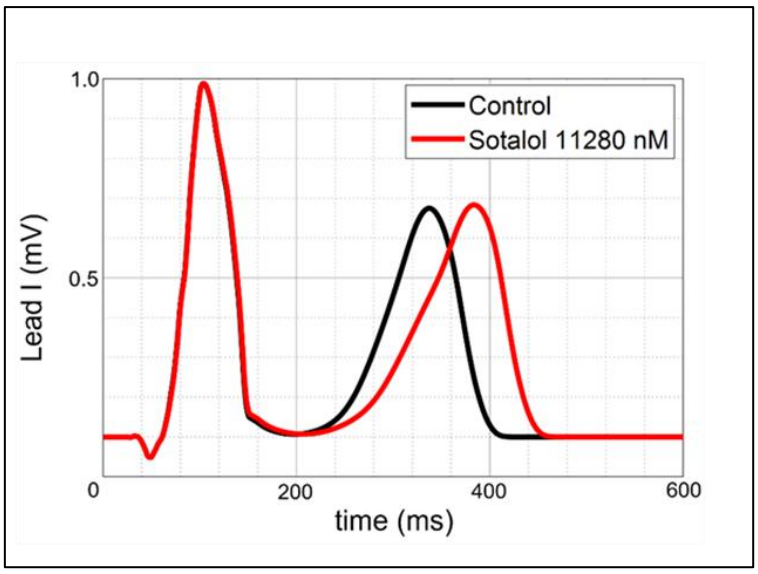

Figure 29: *Simulated ECGs in a biventricular model before (control) and after the administration of the unsafe drug sotalol.*

See details in annex A6.2-UC3-3D (UC3 3D Validation Annex), Assessment section.

4.3 UC3 Validation Uncertainty

4.3.1Model Uncertainty

The uncertainty of model parameters was analysed independently for the three computational models that integrate the TdP tool, and details can be found in the respective annexes.

4.3.2 Comparator Uncertainty

Comparators used in the validation process were different for the three models, meaning that pharmacokinetics, cellular electrophysiology, and tridimensional heart behaviour have their own uncertainty, as explained in the respective annexes:

- A6.2-UC3-PK: UC3 PK Validation Annex
- A6.2-UC3-0D: UC3 0D Validation Annex
- A6.2-UC3-3D: UC3 3D Validation Annex

4.3.3 Sources of Uncertainty

Global model uncertainty should take into account the different uncertainties related with the three parts (PK, cellular and 3D EP) that integrate the computational model. However, uncertainty propagation was not explored from initial inputs to 3D outputs, risking that uncertainty sources increased along the pipeline.

At PK level, we have modelled only the best models with the lowest level of uncertainty. We are currently working to include the residual inter-individual variability in our PK models in order to provide concentration ranges in which the patient's concentration is most likely to be found.

At the cellular level, we designed populations of cellular models representing all types of uncertainties (parameter variability, sampling uncertainty, measurement errors, among others). A distribution of outputs instead of a single number increased prediction value by providing a range of possible results.

At the tissue level, we modelled the simplest representation of the 3D tissue to ensure that the effects of complex geometry (such as complex shapes, heterogeneities, different fibre orientations) does not affect the results. By focusing on the relative change in the ECG parameters, we address the limitation of the model in simulating patient-specific electrophysiology.

4.4 UC3 Model Applicability

Although assessment validation activities were not completed, we can evaluate model applicability considering the strategy we designed and the first results we have obtained.

The in-silico tool to assess drug safety allows to calculate APD90 and QT interval, and provides a classification of drugs considering their torsadogenic risk. Therefore, the computational model was properly conceived to obtain the quantity of interest specified in the QI. However, TdP vulnerability for the validation was not directly evaluated in real patients but extracted from the literature and databases, based on clinical evidences and accepted by experts.

The relevance of validation points to the COU was limited by the available experimental data. On the one hand, each model does not represent a real patient, as cellular EP models were generated randomly within physiological ranges and we used a single heart geometry for all the comparisons. On the other hand, animal models were used in validation activities due to the scarcity of human data. This lack of data also concerned the inability to distinguish between males and females from clinical trials, so predictions could not be validated for each subpopulation based on sex category.

4.5 UC3 Discussion and Future Work

The credibility on the predictive capability of the computational model for proarrhythmic assessment required V&V actions of at least intermediate rigor because the tool was considered to have a medium risk level for the defined COU. Table 10 shows that the score planned to be achieved by validation activities is equal to 3 for all factors except for test conditions. Each credibility factor is the combination of the different actions taken for each of the three individual models that comprise the computational application for drug evaluation, and the final score represents the most restrictive level. The scarcity of comparator conditions for the electrophysiological model caused a low credibility level in this factor, but for the present COU, electrophysiological conditions were less relevant than sample type (drug) to assess TdP risk. Therefore, despite this particular low coverage level, we think that computational model predictions may still be sufficiently credible for decision-making.

Table 10 : Validation and Applicability Credibility Factors Coverage Level for Use Case 3 accounting for PK, 0D, and 3D models (cf. ASME VV40); * indicates validation activities not yet completed.

Model Risk					x		
Credibility Factor Coverage Level			1	2	3	4	5
Validation - Model [Form] *	III				x		
Validation - Model [Inputs] *	III				x		
Validation - Comparator [Test Samples] *	III				x		
Validation - Comparator [Test Conditions] *	II				x		
Validation - Assessment [Input Parameters] *	III				x		
Validation - Assessment [Output Comparison] *	III				x		
Applicability: Relevance of the Quantities of Interest *	III				x		
Applicability: Relevance of the Validation Activities to the COU *	II				x		

The future work for each of the models is as follows:

4.5.1 PK Model

Many pharmacokinetic models can be validated thanks to the availability of therapeutic thresholds, which provide a good understanding of drug efficacy and toxicity levels. However, this validation only reflects the a priori accuracy of the models, and is not satisfactory in the case of drugs with narrow therapeutic margins. For this reason, it is important to carry out higher-level validations for certain drugs requiring a higher level of precision.

To this end, we are seeking to validate additional molecules with validation datasets, enabling external evaluation. However, these data are difficult to obtain.

Another additional step that will take place in the future is to include inter-individual variability in the predictions. This will make it possible to predict the most likely concentration ranges where an individual would be at a given dose, taking into account the variability of the models implemented.
In the context of SimCardioTest, we will perform the entire validation of the molecules made available on the final platform.

4.5.2 EP 0D Model

Multiple parameters integrate the cellular model but only channel conductance and ion-transport proteins were analysed because it is known that genetic variability determines protein quantity, and that pharmacological molecules interact with these proteins limiting ion transport function. Other model parameters could be included in the sensitivity analysis to have a global vision of the model form on outputs, but it has not been planned. However, the analysis of sarcomeric parameters that are part of the mechanical model will be performed, as we plan to integrate mechanics with electrophysiology to improve the predictive power of the computational model for safety drug assessment.

Existing experimental data determined the quality of the comparator. In-vitro drug tests were found for each compound so that the effect of each molecule was validated individually. It is not expected to have new data, but if it came up, we would update the comparator.

To improve current assessment agreement, we planned to include new variables (e.g. mechanical outputs) that may lead to new torsadogenic indices able to improve the classification. The use of population of models is another pending task that would add credibility to predictions by propagating and quantifying uncertainties in the classification and could help determine safe drug concentrations.

4.5.3 EP 3D Model

The 3D EP model has been developed with the goal of eventually simulating patient specific EP at the population level. However, limitations in computational resources has made it necessary to perform 3D simulations on a simple tissue geometry. Future work will focus on increasing performance and efficiency of the software in order to make these types of simulations a possibility. Additionally, the mechanical function of the heart is currently not included in the simulations. This is functionally important as certain drugs are targeted towards improving cardiac function, especially in diseased states. We currently have a preliminary version of the software that can perform fully coupled electromechanical simulations. However, this requires even more computational power compared to EP only simulations. The next steps will be integrating this into the simulator so that we can more fully and accurately represent cardiac function.

5 Conclusion

This report and its annexed documents constitute the SimCardioTest WP6 deliverable D6.2 due in June 2023 (M30). It described all validation activities engaged for assessing the credibility of computational models developed in the frame of Use Cases 1 to 3 (cf. WP2, 3, and 4 respectively). This report is closely linked to SCT deliverable D6.1 which reports the verification activities also supporting the credibility of the models.

In addition, this document describes the uncertainty analysis conducted on the uncertainty sources coming from the validation activities. Finally, it includes a discussion on the Applicability of the validated models.

Validation was conducted on one specific model per each Use Case, corresponding to a pre-selected Question of Interest (QI). All validation activities are conducted according to ASME VV40 standard guidelines. Some of the engaged validation activities are still ongoing at the date of this publication, and will be documented at later time once completed.

For what concerns Use Case 1, validation has been designed for the computational model of a pacemaker in a right ventricular wedge of tissue obtained in sheep hearts. The computational model includes many parameters, some of which have been calibrated in bench experiments, and others may be spatially distributed according to the tissue microstructure, which makes them difficult to identify. In addition, the QI addressed in this context has some well-defined input parameters, which have been very precisely identified, and are comparable in the model and the experiments. Two comparators have been defined, uncertainty sources, and applicability of the model have been

discussed. Overall, the process to validate the computational model has been identified and detailed in this document. Two animal experiments already completed yielded first data sets, and helped us to define this process more accurately, and in particular to adjust the experimental protocol to the calibration of the model and to the comparators. In conclusion, we have designed computations, animal experiments and comparators that are consistent with each other, and consistent with the QI and COU of the computational model. Currently, verification activities are just starting. All activities planned in this document will most likely not be completed in the time frame of this project. We expect comparisons to be available, while quantification and propagation of uncertainty will depend on available resources.

For what concerns Use Case 2, the validation of computational fluid simulations including left atrial appendage occluder devices in the bench-top set-up has been a challenge due to the complexity and the time needed to tune every analysed scenario. However, the initial comparisons between fluid simulation and in-vitro experimental results are very promising, validating the use of the actuators to impose a LA wall motion behaviour obtained from the dCT scans, despite the fact that the blood flow velocities obtained in the in-vitro set-up are lower than expected physiologically. In any case, the performed validation on fluid simulations with LAAO devices is unique due to the data available in SimCardioTest, including a large database of clinical data, in-vitro phantoms, and advanced imaging scans. We have identified the required experiments and quantities of interest to perform reliable comparisons in the defined QI and COU, also establishing the credibility level of all important factors in the VV40 guidelines. Additional uncertainty studies could be beneficial for increasing the overall credibility levels.

For what concerns Use Case 3, we implemented validation activities following VV40 standard guidelines. An independent analysis of the three computational models integrating the drug assessment tool (pharmacokinetics, cellular, and tissue electrophysiology) allowed to focus on the different parameters, inputs, outputs, existing comparators, and uncertainty sources. Executed activities varied depending on the complexity of the model, and we planned all validation steps according to available resources. An intermediate credibility level was achieved with pharmacokinetic and cellular models, and it is expected in tissue models when the software is definitive. Therefore, the computational model could be used to make predictions with the validated drugs, although taking into account that uncontrolled factors beyond validation points might affect results accuracy.

6 Bibliography

[1] V&V40, Assessing Credibility of Computational Modeling Through Verification and Validation: Application to Medical Devices, New York: ASME, 2018.

[2] “cellML,” [Online]. Available: https://models.cellml.org/electrophysiology.

[3] “11th FIMH Conference,” [Online]. Available: https://doi.org/10.1007/978-3-031-35302-4_20.

[4] “Reconstruction of the action potential of ventricular myocardial fibres,” *The Journal of Physiology,* vol. 268 (1), no. DOI: https://doi.org/10.1113/jphysiol.1977.sp011853, pp. 177-210, 1977.

[5] A. Banstola and R. J. N. J., "The Sheep as a Large Animal Model for the Investigation and Treatment of Human Disorders," *Biology,* vol. 11(9), no. DOI: http://dx.doi.org/10.3390/biology11091251, p. 1251, 2022.

[6] K. A. S. Silva and C. A. Emter, "Large Animal Models of Heart Failure," *JACC: Basic to Translational Science,* vol. 5 (8), no. DOI: http://dx.doi.org/10.1016/j.jacbts.2020.04.011, pp. 840-856, 2020.

[7] A. Cresti, M. García-Fernández, H. Sievert and others, "Prevalence of extra-appendage thrombosis in non-valvular atrial fibrillation and atrial flutter in patients undergoing cardioversion: a large transoesophageal echo study," *EuroIntervention,* vol. 15(3), p. e225–e230, 2019.

[8] M. Pons, J. Mill, A. Fernandez-Quilez and others, "Joint Analysis of Morphological Parameters and In Silico Haemodynamics of the Left Atrial Appendage for Thrombogenic Risk Assessment," *Journal of interventional cardiology,* 2022.

[9] A. Sedaghat and G. Nickenig, "Letter by Sedaghat and Nickenig Regarding Article, "device-Related Thrombus after Left Atrial Appendage Closure: Incidence, Predictors, and Outcomes," *doi:10.1161/CIRCULATIONAHA.118.036179,* 2019.

[10] J. Saw, A. Tzikas, S. Shakir and others, "Incidence and clinical impact of device-associated thrombus and peri-device leak following left atrial appendage closure with the amplatzer cardiac plug," *JACC: Cardiovascular Interventions,* vol. 10, p. 391–399, 2017.

[11] L. V. Boersma, B. Schmidt, T. R. Betts and others, "Implant success and safety of left atrial appendage closure with the watchman device: peri-procedural outcomes from the ewolution registry," *European heart journa,* vol. 37, p. 2465–2474, 2016.

[12] A. Sedaghat and others, "Device-Related Thrombus After Left Atrial Appendage Closure: Data on Thrombus Characteristics, Treatment Strategies, and Clinical Outcomes From the EUROC-DRT-Registry," *Circulation. Cardiovascular interventions,* Vols. 14,5, no. e010195, 2021.

[13] I. Chung and G. Y. Lip, "Virchow's triad revisited: Blood constituents," *Pathophysiology of Haemostasis and Thrombosis,* vol. 33, no. doi:10.1159/00008384, p. 449–454, 2003.

[14] O. D. Backer, X. Iriart, J. Kefer and others, "Impact of computational modeling on transcatheter left atrial appendage closure efficiency and outcomes," *JACC: Cardiovascular Interventions,* vol. 16, no. doi:10.1016/j.jcin.2023.01.008, p. 655–666, 2023.

[15] J. Saw, J. P. Lopes, M. Reisman and H. G. Bezerra, "CT Imaging for Percutaneous LAA Closure," *Cham: Springer International Publishing,* no. doi:10.1007/978-3-319-16280-5, p. 117–132, 2016.

[16] A. M. Aguado, A. L. Olivares, E. Silva and others, "In silico optimization of left atrial appendage occluder implantation using interactive and modeling tools," *Frontiers in physiology,* vol. 10, p. 237, 2019.

[17] X. Freixa and others, "Pulmonary ridge coverage and device-related thrombosis after left atrial appendage occlusion," *EuroIntervention : journal of EuroPCR in collaboration with the Working Group on Interventional Cardiology of the European Society of Cardiology,* vol. 16(15), no. doi:10.4244/EIJ-D-20-00886, pp. e1288-e1294, 2021.

[18] A. Santiago, C. Butakoff, B. Eguzkitza and others, "Design and execution of a verification, validation, and uncertainty quantification plan for a numerical model of left ventricular flow after lvad implantation," *PLoS computational biology,* vol. 18, no. e1010141, 2022.

[19] E. Khalili, C. Daversin-Catty, A. Olivares and others, "On the importance of fundamental computational fluid dynamics towards a robust and reliable model of left atrial flows: Is there more than meets the eye?," *arXiv:2302.01716 [physics.flu-dyn],* 2023.

[20] J. Mill, V. Agudelo, A. L. Olivares and others, "Sensitivity analysis of in silico fluid simulations to predict thrombus formation after left atrial appendage occlusion," *Mathematics,* vol. 9 (18), p. 2304, 2021.

[21] G. García-Isla, A. L. Olivares, E. Silva and others, "Sensitivity analysis of geometrical parameters to study haemodynamics and thrombus formation in the left atrial appendage," *nt J Numer Methods Biomed Engineer,* p. e3100, 2018.

[22] R. B. Bird, R. C. Armstrong and O. Hassager, Dynamics of Polymeric Liquids Vol. 1 Ch. 5, John Wiley and Sons, 1987.

[23] M. García-Villalba, L. Rossini, A. Gonzalo and others, "Demonstration of Patient-Specific Simulations to Assess Left Atrial Appendage Thrombogenesis Risk," *Front. Physiol.,* vol. 12, no. DOI: 10.3389/fphys.2021.596596, p. 596, 2021.

[24] C. Albors, A. Olivares, X. Iriart and others, "Impact of Blood Rheological Strategies on the Optimization of Patient-Specific LAAO Configurations for Thrombus Assessment," *In: Bernard, O., Clarysse, P., Duchateau, N., Ohayon, J., Viallon, M. (eds) Functional Imaging and Modeling of the Heart. FIMH 2023. Lecture Notes in Computer Science,* vol. 13958, no. DOI: https://doi.org/10.1007/978-3-031-35302-4_50, 2023.

[25] K. Mendez, D. G. Kennedy, D. D. Wang and others, "Left Atrial Appendage Occlusion: Current Stroke Prevention Strategies and a Shift Toward Data-Driven, Patient-Specific Approaches," *Journal of the Society for Cardiovascular Angiography & Interventions,* vol. 1, no. 5, 2022.

[26] C. Albors and others, "Sensitivity Analysis of Left Atrial Wall Modeling Approaches and Inlet/Outlet Boundary Conditions in Fluid Simulations to Predict Thrombus Formation," *In: , et al. Statistical Atlases and Computational Models of the Heart. Regular and CMRxMotion Challenge Papers. STACOM 2022. Lecture Notes in Computer Science,* vol. 13593, no. DOI: https://doi.org/10.1007/978-3-031-23443-9_17, 2022.

[27] S. F. Nagueh and others, "Recommendations for the evaluation of left ventricular diastolic function by echocardiography," *Eur. J. Echocardiogr,* vol. 10 (2), p. 165–193, 2009.

[28] E. Durán, M. García-Villalba, P. Martínez-Legazpi and others, "Pulmonary vein flow split effects in patient-specific simulations of left atrial flow," *Comput Biol Med,* vol. 163:107128, no. DOI: 10.1016/j.compbiomed.2023.107128, 2023.

[29] J. Mill, V. Agudelo, C. H. Li and others, "Patient-specific flow simulation analysis to predict device-related thrombosis in left atrial appendage occluders," *REC Interv Cardiol,* vol. 3(4), no. DOI: 10.24875/RECICE.M21000224, pp. 278-285, 2021.

[30] Z. Li, B. J. Ridder, X. Han and others, "Assessment of an In Silico Mechanistic Model for Proarrhythmia Risk Prediction Under the CiPA Initiative," *Clin Pharmacol Ther,* vol. 105, no. DOI: https://doi.org/10.1002/CPT.1184, p. 466–475, 2019.

[31] F. Veronesi and others, "Quantification of mitral apparatus dynamics in functional and ischemic mitral regurgitation using real-time 3-dimensional echocardiography," *J. Am. Soc. Echocardiogr,* vol. 21 (4), p. 347–354, 2008.

[32] J. C. Weddell, J. Kwack, P. I. Imoukhuede and others, "Hemodynamic Analysis in an Idealized Artery Tree: Differences in Wall Shear Stress between Newtonian and Non-Newtonian Blood Models," *PLoS One,* vol. 10 (4), no. DOI: 10.1371/journal.pone.0124575, p. e0124575, 2015.

7 Appendices

Detailed implementation of the verification activities and results can be found in the annex documents listed in Table 11.

Table 11: List of Attachments.

Reference	Title
A6.2-UC3-PK	Use Case 3 PK Validation Annex
A6.2-UC3-0D	Use Case 3 0D Validation Annex
A6.2-UC3-3D	Use Case 3 3D Validation Annex

added on 25 September 2025:

ANNEX A (WP6 complement of D6.1 and D6.2)

ANNEX C (WP6 UC3 PK Validation), which cover the additional work carried out between M30 and M54.

This project received funding from the European Union's Horizon 2020 research and innovation program under grant agreement No 101016496

EU Horizon 2020 Research & Innovation Program
Digital transformation in Health and Care
SC1-DTH-06-2020
Grant Agreement No. 101016496

SimCardioTest - Simulation of Cardiac Devices & Drugs for in-silico Testing and Certification

Technical Report

D6.2-UC3-PK: Use Case 3 PK Validation Annex

Work Package 6 (WP6)

Verification, validation, uncertainty quantification & certification

Annex Lead: UPV, Spain
Task Lead: UBx, France
WP Lead: MPC, France

PUBLIC

Document history			
Date	**Version**	**Author(s)**	**Comments**
06/15/2023	V1	S. BAROUDI, K. KOLOSKOFF	Final Draft
29/06/2023	V2	R. SETZU	Format Consolidation
30/06/2023	V3	R. SETZU	Final Version
01/07/2023	V4	R. SETZU M. BARBIER	Format editing

Table of contents

EXECUTIVE SUMMARY

This document is an annex of SimCardioTest deliverable D6.2 and was elaborated for Use Case 3 in the context of drug safety assessment. It contains the technical details for the validation of the pharmacokinetics models.

Acronyms

Table 1: List of Acronyms.

Acronym	Meaning
EXC	ExactCure
MDAPE	Median absolute predictive error
MDPE	Median predictive error
NC	Non-compartmental
PK	Pharmacokinetics
PKPOP	Population pharmacokinetics
RSE	Relative standard error
SCT	SimCardioTest
SE	Standard error
TdP	Torsade de pointes

1. Computational model

Validation activities consist in checking that PK models enable predictions as close as possible to reality, for the different sub-populations likely to receive a given treatment. PK describes the body's effect on drugs, and must be as accurate as possible, since it is used to adapt the dosage regimen of drugs to all patients, taking into account their physical, biological, and demographic characteristics and other differences.

1.1 Model Form

The PK models implemented by EXC are mathematical models describing the kinetics of drugs in the body. The model is built using parameters taken from publications in the scientific literature, and from regulatory agencies. Depending on the availability of literature, and the amount of research carried out on each molecule, EXC implements different types of PK models, classified according to their initial level of evaluation:

1. Model built with NC data coming from PK literature.
2. Model built with NC data from regulators approved data (summary of product characteristics, regulatory agencies documents).
3. Model built from popPK analysis.
4. Model built from popPK analysis and external NC data.
5. Meta-Model built from popPK analysis studies.

The targeted depth – level is 3/5 and is current practice in ExactCure Validation Process. Model whose model form is rate 2/5 can be validated if they met other validation criteria.

1.2 Model Inputs

The model inputs are:

- Mathematical equations (describing the drug kinetics).
- Model parameters (structural parameters, covariates).

However, the term "model inputs" does not cover all the parameters required to run a PK simulation. In fact, additional parameters concerning dosage configuration and patient covariates are required:
- Patients' profiles, defined by their covariates impacting the models, which differ from one model to another.
- Drug dosages, defined by the following parameters, which also differ from one model to another:

- Route (Oral, Rectal, Intravenous, Intramuscular…)
- Form (Tablet, Capsule, Solution…)
- Release process associated with the form (Controlled release, Immediate release…)
- Frequency of administration
- Duration of administration

The model inputs are evaluated according to the following:

1. The parameters of the model are derived from NC data obtained from analysis on few patients or with high variability.
2. The parameters used are derived from NC data obtained from analysis involving large numbers of patients or with low variability.

3. Parameters are obtained from popPK analysis with a relative standard error (RSE) > 30% or taken from the summary of product characteristics or from analysis conducted on many patients with little variability.
4. Parameters are obtained from popPK analysis with a relative standard error (RSE) ≤ 30%.

The targeted depth - level is 3/4 and is current practice in ExactCure Validation Process.

For Validation tests, all these model inputs are encoded following EXC internal declaration (Digital Twin module of EXC medical device ExaMed).

2. Comparator

2.1 Test Samples

The data used to validate the implemented PK models are taken from the literature.
Several levels of test samples are defined as follows:

1. Scattered data from the literature or from the summary of product characteristics, which may be average concentrations, endpoints (e.g., area under the curve, elimination half-life, maximum concentration, time to reach maximum concentration), etc.
2. Efficacy, overexposure, and safety thresholds used for routine therapeutic drug monitoring (TDM) in clinical conditions.
3. External evaluation dataset, which may be derived from partnership projects or open access online, to carry out external evaluations.

The targeted depth – level is 2/3 and is current practice in ExactCure Validation Process.

2.2 Test Conditions

Tests must be performed in conditions where all the specific sub-populations concerned by a drug are covered. Tests must be carried for all specialities of the drug, for all concerned sub-populations, so that the models can be validated in all possible configurations of its use. These conditions depend on the covariates included in the models (and therefore data available for the analysis), as well as on the dose recommendations in force.

Several levels of test conditions are defined as follows:

1. Test conditions were defined with limited data allowing to run simulations for a few standard patients, either because the model does not incorporate all covariates of interest, or because dose recommendations do not cover specific populations that may require dose adaptation.
2. Test conditions were defined with few data allowing to run simulations for a few standard patients and a specific population of interest, which may come from unofficial recommendations (i.e., not published by a regulatory agency) but from literature articles.
3. Test conditions were defined with sufficient data allowing to run simulations for each subpopulation concerned by the drug, but learning dataset is not exhaustive, and leads to extrapolation for patients that were not included in the learning dataset. (e.g., the learning dataset includes young patients only. Simulation for elderly patients leads to extrapolate).
4. Test conditions were defined with sufficient data to run simulations for each patient concerned by the drug, with complete coverage of dosage ranges, and of all sub-populations concerned by the drug.

5. Test conditions were defined with external evaluation dataset. Tests conditions reproduce patient characteristics from the validation dataset to compare with model outputs.

The targeted depth – level is 4/5 and is current practice in ExactCure Validation Process.

3. Assessment

3.1 Equivalency of Input Parameters

The equivalence of input parameters depends on the training dataset of the PK model.
Parameters are equivalent if all doses tested are present in the training dataset, and all patient subpopulations affected by the drug have been covered.
If certain prescribable doses are not included in the training dataset, it is possible to extrapolate with a low risk in the case where the PK of the molecule is linear (response proportional to dose). Most molecules are linear at therapeutic doses.
In cases where sub-populations are not included in the training dataset, extrapolation can only be performed if external data are available to validate it.

Several levels of equivalency of input parameters are defined as follows:

1. The model's training dataset does not cover all the sub-populations concerned by the medication and doses tested. The molecule's PK is not linear over the dose range use in the test conditions. Sub-populations and doses extrapolation can be performed if external data is available to validate it.
2. The model's training dataset does not cover all the sub-populations concerned by the medication and doses tested. The molecule's PK is linear over the dose range use in the test conditions. Sub-populations extrapolation can be performed if external data is available to validate it.
3. The model's training dataset does cover doses tested or PK is linear over the dose range use in the test conditions, but not all the sub-populations concerned by the medication. Sub-populations extrapolation can be performed if external data is available to validate it, or an external validation is carried out and meets validation criteria. (i.e., MDPE ≤ ± 20%, MDAPE ≤ 30%)
4. The model's training dataset does cover all doses or PK is linear over the dose range use in the test conditions and sub-populations concerned by the medication, or an external validation is carried out and meets validation criteria. (i.e., MDPE ≤ ± 20%, MDAPE ≤ 30%)

The targeted depth – level is 3/4 and is current practice in ExactCure Validation Process.

The level 4/4 is achievable provided a PK model learned from a large population is available in the literature, or a meta-model is developed.

3.2 Output Comparison

The comparison of simulation results with validation data is evaluated with the following criteria :

1. Correspondence of model outputs with the results presented in the article from which the model originates.

2. 1 + Correspondence of model outputs with external data available in the literature (T1/2, Cmax, Tmax, AUC)
3. 2 + Correspondence of model outputs with the therapeutic thresholds used in routine clinical therapeutic drug monitoring.
4. 3 + Correspondence of model outputs with an external evaluation dataset or prediction uncertainties. Validation criteria are MDPE ≤ ± 20%, MDAPE ≤ 30%.
5. 3 + Correspondence of model outputs with external evaluation dataset + prediction uncertainties. Validation criteria are MDPE ≤ ± 20%, MDAPE ≤ 30%.

The validation tests are performed for all sub-populations covered by the prescribing information's in the summary of product of the drug.

The targeted depth – level is 3/5 and is current practice in ExactCure Validation Process.

3.3 Conclusion

These general requirements must be met for all EXC PK models. If this is not the case, the validation steps are not satisfying, and the model must be reworked and resubmitted for validation. Validation is performed by another modeler than the one who implemented the model. A manager then ensures that the steps are in line with the defined process of validation.

4. Application of validation processes

4.1 Clozapine

Table 2: Summary of Clozapine validation.

Summary		
Levels	**Notations**	**Comments**
Model form level	3/5	Model built from popPK analysis
Model input level	NA	RSE% were not communicated however this model was successfully validated with an external evaluation
Test samples level	3/3	External database
Tests conditions level	5/5	Test conditions were defined with external evaluation dataset
Equivalency of input parameters level	4/4	All doses and subpopulations of the validation dataset are covered by the training dataset
Output comparison level	4/5	Output comparison met validation criteria
Conclusion: The model is validated since all criteria meet the minimum score required, except for the model input level, which is not applicable, but in this case the model was validated with an external database guaranteeing the accuracy and unbiasedness of the model.		

4.1.1 Model Form

Model form level: 3/5
Model form: Model built from popPK analysis.
Model source(s): Jerling et al [1].

Comment: The implemented PK model is based on a popPK analysis. It is a one-compartment model with first order absorption and elimination.

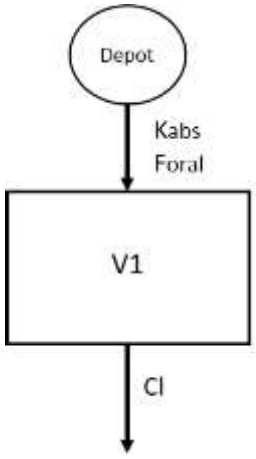

Figure 1: *Model's structure, with one depot compartment, and one central compartment. Kabs, is the absorption rate, Foral the bioavailability V1 the volume of distribution, CL the clearance of elimination.*

4.1.2 Model Inputs

Model inputs level: NA
Model input: NA
Model inputs source(s): Jerling et al [1].
Comment: The evaluation of the model inputs is not applicable for this specific model of Clozapine. However, it is considered as not necessary as the model was successfully evaluated with an external dataset.

	Women			*Men*		
	Median with 25% and 75% quartiles	*Mean*	*Coefficient of variation*	*Median with 25% and 75% quartiles*	*Mean*	*Coefficient of variation*
ka (h^{-1})	1.24 (0.80, 1.50)	1.24	0.42	1.30 (0.87, 1.72)	1.37	0.49
V/F (l)	401 (189, 932)	564	0.8	694 (224, 970)	719	0.79
k (h^{-1})	0.086 (0.037, 0.131)	0.1	0.72	0.083 (0.054, 0.127)	0.095	0.62
CL/F ($l\,h^{-1}$)	28.3 (15.2, 48.6)	39.9	1.22	38.2 (22.0, 60.0)	47.9	0.72

Figure 2: *Clozapine model parameters from Jerling et al [1]. ka is the absorption rate, V/F is the volume of distribution corrected by the bioavailability (F), k is the elimination rate, CL/F is the clearance of elimination corrected by the bioavailability. Picture from [1].*

4.1.3 Test Samples

Test sample level: 3/3
Test sample: External evaluation dataset.
Test samples source(s): Lereclus et al. [2].
Comment: In the context of A. Lereclus PhD thesis, an external dataset for validation (53 patients, 151 observations) was used to evaluate literature models. Jerling et al. [1] was the most performant.

Characteristics	Number or Mean ± SD	Median (Range)
No. of patients (male/female)	53 (41/12)	NA
No. of samples	151	NA
No. of samples per patient	2.77 (±3.90)	1 (1–20)
Age (yr)	38.66 (±11.51)	37 (19–66)
Weight (kg)	81.21 (±19.20)	80 (47–122)
Height (cm)	172.92 (±8.54)	175 (153–185)
Concentration (mg/L)	381 (±296)	287 (36–1504)
Dose (mg)	224.29 (±129.90)	200 (25–625)
Smoker (yes/no)	32/21	NA

Figure 3: *External evaluation dataset patients' characteristics from Lereclus et al., 2022. Picture from [2].*

4.1.4 Test Conditions

Tests conditions level: 5/5
Tests conditions: Test conditions were defined with external evaluation dataset. Tests conditions reproduce patient characteristics from the validation dataset to compare with model outputs.
Tests conditions source(s): Lereclus et al. [2].
Comment: Simulations reproducing physical, biological, and demographic characteristics of patients from an external evaluation dataset were carried out to compare observations and simulations. All situations were covered by the test conditions.

4.1.5 Equivalency of input parameters

Equivalency of input parameters level: 4/4
Equivalency of input parameters: The model's training dataset does cover all doses or PK is linear over the dose range use in the test conditions and sub-populations concerned by the medication, or an external validation is carried out and meets validation criteria. (i.e., MDPE ≤ ± 20%, MDAPE ≤ 30%)
Equivalency of input parameters source(s): Lereclus et al. [2].
Comment: The validation database is covering all patients and doses of the training dataset.

Characteristics	Number or Mean ± SD	Median (Range)
No. of patients (male/female)	53 (41/12)	NA
No. of samples	151	NA
No. of samples per patient	2.77 (±3.90)	1 (1–20)
Age (yr)	38.66 (±11.51)	37 (19–66)
Weight (kg)	81.21 (±19.20)	80 (47–122)
Height (cm)	172.92 (±8.54)	175 (153–185)
Concentration (mg/L)	381 (±296)	287 (36–1504)
Dose (mg)	224.29 (±129.90)	200 (25–625)
Smoker (yes/no)	32/21	NA

Figure 4: *External evaluation dataset. Picture from [2].*

	Women	*Men*
Number of patients	82	159
Number of observations	141	250
Age (years)	39 ± 11 (20–74)	37 ± 9 (20–86)
Total daily dose (mg)	398 ± 160 (50–800)	378 ± 158 (12.5–800)
Dose events per day	2.1 ± 0.8 (1–4)	2.1 ± 0.7 (1–4)
Interval last dose—sampling (h)	12.0 ± 3.0 (2–24)	12.3 ± 3.0 (0.5–24)
Plasma concentration (ng ml^{-1})	515 ± 628 (18–5363)	333 ± 354 (19–3772)

Figure 5: *Model training dataset. Picture from [1].*

4.1.6 Output Comparison

Output comparison level: 4/5
Output comparison: External evaluation dataset.
Output comparison source(s): Lereclus et al. [2].
Comment: The results of an external validation performed by Aurélie Lereclus (151 samples from 53 patients) resulted in **MDPE: -19% / MDAPE 29.4%.** The external validation meets validation criteria.

4.2 Escitalopram

Table 3: Summary of Escitalopram validation.

Summary		
Levels	**Notations**	**Comments**
Model form level	3/5	Model built from popPK analysis
Model input level	4/4	RSE% were <30% for structural parameters
Test samples level	2/3	Therapeutic thresholds
Tests conditions level	3/5	Most conditions could have been tested except renal and hepatic status that were not studied because the training dataset didn't include data on these statuses.
Equivalency of input parameters level	3/4	All doses were covered by the training dataset, but renal and hepatic status was not studied.
Output comparison level	3/5	Model outputs were within therapeutic thresholds.
Conclusion: The model is validated since all criteria meet the minimum score required.		

4.2.1 Model Form

Model form level: 3/5
Model form: Model built from popPK analysis.
Model Source(s): Jin et al. [3].
Comment: The implemented PK model is based on a popPK analysis conducted by Jin et al. [3]. It is a one-compartment model with first order absorption and elimination.

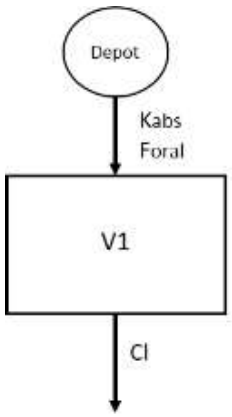

Figure 6: *Model's structure, with one depot compartment, and one central compartment. Kabs, is the absorption rate, Foral the bioavailability V1 the volume of distribution, CL the clearance of elimination.*

4.2.2 Model Inputs

Model inputs level: 4/4
Model input: Parameters are obtained from population pharmacokinetic studies with a relative standard error (RSE) ≤ 30%.
Model inputs source(s): Jin et al. [3].
Comment: The RSE% met validation criteria for all structural parameters.

Parameters	Final Model Estimates	SE%
CL for 2C19 Rapid and Extensive (L/Hr)	26	7.20%
CL for 2C19 IM and PM (L/Hr)	19.8	8.50%
CL for 2C19 missing (L/Hr)	21.5	7.80%
Age on Clearance	CL_1=CL_0*(Age/40) $^{-0.336}$	42.00%
Weight on Clearance	CL_2=CL_1*(Wgt/76) $^{0.333}$	54.10%
V (L)	947	10.20%
BMI on V	V*(BMI/27) $^{1.11}$	49.50%
Ka (hr^{-1})	0.8	N/A
ω_{Cl} %	48.5%	15.10%
ω_{V} %	62.0%	40.30%
ω_{Ka} %	78.9%	87.00%
$\omega_{Cl,V}$ %	9.4%	N/A
$\omega_{Cl,Ka}$ %	47.8%	N/A
$\omega_{V,Ka}$ %	81.3%	N/A
σ_1 %	28.9%	8.80%

Figure 7: *Escitalopram model parameters from Jin et al. [3]. ka is the absorption rate, V/F is the volume of distribution corrected by the bioavailability (F), k is the elimination rate, CL/F is the clearance of elimination corrected by the bioavailability. CL is different for each CYP2C19 type of metabolizer. IM = intermediate metabolizer, PM = poor metabolizer, BMI = body mass index, ω the coefficient of variation of the interindividual variability. σ the coefficient of variation of the residual error. Picture from [3].*

4.2.3 Test Samples

Test sample level: 2/3
Test sample: Efficacy and overexposure thresholds used for routine therapeutic drug monitoring (TDM) in clinical conditions.

- Efficacy threshold was: 0.0065 mg/L
- Safety threshold was: 0.08 mg/L

Test samples source(s): Schulz et al. [4].
Comment: Summary of product characteristics was also used to test the model as mean steady state concentrations were mentioned.

4.2.4 Tests conditions

Tests conditions level: 3/5
Tests condition: Test conditions were defined with sufficient data allowing to run simulations for each subpopulation concerned by the drug, but learning dataset is not exhaustive, and leads to extrapolation for patients that were not included in the learning dataset.
Tests conditions source(s): base-donnees-publique.medicaments.gouv.fr [5]
Comment: According to the test condition source, dose adjustment might be possible in case of renal or hepatic insufficiency. However, it is not possible to combine these cases with other covariates included in the model, that is why, the model cannot cover all subpopulation concern by the drug.

Tests conditions were:

- Test 1: standard patient with 1) minimal usual posology, 2) usual posology, and 3) maximal usual posology
- Test 2: Old patient (80 yo) with 1) recommended usual posology, and 2) maximal usual posology.
- Test 3: Higher BMI patient and low BMI patient with 1) usual posology, and 2) maximal usual posology
- Test 4: slower metabolizer (poor and intermediate) vs standard patient with 1) minimal usual posology 2) usual posology

Where patients are:

- Standard man: weight: 70kg, BMI: 24.2, age: 40, CYP2C19 status: extensive.
- Old patient: 76kg, BMI: 24.2, age: 80, CYP2C19 status: extensive
- Higher BMI patient: weight: 120kg, BMI: 32, age: 40, CYP2C19 status: extensive
- Lower BMI patient: weight: 45kg, BMI: 18, age: 40, CYP2C19 status: extensive
- Slower metabolizer patient: 70kg, BMI: 24.2, age: 40, CYP2C19 status: poor

Where posology are:

- Minimal usual posology: 5mg once daily for a week, and then 10mg daily.
- Usual posology: 10mg once daily.
- Maximal usual posology: 20mg once daily.

4.2.5 Equivalency of input parameters

Equivalency of input parameters level: 3/4
Equivalency of input parameters: The model's training dataset does cover doses tested or PK is linear over the dose range use in the test conditions, but not all the sub-populations concerned by the medication. Sub-populations extrapolation can be performed if external data is available to validate it, or an external validation is carried out and meets validation criteria.
Equivalency of input parameters source(s):

- base-donnees-publique.medicaments.gouv.fr [5],
- *Jin et al. [3].*

Comment: The learning dataset didn't include data on hepatic and renal function of the patients. It was therefore impossible to conclude that the learning dataset covers all sub-populations concerned by the medication. However, it was covering all doses tested.

A daily dose of 5, 10, 15, or 20 mg of escitalopram was prescribed to patients for a minimum of 32 weeks. Patients' characteristics are described in the following table:

Demographics	Pittsburgh Patients	Pisa Patients	All patients
Number of Subjects	105	67	172
Number of Observations	320	153	473
Number of Observations for each subject	3.048	2.2836	2.75
CYP2C19 genotype			
Rapid metabolizers (RM, *17/*17)	4	1	5
Extensive Metabolizers (EM, *17/*1,*1/*1)	54	23	77
Intermediate Metabolizers (IM, *1/*2, *1/*3, *17/*2, *17/*3)	28	15	43
Poor Metabolizers (PM, *2/*2, *3/*3, *2/*3)	3	0	3
Missing	16	28	44
Age, Mean Years ± SD (range)	38.84 ± 12.05 (20.4-64.67)	40.58 ± 11.20 (21-65)	39.52 ± 11.73 (20.41 - 65)
Weight, mean kg ± SD (range)	81.6 ± 20 (31.9 - 139.7)	67.8 ± 15.2 (40-116)	76.25 ± 19.45 (31.9-139.7)
BMI, mean lbs/in2 ± SD (range)	28.20 ± 6.78 (15.55 - 48.26)	24.94 ± 4.52 (16.63-37.41)	26.93 ± 6.20 (15.55 - 48.26)
Sex, n (%)			
Male	47 (45)	7 (10)	54 (31)
Female	58 (55)	60 (90)	118 (69)
Race, n (%)			
White	94 (89)	67 (100)	161 (93)
Black/African American	8 (8)	0 (0)	8 (5)
Asian	3 (3)	0 (0)	3 (2)

Figure 8: *Demographic, biological, physiological characteristics of patients involved in the training dataset of the popPK model from Jin et al. [3]. Picture from [3].*

4.2.6 Output Comparison

Output comparison level: 3/5
Output comparison: Correspondence of model outputs with the therapeutic thresholds used in routine clinical therapeutic drug monitoring.

Output comparison source(s): Schulz et al. [4].
Comment: All patients evaluated were in accordance with thresholds of Schulz et al. [4]. Patients were within therapeutic range for recommended dose for each subpopulation tested.

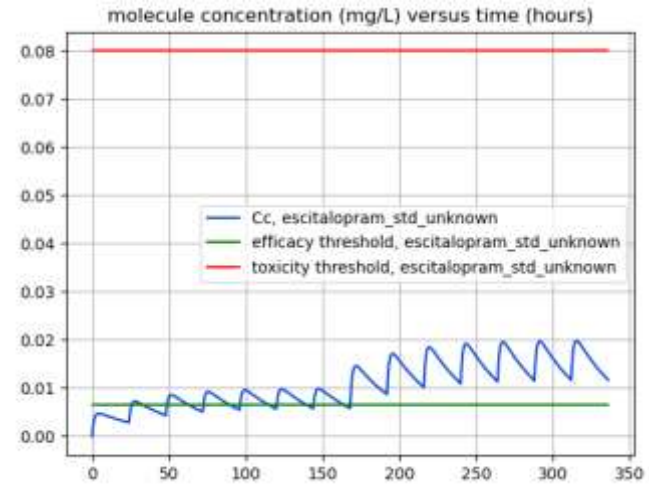

(1)

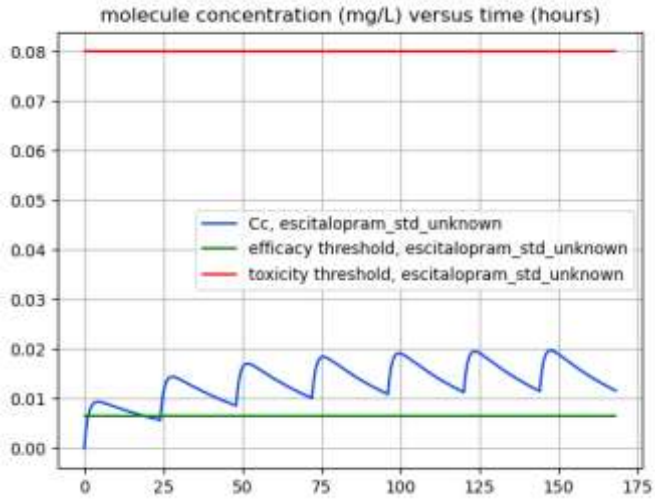

(2)

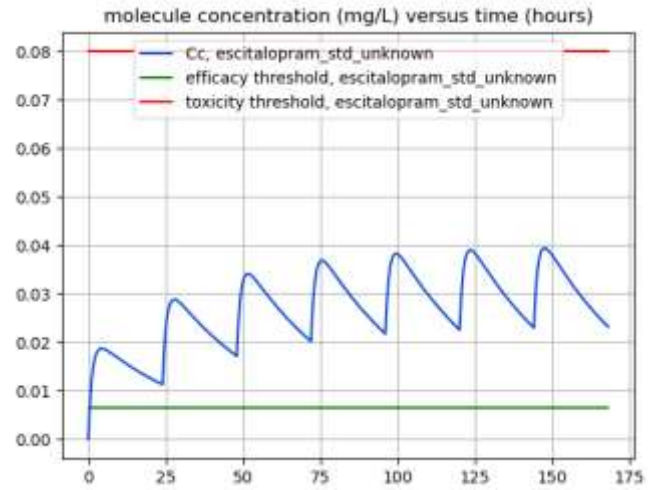

(3)

Figure 9: *Test 1: standard patient with 1) minimal usual posology, 2) usual posology, and 3) maximal usual posology.*

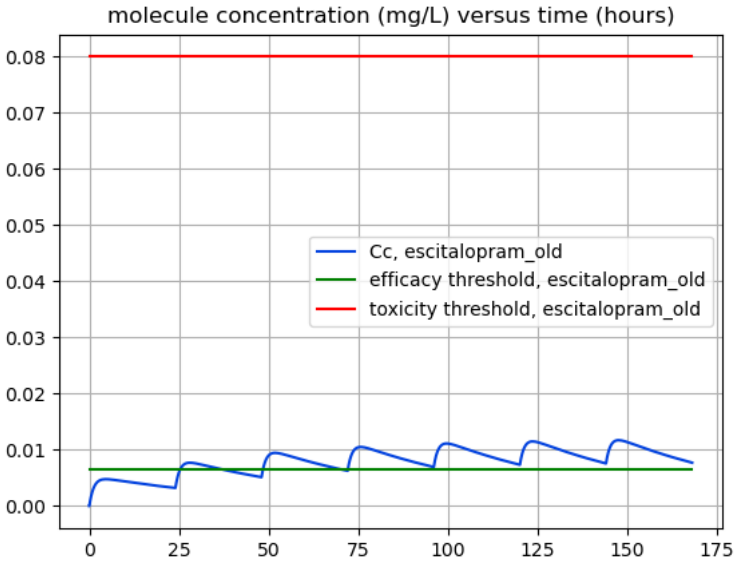

(1)

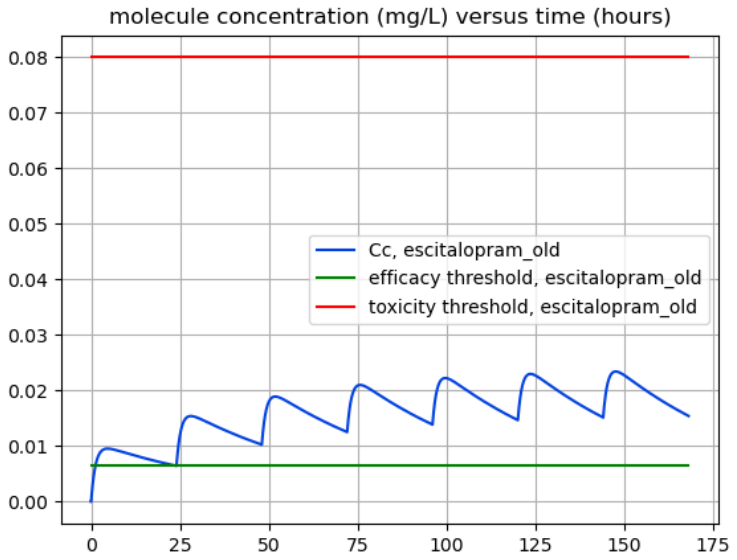

(2)

Figure 10: *Old patient (80 yo) with 1) recommended usual posology, and 2) maximal usual posology.*

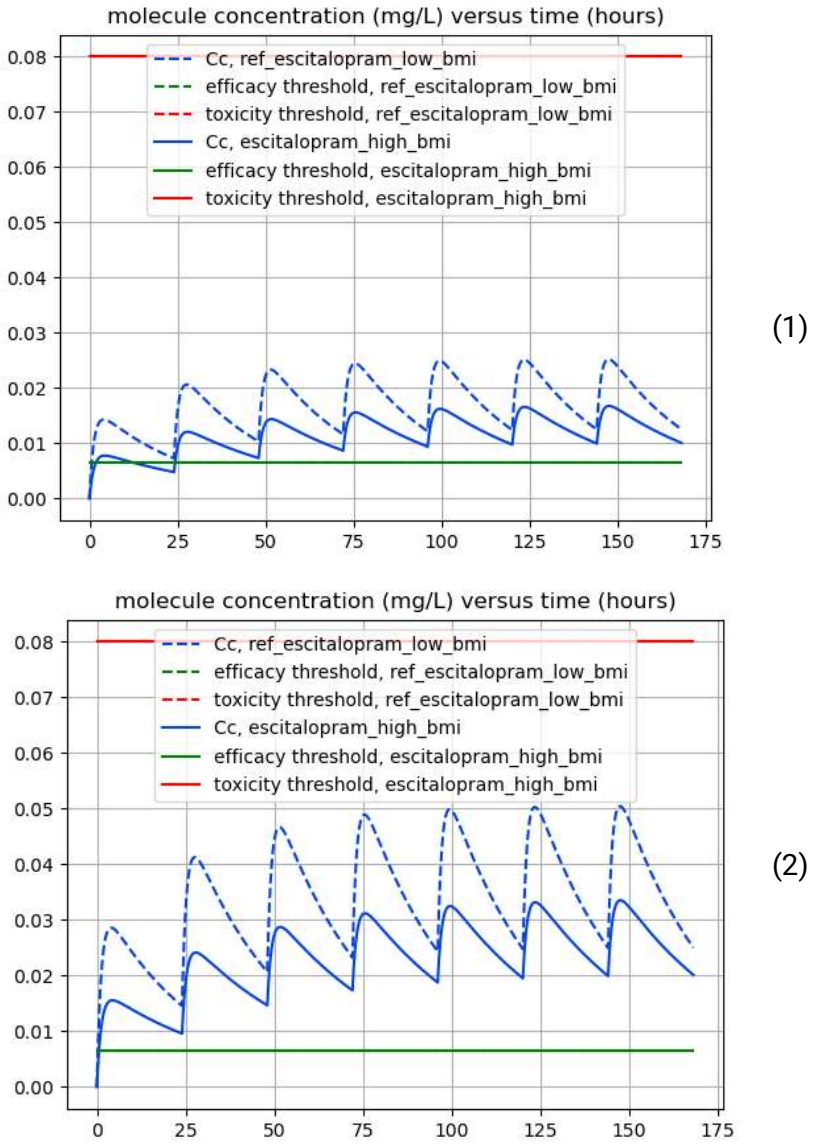

Figure 11: *Test 3: Higher BMI patient and low BMI patient with 1) usual posology, and 2) maximal usual posology.*

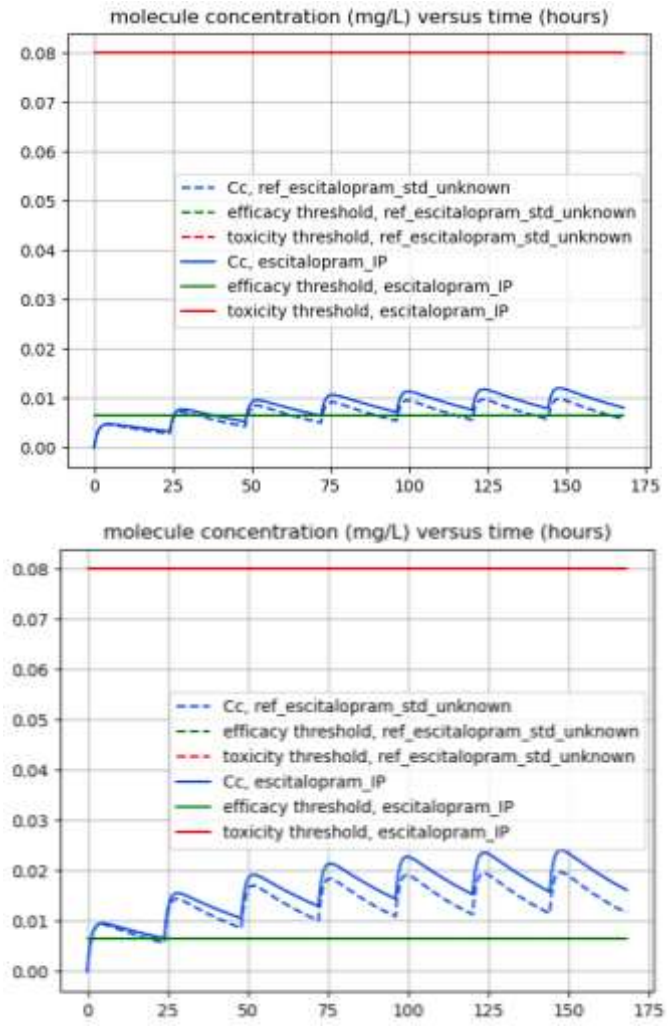

(1)

(2)

Figure 12: *Test 4: slower metabolizer (poor and intermediate) vs standard patient with 1) minimal usual posology 2) usual posology.*

4.3 Risperidone

Table 4: Summary of Risperidone validation.

Summary		
Levels	**Notations**	**Comments**
Model form level	3/5	Model built from popPK analysis
Model input level	4/4	RSE% were <30% for structural parameters
Test samples level	2/3	Therapeutic thresholds
Tests conditions level	4/5	Complete coverage of dosage ranges, and of all sub-populations concerned by the drug.
Equivalency of input parameters level	4/4	The model's training dataset does cover all doses and sub-populations concerned by the medication.
Output comparison level	3/5	Model outputs were within therapeutic thresholds.
Conclusion: The model is validated since all criteria meet the minimum score required.		

4.3.1 Model Form

Model form level: 3/5
Model form: Model built from popPK analysis.
Model Source(s): Thyssen et al. [7].
Comment: The implemented PK model is based on a popPK analysis conducted by Thyssen et al. [7]. It is a two-compartment model with first order absorption and elimination.

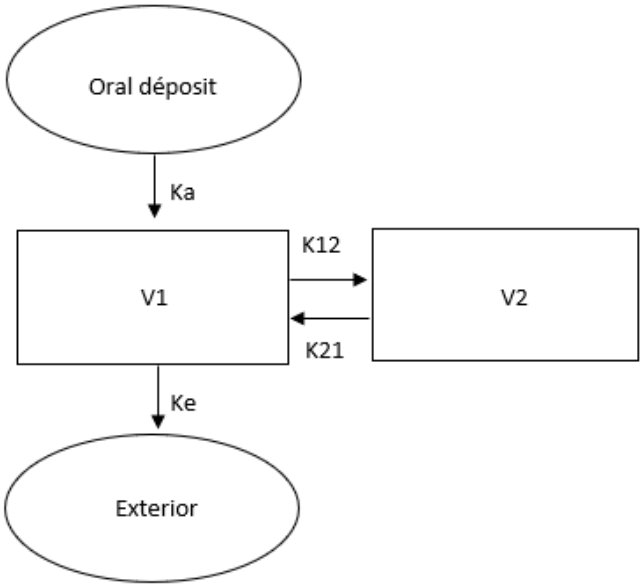

Figure 13: *Model's structure, with depot compartment, central compartment, peripheral compartment, and exterior fictive compartment. Ka is the absorption rate, V1 the volume of the central compartment, V2 the volume of the peripheral compartment, K12 and K21 transfer constant between the 2 compartments, and Ke the elimination rate.*

4.3.2 Model Inputs

Model inputs level: 4/4
Model input: Parameters are obtained from popPK analysis with a relative standard error (RSE) ≤ 30%.
Model inputs source(s): Thyssen et al. [7].
Comment: The RSE% were calculating with the SE and average communicated in the following table:

Parameter	Estimates (SE)	95% CI	%CV
Active antipsychotic fraction			
$CL/F\,(L/h) = (\theta_1 \bullet [WT/70]^{0.75} + \theta_6 \bullet CL_{CR} + \theta_9 \bullet BLAC) \bullet (Age/18.1)^{\theta_{10}}$			
θ_1	4.66 (0.460)	3.76, 5.56	
θ_6	0.00831 (0.00329)	0.00186, 0.01476	
θ_9	0.862 (0.181)	0.507, 1.217	
θ_{10}	−0.172 (0.0310)	−0.233, −0.111	
$V_1/F\,[L] = (\theta_2 + FLAG \bullet \theta_8) \bullet (WT/70)$			
θ_2	137 (7.05)	123, 151	
θ_8	−40.3 (6.83)	−53.7, −26.9	
$V_2/F\,[L] = \theta_3 \bullet (WT/70)$			
θ_3	86.8 (8.02)	71.1, 102.5	
Q/F [L/h]			
θ_4	1.35 (0.0987)	1.16, 1.54	
$k_a\,[h^{-1}]$			
θ_5	2.39 (0.243)	1.91, 2.87	
ALAG1 [h]			
θ_7	0.235 (0.00261)	0.230, 0.240	
$F_1 = 1 + \theta_{11} \bullet GPID$			
θ_{11}	−0.467 (0.145)	−0.751, −0.183	
IIV on CL/F: ω_1^2	0.0586 (0.0159)	0.0274, 0.0898	24.2
IIV on F1: ω_2^2	0.109 (0.0321)	0.0461, 0.172	32.4
IOV on F1	0.156 (0.0446)	0.0686, 0.243	39.5
Residual variability (on log concentration)			
study 6, 7 or 8: σ_1^2 [a]	0.270 (0.0254)	0.220, 0.320	SD 0.52
study 1, 2, 3, 4, 5 or 9: σ_2^2 [a]	0.186 (0.0367)	0.114, 0.258	SD 0.43

Figure 14: *Model parameters from Thyssen et al. [7]. Picture from [7].*

Table 5: Results of RSE% calculation. SE% = standard error, RSE% = residual standard error.

Parameters	SE%	Mean	RSE%
CL/F	0.46	4.66	9.87124464
V1/F	7.05	137	5.1459854
V2/F	7.05	137	5.1459854
Q/F	0.0987	1.35	7.31111111
ka	0.243	2.39	10.167364
ALAG1	0.00261	0.235	1.1106383

Formula used to calculate RSE% was: RSE% = 100 * SE / Mean

4.3.3 Test Samples

Test sample level: 2/3
Test sample: Efficacy and overexposure thresholds used for routine therapeutic drug monitoring (TDM) in clinical conditions.

- Efficacy threshold was: 0.02 mg/L
- Overexposure threshold was: 0.06 mg/L
- Safety threshold was: 0.12 mg/L

Test samples source(s): Schulz et al. [4].
Comment: /

4.3.4 Tests conditions

Tests conditions level: 4/5
Tests condition: Test conditions were defined with sufficient data to run simulations for each patient concerned by the drug, with complete coverage of dosage ranges, and of all sub-populations concerned by the drug.
Tests conditions source(s):

- base-donnees-publique.medicaments.gouv.fr [6].

Comment: /

Tests conditions were :

- Test 1: Standard patient and heavier patient at 1) usual ORAL posology of 4mg 2) maximum posology of 6mg 3) Usual posology of 2mg twice a day.
- Test 2: Standard patient and older patient at 1) usual ORAL posology of 4mg 2) maximum posology of 6mg 3) Minimum posology for elderly 0.5mg twice a day 4) Usual posology of 2mg twice a day.
- Test 3: Standard patient and patient with renal impairment at 1) usual ORAL posology of 4mg 2) maximum posology of 6mg 3) Usual posology of 2mg twice a day.
- Test 4: Standard patient and older patient with lower weight and renal impairment. at 1) usual ORAL posology of 4mg 2) maximum posology of 6mg 3) Minimum posology for elderly 0.5mg twice a day 4) Usual posology of 2mg twice a day
- Test 5: Standard patient and older patient with higher weight and renal impairment. at 1) usual ORAL posology of 4mg 2) maximum posology of 6mg 3) Minimum posology for elderly 0.5mg twice a day 4) Usual posology of 2mg twice a day.

‘

Where patients are:

- Standard patient: weight: 70kg, age: 40, glomerular_filtration_rate: 90 ml/min
- heavier patient: weight: 120kg, age: 40, glomerular_filtration_rate: 90 ml/min
- older patient: weight: 70kg, age: 80, glomerular_filtration_rate: 90 ml/min
- Standard patient with renal impairment: weight: 70kg, age: 40, glomerular_filtration_rate: 15 ml/min.
- Older patient with lower weight and renal impairment: weight: 55kg, age: 80, glomerular_filtration_rate: 15 ml/min.
- older patient with higher weight and renal impairment: weight: 100kg, age: 80, glomerular_filtration_rate: 15 ml/min.

Where posology are:

- usual ORAL posology of 4mg: 4mg/24h
- maximum posology of 6mg: 6mg/24h
- Usual posology of 2mg twice a day: 2mg/12h
- Minimum posology for elderly 0.5mg twice a day : 0.5mg/12h

4.3.5 Equivalency of input parameters

Equivalency of input parameters level: 4/4
Equivalency of input parameters: The model's training dataset does cover all doses and sub-populations concerned by the medication.
Equivalency of input parameters source(s):

- base-donnees-publique.medicaments.gouv.fr [6],
- *Thyssen et al. [7].*

Comment: Model implemented is the one developed and published by the drug manufacturer.

Doses range of test were [0.25/12h - 15mg/24h] which covers all tests.

Parameter	Children [aged 6–12 y]	Adolescents [aged 12–17 y]	Adults [aged >17 y]	All
Subjects [n]	52	252	476	780
Males [n]	34	141	294	469
Females [n]	18	111	182	311
Age [y] [a]	10.7 (6–12)	15.2 (12–17)	32.8 (17–70)	18.1 (6–70)
Race [n]				
Caucasian	35	198	213	446
Black	14	43	106	163
Oriental	0	2	0	2
other	3	9	157	169
Bodyweight [kg] [a]	39 (20–68)	60 (31–103)	65 (35–153)	62 (20–153)
Creatinine clearance [mL/min] [a]	100.6 (54–162)	133.0 (55–254)	112.6 (52–312)	117.6 (52–312)

a Values are expressed as median (range).

Figure 15: *Demographic, biological, physiological characteristics of patients involved in the training dataset of the popPK model. Picture from [7].*

Trial name	Population [n] [a]	Trial design	Dose, dosage form	Pharmacokinetic sampling	Reference
RIS-USA-160	24 children and adolescents (aged 6–17 y) with psychotic and behaviour disorders	Open-label, multicentre, phase I	Flexible dose of 0.25–1.5 or 0.75–1.75 mg/day, bid dosing, tablet	Sampling pre-dose and at 2, 4, 8 and 12 h post-dose	Current study
RIS-BIM-301	106 children and adolescents (aged 10–18 y) with bipolar I disorder	Randomized, placebo-controlled, 3-wk, double-blind, 3-arm, multicentre, phase III	Flexible dose of 0.5–2.5 or 3–6 mg/day, tablet	Sparse sampling on days 7, 14, 21 pre-dose and at ~1 h post-dose	14
RIS-USA-231	261 adolescents (aged 8–17 y) with schizophrenia	Randomized, 8-wk, double-blind, parallel-group, multicentre, phase III	Flexible dose of 0.35–0.6 or 3.5–6 mg/day (depending on bodyweight < or >50 kg), oral solution	Sparse sampling on days 28 and 56 pre-dose and at 1–2 h post-dose	5
RIS-USA-239	119 adults (aged 18–69 y) with bipolar I disorder	Randomized, placebo-controlled, 3-wk, double-blind, parallel-group, multicentre, phase III	Flexible dose of 1–6 mg/day, tablet	Sparse sampling on days 7 and 21 pre-dose and at 1–2 h post-dose	15
RIS-IND-2	140 adults (aged 18–70 y) with bipolar I disorder	Randomized, placebo-controlled, 3-wk, double-blind, parallel-group, multicentre, phase III	Flexible dose of 1–6 mg/day, tablet	Sparse sampling on days 7 and 21 pre-dose and at 1–2 h post-dose	16
RIS-NED-25 [b]	39 healthy adults (aged 20–55 y)	Open-label, randomized, balanced, two-way crossover, bioequivalence, phase I	Single dose of 2 mg, tablet	Rich sampling (pre-dose and up to 96 h post-dose)	17
RIS-P01-103 [b]	40 adults (aged 20–61 y) with schizophrenia	Single-centre, open-label, randomized, two-way crossover, bioequivalence, phase I	Single dose of 4 mg, tablet	Rich sampling (pre-dose and up to 96 h post-dose)	18
RIS-RSA-5 [b]	36 adults (aged 20–60 y) with schizophrenia or schizoaffective disorder	Open-label, randomized, two-way crossover, bioequivalence, phase I	Single dose of 4 mg, tablet	Rich sampling (pre-dose and up to 96 h post-dose)	
R076477-SCH-102	15 adults with schizophrenia or schizoaffective disorder	Open-label, parallel-group, multicentre, phase I	Multiple dosing of 15 mg/day, tablet	Rich sampling (pre-dose and up to 120 h post-dose)	

a Refers to the number of subjects included in the population pharmacokinetic analysis, i.e. subjects treated with oral risperidone (conventional tablet or oral solution) and with accurate dosing and sampling information.

b Only conventional tablet treatment during bioequivalence trials was included in the population pharmacokinetic model.

bid = twice daily.

Figure 16: *Data sources (clinical studies) and dose regimens associated with each study. Picture from [7].*

4.3.6 Output Comparison

Output comparison level: 3/5
Output comparison: Correspondence of model outputs with the therapeutic thresholds used in routine clinical therapeutic drug monitoring.
Output comparison source(s): Schulz et al. [4].
Comment: All patients evaluated were in accordance with thresholds of Schulz et al. [4]. All output results were within therapeutic thresholds.

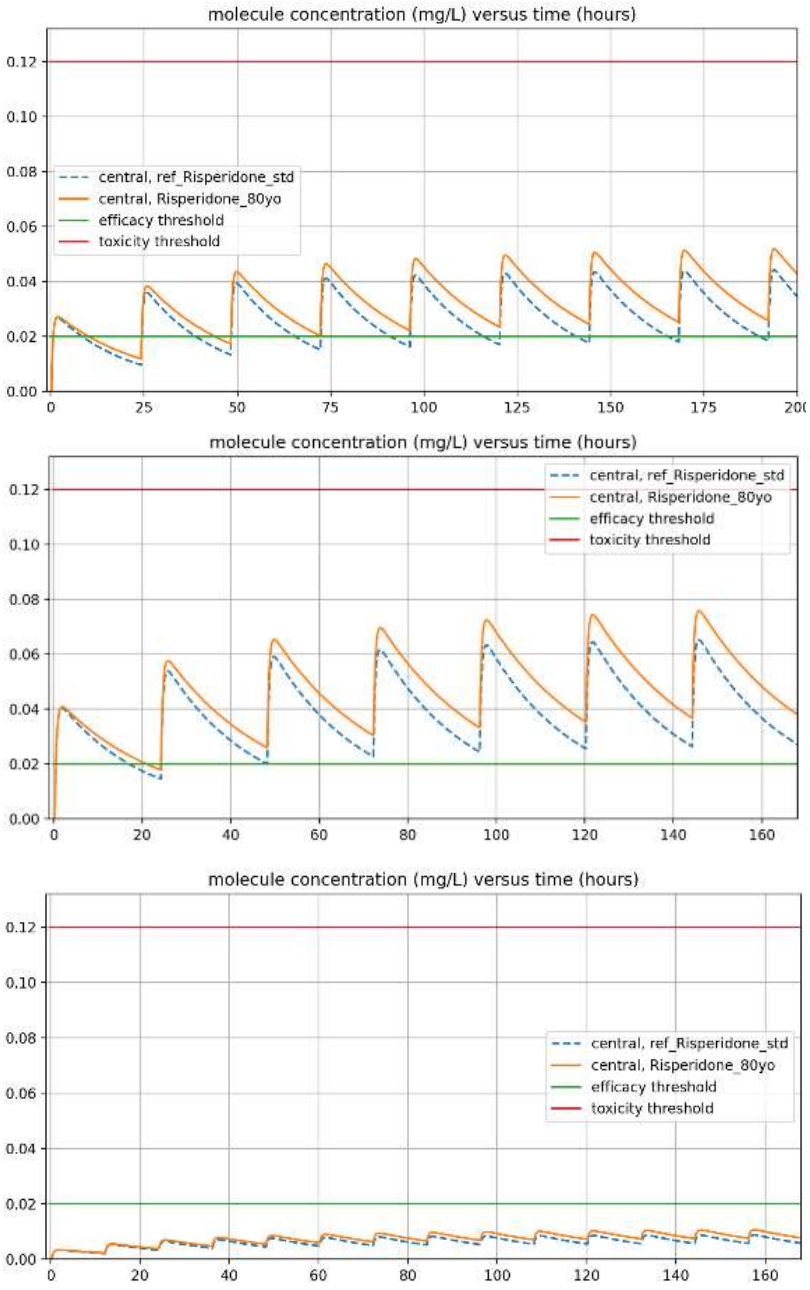

Figure 17: *Test 1: Standard patient and heavier patient at 1) usual ORAL posology of 4mg 2) maximum posology of 6mg 3) Usual posology of 2mg twice a day. Both patients do not reach the therapeutic range. This dosage is just a starting dose for elder patient and might evolute to 2mg/12h.*

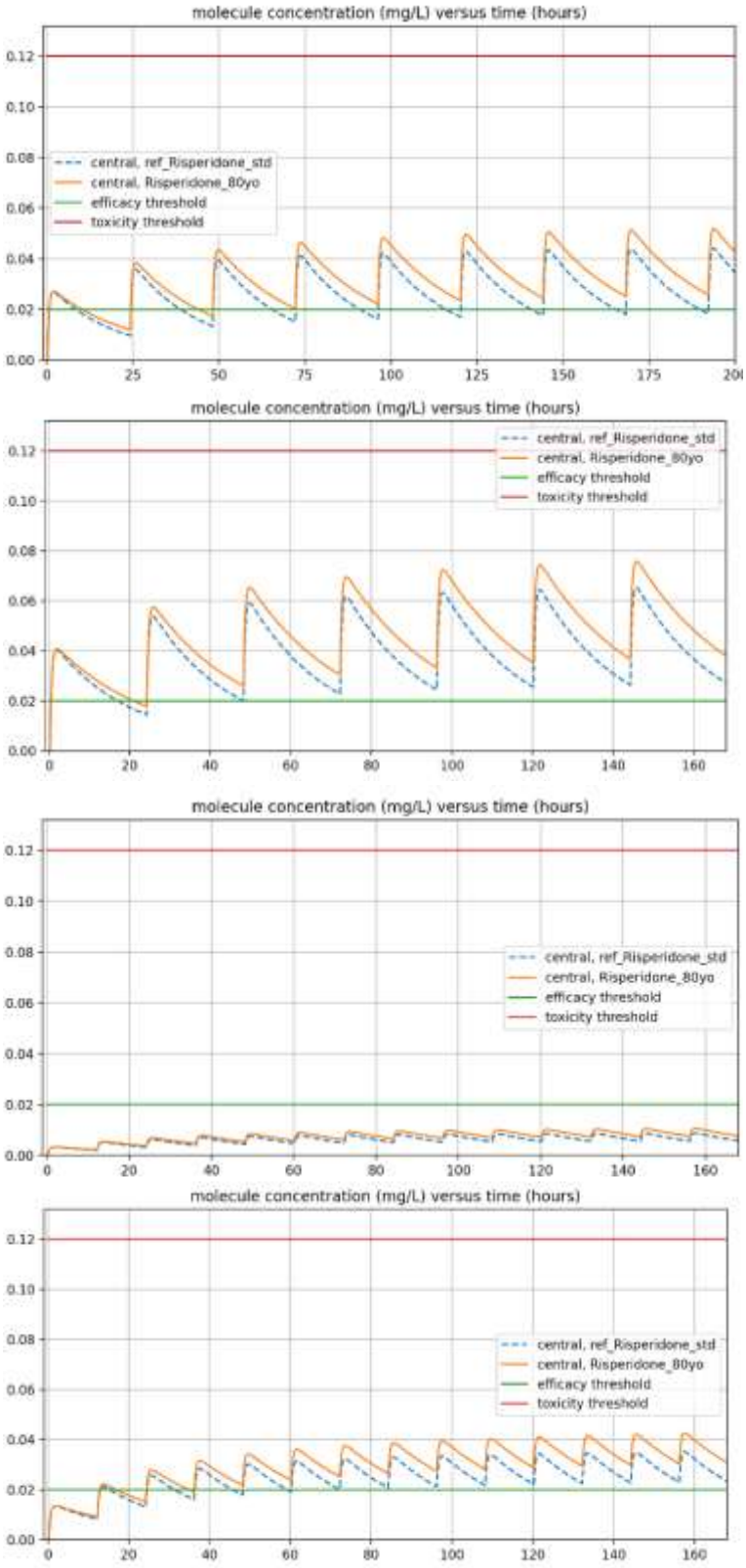

Figure 18: *Test 2: Standard patient and older patient at 1) usual ORAL posology of 4mg 2) maximum posology of 6mg 3) Minimum posology for elderly 0.5mg twice a day. Both patients do not reach the therapeutic range. This dosage is just a starting dose for elder patient and might evolute to 2mg/12h. 4) Usual posology of 2mg twice a day.*

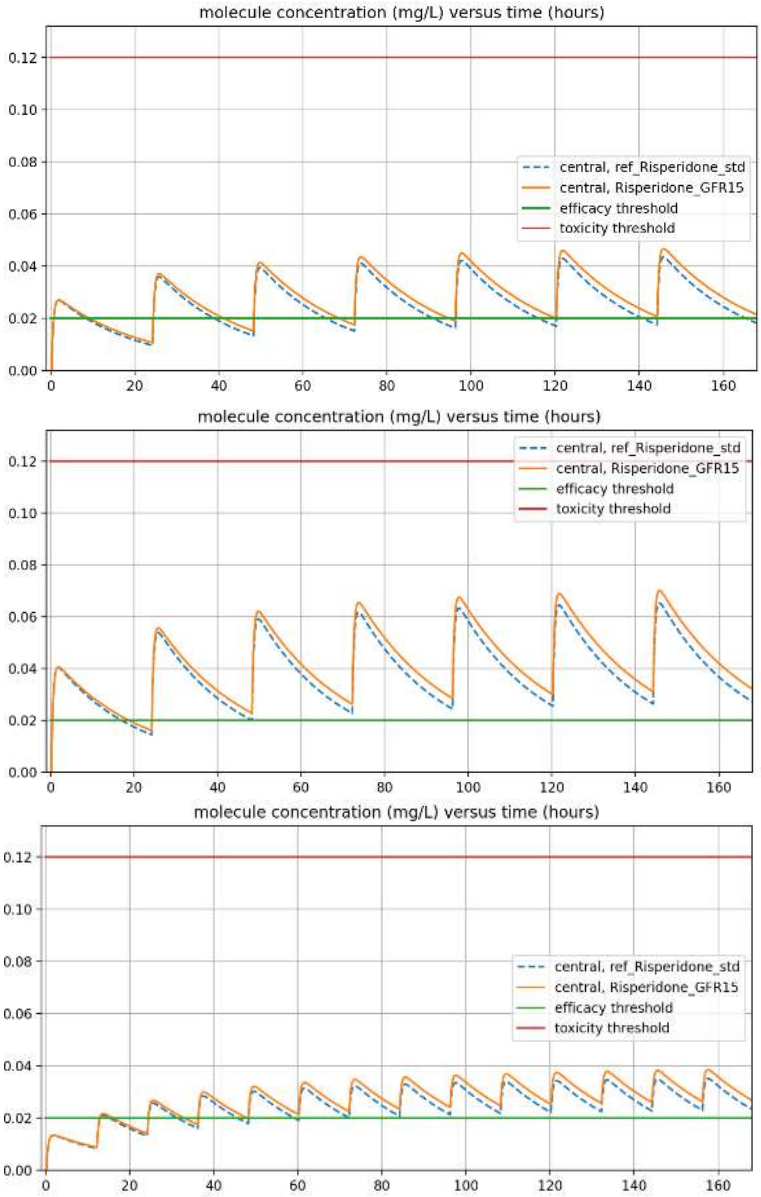

Figure 19: *Test 3: Standard patient and patient with renal impairment at 1) usual ORAL posology of 4mg 2) maximum posology of 6mg 3) Usual posology of 2mg twice a day.*

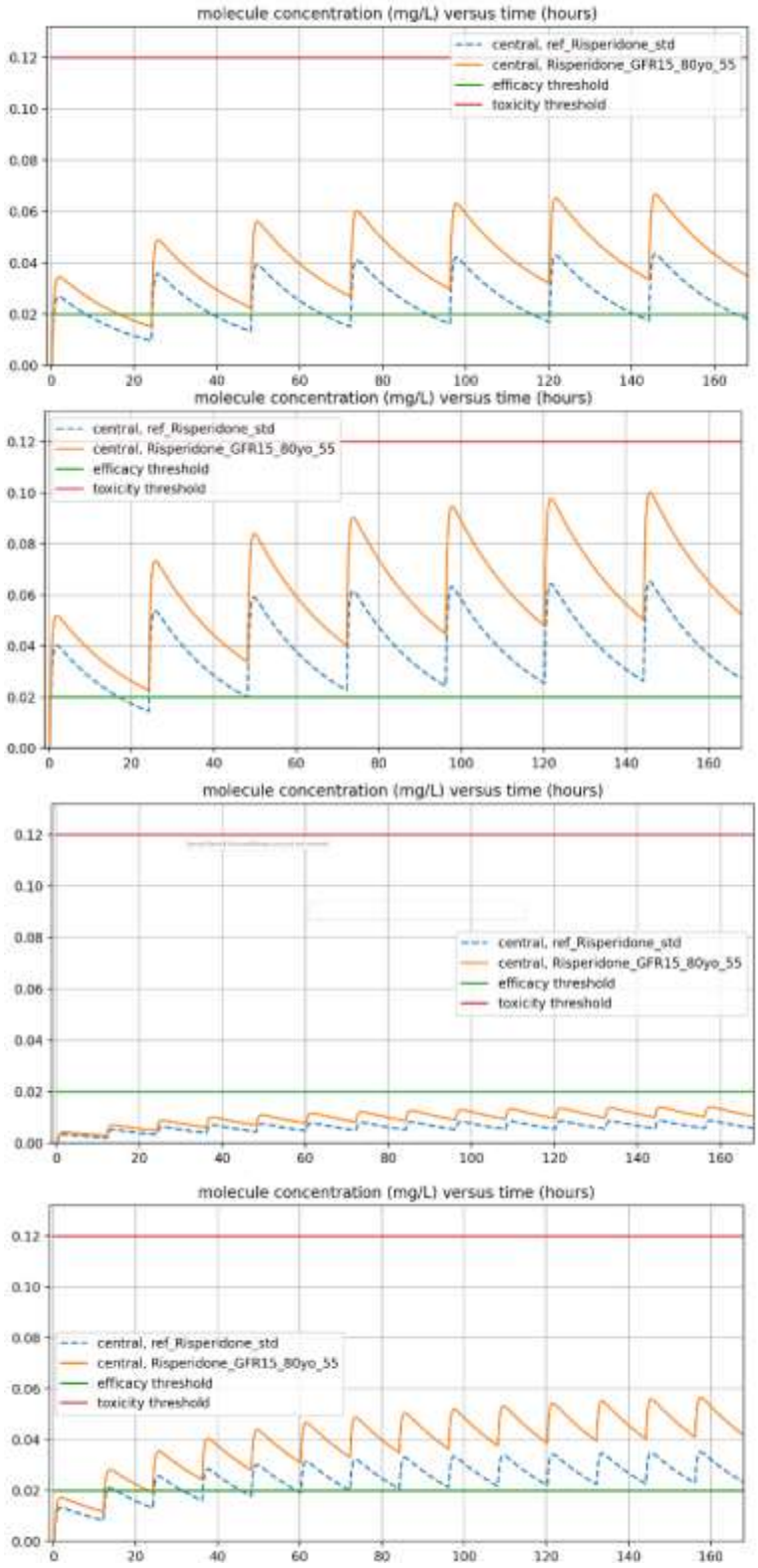

Figure 20: *Test 4: Standard patient and older patient with lower weight and renal impairment. at 1) usual ORAL posology of 4mg 2) maximum posology of 6mg 3) Minimum posology for elderly 0.5mg twice a day 4) Usual posology of 2mg twice a day.*

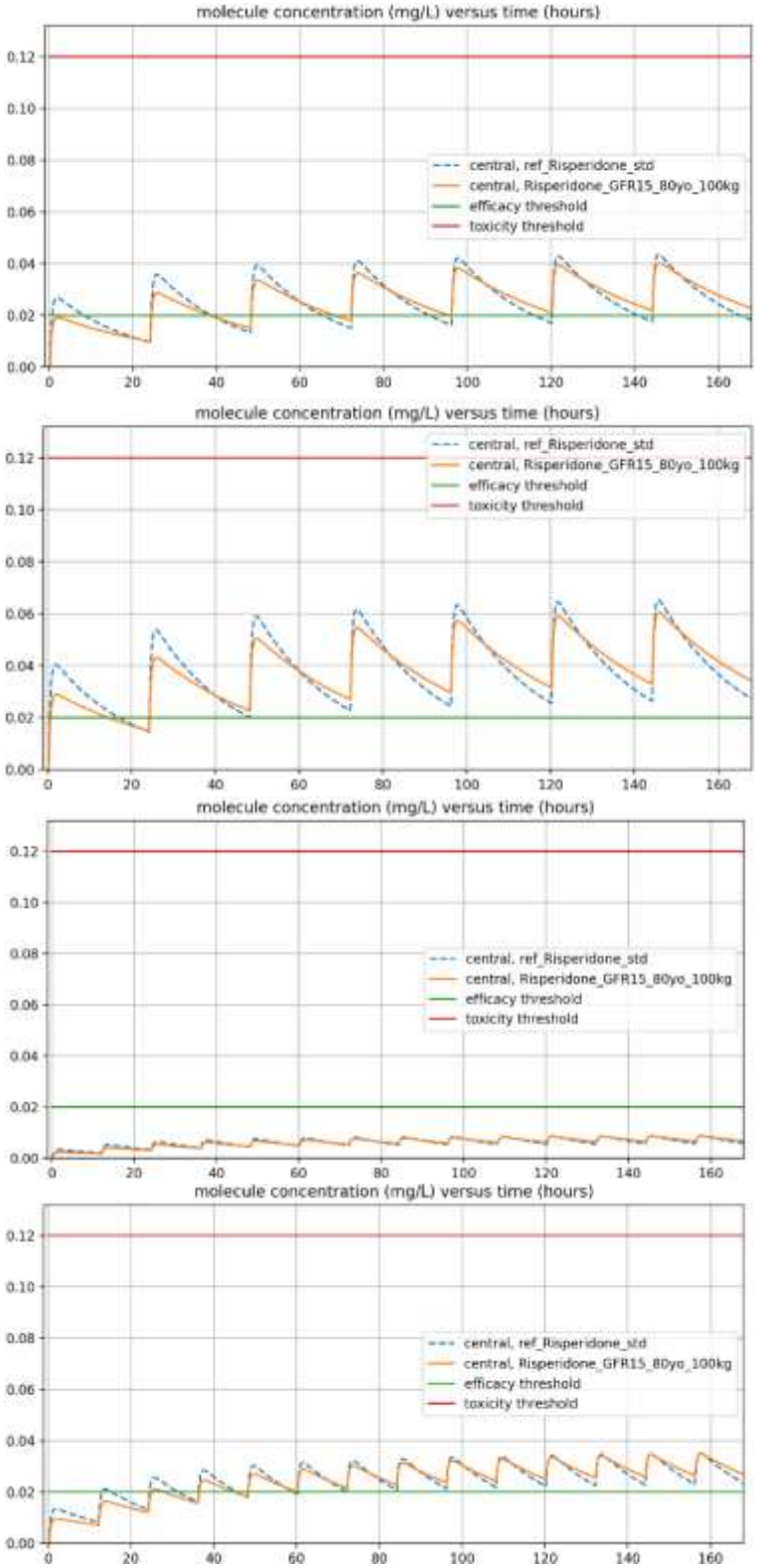

Figure 21: *Test 5: Standard patient and older patient with higher weight and renal impairment. at 1) usual ORAL posology of 4mg 2) maximum posology of 6mg 3) Minimum posology for elderly 0.5mg twice a day. Patients does not reach the therapeutic range but it's just a starting dose that may be increased to 2mg/12h. 4) Usual posology of 2mg twice a day.*

4.4 Carvedilol

Table 6: Summary of Carvedilol validation.

Summary		
Levels	**Notations**	**Comments**
Model form level	3/5	Model built from popPK analysis
Model input level	3/4	RSE% of on parameter is >30%
Test samples level	2/3	Therapeutic thresholds
Tests conditions level	4/5	-
Equivalency of input parameters level	4/4	-
Output comparison level	3/5	Model outputs were within therapeutic thresholds.
Conclusion: The model is validated since all criteria meet the minimum score required.		

4.4.1 Model Form

Model form level: 3/5
Model form: Model built from popPK analysis.
Model Source(s): Nikolic et al. [9].
Comment: The implemented PK model is based on a popPK analysis conducted by Nikolic et al. [9]. It is a one-compartment model with first order absorption and elimination.

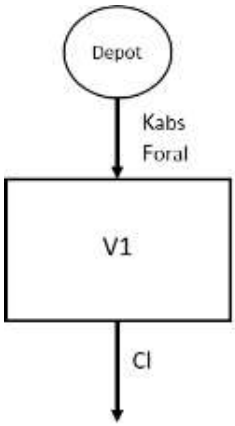

Figure 22: *Model's structure, with one depot compartment, and one central compartment. Kabs, is the absorption rate, Foral the bioavailability V1 the volume of distribution, CL the clearance of elimination.*

4.4.2 Model Inputs

Model inputs level: 3/4
Model input: Parameters are obtained from popPK analysis with a relative standard error (RSE) > 30% or taken from the summary of product characteristics or from analysis conducted on many patients with little variability.
Model inputs source(s): Nikolic et al. [9].
Comment: The RSE% were calculating with the SE and average communicated in the following table:

Model Parameter	Estimated Value	Standard Error (95% Confidence Interval)
Clearance (L/h)—θ_1	10	3.71 2.73–17.27
Volume of distribution (L)—θ_2	832	132.06 573.16–1090.84

Figure 23: *Parameters value from Nikolic et al [9]. popPK analysis. Picture from [9].*

Table 7: Results of RSE% calculation. SE% = standard error, RSE% = residual standard error.

Parameters	SE%	Mean	RSE% [1]
CL	3.71	10	37.1
Vd	132.06	832	15.8725962

[1] RSE% = 100 * SE / Mean

Ka was fixed at 0.81 h-1 according to previous study published by Takekuma et al. [10].

4.4.3 Test Samples

Test sample level: 2/3
Test sample: Efficacy, overexposure, and safety thresholds used for routine therapeutic drug monitoring (TDM) in clinical conditions.

- Efficacy threshold was: 0.02 mg/L
- Safety threshold was: 0.3 mg/L

Test samples source(s): Schulz et al. [4].
Comment: /

4.4.4 Tests conditions

Tests conditions level: 4/5
Tests condition: Test conditions were defined with sufficient data to run simulations for each patient concerned by the drug, with complete coverage of dosage ranges, and of all sub-populations concerned by the drug.
Tests conditions source(s):

- base-donnees-publique.medicaments.gouv.fr [8].

Comment: /
Tests conditions were :

- Test 1: 25mg/12h for: Std patient, smoker patient, and 50 kg patient.
- Test 2: 25mg/12h for: 50kg and 95kg patients smokers and digoxin, and std with digoxin
- Test 3: 25mg/12h AND 50mg/12h for: std patient, 85kg patient, and 120kg patient

Where patients are:

- Std patient: weight: 70, smoker: false, digoxin: false
- Smoker patient: weight: 70, smoker: true, digoxin: false
- 50 kg patient: weight: 50, smoker: false, digoxin: false
- 50 kg patient smoker and digoxin: weight: 70, smoker: true, digoxin: true

- 95 kg patient's smoker and digoxin: weight: 95, smoker: true, digoxin: true
- Std patient with digoxin: weight: 70, smoker: false, digoxin: true
- 85 kg patient: weight: 85, smoker: false, digoxin: false
- 120 kg patient: weight: 120, smoker: false, digoxin: false

4.4.5 Equivalency of Input Parameters

Equivalency of input parameters level: 4/4
Equivalency of input parameters: The model's training dataset does cover all doses or PK is linear over the dose range use in the test conditions and sub-populations concerned by the medication, or an external validation is carried out and meets validation criteria. (i.e., MDPE ≤ ± 20%, MDAPE ≤ 30%).
Equivalency of input parameters source(s):

- base-donnees-publique.medicaments.gouv.fr [8],
- Nikolic et al. [9].

Comment: All subpopulations and doses were covered by in the training dataset.
The total daily doses of carvedilol administered ranged from 3.25 to 25.0 mg twice daily.

Characteristics	Index Set	Range Index	Validation Set	Range Validation
Number of patients	52		14	
Number of observations	55		15	
Gender (male/female)	40/12		9/5	
Total body weight (kg)	77.96 ± 13.46	49–118	71.27 ± 9.20	49–82
Age (years)	63.02 ± 11.95	30–83	60.4 ± 16.53	28–80
Carvedilol dose (mg/day)	12.33 ± 7.55	6.25–50	15.63 ± 11.63	6.25–50
Carvedilol plasma concentration (ng/mL)	7.47 ± 11.99	1–59.07	13.14 ± 11.92	1–35.61
Ejection fraction (%)	37.76 ± 6.16	23–43	37.97 ± 5.13	26–41
Tobacco users	16		2	
Number of patients with *CYP2D6*4* (*wt/*4*)	17		3	
Carvedilol + amiodarone	7		1	
Carvedilol + digoxin	18		2	
Carvedilol + warfarin	25		3	
Carvedilol + aminophyllin	9		2	
Carvedilol + proton pump inhibitors	13		2	

The data are expressed as mean values ± standard deviation (SD; range).

Figure 24: *Demographic, biological, physiological characteristics of patients involved in the training dataset of the Nikolic et al. [9] popPK model. Picture from [9].*

4.4.6 Output Comparison

Output comparison level: 3/5
Output comparison: Correspondence of model outputs with the therapeutic thresholds used in routine clinical therapeutic drug monitoring.
Output comparison source(s): Schulz et al. [4].
Comment: All patients evaluated were in accordance with thresholds of Schulz et al. [4]. Patients were within therapeutic thresholds.

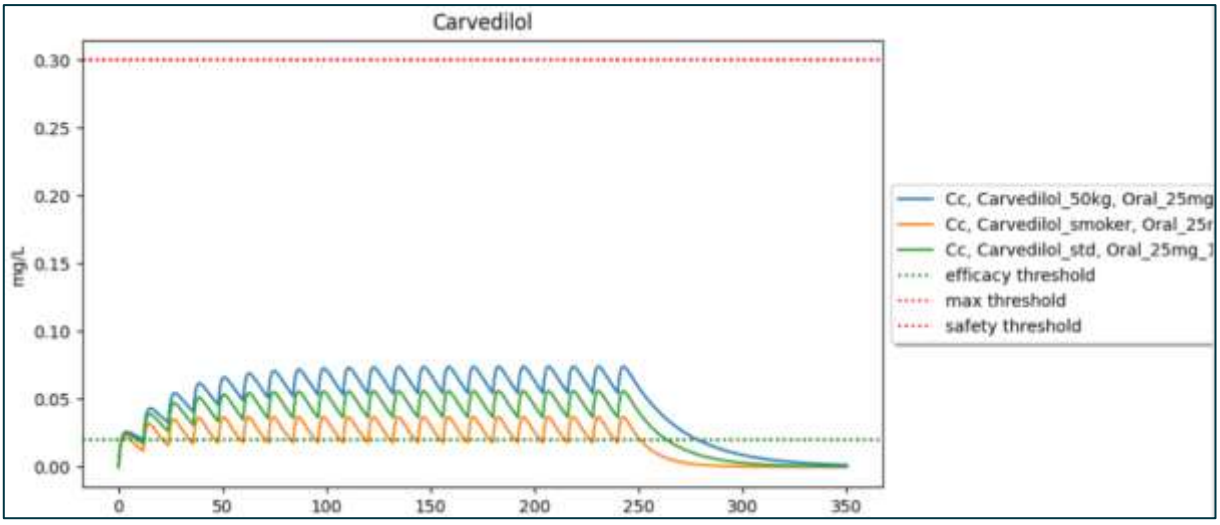

Figure 25: *Test 1: 25mg/12h for: Std patient, smoker patient, and 50 kg patient.*

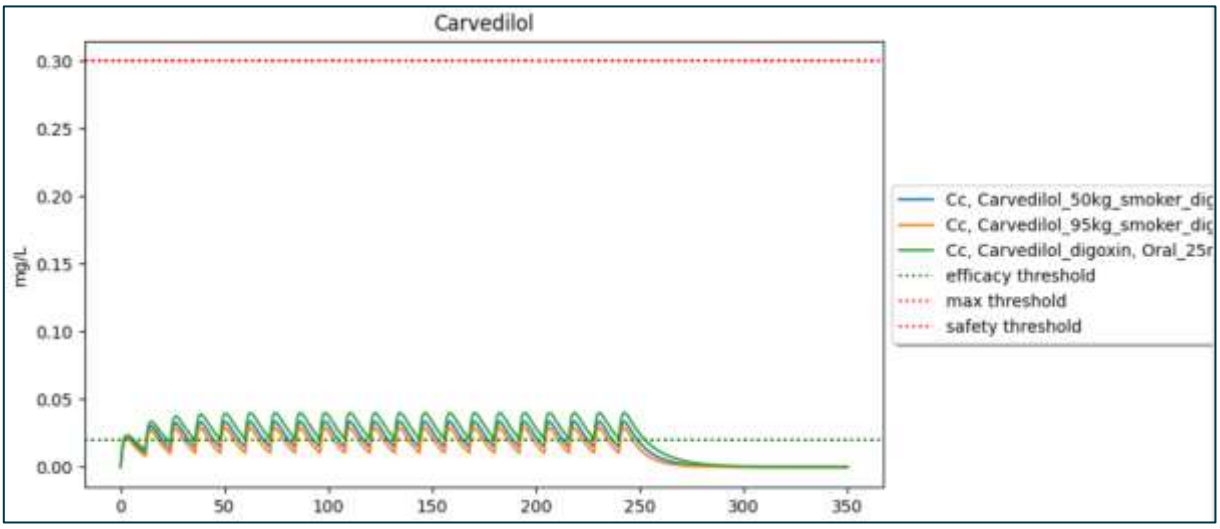

Figure 26: *Test 2: 25mg/12h for: 50kg and 95kg patients smokers and digoxin, and std with digoxin*

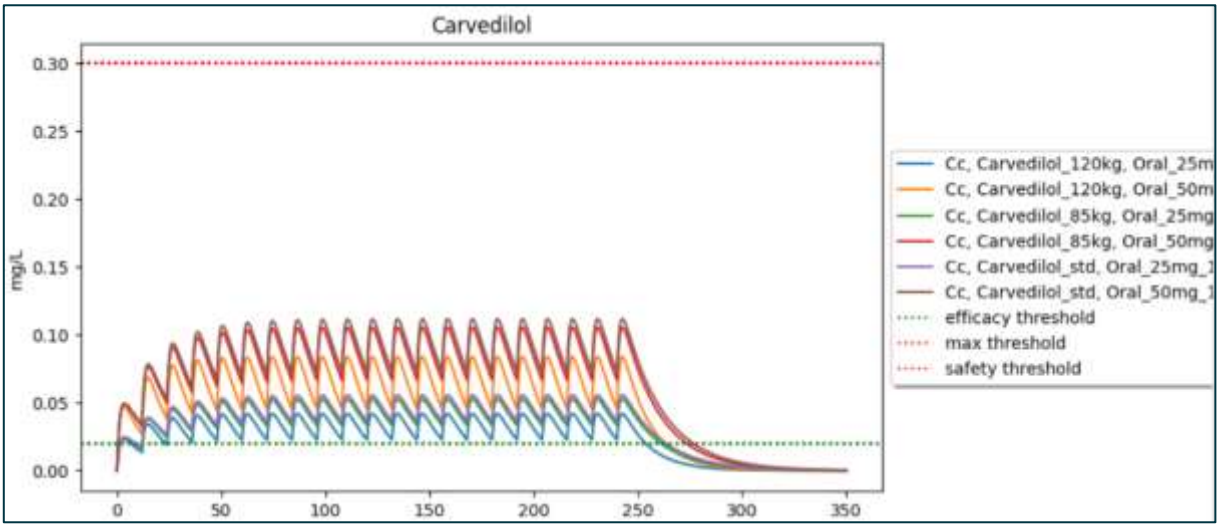

Figure 27: *Test 3: 25mg/12h AND 50mg/12h for: std patient, 85kg patient, and 120kg patient.*

5 Conclusion

This document is an annex of SimCardioTest deliverable D6.2, and reports technical details relative to the validation of the PK numerical model developed for Use Case 3. General conclusions relative to the validation of UC3 numerical model are reported in main deliverable D6.2.

Table 8: List of references per drug.

Drug	References
Clozapine	[1, 2]
Escitalopram	[3, 4, 5]
Risperidone	[4, 6, 7]
Carvedilol	[4, 8, 9, 10]

6 Bibliography

[1] M. Jerling, Y. Merlé, F. Mentré and others, "Population pharmacokinetics of clozapine evaluated with the nonparametric maximum likelihood method,": doi:10.1046/j.1365-2125.1997.t01-1-00606.x, 1997.

[2] A. Lereclus, T. Korchia, C. Riff and others, "Towards Precision Dosing of Clozapine in Schizophrenia: External Evaluation of Population Pharmacokinetic Models and Bayesian Forecasting," Ther Drug Monit, doi:10.1097/FTD.0000000000000987, 2022.

[3] Y. Jin, B. G. Pollock, E. Frank and others, "Effect of age, weight, and CYP2C19 genotype on escitalopram exposure," J Clin Pharmacol. vol. 50(1), p. 62–72, doi: 10.1177/0091270009337946, 2010.

[4] M. Schulz, A. Schmoldt, H. Andersen-Streichert and others, "Revisited: Therapeutic and toxic blood concentrations of more than 1100 drugs and other xenobiotics," Critical Care, vol. 24(1):195, doi: 10.1186/s13054-020-02915-5, 2020.

[5] Base de données publique du médicament (French summary of product)," [Online]. Available: https://base-donnees-publique.medicaments.gouv.fr/affichageDoc.php?specid=68082865&typedoc=R#RcpProp Pharmacodynamiques

[6] "Base de données publique du médicament (French summary of product)," [Online]. https://base-donnees-publique.medicaments.gouv.fr/affichageDoc.php?specid=63605525&typedoc=R#RcpProp Pharmacocinetiques

[7] A. Thyssen, A. Vermeulen, E. Fuseau and others, "Population pharmacokinetics of oral risperidone in children, adolescents and adults with psychiatric disorders," Clinical Pharmacokinetics, vol. 49, p. 465–478, doi:10.2165/11531730-000000000-00000, 2010.

[8] "Base de données publique du médicament (French summary of product)," [Online]. Available : https://base-donnees-publique.medicaments.gouv.fr/affichageDoc.php?specid=61639048&typedoc=R#RcpProp Pharmacocinetiques

[9] V. N. Nikolic, S. M. Jankovic, R. Velickovic-Radovanović, and others, “Population pharmacokinetics of carvedilol in patients with congestive heart failure,” J. Pharm. Sci., vol. 102(8), p. 2851–8, doi:10.1002/jps.23626, 2013.

[10] Y. Takekuma, T. Takenaka, M. Kiyokawa and others, “Evaluation of effects of polymorphism for metabolic enzymes on pharmacokinetics of carvedilol by population pharmacokinetic analysis,” Biol. Pharm. Bull., vol. 30(3), p. 537–542, 2007.

This project received funding from the European Union’s Horizon 2020 research and innovation program under grant agreement No 101016496

EU Horizon 2020 Research & Innovation Program
Digital transformation in Health and Care
SC1-DTH-06-2020
Grant Agreement No. 101016496

SimCardioTest - Simulation of Cardiac Devices & Drugs for in-silico Testing and Certification

Technical Report

D6.2-UC3-0D: Use Case 3 0D Validation Annex

Work Package 6 (WP6)

Verification, validation, uncertainty quantification & certification

Annex Lead: UPV, Spain
Task Lead: UBx, France
WP Lead: MPC, France

PUBLIC

Document history			
Date	**Version**	**Author(s)**	**Comments**
16/06/2023	V1	M. T. MORA	First Draft
19/06/2023	V2	B. TRENOR	Review
21/06/2023	V3	M. T. MORA	Final Draft
29/06/2023	V4	R. SETZU	Format Consolidation
30/06/2023	V5	R. SETZU	Final Version
01/07/2024	V6	R. SETZU M. BARBIER	Format editing

TABLE OF CONTENTS

EXECUTIVE SUMMARY

This document is an annex of SimCardioTest deliverable D6.2 and was elaborated for Use Case 3 in the context of drug safety assessment. It contains the technical details for the validation of the electrophysiological models at the cellular level.

Acronyms

Table 1: List of Acronyms.

Acronym	Meaning
AP	Action Potential
CiPA	Comprehensive in-vitro Proarrhythmia Assay
EFTPC	Effective Free Therapeutic Plasma Concentration
FDA	Food and Drug Administration
iPSC-CM	induced Pluripotent Stem Cell-Derived Cardiomyocytes
ORd	human AP O'Hara-Rudy model
SCT	SimCardioTest
TdP	Torsade de Pointes

1. Computational model

Validation activities focused on the evaluation of the electrophysiological model to assess drug induced arrhythmogenic risk. It is to be noted, that the original O'Hara-Rudy model (ORd, [1]), when published, included a validation process based on multiple comparisons with experimental data. However, since V&V40 strategy was not followed during its development, no specific question of interest was addressed. Therefore, we have performed new validation tests particularized to the present context of use.

1.1 Model Form

The system of equations composing the mathematical model was fixed, but some parameters were evaluated through a sensitivity analysis. Based on the methodology applied in our previous study [2] we analyzed the impact of maximal ion channel conductances and fluxes on some quantities of interest.

In this local sensitivity analysis, 16 parameters varied between ±60% of their baseline values, and the evaluated biomarkers, obtained from the action potential (AP) or the Ca^{2+} transient, were chosen because they were relevant in determining drug TdP-risk in machine learning classifiers [3]. The modulated parameters were the maximal conductances or fluxes of the fast Na^+ current (I_{Na},), the late Na^+ current (I_{NaL}), the transient outward K^+ current (I_{to}), the L-type Ca^{2+} current (I_{CaL}), the rapid delayed rectifier K^+ current (I_{Kr}), the slow delayed rectifier K^+ current (I_{Ks}), the inward rectifier K^+ current (I_{K1}), the Na^+/Ca^{2+} exchange current (I_{NaCa}), the Na^+/K^+ pump current (I_{NaK}), the background currents (I_{Kb}, I_{Nab}, I_{Cab}), the sarcoplasmic reticulum Ca^{2+} release flux via ryanodine receptors (J_{rel}), the sarcoplasmic reticulum Ca^{2+} leak (J_{leak}) and the Ca^{2+} uptake via SERCA pump (J_{SERCA}). The electrophysiological properties were: action potential duration at 90% repolarization (APD_{90}), triangulation 90-30 (T_{90-30}), net charge throughout the AP (qNet), systolic and diastolic intracellular Ca^{2+} concentrations ($[Ca^{2+}]_i$), Ca^{2+} transient duration at 90% ($CaTD_{90}$), and the electromechanical window (EMw), defined as the difference between Ca^{2+} and AP durations.

This simple test (Figure 1) was enough to show the impact I_{Kr} on AP properties and the role of J_{SERCA} on Ca^{2+} biomarkers, as well as to highlight secondary factors such as I_{NaL}, I_{CaL} and I_{NaCa}. No other complex strategies were implemented because the initial results were satisfactory.

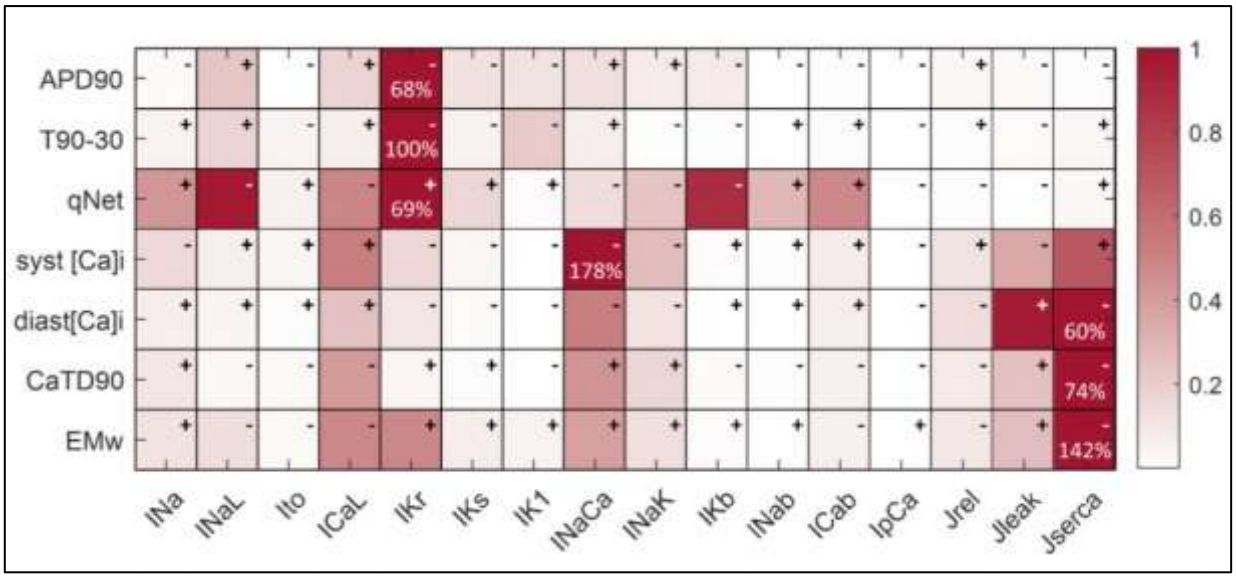

Figure 1: *Model sensitivity analysis. Relative sensitivities for each marker (rows) represented by the color code, being dark red the maximum value and percentages indicate the maximum absolute value. Signs indicate whether the dependency is direct (+) or inverse (-).*

The cellular model reproduces the primary physiological conditions of ventricular myocytes, so simulations were run at 37°C, and extracellular concentrations were set to 140 nM, 5.4 nM, and 1.8 nM for Na^+, K^+, and Ca^{2+}, respectively. Besides, these properties are usually replicated by most of the in vitro experiments, which will facilitate comparisons.

To control system conditions, simulations were initiated from stable initial conditions obtained from the baseline model steady-state. This was merely a rule of thumb, indeed, these constraints did not condition model performance because identical simulations with different initial conditions converged to the same outputs (Figure 2). The cellular AP model did not require other constraints, such as boundary or loading conditions.

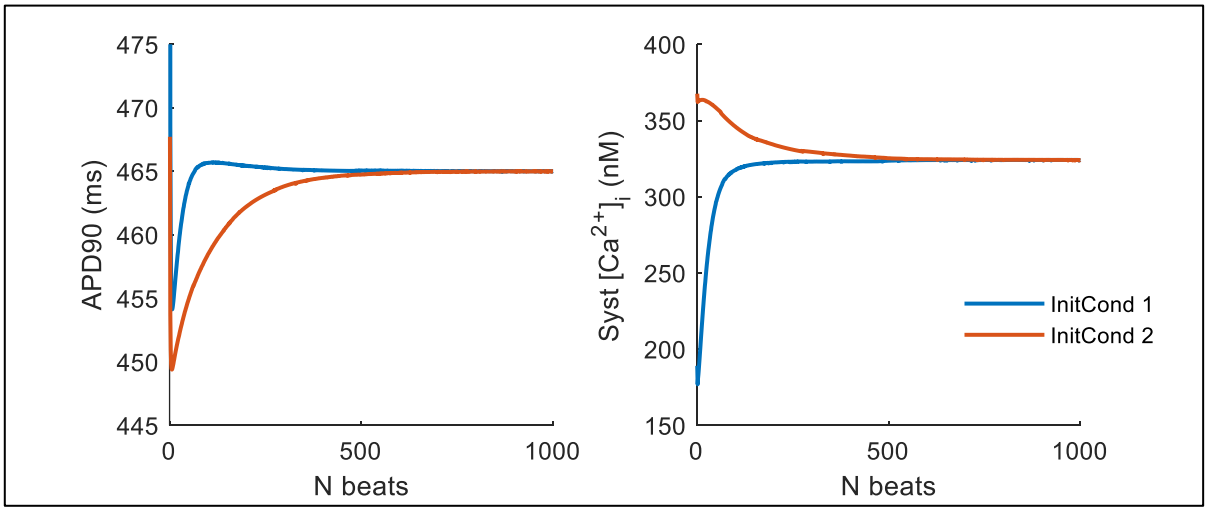

Figure 2: *Effect of initial conditions.*

Most of the uncertainty in model parameters is linked to the diversity within biological populations. For this reason, variability in ion channel conductances to create a heterogeneous population of cellular models was a realistic way of representing the intrinsic natural variability of cardiomyocytes, and we selected 15 parameters for this purpose. Determining real probability distributions for each parameter would be unfeasible, so we assumed that all parameters were independent and normally-distributed, only constrained to be positive. Scaled conductances varied in a range between ±60% of their baseline values, because the standard deviation (σ) of the scaling factors distributions was set to 0.2, assuring that the majority of the population (>99%) was in that range (3σ). Then, a random sampling process ensured the creation of different parameter sets.

Table 2: Biomarkers limits for physiological behaviour.

Biomarker		Min Value	Max Value
APD40 (ms)	AP duration at 40% of repolarization	85	320
APD50 (ms)	AP duration at 50% of repolarization	110	350
APD90 (ms)	AP duration at 90% of repolarization	180	440
Tri90-40 (ms)	AP triangulation	50	150
dV/dtmax (mV/ms)	maximal upstroke velocity	150	1000
Vpeak (mV)	peak voltage	10	55
RMP (mV)	Resting membrane potential	-95	-80
CTD50 (ms)	CaT duration at 50% of recovery	120	420
CTD90 (ms)	CaT duration at 90% of recovery	220	785
[Ca2+]i systolic (μM)	maximal intracellular [Ca2+]	0.26	2.23
[Ca2+]i diastolic (μM)	minimal intracellular [Ca2+]	--	0.40
[Na+]i peak (mM)	maximal intracellular [Na+]	--	39.27
ΔAPD90 (%) under 90% IKs block		-54.4	62
ΔAPD90 (%) under 70% IKr block		32.25	91.94
ΔAPD90 (%) under 50% IK1 block		-5.26	14.86

A further step in setting model parameters consisted of accepting only parameter combinations leading to electrophysiological properties within physiological ranges (Table 3). This calibration approach refines parameter distributions by constraining the range of variability to those that provide physiological outputs.

Figure 3 shows the results of the uncertainty propagation in the control population (without drug). The virtual population of cells presents different electrophysiological phenotypes, including action potential variability, and the result is a distribution of model outputs instead of a single value per biomarker.

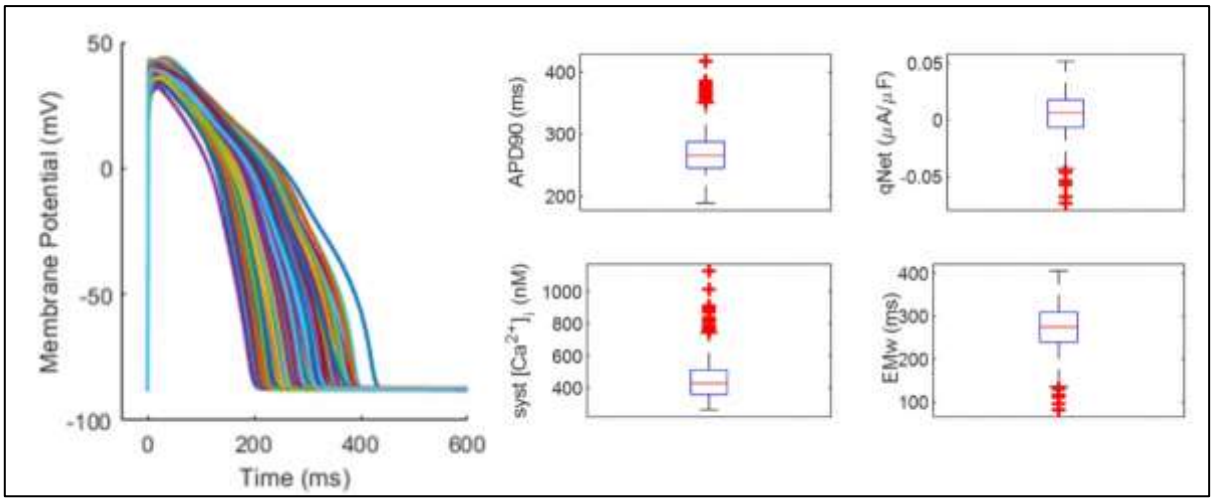

Figure 3: *Uncertainty propagation in the control population. Population of models with biomarkers distributions.*

The aforementioned population of models also accounted for the variability of drug effects, as each individual model of the population showed a different response under the same conditions of a drug due to different cellular parameters.

Figure 4 is an example that illustrates the effect of 0.1 μM of dofetilide on the population of cells.

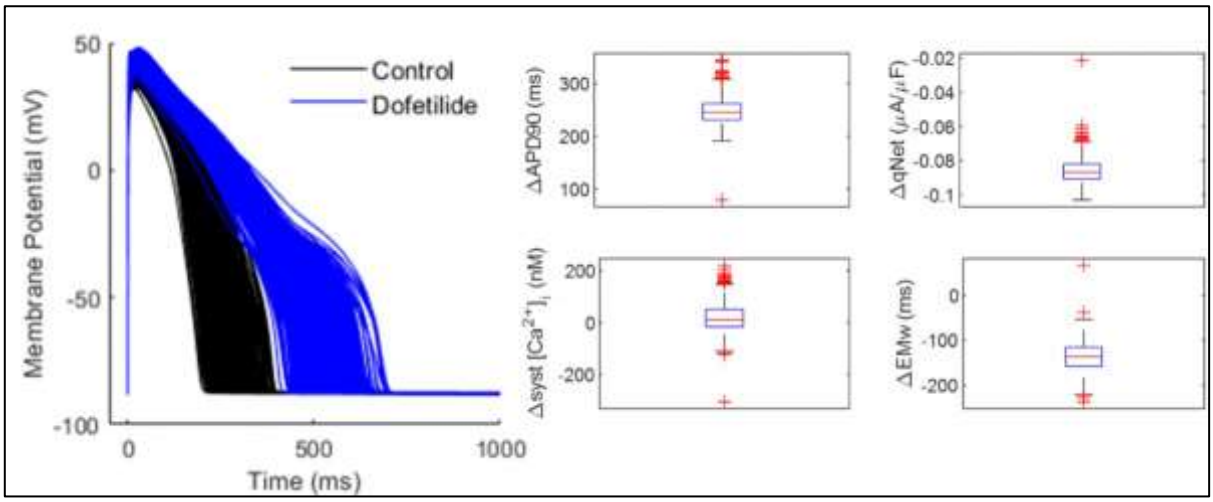

Figure 4: *Uncertainty propagation under the effect of 0.1 μM dofetilide. Action potential variability and distribution of electrophysiological markers changes due to drug application.*

1.2 Model Inputs

Model inputs can be classified into 2 types according to the drug under evaluation and subpopulation selection.

1.2.1 Drugs

During drug assessment, the selection of the molecule and its concentration are main inputs that will determine the model output. Drug modeling is based on a general equation (Equation 1) known

as single block model that is particularized to each drug by means of two parameters (IC_{50} and h), and it is also influenced by the combination of ion currents affected (multi-block model). For known drugs, such as those used in the validation process, all these parameters are predefined in a database. For the evaluation of new drugs, parameters will be provided as model inputs.

$$G_{i,D} = G_i \cdot \left(\frac{1}{1+\left(\frac{[D]}{IC_{50}}\right)^h} \right) \qquad \textit{Equation 1}$$

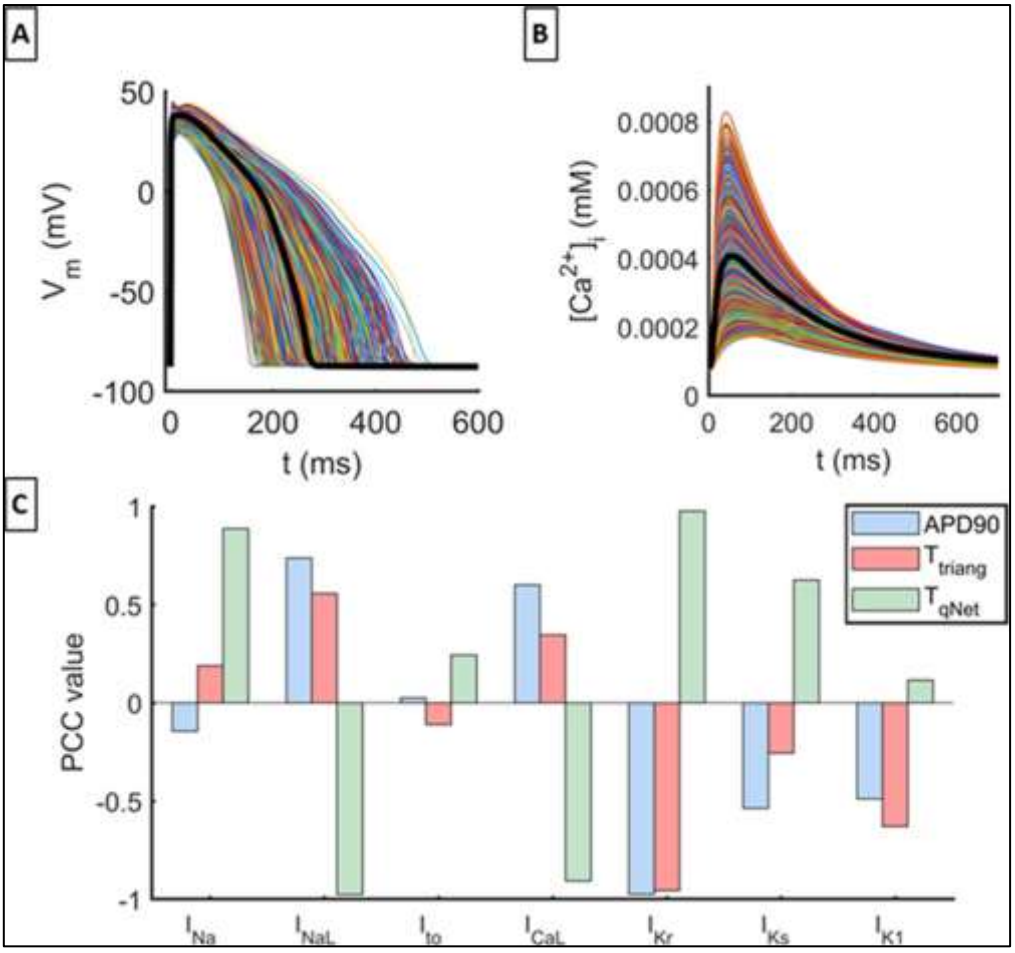

Figure 5: *Sensitivity analysis of electrophysiological characteristics of the action potential to the seven currents involved in drug effects. Effects on action potential and Ca^{2+} transient (upper panels) and sensitivities (PCC values) of APD_{90}, T_{triang} and T_{qNet} to each current. Figure taken from [4].*

Drugs alter electrophysiology by modulating ion channel activity, which means that the effect is modelled as a scalar that modulates ion channel conductances of the cellular model. This perturbation, when multi-channel, usually involves up to seven ionic currents (I_{Kr}, I_{Na}, I_{NaL}, I_{CaL}, I_{K1}, I_{Ks} and I_{to}) according to the CiPA initiative. The individual contribution of these factors has already been explored in the previous sensitivity analysis of the model form (Figure 1). To better focus on model inputs, the partial correlation coefficients (PCC) method was used to analyze the impact of the seven currents linked to drug action.

For this purpose, 1000 virtual drugs were tested on the same cell. Combinations of seven scale factors ranging ±60% were obtained by latin hypercube sampling (LHS) to generate the population. Figure 5A,B illustrates the changes in AP and Ca^{2+} transient exerted by the virtual drugs, representing a wide variability of pharmacological effects. The PCC values for each current and three quantities of interest (APD_{90}, T_{triang}, T_{qNet}) are shown in Figure 5C. T_{qNet} is calculated as the ratio of the net charge carried by I_{Net} (I_{CaL}+ I_{NaL}+ I_{Kr} + I_{Ks} + I_{K1} + I_{to}) when exposed to 10 times the effective free therapeutic plasma concentration (EFTPC) with respect to the net charge in control conditions, and T_{triang} is the ratio between triangulation (APD_{90}-APD_{30}) for a drug concentration of 10 times EFTPC and control model triangulation. The selected biomarkers were three torsadogenic indices we proposed and analyzed in a previous work [4]. Considering all the coefficients, the currents with the more significant impact on TdP risk are I_{Kr}, I_{CaL}, I_{NaL}, and I_{Ks}, consistent with prior results.

A more comprehensive study of model inputs would be quantifying the sensitivity of the quantities of interest to drug parameters, i.e. IC_{50} and h for each ion channel type. However, as Figure 6 shows, drug response covers from minimum (0% channel block) to maximum (100% channel block) effect depending on the concentration. IC_{50} variability modulates the sensitivity of drug response, that is, the concentration needed to achieve the same % block, and hill coefficient h is a measure of the ultrasensitivity by controlling the slope of the curve. Due to drug dependency of results and the wide dispersion of outcomes, we considered that individual sensitivity analyses would not be valuable. Instead, we focused directly on uncertainty.

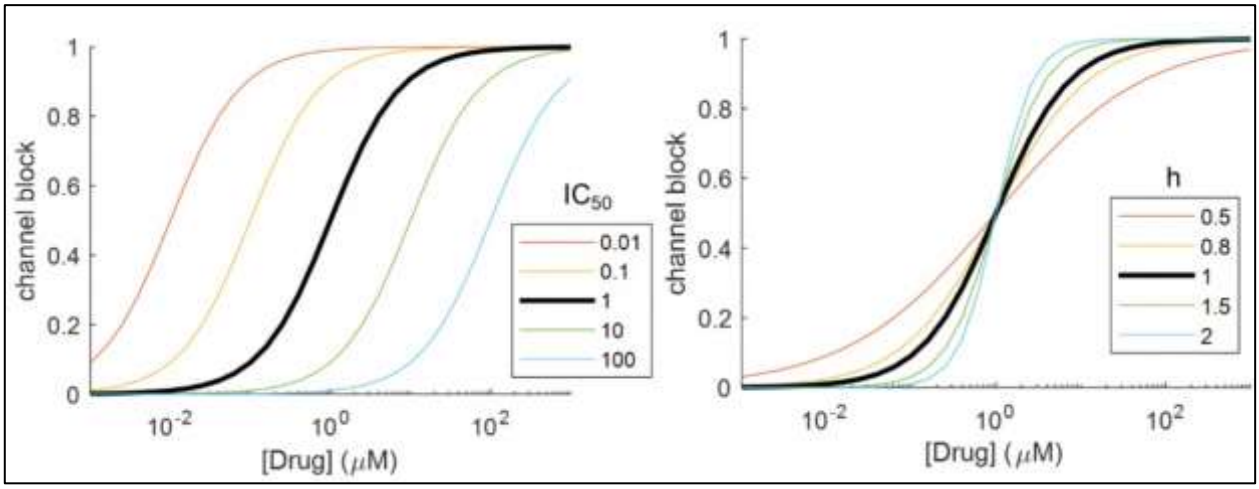

Figure 6: *Effects of drug inputs on the model. IC_{50} and h variability.*

One of the main sources of uncertainty when assessing drug-induced electrophysiological changes is IC_{50} variability among experimental studies. Figure 7A shows the influence of IC_{50} variability (gaussian distribution: N~(pIC_{50}, 0.5)) on APD_{90} in a single cell model. This type of variability due to drug uncertainty was compared to the effect of inter-individual uncertainty, in which a fix IC_{50} was applied to a population of models. The dispersion of APD distributions in Simulation A is narrower than that resulting from inter-individual variability (Figure 7B), except for quinidine. Another remarkable difference is the right skewness of the distributions. When combining both types of variability in one (Figure 7C), the impact of each of the individual procedures on the output is notable,

although the dispersions are not additive. A more exhaustive analysis of this uncertainty assessment can be found in Kopanska et al. work [5] (submitted for publication).

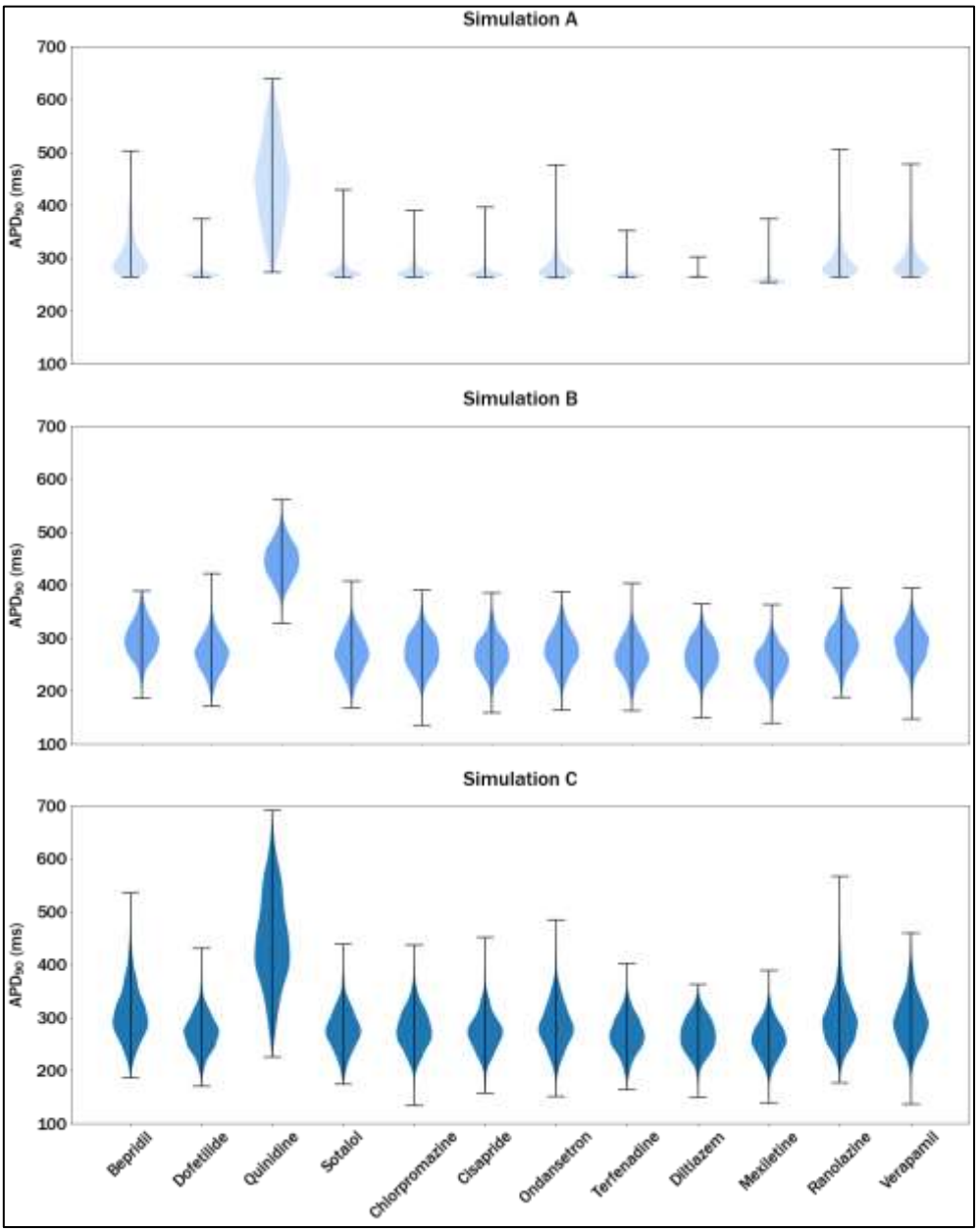

Figure 7: *Violin plots showing distributions of APD_{90} values obtained in different runs of Monte Carlo simulations introducing the following variability types. Simulation A: Experimental variability (Δ-pIC50); Simulation B: Inter-individual variability (Δ-Parameters); Simulation C: Combination of experimental and inter-individual variability. Figure taken from Kopanska et al. [5] (submitted for publication).*

1.2.2 Subpopulation

The other major input is the selected subpopulation, which is a categorical variable. To date, only gender differences were modelled, and the options are male or female.

The uncertainty related to gender is related to the variability in cell parameters present in each group, so we built two different populations, one for male and another for female, to account for electrophysiological variability and sex differences. Former sensitivity analyses of AP model parameters can be used as a reference to know how channel conductances variation affect the outputs.

To generate the populations, we first obtained sex-specific normal distributions of ion channel conductances based on the mean and standard deviations of experimentally measured gene expression levels [6] for a set of 11 ion channels (I_{Kr}, I_{Ks}, I_{K1}, I_{NCX}, I_{Na}, I_{CaL}, I_{to}, I_{pCa}, I_{NaKa}, I_{Kb}, and I_{up}) and calmodulin concentration, which were then translated into conductance scaling factors, as described by Yang et al. [7]. After running simulations, the resulting models exhibited a variability consistent with experimental observations, but a selection was applied to discard models yielding biomarkers out of physiological limits.

The final populations consisted of 300 random models each one taken from the calibrated populations. Figure 8 shows the initial differences between both populations and how each drug can affect differently each subgroup, although effects can be overlapped due to variability.

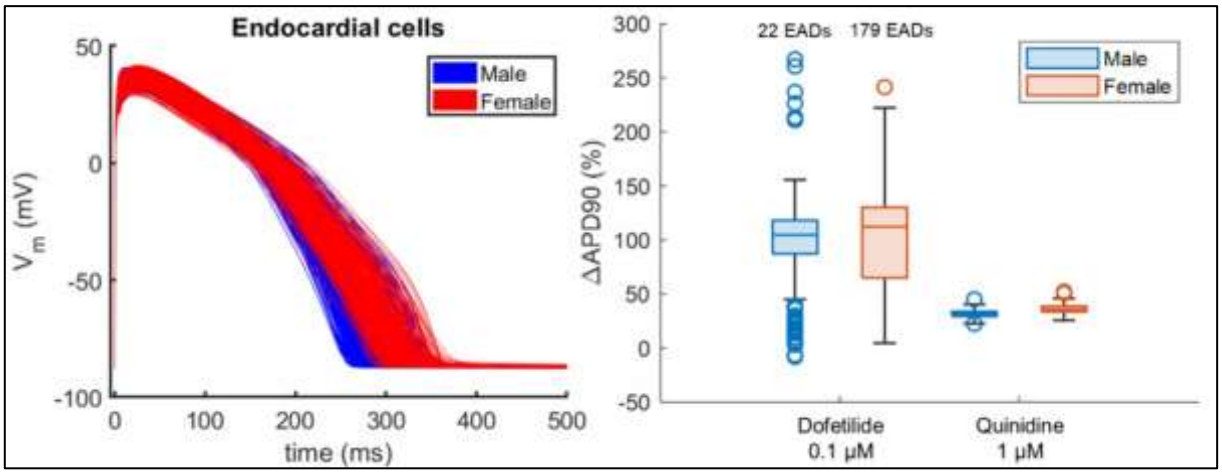

Figure 8: *Input populations and gender differences on proarrhythmic risk markers.*

As stated above, one of the main sources of uncertainty when assessing drug-induced electrophysiological changes is IC_{50} variability among experimental studies, so we further investigated this effect on male and female models. Specifically, we examined the influence of experimental uncertainty in measurements of hERG channel potency, which is the gene encoding I_{Kr} channel, on the final drug effect. We focused on hERG channel due to its strong association with the generation of TdP [8] For this analysis, we selected a representative male model and a representative female model. A constant drug concentration equal to the therapeutic value was used for all the simulations of a given drug, thereby isolating the impact of IC_{50} variability on drug-induced electrophysiological changes. Then, for each drug, we ran simulations in both, the male and the

female models, varying the hERG IC_{50} value among the minimum, median, and maximum values of hERG IC_{50} estimated for each drug by Li et al. [9].

The effect of these inputs on APD_{90} was analyzed, and the biomarker was set to 1000 ms when repolarization abnormalities appeared (Figure 10). In general, drugs do not exhibit significant differences in APD_{90} due to variations in IC_{50} for $I_{Kr,}$ as many values are below 20 ms, with the exception of quinidine which led to repolarization abnormalities. Avoiding this particular case, the maximal difference in APD_{90} between simulations with the minimum and maximum IC_{50} values is 32.5 ms for dofetilide.

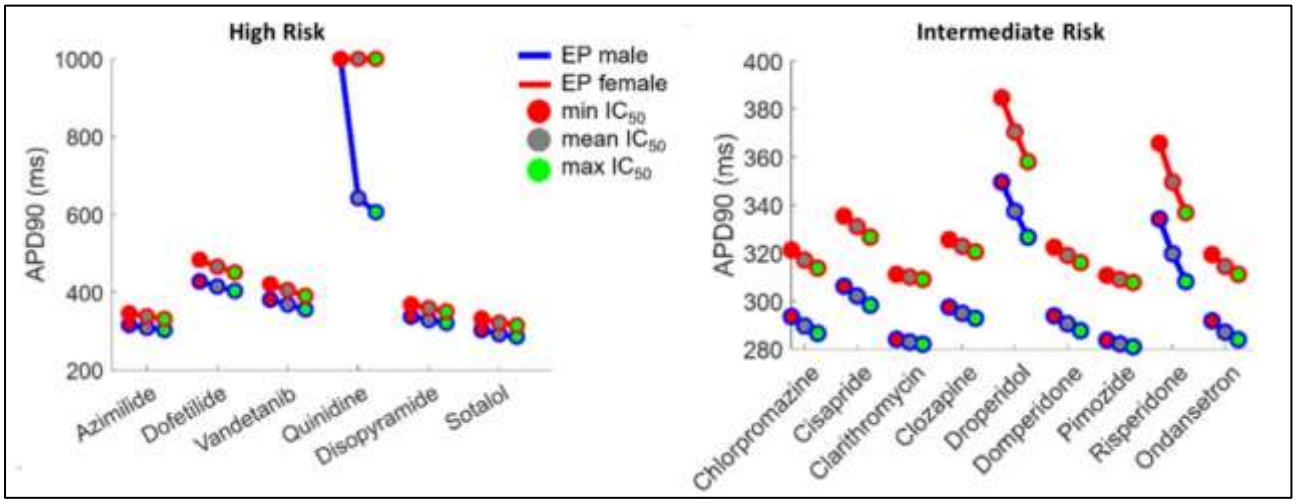

Figure 9: *Sensitivity analysis of APD90 to IKr IC_{50} variability. Figure taken from Llopis-Lorente et al. [10] (submitted for publication).*

2. Comparator

2.1 Test Samples and Conditions

The current regulatory guidelines provided by the FDA for the pharmaceutical industry are ICH E14 and S7B: clinical and non-clinical evaluation of QT/QTc interval prolongation and proarrhythmic potential. It implies the existence of in-vitro assays and clinical trials to test the TdP risk of drugs. Since the in-silico model was developed to improve these experimental tests, we took advantage of available electrophysiological data from the scientific literature to validate the computational application. As a starting point, we selected 22 well-known drugs included in the CiPA initiative [11].

The comparator used for evaluating the effect of drugs at the cellular level consists of diverse pre-clinical experiments that have quantified cellular responses after drug administration. The main quantity of interest is the variation of action potential duration (APD) because it is a cellular surrogate of the QT interval and consequently, a potential biomarker for TdP risk assessment [12]. Figure 10 shows an increasing prolongation of APD as clarithromycin concentration increases, which the model reproduces well. The specific quantity of interest is APD_{90}, that is, the APD measured at 90% of membrane repolarization. Despite standardized protocols, many heterogeneous experimental settings may still cause a wide variability of action potentials among

studies. To solve this issue, we considered the percentage of change instead of absolute values to perform the comparisons.

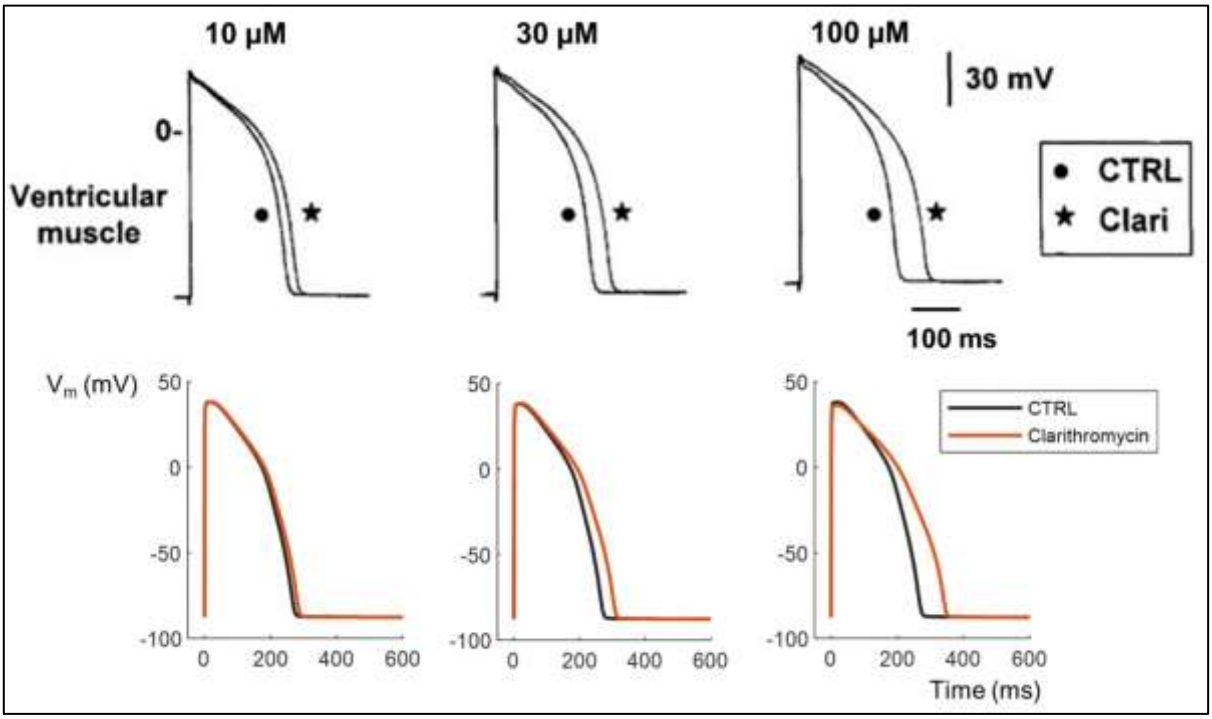

Figure 10: *Action potential prolonging effects of different concentrations of clarithromycin. Simulated results (lower panels) compared to experimental observations extracted from Gluais et al. [13] (upper panels).*

Table 3 summarizes the main characteristics of the different comparators for each drug, according to the experimental study selected. The ground truth about TdP risk has been indicated according to the classification taken into account by the CiPA initiative [11].

Table 3: Experimental references and comparator data. Risk classification follows the criteria stablished for CiPA drugs [11].

Drug Comparator	Samples			
	Type	Concentrations	Conditions	Quantity
High Risk				
Dofetilide [14]	human ventricular trabeculae	0.01 µM, 0.1 µM	1 Hz, 2 Hz	9
Sotalol [14]	human ventricular trabeculae	10 µM, 100 µM	1 Hz, 2 Hz	15
Quinidine [14]	human ventricular trabeculae	1 µM, 10 µM	1 Hz, 2 Hz	15
Disopyramide [15]	rabbit purkinje cells	0.3 – 100 µM	0.2 Hz, 1 Hz	74
Azimilide [16]	canine ventricular myocytes	1 µM, 5 µM	0.33 Hz ,1 Hz	3 – 7
Vandetanib [17]	human iPSC-CM	0.03 µM, 1 µM, 3 µM	Spontaneous	6

Drug Comparator	Samples			
	Type	Concentrations	Conditions	Quantity
Intermediate Risk				
Domperidone [18]	isolated rabbit hearts	0.5 μM, 1 μM, 2 μM	1.11 Hz, 2 Hz, 3.33 Hz	8
Ondansetron [18]	Isolated rabbit hearts	1 μM, 5 μM, 10 μM	1.11 Hz, 2 Hz, 3.33 Hz	10
Chlorpromazine [19]	human iPSC-CM	0.1 – 3 μM	Spontaneous	3 – 5
Cisapride [20]	left ventricular canine midmyocardial myocytes	0.01 – 10 μM	0.5 Hz, 1 Hz	2
Clarithromycin [13]	rabbit ventricular myocytes	3 – 100 μM	1 Hz	9
Pimozide [21]	guinea pig papillary muscle	0.1 μM, 1 μM, 10 μM	0.5 Hz, 1 Hz, 2.5 Hz	6
Risperidone [22]	human ventricular myocardium	0.03 – 10 μM	0.2 Hz, 1 Hz	2 – 4
Droperidol [23]	rabbit purkinje fibers	0.01 – 30 μM	1 Hz	6 – 7
Clozapine [24]	human iPSC-CM	0.1 – 5 μM	Spontaneous	3 cell lines
Low Risk				
Nifedipine [25]	guinea pig ventricular myocardium	0.1 – 30 μM	1 Hz	6
Metoprolol [26]	guinea pig ventricular myocytes	10 μM, 30 μM, 100 μM	0.1 Hz	5
Diltiazem [27]	guinea pig right myocardium	2.2 μM, 22 μM, 110 μM	1.3 Hz	7 – 13
Ranolazine [28]	canine left ventricular myocardium	1 – 100 μM	0.5 Hz	5 – 7
Tamoxifen [29]	rat ventricular myocytes	1 – 3 μM	1 Hz	4
Mexiletine [30]	guinea pig papillary muscles	11.1 μM	0.5 Hz	5 – 6
Loratadine [31]	guinea pig ventricular myocytes	10 μM	0.2 Hz	22

Sample characteristics that vary among the studies are sample type, with variability of cells or tissues and species, the stimulation frequency, and drug concentrations. One important remark is that drug concentrations depend on the molecule and it explains the differences between comparators. Low concentrations tested in the experiments are usually closer to the common therapeutical concentrations, which means that small doses have more weight in model validation than the large ones. Although we would be interested in evaluating and validating specific concentrations for each drug, some experimentalists have highlighted the impossibility to analyse lower concentrations because experimental variability exceeded the magnitude of the effect [14].

Regarding sources of uncertainty, one important factor in biomarker variability is biological variability, which includes both intra-individual variability (different cells from the same heart) and inter-individual variability (different hearts). Britton et al. [14] showed they were of similar magnitude,

contributing similarly to biomarker variability. The widely-used approach to include this uncertainty into in-silico models consists of creating populations of models, through variability in ionic conductances [32].

3. Assessment

3.1 Equivalency of Input Parameters

The computational model uses realistic input parameters, identical to the experimental inputs. Each simulation can be particularized for a drug, for a single or a range of concentrations and for a particular patient. Even some conditions can be introduced as inputs when needed (e.g. heart rate, cell type, etc.). However, more specific inputs, such as IC_{50} and h parameters, and the set of conductances that would characterize a specific patient, cannot be deduced from the comparator data used for validation. To address this problem, we set drug parameters to experimental values obtained from other studies and used an average AP model or a virtual population.

3.2 Output Comparison

We performed two output comparisons: one quantitative and another categorical. We started quantifying the cellular biomarker APD from simulations to measure the prolongation effect of drugs as it is done in in-vitro assays. But heterogeneous experimental conditions found in the literature hampered direct comparisons, and to avoid potential inconsistencies, we decided to compare the percentage of change instead of absolute values.

The results of APD_{90} prolongation are summarized in Figure 11, which compares experimental data with in-silico predicted values. The distance to the diagonal line represents the error of computational results. We only represented 12 out of 22 drugs because we could not find any drug model that reproduced ΔAPD_{90} values provided by the remaining 10 comparators. Despite taking into account all experimental parameter variability, expected ΔAPD_{90} values were not achieved, which might be, in part, due to the low quality data provided by the studies. Furthermore, there is a large heterogeneity among data sets, and samples and conditions used for determining drug model (IC_{50} and h) may greatly differ from samples used to quantify APD, resulting in the observed differences.

Regarding the 12 accepted comparators, at least two points existed for each molecule, as one was used to adjust the model, and the rest to validate it. It should be noted that uncertainty in experiments was not represented here for simplicity, but it would give more margin to results. In addition, we only simulated one model for each comparison, but applying uncertainty to the model would result in a range of predictions that may better represent the experimental variability, as illustrated in Figure 12 for dofetilide.

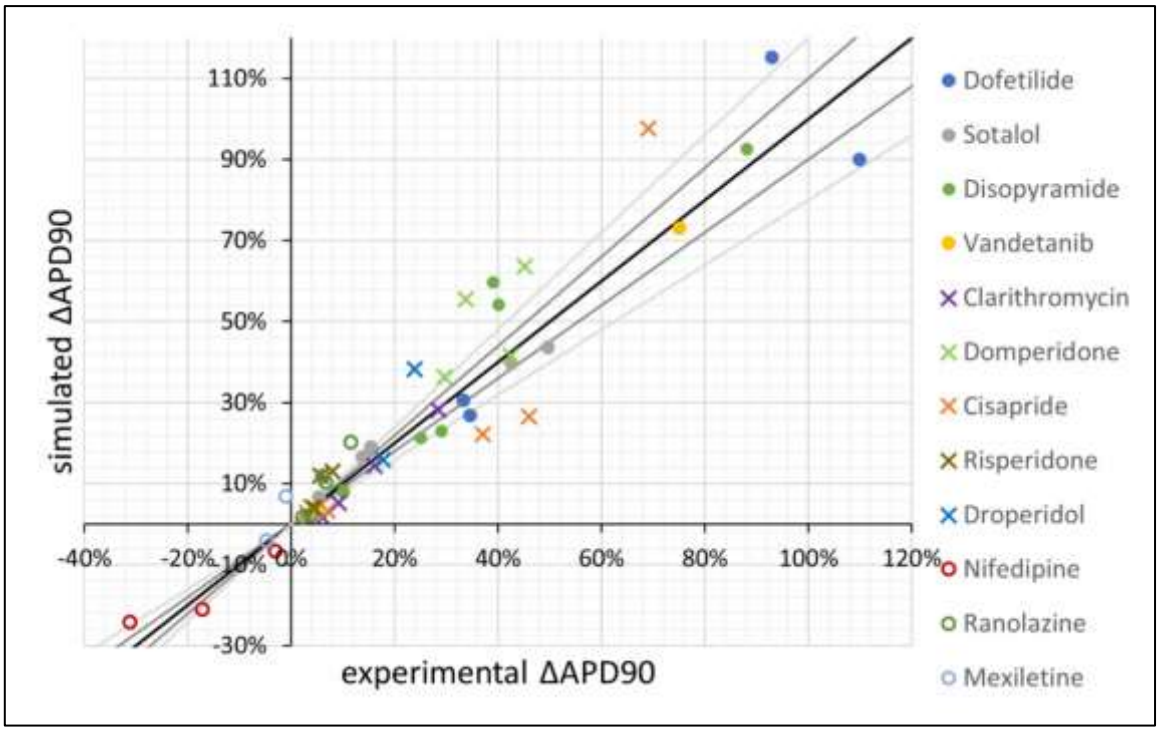

Figure 11: *Output comparison: Action potential duration variation (% ⊿APD90) for high (filled circle), intermediate (cross) and low (empty circle) risk drugs. Diagonal represents complete agreement between experimental and simulated results. Gray lines delimit areas with ±10% (dark lines) and ±20% error (light lines).*

Many factors, apart from model accuracy, can cause the discrepancies with the comparator. The model was developed to evaluate drugs close to the therapeutic range, so the predictive power decreased as drug concentrations get away from these values. Furthermore, we could not control the quality of all datasets, and model results agree with some experimental studies more than with others. Main differences found among experiments are the type of sample used for the tests (isolated myocytes, purkinje cells, ventricular tissue, whole heart, etc) and the origin (species).

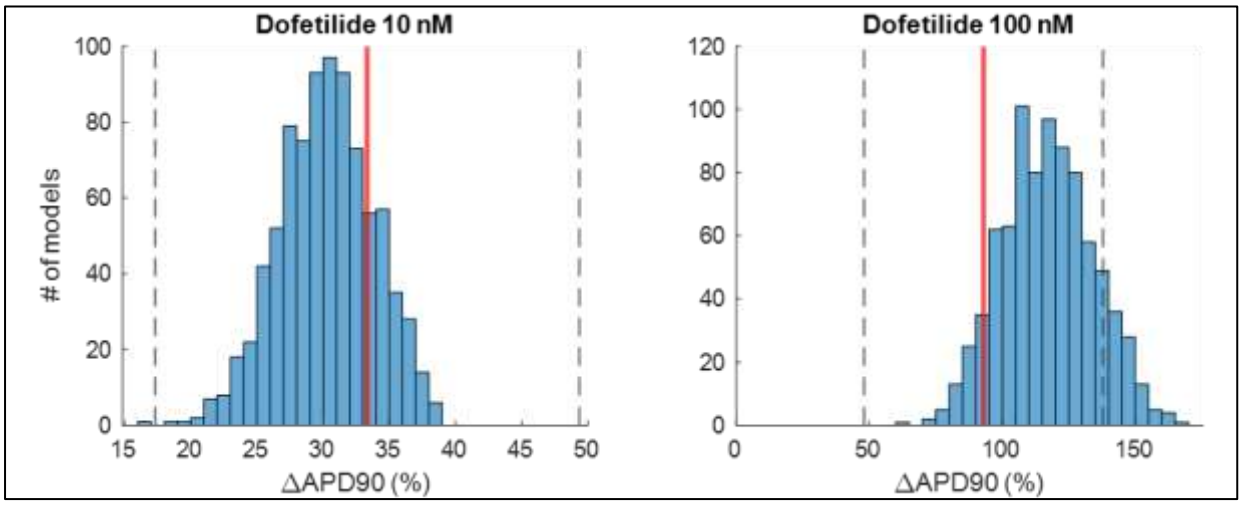

Figure 12: *Output comparison considering uncertainty (population of cellular models). Vertical lines represent experimental values (red: median, grey: ±2SD).*

Drug developers have their standards about the critical APD prolongation, so we did not impose any limit on APD_{90} and let experts apply their criteria to new molecules. However, we developed a binary classifier based on other cellular metrics [4]. It classifies the drugs as safe or unsafe, and these categorical predictions were compared with the ground truth proposed by the CiPA initiative.

A simple classifier consisted in using one torsadogenic index called Tx index [33], defined as the ratio between the concentration of a drug provoking a 10% prolongation of APD_{90} and the EFTPC. The classification, shown in Figure 13, used a Tx threshold equal to 8 so that only molecules having Tx>8 were considered safe. The classification was dependent on drug parameters (IC50 and h), highlighting the effect of drug model uncertainty. We compared simulation studies of safety pharmacology that use the same cellular model but presented differences in drug parameters, due to experimental variability. In Llopis-Lorente et al. [4] study, we worked with median values, Li and colleagues [11] measured new experimental values, and we used Li et al. values with some readjustments to fit APD or QT prolongation (see Annex A6.2_UC3_3D for QT results). All high-risk molecules were classified as unsafe and low risk molecules as safe, with the exception of ranolazine. We usually have considered that intermediate risk drugs should be predicted as unsafe because of their potential TdP risk, and following this criterion the accuracy of the Tx classifier was 77.3%, with four false negatives from the intermediate group.

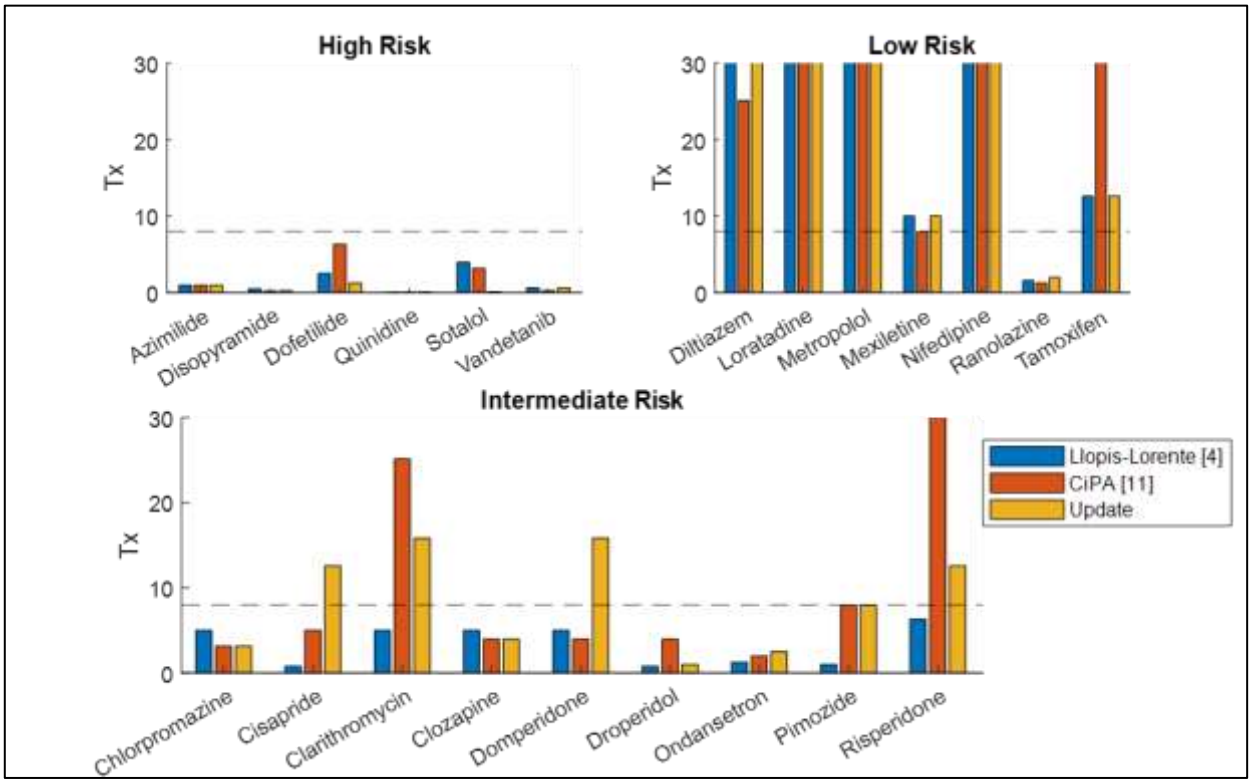

Figure 13: *TdP-risk classification with Tx index. Drugs are separated according to their known risk, and model prediction classifies drugs as unsafe if Tx < 8 and safe if Tx > 8.*

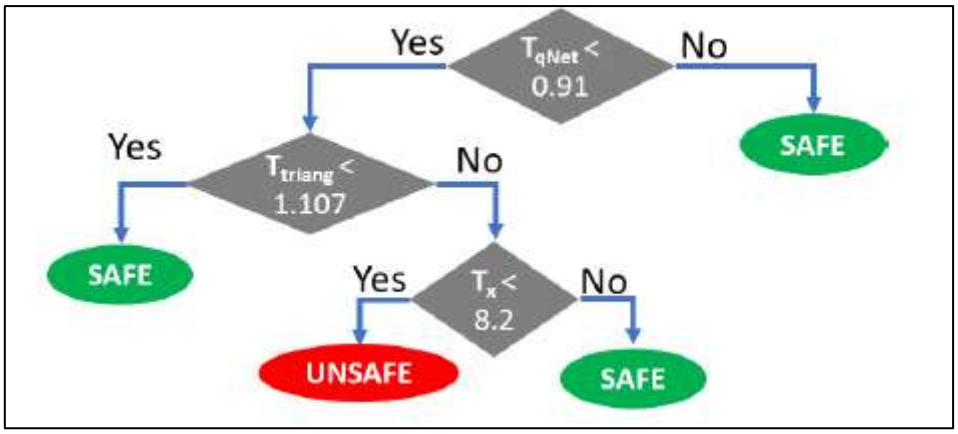

Figure 14: *One decision tree for the binary TdP risk classifier.*
Figure taken from Llopis-Lorente et al. work [4].

A more potent classifier consisted in the combination of 9 decision trees that used three torsadogenic indices: Tx, T_{qnet} and T_{triang} (Figure 14). This classifier increased the prediction accuracy of the 22 drugs to 81.8% by including ranolazine in the safe group. The problem with intermediate risk molecules was depending on drug concentration they could have more or lower risk. For the calculation of all indices we used EFTPC values, which are mean therapeutic values, but we know that depending on patient pharmacokinetics, a similar dose can result in different plasmatic concentrations. For this reason, we additionally evaluated the classifier with low (minimal therapeutic value) and high (toxic values) concentrations, which are specific for each molecule. Results in Table 4 show changes in the classification according to the concentration, but a more exhaustive analysis would be necessary to determine the critical concentration below which each drug would be safe. Limits will also vary due to uncertainty, part of which is related to patient variability, and implementing population of models would provide intervals. Unfortunately, the validation of these results would not be possible due to the unfeasibility to individually analyze the effects of drugs in real patients.

Table 4: Torsadogenic risk prediction of intermediate risk drugs with the decision trees classifier.

Condition	Safe	Unsafe
Low concentration	Chlorpromazine Cisapride Clarithromycin Domperidone Ondansetron Pimozide Risperidone	Clozapine Droperidol
High concentration	Chlorpromazine Clarithromycin	Cisapride Clozapine Domperidone Droperidol Ondansetron Pimozide Risperidone

4. Conclusion

This document is an annex of SimCardioTest deliverable D6.2, and reports technical details relative to the validation of the 0D numerical model developed for Use Case 3. General conclusions relative to the validation of UC3 numerical model are reported in main deliverable D6.2.

5. Bibliography

[1] T. O'Hara, L. Virág, A. Varró, Y. Rudy, Simulation of the undiseased human cardiac ventricular action potential: model formulation and experimental validation., PLoS Comput Biol. 7 (2011) e1002061. https://doi.org/10.1371/journal.pcbi.1002061.

[2] M.T. Mora, J.M. Ferrero, L. Romero, B. Trenor, Sensitivity analysis revealing the effect of modulating ionic mechanisms on calcium dynamics in simulated human heart failure, PLoS One. 12 (2017) e0187739. https://doi.org/10.1371/journal.pone.0187739.

[3] J. Llopis-Lorente, B. Trenor, J. Saiz, Considering population variability of electrophysiological models improves the in silico assessment of drug-induced torsadogenic risk, Comput Methods Programs Biomed. 221 (2022) 106934. https://doi.org/10.1016/J.CMPB.2022.106934.

[4] J. Llopis-Lorente, J. Gomis-Tena, J. Cano, L. Romero, J. Saiz, B. Trenor, In silico classifiers for the assessment of drug proarrhythmicity, J Chem Inf Model. 60 (2020) 5172–5187. https://doi.org/10.1021/acs.jcim.0c00201.

[5] K. Kopańska, P. Rodríguez-Belenguer, J. Llopis-Lorente, B. Trenor, J. Saiz, M. Pastor, Uncertainty assessment of proarrhythmia predictions derived from multi-level in silico models, (Under Preparation). (2023).

[6] N. Gaborit, A. Varro, S. le Bouter, V. Szuts, D. Escande, S. Nattel, S. Demolombe, Gender-related differences in ion-channel and transporter subunit expression in non-diseased human hearts, J Mol Cell Cardiol. 49 (2010) 639–646. https://doi.org/10.1016/J.YJMCC.2010.06.005.

[7] P.C. Yang, C.E. Clancy, In silico prediction of sex-based differences in human susceptibility to cardiac ventricular tachyarrhythmias, Front Physiol. 3 SEP (2012) 360. https://doi.org/10.3389/FPHYS.2012.00360/ABSTRACT.

[8] J. Vicente, R. Zusterzeel, L. Johannesen, J. Mason, P. Sager, V. Patel, M.K. Matta, Z. Li, J. Liu, C. Garnett, N. Stockbridge, I. Zineh, D.G. Strauss, Mechanistic Model-Informed Proarrhythmic Risk Assessment of Drugs: Review of the "CiPA" Initiative and Design of a Prospective Clinical Validation Study, Clin Pharmacol Ther. 103 (2018) 54–66. https://doi.org/10.1002/cpt.896.

[9] Z. Li, B.J. Ridder, X. Han, W.W. Wu, J. Sheng, P.N. Tran, M. Wu, A. Randolph, R.H. Johnstone, G.R. Mirams, Y. Kuryshev, J. Kramer, C. Wu, W.J. Crumb, D.G. Strauss, Assessment of an In Silico Mechanistic Model for Proarrhythmia Risk Prediction Under the CiPA Initiative, Clin Pharmacol Ther. 105 (2019) 466–475. https://doi.org/10.1002/CPT.1184.

[10] J. Llopis-Lorente, S. Baroudi, K. Koloskoff, L. Romero, M.T. Mora, S. Benito, F. Dayan, J. Saiz, B. Trenor, Combining pharmacokinetic and electrophysiological models for early prediction of drug-induced arrhythmogenicity, Computer Methods and Programs in Biomedicine (Submitted for Publication). (2023).

[11] Z. Li, B.J. Ridder, X. Han, W.W. Wu, J. Sheng, P.N. Tran, M. Wu, A. Randolph, R.H. Johnstone, G.R. Mirams, Y. Kuryshev, J. Kramer, C. Wu, W.J. Crumb, D.G. Strauss, Assessment of an In Silico Mechanistic Model for Proarrhythmia Risk Prediction Under the CiPA Initiative, Clin Pharmacol Ther. 105 (2019) 466–475. https://doi.org/10.1002/CPT.1184.

[12] A.S. Bass, G. Tomaselli, R. Bullingham, L.B. Kinter, Drugs effects on ventricular repolarization: A critical evaluation of the strengths and weaknesses of current methodologies and regulatory practices, J Pharmacol Toxicol Methods. 52 (2005) 12–21. https://doi.org/10.1016/j.vascn.2005.04.010.

[13] P. Gluais, M. Bastide, J. Caron, M. Adamantidis, Comparative Effects of Clarithromycin on Action Potential and Ionic Currents from Rabbit Isolated Atrial and Ventricular Myocytes, J Cardiovasc Pharmacol. 41 (2003) 506–517. http://journals.lww.com/cardiovascularpharmbyBhDMf5ePHKav1zEoum1tQfN4a+kJLhEZgbsIH.

[14] O.J. Britton, N. Abi-Gerges, G. Page, A. Ghetti, P.E. Miller, B. Rodriguez, Quantitative comparison of effects of dofetilide, sotalol, quinidine, and verapamil between human ex vivo trabeculae and in silico ventricular models incorporating inter-individual action potential variability, Front Physiol. 8 (2017) 1–19. https://doi.org/10.3389/fphys.2017.00597.

[15] C. Trovato, M. Mohr, F. Schmidt, E. Passini, B. Rodriguez, Cross clinical-experimental-computational qualification of in silico drug trials on human cardiac purkinje cells for proarrhythmia risk prediction, Frontiers in Toxicology. 4 (2022) 124. https://doi.org/10.3389/FTOX.2022.992650.

[16] J.-A. Yao, G.-N. Tseng, Azimilide (NE-10064) Can Prolong or Shorten the Action Potential Duration in Canine Ventricular Myocytes: Dependence on Blockade of K, Ca, and Na Channels, 1997.

[17] H.A. Lee, S.A. Hyun, B. Byun, J.H. Chae, K.S. Kim, Electrophysiological mechanisms of vandetanib-induced cardiotoxicity: Comparison of action potentials in rabbit Purkinje fibers and pluripotent stem cell-derived cardiomyocytes, PLoS One. 13 (2018). https://doi.org/10.1371/journal.pone.0195577.

[18] G. Frommeyer, C. Fischer, C. Ellermann, P.S. Lange, D.G. Dechering, S. Kochhäuser, M. Fehr, L. Eckardt, Severe Proarrhythmic Potential of the Antiemetic Agents Ondansetron and Domperidone, Cardiovasc Toxicol. 17 (2017) 451–457. https://doi.org/10.1007/s12012-017-9403-5.

[19] Y. Yu, M. Zhang, R. Chen, F. Liu, P. Zhou, L. Bu, Y. Xu, L. Zheng, Action potential response of human induced-pluripotent stem cell derived cardiomyocytes to the 28 CiPA compounds: A non-core site data report of the CiPA study, J Pharmacol Toxicol Methods. 98 (2019). https://doi.org/10.1016/j.vascn.2019.04.003.

[20] N. Abi-Gerges, J.P. Valentin, C.E. Pollard, Dog left ventricular midmyocardial myocytes for assessment of drug-induced delayed repolarization: Short-term variability and proarrhythmic potential, Br J Pharmacol. 159 (2010) 77–92. https://doi.org/10.1111/j.1476-5381.2009.00338.x.

[21] S. Hayashi, Y. Kii, M. Tabo, H. Fukuda, T. Itoh, T. Shimosato, H. Amano, M. Saito, H. Morimoto, K. Yamada, A. Kanda, T. Ishitsuka, T. Yamazaki, Y. Kiuchi, S. Taniguchi, T. Mori, S. Shimizu, Y. Tsurubuchi, S.I. Yasuda, S.I. Kitani, C. Shimada, K. Kobayashi, M. Komeno, C. Kasai, T. Hombo, K. Yamamoto, QT PRODACT: A multi-site study of in vitro action potential assays on 21 compounds in isolated guinea-pig papillary muscles, J Pharmacol Sci. 99 (2005) 423–437. https://doi.org/10.1254/jphs.QT-A1.

[22] P. Gluais, M. Bastide, D. Grandmougin, G. Fayad, M. Adamantidis, Risperidone reduces K+ currents in human atrial myocytes and prolongs repolarization in human myocardium, Eur J Pharmacol. 497 (2004) 215–222. https://doi.org/10.1016/j.ejphar.2004.06.046.

[23] M.M. Adamantidis, P. Kerram, J.F. Caron, B.A. Dupuis, Droperidol Exerts Dual Effects on Repolarization and Induces Early Afterdepolarizations and Triggered Activity in Rabbit Purkinje Fibers, THE JOURNAL OF PHARMACOLOGY AND EXPERIMENTAL THERAPEUTICS . 266 (1993) 884–893.

[24] A.M. Da Rocha, J. Creech, E. Thonn, S. Mironov, T.J. Herron, Detection of drug-induced torsades de pointes arrhythmia mechanisms using hiPSC-CM syncytial monolayers in a high-throughput screening voltage sensitive dye assay, Toxicological Sciences. 173 (2020) 402–415. https://doi.org/10.1093/toxsci/kfz235.

[25] A. Bussek, M. Schmidt, J. Bauriedl, U. Ravens, E. Wettwer, H. Lohmann, Cardiac tissue slices with prolonged survival for in vitro drug safety screening, J Pharmacol Toxicol Methods. 66 (2012) 145–151. https://doi.org/10.1016/j.vascn.2011.12.002.

[26] J. Sanchez-Chapula, Effects of metoprolol on action potential and membrane currents in guinea-pig ventricular myocytes, Archives of Pharmacology. 345 (1992) 342–348.

[27] H. Nakajima, M. Hoshiyama, K. Yamashita, A. Kiyomoto, Effect of Diltiazem on electrical and mechanical activity of isolated cardiac ventricular muscle of guinie pig, Japall. J. Piturllacol. 25 (1975) 383–392.

[28] C. Antzelevitch, L. Belardinelli, A.C. Zygmunt, A. Burashnikov, J.M. Di Diego, J.M. Fish, J.M. Cordeiro, G. Thomas, Electrophysiological effects of ranolazine, a novel antianginal agent with antiarrhythmic properties, Circulation. 110 (2004) 904–910. https://doi.org/10.1161/01.CIR.0000139333.83620.5D.

[29] J. He, M.E. Kargacin, G.J. Kargacin, C.A. Ward, G.J. Karga-cin, C.A. Ward, Tamoxifen inhibits Na and K currents in rat ventricular myocytes, Am J Physiol Heart Circ Physiol. 285 (2003) 661–668. https://doi.org/10.1152/ajpheart.00686.2002.-Tamoxifen.

[30] S. Matsuo, H. Kishida, K. Munakata, H. Atarashi, The Effects of Mexiletine on Action Potential Duration and Its Restitution in Guinea Pig Ventricular Muscles, Japan Heart Journal. 26 (1985) 271–287.

[31] C. Davie, J. Pierre-Valentin, C. Pollard, N. Standen, J. Mitcheson, P. Alexander, B. Thong, Comparative pharmacology of guinea pig cardiac myocyte and cloned hERG (IKr) channel, J Cardiovasc Electrophysiol. 15 (2004) 1302–1309. https://doi.org/10.1046/j.1540-8167.2004.04099.x.

[32] O.J. Britton, A. Bueno-Orovio, K. Van Ammel, H.R. Lu, R. Towart, D.J. Gallacher, B. Rodriguez, Experimentally calibrated population of models predicts and explains intersubject variability in cardiac cellular electrophysiology, Proceedings of the National Academy of Sciences. 110 (2013) E2098–E2105. https://doi.org/10.1073/pnas.1304382110.

[33] L. Romero, J. Cano, J. Gomis-Tena, B. Trenor, F. Sanz, M. Pastor, J. Saiz, In Silico QT and APD Prolongation Assay for Early Screening of Drug-Induced Proarrhythmic Risk, J Chem Inf Model. 58 (2018) 867–878. https://doi.org/10.1021/ACS.JCIM.7B00440/ASSET/IMAGES/LARGE/CI-2017-004409_0009.JPEG.

This project received funding from the European Union's Horizon 2020 research and innovation program under grant agreement No 101016496

EU Horizon 2020 Research & Innovation Program
Digital transformation in Health and Care
SC1-DTH-06-2020
Grant Agreement No. 101016496

SimCardioTest - Simulation of Cardiac Devices & Drugs for in-silico Testing and Certification

SIM CARDIO TEST

Technical Report

D6.2-UC3-3D: Use Case 3 3D Validation Annex

Work Package 6 (WP6)

Verification, validation, uncertainty quantification & certification

Annex Lead: UPV, Spain
Task Lead: UBx, France
WP Lead: MPC, France

PUBLIC

Document history			
Date	**Version**	**Author(s)**	**Comments**
12/06/2023	V1	I. VAN HERCK	First Draft
19/06/2023	V2	H. AREVALO	Second Draft
21/06/2023	V3	M. T. MORA	Final Draft
29/06/2023	V4	R. SETZU	Format Consolidation
30/06/2023	V5	R. SETZU	Final Version
01/07/2024	V6	R. SETZU M. BARBIER	Format editing

TABLE OF CONTENTS

EXECUTIVE SUMMARY

This document is an annex of SimCardioTest deliverable D6.2 and was elaborated for Use Case 3 in the context of drug safety assessment. It contains the technical details or planned methods for the validation of the electrophysiological models at the tissue level.

Acronyms

Table 1: List of Acronyms.

Acronym	Meaning
AP	Action potential
IST	InSilicoTrials
SCT	SimCardioTest
TdP	Torsade de pointes

1. Computational model

The most widely used test to assess cardiac electrophysiological health in patients is through the ECG. It is an inexpensive and non-invasive procedure that is widely used to monitor patient cardiac health as well as diagnose diseases. Certain changes in the ECG characteristic are well known to lead to potentially life-threatening cardiac events. Using the inputs from the PK model of the drugs (Annex A6.2_UC3_PK) and the effects it has on the action potential model (Annex A6.2_UC3_0D), we will simulate how this affects propagation in a simplified tissue that can be used to approximate ECG. Thus, the validation activity for simcardems will focus on the simulator's accuracy in predicting the ECG changes that occur after drug intake.

1.1 Model Form

Simcardems solves the monodomain equation which is a PDE that models the propagation of electrical signals in the myocardium. The monodomain equation is typically expressed as:

$$\nabla \cdot (\sigma \nabla V_m) = C_m \frac{\partial V_m}{\partial t} + I_{ion}$$

where: C_m is the membrane capacitance per unit area, V_m is the transmembrane potential, σ is the electrical conductivity of the tissue, and I_{ion} represents the ionic current across the cell membrane. In this application, we will use the model discussed in Annex A6.2_UC3_0D to represent the cellular electrophysiology of the human myocyte.

Pseudo-ECGs will be approximated by using an integral equation proposed by Gima et al [1].

1.2 Model Inputs

The monodomain equation has been widely used to simulate the heart's electrical activity. Thus there is a wide source of values that can be used to represent the different input parameters. For this application, we will use the following values:

- C_m = 1 μF/cm^2 (from literature)
- I_{ion} = O'Hara-Rudy model of the human action potential
- σ = conductivity values obtained from Bishop et al [2].

For the current question of interest, C_m and σ will remain the same throughout all the simulations. The only variable that will change is the I_{ion} which will be modified as discussed in Annex xx. It will represent electrophysiology of different populations as well as the effects of different drugs.
Another model input that will need to be assessed is the geometry of the cardiac tissue. For the validation activity, we will use a realistic torso geometry to assess ECG changes. As preliminary work, we performed sinus simulations with the software ELVIRA [3]. For this simulation, a modified version of the O'Hara et al. model of human ventricular action potential was used [4,5], considering the transmural heterogeneity of the ventricular myocardium. It was included in the biventricular model by defining three different transmural layers for the endocardial, mid-myocardial, and epicardial cells. These layers comprised 17%, 41%, and 42% of ventricular wall thickness, respectively. Longitudinal and transversal conductivities of the tissue were set to 0.24 S/m and 0.0456 S/m, respectively.

For cardiac activation, a Purkinje network was developed and integrated in the biventricular model. For Purkinje cells, we used the model published by Stewart and colleagues [6].
5 beats starting from the steady state cellular conditions were simulated with a basic cycle length of 1000 ms to obtain the steady state at the 3D level under control conditions. Stimuli with an intensity of 900 μA/μF and a duration of 2 ms were applied to the first node of the His bundle.

Drug simulations were run for 5 beats with a basic cycle length of 1000 ms starting from the steady state under control conditions. Stimuli remained the same as the mentioned above (amplitude of 900 μA/μF and duration of 2 ms). Drug effects were simulated via the simple pore block model. QT interval was measured from the onset of the QRS complex to the end of the T-wave (|dV/dt| = 0). The QTc interval measurements were determined in the last beat in the limb lead I.

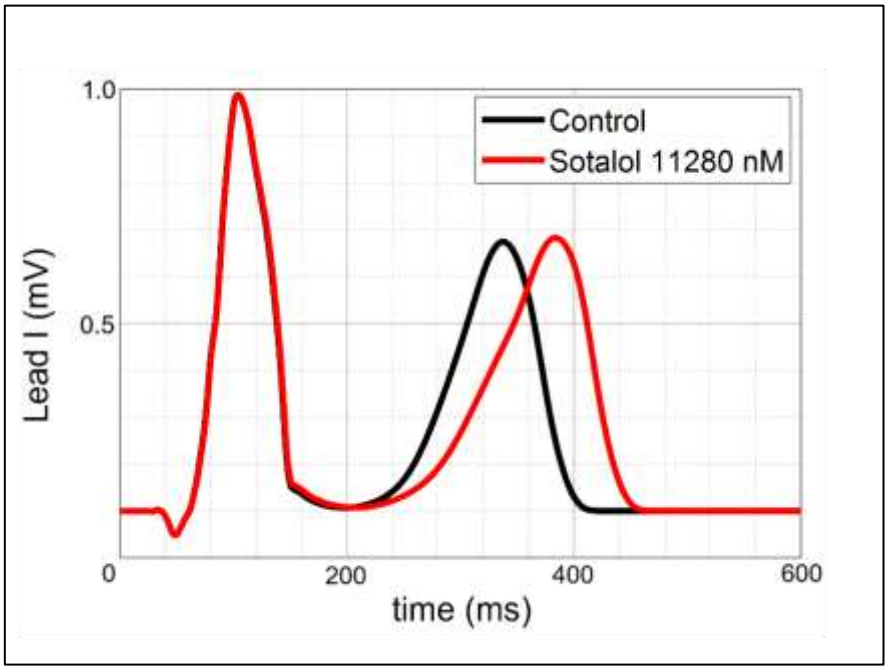

Figure 1: *Comparison the ECG in a biventricular model before (control) and after the administration of sotalol.*

In the actual in-silico trials platform, we will use a simplified tissue slab, as described by Niederer et al [7]. This is done to ensure that the simulations remain computationally tractable. This geometry has been used to benchmark other cardiac electrophysiology solvers and will provide insight into the accuracy of simcardems in simulating electrical propagation in the tissue.

2. Comparator

We will use experimental data taken from the literature, on the arrhythmic risk of drugs, to validate our simulation results. Since the goal is to demonstrate that the simulator can accurately predict the pro-arrhythmic changes caused by certain drugs, we will measure the accuracy of the simulator in predicting ECG changes arising from ingestion of drugs with known pro-arrhythmic effects.

For validation, we will use the following drugs with known QT prolongation:

Table 2: Drugs with known QT prolongation.

	Ref.	Sample Type	Cmax (nM)	% Exp	% Sim
Dofetilide (Intravenous)	[8]	10 males	4.755	26.98	9.41
Dofetilide (Intravenous)*					16.3
Dofetilide (Oral)			1.506	16.40	3.31
Dofetilide (Oral)*					5.9
Clarithromycin	[9]	24 males	874.386	2.81	0
Loratadine	[9]	24 males	0.215	0.75	0
Sotalol	[10]	in-vivo dogs	11280	10.70	11.70
Quinidine	[10]	in-vivo dogs	650	6.80	15.27
Quinidine*			1020	15.10	14.5
Cisapride	[11]	12 subjects (males + females)	2.7471	1.50	0.51
Ondansetron (BCL 900 ms)	[12]	isolated rabbit hearts	1000	15.34	16.52
Domperidone (BCL 900 ms)	[12]	isolated rabbit hearts	500	16.33	25.7
Domperidone* (BCL 900 ms)					19.4

In the table, we present simulation results obtained using the ELVIRA software. The same set of simulations will be performed in simcardems.

3. Assessment

3.1 Equivalency of Input Parameters

Since we do not have access to patient-specific data on the electrophysiological effects of drugs, we must rely on generalized assumptions for our input parameters. Thus, we use values cited from the literature as well as a generic torso model to simulate cardiac ECG.

3.2 Output Comparison

The output of the validation results will be prediction of changes in ECG markers under drugs with known arrhythmic effects. As presented in section 3, we already show pretty good preliminary

results using a different simulator. We aim to have the same level of accuracy when performing validation work with simcardems.

4. Conclusion

This document is an annex of SimCardioTest deliverable D6.2, and reports technical details relative to the validation of the 3D numerical model developed for Use Case 3. General conclusions relative to the validation of UC3 numerical model are reported in main deliverable D6.2.

Here we present the general plan for the validation of the 3D electrophysiological solver simcardems. The level of validation that we aim for is commensurate with the question of interest which is to develop a platform that can accurately determine the pro-arrhythmic effects of drugs in a population. We do not aim to simulate patient-specific electrical activity, which would be a challenging and computationally expensive endeavour, but rather show that our simplified model can accurately simulate the relative changes in the ECG due to drugs. The 3D simulator will integrate the PK models and the 0D models discussed in the previous sections into a simplified electrophysiological geometry. Thus, the validation activities performed in those sections will contribute to the accuracy of simcardems. The validation activity performed at the tissue level will also ensure that the final predictions of the simulator in assessing pro-arrhythmic risk of drugs on the cellular level can be reflected in a 3D myocardial tissue. This validation plan also paves the way for eventual extension of the platform to use realistic cardiac geometries and even torsos to predict drug effect in different populations.

5. Bibliography

1. Gima, Kazutaka, and Yoram Rudy. "Ionic current basis of electrocardiographic waveforms: a model study." *Circulation research* 90.8 (2002): 889-896.
2. Bishop, Martin J., and Gernot Plank. "Representing cardiac bidomain bath-loading effects by an augmented monodomain approach: application to complex ventricular models." *IEEE Transactions on Biomedical Engineering* 58.4 (2011): 1066-1075.
3. Heidenreich EA, Ferrero JM, Doblaré M, Rodríguez JF. Adaptive Macro Finite Elements for the Numerical Solution of Monodomain Equations in Cardiac Electrophysiology. Ann Biomed Eng. 2010;38: 2331–2345. doi:10.1007/s10439-010-9997-2
4. O'Hara T, Virág L, Varró A, Rudy Y. Simulation of the undiseased human cardiac ventricular action potential: model formulation and experimental validation. PLoS Comput Biol. 2011;7: e1002061. doi:10.1371/journal.pcbi.1002061
5. Llopis-Lorente J, Gomis-Tena J, Cano J, Romero L, Saiz J, Trenor B. In silico classifiers for the assessment of drug proarrhythmicity. J Chem Inf Model. 2020;60: 5172–5187. doi:10.1021/acs.jcim.0c00201
6. Stewart P, Aslanidi O v., Noble D, Noble PJ, Boyett MR, Zhang H. Mathematical models of the electrical action potential of Purkinje fibre cells. Philosophical Transactions of the Royal Society A: Mathematical, Physical and Engineering Sciences. 2009;367: 2225–2255. doi:10.1098/RSTA.2008.0283
7. Niederer, Steven A., et al. "Verification of cardiac tissue electrophysiology simulators using an N-version benchmark." *Philosophical Transactions of the Royal Society A: Mathematical, Physical and Engineering Sciences* 369.1954 (2011): 4331-4351.

8. Le Coz F, Funck-Brentano C, Morell T, Ghadanfar MM, Jaillon P. Pharmacokinetic and pharmacodynamic modeling of the effects of oral and intravenous administrations of dofetilide on ventricular repolarization. 1995.
9. Carr RA, Edmonds A, Shi H, Locke CS, Gustavson LE, Craft JC, et al. Steady-State Pharmacokinetics and ElectrocardiographicPharmacodynamics of Clarithromycin and Loratadineafter Individual or Concomitant Administration. Antimicrob Agents Chemother. 1998;42: 3. Available: https://journals.asm.org/journal/aac
10. Himmel HM, Bussek A, Hoffmann M, Beckmann R, Lohmann H, Schmidt M, et al. Field and action potential recordings in heart slices: Correlation with established in vitro and in vivo models. Br J Pharmacol. 2012;166: 276–296. doi:10.1111/j.1476-5381.2011.01775.x
11. Van Haarst AD, Van 'T Klooster GAE, Van Gerven JMA, Schoemaker RC, Van Oene JC, Burggraaf J, et al. The influence of cisapride and clarithromycin on QT intervals in healthy volunteers. Clin Pharmacol Ther. 1998;64: 542–546. doi:10.1016/S0009-9236(98)90137-0
12. Frommeyer G, Fischer C, Ellermann C, Lange PS, Dechering DG, Kochhäuser S, et al. Severe Proarrhythmic Potential of the Antiemetic Agents Ondansetron and Domperidone. Cardiovasc Toxicol. 2017;17: 451–457. doi:10.1007/s12012-017-9403-5

This project received funding from the European Union's Horizon 2020 research and innovation program under grant agreement No 101016496

EU Horizon 2020 Research & Innovation Program
Digital transformation in Health and Care
SC1-DTH-06-2020
Grant Agreement No. 101016496

SimCardioTest - Simulation of Cardiac Devices & Drugs for in-silico Testing and Certification

SIM CARDIO TEST

Technical Annex

Annex A – WP6 complement of D6.1 and D6.2 Technical Reports on Verification, Validation and Uncertainty Quantification for the Use Cases of WP2-4

(Tasks 6.1 and 6.2 – covering M30-M54)

Work Package 6 (WP6)

Verification, validation, uncertainty quantification & certification

WP Lead: MPC, France

PUBLIC

ANNEX A INFORMATION

Annex title	**WP6 complement of D6.1 and D6.2 Technical Reports on Verification, Validation and Uncertainty Quantification for the Use Cases of WP2-4 (Tasks 6.1 and 6.2 – covering M30-M54)**
Description	Report of additional verification, validation and uncertainty quantification activities conducted during M30-M54 period for the different Use Cases (pacing leads, LAAO and drug safety and efficacy)
Lead authors	Romano SETZU (MPC)
Contributors	For UC1 (WP2): Yves COUDIERE, Michael LEGUEBE, Delphine DESHORS (UBx) For UC2 (WP3): Oscar CAMARA, Andy OLIVARES (UPF) For UC3 (WP4): Beatriz TRENOR, Maria Teresa MORA (UPV)
Due date	M54
Submission date	30/06/2025
Comments	-

Document history			
Date	**Version**	**Author(s)**	**Comments**
29/04/2025	V1	R. SETZU	First Draft
30/06/2025	V2	R. SETZU, M. LEGUEBE, A. OLIVARES, M. T. MORA	First consolidated draft including contributions from UC1/2/3
30/07/2025	V4	R. SETZU	Final Version

TABLE OF CONTENTS

EXECUTIVE SUMMARY

This annex summarizes all verification, validation, and uncertainty quantification (VVUQ) activities conducted in the frame of work-package WP6 after the consolidation of deliverables D6.1 and D6.2 in June 2023 (M30) till the end of the SimCardioTest Project in June 2025 (M54) for assessing the credibility of computational models developed within Use Cases 1 to 3 (cf. WP2, 3, and 4 respectively).

This annex is meant to be a self-contained stand-alone document, however, in order to fully comprehend the whole VVUQ activities conducted on the selected computational models since the beginning of the SimCardioTest project, it is recommended to review content of deliverable D6.1 and D6.2 first, as they are often referenced as propaedeutic to this document.

Acronyms

Table 1: List of Acronyms.

Acronym	Meaning
AF	Atrial Fibrillation
ASME	The American Society of Mechanical Engineers
Avg.	Average (abbreviation)
CEPS	Cardiac ElectroPhysiology Solver (cf. Use Case 1)
CFD	Computational Fluid Dynamic
CI	Continuous Integration
CiPA	Comprehensive in-vitro Proarrhythmia Assay (cf. Use Case 3)
COU	Context of Use
CT	Computer Tomography
DE	Discretization Error (in Verification)
DRT	Device-Related Thrombosis
EAB	Exponential Adams-Bashforth
ECG	Electrocardiogram
EP-0D	0D Electrophysiology Model (cf. Use Case 3)
EP-3D	3D Electrophysiology Model (cf. Use Case 3)
EXC	ExactCure
FBE	Forward-Backward Euler
FDA	US Food and Drug Administration
IST	INSILICOTRIALS TECHNOLOGIES SRL Also referring to the Cloud service hosting the models
LA	Left Atrium
LAAO	Left Atrial Appendage Occluder
MOTS	Modified Off-the-Shelf Software
MPC	MICROPORT CRM - SORIN CRM SAS
MV	Mitral Valve
N.A. / n.a.	Not Applicable
NCV	Numerical Code Verification

Acronym	Meaning
NSE	Numerical Solver Error (in Verification)
ODE	Ordinary Differential Equations
OTS	Off-the-Shelf Software
PIV	Particle Image Velocimeter
PK	Pharmacokinetics Model (cf. Use Case 3)
PR	Pulmonary Ridge
PSA	Pacing System Analyzer
PV	Pulmonary Vein
QI	**Question** of Interest
QoI	**Quantity** of Interest
RL	Rush Larsen
SCT	SimCardioTest
SQA	Software Quality Assurance (in Verification)
SRL	SIMULA RESEARCH LABORATORY AS
TAWSS	Time-Averaged Wall Shear Stress
TC	Test Condition (in Validation)
TdP	Torsade de Pointes
TS	Test Sample (in Validation)
UB / U.B.	Uncertainty Budget
UBx	Université de Bordeaux
UC	Use Case
UD	User Developed (Software)
UE	Use Error (in Verification)
UPF	UNIVERSIDAD POMPEU FABRA
UPV	UNIVERSITAT POLITECNICA DE VALENCIA
V&V, VV	Verification & Validation
VVUQ	Verification, Validation, and Uncertainty Quantification
WP	Work Package

Acronym	Meaning
WSS	Wall Shear Stress

Table 2: Table cell background colour-code used across the document to identify and differentiate VV40 items: Verification, Validation, Applicability.

Background Cell Colour-Code
"Light Green" for Verification Items
"Salmon" for Validation Items
"Light Blue" for Applicability Items

1. Introduction

This annex summarizes all verification, validation, and uncertainty quantification (VVUQ) activities conducted in the frame of work-package WP6 after the consolidation of deliverables D6.1 and D6.2 in June 2023 (M30) till the end of the SimCardioTest Project in June 2025 (M54) for assessing the credibility of computational models developed within Use Cases 1 to 3 (cf. WP2, 3, and 4 respectively).
This annex is meant to be a self-contained stand-alone document, however, in order to fully comprehend the whole VVUQ activities conducted on the selected computational models since the beginning of the SimCardioTest project, it is recommended to review content of deliverable D6.1 and D6.2 first, as they are often referenced as propaedeutic to this document.

1.1 Normative Background

Credibility assessment of computational models through VVUQ is paramount for gaining confidence on the models' ability to address the intended Question of Interest in the relevant Context of Use [1]. VVUQ activities on the selected computational models are conducted according to ASME VV40 standard [2]. ASME VV40 organizes the V&V activities in three distinct phases:

- Model Verification
- Model Validation
- Model Applicability

Model Verification comprises those activities meant to demonstrate that the numerical model accurately represents the underlying mathematical model. Model Validation comprises those activities meant to show how well the numerical model represents reality. Finally Model Applicability comprises those activities meant to show the relevance of validation activities to support the use of the numerical model in the selected context of use.
Each V&V activity listed in ASME VV40 addresses a specific credibility factor. All credibility factors contribute to the overall credibility of the numerical model. How well a credibility factor must be investigated depends on the model risk, intended as the result on the importance that the numerical model supposedly has in taking clinical decisions and the severity of clinical consequences in case the model leads to wrong decisions.

1.2 Global V&V Strategy

The selected models will address these specific aspects:

- For Use Case 1 (WP2): Pacing leads electrical performance
- For Use Case 2 (WP3): Left Atrial Appendage Occluders (LAAO) safety
- For Use Case 3 (WP4): Drugs safety

The following sub-sections present the V&V activities undertaken by each Use Case on the selected models.

1.2.1 Model Description

According to ASME VV40 guidelines, for each Use Case and for the selected numerical model the following key concepts are clarified:

- **Device/Drug Description**: the device or drug for which the numerical model is developed
- **Question of Interest**: the question concerning the device/drug safety/efficacy addressed by the selected numerical model

- **Context of Use**: the context in which the numerical model is used in the device/drug life cycle (e.g. device/drug design, validation, clinical use)
- **Model Risk**: the risk related to using the numerical model in the defined context of use

1.2.2 Model Verification

The purpose of Model Verification as intended by ASME VV40 is to demonstrate that the computational model numerical implementation is a robust and accurate representation of the mathematical model describing the phenomenon that the model aims to replicate.
Verification Credibility factors are grouped in two main areas:

- Code Verification
- Calculation Verification

Code Verification credibility factors are intended to demonstrate that the numerical model is developed and runs using robust software and hardware, and correctly implements the underlying mathematical equations which describe the model.
Calculation Verification credibility factors are intended to assess the numerical error associated with the numerical discretization of the mathematical problem, as well as with the implemented numerical solver strategy. In addition, this phase addresses how user errors are handled and possibly mitigated in both model inputs and outputs management.
Table 3 summarizes the Credibility Factors to be addressed in the frame of the computational model validation activities according to ASME VV40.

Table 3: Verification Credibility Factors (cf. ASME VV40).

Activity	Credibility Factor	VV40§
Code Verification	Software Quality Assurance Software functions correctly and gives repeatable results in a specified Hardware/Software environment. (OTS / MOTS / UD)	5.1.1.1
Code Verification	Numerical Code Verification - NCV Demonstrate correct implementation and functioning of algorithms. Compare to analytical solutions.	5.1.1.2
Calculation Verification	Discretization Error Run spatial/temporal grid sensitivity analysis	5.1.2.1
Calculation Verification	Numerical Solver Error Run solver parameters sensitivity analysis	5.1.2.2
Calculation Verification	Use Error [Verify I/O controls in place]	5.1.2.3

1.2.3 Model Validation

The purpose of Model Validation as intended by ASME VV40 is to demonstrate that the computational model provides reliable information about the real-life phenomena it wants to represent.
Validation Credibility factors are grouped in three main areas:

- Computational Model
- Comparator
- Assessment

Computational Model credibility factors are intended to fully describe and quantify the model ability to address its question of interest. Its form, properties and conditions are addressed, as well as its inputs. The investigation includes both sensitivity analysis and uncertainty analysis of these quantities (when applicable) meant to assess the model accuracy.
Comparator credibility factors are intended to fully describe and quantify the comparator(s) used for validating the computational model. Comparators may be of different nature depending on the nature of the numerical model: pre-existing clinical literature data, in-vitro comparators, pre-clinical (animal) or clinical data. There may be one or more comparators addressing different aspects of the numerical model under investigation. Comparator uncertainties are also investigated.
Assessment credibility factors are relative to the actual comparison of the numerical model with the selected comparator. Both inputs and outputs to the comparison are taken into account in this analysis.
Table 4 summarizes the Credibility Factors to be addressed in the frame of the computational model validation activities according to ASME VV40.

NOTE: when multiple items are given for a specific credibility factor, not all of them may be applicable to the numerical model under consideration. Each Use Case will select and justify the credibility factor items to be addressed.

Table 4: Validation Credibility Factors (cf. ASME VV40).

Activity	Credibility Factor	VV40§
Computational Model	Model Form: • Conceptual Formulation of Numerical Model • Mathematical formulation of Numerical Model Address 4 items: • Governing Equations (governing modeled phenomena) • System Configuration (Geometry of device/environment) • System proprieties (Bio. Chem. Phys. Properties) • System conditions (boundary & initial cond.)	5.2.1.1
Computational Model	Model Inputs Address 4 items: • Governing Equations Parameters (governing modeled phenomena) • System Configuration (Geometry of device/environment) • System proprieties (Bio. Chem. Phys. Properties) • System conditions (boundary & initial cond.) Quantification of Sensitivities Quantification of Uncertainties	5.2.1.2

Activity	Credibility Factor	VV40§
Comparator	Test Samples (TS) Address 4 items: • Quantity of TS • Range of Characteristics of TS • Measurements of TS • Uncertainty of TS measurements	5.2.2.1
Comparator	Test Conditions (TC) Address 4 items: • Quantity of TC • Range of TC • Measurements of TC • Uncertainty of TC measurements	5.2.2.2
Assessment	Equivalency of Input Parameters between Numerical Model and Comparator	5.2.3.1
Assessment	Output Comparison Address 4 items: • Quantity • Equivalency of Output Parameters • Rigor of Output Comparison • Agreement of Output Comparison	5.2.3.2

1.2.4 Model Applicability

The ultimate purpose of verifying and validating the numerical model is to gain confidence that the model outputs can be used to make predictions on the represented medical device/drug. However, the validation space (*in primis* the comparator selected for model validation) is a limited representation of the reality which the model aims to replicate.
ASME VV40 predicates an additional analysis, referred to as applicability, meant to assess the relevance of the engaged validation activities to support the use of the numerical model for the selected context of use.
Table 5 summarizes the Credibility Factors to be addressed in the frame of the computational model applicability assessment according to ASME VV40.

Table 5: Model Applicability (cf. ASME VV40).

Activity	Credibility Factor	VV40§
Applicability	Relevance of the Quantities of Interest QoI of Validation may be surrogate to the QoIs of COU	5.3.1
Applicability	Relevance of the Validation Activities to the COU Proximity of Validation Points to COU	5.3.2

1.2.5 Credibility Factors Coverage Level

According to ASME VV40, the model risk is the result of the combination of two factors:

- The ***Decision Consequence***: the clinical consequence of making a wrong decision based on a false prediction of the model

- The ***Model Influence***: the importance of the contribution of the model outcome in making clinical decisions, weighted amongst all other available inputs, such as available literature, design, in-vitro, pre-clinical and clinical information

Decision Consequence can be weighted as:

- **low**: an incorrect decision would not adversely affect patient safety or health, but might result in a nuisance to the physician or have other minor impacts
- **medium**: an incorrect decision could result in minor patient injury or the need for physician intervention, or have other moderate impacts
- **high**: an incorrect decision could result in severe patient injury or death, or have other significant impacts

Model Influence can be weighted as:

- **low**: simulation outputs from the computational model are a minor factor in the decision
- **medium**: simulation outputs from the computational model are a moderate factor in the decision
- **high**: simulation outputs from the computational model are a significant factor in the decision

Figure 1 gives a graphical representation of the Model Risk resulting from the combination of Decision Consequence and Model Influence.

Model influence	**high**	**3**	**4**	**5**
	medium	**2**	**3**	**4**
	low	**1**	**2**	**3**
		low	**medium**	**high**
		Decision consequence		

Figure 1: Model Risk Matrix (cf. ASME VV40).

Each of the credibility factors previously described may be investigated in several ways, each with a different level of investigation. The selected way of investigating each credibility factor may depend on several variables, such as complexity, available knowledge, or available means in the timeframe of this project.

ASME VV40 gives guidance on how to evaluate whether the credibility factors have been sufficiently investigated. For each credibility factor, a score varying from 1 to 5 is given to indicate how deeply the item has been investigated, where 1 means none or little investigation, and 5 means a thorough investigation. The scores are then compared to the model risk level as defined. Whenever a credibility factor coverage level does not match the risk level, a justification is given. This evaluation is summarized in a matrix as shown in Table 6.

Table 6: Credibility Factors Coverage Level (cf. ASME VV40). The model risk level is set to Medium (3) in this table for illustration purposes. The coverage level of the credibility factors is given an arbitrary score on a 1-to-5 scale for illustration purposes.

Model Risk					x		
Credibility Factor Coverage Level		1	2	3	4	5	
Code Verification: Software Quality Assurance	I			x			
Code Verification: Numerical Code Verification - NCV	I			x			
Calculation Verification - Discretization Error	II			x			
Calculation Verification - Numerical Solver Error	II			x			
Calculation Verification - Use Error	III			x			
Validation - Model [Form]	III			x			
Validation - Model [Inputs]	III			x			
Validation - Comparator [Test Samples]	IV			x			
Validation - Comparator [Test Conditions]	IV			x			
Validation - Assessment [Input Parameters]	IV			x			
Validation - Assessment [Output Comparison]	V			x			
Applicability: Relevance of the Quantities of Interest	V			x			
Applicability: Relevance of the Validation Activities to the COU	V			x			

2. Use Case 1

2.1 UC1 Model Summary

2.1.1 Background

The role of a cardiac pacing lead is to effectively stimulate the heart when it is deficient. Current pacemakers offer a wide range of stimulation pulse amplitudes and pulse durations to ensure that the therapy is effectively delivered. However, the higher the stimulation amplitude (and duration), the more energy is drained from the pacemaker battery, which can have an impact on the device longevity. When developing new leads, it is therefore important that the stimulation threshold remains in normal range.

2.1.2 Device Description

Medical devices addressed by the model are cardiac pacing leads. More precisely, their electrical behaviour, and interaction with the cardiac tissue is addressed.

2.1.3 Question of Interest

The Question of Interest addressed by the model is the following:

- What are the stimulation pulse characteristics (voltage amplitude in V and pulse duration in ms) required for a bradycardia lead in bipolar (tip/ring) mode to capture (stimulate) healthy cardiac tissue?

2.1.4 Context of Use

The computational model can be used to help pacing lead manufacturers when developing new products, providing information on the energy levels (pulse amplitudes and durations) required to successfully trigger action potentials and stimulate cardiac tissue.

2.1.5 Model Risk

The following considerations support the assessment of the risk associated with the numerical model.

- Decision Consequence: Low

An error in the model prediction may result in either an underestimation or an overestimation of the energy required to stimulate the cardiac tissue for a given pacing lead design. The clinician will adjust the energy in order to stimulate correctly. An overestimation of the energy by the model has no negative clinical influence on the delivered therapy, as it would result in an increase of the device battery life, which would actually be an unexpected benefit. An underestimation of the energy would have a minor clinical influence, as it would require the physician to increase the programmed therapy energy in order to achieve cardiac stimulation, resulting in a decrease of the expected battery life.

- Model Influence: Medium

Results of simulations with a new design will be systematically compared to those of previous well-established designs. In addition, pre-clinical and clinical data collected during the validation of the new lead design would contribute to corroborate the data provided by the models.

- Model Risk: 2/5 (Low-Medium)

Model Risk is based on Decision Consequence and Model Influence stated above, according to Risk Matrix in Figure 2 (cf. section 1.2.5).

Model influence	**high**	**3**	**4**	**5**
	medium	**2 COU**	**3**	**4**
	low	**1**	**2**	**3**
		low	**medium**	**high**
		Decision consequence		

Figure 2: *Model Risk Matrix (cf. ASME VV40) evaluating the COU included in UC1.*

2.1.6 Model Description

The model aims to reproduce capture threshold detection measurements that are performed ex vivo on a healthy ventricular wedge.

The model includes the tissue and the surrounding electrolyte, the pacing circuit of the device, and a contact model between the device and the tissue. Given a pulse duration and amplitude, it

computes the transmembrane voltage in the cardiac tissue, the electric potential in the tissue and electrolyte, as well as the voltage drops at the tip and ring electrodes.

Simulations are parametrized by:

- Contact properties between the leads and the tissue/electrolyte (modelled by parallel RC-circuits)
- The geometry of both the lead and computational domain
- Micro-structural description of the tissue and its electrical properties
- A model that describes ionic exchanges at the cell membranes

The contact properties are characterized by bench experiments. The geometry and microstructure of the tissue are obtained from 9.4T MR imaging. The shape of the lead is chosen among a family of designs, with the possibility of modifying several parameters (such as inter electrode distance, or radius). The ionic model is chosen from the standardized "cellML" database [3], with parameters adjusted from optical mapping data.
To compute an approximate solution of the model, we need a geometrical mesh of the domain, a spatial discretization scheme (e.g. P1 Lagrange Finite Elements), a time stepping method and an algorithm to solve large linear systems.

In Figure 3 we show the computation of the electric field created by the pacemaker in a slab of passive tissue, which will be the shape of the excitation of the cardiac tissue at the beginning of pacing.

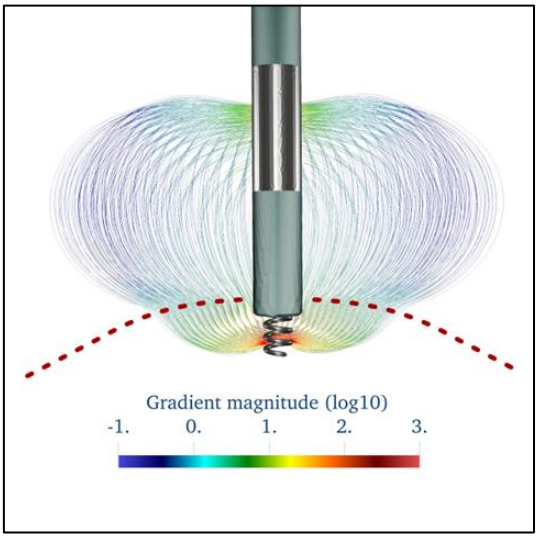

Figure 3: Electric field generated by a pacemaker lead, computed in a computational domain representing blood and a passive tissue, above and below the dotted line, respectively.

Computing the solution for various amplitudes and durations of stimulation allows to locate the so-called Lapicque curve, which is the threshold between capturing and non-capturing stimulations in the amplitude/duration plane (see Figure 4).

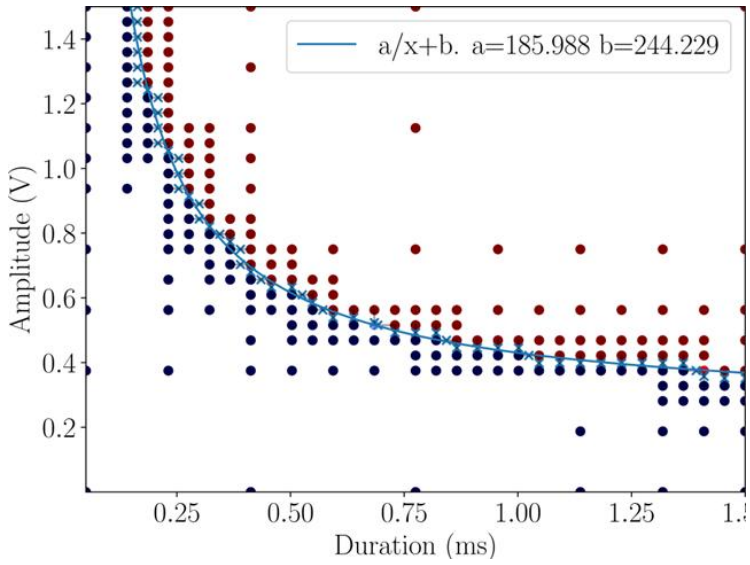

Figure 4: Lapicque Curve obtained from the solutions of an exploratory 0D model. For each blue/red point of the diagram, ie for each pair of amplitude and duration of stimulation, the model computes the response to 5 stimulations, and evaluates whether or not an action potential was triggered after each stimulation. Blue dots are for 0 out of 5 captures, red dots are for 5 out 5 captures.

2.2 UC1 Model Verification – M30-M54 Activities

This section only contains additional Verification activities conducted on UC1 selected computational model during the M30-M54 period. Verification activities conducted during the M1-M30 period are already reported in the UC1 section of deliverable D6.1. Results reported in this section are meant to complete or (in some cases) supersede results of deliverable D6.1. The latter case will be explicitly mentioned, when applicable.

The results presented in this section are focused on the accuracy of our in-house software CEPS, which is used to determine if a piece of cardiac tissue is stimulated by a pacemaker. In particular, we investigate the influence of the discretization of the mesh that represents the pacemaker lead and its surroundings, as well as the chosen time step. Then, we show the influence of the numerical parameters of the linear solver that is used in CEPS.

2.2.1 Discretization Error

2.2.1.1 CEPS Model

The problem which describes the stimulation of cardiac tissue in a bath by a pacemaker has discontinuity properties which prevent from applying standard numerical analysis theorems. In consequence, we present accuracy results on each of the constitutive elements of the problem. Namely, we report the convergence of the results for our implementation of the following items:

- ODE solvers for cardiac ionic models,
- Solvers for the monodomain, bidomain and bidomain-with-bath models which were proposed by Pathmanathan and Gray [4] and approved by the FDA for validation of cardiac electro-physiology software,

- Bidomain model with the Beeler-Reuter ionic model [5], which is used in our pipelines.

Discretization error for ionic models

Before coupling a reaction/diffusion equation to ionic models, we study the convergence of numerical solvers suited for such models. This is performed by suppressing any spatial component from the code. A dedicated executable can be compiled to this aim. CEPS includes several ionic models, which were imported from the CellML repository [3]. They consist of ODE systems for which there exists no fully determined analytic expression. In consequence, we compute a reference solution with a very small time-step and high-order numerical scheme. This reference is used to evaluate the difference with solutions computed with larger time steps and lower order numerical schemes. We report in **Figure 5** the convergence rates of the Forward-Backward Euler (FBE), Rush Larsen (RL) and Exponential Adams-Bashforth (EAB) time schemes, applied to some implemented ionic models (cf CEPS online documentation [1]and references therein). The error is measured in L2([0,100]) norm in time.

[1] CEPS Online Documentation: https://carmen.gitlabpages.inria.fr/ceps/

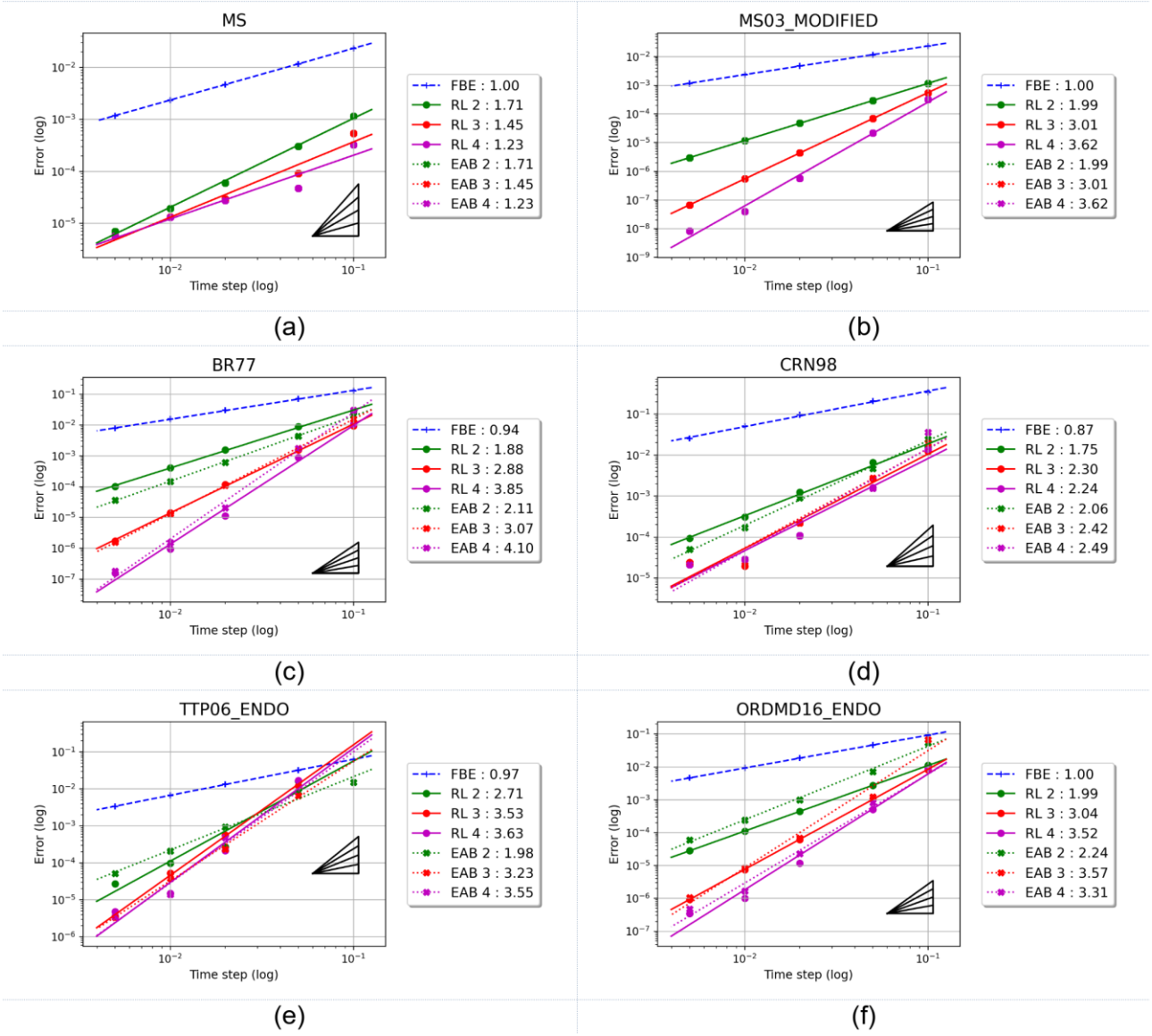

Figure 5: Convergence rates of Forward-Backward-Euler (FBE), Rush-Larsen(RL) and Exponential Adams-Bashforth (EAB) numerical solvers for different ionic models: Mitchell-Scheffer (a), regularized Mitchell-Scheffer (b), Beeler-Reuter (c), Courtemanche-Ramirez-Nattel (d), ten Tuscher-Panvilov (e) and modified O'Hara (f). Numbers in boxes indicate the slope of linear regressions for each set of points, i.e. the measured order of convergence.

Discretization error for the monodomain, bidomain and bidomain-with-bath models

Pathmanathan and Gray [4] introduced a collection of nine manufactured functions which are solutions to the monodomain, bidomain and bidomain-with-bath equations, in computational domains which are 1, 2 and 3 dimensional. The part of the solution that replaces the ionic model follows the same standard as the usual cardiac models. In consequence, the implementation in CEPS was relatively easy. In this document, we report the convergence results of CEPS for the 2D version of the three cardiac problems.

Numerical error is measured relatively to the analytic solution, with all combinations of the following norms:

- In time: value at final time t=1, $L^1([0,1])$ and $L^\infty([0,1])$,
- In space: $L^1(\Omega)$, $L^2(\Omega)$ and $L^\infty(\Omega)$.

Linear solver parameters are set to 10^{-12} for relative and absolute tolerances (cf section 2.2.2.1 for the definition of these parameters). The physical parameters of the model, namely conductivities, membrane capacitance and surface, are set following the instructions given in the FDA verification instructions. Unfortunately, the "ionic" part of this model does not allow to use the ODE solvers that take advantage of the specific form of evolution equations for ionic gate variables. The tests can only be performed with the usual "semi-implicit backward differentiation formula" (SBDF) time schemes for the ionic part.

Given a collection of meshes and time steps, the errors are computed for all combinations of mesh size and time steps. For multi-steps methods, such as SBDF, we replace the result of the first iterations by the analytic solution in order to measure the actual accuracy of the methods, and not that of lower order methods that are used for those first steps. When the fit the errors as the maximum of two linear functions (in log), in both space and time directions. We illustrate this fitting process in **Figure 6**, for the bidomain problem, solved with first order polynomial Lagrange finite elements combined with the SBDF time scheme of order 2. The fitted convergence rates are reported in Table 7, Table 8 and Table 9 for the 2D-monodomain, 2D-bidomain and 2D-bidomain-with-bath problems, respectively.

The convergence rates are in agreement with the numerical methods that were selected. However, order 4 in time is not reached for the SBDF 4 + P2 solver. We identified two reasons. Firstly, our selection of meshes and time steps resulted in errors that were dominated by the error in space for all but three data points. Therefore, the automatic fit leads to loose estimates of the convergence rate. Secondly, our solver is not completely written as a SBDF scheme. At each time step, the ionic current is evaluated explicitly instead of implicitly, to reduce significantly computation time. This adaptation of the numerical scheme comes with a slight loss of accuracy.

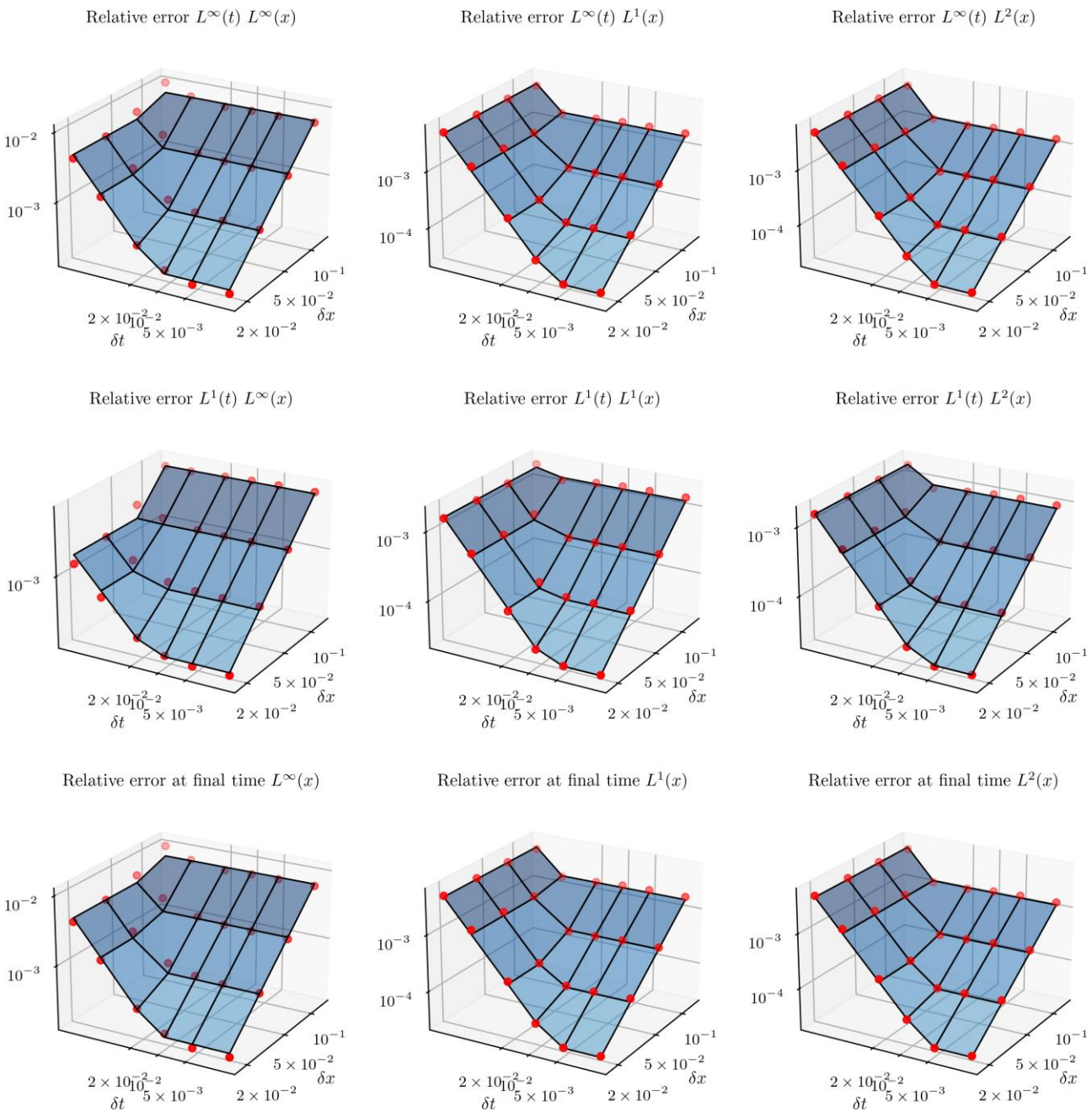

Figure 6: Numerical errors (red dots) with respect to the analytic solution of the manufactured bidomain with bath problem from Pathmanathan and Gray [4], solved with P1 finite elements and SBDF 2 time scheme. The blue surface is the fitted intersection of two planes in δx and δt directions, whose slopes determine the convergence order of the implementation of CEPS.

Table 7: Convergence rates of the 2D monodomain benchmark. Coefficients with stars indicate that no or too few points were generated to accurately measure the convergence rate.

	P1 – SBDF2	P1 – SBDF2	P2 - SBDF4	P2 - SBDF4
Norm	**Spatial cv. rate**	**Time cv. rate**	**Spatial cv. rate**	**Time cv. rate**
$L^\infty([0,1]), L^\infty(\Omega)$	1.86	1.40	2.82	2.16*
$L^\infty([0,1]), L^1(\Omega)$	1.95	1.67	3.22	3.45*
$L^\infty([0,1]), L^2(\Omega)$	1.96	1.67	3.27	3.56*
$L^1([0,1]), L^\infty(\Omega)$	1.78	1.18	2.83	1.07*
$L^1([0,1]), L^1(\Omega)$	1.90	1.35	3.10	2.91*
$L^1([0,1]), L^2(\Omega)$	1.91	1.35	3.11	3.07*
at t=1, $L^\infty(\Omega)$	1.86	1.40	2.82	2.16*
at t=1, $L^1(\Omega)$	1.95	1.67	3.22	3.45*
at t=1, $L^2(\Omega)$	1.96	1.67	3.27	3.56*
Target rate	**2**	**2**	**3**	**4**

Table 8: Convergence rates of the 2D bidomain benchmark. Coefficients with stars indicate that no or too few points were generated to accurately measure the convergence rate.

	P1 – SBDF2	P1 – SBDF2	P2 - SBDF4	P2 - SBDF4
Norm	**Spatial cv. rate**	**Time cv. rate**	**Spatial cv. rate**	**Time cv. rate**
$L^\infty([0,1]), L^\infty(\Omega)$	1.85	1.72	2.88	2.15*
$L^\infty([0,1]), L^1(\Omega)$	2.03	1.62	3.08	3.42*
$L^\infty([0,1]), L^2(\Omega)$	2.01	1.67	3.09	3.52*
$L^1([0,1]), L^\infty(\Omega)$	1.79	1.39	2.86	1.03*
$L^1([0,1]), L^1(\Omega)$	1.94	1.46	3.02	2.87*
$L^1([0,1]), L^2(\Omega)$	1.95	1.47	3.00	3.03*
at t=1, $L^\infty(\Omega)$	1.85	1.72	2.88	2.15*
at t=1, $L^1(\Omega)$	2.03	1.62	3.08	3.42*
at t=1, $L^2(\Omega)$	2.01	1.67	3.09	3.52*
Target rate	**2**	**2**	**3**	**4**

Table 9: Convergence rates of the 2D bidomain with bath benchmark.

	P1 – SBDF2	P1 – SBDF2	P2 - SBDF4	P2 - SBDF4
Norm	**Spatial cv. rate**	**Time cv. rate**	**Spatial cv. rate**	**Time cv. rate**
L∞([0,1]), L∞(Ω)	1.79	1.60	2.88	2.98
L∞([0,1]), L1(Ω)	1.87	1.83	3.08	3.20
L∞([0,1]), L2(Ω)	1.81	1.82	3.09	3.24
$L^1([0,1]), L^\infty(\Omega)$	1.77	1.32	2.86	2.42

	P1 – SBDF2	P1 – SBDF2	P2 - SBDF4	P2 - SBDF4
Norm	**Spatial cv. rate**	**Time cv. rate**	**Spatial cv. rate**	**Time cv. rate**
$L^1([0,1]), L^1(\Omega)$	1.81	1.58	3.02	2.74
$L^1([0,1]), L^2(\Omega)$	1.68	1.56	3.00	2.78
at t=1, $L^\infty(\Omega)$	1.79	1.60	2.88	2.98
at t=1, $L^1(\Omega)$	1.87	1.83	3.08	3.20
at t=1, $L^2(\Omega)$	1.81	1.82	3.09	3.24
Target rate	**2**	**2**	**3**	**4**

Convergence of bidomain model with cardiac ionic model

In this section, we report the accuracy of CEPS when solving the bidomain equations, with a Beeler-Reuter ionic model, which is a usual computation of electrophysiology. Since there is no analytic solution for this problem, we compute numerical errors with respect to a reference solution. This reference is computed with a very fine time step and a high-order numerical scheme. We report in **Figure 7** the convergence towards this solution, for the $L^\infty([0,1]), L^2(\Omega)$ norm. Other norms yield similar results. The convergence rates are in accordance with the selected numerical method, with the exception of order 4 methods, for which we see a deterioration of the convergence rate, between 3 and 4.

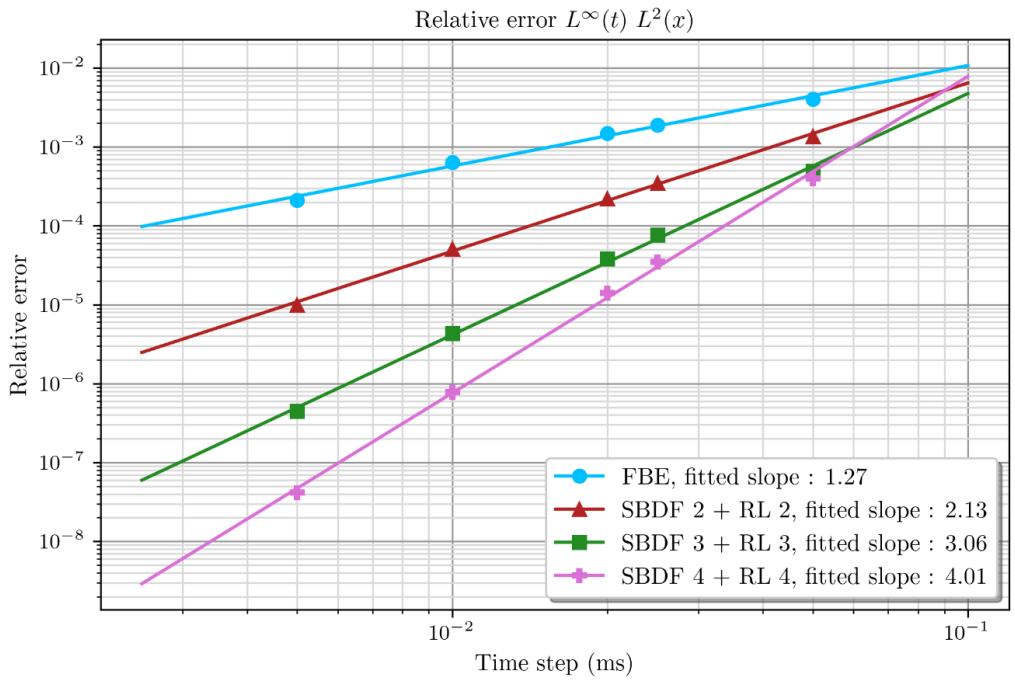

Figure 7: Numerical errors with respect to a reference solution, for the bidomain problem with Beeler-Reuter ionic model.

From each computation, be it the reference or the coarser ones, CEPS extracts the activation map, i.e. for each point of the computational domain, the time when the action potential is detected. On

Figure 8, we show that convergence of activation maps towards the reference map is at best of order 1. This is explained by the simplistic method that is used to detect when a point in tissue is activated.

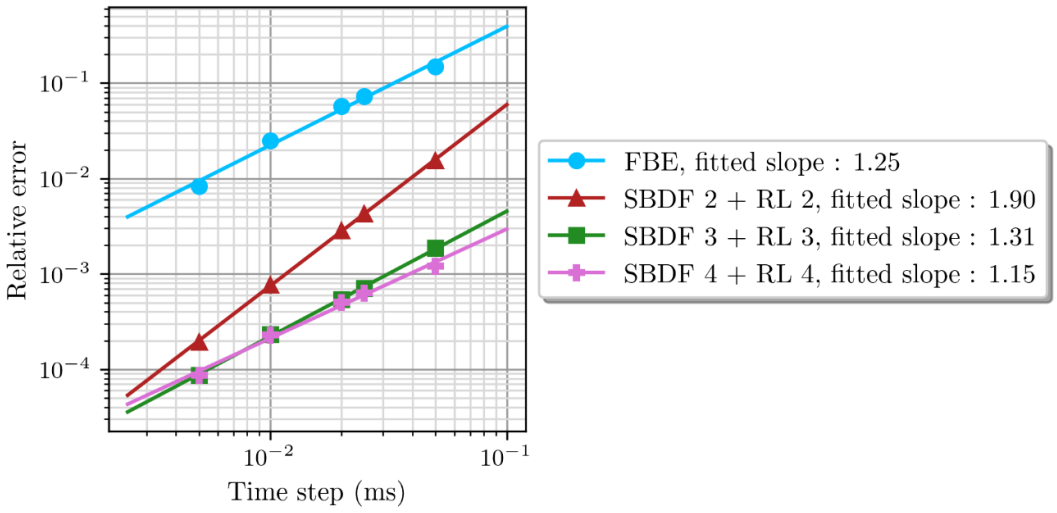

Figure 8: Convergence of activation maps for the bidomain problem with Beeler-Reuter ionic model. Error is measured with respect to the activation map extracted from a reference solution.

2.2.2 Numerical Solver Error

2.2.2.1 CEPS Model

In this section, we modify the few available parameters which tune the linear solver from the library PETSc [2], used by CEPS. We generally use either the Conjugate Gradient (CG), Stabilized Conjugate Gradient (BICGSTAB) or GMRES iterative solvers, as they allow computations in parallel. The stopping criterion used by PETSc is the following: $|r| < \max(\varepsilon_r|r_0|,\varepsilon_a)$, where r is the current residual of the linear system, r_0 is the residual at start, ε_r and ε_a are the relative and absolute tolerances that can be set from the CEPS input file, respectively. Additionally, a maximum number of linear solver iterations can be set. Reaching the maximum of iterations before convergence stops the program.

In this section, we check the influence of the linear solver parameters on the result of the bidomain with bath benchmark problem from section 2.2. Computations are run on a mesh of characteristic size 0.0125, using a SBDF 4 numerical scheme with a time step of 0.01.

[2] PETSc: https://petsc.org/

Error with respect to relative tolerance

ε_a is set to 10^{-20}, and the maximum number of iterations to 5 000. Errors are reported on **Figure 9**.

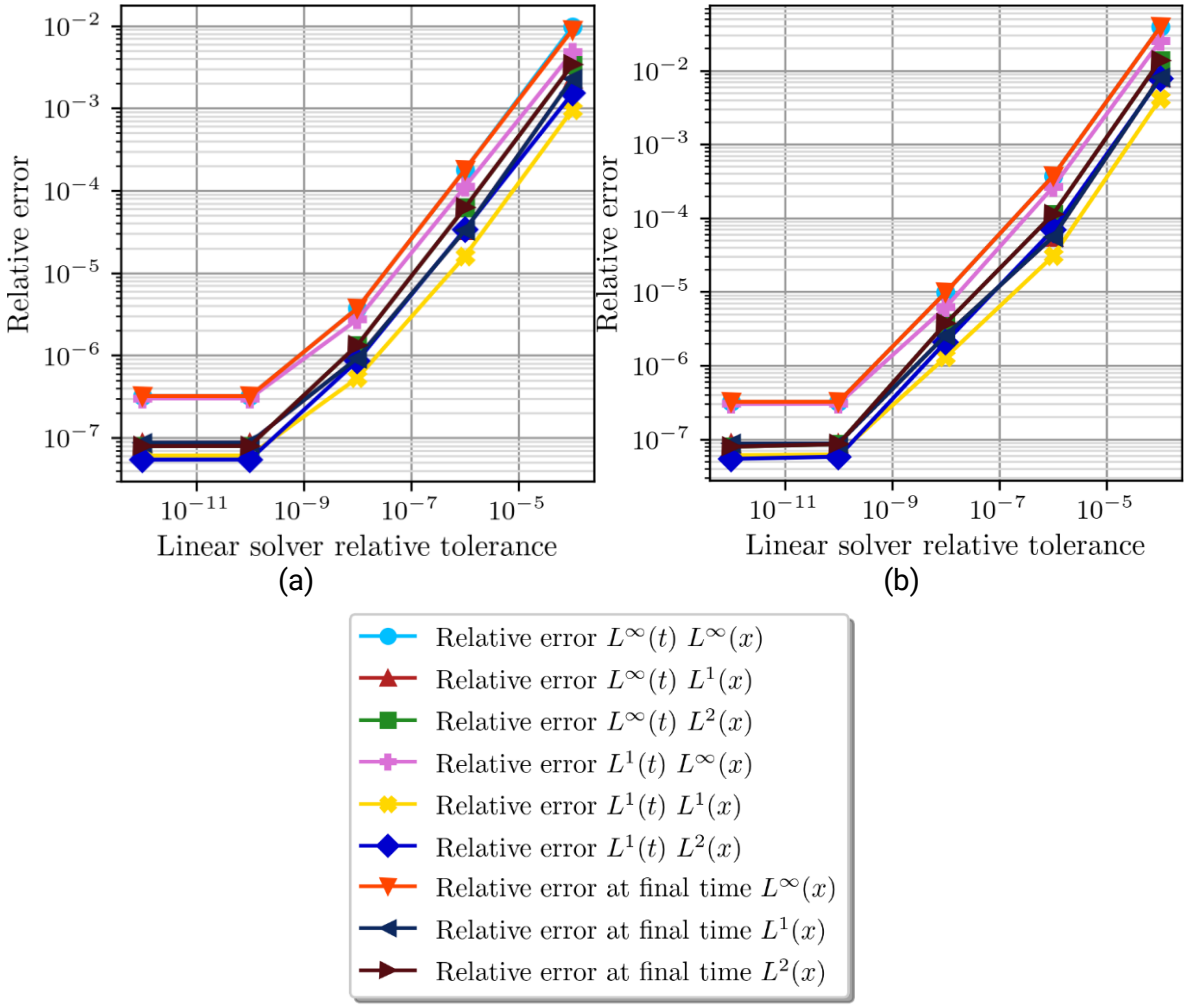

Figure 9: Errors with respect to relative tolerance of linear solver. Bidomain with bath problem, for the BICGSTAB (a) and GMRES (b) linear solver.

Error with respect to absolute tolerance

ε_r is set to 10^{-20}, and the maximum number of iterations to 5 000. Errors are reported on **Figure 10**.

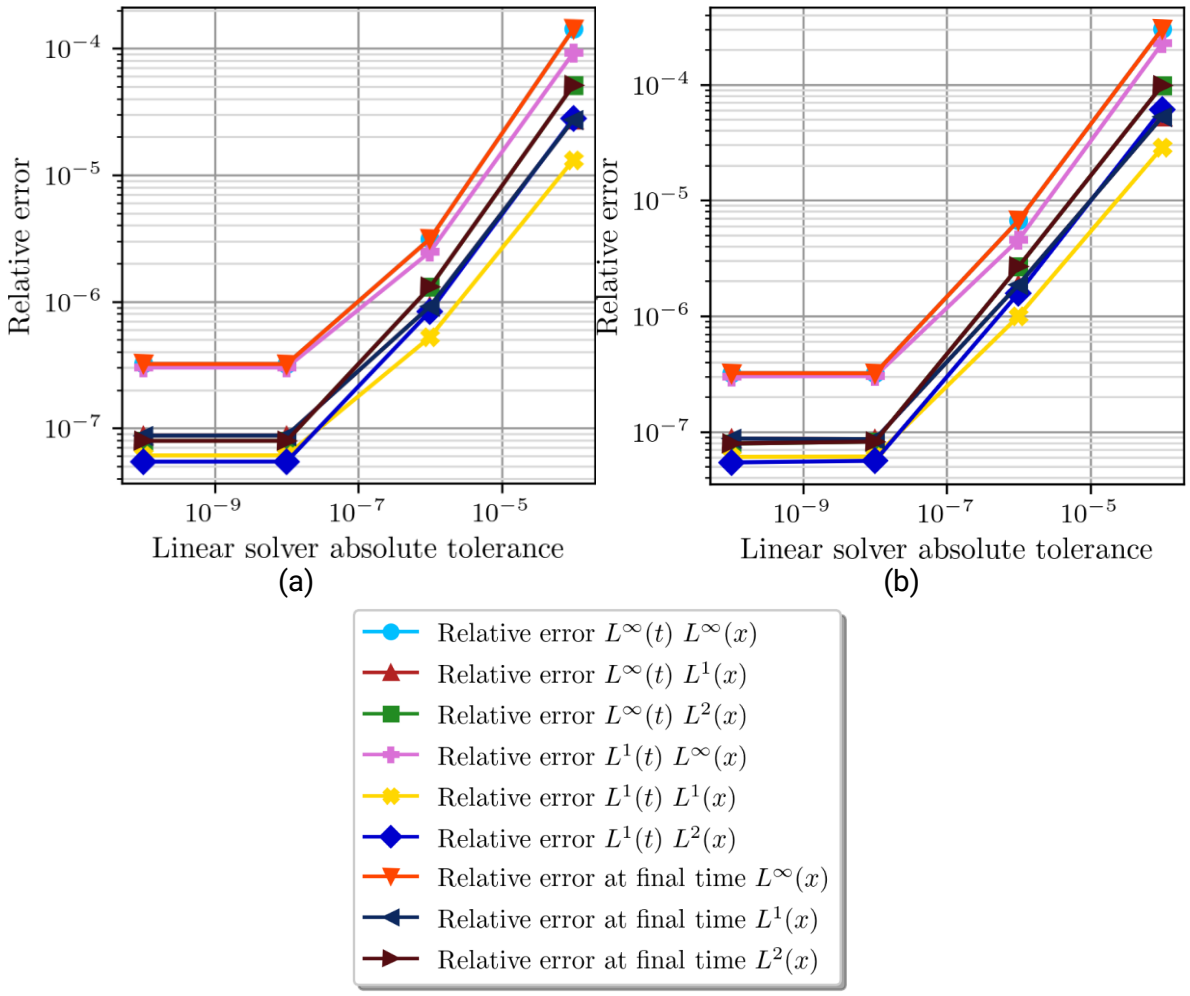

Figure 10: Errors with respect to absolute tolerance of linear solver. Bidomain with bath problem, for the BICGSTAB (a) and GMRES (b) linear solvers.

2.3 UC1 Model Validation – M30-M54 Activities

This section only contains additional Validation activities conducted on UC1 selected computational model during the M30-M54 period. Validation activities conducted during the M1-M30 period are already reported in the UC1 section of deliverable D6.2. Results reported in this section are meant to complete or (in some cases) supersede results of deliverable D6.2. The latter case will be explicitly mentioned, when applicable.

2.3.1 Computational Model Form

The 3D mathematical model that we derived to answer our QI consists of a partial differential equation which is well-known in the electrophysiology community (bidomain with bath), and an ordinary differential equation system that models the circuitry of the pacemaker. The two compartments are coupled via a boundary condition that depends on time, which is not standard for electrophysiology models. To validate our choice of model, we proved mathematically the existence and uniqueness of solutions to our problem, using a generic formalism for pacing devices. This proof is already given in V. Pannetier's PhD thesis [6], and will be submitted as a journal paper.

2.3.2 Computational Model Inputs

The computational model inputs were described in D6.2, UC1 section. The simulation run for model validation used the following additional specifications:

- Geometry of the VEGA lead provided by MPC, and a generic cylindrical domain encompassing the cardiac tissue and bath.
- The contact parameters have values obtained after experimental calibration (see deliverable D2.3), Table 10.
- The conductivity coefficients are taken from the literature, Table 10.
- Parameters from the literature are considered for the ionic model (Beeler-Reuter [5]).
- The initial conditions are set to the equilibrium state of the ionic model.

Table 10: Simulation parameters for the 3D computational model.

Parameter	Symbol	Value	Unit
PSA and contact parameters			
Pulse equivalent capacitance	C	4.97	µF
Opposite discharge equivalent capacitance	C	10.63	µF
Equivalent resistance	R	0.13	kΩ
Tip equivalent capacitance	C_0	18.74	µF
Tip equivalent conductance	G_0	0.5	mS
Ring equivalent capacitance	C_1	5.55	µF
Ring equivalent conductance	G_1	33.33	mS
3D model parameters			
Membrane surface per unit volume	X	2 500	cm
Extracellular conductivity, fiber direction	$\sigma_{e,l}$	3.91	mS cm^{-1}
Extracellular conductivity, transverse direction	$\sigma_{e,t}$	1.97	mS cm^{-1}
Intracellular conductivity, fiber direction	$\sigma_{i,l}$	1.74	mS cm^{-1}
Intracellular conductivity, transverse direction	$\sigma_{i,t}$	0.19	mS cm^{-1}
OD model parameters			
Membrane surface	S_m	15	cm^2
Surface extracellular conductance	g_e	$1.33\,10^{-3}$	mS cm^{-2}
Surface intracellular conductance	g_i	$3.33\,10^{-3}$	mS cm^{-2}

Complete sensitivity analysis was carried out for these contact parameters, and equivalent parameters in a surrogate 0D model (explained in deliverable D2.3), given also in Table 10. Computations with these parameters have been published [7], sensitivity analysis and statistical properties have been documented in deliverable D5.5 (cf. [6] and [8]).

2.3.3 Comparator Description

2.3.3.1 Comparator 1 – Lapicque Curve

We realized computational capture tests with the goal of reproducing experimental Lapicque curves [9].
Since 3D simulations are very expensive computationally, it is impossible to reproduce exactly the experiments that generated Lapicque curves. It is in particular impossible to use the same criterion to determine whether cardiac tissue is captured or not by the pacemaker. During the experiments,

capture is assessed with both an ECG and the expertise of our collaborator in electrophysiology. For 3D simulations, we consider a slab of tissue to be captured when we see an increase of the volume of "activated" tissue (i.e. for which the transmembrane voltage passes an activation threshold), during the first milliseconds after pulse delivery. We also ran simulations with a surrogate 0D model which is significantly less expensive. With this model, we can simulate all the consecutive experimental stimulations. Capture is then determined from the whole time-series of the transmembrane voltage of the in silico experiment.

2.3.4 Comparator – Test Samples

2.3.4.1 Comparator 1 – Lapicque Curve

Experimental Setup and Main Recordings

Cardiac ventricular wedges from sheep aged 1-2 years old were prepared as described in [10] and stretched on a frame to immobilize the tissue in a bath of saline solution **Figure 11** (left). The MICROPORT CRM VEGA bipolar pacing lead was implanted (fully deploying its screw fixture) at a maximum of three locations in the right ventricle (RV), among apex, septum and base, depending on the animal. It is implanted in the RV septum, as shown in **Figure 11**. A total of seven animals were used, including two with an induced infarct scar, Table 11. A pseudo ECG from distant electrodes, and the voltage between the ring to the tip electrodes of the lead were recorded simultaneously by an external device (PowerLab, ADInstruments). The measured voltage has a large deflection during pulses, which last 0.25 ms to 2 ms, as can be seen on **Figure 11** (top-right). We could record these fast events with a sufficient resolution of 100 kHz only for the last five animals.

Table 11: **Summary of animal experiments. The given number of stimulations is an estimate and does not exclude data that could not be used.**

N.	Date	Type	Implantation sites	Generator	Lead(s)	Camera Pixel count	Stim. freq. (BPM)	#stims
1	07/060/2022	healthy	apex	Borea	Vega	100	90	~100
	Pilot experiment. Noise from power outlets in measurements. The tissue slab was placed in the MR scanner in a folded position.							
2	08/11/2022	healthy	apex, base, septum	Borea	Vega	256	90	~320
	No MR scan.							
3	18/10/2023	healthy	apex, septum	Borea	Vega	256	90	~1500
	Ectopic beats with >90bpm frequency.							
4	04/06/2024	infarct	apex, mid	PSA	Vega	256	120	~1500
	Small scar, large moderator band.							
5	05/06/2024	healthy	apex, mid	PSA	Vega, Solia	192	120	~2000
	RAM issues (too much data), optical window was scaled down. Solia lead could not be tested at mid location due to tissue fatigue.							
6	06/06/2024	healthy	mid	PSA	Vega, Solia	192	120	~1000
	Two papillary muscles.							
7	07/06/2024	infarct	apex, mid	PSA	Vega	256	120	~1500
	Recurring ventricular tachycardia, lower signal to noise ratio in ECG. Lots of fat.							

Experimental Capture Test

Capture is detected by applying pulse trains of fixed duration D, and decreasing the voltage V from train pulse to train pulse, starting by capturing values until capture is lost. The actual threshold is located in the interval between the last value that captures V^c (D), and the first value that loses capture V_c (D). Capture occurs when an action potential has been triggered by the pulse, as observed on the pseudo ECG. **Figure 11** (top-right), shows such a transition from capturing (V^c = 0.5 V) to non capturing (V_c = 0.4 V), using trains of eight pulses of duration D = 1 ms at 1.5 Hz. As a consequence, the accuracy of the localization of the curve depends on the time and voltage resolution of the pulse generator. We report here capture data recorded with a Pacing System Analyzer (PSA) instead of a traditional pacemaker, because of its higher voltage and time resolution. Example experimental Lapicque curves obtained by this process with trains of eight pulses at 1 or 1.5 Hz are reported on **Figure 13**, where the coloured region are between the upper and lower bounds V^c and V_c. Data shows curves for several healthy implantation sites stimulated by the PSA, with recorded voltages at 100 kHz. For instance, for each of the 24 durations allowed by the PSA, searching for the threshold requires to pace the tissue 56 times on average (i.e. to test 7 amplitudes with trains of 8 pulses each). The total duration to obtain the Lapicque curve at a single site is around 30 min.

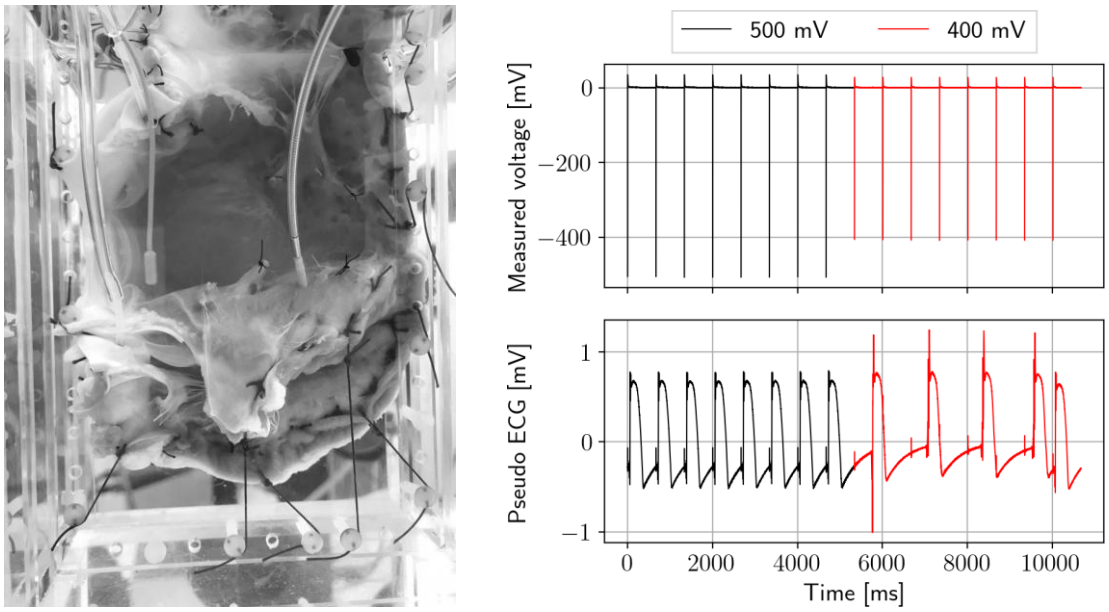

Figure 11: Photography of the tissue preparation in sheep heart #3 experiment (left), measured voltage at device pins (top-right), and the corresponding pseudo ECG recorded (bottom-right) during a threshold search, with a pulse duration of 1 ms. The pulses with amplitude of 0.4 V (in red) resulted in non-capturing stimulations. The action potentials in red are those of ectopic beats. This is deduced from their asynchronicity with the pacemaker stimulations, and corroborated with optical maps (not shown here).

2.3.4.2 Comparator 2 – Optical Map

In parallel of the capture tests described in the previous section, propagation of the action potential on the surface of the endocardium and epicardium were recorded for each sheep, using standard optical mapping techniques [10], as shown on **Figure 12** (left). Additionally, we imaged the structure of the tissue at high resolution using 9.4T MR, for the sheep #4 to 7. We do not have the images of sheep #1 to 3 as they were used to alleviate the technical difficulties of the procedure. An example of the segmentation of the ventricle of sheep #4 is given on **Figure 12** (right). As shown, the ventricle was put back into its resting state in order to fit into the small bore of the MR machine. Unfortunately, this prevents us from comparing directly experimental activation maps with simulated ones, which can only be computed on the folded ventricle mesh. The deformation is too large to project activation data onto the mesh.

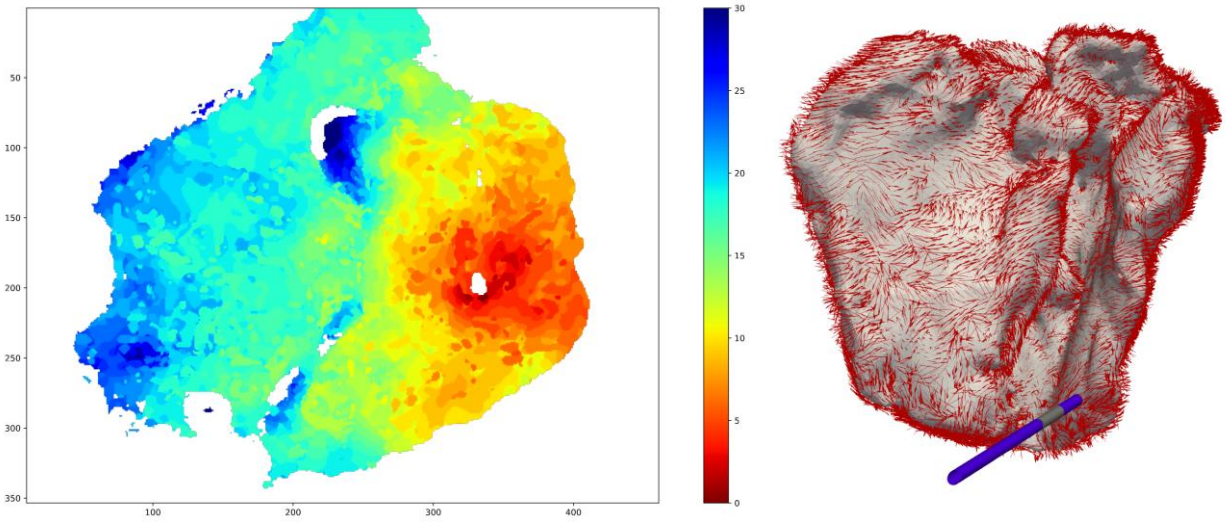

Figure 12: Left: endocardial activation map obtained from sheep #1 experiments. Right: segmented mesh from sheep #4, with fibre direction imported from the MR sequences. The pacemaker lead has been added to the mesh.

2.3.5 Output Comparison

2.3.5.1 Comparator 1 – Lapicque Curve

The Lapicque curves obtained with both models are reported in **Figure 13**, as well as some curves from the sheep experiments. The threshold curves vary significantly, even for the same animal. This variability can be explained by the variability between animals, the tissue structure at the implantation sites, by uncertainty on the insertion depth, and by the degradation of the myocardium during an experiment that lasts several hours. Our model has not been calibrated yet, and hence cannot explain these variations. However, simulations provide curves with a profile similar to the experimental ones, and with the correct order of magnitude, even with standard parameters. This semi-quantitative agreement is encouraging for the forthcoming work of calibrating the models to this data.

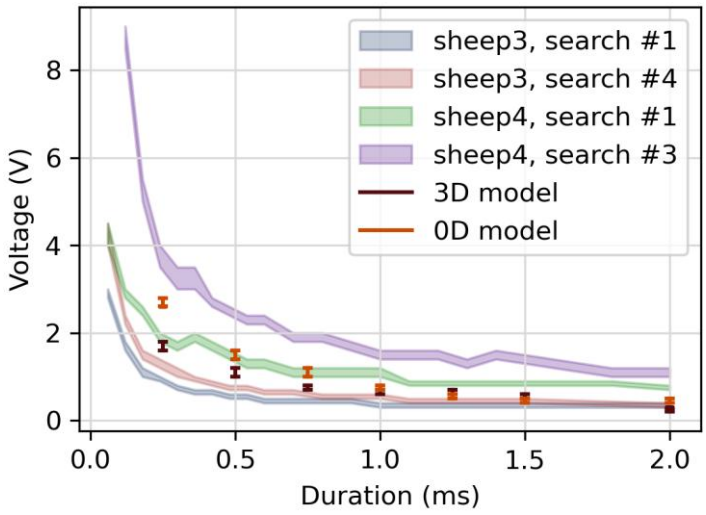

Figure 13: Experimental stimulation threshold detection intervals (filled), for two out of seven sheep ventricles. Search numbers indicate different implantation sites. Intervals marked with brackets are from the computational models.

2.4 UC1 Uncertainty Quantification – M30-M54 Activities

No additional specific Uncertainty Quantification (UQ) activities were conducted during M30-M54 in the frame of UC1 model credibility assessment. Uncertainty Quantification results and discussion in deliverable D6.2 apply. Moreover, sensitivity analysis results and statistical studies detailed in deliverable D5.5 provide a first analysis of the effect of some sources of uncertainty, notably the device parameters and conductivity coefficients.

2.5 UC1 Model Applicability – M30-M54 Activities

No additional specific Model Applicability activities were conducted during M30-M54 in the frame of UC1 model credibility assessment. Applicability discussion in deliverable D6.2 apply.

2.6 UC1 Discussion

We have been able to entirely execute the verification activities initiated in deliverable D6.1, and even add additional verification activities, e.g. running the FDA tests on manufactured solutions. The validation activities have been carried out, and we obtained satisfactory results for comparator 1 (Lapicques curves) with biological parameters (ionic ones, and tissue conductivity) from the literature.

Comparator 2 (optical maps) could not be setup for technical reasons: the deformation of the tissue sample between optical ex-vivo experiments and final post-mortem structure imaging is too large for standard registration tools to apply, so that the comparison was not possible. The computational software code has been delivered to IST for integration on the web-based platform, where verification tests will be also executed to ensure that the integrated model performs ad intended, and that the integration process did not affect the numerical outcome and the credibility level of the model.

A complementary statistical analysis has been carried out and has been explained in deliverable D5.5. It tends to show that a deterministic comparator, like comparator 1, badly accounts for the high variability across biological samples. This is especially true for capture, because it is a threshold, so that it probably follows a Bernoulli law, with a bimodal distribution of the output. In the context of threshold detection, a goal-oriented statistical comparator would be more relevant. For instance, comparing the probability of capture at one (or a few) relevant points of the Lapicque plane would be of interest. Finally, this issue concerning the comparison methodology is a known bias of ASME V&V40 approach, as also discussed in deliverable D6.4.

Table 12: Credibility Factors Coverage Level for Use Case 1 (cf. ASME VV40).

Model Risk				x			
Credibility Factor Coverage Level		1	2	3	4	5	
Code Verification: Software Quality Assurance	V		x				
Code Verification: Numerical Code Verification - NCV	V		x				
Calculation Verification - Discretization Error	V		x				
Calculation Verification - Numerical Solver Error	V		x				
Calculation Verification - Use Error	IV		x				
Validation - Model [Form]	III		x				
Validation - Model [Inputs]	III		x				
Validation - Comparator [Test Samples] [3]	II		x				
Validation - Comparator [Test Conditions]	II		x				
Validation - Assessment [Input Parameters]	III		x				
Validation - Assessment [Output Comparison]	II		x				
Applicability: Relevance of the Quantities of Interest	V		x				
Applicability: Relevance of the Validation Activities to the COU	V		x				

2.7 UC1 – VVUQ Publications

This section lists all scientific publications relating to the UC1 VVUQ activities conducted within the frame of the SimCardioTest project.

Table 13: UC1 – List of publications related to VVUQ activities.

Reference	VVUQ Topic
Pannetier et al. (FIMH 2025) [7]	Validation
Pannetier et al. (FIMH 2023) [9]	Validation
Pannetier et al. (CANUM 2024) [11]	Validation

[3] Initially set to "Level IV", the coverage level for the Validation - Comparator [Test Samples] credibility factor has been decreased to "Level II" to account for all the technical difficulties encountered during the real experiments and the fact that one animal intended for the validation died before testing (thus diminishing the initial sample size). The new coverage level is still sufficient to cover the assessed model risk.

Reference	VVUQ Topic
Pannetier (PhD) [6]	Validation, Verification, Uncertainty Quantification
Pannetier et al. (CINC 2024) [8]	Uncertainty Quantification
Pannetier et al. (VPH 2024) [12]	Validation
Leguèbe (draft) [13]	Verification

3. Use Case 2

3.1 UC2 Model Summary

3.1.1 Background

Atrial fibrillation (AF) is considered the most common of human arrhythmias. AF is currently seen as a marker of an increased risk of stroke since it favours thrombus formation inside the left atrium (LA). Around 99% of thrombi in non-valvular AF are formed in the left atrial appendage (LAA) [14]. LAA shapes are complex and have a high degree of anatomical variability among the population [15]. Percutaneous left atrial appendage occlusion (LAAO) can be an efficient strategy to prevent cardioembolic events in selected non-valvular AF patients, as an alternative to life-long oral anticoagulation (OAC) [16], as shown in large clinical trials (ACP Multicentre [17], EWOLUTION [18]), where LAAO procedures demonstrated non-inferiority. However, a successful implantation of LAAO devices remains a challenge in some cases, due to the complexity of LA geometry. Sub-optimal LAAO settings can lead to device-related thrombosis (DRT), i.e., a thrombus formed at the device, becoming a major concern [19] since it can lead to stroke. Based on the Virchow's triad, three factors are thought to contribute to thrombus formation: hypercoagulability, endothelial injury (replaced by a nitinol surface after LAAO) and blood stasis [20]. Related to the latter, key hemodynamic factors with demonstrated influence in thrombus formation in LAAO include (see Figure 14):

1. Occluder design and position: The geometry and characteristics of the occluder device can impact the flow patterns in the left atrium. Different occluder designs, such as shape, size, and surface properties, can influence the likelihood of thrombus formation. The position and alignment of the occluder within the left atrium can affect the flow patterns and the likelihood of thrombus formation. For instance, covering the pulmonary ridge (see Figure 15) may have a protective effect regarding DRT. Studying different occluder positions can help determining the optimal placement to minimize the DRT risk.

2. Blood flow velocity: Areas with low flow velocity or regions of recirculation may be prone to stasis and clot formation.

3. Blood viscosity: Altering the viscosity can provide insights into how changes in blood composition or conditions, such as hematocrit or temperature, affect thrombus formation. Parameters related to blood coagulation, such as platelet activation or coagulation cascade dynamics, can be simulated to understand their impact on thrombus formation.

4. Wall shear stress: Wall shear stress is the frictional force exerted by the flowing blood on the atrial wall. Low wall shear stress regions can be associated to thrombus formation. Evaluating different wall shear stress levels can help identify critical areas. Wall injuries due to abnormal stresses can also be caused by the device deployment.

To avoid blood stasis, it is crucial to properly choose the type of device and the position where the device is going to be deployed. Thus, different planning tools has emerged to find the optimal device configuration for each patient such as the commercial products from FEOPS [21] and Pie Medical [22], or the VIDAA platform [23], developed by UPF. However, none of these solutions include functional information on blood stasis, which is key for assessing the risk of DRT. In-silico computational fluid dynamic (CFD) can help to describe and relate patient-specific LA/LAA morphology and complex hemodynamics to understand the mechanism behind thrombus formation. Moreover, computational models of the blood flow can be used to predict the effectiveness of LAAO devices, to evaluate new device designs, and to better understand clinical outcomes such as DRT.

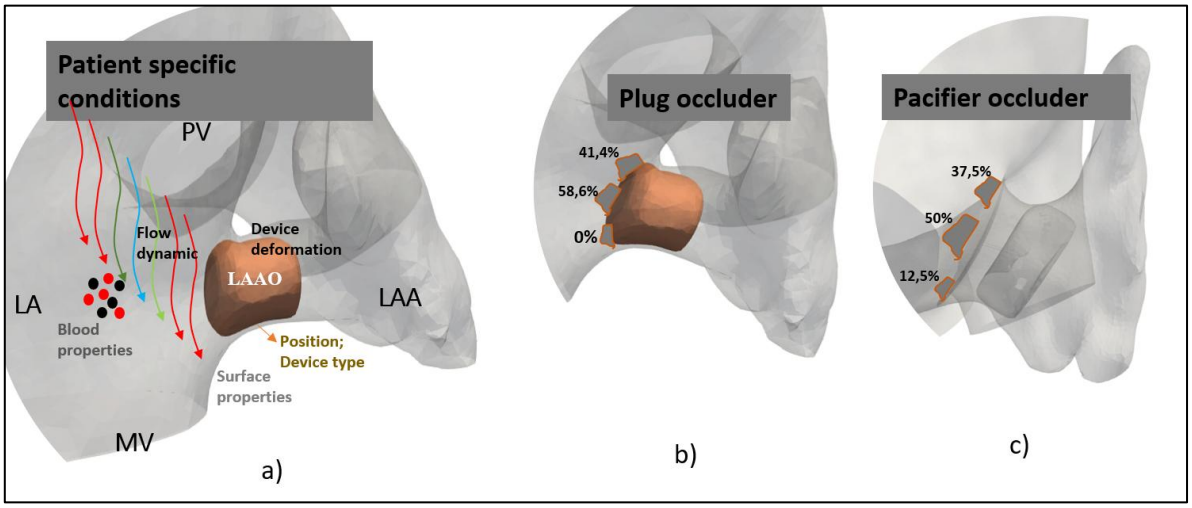

Figure 14: a) Principal factors associated to thrombus formation, including blood properties, device type and positioning. b,c) Percentages of device-related thrombus (DRT) in different parts of the device, reported in Sedaghat et al. [19] for the plug- and pacifier-type of occluder devices (b and c, respectively). LAAO: left atrial appendage occluder. MV: mitral valve. PV: pulmonary veins.

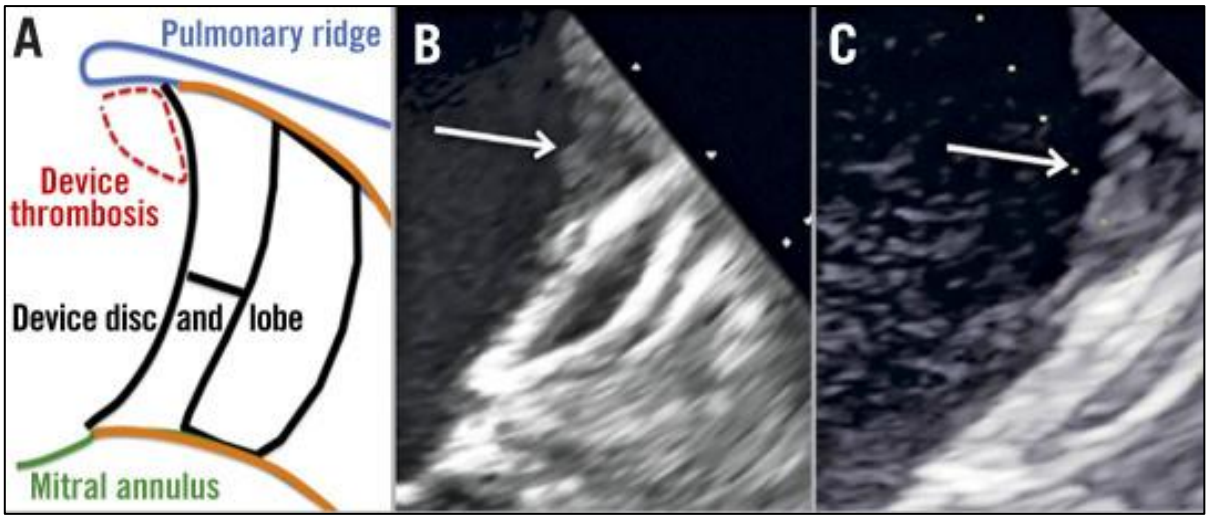

Figure 15: Influence of covering the pulmonary ridge (PR) for avoiding device-related thrombosis, from Freixa et al. ***[24].*** *The arrows point to uncovered PR where thrombus is found after left atrial appendage occluder implantation.*

3.1.2 Device Description

Left atrial appendage closure devices (see Figure 16) are used to reduce the risk of stroke in patients with atrial fibrillation by occluding or sealing off the left atrial appendage, which is a small pouch-like structure in the heart where blood clots can form. Here are two commonly used device types:

1. Plug-Type Devices
   - Plug-type left atrial appendage occluders are designed to completely seal off the left atrial appendage (LAA). These devices typically consist of a self-expanding frame or mesh structure that fills and completely occludes the LAA, preventing blood flow into the appendage. The frame or mesh is often covered with a fabric or membrane material to enhance closure.
   - The Watchman device is an example of a plug-type occluder. It is developed by Boston Scientific, and it is a fabric-covered, self-expanding nitinol frame with fixation barbs. It is delivered through a minimally invasive procedure and placed in the left atrial appendage to block blood flow, thereby preventing blood clots from forming and potentially causing a stroke.

2. Pacifier-Type Devices
   - Pacifier-type left atrial appendage occluders, as the name suggests, partially occlude the LAA while allowing some blood flow to continue. These devices have a central channel or opening that allows limited blood flow through the LAA while reducing the risk of blood clot formation. This design is intended to maintain some physiological flow patterns and potentially reduce the risk of complications associated with complete occlusion.
   - The Amplatzer Amulet device is an example of a pacifier-type occluder. It is manufactured by Abbott and it consists of a self-expanding nitinol frame covered with a permeable polyester fabric. Similar to the Watchman, it is implanted in the left atrial appendage to close it off and reduce the risk of stroke.

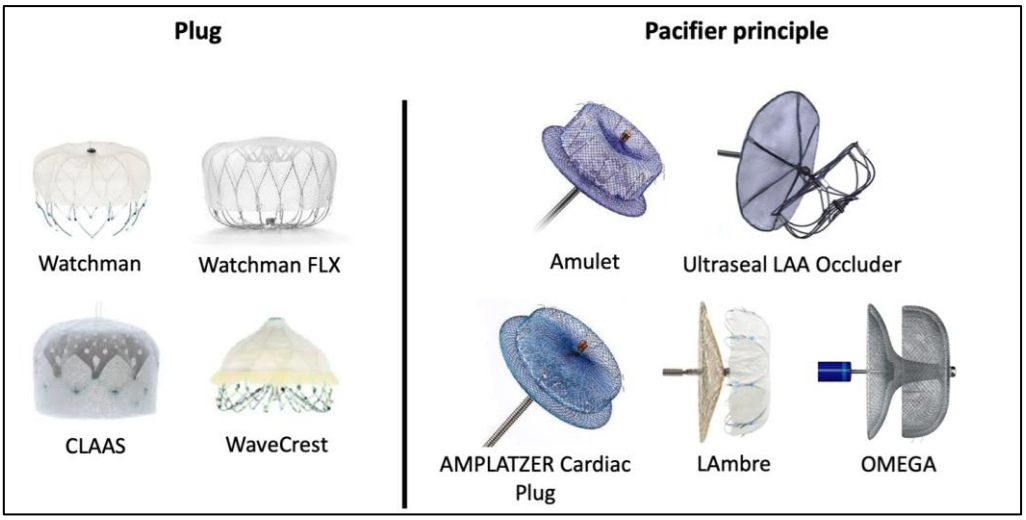

Figure 16: Types of left atrial appendage devices, classified as plug or pacifier types. The most used devices are the Watchman and Watchman FLX (plug-type), developed by Boston Scientific (left), and the Amplatzer Amulet device (pacifier-type), manufactured by Abbott (right).

3.1.3 Question of Interest

Several relevant questions of interest (QI) can be answered by computational fluid simulations applied to left atrial appendage occluder devices, encompassing different aspects of the device design and applicability. The different stakeholders involved in SimCardioTest, including device manufacturers, clinicians and academic partners defined multiple QIs during the project, which were ranked based on the most critical aspects to study in relation to possible adverse events during the implantation, especially regarding DRT. The QI that had the maximum level of priority and feasibility, being selected to guide the V&V exercise of Use Case 2 according to ASME VV40 guidelines, is the following:

- Does covering of the pulmonary ridge with a LAAO device (plug or pacifier) relate with the likelihood of low blood flow velocities around the device and induce the device-related thrombus (DRT)?

The QI above follows the formulation found in pioneering V&V works on cardiac devices [25] and studies the influence of device settings (type and position) in relation to DRT by measuring low blood flow velocities.

3.1.4 Context of Use

From the selected QI, two different Contexts of Use (COU), assessing the device performance, were defined. These COUs have different level of influence on the decision of whether the covering of the pulmonary ridge (PR) with the LAAO device is equivalent to or better than placing it deeper into the LAA (i.e., with an uncovered PR). In both cases, the computational model is used to assess blood flow velocities near the device. The performed evaluations are based on two different cohorts, depending on the COU. In the first COU, pre-operative and follow-up imaging data from twenty patients who underwent LAAO has been used, half of them suffering DRT. The second COU is based on a set of two patient-specific geometries obtained from clinical cases: one suffer from AF, and the other acts as a control case.

- **COU1** - Performance evaluation with computational fluid simulations only. Computational modelling is used to identify low blood flow velocities near the device, placed in a proximal or distal position (e.g., covering or not the PR) with both device types (i.e., plug and pacifier). There is no supporting data from in-vitro testing available for assessing the performance of the occluder devices.

- **COU2** - Performance evaluation with computational fluid simulations and in-vitro data. In addition to in-silico experiments, in-vitro testing is conducted to create additional evidence on whether the covering of the PR is critical for DRT with both types of device.

3.1.5 Model Risk

The following considerations support the assessment of the risk associated with the numerical model.

- Decision Consequence: Medium

Based on VV40 guidelines, both COUs have a Medium consequence since the intended users are engineers from manufacturers, using computational fluid simulations and in-vitro testing experiments to optimize the design of next-generation occluder devices and provide better implantation guidelines to prevent DRT. If simulations and experiments are incorrect (i.e., under- or over-estimating the risk of DRT), they could lead to sub-optimal design of new devices and recommendations, potentially increasing abnormal events after implantation such as device embolization, DRT or peri-device leaks.

- Model Influence for COU 1: High
- Model Influence for COU 2: Medium

Based on VV40 guidelines, COU1 has a High influence because the computational model results are the only ones informing the decision. COU2 has a Medium influence because supporting data from in-vitro testing complement the computational modelling studies.

- Model Risk for COU 1: 4/5 (Medium-High)
- Model Risk for COU 2: 3/5 (Medium-Medium)

Model Risk is based on Decision Consequence and Model Influence stated above, according to Risk Matrix in Figure 17 (cf. section 1.2.5).

Model influence	**high**	**3**	**4 COU1**	**5**
	medium	**2**	**3 COU2**	**4**
	low	**1**	**2**	**3**
		low	**medium**	**high**
		Decision consequence		

Figure 17: Model Risk Matrix (cf. ASME VV40) evaluating the COU1 and COU2 included in UC2.

3.1.6 Model Description

Simulating blood flow in the left atrium with an implanted occluder device can indeed facilitate the identification of the parameters that may contribute to thrombus formation. By conducting blood flow simulations with the occluder device in place, researchers can explore the impact of various factors, such as the shape or position of the device, on flow characteristics and the potential for thrombus formation. The initial step involves processing patient-specific medical images to extract a three-dimensional model, followed by the building of an appropriate 3D volumetric mesh. In COU1, for each left atrial geometry, the two studied device positions (covering and uncovering the pulmonary ridge) have been previously defined. In COU2, fluid simulations from two patients are compared with an in-vitro setup. The blood flow magnitude and directions will serve as the primary parameters evaluated in the current V&V study, for detecting blood stagnation zones around the LAAO device.

As a previously required step for VV40 analysis of flow simulations with LAAO devices, verification and validation experiments to assess the credibility of blood flow simulations in the left atria without a device are also required. In SimCardioTest, we performed the largest VV40 study available in literature for such type of simulations, testing several numerical parameters in mesh and time-step convergence analysis, as reported in SCT deliverable D3.2, and recently published [26]. This study contributed to identify most of the numerical parameters to be used in fluid simulations of the left atria. The rest of the document will mainly focus on the complementary VV40 experiments performed on simulations including LAAO devices.

3.2 UC2 Model Verification – M30-M54 Activities

No additional specific Verification activities were conducted during M30-M54 in the frame of UC2 model credibility assessment. Verification results and discussion in deliverable D6.2 apply.

3.3 UC2 Model Validation – M30-M54 Activities

This section only contains additional Validation activities conducted on UC2 selected computational model during the M30-M54 period. Validation activities conducted during the M1-M30 period are already reported in the UC2 section of deliverable D6.2. Results reported in this section are meant to complete or (in some cases) supersede results of deliverable D6.2. The latter case will be explicitly mentioned, when applicable.

3.3.1 Comparator – Test Conditions and Validation Results from the In-Vitro Set-Up developed in MIT

As we mentioned in deliverable D6.2, one of the most important advantages of the in vitro experimental set-up developed by MIT is the ability to include left atrial movement, thereby differentiating between movements for patients with atrial fibrillation and healthy atrial movements. The motion generated from the placement of actuators along these key regions, guided by fibre orientation, was validated through M-mode ultrasound imaging (**Figure 18**a). The input pressure for these actuators was systematically varied from 0 to 40 psi to assess the range of wall displacement. Ultrasound imaging (**Figure 18**b) confirmed the effectiveness of individual actuators in producing tunable wall motion. These results demonstrated that the actuators could reliably replicate both

healthy and AF contractile behaviour. This biomimetic contractile motion can support the ejection of blood from the LA and LAA and prevent stagnation, critical for reducing thrombus formation in healthy physiology.

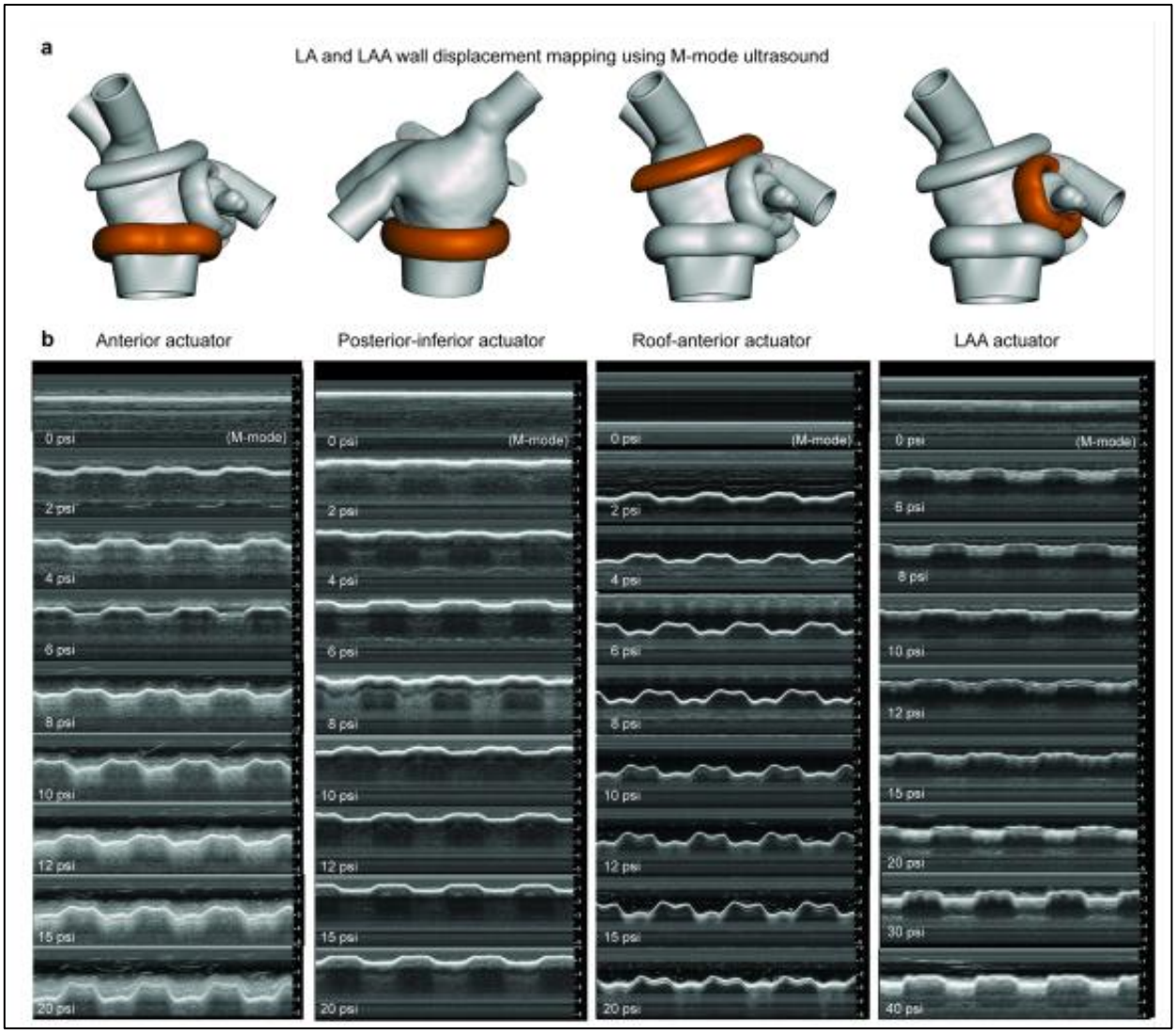

Figure 18: Soft robotic actuator positioning influences left atrium (LA) and left atrial appendage (LAA) wall motion and displacement under varying pressures. (a) Different configurations of soft robotic actuators wrapped around the LA and LAA structures at distinct anatomical orientations (highlighted in orange), impacting the extent of wall motion and direction of simulated atrial contraction. (b) M-mode ultrasound images capturing wall displacement at increasing actuator pressures ***[27]****.*

The circulatory flow loop developed by MIT was specifically designed to simulate systemic circulation, incorporating adjustable parameters such as preload, afterload, vascular compliance, and resistance (**Figure 19**). The system utilized two clinically standard mechanical valves (mitral and aortic) to ensure unidirectional flow through the circuit, with the soft robotic LV functioning as the primary pump to drive fluid flow. The actuation of soft robotic elements on the LA and LAA successfully replicates the atrial kick, a dynamic contraction crucial for active ventricular filling, which cannot be achieved with passive 3D-printed models. The soft robotic LV generated biphasic

ventricular pressures (120/6 mmHg) and drove systemic circulation, producing phasic aortic systemic pressures of 115/60 mmHg at a sinus rhythm of 60 bpm. When combined with the soft robotic LA, the system reproduced physiologically accurate flow waveforms for left-sided circulation. The system demonstrates alternating mitral and aortic flow, with a cardiac outflow of over 5 L/min. The mitral valve flow waveform exhibited distinct E and A wave regions, representing passive ventricular filling during early diastole and active filling driven by atrial contraction, respectively. These findings confirm the capability of the soft robotic LA to contribute to active ventricular filling, mimicking the functional role of atrial contraction in the cardiac cycle. Pulsed wave Doppler imaging was used to measure fluid flow velocities in the soft robotic LA, visualizing E and A wave patterns associated with mitral flow.

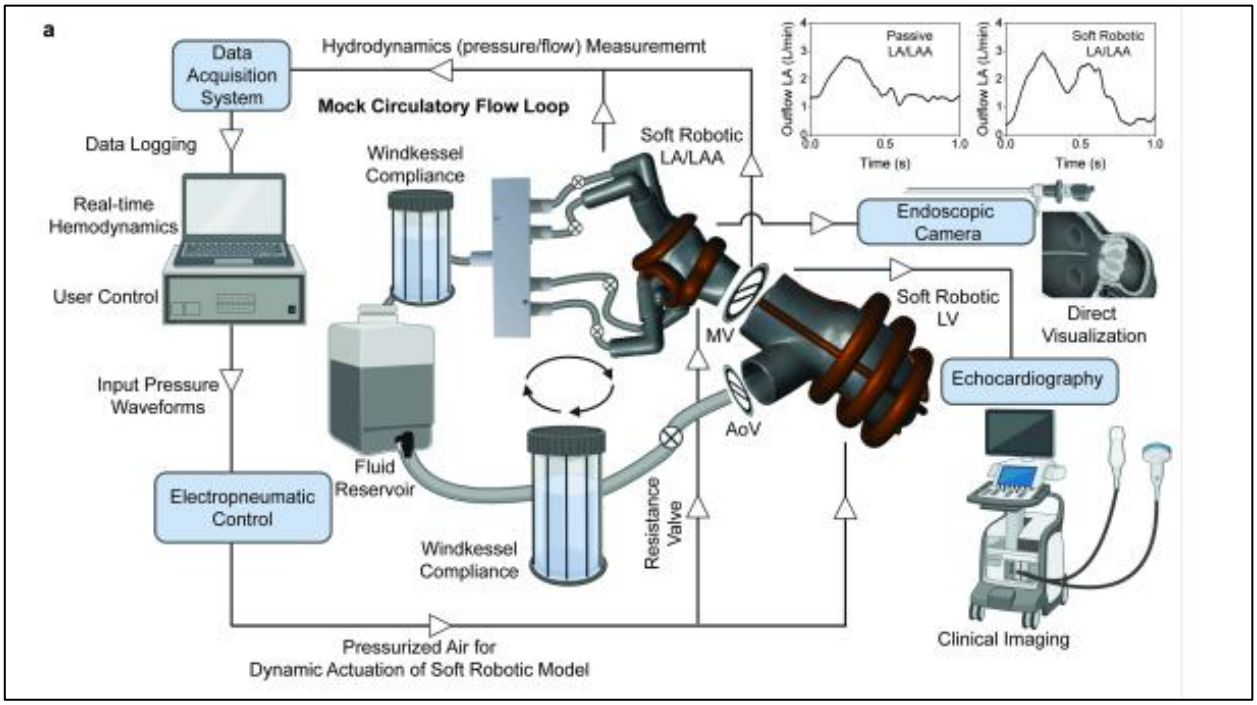

Figure 19: A mock circulatory flow loop enables hemodynamic measurements in the soft robotic left heart simulator. (a) Schematic of the mock circulatory flow loop with components to replicate cardiac and vascular hemodynamics, including the soft robotic left atrium (LA) left atrial appendage (LAA), and left ventricle (LV) models. The circuit includes mechanical mitral valve (MV) and aortic valve (AoV) components, which are essential for simulating unidirectional flow [27].

Figure 20 shows the patient model used in the experiments, where an initial planning was performed using VIDAA software and then a mesh cut. The resulting geometry was 3D printed with the materials and technology described in previous deliverables. The locations where the measurements were acquired are marked in the figure; this proved to be relevant for comparison purposes. Therefore, results are shown with pulmonary vein lengths with normal dimensions and others with elongated dimensions that represent the area where the measurements were actually taken. The experimental and simulation results show better fits in the models with elongated veins, as shown in **Figure 21**.

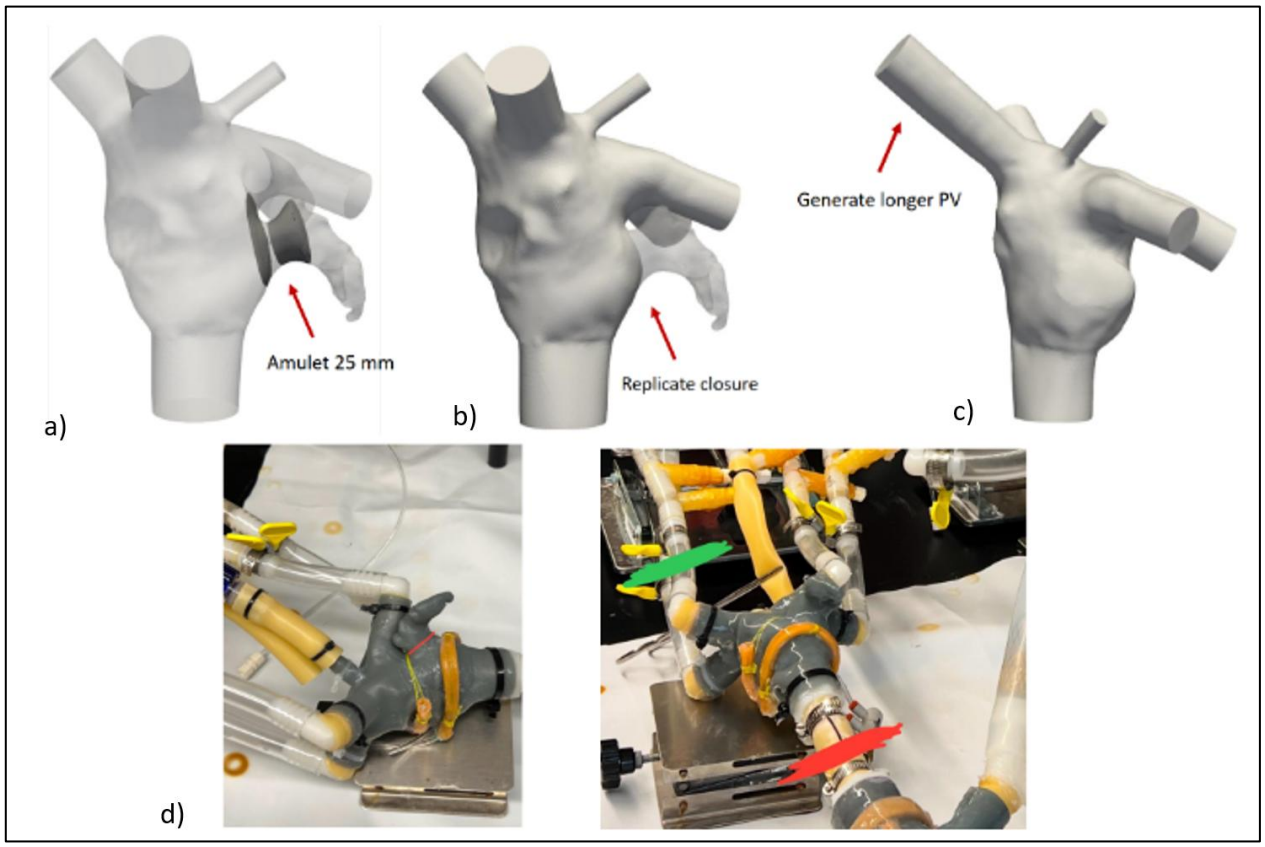

Figure 20: a) Left atrial model with occluder. b) Approximation of the 3D atrium with the occluder, printed for in vitro testing. c) Subsequent adaptation of the CFD model with the generation of longer PV to obtain parameters in areas similar to those measured in the (d) in vitro test (marked in green and red).

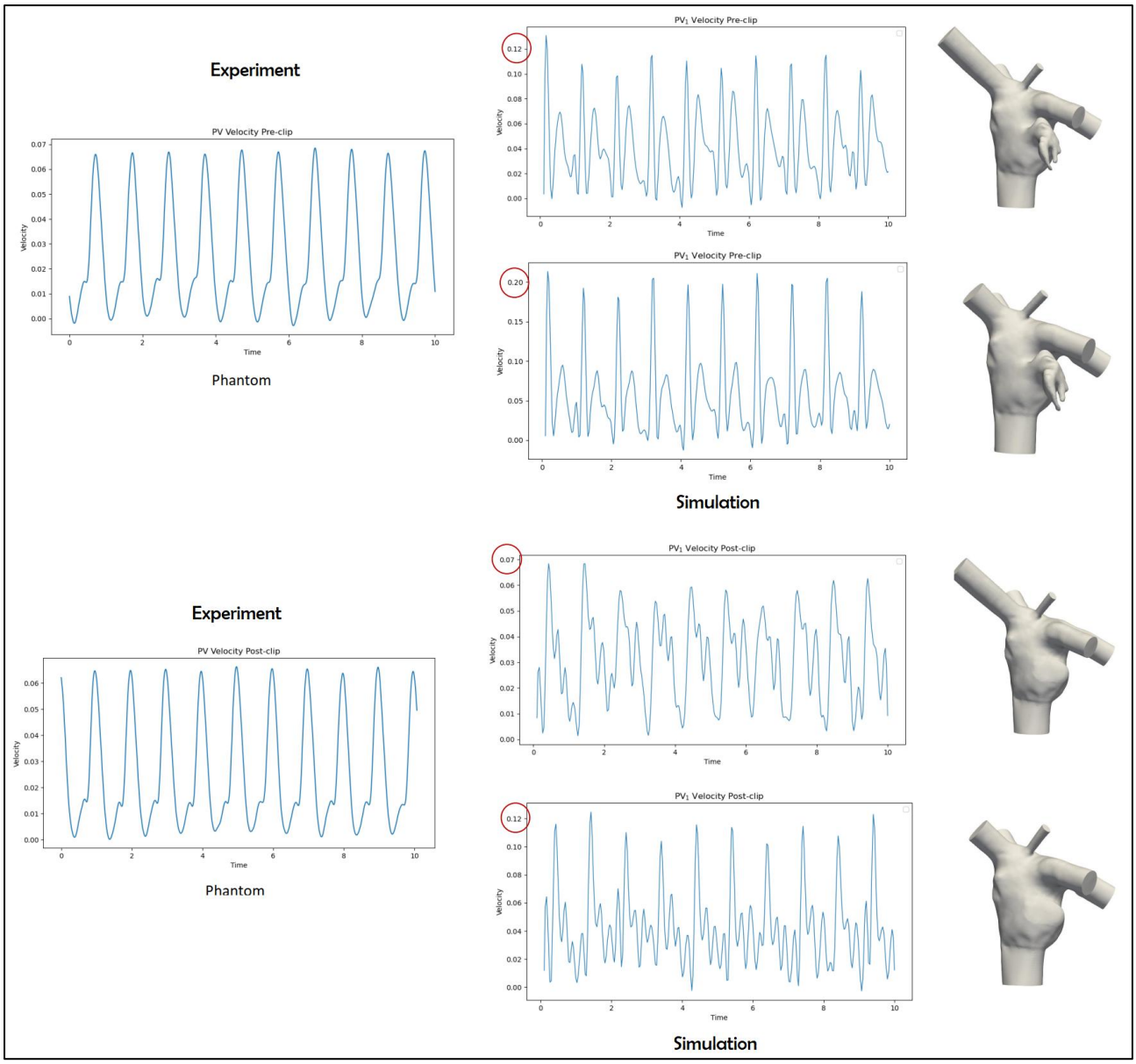

Figure 21: Comparative results of pulmonary vein velocities before and after LAAO implantation measurements in experiments and simulations. The elongated veins and their original configuration were compared in order to obtain a better calibration of the results in relation to where the sensors were placed.

3.3.2 Comparator – Test Conditions and Validation Results from the In-Vitro Set-Up developed in BioCardioLab

In collaboration with BioCardioLab (Massa, Italy) a new left atria simulator for the fluid dynamic was created. Using computed tomography (CT) images, a three-dimensional LA with LAA model was generated and then properly fabricated. The model was integrated into a mock circulatory loop, and fluid dynamic under physiological conditions was evaluated using particle image velocimeter (PIV) technique.

The model of the LA phantom was obtained by segmenting the CT dataset, the same patient using in the others experiments with MIT. The phantom was realized in Sylgard 184 silicone (Dow, Wiesbaden, Germany), given its optical properties and its compliance (Young's modulus of 2 MPa and Poisson modulus of 0.495) with the PIV technique. Two molds were designed and realized to manufacture the silicone phantom, the inner core and the external mold (**Figure 22** b-c). The inner core consists of the inner surfaces of the phantom. It was made of ABS using Fused Deposition Modeling (**Figure 22**d) and then underwent acetone vapours treatment to obtain smooth surfaces suitable for PIV investigation. The external mold was designed by outwarding the external surfaces of the model, to obtain a mold thickness of 5 mm. Given the phantom undercuts, to allow an easy molds assembly and the silicone phantom demolding, the outer mold was subdivided in six subcomponents. The outer mold subcomponents were manufactured using stereolithography techniques with Clear v4 resin (**Figure 22**e)

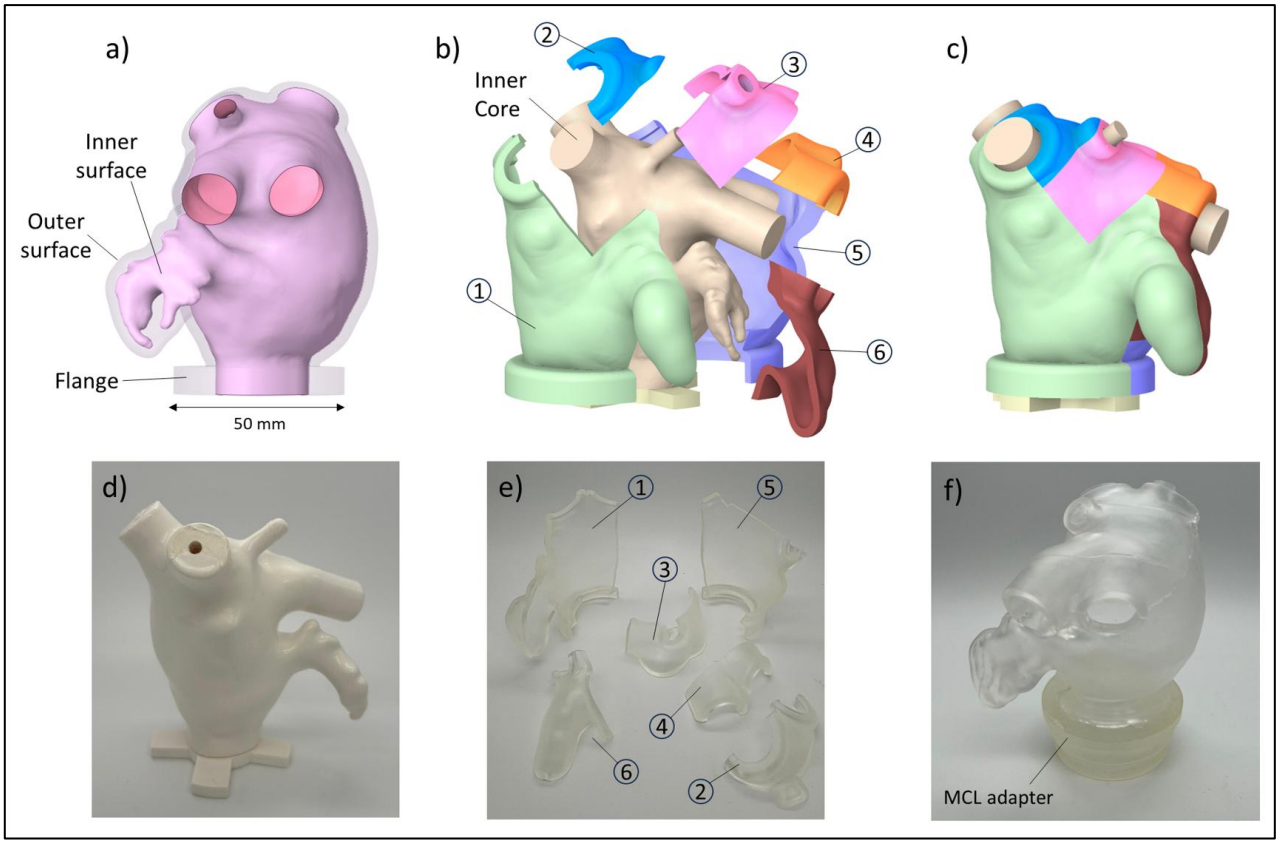

Figure 22: a) Phantom of left atrium (LA) and molds design and fabrication: b) LA phantom model , exploded view of the inner core and the outer mold subcomponents (1-6) , c) molds assembly, d) realized inner core , e) outer molds subcomponents (1-6) and f) silicone LA phantom.

The phantom required 65 g of material obtained by mixing the silicone and the curing agent with a ratio of 10:1. The material was then poured into the molds in three steps to prevent air bubbles from being trapped in thick layers. The silicone was then cured at 65°C for 24 hours. After curing, the phantom was demolded from the outer mold and the inner core was dissolved by an acetone bath (**Figure 22**f). An adapter was designed and realized in Clear resin to allow the connection of the phantom to the mock circulatory loop.

Mock Circulatory Loop and PIV Setup

The fluid dynamic experiments on the phantom were conducted using a mock circulatory loop integrated with a PIV system. An overview of the experimental setup is shown in **Figure 23**. Regarding the boundary conditions imposed on the phantom, a constant pressure of 0 mmHg was applied at the pulmonary veins using an atmospheric reservoir in which the phantom was positioned and secured. A time-varying mitral flow profile was imposed at the phantom's mitral outlet using a pulsatile piston pump. This setup replicated the healthy physiological mitral waveform from and imposed a cardiac output of 5.92 L/min, which was estimated from CT-derived left ventricular volumes and heart rate. A flow sensor (CO.55/190 V2.0, Sonotec) was installed to measure the flow rate at the mitral inlet accurately. The PIV system captured the velocity field within the phantom, enabling detailed analysis of fluid dynamics.
The PIV system featured a pulsed high-power LED system as the illumination source. A fibre optic line light with a cylindrical lens was used to form the light sheet required for experiments. Images were acquired using a high-speed camera. Both the camera and the light-generating components were mounted on an optical cage system (Thorlabs, USA), which was attached to a 2D motorized XY translation stage (PLSXY, Thorlabs, USA). This setup enabled control over the system's height, depth, and alignment relative to the phantom. A working fluid composed of water (44%), glycerine (34%), and urea (22%) was adopted to match the refractive index of Sylgard silicone. This mixture simultaneously maintained the density ρ (1060 kg/m3) and the dynamic viscosity μ (0.0035 Pa-s) of the blood. The flow was seeded with hollow spherical particles with 10 μm in diameter and density of 1100 kg/m3, to perform the PIV.

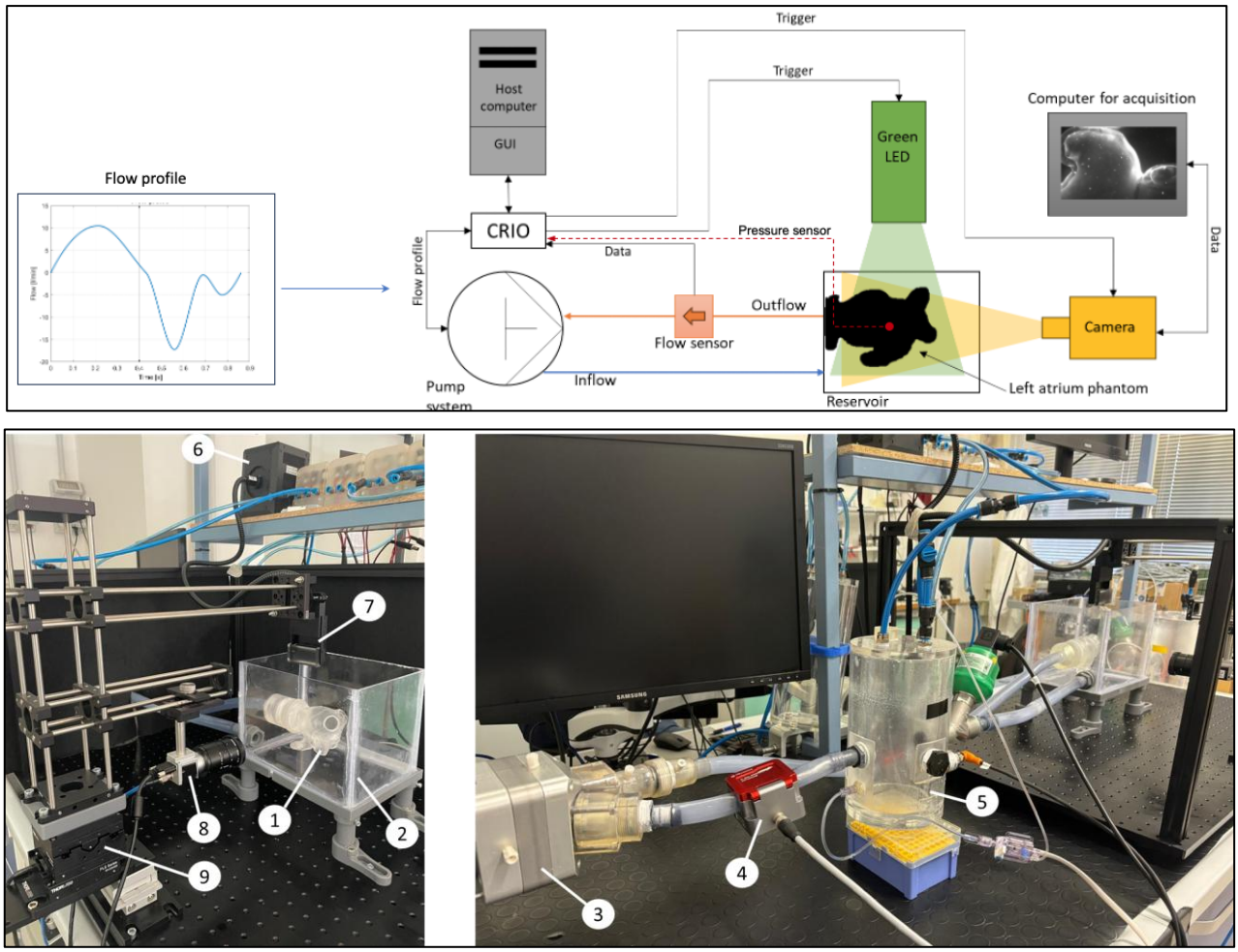

Figure 23: Mock circulatory loop: (1) left atrium phantom model, (2) reservoir, (3) piston pump, (4) flow sensor, (5) hybrid chamber, (6) LED illuminator, (7) Cylindrical lens, (8) camera and (9) translational stage.

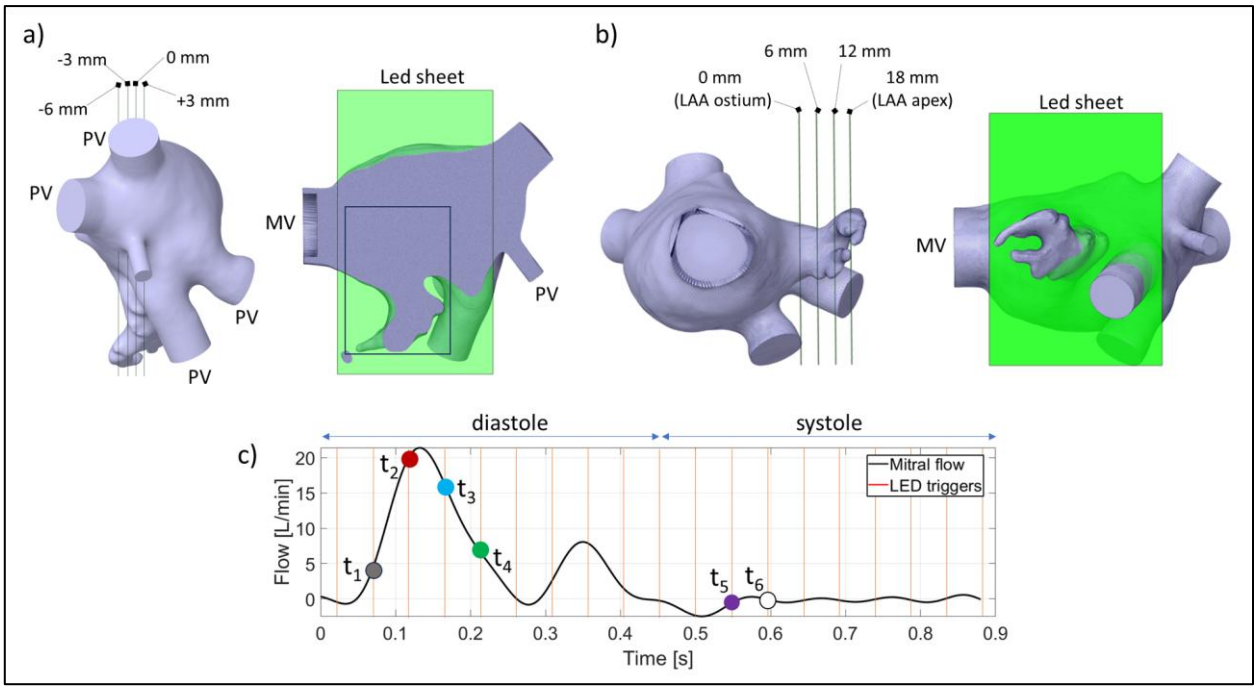

Figure 24: PIV acquisition planes of the left atrial appendage region: longitudinal plane a) with depths reference (-6 mm, -3 mm, 0 mm, +3 mm) and transversal plane b) with depths reference (0 mm, 6 mm, 12 mm, 18 mm). Mitral valve outlet (MV) and pulmonary veins (PV) inlets are reported. Imposed transient mitral flow in a cardiac cycle c) with led triggers and evaluated instants (t1 = 75 ms, t2 = 118 ms, t3 = 160 ms, t4 = 204 ms, t5 = 506 ms, t6 = 549 ms).

Fluid Model Simulate the In Vitro Condition

To further complement the experimental observations, a proof-of-concept CFD model was developed to simulate the flow dynamics under analogous conditions. The CFD simulation was performed using Ansys Fluent 2022 solver (ANSYS Inc, USA). Blood rheology was modelled as an incompressible Newtonian fluid with a density of ρ = 1060 kg m−3 and a viscosity of μ = 0.0035 kg/m·s, assuming a laminar flow regime. The outlet boundary condition was defined by the mitral flow profile of the PIV setup, while zero pressure was set to the pulmonary vein inlets, ensuring alignment with the experimental mock circulatory loop.

Preliminary Results

The phase averaged magnitude of the velocity at the 0 mm longitudinal location in different instants of the cardiac cycle is reported in **Figure 25**. The velocity is synchronous with the mitral flow throughout the cardiac cycle. During the acceleration phase (t1, t2) the fluid velocity increases reaching its maximum velocity (equal to 0.44 m/s), coinciding with the mitral E peak instant. During this phase, a parabolic velocity profile is observed near the mitral valve outlet, and a high-velocity channel appears at the pulmonary vein inlet; conversely, the velocity in the LAA remains near zero. As the cardiac cycle progresses (t3, t4), the deceleration of the PV channel combined with the low velocity in the LAA contributes to the formation of a vortex at the ostium, followed by a gradual slowing of the flow. At the systole phase (t5), the flow velocity becomes negligible in all regions of LA. Regarding the spatial distribution of the velocity field, the magnitude decreases from the atrium centre to the ostium and the LAA (**Figure 25**). Within the LAA, flow velocities remain near zero

throughout the cardiac cycle creating a zone of stagnation. **Figure 25** depicts the phase averaged velocity magnitude at the different transversal depths, over the cardiac cycle. The transversal velocities reach the maximum value (0.06 m/s) at the ostium (0 mm) and decrease to the LAA apex location. This trend is confirmed by the bulk velocity, computed in the transverse region of interest in the LAA, which decreases from 0.021 m/s at the ostium to 0.001 m/s at the LAA apex. The maximum LA displacement measured from the PIV images was 0.25 mm.

The velocity ranges are in agreement with the in-vivo measurements from MRI echocardiography. During the acceleration phase, the velocity peak corresponds with the peak of mitral inflow. The subsequent formation of vortices at the ostium demonstrates the relationship between morphological and spatial gradient of the velocity. The transversal plane analysis complements these findings by illustrating the directional dependency of flow velocities. Lower maximum velocities observed in transversal planes (**Figure 25**) indicate predominant flow along the longitudinal axis, driven by pulmonary vein inflow and mitral valve outflow. The reduction in transversal velocity magnitude and the increasing temporal delay of velocity peaks relative to mitral flow in distal regions highlight kinetic energy dissipation.

The PIV system captured the velocity field within the phantom, enabling a detailed analysis of the fluid dynamics. In addition, a preliminary proof-of-concept CFD simulation with the same boundary conditions was performed as a parallel analysis. The initial results from the computational simulation, presented in **Figure 25** and in **Figure 26**, were compared to the experimental results to demonstrate the potential of the experimental dataset to serve as a benchmark for the future validation for LAAO intervention and detecting DRT.

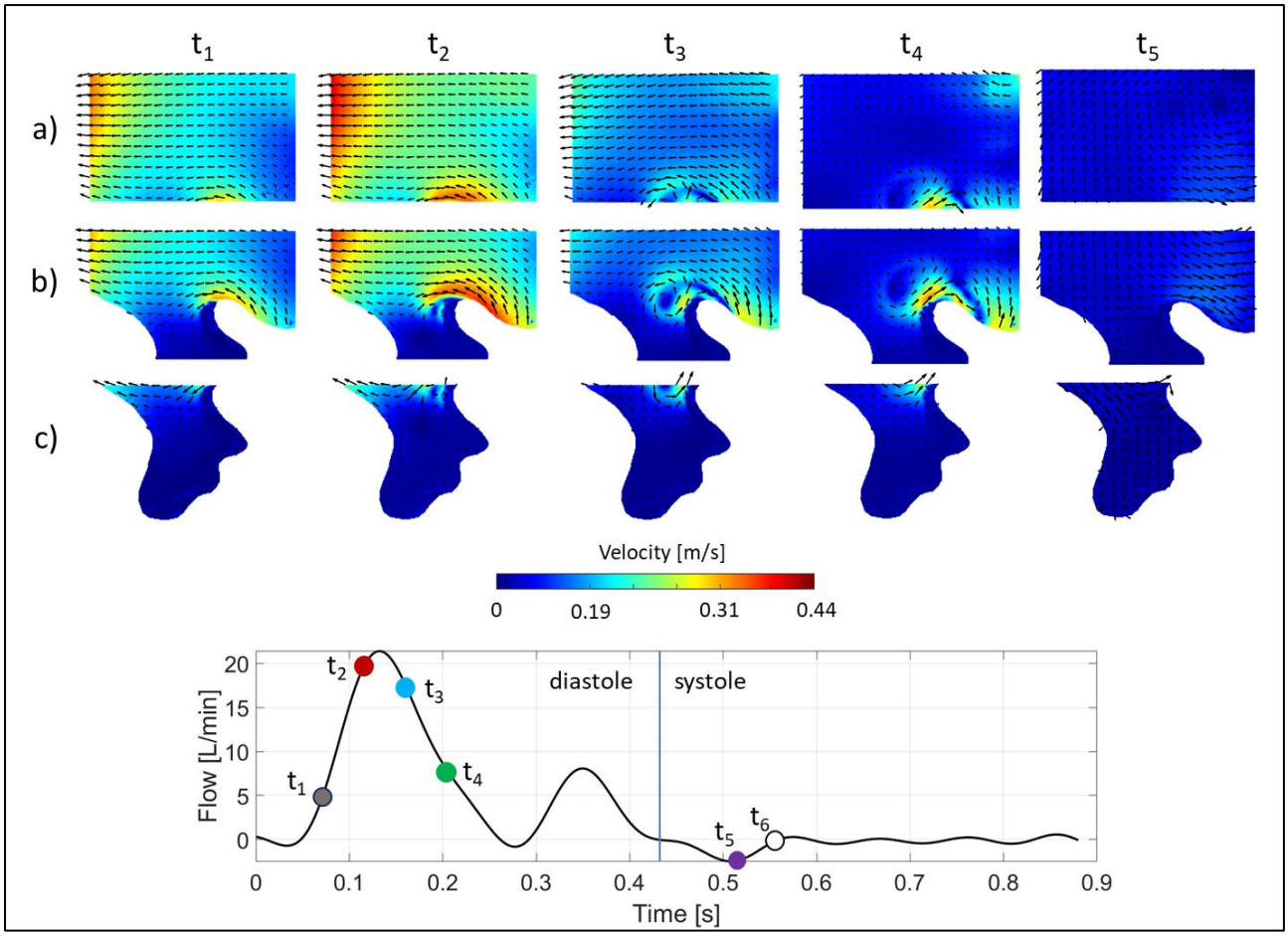

Figure 25: a) Phase average velocity field at the 0 mm longitudinal plane in left atrium (LA) a), Ostium b) and left atrial appendage (LAA) c) views, during the cardiac cycle (t1 = 75ms, t2 = 118ms, t3 = 160ms, t4 = 204ms, t5 = 506ms).

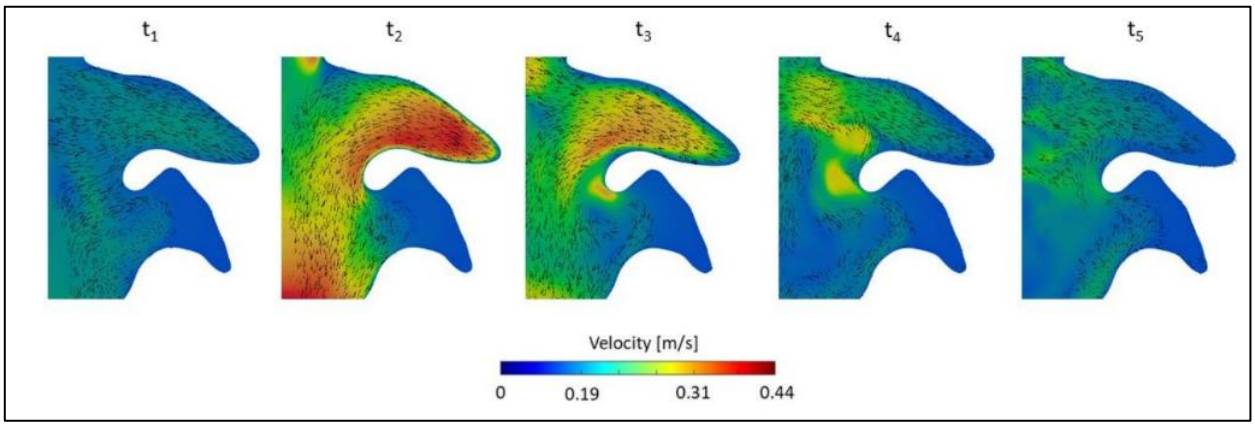

Figure 26: Velocity Magnitude field from CFD in a) longitudinal plane during the cardiac cycle (t1 = 75ms, t3 = 160ms, t4 = 204ms, t5 = 506ms).

In accordance with the guidelines (V&V40), the obtained data potentially represent the benchmark required to fully validate numerical methods, ensuring their accuracy and reliability in replicating the complex fluid dynamics within LAA models, as already demonstrated in different cardiovascular districts. The presented setup can potentially represent the basis for the development of new numerical methods to provide insights in the clinical context. Additionally, the experimental setup could be used to explore different clinical scenarios, such as the LAA closure procedures and their efficacy (estimation of device related thrombus and peri device leak risks), in a controlled environment. Velocity fields-derived metrics, such as kinetic energies and shear stresses, could be processed from the experimental datasets to serve as a reference for verifications. By offering a validated dataset with metrics, this study would potentially establish the basis for collaborative challenges within the scientific community, to increase realism and predictive power of computational modelling techniques. Future developments will overcome limitations related to wall movement neglection and constant pressure conditions at the pulmonary veins. Further improvements will include a complete left heart phantom, with both atrium and ventricle, the study of the fluid dynamic behaviour of the left atrial appendage occluder devices and the analysis of additional patient specific LA and LAA morphologies.

3.4 UC2 Validation Uncertainty – M30-M54 Activities

This section only contains additional Uncertainty Quantification (UQ) activities conducted on UC2 selected computational model during the M30-M54 period. UQ activities conducted during the M1-M30 period are already reported in the UC2 section of deliverable D6.2. Results reported in this section are meant to complete or (in some cases) supersede results of deliverable D6.2. The latter case will be explicitly mentioned, when applicable.

Large-Scale Sensitivity Analysis of Modelling Settings Influencing Hemodynamics after Left Atrial Appendage Occlusion

During the SimCardioTest project the numbers of fluid simulations reached around 2,100. The last study developed in the scope of the virtual population to increase the number of cases was conducted resulting in a total of 1,000 CFD simulations. For that, a selected dataset of 50 atrial fibrillation (AF) patients from CHU Bordeaux (France) was analysed. For each patient-specific left atrium (LA), two occluders, Amplatzer Amulet and Watchman FLX, were implanted in two positions: either covering or uncovering the pulmonary ridge (PR), a key factor in device related thrombus formation. Computational fluid dynamics (CFD) simulations were conducted in Ansys Fluent 2021R2 (ANSYS Inc, US) under five modelling conditions: (1) blood modelled as a Newtonian fluid (AF Newtonian); (2) blood modelled as a non-Newtonian fluid (AF non-Newtonian); (3) inclusion of the A-wave in the mitral velocity profile (No-AF Newtonian); (4) scaling the outlet velocity profile by 1.25 (high-velocity AF Newtonian); and (5) scaling the outlet velocity profile by 0.75 (low-velocity AF Newtonian). **Figure 27** shows that AF conditions resulted in lower velocities near the device, while No-AF increased both flow velocity and complexity near the device. The non-Newtonian model caused slight velocity variations, but its overall impact was minimal in comparison with the Newtonian model under same physiological conditions. In contrast, higher velocity enhanced both flow activity and complexity, reducing flow recirculations around the LAAO device and increasing the washout from the device region.

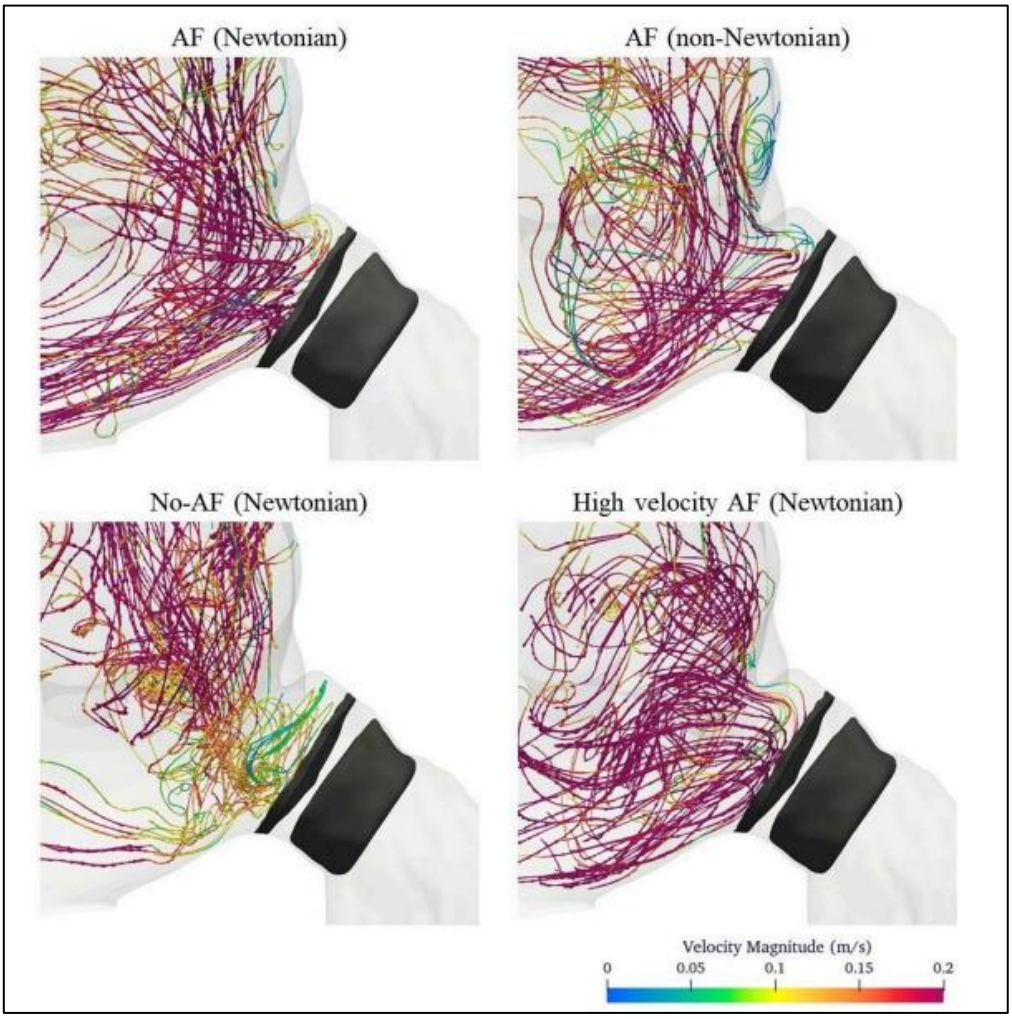

Figure 27: Simulated flow patterns at late diastole for four modelling conditions (case 44, Amplatzer Amulet with the PR uncovered).

Initiative: FLAMES Workshop – Fluid Simulations of the Left Atrium with Multi-Source Experimental Data

As part of ongoing efforts to advance cardiovascular hemodynamic modelling, the FLAMES Workshop (Fluid Simulations of the Left Atrium with Multi-source Experimental Data) has been launched. This initiative aims to establish best practices for fluid simulations of the left atrium through collaborative efforts based on a shared dataset.
The organizers have compiled a comprehensive validation dataset that integrates multiple imaging modalities. This dataset will enable the scientific community to conduct verification and benchmarking studies, identify the most promising modelling strategies, and address current challenges in the field. The available data include:

- In vitro data from particle image velocimetry (PIV) experiments, collected and curated by BioCardioLab, Fondazione Toscana G. Monasterio (Massa, Italy),
- 4D flow magnetic resonance imaging (MRI) data, collected by Hospital Clínic de Barcelona and curated by Universitat Pompeu Fabra (Barcelona, Spain),

- Dynamic opacity computed tomography (CT) data, collected by the University of California San Diego (La Jolla, USA) and curated by the University of Washington (Seattle, USA).

Beyond technical benchmarking, the workshop also addresses a critical but often overlooked source of variability in simulation: **the role of the user** in the modelling process. One of the main challenges in verification and validation lies in evaluating how user expertise—or lack thereof—can introduce modelling errors that become intertwined with numerical uncertainties. To explore this aspect, the FLAMES Workshop is designed as an open platform, encouraging participation from research groups with varying levels of experience in atrial flow simulation and experimentation. This collaborative setting allows us to assess how user-dependent factors impact simulation results and to better understand the cumulative uncertainties arising simply from differences in model construction approaches.

Workshop outcomes and methodologies will be presented in a dedicated session at the FIMH25 conference (June 1–5, Texas, USA), with hybrid participation options available. A second in-person meeting will take place during the CMBBE25 conference (September 3–5, Barcelona, Spain).

The primary output of the workshop will be a co-authored scientific publication summarizing key lessons learned. All methodologies will be anonymized to emphasize collective insights and foster community-driven progress rather than individual performance metrics.

3.5 UC2 Model Applicability – M30-M54 Activities

The IDEAL-LAAC (Impact of Flow Dynamics according to Device Implant Depth after Left Atrial Appendage Occlusion) study, led by UPF, included a cohort of 285 patients who underwent LAAC across 10 centres in Europe and North America between January 2019 and October 2023. Eligible patients received either Watchman or Amulet devices, had follow-up cardiac CT imaging, and pulsed-wave Doppler assessment of the mitral valve within six months of the CT scan. A final core dataset of over 250 patients was compiled, maintaining an approximately 1:10 ratio between cases with device-related thrombus (DRT) and those without, to ensure sufficient statistical power given the low incidence of DRT. All patients provided informed consent, and the study adhered to local ethics requirements and the Declaration of Helsinki.

To evaluate the impact of device positioning on flow dynamics, patients were stratified into proximal and distal implant groups based on the depth of the device relative to the pulmonary ridge (PR). Definitions of proximal implantation varied by device type: for lobe/disc devices, the disc had to be positioned at the level of the PR; for single-lobe devices, a proximal implant was defined as a position within <10 mm from the PR. Any device placement outside these criteria was considered distal. Device success was defined as complete deployment within the LAA, while DRT was identified via CT as thrombus adherent to the atrial surface of the device. Other procedural outcomes were classified using established consensus definitions.

The primary objective of the study was to analyse flow dynamic differences between proximal and distal device implants using computational simulations. These simulations provide valuable insights into how implantation depth affects intra-atrial blood flow, particularly in relation to thrombus formation. Secondary analyses included a more granular evaluation of flow dynamics across incremental depth categories and a comparison of flow patterns in patients with and without DRT. The results from these simulations can inform optimal implantation strategies, improve device positioning protocols, and potentially reduce the incidence of post-procedural thrombus formation.

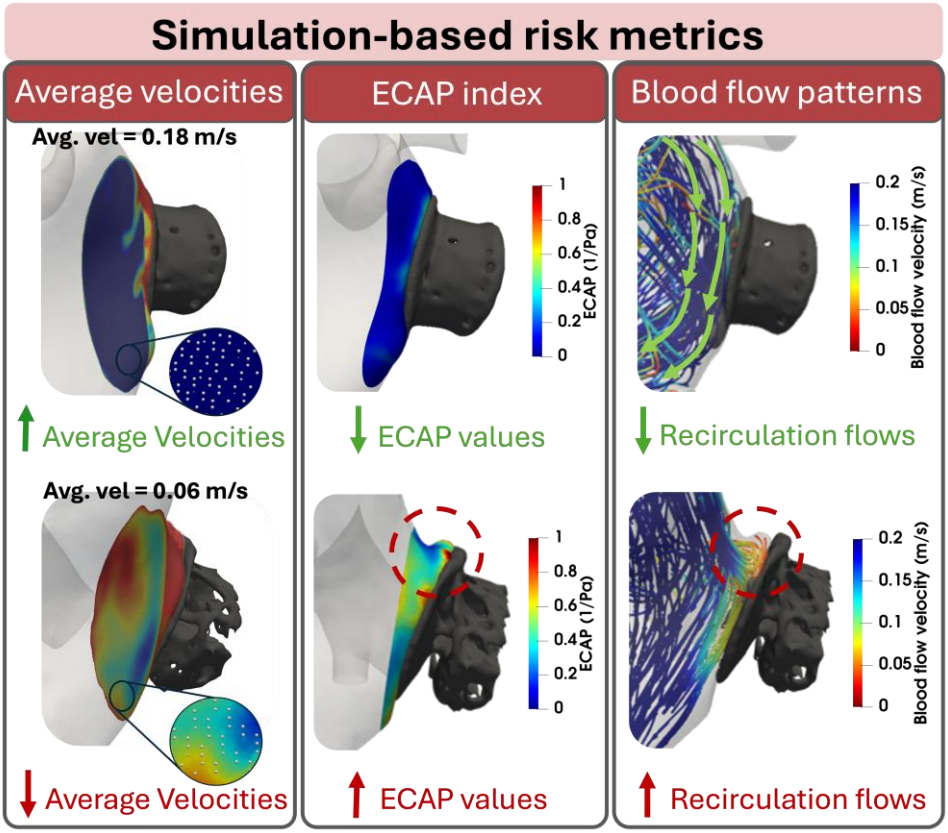

Figure 28: Main risk metrics used for thrombus detection in the IDEAL study. The example shown in the upper part illustrates an LAAO safety scenario with high blood velocity, low ECAP, and laminar flow patterns. The lower part shows a poorly positioned device, indicated by a poor index and a high probability of DRT.

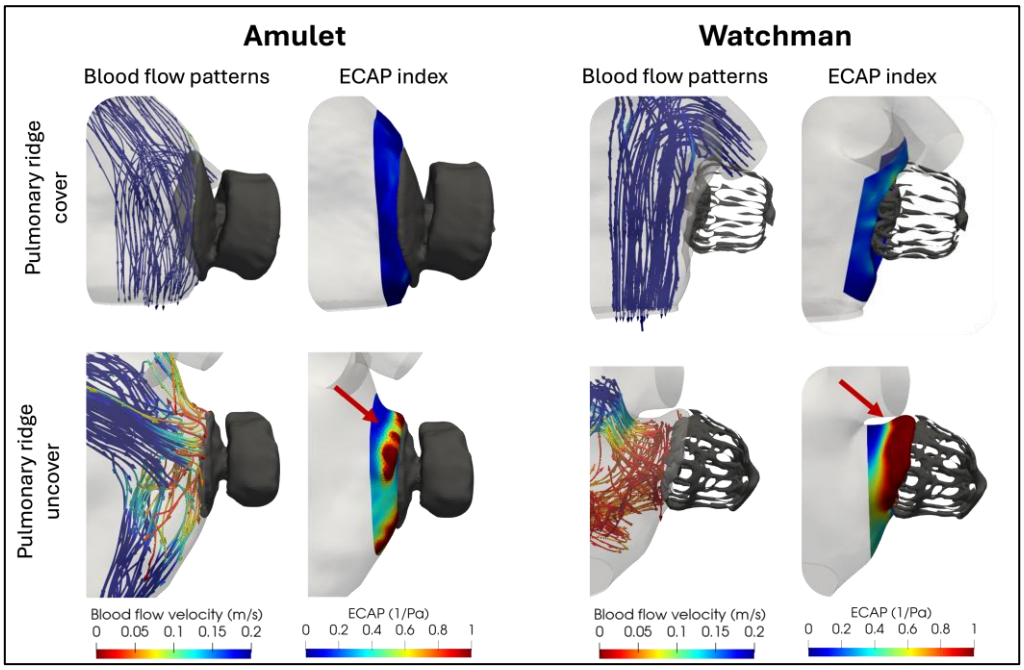

Figure 29: Patients with uncovers and covers pulmonary veins. Results show the importance to take in account the position and type of the device.

In addition, we have participated in several live cases where doctors have used our simulations to support their decisions, examples in CSI congress Frankfurt 2025, LAAO Summit 2025, CSCEstructural, CSI Focus LAA Congress, etc. (**Figure 30**).

Figure 30: Live CSI congress Frankfurt 2025. A successful live case was performed from the University Hospital of Salamanca, where our simulations was used for the preprocedural planning of a left atrial appendage closure with an Amulet device from Abbott, achieving an excellent result.

3.6 UC2 Discussion

During this period, the primary focus has been on consolidating previously obtained results. First, the number of simulations has been increased to approximately 2100, using the parameters established in the verification study. This extensive set of simulations forms a comprehensive virtual database, which will be subjected to statistical analysis in the near future. Regarding validation, significant progress has been made with the initial setup developed by MIT, yielding high-quality fluid dynamics results, including atrial motion and physiological flow conditions. Additionally, a comparative analysis has been initiated with a second experimental setup at BioCardioLab. Preliminary findings from this comparison are promising and will enable a more detailed investigation of local velocity behaviours, with the ultimate goal of improving our understanding of the left atrial appendage occlusion (LAAO) procedure. Progress has also been made in enhancing the credibility and applicability of the models, which are now employed in retrospective analyses to determine device-related thrombosis (DRT), as well as to identify the optimal device positioning in cases involving real-time clinical interventions.

Table 14: Credibility Factors Coverage Level for Use Case 2 – COU1 (cf. ASME VV40).

Model Risk					x	
Credibility Factor Coverage Level		1	2	3	4	5
Code Verification: Software Quality Assurance	V				x	
Code Verification: Numerical Code Verification - NCV	V				x	
Calculation Verification - Discretization Error	V				x	
Calculation Verification - Numerical Solver Error	V				x	
Calculation Verification - Use Error *	III				x	

Validation - Model [Form]	III					x	
Validation - Model [Inputs]	III					x	
Validation - Comparator [Test Samples]	III					x	
Validation - Comparator [Test Conditions]	I					x	
Validation - Assessment [Input Parameters]	III					x	
Validation - Assessment [Output Comparison]	IV					x	
Applicability: Relevance of the Quantities of Interest	V					x	
Applicability: Relevance of the Validation Activities to the COU	IV					x	

Table 15: Credibility Factors Coverage Level for Use Case 2 – COU2 (cf. ASME VV40).

Model Risk					x		
Credibility Factor Coverage Level			1	2	3	4	5
Code Verification: Software Quality Assurance	V				x		
Code Verification: Numerical Code Verification - NCV	V				x		
Calculation Verification - Discretization Error	V				x		
Calculation Verification - Numerical Solver Error	V				x		
Calculation Verification - Use Error	III				x		
Validation - Model [Form]	III				x		
Validation - Model [Inputs]	III				x		
Validation - Comparator [Test Samples]	I				x		
Validation - Comparator [Test Conditions]	III				x		
Validation - Assessment [Input Parameters]	V				x		
Validation - Assessment [Output Comparison]	V				x		
Applicability: Relevance of the Quantities of Interest	V				x		
Applicability: Relevance of the Validation Activities to the COU	IV				x		

3.7 UC2 – VVUQ Publications

This section lists all scientific publications relating to the UC2 VVUQ activities conducted within the frame of the SimCardioTest project.

Table 16: UC2 – List of publications related to VVUQ activities.

Reference	VVUQ Topic
Albors et al. 2022 [28]	Verification
Albors et al. 2023 [29]	Verification
Mill et al. 2024 [30]	Verification, Uncertainty quantification
Khalili et al. 2024 [31]	Verification
Albors et al. 2024 [32]	Validation, Applicability

Reference	VVUQ Topic
Olivares et al. (draft) [33]	Verification, Validation, Uncertainty Quantification
Gasparotti et al. 2025 [34]	Validation
Roche et al. 2025 (preprint) [27]	Validation
Albors et al. (draft) [35]	Clinical Validation
Casademunt et al. 2025 [36]	Clinical Validation, Uncertainty Quantification
Barrouhou et al. 2025 [37]	Verification, Uncertainty Quantification
Albors et al. 2025 [38]	Verification, Applicability
Kjeldsberg et al. 2024 [39]	Verification

4. Use Case 3

4.1 UC3 Model Summary

4.1.1 Background

Safety pharmacology studies evaluate cardiac risks induced by drugs. Since Torsade de Pointes (TdP), a well-known malignant arrhythmia, was related to pharmacological effects, regulatory guidelines have looked for biomarkers able to identify arrhythmogenic effects of drugs in order to withdraw them from the development process. Consequently, research efforts to ensure the safety of new molecules have become time-consuming and expensive for drug developers, delaying the release of new medicines into the market. Besides, initial tests focused on hERG (human ether-à-go-go related gene) activity and in vitro repolarization assays limited the development of potentially beneficial compounds, and the increasing attrition rate urged the design of new strategies.

The first initiative to include in-silico models was the Comprehensive in-vitro Proarrhythmia Assay (CiPA), which proposed integrating drug effects obtained in-vitro into a cardiomyocyte model to predict TdP risk. Furthermore, the continuous development of new models opens the possibility to personalize computer simulations to optimize drug therapy.

4.1.2 Drug Description

Drugs are chemical compounds that exert a therapeutic action by modulating physiology. Besides the therapeutic effects, undesirable secondary effects can alter the normal functioning of different organs, including the heart.

Some molecules can modulate cardiac function by interacting with cellular mechanisms. Specifically, molecules that induce critical changes in ion channel permeability alter myocyte electrical activity, causing changes in heart rhythm with potentially fatal consequences. For this reason, drug developers need to perform safety pharmacology tests to evaluate drug candidates.

Before reaching cardiac tissue, drugs undergo a series of processes inside the body from its administration, including a distribution phase. Pharmacokinetics describes all these steps inside a

living organism until the complete elimination of the substance, but interactions between each chemical compound and each organism differ. Pharmacokinetic processes are influenced by many external variables such as gender, age, weight, and previous pathologies, and the analysis of all the contributors is needed to determine the better therapeutic dose and route of administration.

Integrating pharmacokinetics and electrophysiology studies in drug assessment allows a more complete and personalized evaluation of the proarrhythmic risk by including the dosage and specific characteristics of the patient.

4.1.3 Question of Interest

The Question of Interest addressed by the model is the following:

- What is the maximum concentration/dose regimen of a drug to assure TdP-related safety in a population of healthy subjects?

4.1.4 Context of Use

A human electrophysiological (EP) model with pharmacokinetics (PK) can be used at early phases of drug development to obtain biomarkers that guide in selecting drugs and doses without TdP-risk for each subpopulation (male/ female/ age). This computational model is not intended to replace in vitro or animal experiments but to enrich and complement them by predicting additional outcomes. The goal of the in-silico trials is to help in designing clinical trials, to reduce the number of participants and protect them from suffering malignant arrhythmogenic events.

TdP-risk index is a metric obtained from a single or a set of electrophysiological biomarkers. By using appropriate threshold values, it performs a binary classification (safe/unsafe).

Quantities of Interest (QoI)

To obtain TdP-risk index, we considered action potential duration (APD90) and QT interval as the main indicators. Secondary biomarkers were calculated to improve predictions.

4.1.5 Model Risk

The following considerations support the assessment of the risk associated with the numerical model.

- Decision Consequence: Medium

An incorrect prediction with the computational model can have a risk on the development of the clinical trial if torsadogenic concentrations were administered. Low concentrations, on the other hand, do not have negative electrophysiological consequences.

- Model Influence: Medium

The model will complement preclinical and non-clinical (animal) experimental data and will help to design and refine the inclusion criteria and dosage in posterior clinical trials. In vitro and in vivo tests will still be required, but the number of participants in clinical trials as well as malignant

arrhythmogenic events can be reduced. Therefore, the model will act as a complementary approach in determining safe drug concentrations.

- Model Risk: 3/5 (Medium-Medium)

Model Risk is based on Decision Consequence and Model Influence stated above, according to Risk Matrix in Figure 31 (cf. section 1.2.5).

Model influence	**high**	**3**	**4**	**5**
	medium	**2**	**3 COU**	**4**
	low	**1**	**2**	**3**
		low	**medium**	**high**
		Decision consequence		

Figure 31: Model Risk Matrix (cf. ASME VV40) evaluating the COU included in UC3.

4.1.6 Model Description

The computational model for proarrhythmia risk prediction integrates the following steps:

- Pharmacokinetics
- Heart electrophysiology
- Cardiac mechanics

One particular aspect of this in-silico strategy we propose for drug assessment is the inclusion of patient characteristics to optimize predictions.

The model pipeline initiates with drug pharmacokinetics, which consists of obtaining the plasmatic concentration following a specific compound dosage. This concentration is used as the input of the cellular model to simulate the drug effect on myocyte electrophysiology based on the interaction of the pharmacological molecule with ion channels. The last step of the computational model is to simulate and predict the electrophysiological activity in the whole heart.

Verification activities were evaluated separately in each computational model because the tools were developed independently.

4.1.7 UC3 Stakeholder Update

ExactCure terminated its participation before the end of the SimCardioTest project and related V&V activities on pharmacokinetics finished 10 months beforehand. Although UC3 had pharmacokinetics as the first step in the workflow, electrophysiological simulations can be conducted with input data collected from literature and the independent validation approach allowed to complete EP activities despite the departure of ExactCure.

4.2 UC3 Model Verification – M30-M54 Activities

This section only contains additional Verification activities conducted on UC3 selected computational model during the M30-M54 period. Verification activities conducted during the M1-M30 period are already reported in the UC3 section of deliverable D6.1. Results reported in this section are meant to complete or (in some cases) supersede results of deliverable D6.1. The latter case will be explicitly mentioned, when applicable.

4.2.1 PK Model

4.2.1.1 Numerical Solver Error

Quantities of interest (concentrations) sensitivities to tolerances level have been expanded for the following molecules/models in the COU: Cisapride, Quinidine, Pimozide, Azimilide and Dofetilide. The complete report can be found in Annex B.

4.3 UC1 Model Validation – M30-M54 Activities

This section only contains additional Validation activities conducted on UC3 selected computational model during the M30-M54 period. Validation activities conducted during the M1-M30 period are already reported in the UC3 section of deliverable D6.2. Results reported in this section are meant to complete or (in some cases) supersede results of deliverable D6.2. The latter case will be explicitly mentioned, when applicable.

4.3.1 PK Model Validation

Model form and input sources, test samples and conditions, equivalency of input parameters and output comparisons were expanded and detailed for the following molecules: Azimilide, Chlorpromazine, Cisapride, Clarythromycin, Sotalol, Disopyramide, Dofetilide, Domperidone, Droperidol, Flecainide, Metronidazole, Mexiletine, Nicorandil, Ondansetron, Pimozide, Quinidine and Vandetanib. New quantification of sensitivities and uncertainties was included for the 21 drugs included in the report. All the details can be found in Annex C.

4.3.2 EP (0D and 3D) Model Validation

4.3.2.1 Comparators description, samples and conditions

The initial list of 22 drugs was updated with the cellular comparators for the remaining 6 drugs to complete the 28 compounds included in the CiPA initiative [40], including the clinical TdP-risk category assigned by a committee of experts.

Table 17: Experimental comparators from the literature that provide 0D electrophysiological data for the molecules under study. TdP-risk categories according to the criterion stablished for CiPA drugs [40].

Drug Comparator		Samples			
Molecule	**Ref.**	**Type**	**Concentrations**	**Conditions**	**Quantity**
High Risk					
Bepridil	[41]	guinea pig ventricular papillary muscles	1 μM, 4 μM, 10 μM, 20 μM	0.1 – 5 Hz	4
Ibutilide	[42]	dog left ventricle muscle	1 μM	0.25 Hz, 0.67 Hz, 2 Hz	5
Intermediate Risk					
Astemizole	[43]	isolated guinea pig ventricular myocytes	$0.3 \cdot 10^{-3}$ μM, 10^{-3} μM	1 Hz, 3Hz	4
Terfenadine	[44]	hiPSC-CM	3 μM, 10 μM, 30 μM, 100 μM	1 Hz	6
Low Risk					
Nitrendipine	[45]	hiPSC-CM	0.01 μM - 0.3 μM	1 Hz	3-5
Verapamil	[44]	hiPSC-CM	0.03 μM - 3 μM	1 Hz	7

The characteristics of the new comparators used to assess APD variation, which correspond to the experimental settings of several preclinical in-vitro studies found in the literature, are summarized in Table 17. Molecules are categorized according to their clinical TdP-risk label.

A new set of comparators was introduced to make use of the electrophysiological model in a ventricular geometry (3D model) and provide new outputs based on the simulation of the electrocardiogram (ECG), which are more comparable to the clinics. Data were obtained from sources different to the cellular ones, since the experimental settings to obtain the ECG differ. After thorough search to find clinical human data in the literature, Table 18 summarizes the selected comparators. The main criterion for their selection was that published information provided quantitative details about the critical input and output parameters needed to replicate during the simulations, as detailed below. This explains that some comparators were preclinical and with animal models.

Due to the computational cost of 3D simulations, a single dose and a single condition was compared for each molecule, those closer to the therapeutic scenarios when possible. Drugs without available comparators were nevertheless simulated, because we can qualitatively validate the outputs according to their TdP-risk category.

Table 18: Experimental comparators from the literature that provide 3D electrophysiological data for the molecules under study. TdP-risk categories according to the criterion stablished for CiPA drugs [40].

Drug Comparator		Samples			
Molecule	**Ref.**	**Type**	**Quantity**	**Settings**	**Effective C_{max}**
High Risk					
Bepridil	[46]	males	12	12-lead ECG QT interval on lead II 71 beats/min	23.5 nM
Disopyramide	[47]	beagle dogs of either sex	6	Lead II ECG Bazett-corrected QT interval (QTcB)	11782.9 nM
Dofetilide	[48]	males	10	Leads V2, V5, and V6 Fridericia-corrected QT interval (QTcF)	4.76 nM
Ibutilide	[49]	patients with AF or flutter	266	12-lead ECG corrected QT interval (QTc)	92.8 nM
Quinidine	[50]	beagle dogs of either sex	5-6	Lead II ECG Van de Water-corrected QT interval (QTcV)	1020 nM
Sotalol	[50]	beagle dogs of either sex	5-6	Lead II ECG Van de Water-corrected QT interval (QTcV)	11280 nM
Vandetanib	[51]	males and females	18 (11:7)	12-lead ECG QTc interval	269.7 nM
Azimilide	-				122.0 nM
Intermediate Risk					
Astemizole	[52]	guinea pig hearts	5-10	pseudoECG constant RR	100 nM
Cisapride	[53]	males and females	12	12-lead ECG automatic QTcB interval	2.75 nM
Clarithromycin	[54]	males	23	12-lead ECG automatic QTcB interval	874.4 nM
Clozapine	[55]	males and females	82 (58:24)	12-lead ECG QTcB interval on leads II, V2, and V3	28.0 nM
Domperidone	[56]	isolated rabbit hearts	8	BCL = 900 ms	500 nM
Droperidol	[57]	males and females	16 (8:8)	12-lead ECG QTcF interval	37.7 nM
Ondansetron	[56]	isolated rabbit hearts	10	BCL = 900 ms	1000 nM
Pimozide	[58]	males and females	12 (7:5)	ECG machine QTcF, with tangent defining the end of the T-wave	0.095 nM

Drug Comparator		Samples			
Molecule	**Ref.**	**Type**	**Quantity**	**Settings**	**Effective C_{max}**
Risperidone	[59]	males and females	28 (22:6)	12-lead ECG QTc interval	17.2 nM
Terfenadine	[52]	guinea pig hearts	5-10	pseudoECG constant RR	100 nM
Chlorpromazine	-				78.4 nM
Low Risk					
Loratadine	[54]	males	24	12-lead ECG automatic QTcB interval	0.215 nM
Ranolazine	[60]	humans	22	12-lead ECG QTcF interval on lead II, with tangent defining the end of the T-wave	3288.6 nM
Verapamil	[60]	humans	22	12-lead ECG QTcF interval on lead II, with tangent defining the end of the T-wave	25.8 nM
Diltiazem	-				188.0 nM
Metoprolol	-				493.3 nM
Mexiletine	-				3359.8 nM
Nifedipine	-				100 nM
Nitrendipine	-				3.03 nM
Tamoxifen	-				7.04 nM

For TdP-risk assessment, the measurement of QT prolongation on the ECG is critical, because it is a main biomarker altered with drugs, as proposed by the pharmaceutical guidelines ICH S7B and E14 [61]. Our model is able to reproduce pseudo-ECGs, which is the electrical potential on the leads located on a torso but without computing the conductivity of the organs (**Figure 32**). Although different in amplitude, the pseudo-ECG and ECG have equivalent durations and main complexes match in time, which allowed us to compute the QT interval with less computational cost. As mentioned above, heterogeneous experimental settings and calculation methods may cause a wide variability in QT intervals among studies. To solve this issue, we considered the percentage of change instead of absolute variation values, as performed at the cellular level with APD comparisons.

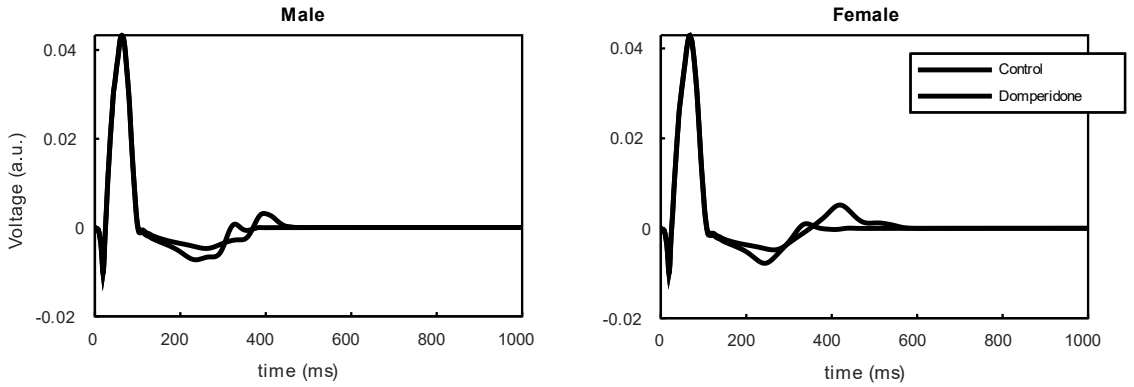

Figure 32: In silico pseudo-ECGs illustrating QT prolongation under the effect of Domperidone. One male and one female cellular models simulated in the biventricular geometry.

After validating drug effects, through 0D and 3D simulations, we applied a machine learning classifier based on Support Vector Machine for safety assessment. The main objective of this supervised learning approach is quantifying the predictive capacity of the validated mathematical model to classify the CiPA drugs according their TdP-risk category. As well as the risk labels (ground truth of reference), the training and validation sets were designated by a team of experts in the original work where the 28 known drugs were chosen [40], and we followed the same criterion. The features we used for classification were in-silico cellular biomarkers from populations as described in our previous work [62], with the difference that we generated two specific subpopulations, one for males and one for females [63]. This classifier has not been performed with experimental data, which means that does not exist an equivalent comparator per se, but we know the TdP-risk labels for the 28 CiPA drugs to evaluate the accuracy of predictions.

4.3.2.2 Equivalence of Input Parameters

Input parameters of the 0D model did not change. The unique update was applying different genotypic profiles in cell parameters to create populations of males and females for all the comparators, based on observed experimental data that differentiate control cellular properties between both sexes.

Regarding the 3D model, as it is an extension of the cellular model, it depends on the same input parameters: electrophysiological genotype and drug parameters. Three-dimensional new inputs are the ventricular mesh and all its properties to compute the electrical potential propagation. However, we used a generic geometry, parameterized in a previous study [63], for all the comparisons because experimental studies do not provide anatomical details about the hearts. Similarly, a single representative male and female electrophysiological profile from the cellular population were selected, given that this specific information is unknown.

The main drug-related input in the electrophysiological model is the effective plasmatic concentration, while IC50 and h parameters are inherited from the cellular model and they are specific for each molecule and ion channel. The comparators that quantify drug effects on the ECG usually provide the administered dose. Although PK models could predict plasmatic concentration from dose data, we used as input the maximal plasmatic concentration reported in the studies. It is

typically provided in ng/mL, and a minor direct transformation was necessary to convert it in effective concentration (nM), by means of molecular weight and binding fraction values, accessible data in drug databases [64].

4.3.2.3 Output Comparison

0D Model

Simulated drug-induced APD90 variation was directly compared to experimental APD variation for the new set of drug comparators (**Figure 33**), as previously done with 22 drugs. This time, we included the uncertainty linked to the experimental variability as horizontal error bars. There is at least one point for each drug whose interval reaches the diagonal, indicating the accuracy of predictions.

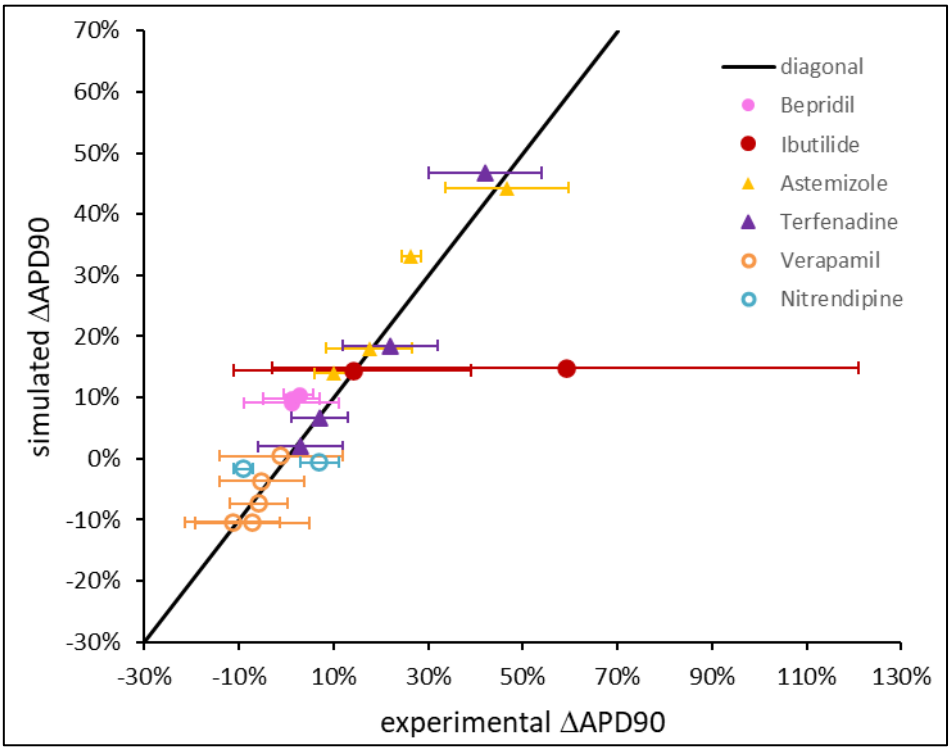

Figure 33: Output comparison: variation of action potential duration (% ΔAPD90) for high (filled circle), intermediate (triangle) and low (empty circle) TdP-risk drugs. Diagonal represents complete agreement between experimental and simulated results. Horizontal error bars denote experimental uncertainty.

Simulations can also reproduce output variability through input variability. It is the case of population of cell models, and we particularly created specific subpopulations, one for males and one for females. They were used to compare all drug effects also on APD. Although experimental data provided by the comparators was not specific for any of these subpopulations, this variability allows to examine how uncertainty due to patient characteristics (genomics) is propagated to the results.

Unlike **Figure 33**, in which drug effect is a single point, histograms of **Figure 34** show the variability in ΔAPD caused by drugs, divided in two subgroups. For these comparisons, a single concentration

per drug was evaluated; we selected the closest to the therapeutic value. The accuracy of predictions is dictated by the degree of overlap between histograms (model results) and the experimental range represented shaded areas. After applying variability is more probable that simulated results reach observed experimental bounds.

Depending on the drug comparator, output agreement quality differs. For molecules such as dofetilide, astemizole or nifedipine, despite the differences in means between experimental comparators, both populations are inside limits. Others are partially inside range, such as cisapride and diltiazem. When discrepancies are present, the causes have to be analysed one by one. For instance, the reduction in APD with metoprolol was not reproduced by the model, but as it is a low-risk drug, the lack of ΔAPD computed may be sufficient for safety prediction. In the case of chlorpromazine, instead, the in silico APD increase versus the experimental reduction needs further elucidation.

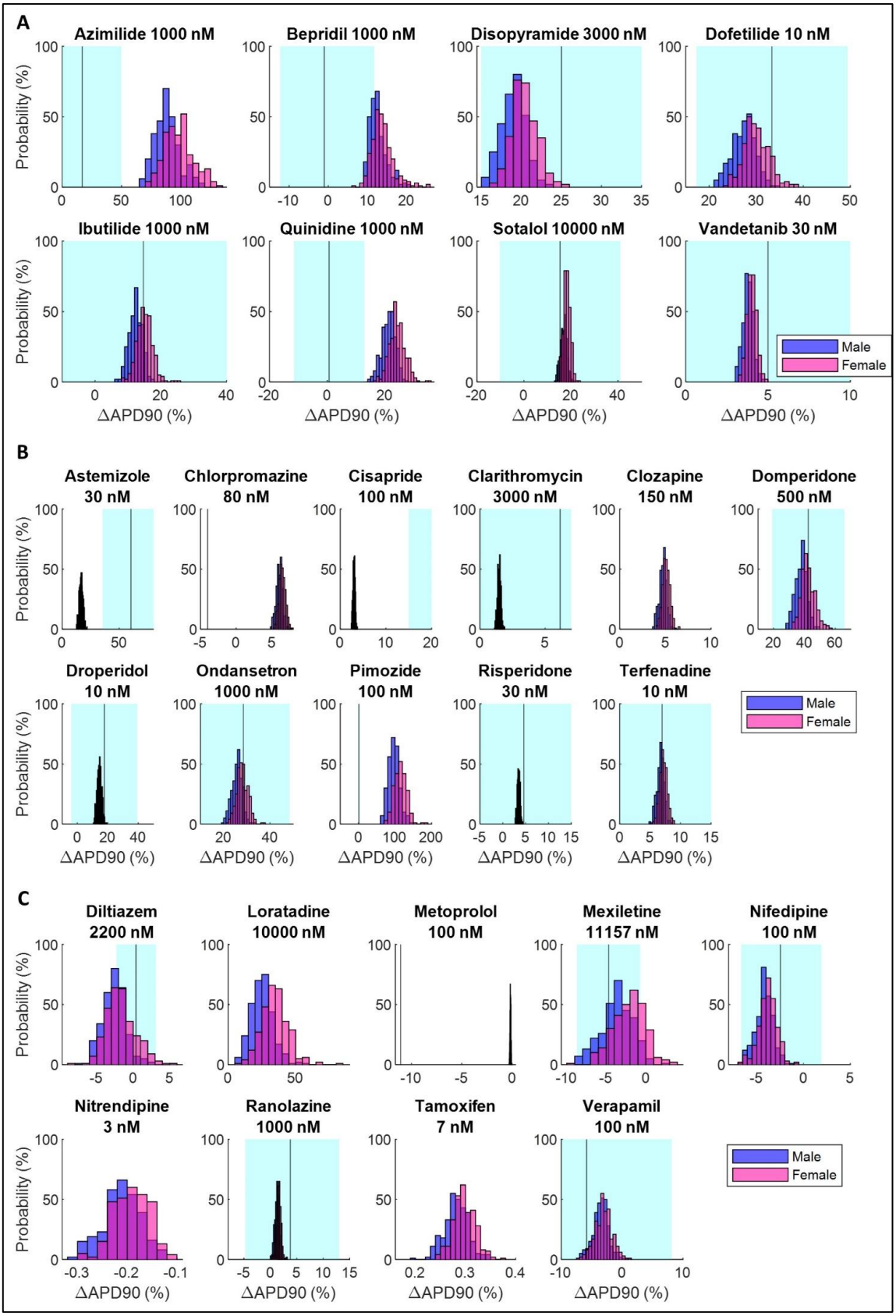

Figure 34: Output comparison in populations of cellular models divided in two subgroups by sex. A) High TdP-Risk drugs, B) Intermediate TdP-Risk drugs, C) Low TdP-Risk drugs. Shaded areas represent the experimental range, where the vertical line stands for the mean. ΔAPD90: variation of action potential duration.

3D Model

The numerical model is able to simulate an electrical signal equivalent to the ECG obtained in clinics, which allows the direct comparison between outputs. Changes on the QT interval quantified from the ECG was the only biomarker considered at the organ level to assess drug effects. Depending on the study, QT quantification varies, but the most common is an automatic value provided by the electrocardiograph based on 12-lead ECG and with heart rate correction. In our simulations, we used a constant heart rate of 1 Hz and quantified the QT on lead I.

Comparisons between in-vivo and in-silico data were evaluated molecule by molecule, similarly to the 0D comparisons, and the level of agreement obtained with the computational models can be observed in **Figure 35**. Although experimental comparators provide a mean value, we also considered the variability reported by the studies and we included it as an uncertainty interval. In-silico QT variation was considered valid if it fell within the clinical range or the distance to the limits was less than 5%. Drugs without a comparator can also be evaluated, and they perform well because ΔQT is larger in molecules from the high-risk group than in compounds with low risk, while a moderate effect is more common in the intermediate group.

Simulations were run with a single male model and a single female model selected from the population of cells, which led to two in-silico ΔQT values, although the real comparator does not distinguish sex-related effects. In fact, depending on the comparator, women may be included or not in the study, but they are usually underrepresented in clinical trials. This means that the validation should be flexible with subgroup results. Differences between male and female were considered part of the uncertainty propagated to outputs when the ionic profile differs between individuals.

Output comparisons displayed in **Figure 35** were inside the acceptable range.

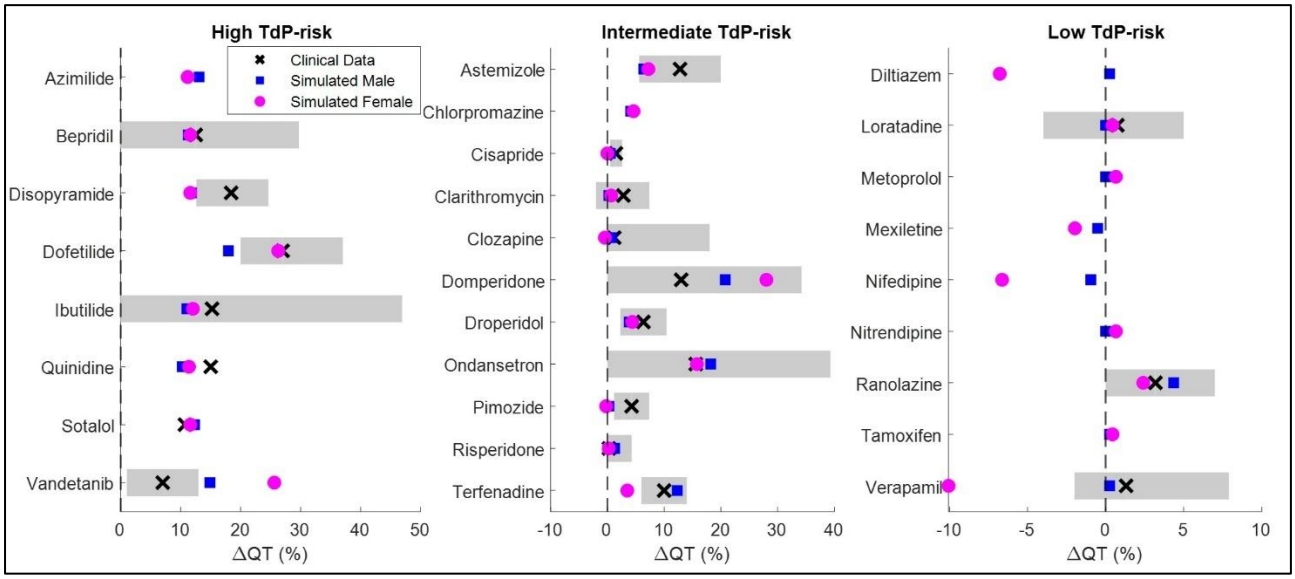

Figure 35: Comparison of in silico QT variation (ΔQT) with clinical data for 28 CiPA drugs. Simulated QT computed for one representative male and one representative female model from the population. Shaded areas represent the experimental range.

Machine Learning Classification

The quality of the classifier is evaluated with performance metrics (**Figure 36**). An accuracy of 87.5 % is obtained with the validation dataset of 16 molecules because there were two low TdP-risk drugs, loratadine and tamoxifen, misclassified as intermediate risk. The same performance metrics are obtained for the male and female populations, although TdP-scores were slightly larger in females. However, such differences were not enough to alter the classification results of any drug after using the same TdP thresholds to separate categories.

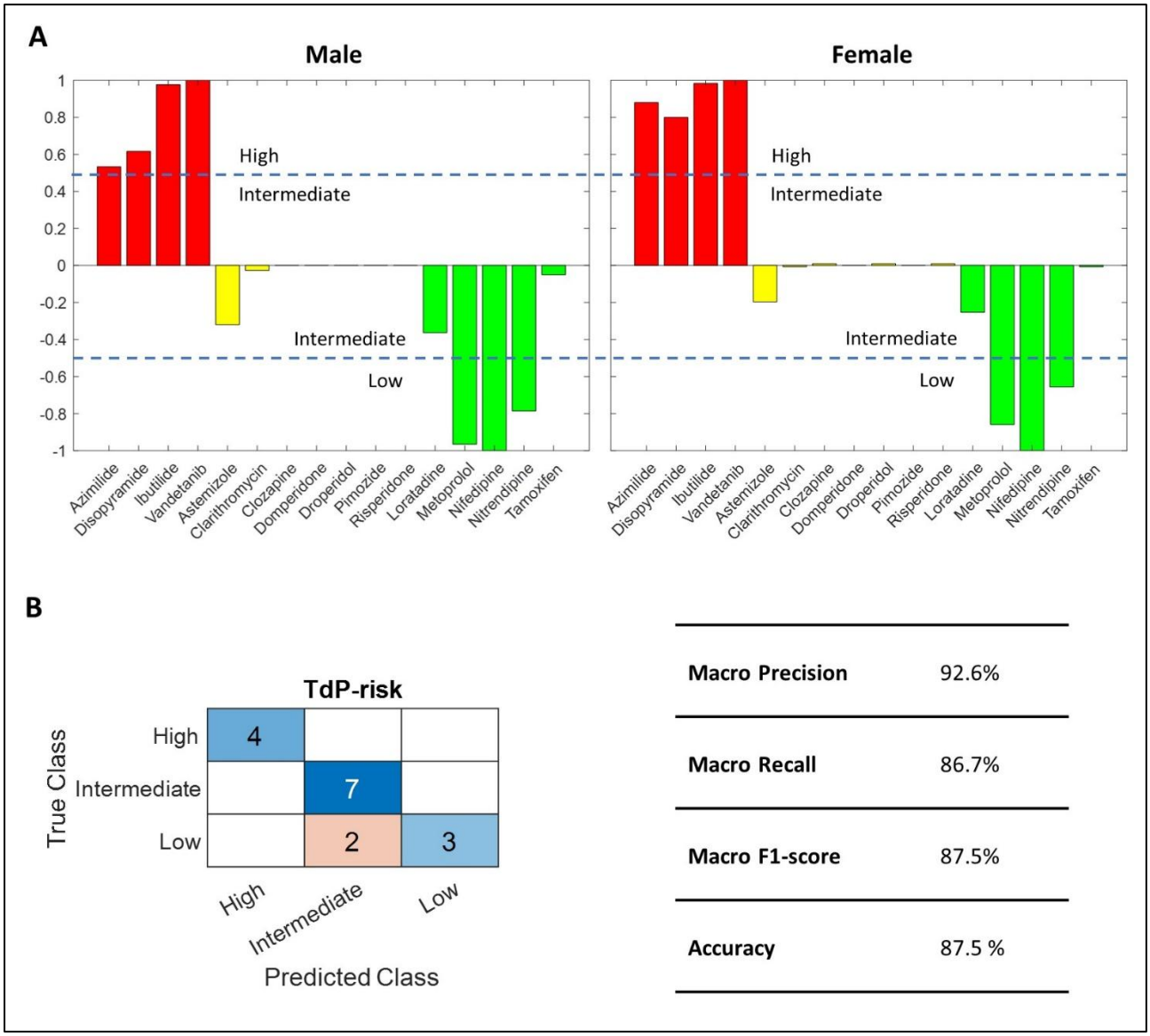

Figure 36: Classification results for the validation dataset of 16 drugs in male and female populations. A) TdP-score graphs and B) performance metrics (same results for males and females).

The predictive power of this machine learning model depends, in part, on the in-silico data provided. In this case, the electrophysiological features used for classification were obtained after validating drug-induced QT prolongations. If only APD prolongation was validated, the classifier performed

with a smaller accuracy (75%). This finding suggests that QT comparators are more reliable to validate drug parameters than cellular comparators.

4.4 UC1 Validation Uncertainty – M30-M54 Activities

This section only contains additional Uncertainty Quantification (UQ) activities conducted on UC3 selected computational model during the M30-M54 period. UQ activities conducted during the M1-M30 period are already reported in the UC3 section of deliverable D6.2. Results reported in this section are meant to complete or (in some cases) supersede results of deliverable D6.2. The latter case will be explicitly mentioned, when applicable.

4.4.1 Comparator Uncertainty

4.4.1.1 PK Model

New data about the uncertainty in PK comparators can be found in Annex C.

4.4.1.2 EP (0D and 3D) Model

Experimental uncertainty in published studies is usually presented in the form of standard deviation or standard error of the mean. We used this data to estimate the intervals for APD and QT variation that help inform about the accuracy of simulation outputs. The expected ranges are specific for each drug scenario and are illustrated in **Figure 34** and **Figure 35** as shaded areas.

4.4.2 Sources of Uncertainty

The populations of cellular models were designed to account for biological uncertainty with the purpose to study how this input variability is propagated to in silico outputs and how these biomarkers match with the uncertainty reported experimentally. The computational cost required to conduct population of models was only feasible at the cellular level, and **Figure 34** illustrates variability effects on APD for the 28 CiPA drugs.

Another uncertainty source is related to drug parameters. There are different studies that have evaluated dose-current blockage effects in their laboratories, leading to multiple possible IC50 values, whose range can span even up to two orders of magnitude (**Figure 37**). The comparators were useful to set the most appropriate parameters, contrasting first with reported cellular APD prolongation and validating later with the QT interval at the organ level. However, moving from 0D to 3D simulations with the same parameters was challenging because outputs did not always align with the expected results. In these cases, 3D comparators prevail because we found that safety assessment performed better after having validating with ECG data.

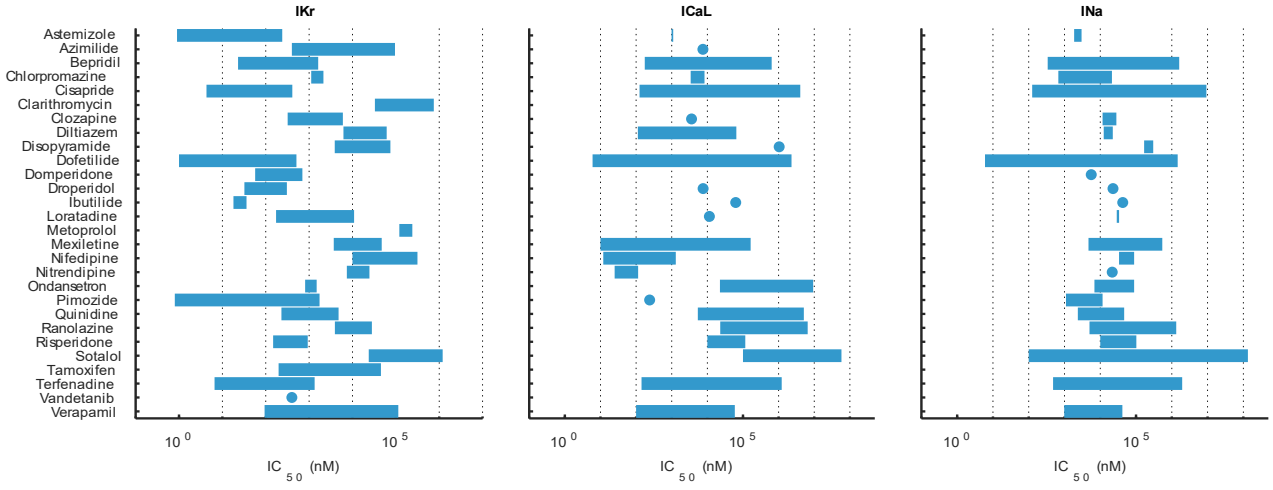

Figure 37: Variability range of IC50 for IKr, ICaL, and INa, based on values reported across multiple studies.

4.5 UC3 Model Applicability – M30-M54 Activities

Our models are part of an in-silico tool for drug safety assessment, which allows to calculate APD90 and QT interval, and provides a classification of drugs considering their torsadogenic risk. Therefore, the computational model was properly conceived to obtain relevant quantities of interest and to answer the Question of Interest.

The only concern is that in-silico predictions are not directly related with real patients, but they provide an estimation on how drugs could perform on a population, and particularly in two subgroups differentiated by sex. Cellular models were virtually generated based on reported data and validation was performed against general metrics gathered from the literature. This implies that, despite the suitability of the validation activities to the context of use, the model domain is large and uncertainty plays an important role. For instance, the experimental comparators did not provide sex differences in biomarkers or TdP risk, so the individual outputs from the numerical models had to be evaluated with the same reference data. In fact, the ground truth for each of the 28 drugs under study is a single TdP-risk label, based on clinical evidence and expert consensus on the effects of the molecule on patients.

To guarantee greater applicability, we attempted to apply two specific comparators per drug, one cellular and other at the organ level, with concentrations close to the therapeutic values. Currently, the relevance of validation points to the COU is limited by the available experimental data, but the methodology here proposed ensures minimal differences between the validation activities and the context of use, and it can be extended to other pharmacological molecules.

4.6 UC3 Discussion

The credibility on the predictive capability of the computational model for proarrhythmic assessment required V&V actions of at least intermediate rigor because the tool was considered to have a medium risk level for the defined COU. Table 9 shows that the score planned to be achieved by validation activities is equal to 3 for all factors except for test conditions. Each credibility factor is the combination of the different actions taken for each of the three individual models that comprise the computational application for drug evaluation, and the final score represents the most

restrictive level. The scarcity of comparator conditions for the electrophysiological model caused a low credibility level in this factor, but for the present COU, electrophysiological conditions were less relevant than sample type (drug) to assess TdP risk. Therefore, despite this particular low coverage level, we think that computational model predictions may still be sufficiently credible for decision-making.

4.6.1 PK Model

Many pharmacokinetic models can be validated thanks to the availability of therapeutic thresholds, which provide a good understanding of drug efficacy and toxicity levels. However, this validation only reflects the a priori accuracy of the models, and is not satisfactory in the case of drugs with narrow therapeutic margins. For this reason, it is important to carry out higher-level validations for certain drugs requiring a higher level of precision.

Validation datasets are difficult to obtain, however, after a thorough search, we found the external comparators needed to complete the list of molecules.

Another additional step incorporated to the validation pipeline was to include inter-individual variability in the predictions. This makes it possible to predict the most likely concentration ranges where an individual would be at a given dose, taking into account the variability of the models implemented. In the context of SimCardioTest, we conducted the entire PK validation of the molecules included for EP assessment.

4.6.2 EP (0D and 3D) Model

With the aim to gain credibility in assessing the TdP risk in drugs, several validation activities have been conducted with the EP model, some of them expanded in this last term with more elaborated outputs regarding the computational cost. Multiple parameters integrate the cellular model but only channel conductance and ion-transport proteins have been analysed as part of the genetic variability determined by protein quantity and function, and because most of the electrophysiological effects induced by pharmacological compounds are linked to the alteration of ion currents. Drug effects were evaluated at the cellular an organ level to obtain in silico biomarkers that can be directly compared with in-vitro and in vivo metrics. Available experimental data from previous published studies were the base for the validation process. We sought in-vitro drug tests to compare APD prolongation and clinical studies reporting changes in QT for each compound. Populations of cellular models show the output variability and two representative sex-differentiated models illustrate differences in the ECG between males and females.
After validating the drug models with key electrophysiological features, a classification tool is implemented to predict the torsadogenic risk of each molecule. This last step strengthens the validation process by directly targeting the question of interest and providing a risk label to each molecule, which allows to identify safe compounds and suggests those that should be discarded because of their TdP risk.

Table 19: Verification Credibility Factors Coverage Level for Use Case 3 (cf. ASME VV40).

Model Risk					x		
Credibility Factor Coverage Level		1	2	3	4	5	
Code Verification: Software Quality Assurance	III			x			
Code Verification: Numerical Code Verification - NCV	IV			x			
Calculation Verification - Discretization Error	III			x			
Calculation Verification - Numerical Solver Error	III			x			
Calculation Verification - Use Error	IV			x			
Validation - Model [Form]	III			x			
Validation - Model [Inputs]	III			x			
Validation - Comparator [Test Samples]	III			x			
Validation - Comparator [Test Conditions]	II			x			
Validation - Assessment [Input Parameters]	III			x			
Validation - Assessment [Output Comparison]	III			x			
Applicability: Relevance of the Quantities of Interest	III			x			
Applicability: Relevance of the Validation Activities to the COU	II			x			

4.7 UC3 – VVUQ Publications

This section lists all scientific publications relating to the UC3 VVUQ activities conducted within the frame of the SimCardioTest project.

Table 20: UC3 – **List of publications related to VVUQ activities**.

Title	VVUQ Topic
Mora MT. (draft) [65]	Validation, Uncertainty Quantification

5. Conclusion

This annex describes all validation, verification, and uncertainty quantification (VVUQ) activities engaged within the SimCardioTest project between M30 (June 2023) and M54 (June 2025) for assessing the credibility of computational models developed in the frame of Use Cases 1 to 3 (cf. WP2, 3, and 4 respectively). This annex follows and completes project deliverables D6.1 and D6.2 issued in June 2023 (M30).

VVUQ activities were conducted on the same computational models introduced in deliverables D6.1 and D6.2, one specific model per each Use Case, corresponding to a pre-selected Question of Interest (QI). All VVUQ activities were conducted according to ASME VV40 standard guidelines.

For what concerns Use Case 1, the activities were completed satisfactorily, ensuring credibility of the model in the sense of the ASME VVUQ framework. Some technical limitations were encountered, which do not endanger the credibility of this work. Verification activities made our software code

more visible and robust, and its continuous development process extremely healthy. Limitations were identified in the formulation of the comparators, which can be considered as induced by the ASME guideline itself. It prompts, for a threshold detection test, to consider goal-oriented criteria, such as the probability of capture at a given point as a more relevant indication for validation activities.

For what concerns Use Case 2, all planned activities related to Verification, Validation, and Uncertainty Quantification (VVUQ) have been successfully completed. Nonetheless, we recognize that clinical validation requires a significantly broader scope of experimentation and verification efforts. Based on the work conducted throughout the duration of the project, we draw the following key conclusions:

- A numerically stable configuration was established with respect to both discretization schemes and numerical methods, specifically within the Ansys Fluent software environment.
- Atrial motion dynamics were incorporated into the simulations, supported by experimental validation. This advancement enabled the application of motion profiles from patients with atrial fibrillation and facilitated comparative analyses with those from healthy individuals.
- Hemodynamic indices related to thrombus formation in the vicinity of left atrial appendage occlusion (LAAO) devices were analysed, providing insights into the influence of device type, positioning, and patient-specific conditions.
- Initial validation of both global and localized flow parameters was undertaken using diverse experimental setups.
- The developed simulation framework was applied to real-world clinical cases, including both retrospective analyses and preliminary prospective (live) studies.

For what concerns Use Case 3, we implemented validation activities following VV40 standard guidelines in a model used to assess the torsadogenic risk of drugs. An independent analysis of the three computational models integrating the drug assessment tool (pharmacokinetics, cellular, and tissue electrophysiology) allowed to focus on the different parameters, inputs, outputs, existing comparators, and uncertainty sources. Executed activities varied depending on the complexity of the model, and we planned all validation steps according to available resources. An intermediate credibility level was achieved after conducting all the tasks in pharmacokinetics and electrophysiological models. This methodology provides robustness to the study results and, although TdP-risk predictions were based on known and validated drugs, the approach can be extended to new molecules.

For each Use Case, a list of scientific publications related to VVUQ activities engaged during the SimCardioTest project is also given.

6. Bibliography

[1] R. Setzu, A. Olivares, J. Mill and others, “Building credibility of computational models in cardiovascular medicine through verification and validation,” *EDMA,* vol. 19, pp. 86-90, 2024.

[2] V&V40, “Assessing Credibility of Computational Modeling Through Verification and Validation: Application to Medical Devices,” ASME, New York, 2018.

[3] "cellML database," [Online]. Available: https://models.cellml.org/electrophysiology.

[4] P. Pathmanathan and R. A. Gray, "Verification of computational models of cardiac electrophysiology," *International Journal for Numerical Methods in Biomedical Engineering,* vol. 30 (5), no. DOI: 10.1002/cnm.2615, p. 525–544, 2014.

[5] G. W. Beeler and H. Reuter, "Reconstruction of the action potential of ventricular myocardial fibres," *The Journal of Physiology,* vol. 268 (1), no. https://pubmed.ncbi.nlm.nih.gov/874889/, p. 177–210, 1977.

[6] V. Pannetier, Simulations numériques standardisées de dispositifs de stimulation électrique cardiaque, PhD Thesis (in French), Université de Bordeaux, 2024.

[7] V. Pannetier, M. Leguèbe, Y. Coudière and others, "Towards validation of two computational models of artificial pacemakers," *Accepted at Functional Imaging and Modeling of the Heart (FIMH),* 2025.

[8] V. Pannetier, M. Leguèbe, Y. Coudière and others, "Sensitivity Analysis in a Rescaled 0D Pacemaker-Bimembrane Model," *Computing in Cardiology (CINC) Conference,* no. doi: 10.22489/CinC.2024.317, 2024.

[9] V. Pannetier, M. Leguèbe, Y. Coudière and others, "Modeling Cardiac Stimulation by a Pacemaker, with Accurate Tissue-Electrode Interface," *Functional Imaging and Modeling of the Heart,* no. doi:10.1007/978-3-031-35302-4_20, p. 194203, 2023.

[10] R. D. Walton, A. Pashaei, M. E. Martinez and others, "Compartmentalized Structure of the Moderator Band Provides a Unique Substrate for Macroreentrant Ventricular Tachycardia," *Circulation: Arrhythmia and Electrophysiology,* vol. 11 (8), no. https://doi.org/10.1161/circep.117.005913, p. e005913, 2018.

[11] V. Pannetier, Y. Coudière and M. Leguèbe, "Bidomain Model Coupled To A Realistic Multi-Electrode Device In Cardiac Electrophysiology," *Congrès National d'Analyse Numérique (CANUM),* no. https://inria.hal.science/hal-04610592v1, 2024.

[12] V. Pannetier, M. Leguèbe, Y. Coudière and others, "Determination of stimulation threshold in a 3D model of a pacemaker," *Virtual Physiological Human (VPH) conference,* 2024.

[13] M. Leguèbe and others, "CEPS : Cardiac Electrophysiology Solver," *Draft submitted to Journal of Open Source Software,* 2025.

[14] A. Cresti, M. García-Fernández, H. Sievert and others, "Prevalence of extra-appendage thrombosis in non-valvular atrial fibrillation and atrial flutter in patients undergoing cardioversion: a large transoesophageal echo study," *EuroIntervention,* vol. 15(3), p. e225–e230, 2019.

[15] M. Pons, J. Mill, A. Fernandez-Quilez and others, "Joint Analysis of Morphological Parameters and In Silico Haemodynamics of the Left Atrial Appendage for Thrombogenic Risk Assessment," *Journal of interventional cardiology,* 2022.

[16] A. Sedaghat and G. Nickenig, "Letter by Sedaghat and Nickenig Regarding Article, "device-Related Thrombus after Left Atrial Appendage Closure: Incidence, Predictors, and Outcomes," *doi:10.1161/CIRCULATIONAHA.118.036179,* 2019.

[17] J. Saw, A. Tzikas, S. Shakir and others, "Incidence and clinical impact of device-associated thrombus and peri-device leak following left atrial appendage closure with the amplatzer cardiac plug," *JACC: Cardiovascular Interventions,* vol. 10, p. 391–399, 2017.

[18] L. V. Boersma, B. Schmidt, T. R. Betts and others, "Implant success and safety of left atrial appendage closure with the watchman device: peri-procedural outcomes from the ewolution registry," *European heart journa,* vol. 37, p. 2465–2474, 2016.

[19] A. Sedaghat and others, "Device-Related Thrombus After Left Atrial Appendage Closure: Data on Thrombus Characteristics, Treatment Strategies, and Clinical Outcomes From the EUROC-DRT-Registry," *Circulation. Cardiovascular interventions,* Vols. 14,5, no. e010195, 2021.

[20] I. Chung and G. Y. Lip, "Virchow's triad revisited: Blood constituents," *Pathophysiology of Haemostasis and Thrombosis,* vol. 33, no. doi:10.1159/00008384, p. 449–454, 2003.

[21] O. D. Backer, X. Iriart, J. Kefer and others, "Impact of computational modeling on transcatheter left atrial appendage closure efficiency and outcomes," *JACC: Cardiovascular Interventions,* vol. 16, no. doi:10.1016/j.jcin.2023.01.008, p. 655–666, 2023.

[22] J. Saw, J. P. Lopes, M. Reisman and H. G. Bezerra, "CT Imaging for Percutaneous LAA Closure," *Cham: Springer International Publishing,* no. doi:10.1007/978-3-319-16280-5, p. 117–132, 2016.

[23] A. M. Aguado, A. L. Olivares, E. Silva and others, "In silico optimization of left atrial appendage occluder implantation using interactive and modeling tools," *Frontiers in physiology,* vol. 10, p. 237, 2019.

[24] X. Freixa and others, "Pulmonary ridge coverage and device-related thrombosis after left atrial appendage occlusion," *EuroIntervention : journal of EuroPCR in collaboration with the Working Group on Interventional Cardiology of the European Society of Cardiology,* vol. 16(15), no. doi:10.4244/EIJ-D-20-00886, pp. e1288-e1294, 2021.

[25] A. Santiago, C. Butakoff, B. Eguzkitza and others, "Design and execution of a verification, validation, and uncertainty quantification plan for a numerical model of left ventricular flow after lvad implantation," *PLoS computational biology,* vol. 18, no. e1010141, 2022.

[26] E. Khalili, C. Daversin-Catty, A. Olivares and others, "On the importance of fundamental computational fluid dynamics towards a robust and reliable model of left atrial flows: Is there more than meets the eye?," *arXiv:2302.01716 [physics.flu-dyn],* 2023.

[27] E. Roche, M. Singh, K. Mendez and others, "Integrating soft robotics and computational models to study left atrial hemodynamics and device testing in sinus rhythm and atrial fibrillation," *Research Square,* vol. PREPRINT (Version 1), no. DOI: 10.21203/rs.3.rs-6283242/v1.

[28] C. Albors, J. Mill, H. A. Kjeldsberg and others, "Sensitivity Analysis of Left Atrial Wall Modeling Approaches and Inlet/Outlet Boundary Conditions in Fluid Simulations to Predict Thrombus Formation," in *Statistical Atlases and Computational Models of the Heart. Regular and CMRxMotion Challenge Papers (STACOM 2022)*, 2022.

[29] C. Albors, A. L. Olivares, X. Iriart and others, "Impact of Blood Rheological Strategies on the Optimization of Patient-Specific LAAO Configurations for Thrombus Assessment," in *Functional Imaging and Modeling of the Heart (FIMH 2023)*, 2023.

[30] J. Mill, J. Harrison, M. Saiz-Vivo and others, "The role of the pulmonary veins on left atrial flow patterns and thrombus formation," *Sci Rep,* vol. 14, no. https://doi.org/10.1038/s41598-024-56658-2, p. 5860, 2024.

[31] E. Khalili, C. Daversin-Catty, A. L. Olivares and others, "On the importance of fundamental computational fluid dynamics toward a robust and reliable model of left atrial flows,"

Internatioanl Journal for Numerical Methods in Biomedical Engineering, vol. 40 (4), no. https://doi.org/10.1002/cnm.3804, p. e3804, 2024.

[32] C. Albors, J. Mill, A. L. Olivares and others, "Impact of occluder device configurations in in-silico left atrial hemodynamics for the analysis of device-related thrombus," *PLoS Comput Biol,* vol. 20 (9), no. doi: 10.1371/journal.pcbi.1011546, p. e1011546, 2024.

[33] A. Olivares and others, "Verification and validation pipeline of fluid simulations for optimising left atrial appendage occluder implantations: design and initial experiments," *draft*.

[34] E. Gasparotti, E. Vignali, R. Marangoni and others, "An Experimental Setup for the Analysis of Patient-Specific Left Atrial Appendage with Particle Image Velocimetry Investigation," *Functional Imaging and Modeling of the Heart* , no. DOI:10.1007/978-3-031-94559-5_17, pp. 186-196, 2025.

[35] C. Albors and others, "Impact of Flow Dynamics according to Device Implant Depth after Left Atrial Appendage Occlusion," *draft*.

[36] P. Casademunt and others, "Flow component analysis to study haemodynamic," in *CMBEE2025*, 2025.

[37] M. Barrouhou and others, "Large-scale sensitivity analysis of modeling settings influencing Hemodynamics after left atrial appendage occlusion," in *CMBEE2025*, 2025.

[38] C. Albors, N. Arrarte Terreros, M. Saiz and others, "In silico estimation of thrombogenic risk after left atrial appendage excision: Towards digital twins in atrial fibrillation," *Computers in biology and medicine,* vol. 194, no. DOI:10.1016/j.compbiomed.2025.110483, p. 110483, 2025.

[39] H. Kjeldsberg, C. Albors, J. Mill and others, "Impact of left atrial wall motion assumptions in fluid simulations on proposed predictors of thrombus formation," *International Journal for Numerical Methods in Biomedical Engineering,* vol. 40 (6), no. DOI:10.1002/cnm.3825, 2024.

[40] Z. Li, B. J. Ridder, X. Han and others, "Assessment of an In Silico Mechanistic Model for Proarrhythmia Risk Prediction Under the CiPA Initiative," *Clinical Pharmacology & Therapeutics,* vol. 105, no. 2, pp. 466-475, 2 2019.

[41] S. Nobe, M. Aomine and M. Arita, "Bepridil prolongs the action potential duration of guinea pig ventricular muscle only at rapid rates of stimulation," *General Pharmacology: The Vascular System,* vol. 24, no. 5, pp. 1187-1196, 9 1993.

[42] S. C. Verduyn, J. G. M. Jungschleger, M. Stengl and others, "Electrophysiological and proarrhythmic parameters in transmural canine left-ventricular needle biopsies.," *Pflugers Archiv : European journal of physiology,* vol. 449, no. 1, pp. 115-22, 10 2004.

[43] J. J. Salata, N. K. Jurkiewicz, A. A. Wallace, R. F. Stupienski, P. J. Guinosso and J. J. Lynch, "Cardiac Electrophysiological Actions of the Histamine H r Receptor Antagonists Astemizole and Terfenadine Compared With Chlorpheniramine and Pyrilamine," 1995.

[44] J. K. Gibson, Y. Yue, J. Bronson and others, "Human stem cell-derived cardiomyocytes detect drug-mediated changes in action potentials and ion currents," *Journal of Pharmacological and Toxicological Methods,* vol. 70, no. 3, pp. 255-267, 11 2014.

[45] Y. Yu, M. Zhang, R. Chen and others, "Action potential response of human induced-pluripotent stem cell derived cardiomyocytes to the 28 CiPA compounds: A non-core site data report of the CiPA study," *Journal of Pharmacological and Toxicological Methods,* vol. 98, 7 2019.

[46] B. Lecocq, V. Lecocq, P.-L. Prost and others, "Effects of bepridil and CERM 4205 (ORG 30701) on the relation between cardiac cycle length and QT duration in healthy volunteers," *The American Journal of Cardiology,* vol. 66, no. 5, pp. 636-641, 5 1990.

[47] S. Miyamoto, B. M. Zhu, T. Teramatsu and others, "QT-prolonging class I drug, disopyramide, does not aggravate but suppresses adrenaline-induced arrhythmias. Comparison with cibenzoline and pilsicainide," *European Journal of Pharmacology,* vol. 400, no. 2-3, pp. 263-269, 5 2000.

[48] F. L. Coz, C. Funck-Brentano, T. Morell and others, "Pharmacokinetic and pharmacodynamic modeling of the effects of oral and intravenous administrations of dofetilide on ventricular repolarization," *Clinical pharmacology and therapeutics,* vol. 57, no. 5, pp. 533-542, 1995.

[49] B. S. Stambler, M. A. Wood, K. A. Ellenbogen and others, "Efficacy and safety of repeated intravenous doses of ibutilide for rapid conversion of atrial flutter or fibrillation," *Circulation,* vol. 94, no. 7, pp. 1613-1621, 5 1996.

[50] H. M. Himmel, A. Bussek, M. Hoffmann and others, "Field and action potential recordings in heart slices: correlation with established in vitro and in vivo models," *British journal of pharmacology,* vol. 166, no. 1, pp. 276-296, 5 2012.

[51] K. Kiura, K. Nakagawa, T. Shinkai and others, "A Randomized, Double-Blind, Phase IIa Dose-Finding Study of Vandetanib (ZD6474) in Japanese Patients With Non-Small Cell Lung Cancer," *Journal of Thoracic Oncology,* vol. 3, no. 4, pp. 386-393, 5 2008.

[52] L. Testai, M. C. Breschi, E. Martinotti and V. Calderone, "QT prolongation in guinea pigs for preliminary screening of torsadogenicity of drugs and drug-candidates. II," *Journal of applied toxicology : JAT,* vol. 27, no. 3, pp. 270-275, 5 2007.

[53] A. D. V. Haarst, G. A. E. V. '. Klooster, J. M. A. V. Gerven and others, "The influence of cisapride and clarithromycin on QT intervals in healthy volunteers," *Clinical pharmacology and therapeutics,* vol. 64, no. 5, pp. 542-546, 1998.

[54] R. A. Carr, A. Edmonds, H. Shi and others, "Steady-state pharmacokinetics and electrocardiographic pharmacodynamics of clarithromycin and loratadine after individual or concomitant administration," *Antimicrobial agents and chemotherapy,* vol. 42, no. 5, pp. 1176-1180, 1998.

[55] I. Grande, A. Pons, I. Baeza and others, "QTc prolongation: is clozapine safe? Study of 82 cases before and after clozapine treatment," *Human psychopharmacology,* vol. 26, no. 6, pp. 397-403, 5 2011.

[56] G. Frommeyer, C. Fischer, C. Ellermann and others, "Severe Proarrhythmic Potential of the Antiemetic Agents Ondansetron and Domperidone," *Cardiovascular toxicology,* vol. 17, no. 4, pp. 451-457, 5 2017.

[57] B. Charbit, J. C. Alvarez, E. Dasque and others, "Droperidol and ondansetron-induced QT interval prolongation: a clinical drug interaction study," *Anesthesiology,* vol. 109, no. 2, pp. 206-212, 2008.

[58] Z. Desta, T. Kerbusch and D. A. Flockhart, "Effect of clarithromycin on the pharmacokinetics and pharmacodynamics of pimozide in healthy poor and extensive metabolizers of cytochrome P450 2D6 (CYP2D6)," *Clinical pharmacology and therapeutics,* vol. 65, no. 1, pp. 10-20, 1999.

[59] E. P. Harrigan, J. J. Miceli, R. Anziano and others, "A randomized evaluation of the effects of six antipsychotic agents on QTc, in the absence and presence of metabolic inhibition," *Journal of clinical psychopharmacology,* vol. 24, no. 1, pp. 62-69, 5 2004.

[60] L. Johannesen, J. Vicente, J. W. Mason and others, "Differentiating Drug-Induced Multichannel Block on the Electrocardiogram: Randomized Study of Dofetilide, Quinidine, Ranolazine, and Verapamil," *Clinical Pharmacology & Therapeutics,* vol. 96, no. 5, pp. 549-558, 5 2014.

[61] B. Darpo, "The thorough QT/QTc study 4 years after the implementation of the ICH E14 guidance," *British Journal of Pharmacology,* vol. 159, no. 1, pp. 49-57, 1 2010.

[62] J. Llopis-Lorente, B. Trenor and J. Saiz, "Considering population variability of electrophysiological models improves the in silico assessment of drug-induced torsadogenic risk," *Computer Methods and Programs in Biomedicine,* vol. 221, p. 106934, 6 2022.

[63] J. Llopis-Lorente, S. Baroudi, K. Koloskoff and others, "Combining pharmacokinetic and electrophysiological models for early prediction of drug-induced arrhythmogenicity," *Computer Methods and Programs in Biomedicine,* vol. 242, p. 107860, 12 2023.

[64] C. Knox, M. Wilson, C. M. Klinger and others, "DrugBank 6.0: the DrugBank Knowledgebase for 2024," *Nucleic Acids Research,* vol. 52, no. D1, pp. D1265-D1275, 1 2024.

[65] M. Mora, C. Ortigosa, H. Finsberg and others, "Refinement of electrophysiological drug safety assessment through validation-readjustment strategies," *draft*.

This project received funding from the European Union's Horizon 2020 research and innovation program under grant agreement No 101016496

EU Horizon 2020 Research & Innovation Program
Digital transformation in Health and Care
SC1-DTH-06-2020
Grant Agreement No. 101016496

SimCardioTest - Simulation of Cardiac Devices & Drugs for in-silico Testing and Certification

SIM CARDIO TEST

Technical Annex

Annex C – WP6 UC3 PK Validation
(complement to WP6 Task 6.2 – including M30-M54 activities)

Work Package 6 (WP6)
Verification, validation, uncertainty quantification & certification

WP Lead: MPC, France

PUBLIC

Document history			
Date	**Version**	**Author(s)**	**Comments**
06/15/2023	V1	S. BAROUDI, K. KOLOSKOFF	Final Draft
29/06/2023	V2	R. SETZU	Format Consolidation
30/06/2023	V3	R. SETZU	Final Version
01/07/2023	V4	R. SETZU	Format editing
23/07/2024	V5	S. BAROUDI, R. LESTREZ	Content editing
30-06-2024	V6	R. SETZU	Format editing Highlighted M36-M54 new content

Table Of Contents

Executive Summary

This technical annex expands on Annex A6.2-UC3-PK which was initially included in the SimCardioTest WP6 deliverable D6.2 and elaborated for Use Case 3 in the context of drug safety assessment. It completes the original annex with the work performed after M30 till the completion of the UC3 validation activities of the PK models in scope.

Acronyms

Table 1. *List of acronyms.*

Acronym	Meaning
EXC	ExactCure
ANSM	Agence nationale de sécurité du médicament et des produits de santé
IIV	Interindividual variability
RV	Residual variability
MDAPE	Median absolute predictive error
MDPE	Median predictive error
NC	Non-compartmental
PK	Pharmacokinetics
PKPOP	Population pharmacokinetics
RSE	Relative standard error
SCT	SimCardioTest
SE	Standard error
TdP	Torsade de pointes
GFR	Glomerular filtration rate
Cmax	Maximum concentration
Tmax	Time to reach the maximum concentration
AUC	Area under the curve
T1/2	Half-life of elimination
Vd	Distribution volume
V1	Central volume
V2	Peripheral volume
F	Bioavailability
ka	Absorption rate
ke	Elimination rate

1. Computational Model

Validation activities consist of verifying that pharmacokinetic (PK) models enable predictions as close as possible to reality for the different sub-populations likely to receive a given treatment. The validation of these models is essential to ensure that the underlying model assumptions are correct and that the sensitivities and uncertainties of the PK model are well understood.
Pharmacokinetics, which describes the body's effect on drugs, must be as accurate as possible because it is used to adapt the dosage regimen of drugs to all patients, considering their physical, biological, and demographic characteristics, as well as other individual differences.
Thus, appropriate validation activities require rigorous attention to both the PK model and the comparators, with a thorough evaluation of the simulation results to ensure the accuracy and reliability of predictions under varied conditions. The following sections will describe aspects of the validation process in more detail.

1.1 Model Form

The PK models implemented by EXC are mathematical models characterizing the kinetics of drugs in the body. The model is established using parameters sourced from scientific literature and summary of product characteristics published on regulatory agencies website (FDA, EMA, ANSM, etc.). Depending on the availability of literature and the extent of research carried out on each molecule, EXC implements different types of PK models, classified according to their initial level of evaluation:

1. Model built with non-compartmental data (NC) data from pharmacokinetic literature.
2. Model built with NC data from regulators' approved data. (summary of product characteristics, regulatory agencies documents).
3. Model built from population pharmacokinetics (popPK) analysis.
4. Model built from popPK analysis and external NC data.
5. Meta-Model built from popPK analysis studies.

The targeted depth – level is 3/5 and is current practice in ExactCure Validation Process. Models whose "model form" is rated 2/5 can be validated if they meet other validation criteria.

1.2 Model Inputs

The model inputs to run a PK simulation are:

- Mathematical equations (describing the drug kinetics).
- Model parameters (structural parameters, covariates).
- Model conditions (additional parameters concerning dosage configuration and patient covariates are required):
    - Patients' profiles, defined by their covariates impacting the models, which differ from one model to another.

- Drug dosages, defined by the following parameters, which also differ from one model to another:
    - Route (Oral, Rectal, Intravenous, Intramuscular, etc.)
    - Form (Tablet, Capsule, Solution, etc.)
    - Release process associated with the form (Controlled release, Immediate release, etc.)
    - Frequency of administration
    - Duration of administration

1.2.1 Model inputs sources

The model inputs are evaluated according to the following criteria:

1. The parameters of the model are derived from NC data obtained from analysis on few patients or with high variability.
2. The parameters used are derived from NC data from regulatory agencies or obtained from analysis involving large numbers of patients or with low variability.
3. Parameters are obtained from popPK analysis with a relative standard error (RSE) > 30% or taken from the summary of product characteristics or from analysis conducted on many patients with little variability.
4. Parameters are obtained from popPK analysis with a relative standard error (RSE) ≤ 30%.

The targeted depth - level is 3/4 and is current practice in the ExactCure Validation Process.

For Validation tests, all these model inputs are encoded following EXC internal declaration (Digital Twin module of EXC medical device ExaMed).

1.2.2 Quantification of sensitivities

Quantification of sensitivities involves examining the degree of sensitivity of the model outputs to the model inputs. A comprehensive sensitivity analysis was performed to assess whether a ±10% change in parameters results in appropriate changes in the outputs.

For each model, parameters should influence the simulation results in an expected way. If the behaviour of the results aligns with the expected direction of the parameter modifications, there are no contraindications for validation. The model is not validated if a parameter modification leads to unexpected behaviour. Behaviour on Cmax and AUC were used as standards outputs for the sensitivity analysis:

Table 2. Expected behaviour of simulation outputs (Cmax and AUC) of the sensitivity analysis from PK parameters.

Expected behavior								
	ka		F		V		CL	
	-10%	+10%	-10%	+10%	-10%	+10%	-10%	+10%
Cmax	↓	↑	↓	↑	↑	↓	↑	↓
AUC	=	=	↓	↑	=	=	↑	↓

ka: absorption rate constant, F: bioavailability, V: volume of distribution, and CL: clearance of elimination. Symbols were ↓ for decrease, ↑ for increase, = for no significant impact.

1.2.3 Quantification of uncertainties

Quantification of uncertainties involves identifying and quantifying uncertainties on model parameters and propagating them into simulation results.
Different levels of uncertainties exist in models :

1. The model inputs are fixed parameters from NC literature.
2. The model inputs are parameters from NC literature with ranges used to propagate uncertainties.

3. The model has been built with popPK data : uncertainties are quantified as interindividual variability (IIV) and residual variability (RV).

For each model, the model inputs are described in model inputs sources section. Simulations with propagation of uncertainties are shown in quantification of uncertainties section.

The steps of quantification of sensitivities and uncertainties will be performed separately at the end of the document.

2. Comparator

2.1 Test Samples

The data used to validate the implemented PK models are taken from the literature.
Several levels of test samples are defined as follows:

1. Scattered data from the literature or from the summary of product characteristics, which may be average concentrations, endpoints (e.g., area under the curve, elimination half-life, maximum concentration, time to reach maximum concentration), etc.
2. Efficacy, overexposure, and safety thresholds used for routine therapeutic drug monitoring (TDM) in clinical settings, or thresholds reflecting specific expected events (such as efficacy or toxicity) that may occur at these levels of exposure.
3. External evaluation dataset, which may be derived from partnership projects or open access online, to carry out external evaluations.

The targeted depth – level is 2/3 and is current practice in ExactCure Validation Process.

2.2 Test Conditions

Tests must be performed in conditions where all the specific sub-populations concerned by a drug are covered. Tests must be carried out for all formulations of the drug, for all concerned sub-populations, so that the models can be validated in all possible configurations of its use. These conditions depend on the covariates included in the models (and therefore the data available for the analysis), as well as on the dose recommendations in force.

Several levels of test conditions are defined as follows:

1. Test conditions were defined with limited data allowing to run simulations for a few standard patients, either because the model does not incorporate all covariates of interest, or because dose recommendations do not cover specific populations that may require dose adaptation.
2. Test conditions were defined with few data allowing to run simulations for a few standard patients and a specific population of interest, which may come from unofficial recommendations (i.e., not published by a regulatory agency) but from literature articles.
3. Test conditions were defined with sufficient data allowing to run simulations for each subpopulation concerned by the drug, but learning dataset is not exhaustive, and leads to extrapolation for patients that were not included in the learning dataset. (e.g., the learning dataset includes young patients only. Simulation for elderly patients leads to extrapolate).
4. Test conditions were defined with sufficient data to run simulations for each patient concerned by the drug, with complete coverage of dosage ranges, and of all sub-populations concerned by the drug.

5. Test conditions were defined with external evaluation dataset. Tests conditions reproduce patients' characteristics from the validation dataset to compare with model outputs.

The targeted depth – level is 4/5 and is current practice in ExactCure Validation Process.

3. Assessment

3.1 Equivalency of Input Parameters

The equivalence of input parameters depends on the training dataset of the PK model.
Parameters are equivalent if all doses tested are present in the training dataset, and all patient subpopulations affected by the drug have been covered.
If certain prescribable doses are not included in the training dataset, it is possible to extrapolate with a low risk in the case where the PK of the molecule is linear (response proportional to dose). Most molecules are linear at therapeutic doses.
In cases where sub-populations are not included in the training dataset, extrapolation can only be performed if external data are available to validate it.

Several levels of equivalency of input parameters are defined as follows:

1. The model's training dataset does not cover all the sub-populations concerned by the medication and doses tested. The molecule's PK is not linear over the dose range used in the test conditions. Sub-populations and doses extrapolation can be performed if external data is available to validate it.
2. The model's training dataset does not cover all the sub-populations concerned by the medication and doses tested. The molecule's PK is linear over the dose range used in the test conditions. Sub-populations extrapolation can be performed if external data is available to validate it.
3. The model's training dataset does covers doses tested or PK is linear over the dose range used in the test conditions, but not all the sub-populations concerned by the medication. Sub-populations extrapolation can be performed if external data is available to validate it, or an external validation is carried out and meets validation criteria. (i.e., MDPE ≤ ± 20%, MDAPE ≤ 30%)
4. The model's training dataset does cover all doses or PK is linear over the dose range used in the test conditions and sub-populations concerned by the medication, or an external validation is carried out and meets validation criteria. (i.e., MDPE ≤ ± 20%, MDAPE ≤ 30%)

The targeted depth – level is 3/4 and is current practice in ExactCure Validation Process.

The level 4/4 is achievable provided a PK model learned from a large population is available in the literature, or a meta-model is developed.

3.2 Output Comparison

The comparison of simulation results with validation data is evaluated with the following criteria:

1. Correspondence of model outputs with the results presented in the article from which the model originates.
2. Correspondence of model outputs with external data available in the literature (T1/2, Cmax, Tmax, AUC)
3. Correspondence of model outputs with the therapeutic thresholds used in routine clinical therapeutic drug monitoring or thresholds reflecting specific expected events (such as efficacy or toxicity) that may occur at these levels of exposure.
4. Correspondence of model outputs with an external evaluation dataset or prediction uncertainties. Validation criteria are MDPE ≤ ± 20%, MDAPE ≤ 30%.
5. Correspondence of model outputs with an external evaluation dataset + prediction uncertainties. Validation criteria are MDPE ≤ ± 20%, MDAPE ≤ 30%.

The validation tests are performed for all sub-populations covered by the prescribing information's in the summary of product of the drug.

The targeted depth – level is 3/5 and is current practice in ExactCure Validation Process.

4/4 is achievable provided a PK model learned from a large population is available in the literature, or a meta-model is developed.

3.3 Conclusion

These general requirements must be met for all EXC PK models. If this is not the case, the validation steps are not satisfactory, and the model must be reworked and resubmitted for validation. Validation is performed by another modeler other than the one who implemented the model. A manager then ensures that the steps are in line with the defined process of validation.

4. Application of validation processes

4.1 Clozapine

Table 3. Summary of clozapine validation.

Summary		
Levels	**Notations**	**Comments**
Model form level	3/5	Model built from popPK analysis
Model inputs sources level	NA	RSE% were not communicated however this model was successfully validated with an external evaluation
Test samples level	3/3	External database
Tests conditions level	5/5	Test conditions were defined with external evaluation dataset

Equivalency of input parameters level	4/4	All doses and subpopulations of the validation dataset are covered by the training dataset
Output comparison level	4/5	Output comparison met validation criteria
Conclusion: The model is validated since all criteria meet the minimum score required, except for the Model inputs sources level, which is not applicable, but in this case the model was validated with an external database guaranteeing the accuracy and unbiasedness of the model.		

4.1.1 Model Form

Model form level: 3/5
Model form: model built from popPK analysis.
Model source(s): Jerling et al [1]
Comment: the implemented PK model is based on a popPK analysis. It is a one-compartment model with first order absorption and elimination.

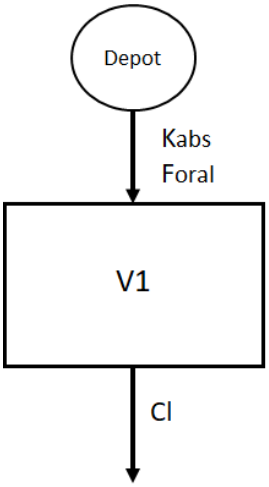

Figure 1. *Model's structure, with one depot compartment, and one central compartment. Kabs, is the absorption rate, Foral the bioavailability V1 the volume of distribution, CL the clearance of elimination.*

4.1.2 Model inputs sources

Model inputs sources level: NA
Model input: NA
Model inputs source(s): Jerling et al [1]
Comment: even though the parameters are derived from a population pharmacokinetic (popPK) study, the evaluation of the model inputs is not directly applicable to this specific model of clozapine. However, the model was successfully validated using an external dataset, providing a clear indication of the accuracy and relevance of the parameters.
Models inputs were directly taken from Jerling et al [1], as shown in the following figure.

	Women			Men		
	Median with 25% and 75% quartiles	*Mean*	*Coefficient of variation*	*Median with 25% and 75% quartiles*	*Mean*	*Coefficient of variation*
ka (h^{-1})	1.24 (0.80, 1.50)	1.24	0.42	1.30 (0.87, 1.72)	1.37	0.49
V/F (l)	401 (189, 932)	564	0.8	694 (224, 970)	719	0.79
k (h^{-1})	0.086 (0.037, 0.131)	0.1	0.72	0.083 (0.054, 0.127)	0.095	0.62
CL/*F* ($l\,h^{-1}$)	28.3 (15.2, 48.6)	39.9	1.22	38.2 (22.0, 60.0)	47.9	0.72

Figure 2. Clozapine model parameters from Jerling et al [1]. ka is the absorption rate, V/F is the volume of distribution corrected by the bioavailability (F), k is the elimination rate, CL/F is the clearance of elimination corrected by the bioavailability. Picture from [1].

4.1.3 Quantification of sensitivities

Table 4. Analysis of the sensitivity of Cmax and AUC for clozapine by varying absorption rate constant (ka), bioavailability (F), volume of distribution (V), and clearance of elimination (CL).

Sensitivity analysis												
	ka			F			V			CL		
	-10%	ref	+10%	-10%	ref	+10%	-10%	ref	+10%	-10%	ref	+10%
Cmax	0.1494	0.1510	0.1524	0.1359	0.1510	0.1661	0.1591	0.1510	0.1445	0.1598	0.1510	0.1439
Expected behavior	Yes		Yes	Yes		Yes	Yes		Yes	Yes		Yes
AUC	10.32	10.32	10.32	9.289	10.32	11.35	10.36	10.32	10.28	11.41	10.32	9.413
Expected behavior	Yes		Yes	Yes		Yes	Yes		Yes	Yes		Yes

Conclusion: The sensitivity analysis did not indicate any discrepancies in the expected behavior of the outputs studied, thereby confirming that there is no obstacle to the model's validation.

4.1.4 Quantification of uncertainties

Introduction

The model has been built with popPK data : uncertainties are quantified with median and quartiles.

Propagation in simulation results

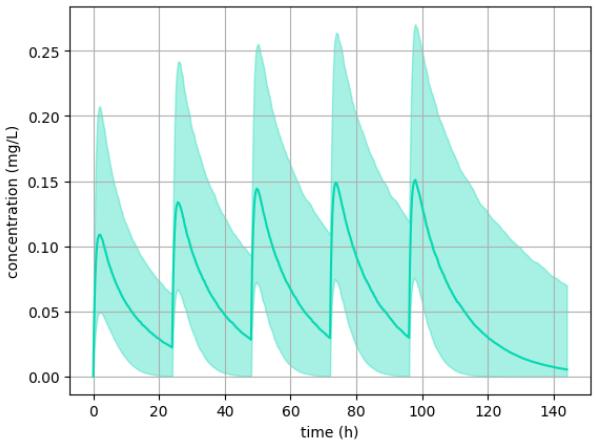

Figure 3. quantification of uncertainties for clozapine

4.1.5 Test Samples

Test sample level: 3/3
Test sample: external evaluation dataset.
Test samples source(s): Lereclus et al. [2].
Comment: in the context of A. Lereclus PhD thesis (ExactCure collaborator), an external dataset for validation (53 patients, 151 observations) was used to evaluate literature models. Jerling et al. [1] was the most performant.

Characteristics	Number or Mean ± SD	Median (Range)
No. of patients (male/female)	53 (41/12)	NA
No. of samples	151	NA
No. of samples per patient	2.77 (±3.90)	1 (1–20)
Age (yr)	38.66 (±11.51)	37 (19–66)
Weight (kg)	81.21 (±19.20)	80 (47–122)
Height (cm)	172.92 (±8.54)	175 (153–185)
Concentration (mg/L)	381 (±296)	287 (36–1504)
Dose (mg)	224.29 (±129.90)	200 (25–625)
Smoker (yes/no)	32/21	NA

Figure 4. External evaluation dataset patients' characteristics from Lereclus et al., 2022. Picture from [2].

4.1.6 Test Conditions

Tests conditions level: 5/5
Tests conditions: test conditions were defined with external evaluation dataset. Tests conditions reproduce patients' characteristics from the validation dataset to compare with model outputs.
Tests conditions source(s): Lereclus et al. [2].
Comment: simulations reproducing physical, biological, and demographic characteristics of patients from an external evaluation dataset were carried out to compare observations and simulations. All situations were covered by the test conditions.

4.1.7 Equivalency of input parameters

Equivalency of input parameters level: 4/4

Equivalency of input parameters: the model's training dataset does cover all doses or PK is linear over the dose range used in the test conditions and sub-populations concerned by the medication, or an external validation is carried out and meets validation criteria. (i.e., MDPE ≤ ± 20%, MDAPE ≤ 30%)
Equivalency of input parameters source(s): Lereclus et al. [2]
Comment: the validation database is covering all patients and doses of the training dataset.

Characteristics	Number or Mean ± SD	Median (Range)
No. of patients (male/female)	53 (41/12)	NA
No. of samples	151	NA
No. of samples per patient	2.77 (±3.90)	1 (1–20)
Age (yr)	38.66 (±11.51)	37 (19–66)
Weight (kg)	81.21 (±19.20)	80 (47–122)
Height (cm)	172.92 (±8.54)	175 (153–185)
Concentration (mg/L)	381 (±296)	287 (36–1504)
Dose (mg)	224.29 (±129.90)	200 (25–625)
Smoker (yes/no)	32/21	NA

Figure 5. External evaluation dataset. Picture from [2].

	Women	*Men*
Number of patients	82	159
Number of observations	141	250
Age (years)	39 ± 11 (20–74)	37 ± 9 (20–86)
Total daily dose (mg)	398 ± 160 (50–800)	378 ± 158 (12.5–800)
Dose events per day	2.1 ± 0.8 (1–4)	2.1 ± 0.7 (1–4)
Interval last dose—sampling (h)	12.0 ± 3.0 (2–24)	12.3 ± 3.0 (0.5–24)
Plasma concentration (ng ml^{-1})	515 ± 628 (18–5363)	333 ± 354 (19–3772)

Figure 6. Model training dataset. Picture from [1].

4.1.8 Output Comparison

Output comparison level: 4/5
Output comparison: external evaluation dataset.
Output comparison source(s): Lereclus et al. [2]
Comment: the results of an external validation performed by Aurélie Lereclus (151 samples from 53 patients) resulted in median predictive error (MDPE) of -19% and median absolute predictive error (MDAPE) of 29.4%. The external validation meets validation criteria.

4.2 Escitalopram

Table 5. Summary of escitalopram validation.

Summary		
Levels	**Notations**	**Comments**
Model form level	3/5	Model built from popPK analysis
Model inputs sources level	3/4	RSE% were >30% for structural parameters
Test samples level	2/3	Therapeutic thresholds
Tests conditions level	3/5	Most conditions could have been tested except renal and hepatic status that were not studied because the training dataset didn't include data on these statuses.
Equivalency of input parameters level	3/4	All doses were covered by the training dataset, but renal and hepatic status was not studied.
Output comparison level	3/5	Model outputs were within therapeutic thresholds.
Conclusion: The model is validated since all criteria meet the minimum score required.		

4.2.1 Model Form

Model form level: 3/5
Model form: model built from popPK analysis.
Model Source(s): Jin et al. [3]
Comment: the implemented PK model is based on a popPK analysis conducted by Jin et al. [3]. It is a one-compartment model with first order absorption and elimination.

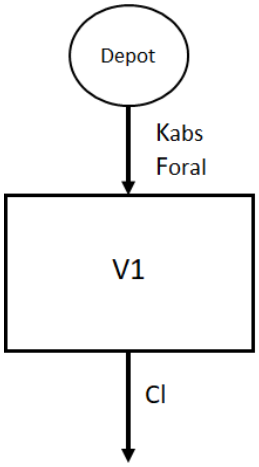

Figure 7. *Model's structure, with one depot compartment, and one central compartment. Kabs, is the absorption rate, Foral the bioavailability V1 the volume of distribution, CL the clearance of elimination.*

4.2.2 Model inputs sources

Model inputs sources level: 3/4
Model input: parameters are obtained from popPK analysis with a relative standard error (RSE) > 30% or taken from the summary of product characteristics or from analysis conducted on many patients with little variability.
Model inputs source(s): Jin et al. [3].
Comment: /

Parameters	Final Model Estimates	SE%
CL for 2C19 Rapid and Extensive (L/Hr)	26	7.20%
CL for 2C19 IM and PM (L/Hr)	19.8	8.50%
CL for 2C19 missing (L/Hr)	21.5	7.80%
Age on Clearance	$CL_1=CL_0*(Age/40)^{-0.336}$	42.00%
Weight on Clearance	$CL_2=CL_1*(Wgt/76)^{0.333}$	54.10%
V (L)	947	10.20%
BMI on V	$V*(BMI/27)^{1.11}$	49.50%
Ka (hr^{-1})	0.8	N/A
ω_{cl} %	48.5%	15.10%
ω_{v} %	62.0%	40.30%
ω_{Ka} %	78.9%	87.00%
$\omega_{cl,v}$ %	9.4%	N/A
$\omega_{cl,Ka}$ %	47.8%	N/A
$\omega_{v,Ka}$ %	81.3%	N/A
σ_1 %	28.9%	8.80%

Figure 8. Escitalopram model parameters from Jin et al. [3]. ka is the absorption rate, V/F is the volume of distribution corrected by the bioavailability (F), k is the elimination rate, CL/F is the clearance of elimination corrected by the bioavailability. CL is different for each CYP2C19 type of metabolizer. IM = intermediate metabolizer, PM = poor metabolizer, BMI = body mass index, ω the coefficient of variation of the interindividual variability. σ the coefficient of variation of the residual error. Picture from [3].

4.2.3 Quantification of sensitivities

***Table 6**. Analysis of the sensitivity of Cmax and AUC for escitalopram by varying absorption rate constant (ka), bioavailability (F), volume of distribution (V), and clearance of elimination (CL).*

Sensitivity analysis												
	ka			F			V			CL		
	-10%	ref	+10%	-10%	ref	+10%	-10%	ref	+10%	-10%	ref	+10%
Cmax	0.02854	0.02873	0.02890	0.02586	0.02873	0.03160	0.02975	0.02873	0.02781	0.03079	0.02873	0.02696
Expected behavior	Yes		Yes	Yes		Yes	Yes		Yes	Yes		Yes
AUC	2.878	2.878	2.878	2.591	2.878	3.166	2.881	2.878	2.875	3.194	2.878	2.619
Expected behavior	Yes		Yes	Yes		Yes	Yes		Yes	Yes		Yes

Conclusion: The sensitivity analysis did not indicate any discrepancies in the expected behavior of the outputs studied, thereby confirming that there is no obstacle to the model's validation.

4.2.4 Quantification of uncertainties

Introduction

The model has been built with popPK data : uncertainties were quantified as interindividual variability (IIV) and residual variability (RV).

Propagation in simulation results

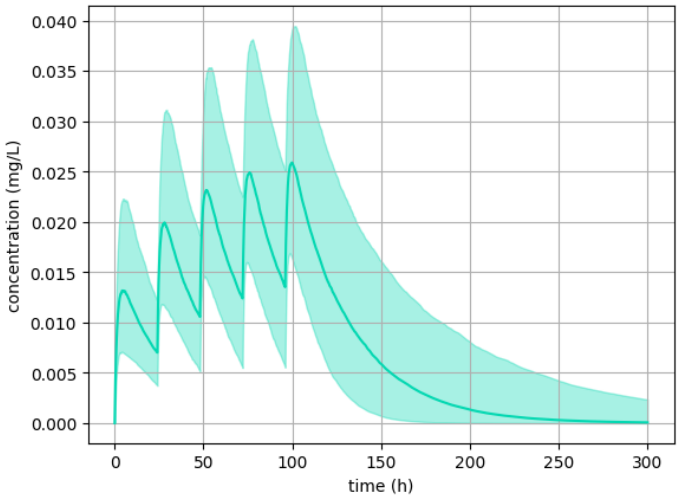

Figure 9. quantification of uncertainties for escitalopram

4.2.5 Test Samples

Test sample level: 2/3

Test sample: efficacy, overexposure, and safety thresholds used for routine therapeutic drug monitoring (TDM) in clinical settings, or thresholds reflecting specific expected events (such as efficacy or toxicity) that may occur at these levels of exposure.

- Efficacy threshold was: 0.0065 mg/L
- Safety threshold was: 0.08 mg/L

Test samples source(s): Schulz et al. [4]

Comment: /

4.2.6 Tests conditions

Tests conditions level: 3/5

Tests condition: test conditions were defined with sufficient data allowing to run simulations for each subpopulation concerned by the drug, but learning dataset is not exhaustive, and leads to extrapolation for patients that were not included in the learning dataset.

Tests conditions source(s): summary of product characteristics [5]

Comment: according to the test condition source, dose adjustment might be possible in case of renal or hepatic insufficiency. However, it is not possible to combine these cases with other covariates included in the model, that is why, the model cannot cover all subpopulation concern by the drug.

Tests conditions were:

Test 1:

- Dosage: 5mg/24h for a week, then 10mg/24h or 10mg/24h or 20mg/24h

- Groups: patient with weight of 70kg, BMI of 24.2, age of 40 years, and CYP2C19 extensive metabolizer profile.

Test 2:

- Dosage: 5mg/24h or 10mg/24h
- Groups: patient of 80 years old.

Test 3:

- Dosage: 10mg/24h or 20mg/24h
- Groups: patient with weight of 100kg, and 50kg.

Test 4:

- Dosage: 5mg/24h or 10mg/24h
- Groups: patient with CYP2C19 poor metabolizer profile.

4.2.7 Equivalency of input parameters

Equivalency of input parameters level: 3/4
Equivalency of input parameters: the model's training dataset does cover doses tested or PK is linear over the dose range used in the test conditions, but not all the sub-populations concerned by the medication. Sub-populations extrapolation can be performed if external data is available to validate it, or an external validation is carried out and meets validation criteria.
Equivalency of input parameters source(s): summary of product characteristics [5], Jin et al. [3].
Comment: the learning dataset didn't include data on hepatic and renal function of the patients. It was therefore impossible to conclude that the learning dataset covers all sub-populations concerned by the medication. However, it was covering all doses tested.

4.2.8 Output Comparison

Output comparison level: 3/5
Output comparison: correspondence of model outputs with the therapeutic thresholds used in routine clinical therapeutic drug monitoring or thresholds reflecting specific expected events (such as efficacy or toxicity) that may occur at these levels of exposure.
Output comparison source(s): Schulz et al. [4]
Comment: all patients evaluated were in accordance with thresholds of Schulz et al. [4] Patients were within therapeutic range for recommended dose for each subpopulation tested.

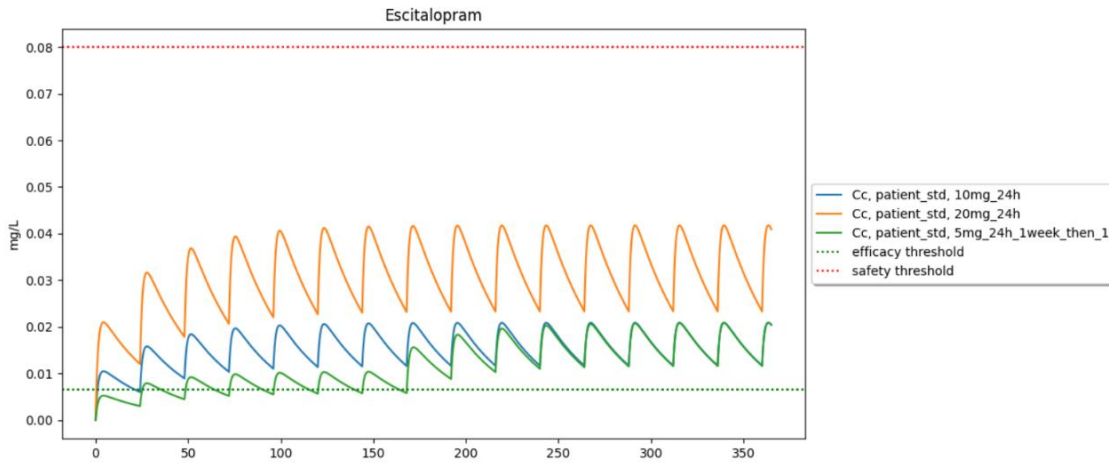

Figure 10. Test 1: standard patient with 5mg/24h for a week, then 10mg/24h or 10mg/24h or 20mg/24h

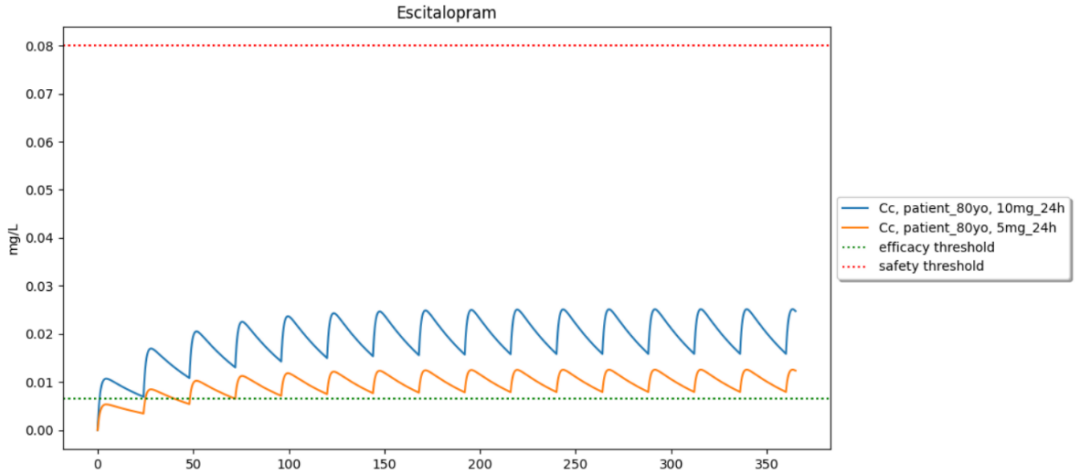

Figure 11. Test 2: older patient of 80 years old with 5mg/24h or 10mg/24h

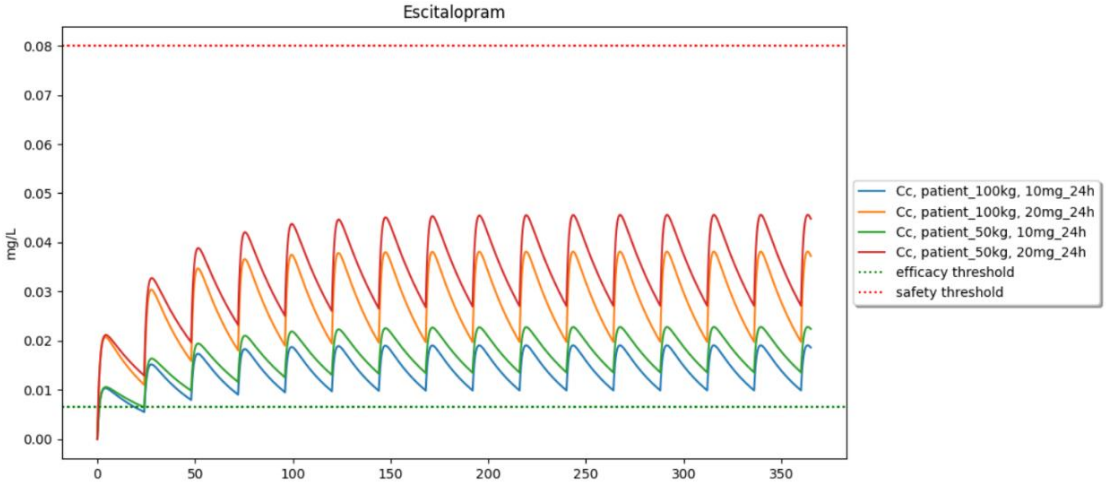

Figure 12. *Test 3: 50 and 100kg patients with 10mg/24h or 20mg/24h*

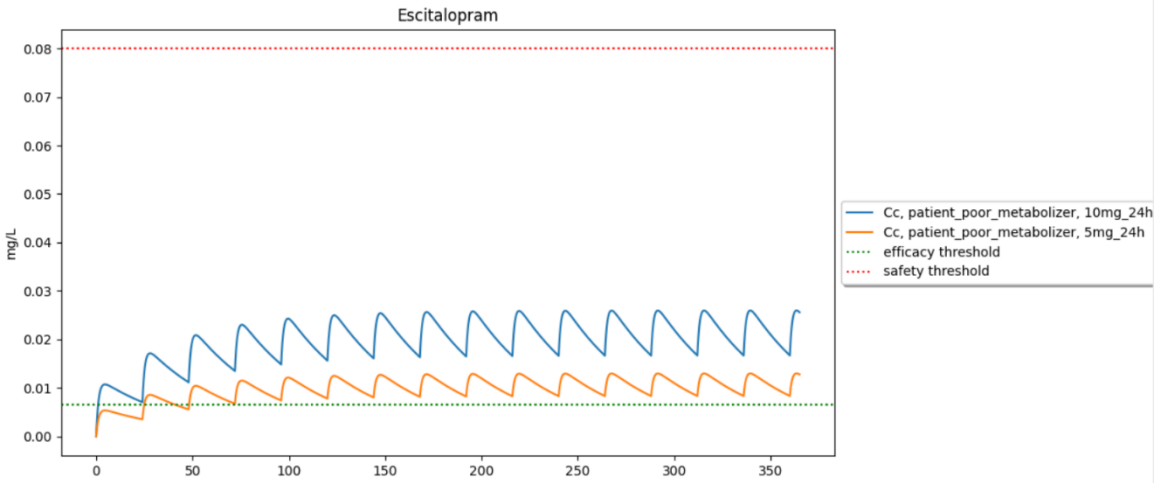

Figure 13. *Test 4: CYP2C19 poor metaboliser patient with 5mg/24h or 10mg/24h*

4.3 Risperidone

Table 7. Summary of risperidone validation.

Summary		
Levels	**Notations**	**Comments**
Model form level	3/5	Model built from popPK analysis
Model inputs sources level	4/4	RSE% were <30% for structural parameters
Test samples level	2/3	Therapeutic thresholds
Tests conditions level	4/5	Complete coverage of dosage ranges, and of all sub-populations concerned by the drug.
Equivalency of input parameters level	4/4	The model's training dataset does cover all doses and sub-populations concerned by the medication.
Output comparison level	3/5	Model outputs were within therapeutic thresholds.
Conclusion: The model is validated since all criteria meet the minimum score required.		

4.3.1 Model Form

Model form level: 3/5
Model form: model built from popPK analysis.
Model Source(s): Thyssen et al. [6].
Comment: the implemented PK model is based on a popPK analysis conducted by Thyssen et al. [7]. It is a two-compartment model with first order absorption and elimination.

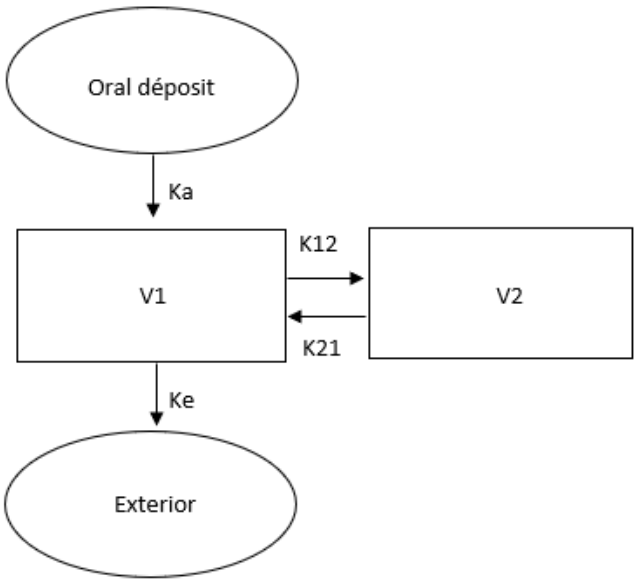

Figure 14. Model's structure, with depot compartment, central compartment, peripheral compartment, and exterior fictive compartment. Ka is the absorption rate, V1 the volume of the central compartment, V2 the volume of the peripheral compartment, K12 and K21 transfer constant between the 2 compartments, and Ke the elimination rate.

4.3.2 Model inputs sources

Model inputs sources level: 4/4
Model input: parameters are obtained from popPK analysis with a relative standard error (RSE) ≤ 30%.
Model inputs source(s): Thyssen et al. [6].
Comment: /
Parameters were directly taken from the source:

Parameter	Estimates (SE)	95% CI	%CV
Active antipsychotic fraction			
$CL/F\,(L/h) = (\theta_1 \bullet [WT/70]^{0.75} + \theta_6 \bullet CL_{CR} + \theta_9 \bullet BLAC) \bullet (Age/18.1)^{\theta_{10}}$			
θ_1	4.66 (0.460)	3.76, 5.56	
θ_6	0.00831 (0.00329)	0.00186, 0.01476	
θ_9	0.862 (0.181)	0.507, 1.217	
θ_{10}	−0.172 (0.0310)	−0.233, −0.111	
$V_1/F\,[L] = (\theta_2 + FLAG \bullet \theta_8) \bullet (WT/70)$			
θ_2	137 (7.05)	123, 151	
θ_8	−40.3 (6.83)	−53.7, −26.9	
$V_2/F\,[L] = \theta_3 \bullet (WT/70)$			
θ_3	86.8 (8.02)	71.1, 102.5	
Q/F [L/h]			
θ_4	1.35 (0.0987)	1.16, 1.54	
k_a [h^{-1}]			
θ_5	2.39 (0.243)	1.91, 2.87	
ALAG1 [h]			
θ_7	0.235 (0.00261)	0.230, 0.240	
$F_1 = 1 + \theta_{11} \bullet GPID$			
θ_{11}	−0.467 (0.145)	−0.751, −0.183	
IIV on CL/F: ω_1^2	0.0586 (0.0159)	0.0274, 0.0898	24.2
IIV on F1: ω_2^2	0.109 (0.0321)	0.0461, 0.172	32.4
IOV on F1	0.156 (0.0446)	0.0686, 0.243	39.5
Residual variability (on log concentration)			
study 6, 7 or 8: σ_1^2 [a]	0.270 (0.0254)	0.220, 0.320	SD 0.52
study 1, 2, 3, 4, 5 or 9: σ_2^2 [a]	0.186 (0.0367)	0.114, 0.258	SD 0.43

Figure 15. Model parameters from Thyssen et al. [6] Picture from Thyssen et al. [6]

the RSE% were calculating with the SE and average communicated in the following table:

Table 8. *Results of RSE% calculation.*

Parameters	SE%	Mean	RSE%
CL/F	0.46	4.66	9.87124464
V1/F	7.05	137	5.1459854
V2/F	7.05	137	5.1459854
Q/F	0.0987	1.35	7.31111111
ka	0.243	2.39	10.167364
ALAG1	0.00261	0.235	1.1106383

SE% = standard error, RSE% = residual standard error.
Formula used to calculate RSE% was: RSE% = 100 * SE / Mean

4.3.3 Quantification of sensitivities

Table 9. Analysis of the sensitivity of Cmax and AUC for risperidone by varying absorption rate constant (ka), bioavailability (F), volume of distribution (V), and clearance of elimination (CL).

Sensitivity analysis												
	ka			F			V			CL		
	-10%	ref	+10%	-10%	ref	+10%	-10%	ref	+10%	-10%	ref	+10%
Cmax	0.04034	0.04051	0.04066	0.03646	0.04051	0.04456	0.04229	0.04051	0.03889	0.04259	0.04051	0.03863
Expected behavior	Yes		Yes	Yes		Yes	Yes		Yes	Yes		Yes
AUC	2.596	2.596	2.596	2.337	2.596	2.856	2.600	2.596	2.592	2.871	2.596	2.368
Expected behavior	Yes		Yes	Yes		Yes	Yes		Yes	Yes		Yes

Conclusion: The sensitivity analysis did not indicate any discrepancies in the expected behavior of the outputs studied, thereby confirming that there is no obstacle to the model's validation.

4.3.4 Quantification of uncertainties

Introduction

The model has been built with popPK data : uncertainties were quantified as interindividual variability (IIV) and residual variability (RV).

Propagation in simulation results

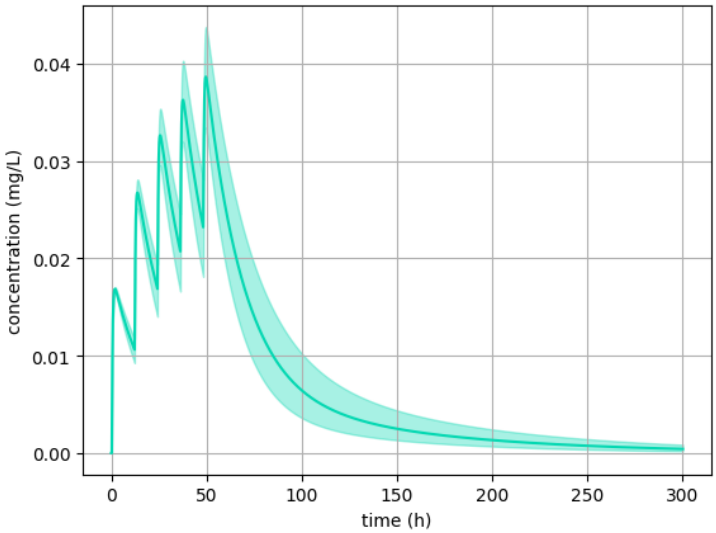

Figure 16. quantification of uncertainties for risperidone

4.3.5 Test Samples

Test sample level: 2/3

Test sample: efficacy, overexposure, and safety thresholds used for routine therapeutic drug monitoring (TDM) in clinical settings, or thresholds reflecting specific expected events (such as efficacy or toxicity) that may occur at these levels of exposure.

- Efficacy threshold was: 0.02 mg/L
- Overexposure threshold was: 0.06 mg/L
- Safety threshold was: 0.12 mg/L

Test samples source(s): Schulz et al. [4]
Comment: /

4.3.6 Tests conditions

Tests conditions level: 4/5
Tests condition: test conditions were defined with sufficient data to run simulations for each patient concerned by the drug, with complete coverage of dosage ranges, and of all sub-populations concerned by the drug.
Tests conditions source(s): summary of product characteristics [7]
Comment: /
Tests conditions were:
Test 1:

- Dosage: 4mg/24h, 6mg/24h, 2mg/12h
- Groups: standard patient (70kg, 40 years old, glomerular_filtration_rate: 90 ml/min/1.73m²) and patient of 120kg.

Test 2:

- Dosage: 4mg/24h, 6mg/24h, 0.5mg/12h, 2mg/12h
- Groups: standard patient and patient of 80 years old.

Test 3:

- Dosage: 4mg/24h, 6mg/24h, 2mg/12h
- Groups: standard patient and patient with glomerular_filtration_rate: 15 ml/min/1.73m²

Test 4:

- Dosage: 4mg/24h, 6mg/24h, 0.5mg/12h, 2mg/12h
- Groups: patient of 80 years old, 55kg and with glomerular_filtration_rate: 15 ml/min/1.73m² and patient of 80 years old, 100kg and with glomerular_filtration_rate: 15 ml/min/1.73m²

4.3.7 Equivalency of input parameters

Equivalency of input parameters level: 4/4
Equivalency of input parameters: the model's training dataset does cover all doses and sub-populations concerned by the medication.
Equivalency of input parameters source(s): summary of product characteristics [7], Thyssen et al. [6]
Comment: model implemented is the one developed and published by the drug manufacturer.

4.3.8 Output Comparison

Output comparison level: 3/5
Output comparison: correspondence of model outputs with the therapeutic thresholds used in routine clinical therapeutic drug monitoring or thresholds reflecting specific expected events (such as efficacy or toxicity) that may occur at these levels of exposure.
Output comparison source(s): Schulz et al. [4]
Comment: all patients evaluated were in accordance with thresholds of Schulz et al. [4] All output results were within therapeutic thresholds. (Evaluation is on Cmax) Only 0.5mg/12h posology for elderly patients is under efficacy threshold: this is a starting posology to assess the tolerance before using the 2mg/12h dosing regimen.

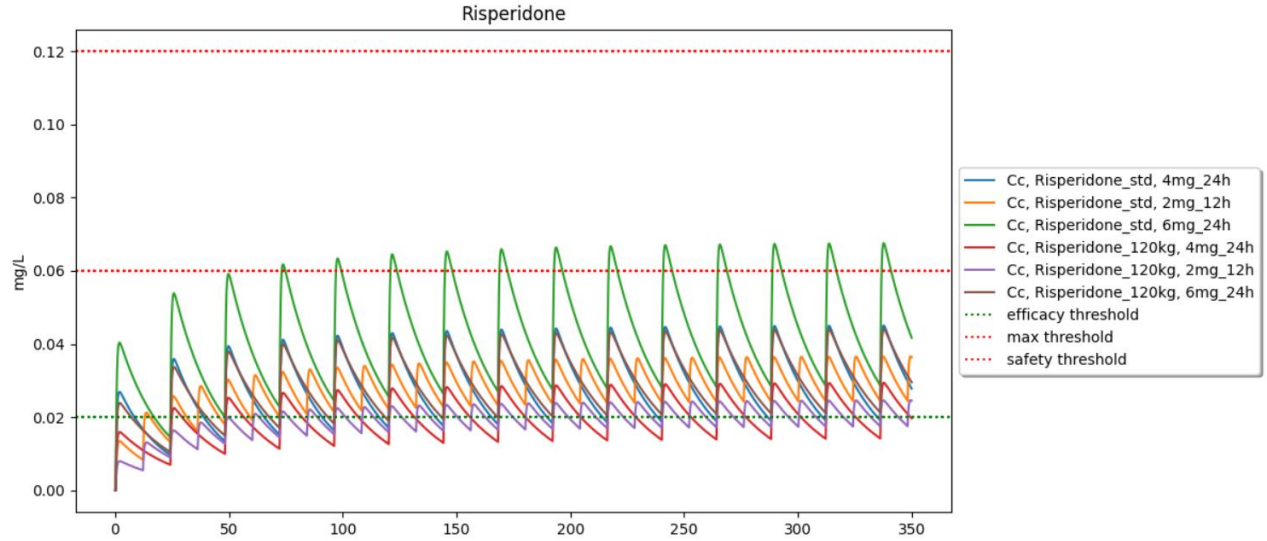

Figure 17. Test 1: Standard patient and 120kg patient at 4mg/24h, 6mg/24h, 2mg/12h

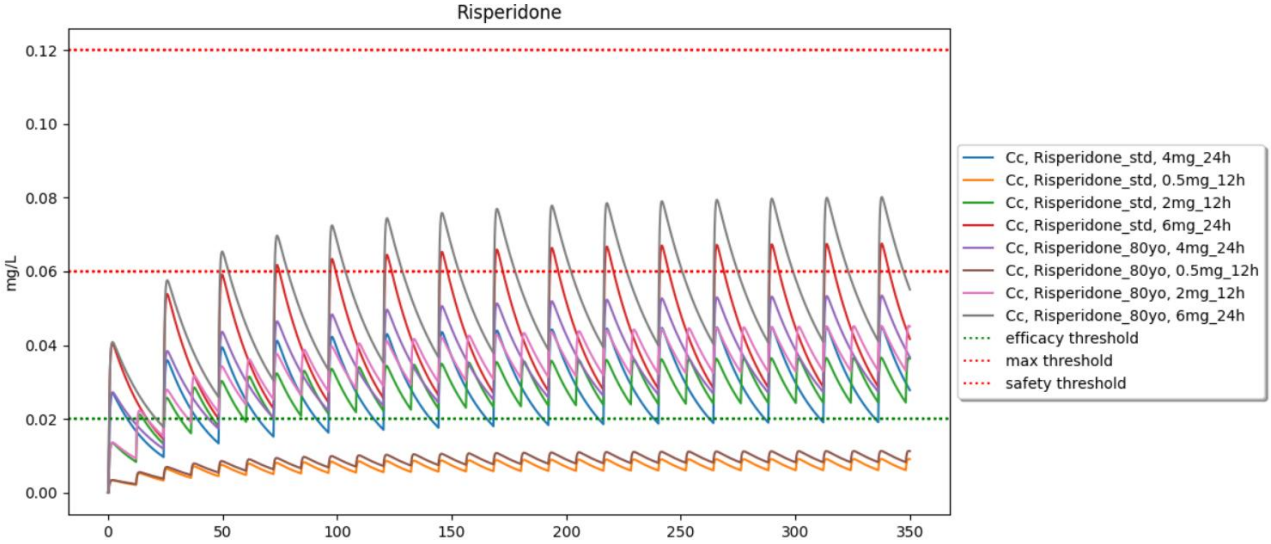

Figure 18. Test 2: Standard patient and 80 years old patient at 4mg/24h, 6mg/24h, 0.5mg/12h, 2mg/12h

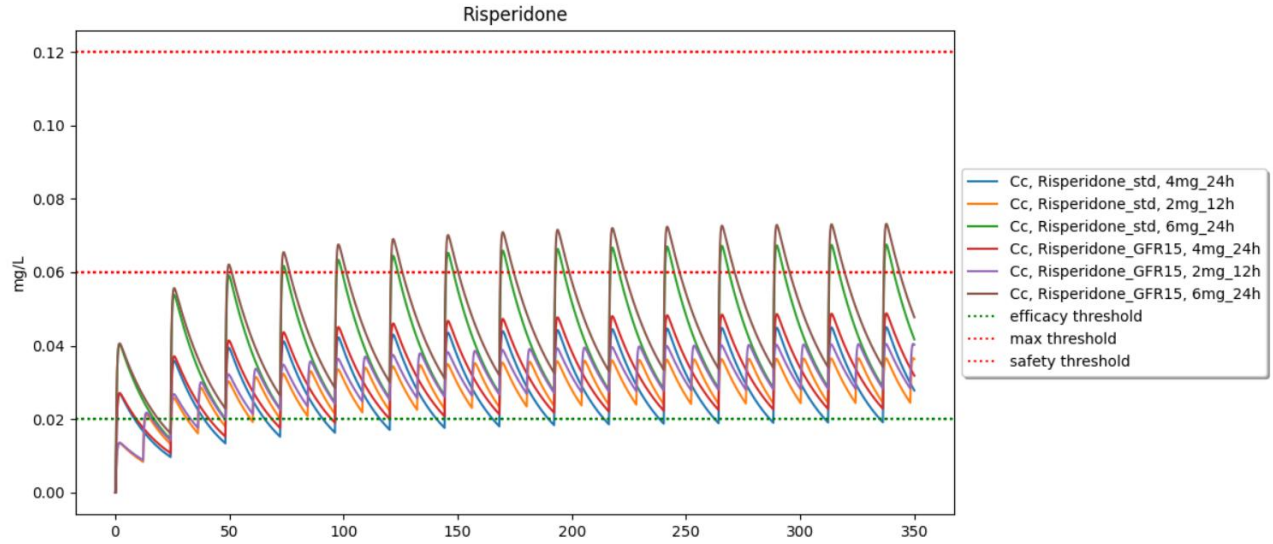

Figure 19. Test 3: Standard patient and renal impaired patient at 4mg/24h, 6mg/24h, 2mg/12h

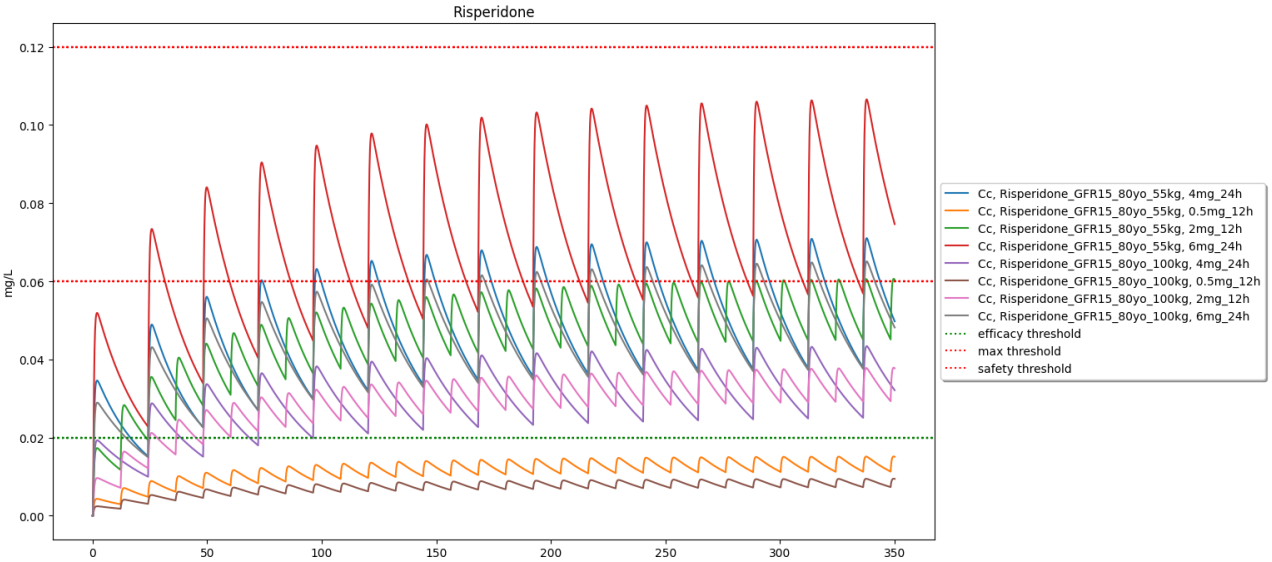

Figure 20. Test 4: patient of 80 years old, 55kg and with glomerular_filtration_rate: 15 ml/min/1.73m² and patient of 80 years old, 100kg and with glomerular_filtration_rate: 15 ml/min/1.73m² at 4mg/24h, 6mg/24h, 0.5mg/12h, 2mg/12h

4.4 Carvedilol

Table 10. Summary of carvedilol validation.

Summary		
Levels	**Notations**	**Comments**
Model form level	3/5	Model built from popPK analysis
Model inputs sources level	3/4	RSE% on parameters are >30%
Test samples level	2/3	Therapeutic thresholds
Tests conditions level	4/5	-
Equivalency of input parameters level	4/4	-

Output comparison level	3/5	Model outputs were within therapeutic thresholds.
Conclusion: The model is validated since all criteria meet the minimum score required.		

4.4.1 Model Form

Model form level: 3/5
Model form: model built from popPK analysis.
Model Source(s): Nikolic et al. [8]
Comment: the implemented PK model is based on a popPK analysis conducted by Nikolic et al. [8] It is a one-compartment model with first order absorption and elimination.

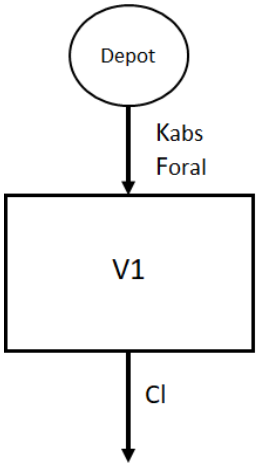

Figure 21. Model's structure, with one depot compartment, and one central compartment. Kabs, is the absorption rate, Foral the bioavailability V1 the volume of distribution, CL the clearance of elimination.

4.4.2 Model inputs sources

Model inputs sources level: 3/4
Model input: parameters are obtained from popPK analysis with a relative standard error (RSE) > 30% or taken from the summary of product characteristics or from analysis conducted on many patients with little variability.
Model inputs source(s): Nikolic et al. [8]
Comment: /

Model Parameter	Estimated Value	Standard Error (95% Confidence Interval)
Clearance (L/h)—θ_1	10	3.71 2.73–17.27
Volume of distribution (L)—θ_2	832	132.06 573.16–1090.84

Figure 22. Parameters' values from Nikolic et al. [8] popPK analysis. Picture from Nikolic et al. [8]

The RSE% were calculating with the SE and average communicated in the following table:

Table 11. *Results of RSE% calculation.*

Parameters	SE%	Mean	RSE%
CL	3.71	10	37.1
Vd	132.06	832	15.8725962

*SE% = standard error, RSE% = residual standard error. RSE% = 100 * SE / Mean*

Ka was fixed at 0.81 h-1 according to previous study published by Takekuma et al. [9]

4.4.3 Quantification of sensitivities

Table 12. Analysis of the sensitivity of Cmax and AUC for carvedilol by varying absorption rate constant (ka), bioavailability (F), volume of distribution (V), and clearance of elimination (CL).

Sensitivity analysis												
	ka			F			V			CL		
	-10%	ref	+10%	-10%	ref	+10%	-10%	ref	+10%	-10%	ref	+10%
Cmax	0.05602	0.05647	0.05687	0.05082	0.05647	0.06212	0.05833	0.05647	0.05472	0.06059	0.05647	0.05287
Expected behavior	Yes		Yes	Yes		Yes	Yes		Yes	Yes		Yes
AUC	3.092	3.092	3.092	2.782	3.092	3.401	3.092	3.092	3.092	3.435	3.092	2.811
Expected behavior	Yes		Yes	Yes		Yes	Yes		Yes	Yes		Yes

Conclusion: The sensitivity analysis did not indicate any discrepancies in the expected behavior of the outputs studied, thereby confirming that there is no obstacle to the model's validation.

4.4.4 Quantification of uncertainties

Introduction

The model has been built with popPK data : uncertainties were quantified as interindividual variability (IIV) and residual variability (RV).

Propagation in simulation results

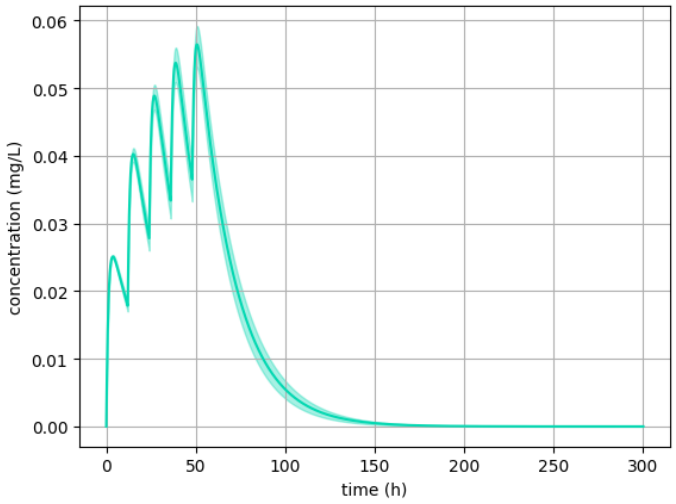

Figure 23. quantification of uncertainties for carvedilol

4.4.5 Test Samples

Test sample level: 2/3
Test sample: efficacy, overexposure, and safety thresholds used for routine therapeutic drug monitoring (TDM) in clinical settings, or thresholds reflecting specific expected events (such as efficacy or toxicity) that may occur at these levels of exposure.

- Efficacy threshold was: 0.02 mg/L
- Safety threshold was: 0.3 mg/L

Test samples source(s): Schulz et al. [4]
Comment: /

4.4.6 Tests conditions

Tests conditions level: 4/5
Tests condition: test conditions were defined with sufficient data to run simulations for each patient concerned by the drug, with complete coverage of dosage ranges, and of all sub-populations concerned by the drug.
Tests conditions source(s): summary of product characteristics [10]
Comment: /
Tests conditions were:
Test 1:

- Dosage: 25mg/12h
- Groups: standard patient, smoker patient, and 50 kg patient.

Test 2:

- Dosage: 25mg/12h
- Groups: 50kg and 95kg patients' smokers and digoxin, and standard patient with digoxin

Test 3:

- Dosage: 25mg/12h, 50mg/12h
- Groups: std patient, 85kg patient, and 120kg patient

4.4.7 Equivalency of Input Parameters

Equivalency of input parameters level: 4/4
Equivalency of input parameters: the model's training dataset does cover all doses or PK is linear over the dose range used in the test conditions and sub-populations concerned by the medication, or an external validation is carried out and meets validation criteria. (i.e., MDPE ≤ ± 20%, MDAPE ≤ 30%).
Equivalency of input parameters source(s): summary of product characteristics [10], Nikolic et al. [8]
Comment: all subpopulations and doses were covered by in the training dataset.

4.4.8 Output Comparison

Output comparison level: 3/5
Output comparison: correspondence of model outputs with the therapeutic thresholds used in routine clinical therapeutic drug monitoring or thresholds reflecting specific expected events (such as efficacy or toxicity) that may occur at these levels of exposure.
Output comparison source(s): Schulz et al. [4]
Comment: all patients evaluated were in accordance with thresholds of Schulz et al. [4]

Simulation outputs were within therapeutic thresholds.

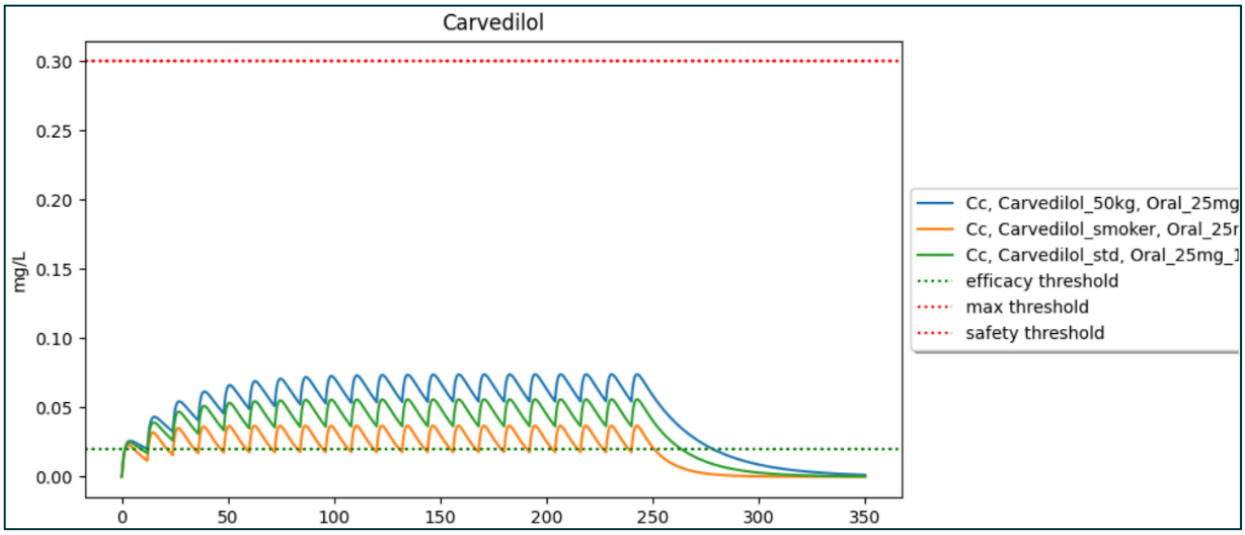

Figure 24. Test 1: 25mg/12h for standard patient, smoker patient, and 50 kg patient.

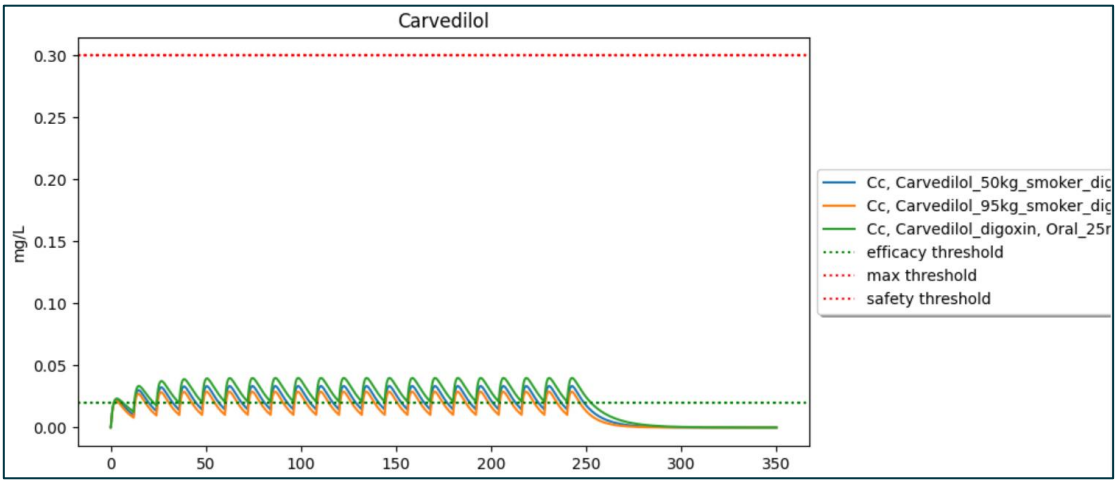

Figure 25. Test 2: 25mg/12h for: 50kg and 95kg patients' smokers and digoxin, and std with digoxin.

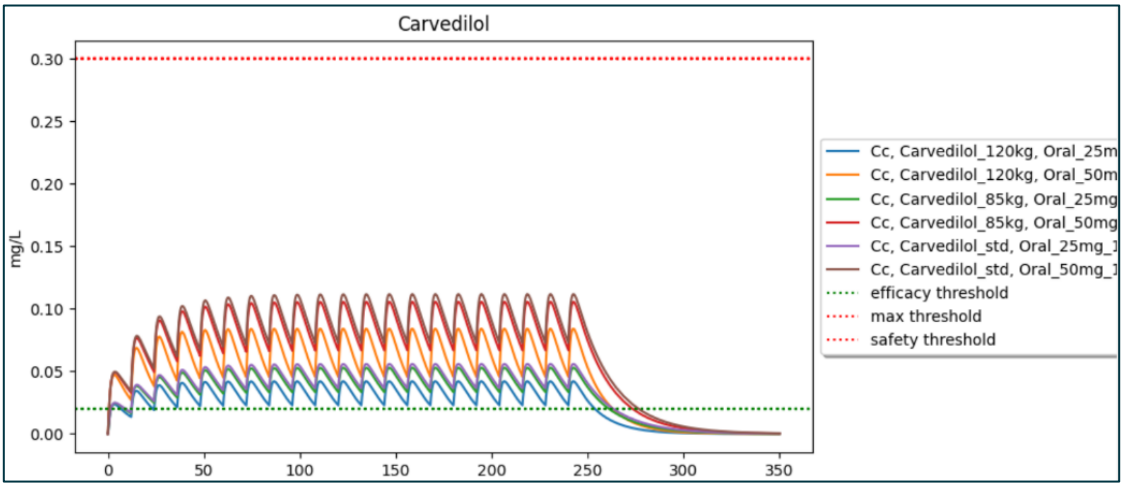

Figure 26. Test 3: 25mg/12h and 50mg/12h for: std patient, 85kg patient, and 120kg patient.

4.5 Azimilide (New)

Table 13. Summary of azimilide validation.

Summary		
Levels	**Notations**	**Comments**
Model form level	3/5	Model built from popPK analysis
Model inputs sources level	3/4	RSE% on parameters are >30%
Test samples level	2/3	Therapeutic thresholds
Tests conditions level	4/5	-
Equivalency of input parameters level	NA	This drug is not yet on the market
Output comparison level	3/5	Model outputs were within therapeutic thresholds.
Conclusion: The model is validated since all applicable criteria meet the minimum score required.		

4.5.1 Model Form

Model form level: 3/5
Model form: model built from popPK analysis.
Model Source(s): Philips et al. [11]
Comment: the implemented PK model is based on a popPK analysis conducted by Philips et al. [11] It is a one-compartment model with first order absorption and elimination.

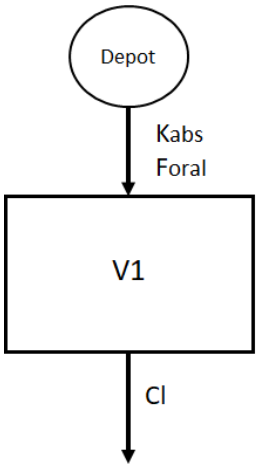

Figure 27. Model's structure, with one depot compartment, and one central compartment. Kabs, is the absorption rate, Foral the bioavailability V1 the volume of distribution, CL the clearance of elimination.

4.5.2 Model inputs sources

Model inputs sources level: 3/4
Model input: parameters are obtained from popPK analysis with a relative standard error (RSE) > 30% or taken from the summary of product characteristics or from analysis conducted on many patients with little variability.
Model inputs source(s): Philips et al. [11]

Comment: the RSE% are directly communicated by the authors in the following table (as %SEM, standard error of the mean)

Parameter	Population mean		Magnitude of interindividual variability (%CV)	
	Final estimate	%SEM	Final estimate	%SEM
Ka (L/h)	0.497	22.3	55.14	167.8
CL (L/h · kg)	3.92	12.3	21.79	10.9
V (L/unit BIL)	717	13.0	34.21	17.8
MALE-CL	0.171	21.3		
Current TOB-CL	0.155	39.7		
WTKG-CL	0.208	17.5		
WTKG-V	9.88	18.3		
BIL-V	0.348	25.9		
*Residual variability**				
σ_1^2	0.0248	18.3		
$\left(\frac{\sigma_2}{\sigma_1}\right)$	216	27.5		
Covariance of CL and V†	0.0432	14.4		

CV, Coefficient of variation; Ka, absorption rate constant; CL, apparent oral clearance; V, apparent volume of the central compartment. Minimum value of objective function = 20646.242.

Figure 28. Parameters value from Philips et al. [11] popPK analysis. Picture from [11]

Only one parameter, the effect of smoker status on the clearance of elimination was >30%. Other parameters were estimated with RSE% <30%.

4.5.3 Quantification of sensitivities

Table 14. Analysis of the sensitivity of Cmax and AUC for azimilide by varying absorption rate constant (ka), bioavailability (F), volume of distribution (V), and clearance of elimination (CL).

Sensitivity analysis												
	ka			F			V			CL		
	-10%	ref	+10%	-10%	ref	+10%	-10%	ref	+10%	-10%	ref	+10%
Cmax	0.7157	0.7177	0.7196	0.646	0.7177	0.7895	0.7277	0.7177	0.7077	0.7851	0.7177	0.6607
Expected behavior	Yes		Yes	Yes		Yes	Yes		Yes	Yes		Yes
AUC	295.7	295.7	295.7	266.2	295.7	325.3	295.9	295.7	295.5	328.3	295.7	269.0
Expected behavior	Yes		Yes	Yes		Yes	Yes		Yes	Yes		Yes

Conclusion: The sensitivity analysis did not indicate any discrepancies in the expected behavior of the outputs studied, thereby confirming that there is no obstacle to the model's validation.

4.5.4 Quantification of uncertainties

Introduction

The model has been built with popPK data : uncertainties were quantified as interindividual variability (IIV) and residual variability (RV).

Propagation in simulation results

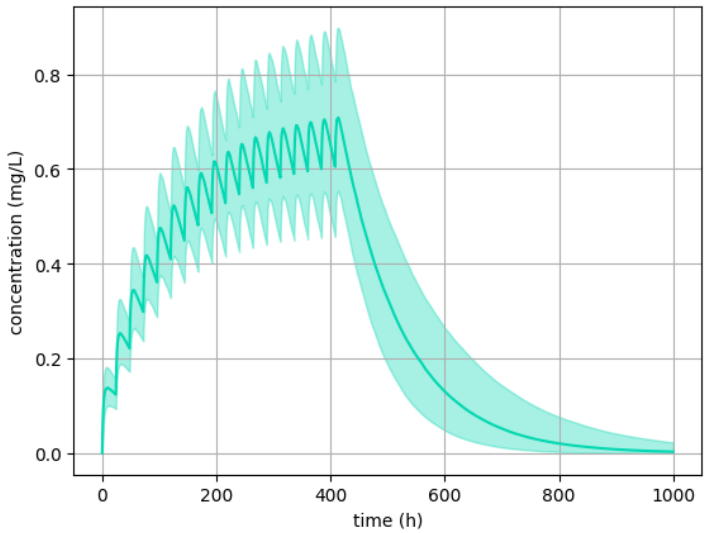

Figure 29. quantification of uncertainties for azimilide

4.5.5 Test Samples

Test sample level: 2/3

Test sample: efficacy, overexposure, and safety thresholds used for routine therapeutic drug monitoring (TDM) in clinical settings, or thresholds reflecting specific expected events (such as efficacy or toxicity) that may occur at these levels of exposure.

- Efficacy threshold was: 0.186 mg/L
- Overexposure threshold was: 1.03 mg/L

Test samples source(s): Corey et al. [12]

Comment: /

4.5.6 Tests conditions

Tests conditions level: 4/5

Tests condition: test conditions were defined with sufficient data to run simulations for each patient concerned by the drug, with complete coverage of dosage ranges, and of all sub-populations concerned by the drug.

Tests conditions source(s):

- Corey et al. [12].

Comment: /

Test conditions were:

Test 1:

- Dosage: 35 mg/24h
- Groups: 1/ patients weighing 50 kg, 70 kg, 100 kg, and smoker patients. 2/ Female patients, female smokers, female patients with weights of 50 kg and 100 kg. 3/ Female smokers weighing 50 kg and 100 kg.

Test 2:

- Dosage: 100 mg/24h
- Groups: patients weighing 50 kg, 70 kg, 100 kg, and smoker patients, female patients, female smokers, female patients with weights of 50 kg and 100 kg, female smokers weighing 50 kg and 100 kg.

Test 3:

- Dosage: 150 mg/24h
- Groups: patients weighing 50 kg, 70 kg, 100 kg, and smoker patients, female patients, female smokers, female patients with weights of 50 kg and 100 kg, female smokers weighing 50 kg and 100 kg.

Test 4:

- Dosage: 200 mg/24h
- Groups: patients weighing 50 kg, 70 kg, 100 kg, and smoker patients, female patients, female smokers, female patients with weights of 50 kg and 100 kg, female smokers weighing 50 kg and 100 kg.

4.5.7 Equivalency of Input Parameters

Equivalency of input parameters level: NA
Equivalency of input parameters: NA
Equivalency of input parameters source(s): NA
Comment: Azimilide is an experimental drug not yet authorized for use in any market, it's still in clinical trial phases.

4.5.8 Output Comparison

Output comparison level: 3/5
Output comparison: correspondence of model outputs with the therapeutic thresholds used in routine clinical therapeutic drug monitoring or thresholds reflecting specific expected events (such as efficacy or toxicity) that may occur at these levels of exposure.
Output comparison source(s): Corey et al. [12].
Comment: even if the drug is not yet on the market, therapeutic thresholds could be extracted from Corey et al. [12] by using the steady-state through concentration as reference range for therapeutic monitoring waiting for more precise ranges with a potential clinical use. This range allows to assess a model outputs comparison. The model outputs were within therapeutic thresholds for appropriate doses. For instance, a patient with a weight at 100kg was not in thresholds with a starting dose of 35mg/day but was within therapeutic range with higher doses ; on the opposite, women of 50kg were above overexposure threshold with 150mg/day, but the dose is not appropriate for this patient. 100mg/day is the maximal dose this patient should receive.

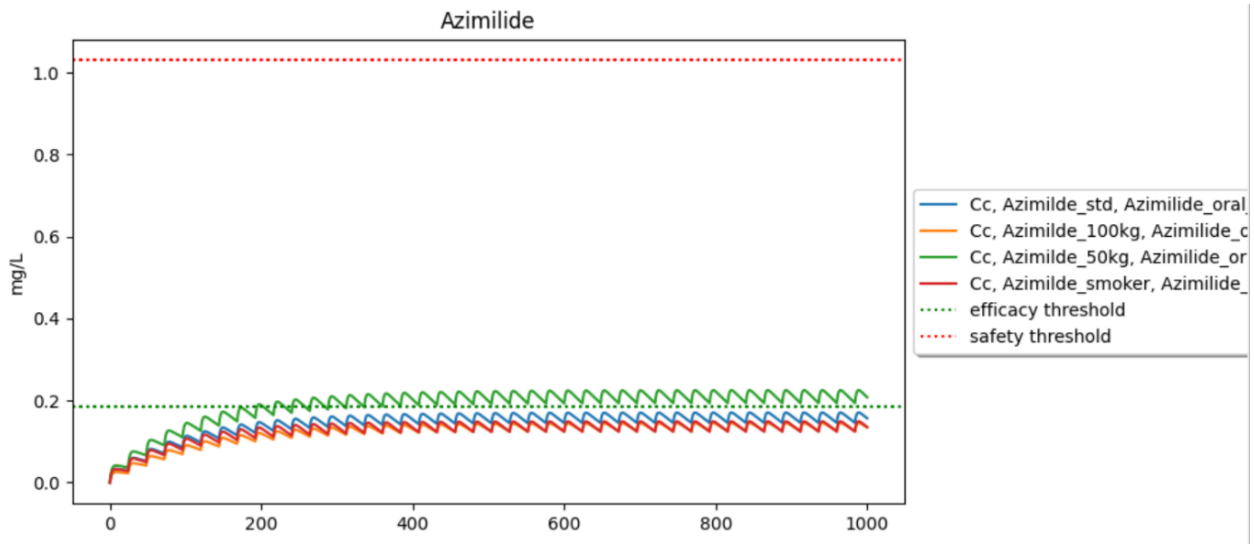

Figure 30. Test 1.1: 35 mg/24h for standard patients weighing 50 kg, 70 kg, 100 kg, and smoker

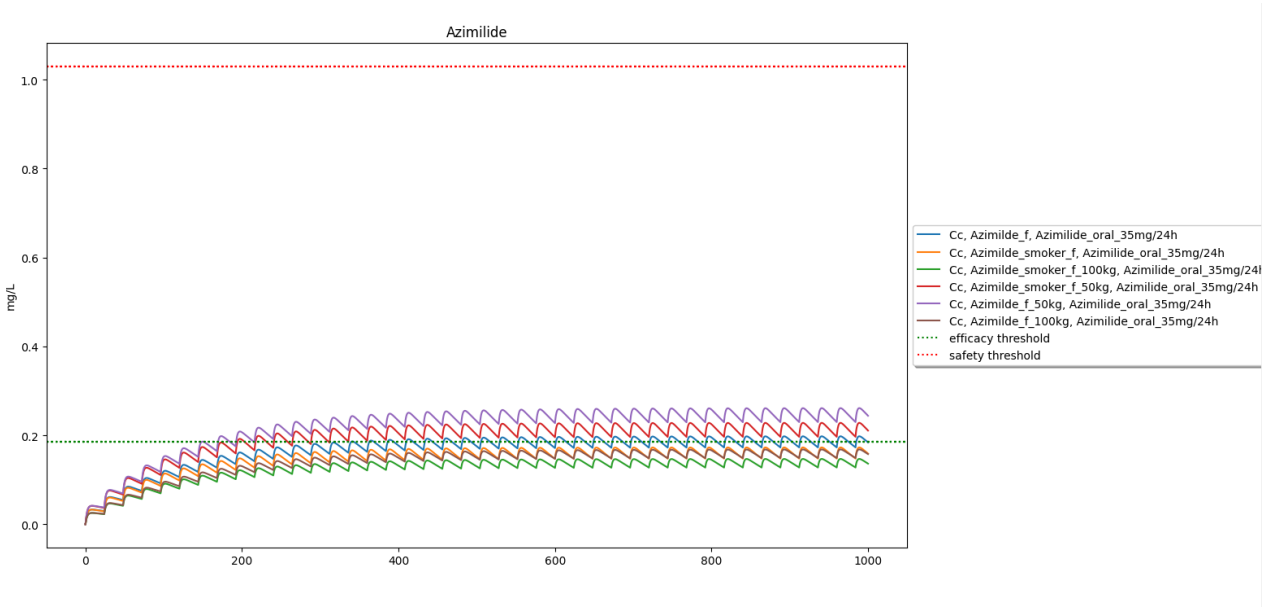

patients.

Figure 31. Test 1.2 and 1.3: 35 mg/24h for female patients, female smokers, female patients weighing 50 kg and 100 kg. 35 mg/24h for female smokers weighing 50 kg and 100 kg.

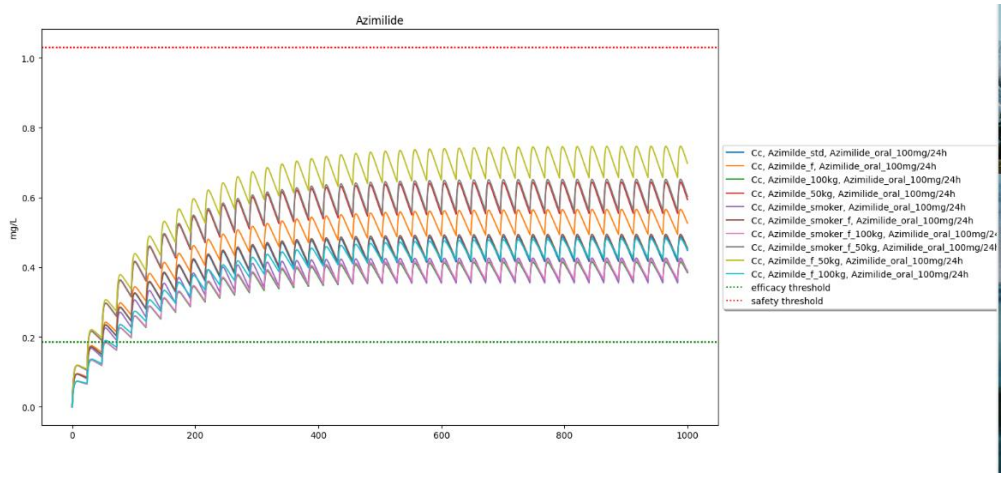

Figure 32. Test 2: 100 mg/24h for standard patients weighing 50 kg, 70 kg, 100 kg, and smoker patients, female patients, female smokers, female patients weighing 50 kg and 100 kg, female smokers weighing 50 kg and 100 kg.

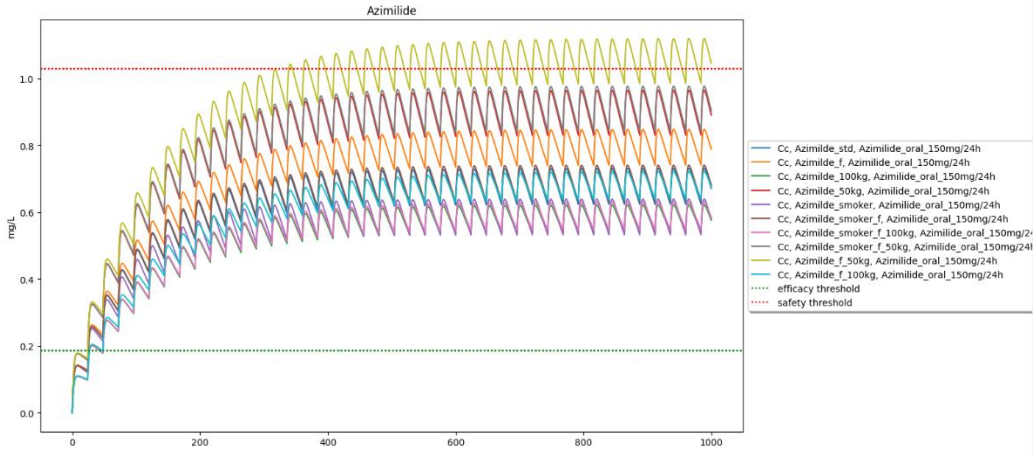

Figure 33. Test 3: 150 mg/24h for standard patients weighing 50 kg, 70 kg, 100 kg, and smoker patients, female patients, female smokers, female patients weighing 50 kg and 100 kg, female smokers weighing 50 kg and 100 kg.

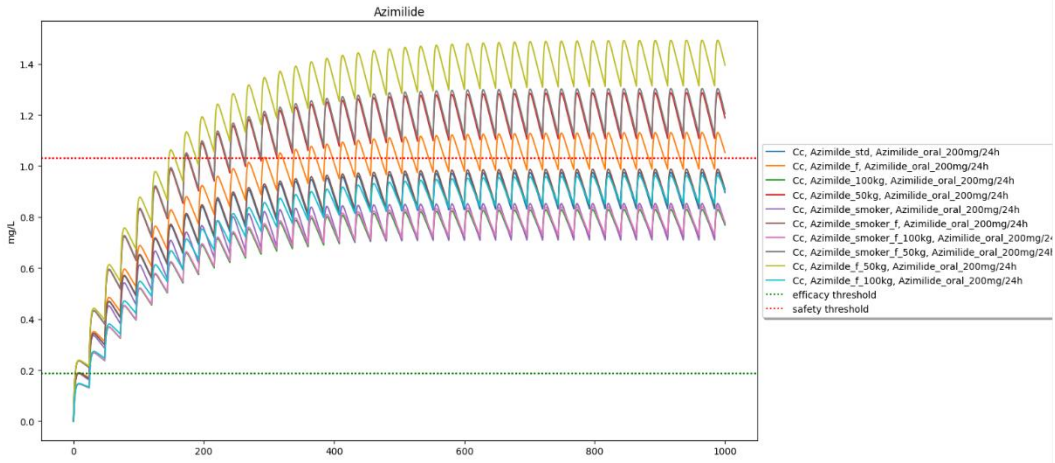

Figure 34. Test 4: 200 mg/24h for standard patients weighing 50 kg, 70 kg, 100 kg, and smoker patients, female patients, female smokers, female patients weighing 50 kg and 100 kg, female smokers weighing 50 kg and 100 kg.

4.6 Chlorpromazine (New)

Table 15. Summary of chlorpromazine validation.

Summary		
Levels	**Notations**	**Comments**
Model form level	2/5	One-compartment model built from NC data
Model inputs sources level	2/4	Parameters comes from NC data
Test samples level	2/3	Therapeutic thresholds
Tests conditions level	4/5	-
Equivalency of input parameters level	4/4	all doses and sub-populations concerned by the medication are covered by the simulations. PK is linear in the dose range.
Output comparison level	3/5	Model outputs were within therapeutic thresholds.
Conclusion: The model is validated since all criteria meet the minimum score required. Model inputs sources level can't be increased at the targeted depth level 3/4 as no popPK model was available in literature.		

4.6.1 Model Form

Model form level: 2/5
Model form: model built with NC data from regulators approved data (summary of product characteristics, regulatory agencies documents).
Model Source(s): Goodman and Gilman et al. [13]
Comment: The model parameters were calibrated with summary of product characteristics non-compartmental data. The V, CL, kabs and F were calibrated or directly taken from the source and constitutes a one-compartment model.

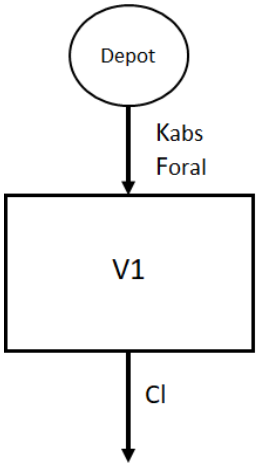

Figure 35. Model's structure, with one depot compartment, and one central compartment. Kabs, is the absorption rate, Foral the bioavailability V1 the volume of distribution, CL the clearance of elimination.

4.6.2 Model inputs sources

Model inputs sources level: 2/4
Model input: The parameters used are derived from NC data from regulatory agencies or obtained from analysis involving large numbers of patients or with low variability.
Model inputs source(s): Goodman and Gilman et al. [13]
Comment:

BIOAVAILABILITY (ORAL) (%)	URINARY EXCRETION (%)	BOUND IN PLASMA (%)	CLEARANCE (mL/min/kg)	VOL. DIST. (L/kg)	HALF-LIFE (hours)	PEAK TIME (h)	PEAK CONCENTRATION
Chlorpromazine[a]							
32 ± 19[b]	<1	95–98	8.6 ± 2.9[c]	21 ± 9[c]	30 ± 7[c]	1–4[d]	25–150 ng/mL[d]
			↓ Child				

[a]Active metabolites, 7-hydroxychlorpromazine ($t_{1/2}$ = 25 ± 15 h) and possibly chlorpromazine *N*-oxide, yield AUCs comparable to the parent drug (single doses). [b]After a single dose. Bioavailability may decrease to ~ 20% with repeated dosing. [c]CL/F, V_{area}, and terminal $t_{1/2}$ following intramuscular administration. [d] Following a 100-mg oral dose given twice a day for 33 days to adult patients. Neurotoxicity (tremors and convulsions) occurs at concentrations of 750–1000 ng/mL.
Reference: Dahl SG, et al. Pharmacokinetics of chlorpromazine after single and chronic dosage. *Clin Pharmacol Ther*, **1977**, *21*:437–448.

Figure 36. Parameters value from Goodman and Gilman et al. [13]. *Picture from Goodman and Gilman et al.* [13]

4.6.3 Quantification of sensitivities

Table 16. Analysis of the sensitivity of Cmax and AUC for chlorpromazine by varying absorption rate constant (ka), bioavailability (F), volume of distribution (V), and clearance of elimination (CL).

Sensitivity analysis												
	ka			F			V			CL		
	-10%	ref	+10%	-10%	ref	+10%	-10%	ref	+10%	-10%	ref	+10%
Cmax	0.04089	0.04109	0.04127	0.03698	0.04109	0.04520	0.04543	0.04109	0.03751	0.04128	0.04109	0.04091
Expected behavior	Yes		Yes	Yes		Yes	Yes		Yes	Yes		Yes
AUC	1.884	1.884	1.884	1.696	1.884	2.073	1.884	1.884	1.884	2.094	1.884	1.713
Expected behavior	Yes		Yes	Yes		Yes	Yes		Yes	Yes		Yes

Conclusion: The sensitivity analysis did not indicate any discrepancies in the expected behavior of the outputs studied, thereby confirming that there is no obstacle to the model's validation.

4.6.4 Quantification of uncertainties

Introduction
The model inputs were parameters from NC literature with ranges used to propagate uncertainties. Uncertainties were propagated using ranges of values and standard deviations.
Propagation in simulation results

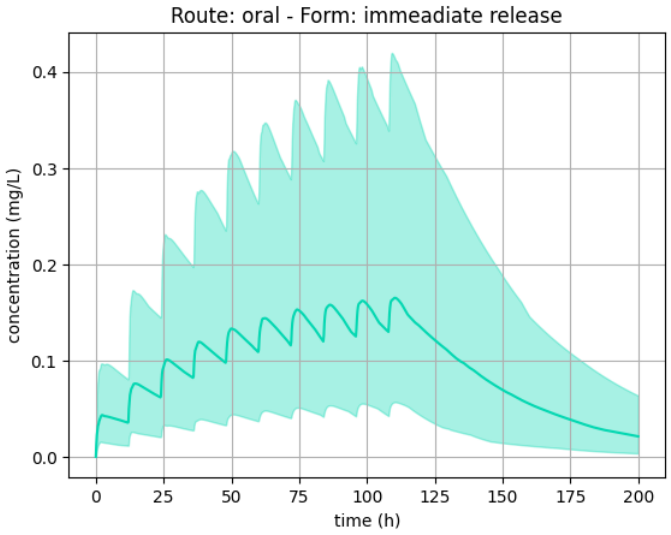

Figure 37. quantification of uncertainties for chlorpromazine

4.6.5 Test Samples

Test sample level: 2/3
Test sample: efficacy, overexposure, and safety thresholds used for routine therapeutic drug monitoring (TDM) in clinical settings, or thresholds reflecting specific expected events (such as efficacy or toxicity) that may occur at these levels of exposure.

- Efficacy threshold was: 0.03 mg/L
- Safety threshold was: 0.6 mg/L

Test samples source(s): Schulz et al. [4]
Comment: /

4.6.6 Tests conditions

Tests conditions level: 4/5
Tests condition: test conditions were defined with sufficient data to run simulations for each patient concerned by the drug, with complete coverage of dosage ranges, and of all sub-populations concerned by the drug.
Tests conditions source(s): summary of product characteristics [14]
Comment: /
Test conditions were:
Test 1:

- Dosage: 12.5 mg/12h
- Groups: Standard patients weighing 50 kg, 70 kg (standard), 100 kg, and children of 20kg and 30kg.

Test 2:

- Dosage: 25 mg/12h

Groups: Standard patients weighing 50 kg, 70 kg (standard), 100 kg, and children of 20kg and 30kg.
Test 3:

- Dosage: 50 mg/12h

Groups: Standard patients weighing 50 kg, 70 kg (standard), 100 kg, and children of 20kg and 30kg.
Test 4:

- Dosage: 100 mg/12h

Groups: Standard patients weighing 50 kg, 70 kg (standard), 100 kg, and children of 20kg and 30kg.

Test 5:

- Dosage: 150 mg/12h

Groups: Standard patients weighing 50 kg, 70 kg (standard), 100 kg, and children of 20kg and 30kg.

Test 6:

- Dosage: 300 mg/12h

Groups: Standard patients weighing 50 kg, 70 kg (standard), 100 kg, and children of 20kg and 30kg.

4.6.7 Equivalency of Input Parameters

Equivalency of input parameters level: 4/4

Equivalency of input parameters: the model's training dataset does cover all doses or PK is linear over the dose range used in the test conditions and sub-populations concerned by the medication, or an external validation is carried out and meets validation criteria. (i.e., MDPE ≤ ± 20%, MDAPE ≤ 30%)

Equivalency of input parameters source(s): summary of product characteristics [14] and Brunton LL et al. [13].

Comment: chlorpromazine simulation outputs were tested with summary of products dosing regimen covering all indications.

4.6.8 Output Comparison

Output comparison level: 3/5

Output comparison: correspondence of model outputs with the therapeutic thresholds used in routine clinical therapeutic drug monitoring or thresholds reflecting specific expected events (such as efficacy or toxicity) that may occur at these levels of exposure.

Output comparison source(s): Schulz et al. [4]

Comment: summary of product was used to extract dosing regimen data, and simulation outputs were compared to therapeutic ranges from Schulz et al. [4]. The simulation results were consistent with the expected behaviour: patients with low body weight and young children exhibit higher concentrations, reaching the efficacy threshold at lower doses compared to patients with higher body weight, while they surpass the safety threshold more quickly. Conversely, patients with higher body weight require higher doses to reach therapeutic concentrations. For example, the dosage of 12.5 mg every 12 hours is only an initial step in the progressive dose escalation strategy.

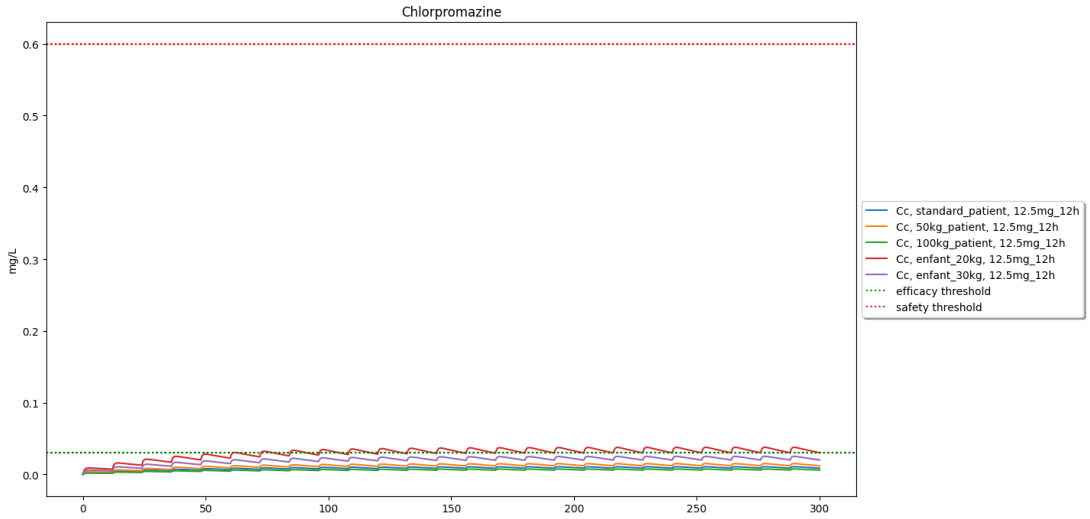

Figure 38. Test 1: 12.5 mg per 12 hours for standard patients of 50,70,100kg and children's patients of 20, 30kg.

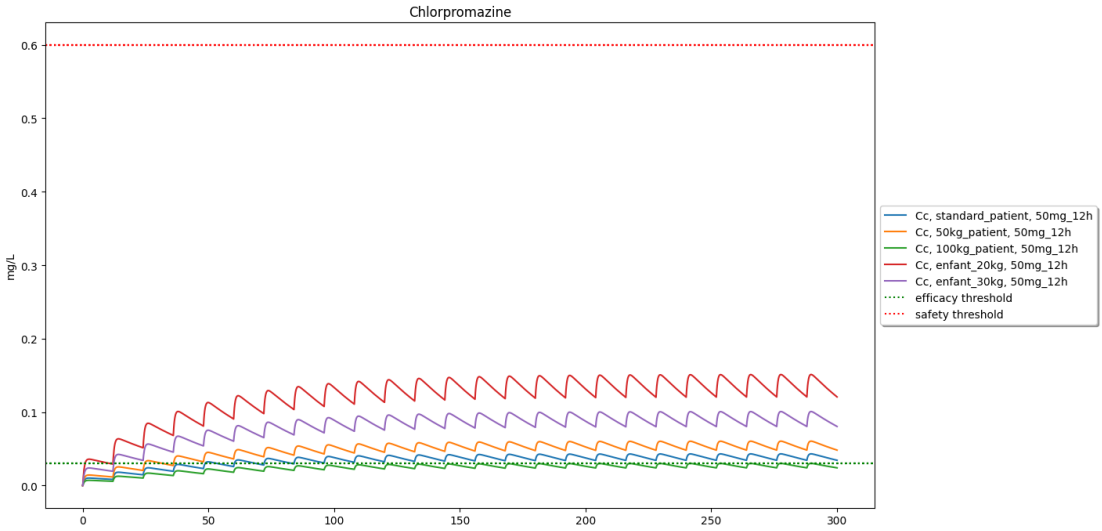

Figure 39. Test 2: 25 mg per 12 hours for standard patients of 50,70,100kg and children's patients of 20, 30kg.

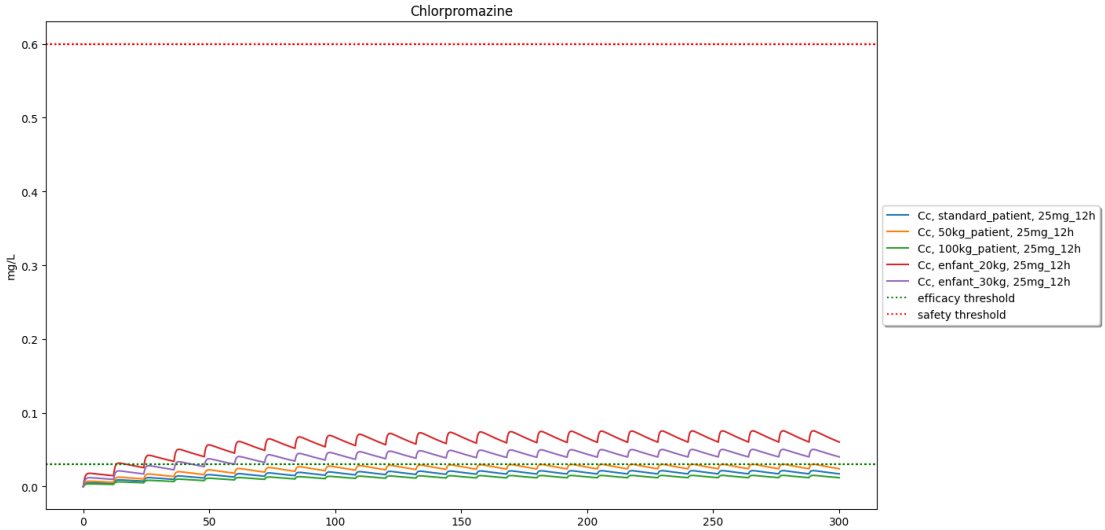

Figure 40. Test 3: 50 mg per 12 hours for standard patients of 50,70,100kg and children's patients of 20, 30kg.

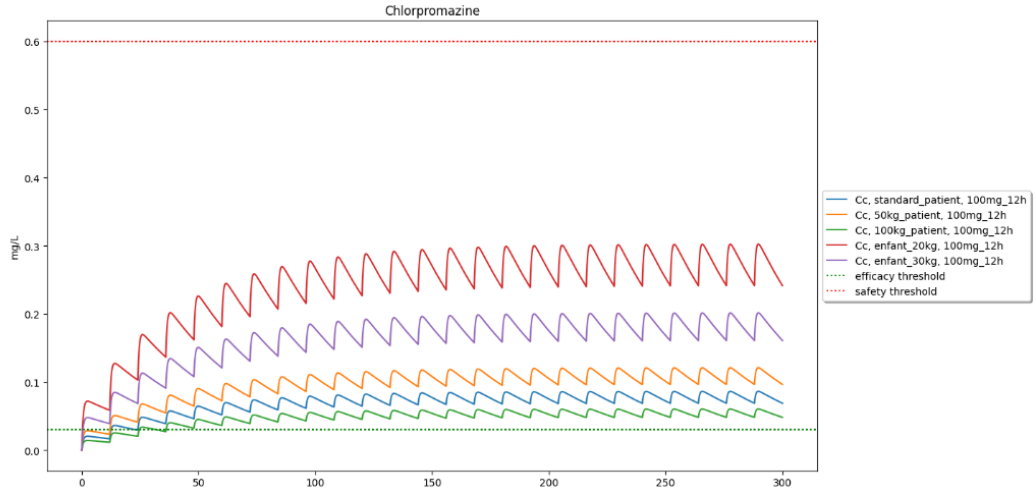

Figure 41. Test 4: 100 mg per 12 hours for standard patients of 50,70,100kg and children's patients of 20, 30kg.

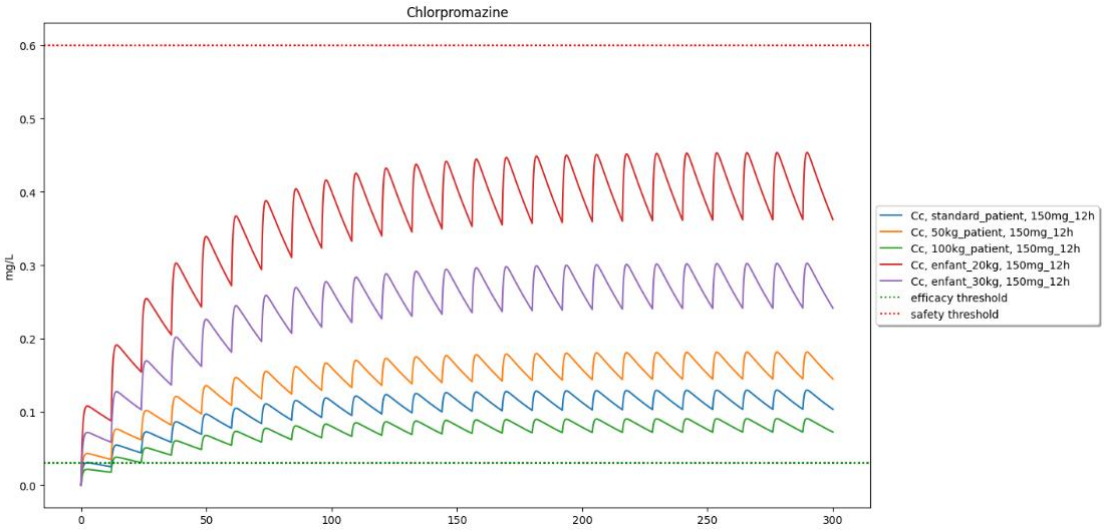

Figure 42. Test 5: 150 mg per 12 hours for standard patients of 50,70,100kg and children's patients of 20, 30kg.

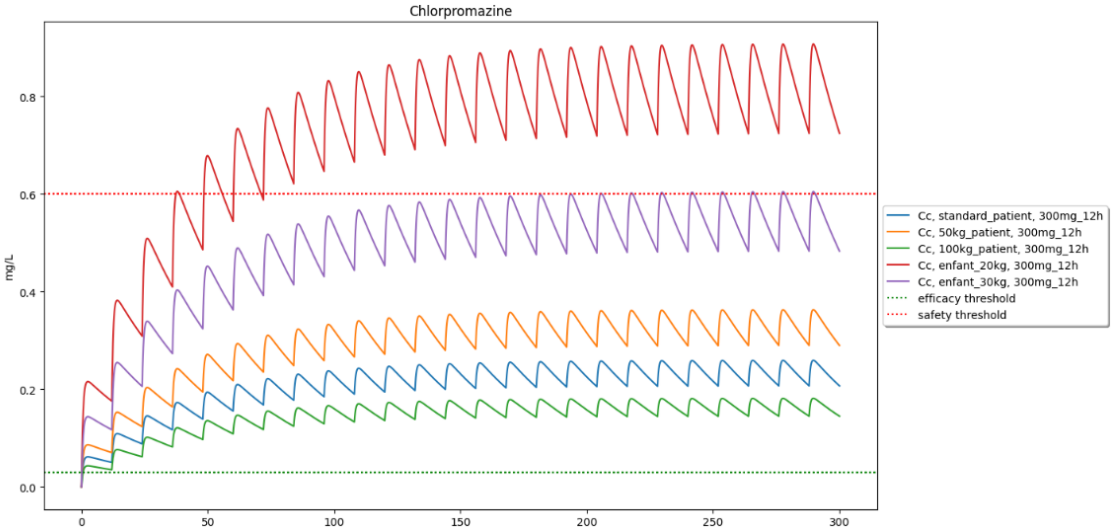

Figure 43. Test 6: 300 mg per 12 hours for standard patients of 50,70,100kg and children's patients of 20, 30kg.

4.7 Cisapride (New)

Table 17. Summary of cisapride validation.

Summary		
Levels	**Notations**	**Comments**
Model form level	4/5	Model built from popPK analysis and NC data.
Model inputs sources level	3/4	RSE% on parameters are >30%
Test samples level	2/3	Therapeutic thresholds
Tests conditions level	4/5	-
Equivalency of input parameters level	NA	This drug is not yet on the market
Output comparison level	3/5	Model outputs were within therapeutic thresholds.
Conclusion: The model is validated since all applicable criteria meet the minimum score required.		

4.7.1 Model Form

Model form level: 4/5
Model form: Model built from popPK analysis and external NC data.
Model Source(s): Prechagoon et al. [15], Arona et al. [16], summary of product characteristics from ANSM, 2005 [17]
Comment: The implemented PK model is based on a popPK analysis from Prechagoon et al. [15]. This model was applicable only for very young kids with maximum weight of 6.5kg (to avoid overextrapolation). The model was calibrated for children with weight > 6.5kg with NC data from summary of product characteristics from ANSM, 2005 [17] and Arona et al. [16]. It was a one-compartment model with first order absorption and elimination rate.

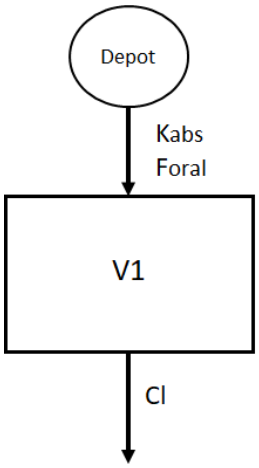

Figure 44. Model's structure, with one depot compartment, and one central compartment. Kabs, is the absorption rate, Foral the bioavailability V1 the volume of distribution, CL the clearance of elimination.

4.7.2 Model inputs sources

Model inputs sources level: 3/4
Model input: Parameters are obtained from popPK analysis with a relative standard error (RSE) > 30% or taken from the summary of product characteristics or from analysis conducted on many patients with little variability.
Model inputs source(s): Prechagoon et al. [15], Arona et al. [16], summary of product characteristics from ANSM, 2005 [17]
Comment:

- the RSE% of Prechagoon et al. [15] are directly communicated by the authors in the following table (as %CV, coefficient of variation)

Parameter (units)	*Typical value*	*s.e. of parameter estimate (CV%)#*
Structural parameters		
CL/F ($l\,h^{-1}\,kg^{-1}$)	0.538	7.6
V/F (l)	21.9	31.7
Ka (h^{-1})	2.58	34.9
Variance parameters		
Interindividual CV(%) in CL/F	34.5	47.6
Interindividual CV(%) in V/F	84.3	35.5
Intraindividual variance	0.154	22.5
Derived parameters		
Clearance ($ml\,min^{-1}\,kg^{-1}$)	9.0	–
Absorption half-life (min)	16.1	–
Elimination half-life (h)*	11.5	–

Figure 45. Parameters value from Prechagoon et al. [15] popPK analysis. Picture from [15].

- Other parameters from Arona et al. ***[16]***, summary of product from ANSM, 2005 ***[17]*** were :
    - ANSM ***[17]*** : F : 0.45, CL : 0.16635 * weight (liters per hour).
    - Arona et al. ***[16]***: V : 2.4 * weight (Liters).

4.7.3 Quantification of sensitivities

Table 18. Analysis of the sensitivity of Cmax and AUC for cisapride by varying absorption rate constant (ka), bioavailability (F), volume of distribution (V), and clearance of elimination (CL).

Sensitivity analysis												
	ka			F			V			CL		
	-10%	ref	+10%	-10%	ref	+10%	-10%	ref	+10%	-10%	ref	+10%
Cmax	0.6357	0.6414	0.6467	0.5772	0.6414	0.7055	0.6628	0.6414	0.6242	0.6916	0.6414	0.6006
Expected behavior	Yes		Yes	Yes		Yes	Yes		Yes	Yes		Yes
AUC	40.79	40.79	40.79	36.71	40.79	44.87	40.80	40.79	40.79	45.32	40.79	37.09
Expected behavior	Yes		Yes	Yes		Yes	Yes		Yes	Yes		Yes

Conclusion: The sensitivity analysis did not indicate any discrepancies in the expected behavior of the outputs studied, thereby confirming that there is no obstacle to the model's validation.

4.7.4 Quantification of uncertainties

Introduction
The model has been built with popPK data : uncertainties were quantified as interindividual variability (IIV) and residual variability (RV).
Propagation in simulation results

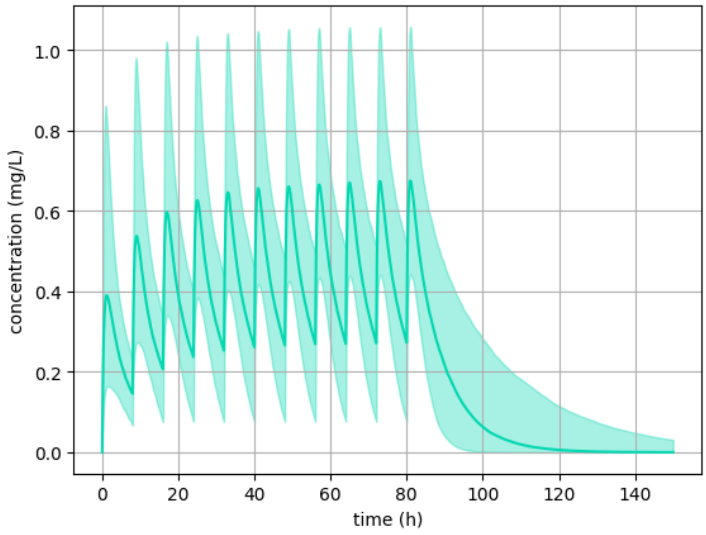

Figure 46. quantification of uncertainties for cisapride

est Samples
Test sample level: 2/3
Test sample: Efficacy, overexposure, and safety thresholds used for routine therapeutic drug monitoring (TDM) in clinical settings, or thresholds reflecting specific expected events (such as efficacy or toxicity) that may occur at these levels of exposure.

- Efficacy threshold was: 0.01 mg/L
- Overexposure threshold was: 0.115 mg/L

Test samples source(s): Benatar et al. [18], summary of product characteristics from ANSM, 2005 [17].
Comment: efficacy threshold was taken from summary of product characteristics [17] and safety threshold from Benatar et al. [18]

4.7.5 Tests conditions

Tests conditions level: 4/5
Tests condition: Test conditions were defined with sufficient data to run simulations for each patient concerned by the drug, with complete coverage of dosage ranges, and of all sub-populations concerned by the drug. However, as the drug is no longer on the market, the tests were performed with ancient dosing regimen from ANSM summary of product of 2005 [17].
Tests conditions source(s):
ANSM summary of product of 2005 [17].
Comment: /

Test conditions were :

Test 1:
- Dosage: 0.4 mg/8h
- Children of 2 kg

Test 2:
- Dosage: 1 mg/8h
- Children of 5 kg

Test 3:
- Dosage: 2 mg/8h
- Children of 10 kg

Test 4:
- Dosage: 5 mg/8h
- Children of 25 kg

Test 5:
- Dosage: 7 mg/8h
- Children of 35 kg

4.7.6 Equivalency of Input Parameters

Equivalency of input parameters level: NA
Equivalency of input parameters: NA
Equivalency of input parameters source(s): NA
Comment: Azimilide is an experimental drug not yet authorized for use in any market, it's still in clinical trial phases.

4.7.7 Output Comparison

Output comparison level: 3/5
Output comparison: Correspondence of model outputs with the therapeutic thresholds used in routine clinical therapeutic drug monitoring or thresholds reflecting specific expected events (such as efficacy or toxicity) that may occur at these levels of exposure.
Output comparison source(s): Benatar et al. [18], summary of product characteristics from ANSM, 2005 [17].
Comment: Even if the drug is not yet on the market, therapeutic thresholds could be extracted from Corey et al. [12] by using the steady-state through concentration as reference range for therapeutic monitoring waiting for more precise ranges with a potential clinical use. This range allows to assess a model outputs comparison. The model outputs were within therapeutic thresholds for appropriate doses. For instance, a patient with a weight at 100kg was not in thresholds with a starting dose of 35mg/day but was within therapeutic range with higher doses ; on the opposite, women of 50kg were above overexposure threshold with 150mg/day, but the dose is not appropriate for this patient. 100mg/day is the maximal dose this patient should receive.

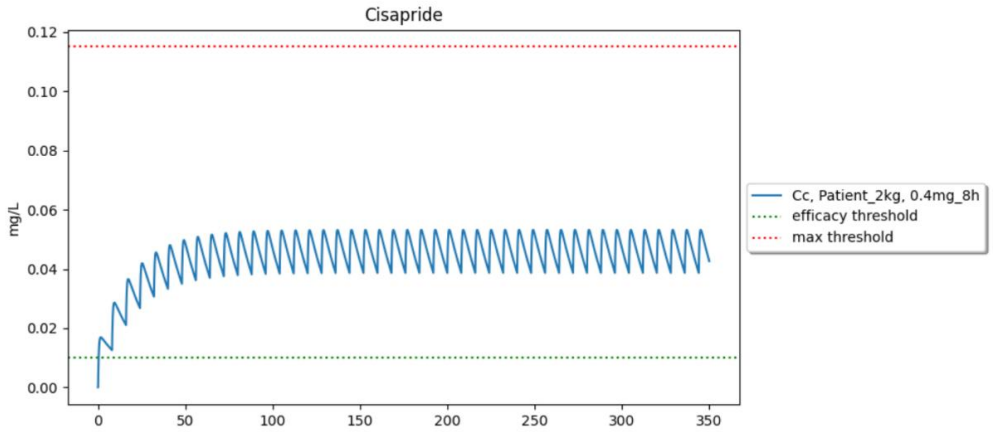

Figure 47. Test 1: 0.4mg/8h, children weighing 2kg.

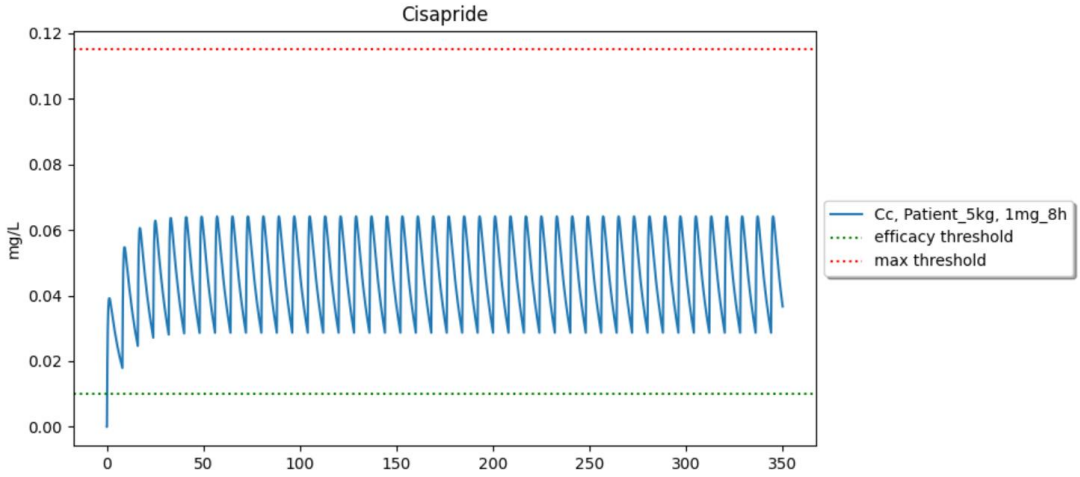

Figure 48. Test 2: 1mg/8h, children weighing 5kg.

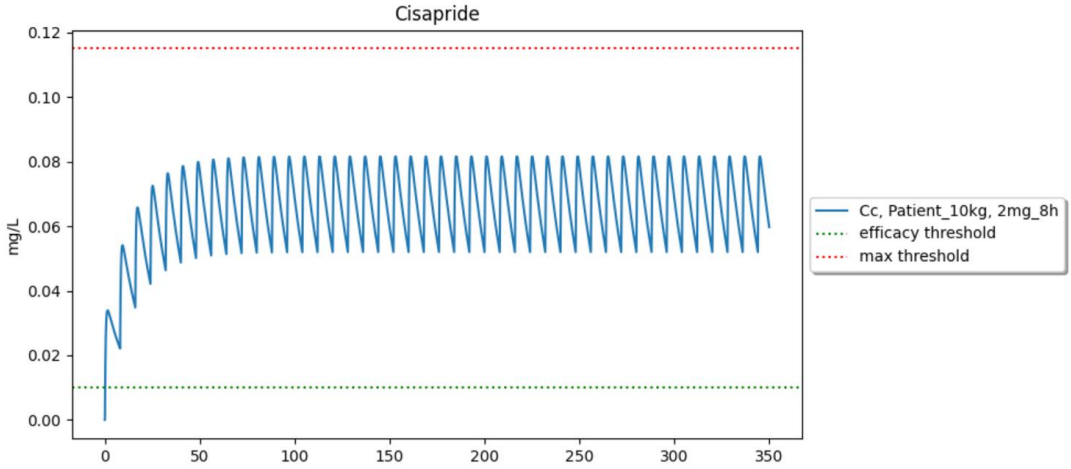

Figure 49. Test 3: 2mg/8h, children weighing 10kg.

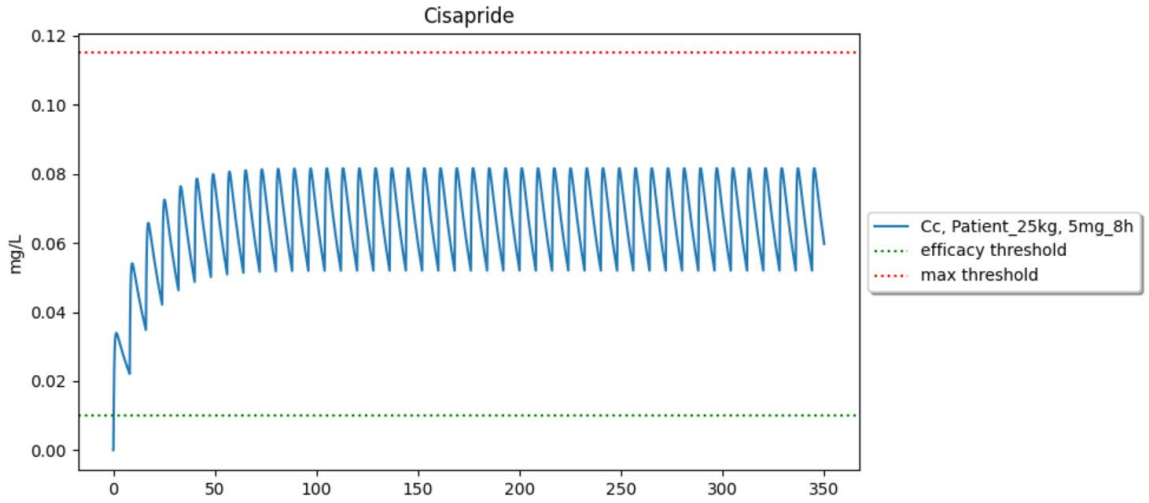

Figure 50. Test 4: 5mg/8h, children weighing 25kg.

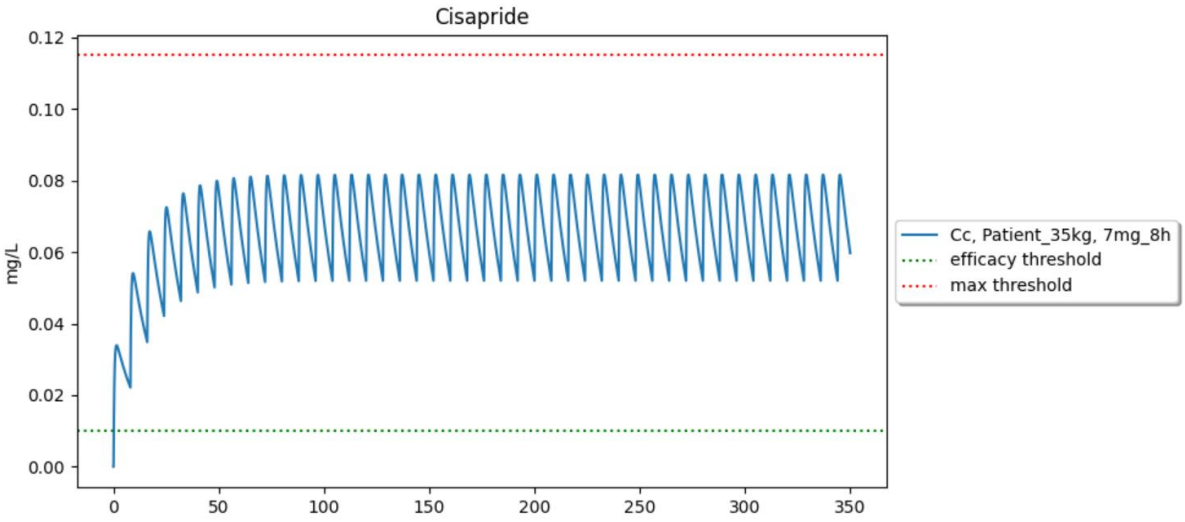

Figure 51. Test 5: 7mg/8h, children weighing 35kg.

4.8 Clarithromycin (New)

Table 19. Summary of clarithromycin validation.

Summary		
Levels	**Notations**	**Comments**
Model form level	2/5	One-compartment model built from NC data
Model inputs sources level	2/4	Parameters comes from NC data
Test samples level	2/3	Therapeutic thresholds
Tests conditions level	4/5	-
Equivalency of input parameters level	4/4	all doses and sub-populations concerned by the medication are covered by the simulations. PK is linear in the dose range.
Output comparison level	3/5	Model outputs were within therapeutic thresholds.

Conclusion: The model is validated since all criteria meet the minimum score required. Model inputs sources level can't be increased at the targeted depth level 3/4 as no popPK model was available in literature.

4.8.1 Model Form

Model form level: 2/5
Model form: model built with NC data from regulators approved data (summary of product characteristics, regulatory agencies documents).
Model Source(s): summary of product characteristics [19].
Comment: a one-compartment model was calibrated with non-compartmental data.

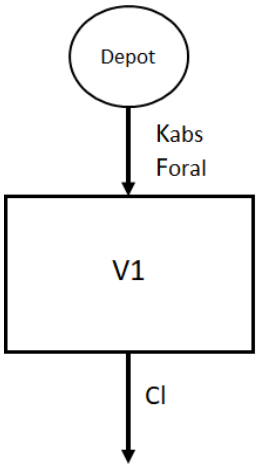

Figure 52. Model's structure, with one depot compartment, and one central compartment. Kabs, is the absorption rate, Foral the bioavailability V1 the volume of distribution, CL the clearance of elimination.

4.8.2 Model inputs sources

Model inputs sources level: 2/4
Model input: The parameters used are derived from NC data from regulatory agencies or obtained from analysis involving large numbers of patients or with low variability.
Model inputs source(s): summary of product characteristics [19].
Comment: NC data used for the calibration were F for immediate and controlled release: 0.55, V: 3 Liters/kg (interval: 2-4L/kg), T1/2: 3.8 hours, Tmax for immediate release: 1.7 hours, Tmax for controlled release: 5.6 hours. Recalibration of T1/2 by a factor 2 was performed when patients had an age >65 years old.

4.8.3 Quantification of sensitivities

Table 20. Analysis of the sensitivity of Cmax and AUC for clarithromycin by varying absorption rate constant (ka for immediate and controlled release), bioavailability (F), volume of distribution (V), and clearance of elimination (CL).

Sensitivity analysis									
	Ka IR			Ka CR			CL		
	-10%	ref	+10%	-10%	ref	+10%	-10%	ref	+10%
Cmax	0.9394	0.9604	0.9787	0.4466	0.4715	0.4945	0.9806	0.9604	0.9414

Expected behavior	Yes		Yes	Yes		Yes	Yes		Yes
AUC	7.179	7.179	7.179	7.179	7.179	7.179	7.977	7.179	6.526
Expected behavior	Yes		Yes	Yes		Yes	Yes		Yes

	F			**V**		
	-10%	**ref**	**-10%**	**-10%**	**ref**	**+10%**
Cmax	0.8643	0.9604	1.0564	1.0437	0.9604	0.8898
Expected behavior	Yes		Yes	Yes		Yes
AUC	6.461	7.179	7.897	7.179	7.179	7.179
Expected behavior	Yes		Yes	Yes		Yes

Conclusion: The sensitivity analysis did not indicate any discrepancies in the expected behavior of the outputs studied, thereby confirming that there is no obstacle to the model's validation.

4.8.4 Quantification of uncertainties

Introduction

The model inputs were parameters from NC literature with ranges used to propagate uncertainties. Uncertainties were propagated using ranges of values.

Propagation in simulation results

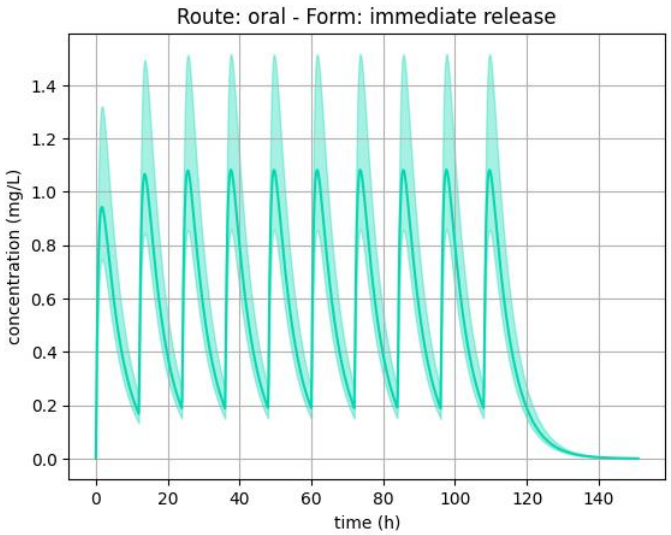

Figure 53. quantification of uncertainties for clarithromycin immediate release formulation.

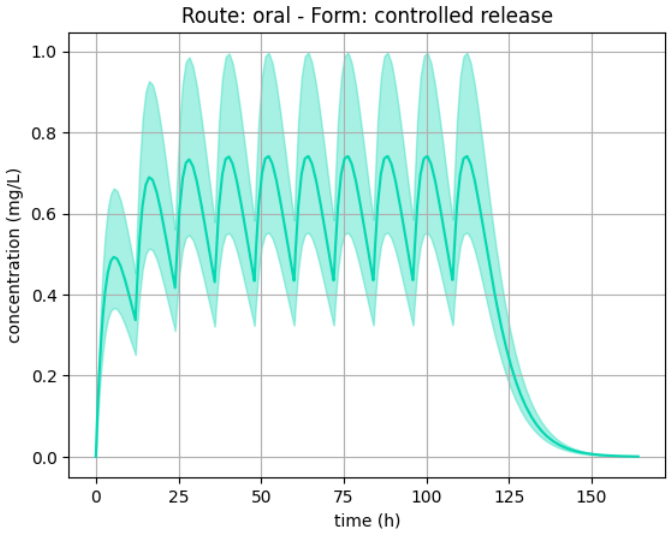

Figure 54. quantification of uncertainties for clarithromycin controlled release formulation.

4.8.5 Test Samples

Test sample level: 2/3
Test sample: Efficacy, overexposure, and safety thresholds used for routine therapeutic drug monitoring (TDM) in clinical settings, or thresholds reflecting specific expected events (such as efficacy or toxicity) that may occur at these levels of exposure.

- Efficacy threshold was: 0.2 mg/L
- Safety threshold was: 7 mg/L

Test samples source(s): Schulz et al. [4]
Comment: /

4.8.6 Tests conditions

Tests conditions level: 4/5
Tests condition: Test conditions were defined with sufficient data to run simulations for each patient concerned by the drug, with complete coverage of dosage ranges, and of all sub-populations concerned by the drug.
Tests conditions source(s): summary of product characteristics [19]
Comment: /
Test conditions were:
Test 1:

- Dosage: 250 mg/12h orally (immediate released form)
- Groups: Standard patients weighing 50 kg, 70 kg (standard), 100 kg, and older patients of 50 kg, 70 kg, 100 kg

Test 2:

- Dosage: 500 mg/12h orally (immediate released form)
- Groups: Standard patients weighing 50 kg, 70 kg (standard), 100 kg, and children of 20kg and 30kg.

Test 3:

- Dosage: 500 mg/24h orally (control released form)

Groups: Standard patients weighing 50 kg, 70 kg (standard), 100 kg, and children of 20kg and 30kg.

Test 4:

- Dosage: 1000 mg/24h orally (control released form)
- Groups: Standard patients weighing 50 kg, 70 kg (standard), 100 kg, and children of 20kg and 30kg.

Test 5:

- Dosage: 250 mg/12h intravenous
- Groups: Standard patients weighing 50 kg, 70 kg (standard), 100 kg, and children of 20kg and 30kg.

Test 6:

- Dosage: 500 mg/12h intravenous
- Groups: Standard patients weighing 50 kg, 70 kg (standard), 100 kg, and children of 20kg and 30kg.

4.8.7 Equivalency of Input Parameters

Equivalency of input parameters level: 4/4
Equivalency of input parameters: The model's training dataset does cover all doses or PK is linear over the dose range used in the test conditions and sub-populations concerned by the medication, or an external validation is carried out and meets validation criteria. (i.e., MDPE ≤ ± 20%, MDAPE ≤ 30%)
Equivalency of input parameters source(s): summary of product characteristics [19]
Comment: Clarithromycin simulation outputs were tested with summary of products dosing regimen covering all indications.

4.8.8 Output Comparison

Output comparison level: 3/5
Output comparison: Correspondence of model outputs with the therapeutic thresholds used in routine clinical therapeutic drug monitoring or thresholds reflecting specific expected events (such as efficacy or toxicity) that may occur at these levels of exposure.
Output comparison source(s): Schulz et al. [4]
Comment: summary of product [19] was used to extract dosing regimen data, and simulation outputs were compared to therapeutic ranges from Schulz et al. [4]. The simulation results were consistent with the expected behaviour.

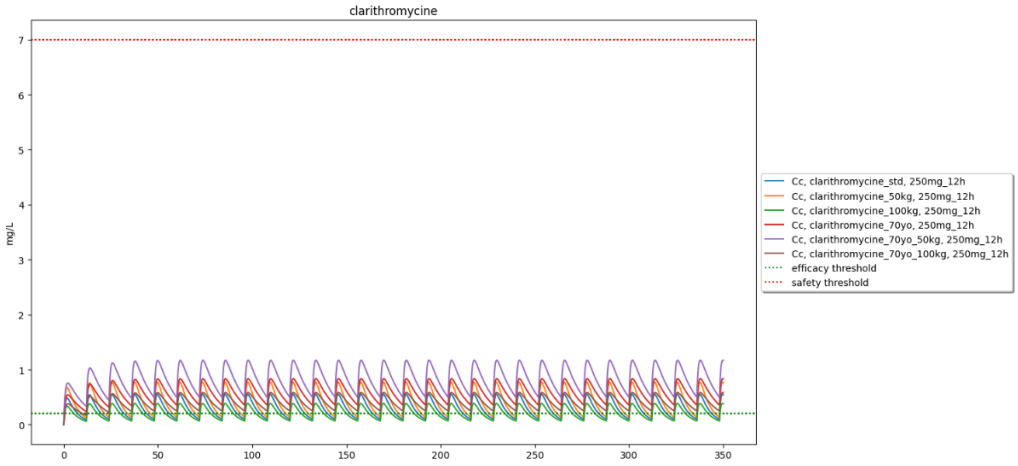

Figure 55. Test 1: 250 mg per 12 hours orally (immediate released) for standard patients weighing 50 kg, 70 kg (standard), 100 kg, and older patients of 50 kg, 70 kg (standard), 100 kg.

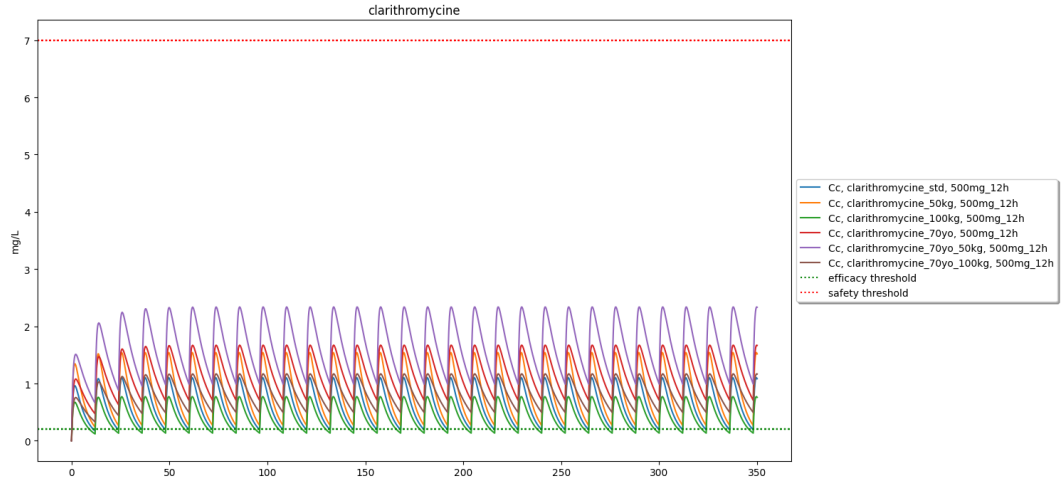

Figure 56. Test 2: 500 mg per 12 hours orally (immediate released) for standard patients weighing 50 kg, 70 kg (standard), 100 kg, and older patients of 50 kg, 70 kg (standard), 100 kg.

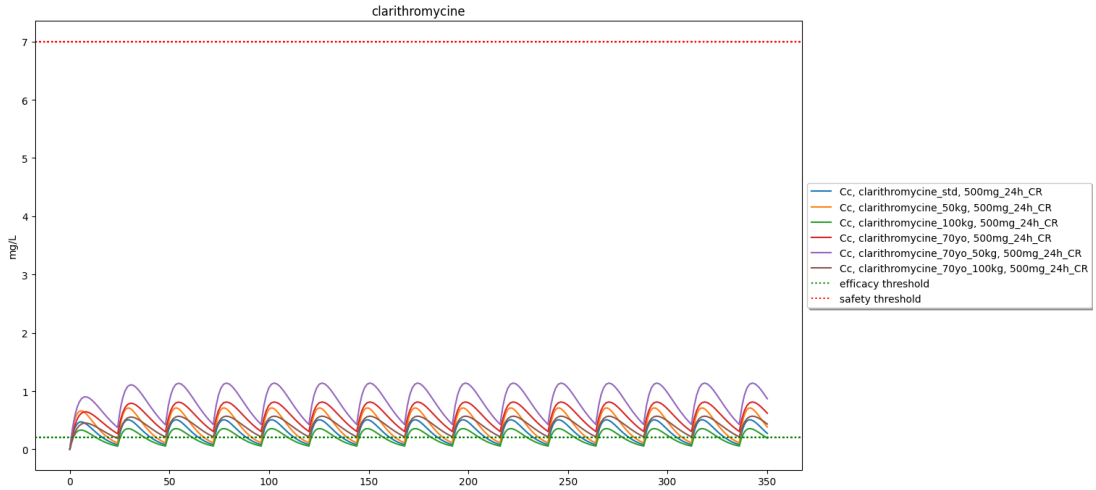

Figure 57. Test 3: 500 mg per 24 hours orally (control released) for standard patients weighing 50 kg, 70 kg (standard), 100 kg, and older patients of 50 kg, 70 kg (standard), 100 kg.

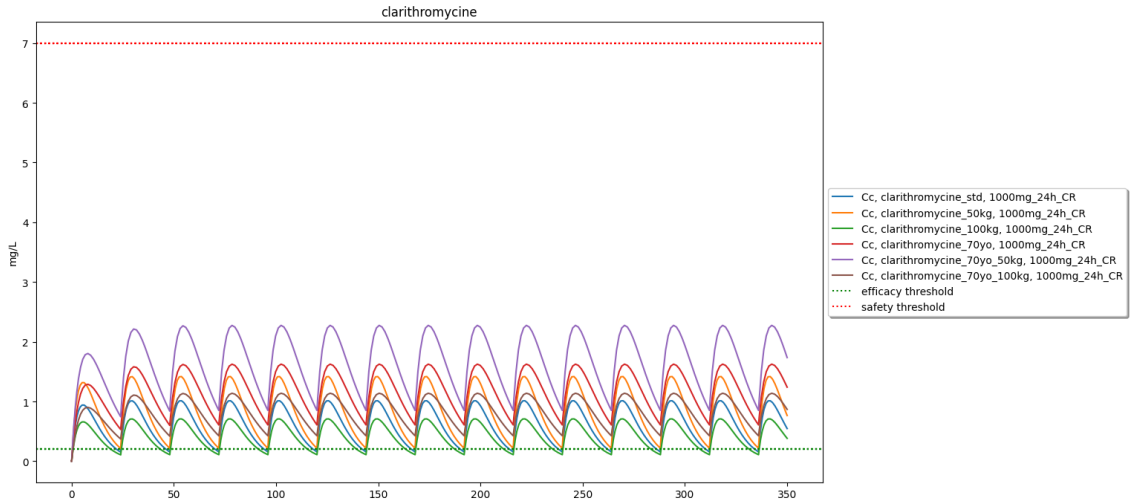

Figure 58. Test 4: 1000 mg per 24 hours orally (control released) for standard patients weighing 50 kg, 70 kg (standard), 100 kg, and older patients of 50 kg, 70 kg (standard), 100 kg.

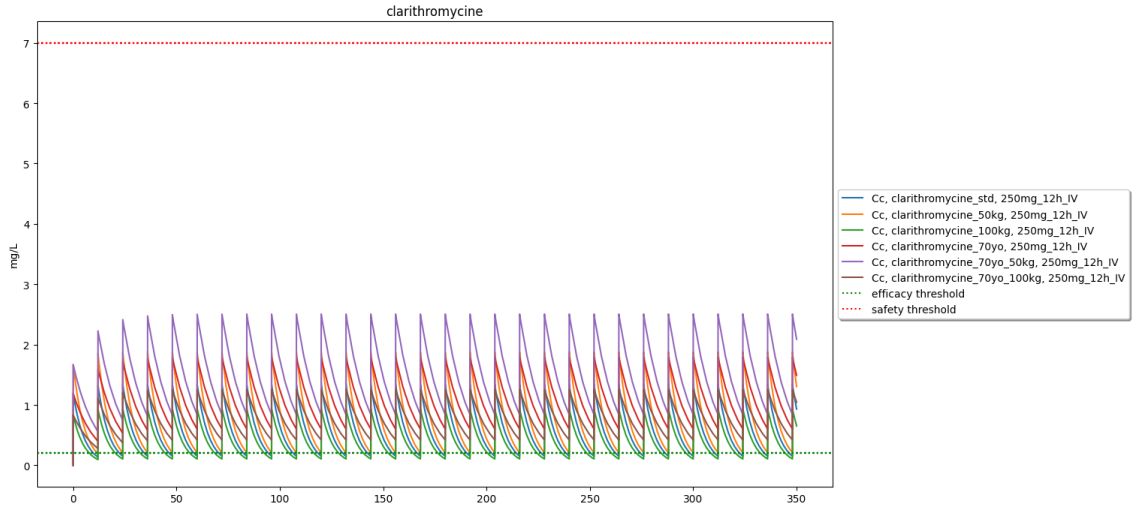

Figure 59. Test 5: 250 mg per 12 hours intravenous for standard patients weighing 50 kg, 70 kg (standard), 100 kg, and older patients of 50 kg, 70 kg (standard), 100 kg.

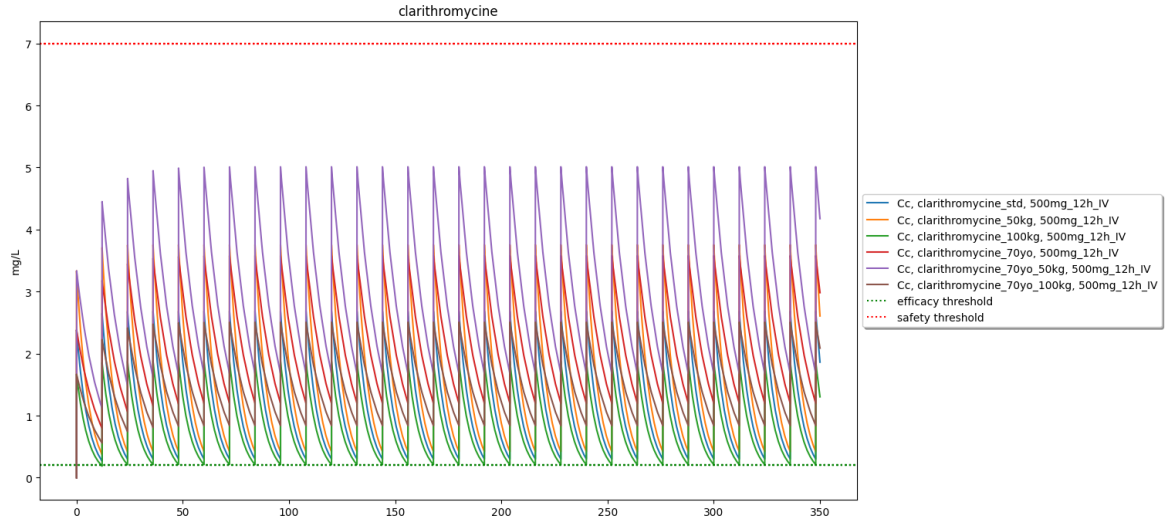

Figure 60. Test 6: 500 mg per 12 hours intravenous for standard patients weighing 50 kg, 70 kg (standard), 100 kg, and older patients of 50 kg, 70 kg (standard), 100 kg.

4.9 Sotalol (New)

Table 21. Summary of sotalol validation.

Summary		
Levels	**Notations**	**Comments**
Model form level	2/5	One-compartment model built from NC data
Model inputs sources level	2/4	Parameters comes from NC data
Test samples level	2/3	Therapeutic thresholds
Tests conditions level	4/5	-
Equivalency of input parameters level	4/4	all doses and sub-populations concerned by the medication are covered by the simulations. PK is linear in the dose range.
Output comparison level	3/5	Model outputs were within therapeutic thresholds.

Conclusion: The model is validated since all criteria meet the minimum score required. Model inputs sources level can't be increased at the targeted depth level 3/4 as no popPK model was available in literature.

4.9.1 Model Form

Model form level: 2/5
Model form: model built with NC data from regulators approved data (summary of product characteristics, regulatory agencies documents).
Model Source(s): summary of product characteristics [20], Brunton LL et al. [13].
Comment: The model parameters were calibrated with non-compartmental data. The V, CL, kabs and F were calibrated or directly taken from the source and constitutes a one-compartment model. Data from Brunton LL et al. [13] were used, but the data are consistent with Sotalol Summary of product characteristics [20].

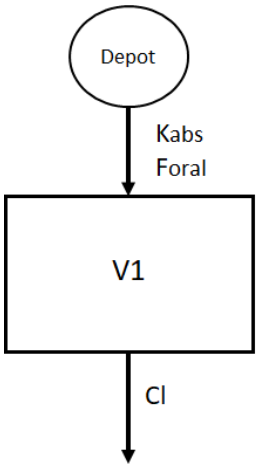

Figure 61. Model's structure, with one depot compartment, and one central compartment. Kabs, is the absorption rate, Foral the bioavailability V1 the volume of distribution, CL the clearance of elimination.

4.9.2 Model inputs sources

Model inputs sources level: 2/4
Model input: the parameters used are derived from NC data from regulatory agencies or obtained from analysis involving large numbers of patients or with low variability.
Model inputs source(s): summary of product characteristics [20], Brunton LL et al. [13].
Comment:

BIOAVAILABILITY (ORAL) (%)	URINARY EXCRETION (%)	BOUND IN PLASMA (%)	CLEARANCE (mL/min/kg)	VOL. DIST. (L/kg)	HALF-LIFE (hours)	PEAK TIME (h)	PEAK CONCENTRATION
Sotalol[a]							
60–100	70 ± 15	Negligible	2.20 ± 0.67	1.21 ± 0.17	7.18 ± 1.30	3.1 ± 0.6	1.0 ± 0.5 μg/mL[b]
			↓ RD		↑ RD		

[a]Sotalol is available as a racemate. The enantiomers contribute equally to sotalol's antiarrhythmic action; hence, pharmacokinetic parameters for total enantiomeric mixture are reported herein. β Adrenoreceptor blockade resides solely with *S*-(–)-isomer. [b]Following 80-mg, twice-a-day dosing to steady state.

References: Berglund G, et al. Pharmacokinetics of sotalol after chronic administration to patients with renal insufficiency. *Eur J Clin Pharmacol*, **1980**, *18*:321–326. Kimura M, et al. Pharmacokinetics and pharmacodynamics of (+)-sotalol in healthy male volunteers. *Br J Clin Pharmacol*, **1996**, *42*:583–588. Poirier JM, et al. The pharmacokinetics of d-sotalol and d,l-sotalol in healthy volunteers. *Eur J Clin Pharmacol*, **1990**, *38*:579–582.

Figure 62. Parameters value from Brunton LL et al. [13]. *Picture from* [13,21].

4.9.3 Quantification of sensitivities

Table 22. Analysis of the sensitivity of Cmax and AUC for sotalol by varying absorption rate constant (ka), bioavailability (F), volume of distribution (V), and clearance of elimination (CL).

Sensitivity analysis												
	ka			F			V			CL		
	-10%	ref	+10%	-10%	ref	+10%	-10%	ref	+10%	-10%	ref	+10%
Cmax	1.097	1.120	1.141	1.008	1.120	1.232	1.218	1.120	1.037	1.143	1.120	1.099
Expected behavior	Yes		Yes	Yes		Yes	Yes		Yes	Yes		Yes
AUC	15.65	15.65	15.65	14.09	15.65	17.22	15.65	15.65	15.65	17.39	15.65	14.23
Expected behavior	Yes		Yes	Yes		Yes	Yes		Yes	Yes		Yes

Conclusion: The sensitivity analysis did not indicate any discrepancies in the expected behavior of the outputs studied, thereby confirming that there is no obstacle to the model's validation.

4.9.4 Quantification of uncertainties

Introduction

The model inputs were parameters from NC literature with ranges used to propagate uncertainties. Uncertainties were propagated using standard deviations.

Propagation in simulation results

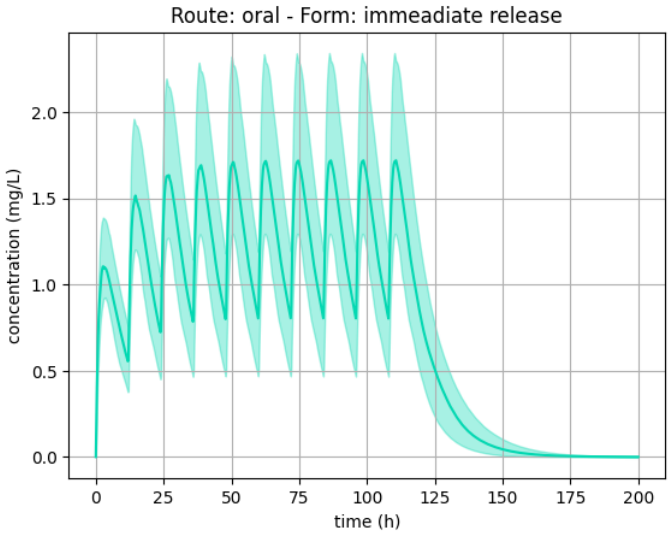

Figure 63. quantification of uncertainties for sotalol

4.9.5 Test Samples

Test sample level: 2/3

Test sample: efficacy, overexposure, and safety thresholds used for routine therapeutic drug monitoring (TDM) in clinical settings, or thresholds reflecting specific expected events (such as efficacy or toxicity) that may occur at these levels of exposure.

- Efficacy threshold was: 0.5 mg/L
- Safety threshold was: 4 mg/L

Test samples source(s): Schulz et al. [4]
Comment: /

4.9.6 Tests conditions

Tests conditions level: 4/5
Tests condition: test conditions were defined with sufficient data to run simulations for each patient concerned by the drug, with complete coverage of dosage ranges, and of all sub-populations concerned by the drug.
Tests conditions source(s): summary of product characteristics [20]
Comment: /
Test conditions were:
Test 1:
- Dosage: 40 mg/12h
- Groups: Standard patients weighing 50 kg, 70 kg (standard), 100 kg, and patients with GFR at 10, 35, 65 weighing 50, 70 and 100kg.

Test 2:
- Dosage: 80 mg/12h
- Groups: Standard patients weighing 50 kg, 70 kg (standard), 100 kg, and patients with GFR at 10, 35, 65 weighing 50, 70 and 100kg.

Test 3:
- Dosage: 160 mg/12h
- Groups: Standard patients weighing 50 kg, 70 kg (standard), 100 kg, and patients with GFR at 10, 35, 65 weighing 50, 70 and 100kg.

Test 4:
- Dosage: 240 mg/12h
- Groups: Standard patients weighing 50 kg, 70 kg (standard), 100 kg, and patients with GFR at 10, 35, 65 weighing 50, 70 and 100kg.

4.9.7 Equivalency of Input Parameters

Equivalency of input parameters level: 4/4
Equivalency of input parameters: the model's training dataset does cover all doses or PK is linear over the dose range used in the test conditions and sub-populations concerned by the medication, or an external validation is carried out and meets validation criteria. (i.e., MDPE ≤ ± 20%, MDAPE ≤ 30%)
Equivalency of input parameters source(s): summary of product characteristics [20].
Comment: sotalol simulation outputs were tested with summary of products dosing regimen covering all patients.

4.9.8 Output Comparison

Output comparison level: 3/5
Output comparison: correspondence of model outputs with the therapeutic thresholds used in routine clinical therapeutic drug monitoring or thresholds reflecting specific expected events (such as efficacy or toxicity) that may occur at these levels of exposure.
Output comparison source(s): Schulz et al. [4]

Comment: summary of product was used to extract dosing regimen data, and simulation outputs were compared to therapeutic ranges from Schulz et al. [4]. The simulation results were consistent with the expected behaviour: patients with low body weight and low glomerular filtration rate exhibit higher concentrations, reaching the efficacy threshold at lower doses compared to patients with higher body weight, while they surpass the safety threshold more quickly. Conversely, patients with higher body weight require higher doses to reach therapeutic concentrations. The dosing regimen described as usually effective for most of the population are 80mg or 160mg per 12 hours. The only patients above safety range at 160mg per 12 hours were 10kg patients with glomerular filtration rate at 10 mL/min/1.73m². Recommendations for patients with glomerular filtration rate between 10 and 30 mL/min/1.73m² is to reduce the dose at ¼ of the standard posology, which is 40mg per 12 hours. At this posology, patients of 50, 70 and 100kg with a glomerular filtration rate at 10 mL/min/1.73m² are within therapeutic thresholds.

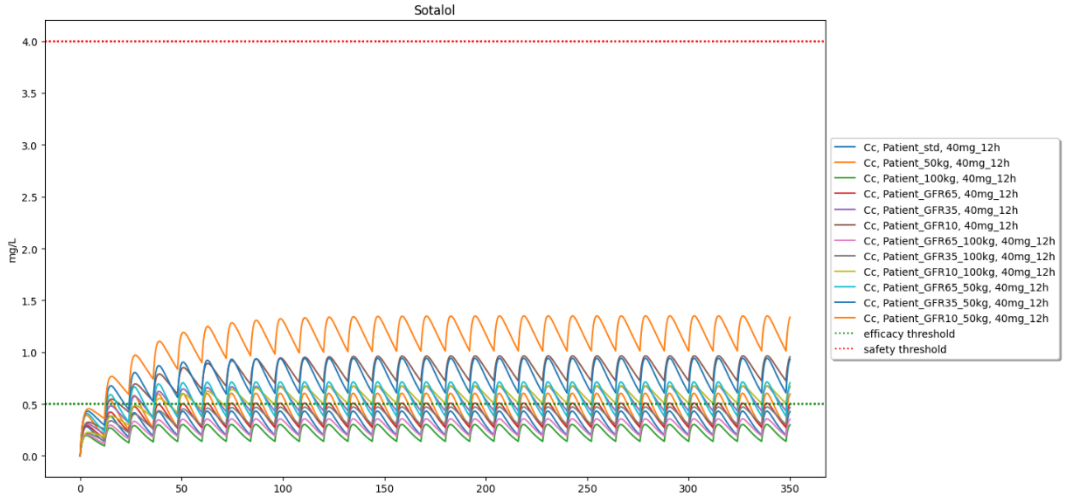

Figure 64. Test 1: 12.5 mg per 12 hours for standard patients of 50,70,100kg and children's patients of 20, 30kg.

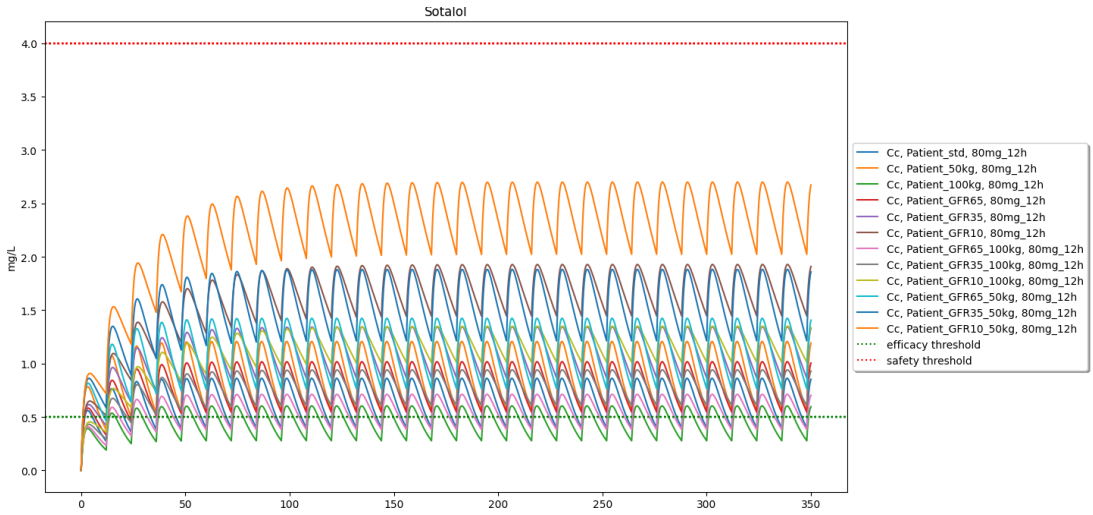

Figure 65. Test 2: 25 mg per 12 hours for standard patients of 50,70,100kg and children's patients of 20, 30kg.

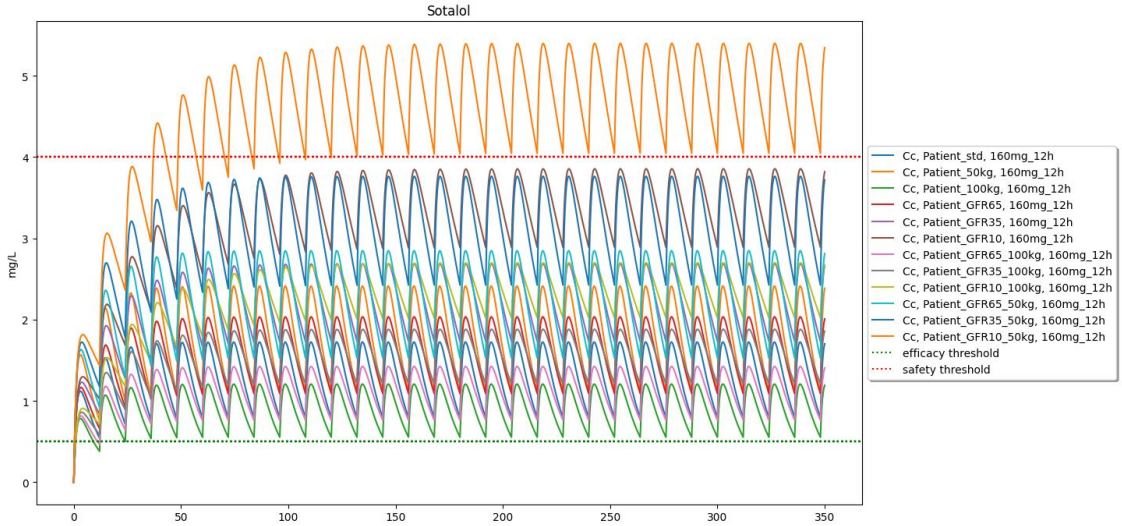

Figure 66. Test 3: 50 mg per 12 hours for standard patients of 50,70,100kg and children's patients of 20, 30kg.

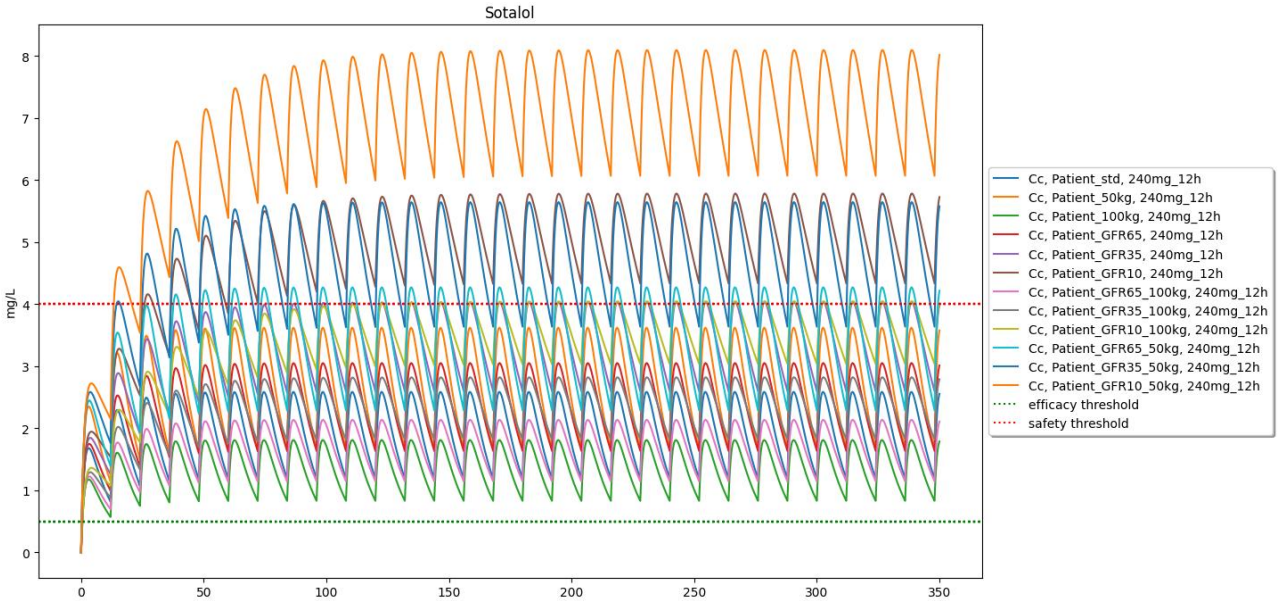

Figure 67. Test 4: 100 mg per 12 hours for standard patients of 50,70,100kg and children's patients of 20, 30kg.

4.10 Disopyramide (New)

Table 23. Summary of disopyramide validation.

Summary		
Levels	**Notations**	**Comments**
Model form level	2/5	Model built from NC data from regulators approved data
Model inputs sources level	2/4	Parameters comes from NC analysis from regulators data
Test samples level	2/3	Therapeutic thresholds
Tests conditions level	4/5	-
Equivalency of input parameters level	4/4	all doses and sub-populations concerned by the medication are covered by the simulations. PK is linear in the dose range.
Output comparison level	3/5	Model outputs were within therapeutic thresholds.
Conclusion: The model is validated since all criteria meet the minimum score required. Model inputs sources level can't be increased at the targeted depth level 3/4 as no popPK model was available in literature.		

4.10.1 Model Form

Model form level: 2/5
Model form: model built with NC data from regulators approved data (summary of product characteristics, regulatory agencies documents).
Model Source(s): summary of product characteristics for disopyramide immediate [22] and control released [23] formulations.
Comment: the model parameters were calibrated with non-compartmental data. The V, CL, kabs and F were calibrated or directly taken from the source and constitutes a one-compartment model.

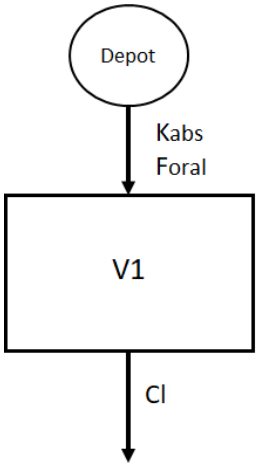

Figure 68. Model's structure, with one depot compartment, and one central compartment. Kabs, is the absorption rate, Foral the bioavailability V1 the volume of distribution, CL the clearance of elimination.

4.10.2 Model inputs sources

Model inputs sources level: 2/4
Model input: the parameters used are derived from NC data from regulatory agencies or obtained from analysis involving large numbers of patients or with low variability.
Model inputs source(s): summary of product characteristics for disopyramide immediate [22] and control released [23] formulations.
Comment:

- parameters were :
    - F : 0.95 (interval: 0.9 – 1), V : 0.75 L/kg (interval: 0.5L/kg – 1L/kg), T1/2 of elimination : 6.3 hours(interval: 4.4 – 7.8).
    - For immediate release : Tmax was 1.5 hours.
    - For controlled release : Tmax was 4.5 hours.

4.10.3 Quantification of sensitivities

Table 24. Analysis of the sensitivity of Cmax and AUC for disopyramide by varying absorption rate constant (ka for immediate and controlled release formulations), bioavailability (F for immediate and controlled release formulations), volume of distribution (V), and clearance of elimination (CL).

Sensitivity analysis									
	ka IR			ka CR			F IR		
	-10%	ref	+10%	-10%	ref	+10%	-10%	ref	+10%
Cmax	1.515	1.534	1.551	2.670	2.757	2.835	1.381	1.534	1.688
Expected behavior	Yes		Yes	Yes		Yes	Yes		Yes
AUC	16.45	16.45	16.45	41.12	41.12	41.12	14.8	16.45	18.09
Expected behavior	Yes		Yes	Yes		Yes	Yes		Yes
	F CR			V			CL		
	-10%	ref	-10%	ref	+10%	+10%	-10%	ref	+10%
Cmax	2.482	2.757	3.033	1.683	1.534	1.410	1.553	1.534	1.517
Expected behavior	Yes		Yes	Yes		Yes	Yes		Yes
AUC	37.01	41.12	45.23	16.45	16.45	16.45	18.27	16.45	14.95
Expected behavior	Yes		Yes	Yes		Yes	Yes		Yes

Conclusion: The sensitivity analysis did not indicate any discrepancies in the expected behavior of the outputs studied, thereby confirming that there is no obstacle to the model's validation.

4.10.4 Quantification of uncertainties

Introduction

The model inputs were parameters from NC literature with ranges used to propagate uncertainties. Uncertainties were propagated using ranges of values.

Propagation in simulation results

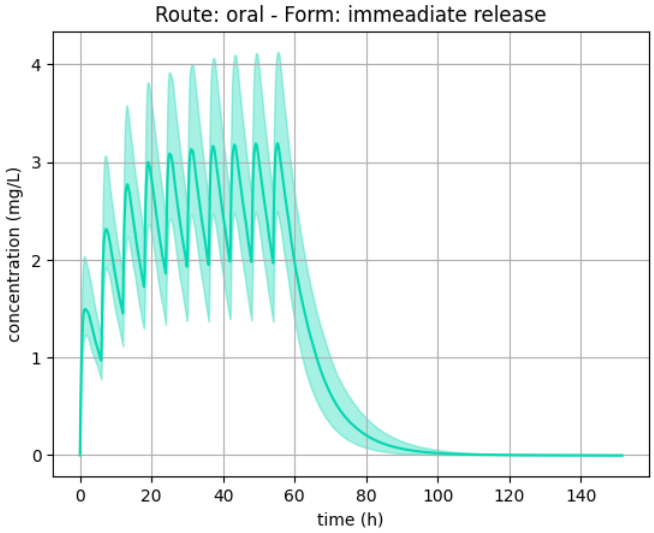

Figure 69. quantification of uncertainties for disopyramide immediate release formulation

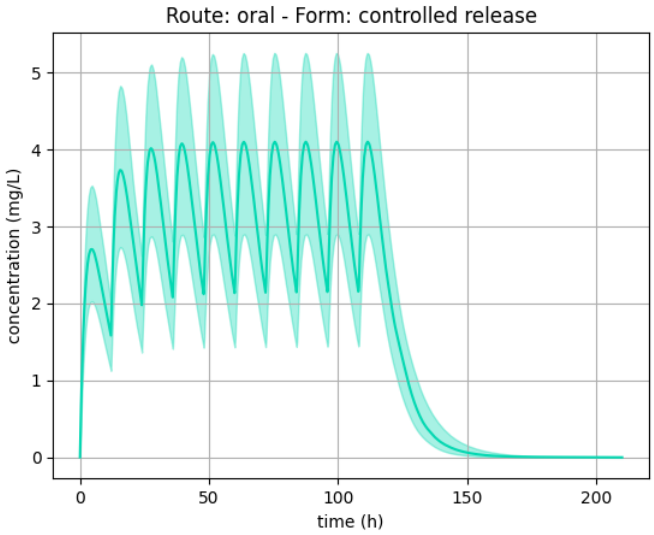

Figure 70. quantification of uncertainties for disopyramide controlled release formulation

4.10.5 Test Samples

Test sample level: 2/3

Test sample: efficacy, overexposure, and safety thresholds used for routine therapeutic drug monitoring (TDM) in clinical settings, or thresholds reflecting specific expected events (such as efficacy or toxicity) that may occur at these levels of exposure.

- Efficacy threshold was: 2 mg/L
- Overexposure threshold was: 7 mg/L
- Safety threshold was: 9 mg/L

Test samples source(s): Schulz et al. [4], summary of product characteristics [22]

Comment: the efficacy and overexposure thresholds come from Schulz et al. [4]. The safety threshold was fixed at 9mg/L according to data from summary of product characteristics [22].

4.10.6 Tests conditions

Tests conditions level: 4/5
Tests condition: test conditions were defined with sufficient data to run simulations for each patient concerned by the drug, with complete coverage of dosage ranges, and of all sub-populations concerned by the drug.
Tests conditions source(s): summary of product characteristics for disopyramide immediate [22] and control released [23] formulations.
Comment: /
Test conditions were:
Test 1:
- Dosage: 100 mg/6h
- Groups: Standard patients weighing 50 kg, 70 kg (standard), 100 kg.

Test 2:
- Dosage: 150 mg/6h
- Groups: Standard patients weighing 50 kg, 70 kg (standard), 100 kg.

Test 3:
- Dosage: 100 mg/8h
- Groups: patients with GFR40 weighing 50 kg, 70 kg (standard), 100 kg.

Test 4:
- Dosage: 100 mg/12h
- Groups: patients with GFR20 weighing 50 kg, 70 kg (standard), 100 kg.

Test 5:
- Dosage: 100 mg/24h
- Groups: patients with GFR5 weighing 50 kg, 70 kg (standard), 100 kg.

Test 6:
- Dosage: 250 mg/12h and 375mg/12h
- Groups: standard patients weighing 50 kg, 70 kg (standard), 100 kg.

4.10.7 Equivalency of Input Parameters

Equivalency of input parameters level: 4/4
Equivalency of input parameters: the model's training dataset does cover all doses or PK is linear over the dose range used in the test conditions and sub-populations concerned by the medication, or an external validation is carried out and meets validation criteria. (i.e., MDPE ≤ ± 20%, MDAPE ≤ 30%)
Equivalency of input parameters source(s): summary of product characteristics for disopyramide immediate [22] and control released [23] formulations.
Comment: Disopyramide simulation outputs were tested with summary of products dosing regimen covering all patients.

4.10.8 Output Comparison

Output comparison level: 3/5
Output comparison: correspondence of model outputs with the therapeutic thresholds used in routine clinical therapeutic drug monitoring or thresholds reflecting specific expected events (such as efficacy or toxicity) that may occur at these levels of exposure.
Output comparison source(s): Schulz et al. [4]
Comment: summary of product was used to extract dosing regimen data, and simulation outputs were compared to therapeutic ranges from Schulz et al. [4]. The simulation results were consistent with the expected behaviour. Most of patients are within therapeutic thresholds. Patients with hight weight (100kg) should receive an increased dose (150mg/6 hours instead of 100mg). Patients with low weight (50kg) should receive a reduced dose with controlled release formulation (375mg/12 hours is to be avoided, even if the safety threshold is not reached).

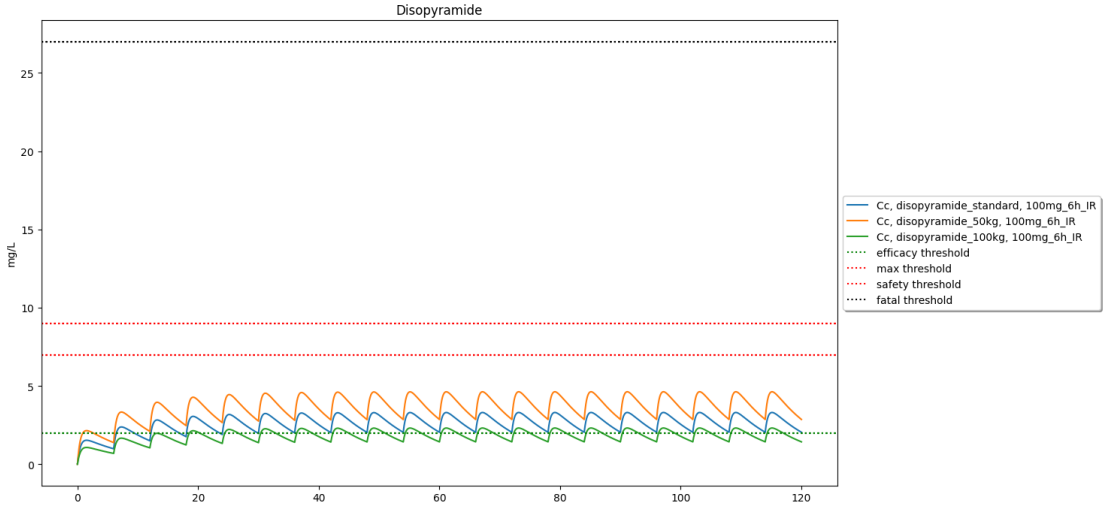

Figure 71. Test 1: 100mg/6 hours for standard patients of 50, 70, 100kg.

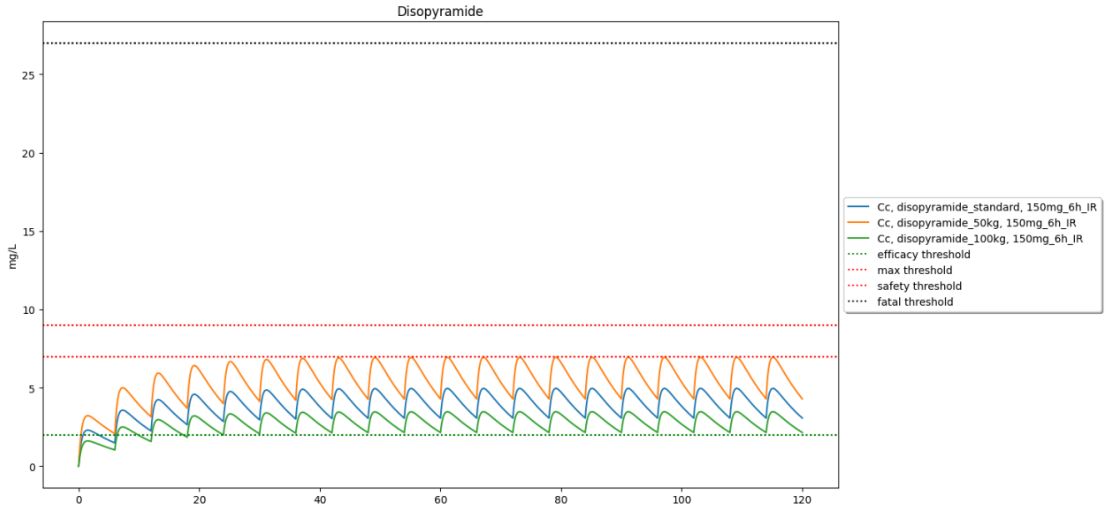

Figure 72. Test 2: 150mg/6 hours for standard patients of 50, 70, 100kg.

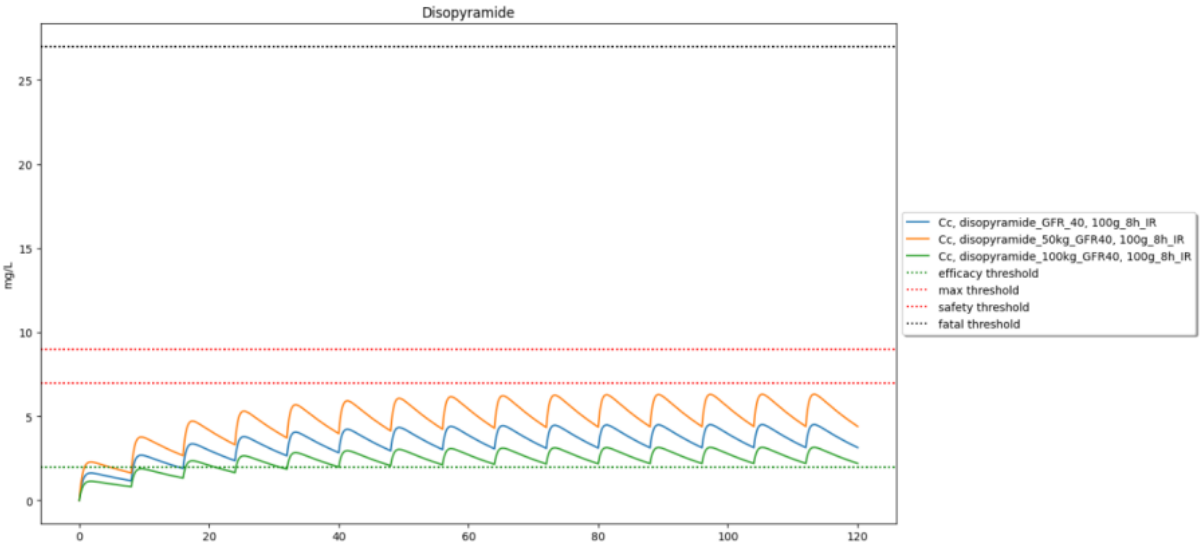

Figure 73. Test 3: 100mg/8 hours for patients of 50, 70, 100kg with glomerular filtration rate of 40mL/min/1.73m².

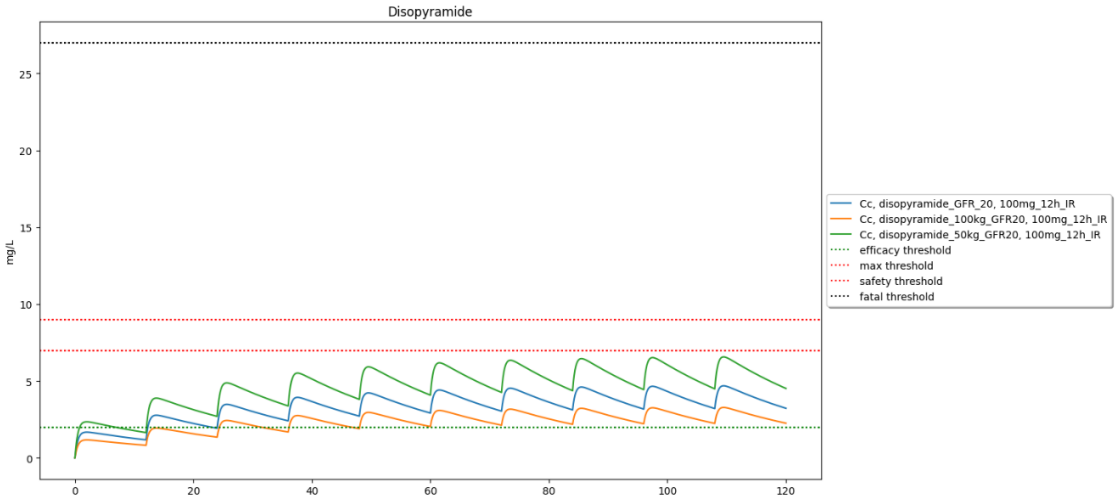

Figure 74. Test 4: 100mg/12 hours for patients of 50, 70, 100kg with glomerular filtration rate of 20mL/min/1.73m².

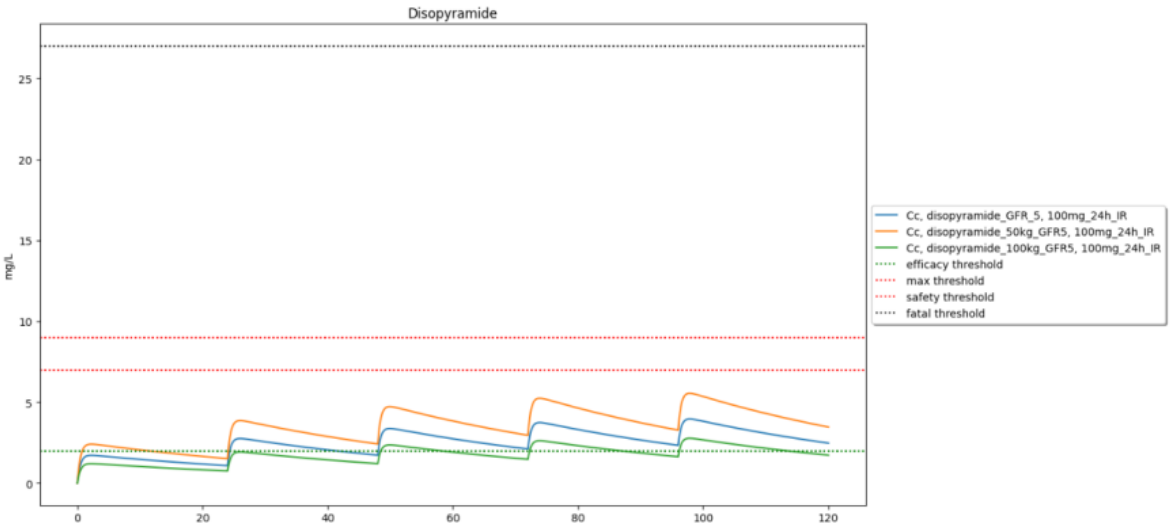

Figure 75. Test 5: 100mg/24 hours for patients of 50, 70, 100kg with glomerular filtration rate of 5mL/min/1.73m².

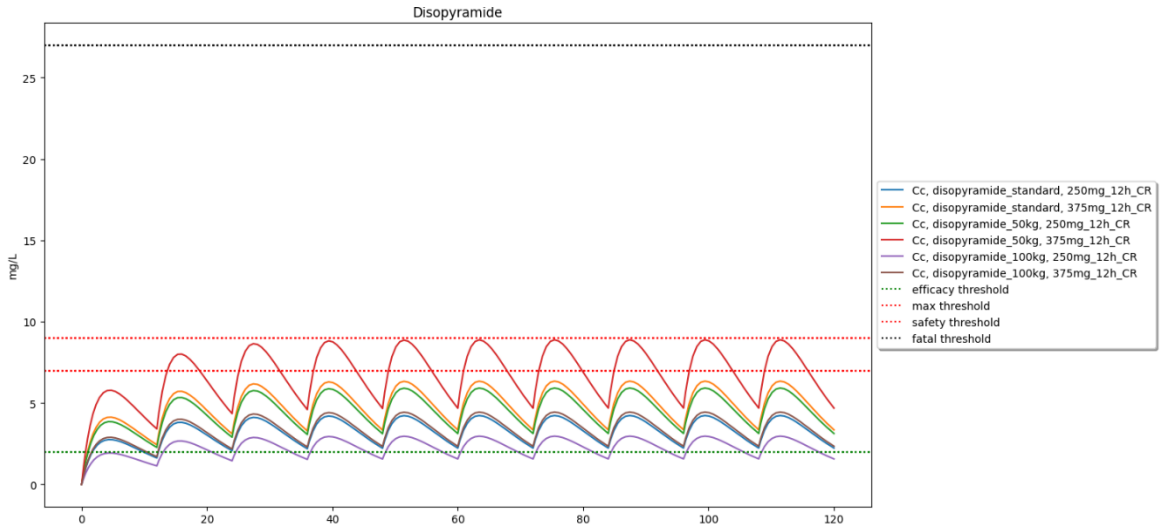

Figure 76. Test 6: controlled release formulation at 250mg/12hours and 375mg/12hours for standard patients weighing 50, 70 and 100kg.

4.11 Dofetilide (New)

Table 25. Summary of dofetilide validation.

Summary		
Levels	**Notations**	**Comments**
Model form level	2/5	One-compartment model built from NC data
Model inputs sources level	2/4	Parameters comes from NC data
Test samples level	2/3	Therapeutic thresholds
Tests conditions level	4/5	-
Equivalency of input parameters level	4/4	all doses and sub-populations concerned by the medication are covered by the simulations. PK is linear in the dose range.
Output comparison level	3/5	Model outputs were within therapeutic thresholds.
Conclusion: The model is validated since all criteria meet the minimum score required. Model inputs sources level can't be increased at the targeted depth level 3/4 as no popPK model was available in literature.		

4.11.1 Model Form

Model form level: 2/5
Model form: model built with NC data from regulators approved data (summary of product characteristics, regulatory agencies documents).
Model Source(s): summary of product characteristics [24], summarized by Medscape [25]
Comment: the model parameters were calibrated with summary of product characteristics non-compartmental data. The V, CL, kabs and F were calibrated or directly taken from the source and constitutes a one-compartment model.

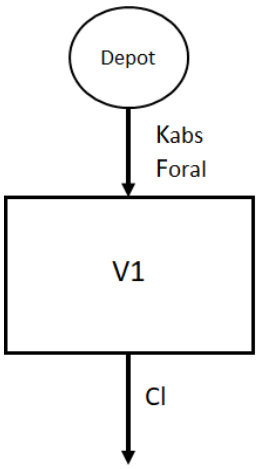

Figure 77. Model's structure, with one depot compartment, and one central compartment. Kabs, is the absorption rate, Foral the bioavailability V1 the volume of distribution, CL the clearance of elimination.

4.11.2 Model inputs sources

Model inputs sources level: 2/4
Model input: the parameters used are derived from NC data from regulatory agencies or obtained from analysis involving large numbers of patients or with low variability.
Model inputs source(s): summary of product characteristics [24], summarized by Medscape [25]

Comment:

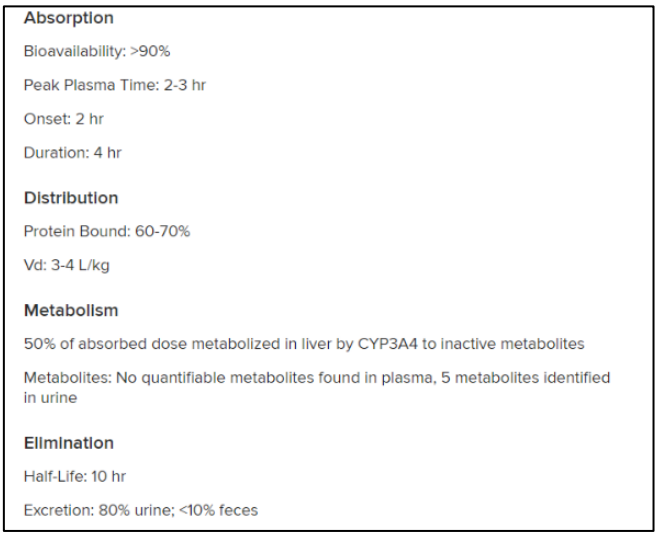
Absorption

Bioavailability: >90%

Peak Plasma Time: 2-3 hr

Onset: 2 hr

Duration: 4 hr

Distribution

Protein Bound: 60-70%

Vd: 3-4 L/kg

Metabolism

50% of absorbed dose metabolized in liver by CYP3A4 to inactive metabolites

Metabolites: No quantifiable metabolites found in plasma, 5 metabolites identified in urine

Elimination

Half-Life: 10 hr

Excretion: 80% urine; <10% feces

Figure 78. Parameters value from summary of product characteristics [24], summarized by Medscape [25]. Picture from Medscape [25].

Recalibration of CL by a factor 0.85 was performed when patients were female. Also, ke (elimination rate) was recalibrated to include the GFR covariate using the urinary fraction of 80% with the following formula: "(1-0.80*(1-GFR/90))".

4.11.3 Quantification of sensitivities

***Table 26*. Analysis of the sensitivity of Cmax and AUC for dofetilide by varying absorption rate constant (ka), bioavailability (F), volume of distribution (V), and clearance of elimination (CL).**

Sensitivity analysis						
	ka			F		
	-10%	ref	+10%	-10%	ref	+10%
Cmax	0.001778	0.001802	0.001823	0.001622	0.001802	0.001982
Expected behavior	Yes		Yes	Yes		Yes
AUC	0.03091	0.03091	0.03091	0.02782	0.03091	0.03401
Expected behavior	Yes		Yes	Yes		Yes
	V			CL		
	-10%	ref	+10%	-10%	ref	+10%
Cmax	0.001975	0.001802	0.001657	0.001825	0.001802	0.001780
Expected behavior	Yes		Yes	Yes		Yes
AUC	0.03091	0.03091	0.03091	0.03435	0.03091	0.0281
Expected behavior	Yes		Yes	Yes		Yes

Conclusion: The sensitivity analysis did not indicate any discrepancies in the expected behavior of the outputs studied, thereby confirming that there is no obstacle to the model's validation.

4.11.4 Quantification of uncertainties

Introduction

The model inputs were fixed parameters from NC literature, except for Tmax which was described with a range of 2 to 3 hours. It has no great impact when propagating uncertainties.

Propagation in simulation results

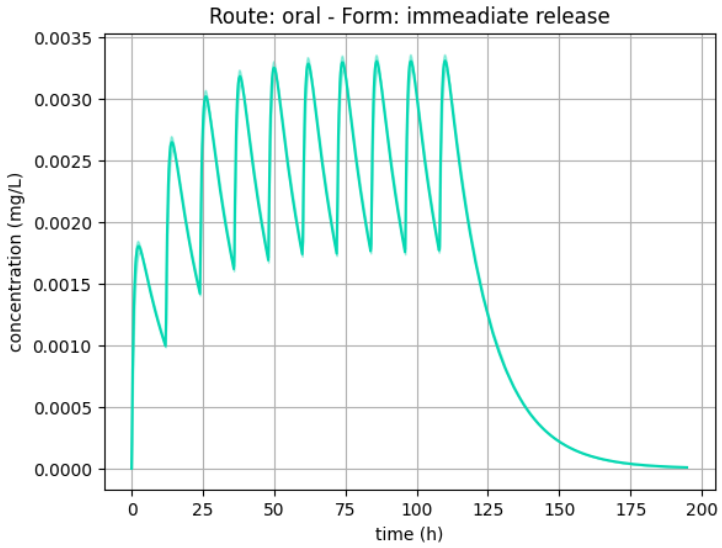

Figure 79. quantification of uncertainties for dofetilide

4.11.5 Test Samples

Test sample level: 2/3
Test sample: efficacy, overexposure, and safety thresholds used for routine therapeutic drug monitoring (TDM) in clinical settings, or thresholds reflecting specific expected events (such as efficacy or toxicity) that may occur at these levels of exposure.

- Efficacy threshold was: 0.001 mg/L
- Safety threshold was: 0.0055 mg/L

Test samples source(s): Schulz et al. [4], Summary of product characteristics [24]
Comment: the efficacy threshold comes from the summary of product characteristics [24], while the overexposure threshold from Schulz et al. [4].

4.11.6 Tests conditions

Tests conditions level: 4/5
Tests condition: test conditions were defined with sufficient data to run simulations for each patient concerned by the drug, with complete coverage of dosage ranges, and of all sub-populations concerned by the drug.
Tests conditions source(s): summary of product characteristics [24], summarized by Medscape [25]
Comment: /
Test conditions were:
Test 1:

- Dosage: 0.5 mg/12h
- Groups: patients male and female weighing 50 kg, 70 kg (standard), 100kg.

Test 2:

- Dosage: 0.25 mg/12h
- Groups: patients male and female weighing 50 kg, 70 kg (standard), 100kg with GFR of 50mL/min/1.73m².

Test 3:

- Dosage: 0.125 mg/12h
- Groups: patients male and female weighing 50 kg, 70 kg (standard), 100kg with GFR of 30mL/min/1.73m².

4.11.7 Equivalency of Input Parameters

Equivalency of input parameters level: 4/4
Equivalency of input parameters: the model's training dataset does cover all doses or PK is linear over the dose range used in the test conditions and sub-populations concerned by the medication, or an external validation is carried out and meets validation criteria. (i.e., MDPE ≤ ± 20%, MDAPE ≤ 30%)
Equivalency of input parameters source(s): summary of product characteristics [24], summarized by Medscape [25]
Comment: Dofetilide simulation outputs were tested with summary of products dosing regimen covering all indications.

4.11.8 Output Comparison

Output comparison level: 3/5
Output comparison: correspondence of model outputs with the therapeutic thresholds used in routine clinical therapeutic drug monitoring or thresholds reflecting specific expected events (such as efficacy or toxicity) that may occur at these levels of exposure.
Output comparison source(s): Schulz et al. [4], Summary of product characteristics [24]
Comment: summary of product was used to extract dosing regimen data, and simulation outputs were compared to therapeutic thresholds.
The simulation results were all within therapeutic thresholds.

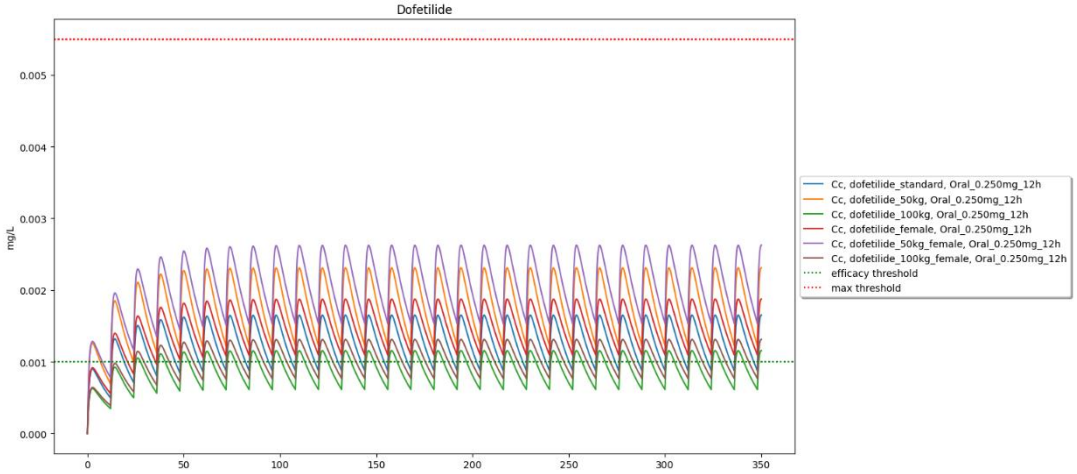

Figure 80. Test 1: 0.5mg per 12 hours for patient's male and female weighing 50 kg, 70 kg, 100kg.

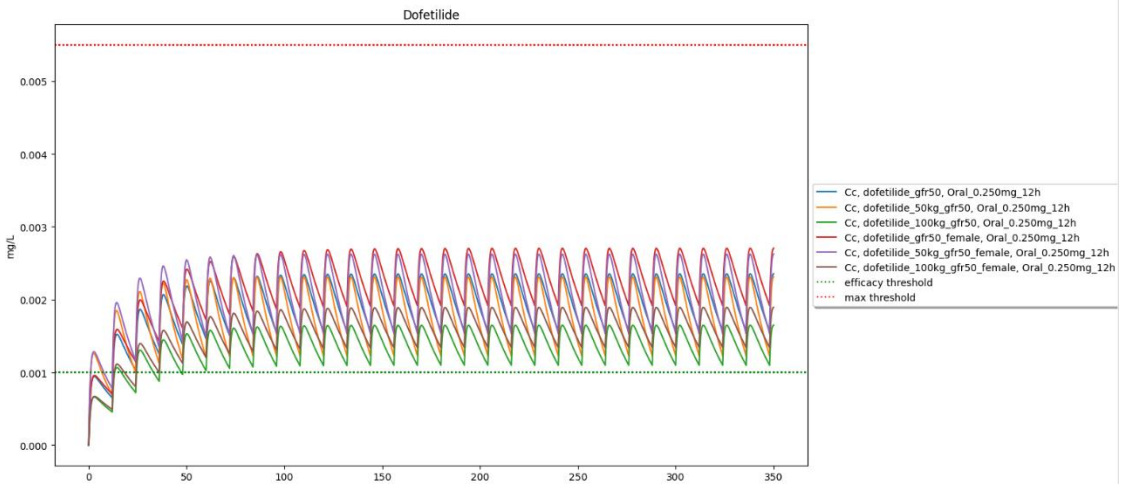

Figure 81. Test 2: 0.25 mg per 12 hours for patient's male and female weighing 50 kg, 70 kg, 100kg with GFR of 50mL/min/1.73m².

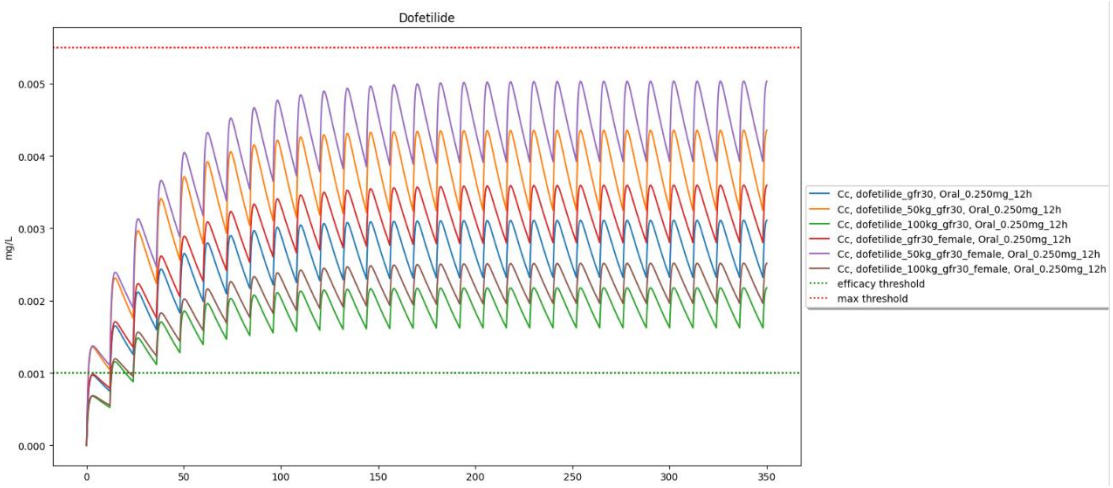

Figure 82. Test 3: 0.125 mg per 12 hours for patient's male and female weighing 50 kg, 70 kg, 100kg with GFR of 30mL/min/1.73m².

4.12 Domperidone (New)

Table 27. Summary of domperidone validation.

Summary		
Levels	**Notations**	**Comments**
Model form level	2/5	One-compartment model built from NC data
Model inputs sources level	2/4	Parameters comes from NC data
Test samples level	2/3	Therapeutic thresholds
Tests conditions level	4/5	-
Equivalency of input parameters level	4/4	all doses and sub-populations concerned by the medication are covered by the simulations. PK is linear in the dose range.
Output comparison level	3/5	Model outputs were within therapeutic thresholds.
Conclusion: The model is validated since all criteria meet the minimum score required. Model inputs sources level can't be increased at the targeted depth level 3/4 as no popPK model was available in literature.		

4.12.1 Model Form

Model form level: 2/5
Model form: model built with NC data from regulators approved data (summary of product characteristics, regulatory agencies documents).
Model Source(s): summary of product characteristics [26], Helmy et al. [27]
Comment: the model parameters were calibrated with non-compartmental data from Helmy et al. [27]. The V, CL, kabs and F were calibrated from the source and constitutes a one-compartment model. Absorption was calibrated for domperidone suspension and tablet with different parameters from the same source. Then, two absorption rates (ka) were calibrated.

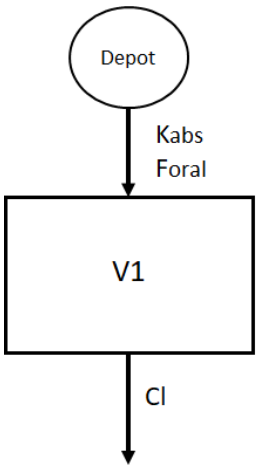

Figure 83. Model's structure, with one depot compartment, and one central compartment. Kabs, is the absorption rate, Foral the bioavailability V1 the volume of distribution, CL the clearance of elimination.

4.12.2 Model inputs sources

Model inputs sources level: 2/4
Model input: the parameters used are derived from NC data from regulatory agencies or obtained from analysis involving large numbers of patients or with low variability.
Model inputs source(s): summary of product characteristics [26], Helmy et al. [27]

Comment:

Parameters	Domperidone Suspension (Mean ± SD)	Domperidone Tablet (Mean ± SD)	90% Confidence Interval, Point Estimate (Lower Limit–Upper Limit)
C_{max} (ng/mL)	43.0 ± 13.2	39.6 ± 11.5	0.94 (0.81–1.1)
t_{max} (hour)	0.9 ± 0.2	1.2 ± 0.4	
$AUC_{0\rightarrow t}$ (ng h/mL)	249.5 ± 84.7	202.8 ± 70.1	0.89 (0.80–0.98)
$AUC_{0\rightarrow\infty}$ (ng h/mL)	298.3 ± 101.4	247.7 ± 72.1	0.89 (0.81–0.96)
$t_{1/2}$ (hour)	8.1 ± 2.4	7.9 ± 2.1	

C_{max}, peak plasma concentration; t_{max}, time to reach peak plasma concentration; $AUC_{0-\infty}$, area under the concentration–time curve from zero to infinity; AUC_{0-t}, area under the concentration–time curve from zero to the last measurable plasma concentration; $AUC_{t-\infty}$, area under the concentration–time curve from the last measurable concentration to infinity; and $t_{1/2}$, elimination half-life.

Figure 84. Parameters value from Helmy et al. [27]. Picture is from Helmy et al. [27].

F was 1 for oral solution and 0.831 for oral tablet. Parameters used as model inputs for calibration were consistent with summary of product characteristics [26]. T1/2 recalibration by a factor 2.81 was performed for patient with GFR < 30 mL/min/1.73m² according to data from summary of product characteristics [26].

4.12.3 Quantification of sensitivities

***Table 28*. Analysis of the sensitivity of Cmax and AUC for domperidone by varying absorption rate constant (ka for tablet and solution), bioavailability (F for tablet and solution), volume of distribution (V), and clearance of elimination (CL).**

Sensitivity analysis									
	ka solution			ka tablet			F solution		
	-10%	ref	+10%	-10%	ref	+10%	-10%	ref	+10%
Cmax	0.02136	0.02150	0.02162	0.01961	0.01978	0.01992	0.01935	0.02150	0.02365
Expected behavior	Yes		Yes	Yes		Yes	Yes		Yes
AUC	0.2683	0.2683	0.2683	0.2533	0.2533	0.2533	0.2414	0.2683	0.2951
Expected behavior	Yes		Yes	Yes		Yes	Yes		Yes
	F tablet			V			CL		
	-10%	ref	-10%	ref	+10%	+10%	-10%	ref	+10%
Cmax	0.01780	0.01978	0.02176	0.02373	0.02150	0.01965	0.02163	0.02150	0.02137
Expected behavior	Yes		Yes	Yes		Yes	Yes		Yes
AUC	0.2280	0.2533	0.2787	0.2683	0.2683	0.2683	0.2981	0.2683	0.2439
Expected behavior	Yes		Yes	Yes		Yes	Yes		Yes

Conclusion: The sensitivity analysis did not indicate any discrepancies in the expected behavior of the outputs studied, thereby confirming that there is no obstacle to the model's validation.

4.12.4 Quantification of uncertainties

Introduction

The model inputs were parameters from NC literature with ranges used to propagate uncertainties. Uncertainties were propagated using standard deviations.

Propagation in simulation results

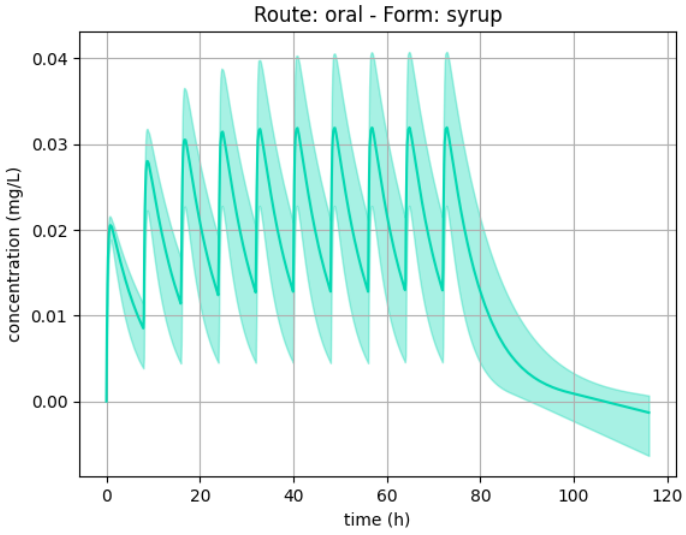

Figure 85. quantification of uncertainties for domperidone

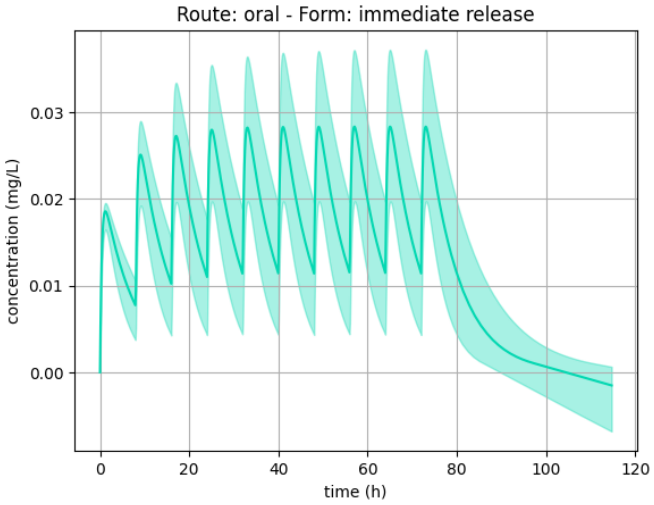

Figure 86. quantification of uncertainties for domperidone

4.12.5 Test Samples

Test sample level: 2/3
Test sample: efficacy, overexposure, and safety thresholds used for routine therapeutic drug monitoring (TDM) in clinical settings, or thresholds reflecting specific expected events (such as efficacy or toxicity) that may occur at these levels of exposure.

- Efficacy threshold was: 0.01 mg/L
- Overexposure threshold was: 0.1 mg/L
- Safety threshold was: 0.2 mg/L

Test samples source(s): Schulz et al. [4]
Comment: /

4.12.6 Tests conditions

Tests conditions level: 4/5
Tests condition: test conditions were defined with sufficient data to run simulations for each patient concerned by the drug, with complete coverage of dosage ranges, and of all sub-populations concerned by the drug.
Tests conditions source(s): summary of product characteristics [26]
Comment: /
Test conditions were:
Test 1:

- Dosage: 10mg/8h, oral solution
- Groups: standard patient and patient with GFR at 20 mL/min/1.73m²

Test 2:

- Dosage: 10mg/24h, oral solution
- Groups: patient with GFR at 20 mL/min/1.73m²

Test 3:

- Dosage: 10mg/8h, oral tablet
- Groups: standard patient and patient with GFR at 20 mL/min/1.73m²

Test 4:

- Dosage: 10mg/24h, oral tablet
- Groups: patient with GFR at 20 mL/min/1.73m²

4.12.7 Equivalency of Input Parameters

Equivalency of input parameters level: 4/4
Equivalency of input parameters: the model's training dataset does cover all doses or PK is linear over the dose range used in the test conditions and sub-populations concerned by the medication, or an external validation is carried out and meets validation criteria. (i.e., MDPE ≤ ± 20%, MDAPE ≤ 30%)
Equivalency of input parameters source(s): summary of product characteristics [26]
Comment: domperidone simulation outputs were tested with summary of products dosing regimen covering all indications.

4.12.8 Output Comparison

Output comparison level: 3/5
Output comparison: correspondence of model outputs with the therapeutic thresholds used in routine clinical therapeutic drug monitoring or thresholds reflecting specific expected events (such as efficacy or toxicity) that may occur at these levels of exposure.
Output comparison source(s): Schulz et al. [4]
Comment: summary of product was used to extract dosing regimen data, and simulation outputs were compared to therapeutic thresholds.
The simulation results were all within therapeutic thresholds.

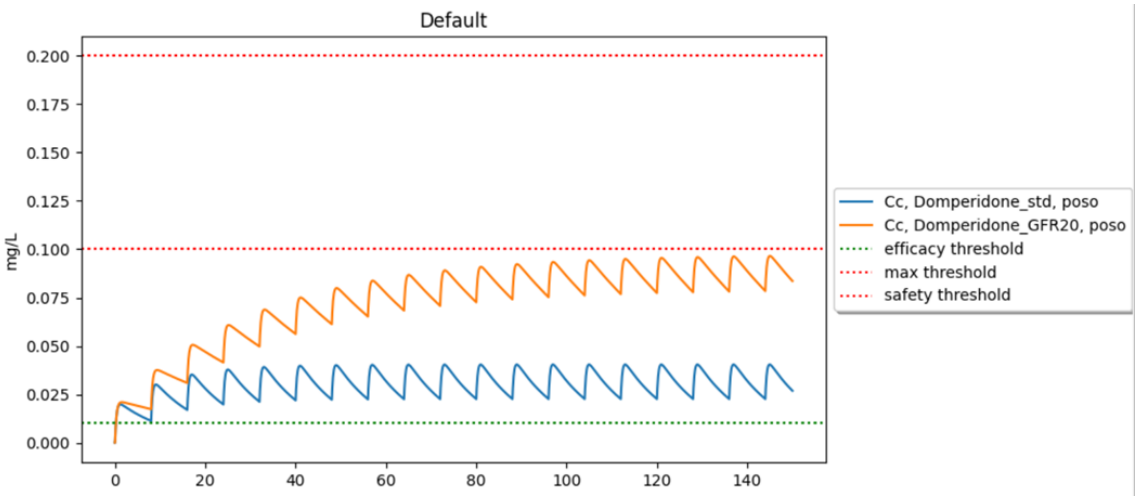

Figure 87. Test 1: 10mg per 8 hours for standard patient and patient with GFR at 20 mL/min/1.73m², oral solution

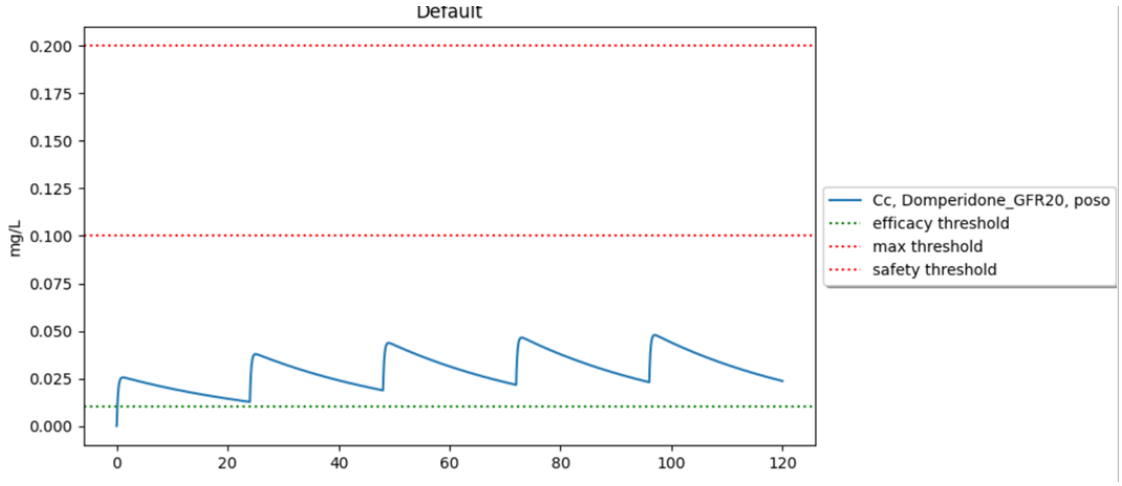

Figure 88. Test 2: 10mg per 24 hours for patient with GFR at 20 mL/min/1.73m², oral solution

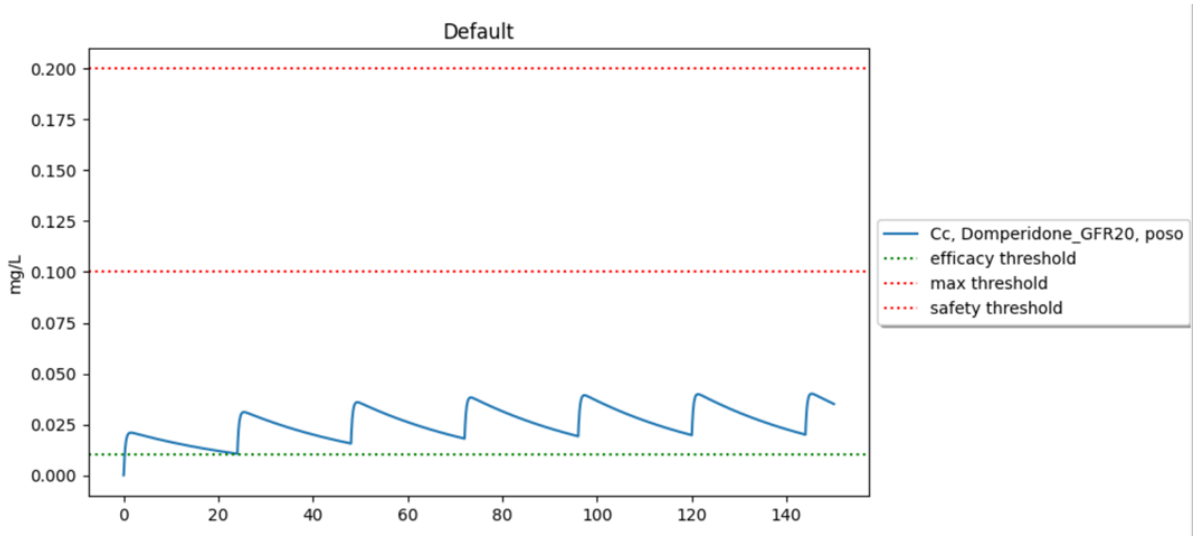

Figure 89. Test 3: 10mg per 8 hours for standard patient and patient with GFR at 20 mL/min/1.73m², oral tablet

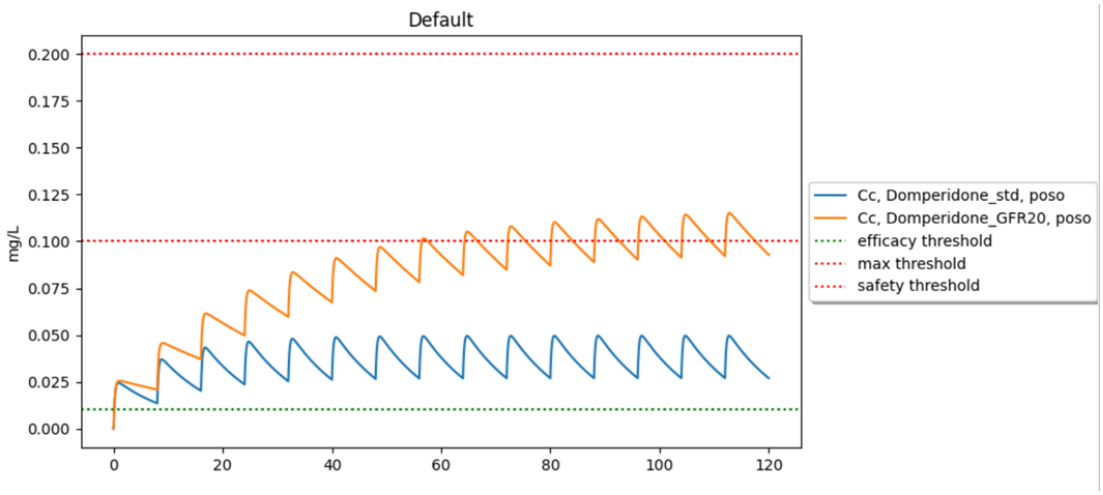

Figure 90. Test 4: 10mg per 24 hours for patient with GFR at 20 mL/min/1.73m², oral tablet

4.13 Droperidol (New)

Table 29. Summary of droperidol validation.

Summary		
Levels	**Notations**	**Comments**
Model form level	3/5	Model built from popPK analysis
Model inputs sources level	3/4	RSE% on parameters are >30%
Test samples level	2/3	Therapeutic thresholds
Tests conditions level	4/5	-
Equivalency of input parameters level	4/4	all doses and sub-populations concerned by the medication are covered by the simulations. PK is linear in the dose range.
Output comparison level	3/5	Model outputs were within therapeutic thresholds.
Conclusion: The model is validated since all applicable criteria meet the minimum score required.		

4.13.1 Model Form

Model form level: 3/5
Model form: model built from popPK analysis.
Model Source(s): Foo etal. [28]
Comment: the implemented PK model is based on a popPK analysis conducted by Foo etal. [28]. It is a one-compartment model with first order absorption and elimination.

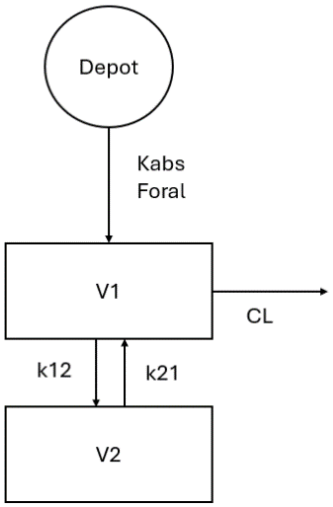

Figure 91. Model's structure, with one depot compartment, and one central compartment. Kabs, is the absorption rate, Foral the bioavailability V1 the volume of central compartment, V2 the volume of peripheral compartment and CL the clearance of elimination. K21 et K12 are transfer compartment between central and peripheral compartment.

4.13.2 Model inputs sources

Model inputs sources level: 3/4
Model input: parameters are obtained from popPK analysis with a relative standard error (RSE) > 30% or taken from the summary of product characteristics or from analysis conducted on many patients with little variability.
Model inputs source(s): Foo etal. [28]
Comment:

	Parameter estimate (95% CI)	Between subject variability CV% (95% CI)
CL ($l\ h^{-1}$)	41.9 (34.8–49.0)	51% (31.2–64.4%)
Vp (l)	73.6 (51.1–96.1)	51%[a] (31.2–64.4%)
k_a (l^{-1})	10 F (–)	100% (–)
Q ($l\ h^{-1}$)	71.5 (42.3–100.7)	–
Vp (l)	79.8 (58.8–100.8)	–
σ (CV%)	22% (8.5–30.3%)	
σ_{add} ($\mu g\ l^{-1}$)	0.0001 F	

Figure 92. Parameters value from Foo etal. [28]. Picture from Foo etal. [28].

An error was found in the figure. “Vp” which refers to the peripheral volume was used twice. The first “Vp” should have been “Vc”.

4.13.3 Quantification of sensitivities

***Table 30*. Analysis of the sensitivity of Cmax and AUC for droperidol by varying absorption rate constant (ka), bioavailability (F), volume of distribution (V), and clearance of elimination (CL).**

Sensitivity analysis												
	ka			F			V			CL		
	-10%	ref	+10%	-10%	ref	+10%	-10%	ref	+10%	-10%	ref	+10%
Cmax	0.05452	0.05599	0.05715	0.05039	0.05599	0.06159	0.05994	0.05599	0.05266	0.05797	0.05599	0.05437
Expected behavior	Yes		Yes	Yes		Yes	Yes		Yes	Yes		Yes
AUC	0.7104	0.7101	0.7098	0.6391	0.7101	0.7811	0.7100	0.7101	0.7101	0.7885	0.7101	0.6458
Expected behavior	Yes		Yes	Yes		Yes	Yes		Yes	Yes		Yes

Conclusion: The sensitivity analysis did not indicate any discrepancies in the expected behavior of the outputs studied, thereby confirming that there is no obstacle to the model's validation.

4.13.4 Quantification of uncertainties

Introduction

The model has been built with popPK data : uncertainties were quantified as interindividual variability (IIV) and residual variability (RV).

Propagation in simulation results

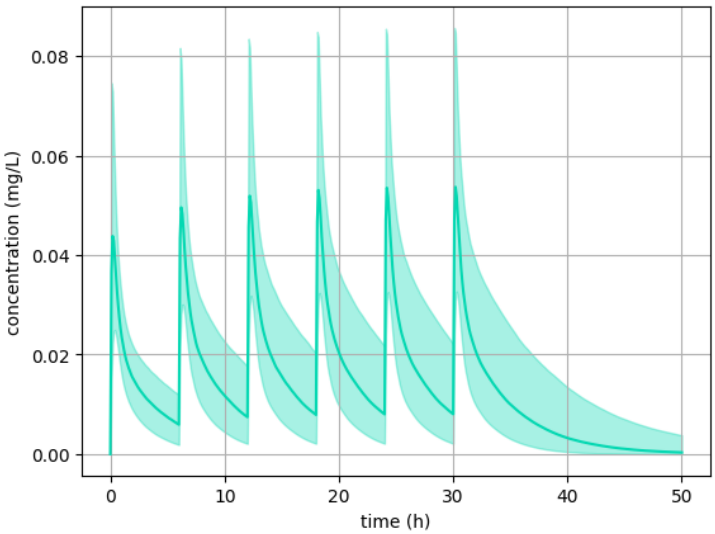

Figure 93. quantification of uncertainties for droperidol

4.13.5 Test Samples

Test sample level: 2/3

Test sample: efficacy, overexposure, and safety thresholds used for routine therapeutic drug monitoring (TDM) in clinical settings, or thresholds reflecting specific expected events (such as efficacy or toxicity) that may occur at these levels of exposure.

- Efficacy threshold was: 0.005 mg/L
- Overexposure threshold was: 0.05 mg/L
- Toxic threshold was: 0.225 mg/L

Test samples source(s): Schulz et al. [4], Foo etal. [28], Fischler et al. [29]

Comment: /

4.13.6 Tests conditions

Tests conditions level: 4/5

Tests condition: test conditions were defined with sufficient data to run simulations for each patient concerned by the drug, with complete coverage of dosage ranges, and of all sub-populations concerned by the drug.

Tests conditions source(s): summary of product characteristics of immediate release formulation [30]

Comment: /

Test conditions were:

Test 1:

- Dosage: 5 mg/6h
- Groups: Standard patients weighing 50 kg, 70 kg, 100 kg.

Test 2:
- Dosage: 5 mg/4h
- Groups: Standard patients weighing 50 kg, 70 kg, 100 kg.

Test 3:
- Dosage: 5 mg/6h
- Groups: Children patients weighing 35 kg, 25 kg.

Test 4:
- Dosage: 2.5 mg/6h
- Groups: Children patients weighing 35 kg, 25 kg.

Test 5:
- Dosage: 5mg once, 5mg 15 minutes later. (injection posology in case of clinical inefficiency)
- Groups: Standard patients weighing 70kg.

4.13.7 Equivalency of Input Parameters

Equivalency of input parameters level: 4/4
Equivalency of input parameters: The model's training dataset does cover all doses or PK is linear over the dose range used in the test conditions and sub-populations concerned by the medication, or an external validation is carried out and meets validation criteria. (i.e., MDPE ≤ ± 20%, MDAPE ≤ 30%)
Equivalency of input parameters source(s): summary of product characteristics of immediate release formulation [30]
Comment: Droperidol simulation outputs were tested with summary of products dosing regimen covering all indications.

4.13.8 Output Comparison

Output comparison level: 3/5
Output comparison: Correspondence of model outputs with the therapeutic thresholds used in routine clinical therapeutic drug monitoring or thresholds reflecting specific expected events (such as efficacy or toxicity) that may occur at these levels of exposure.
Output comparison source(s): Schulz et al. [4], Foo etal. [28], Fischler et al. [29]
Comment: All patients are within therapeutic – safety threshold, even if patients reach overexposure thresholds with standard posologies. Droperidol exists as intramuscular (IM) and intravenous (IV) formulation. Only IM formulation was implemented.

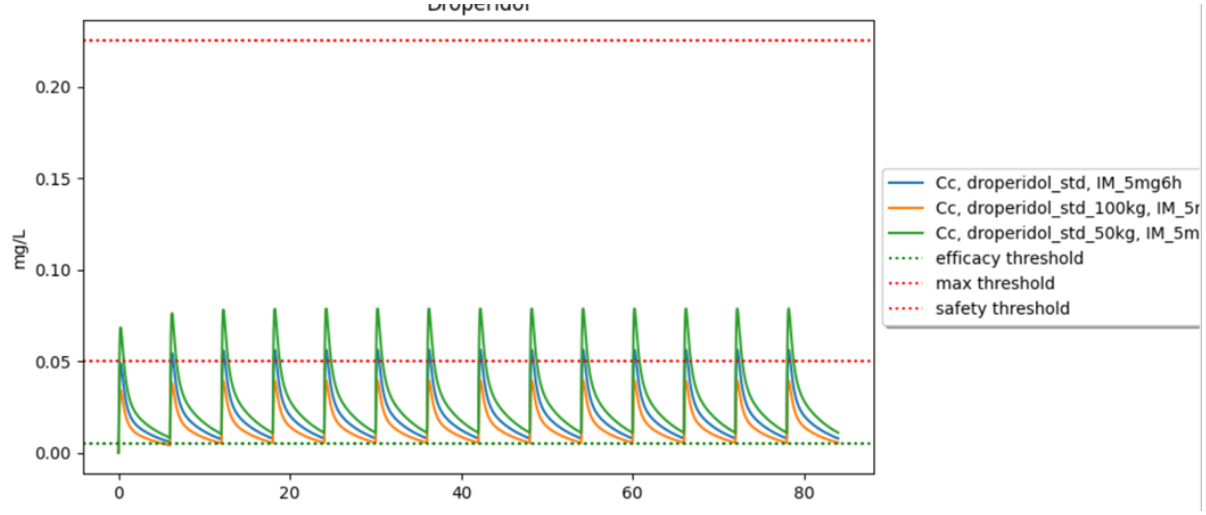

Figure 94. Test 1: 5 mg/6h for standard patients weighing 50 kg, 70 kg, 100 kg.

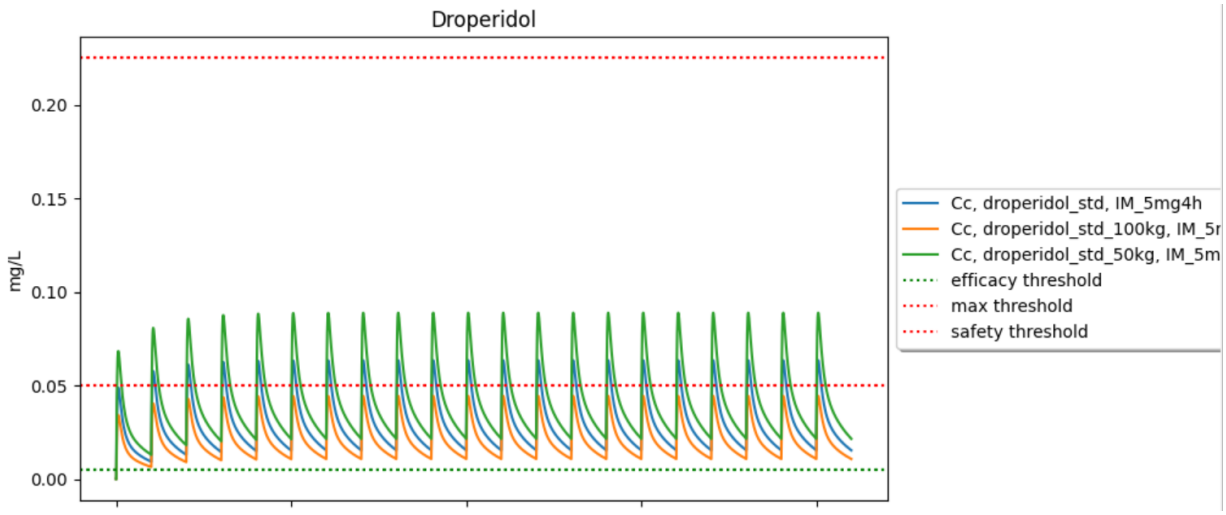

Figure 95. Test 2: 5 mg/4h for standard patients weighing 50 kg, 70 kg, 100 kg.

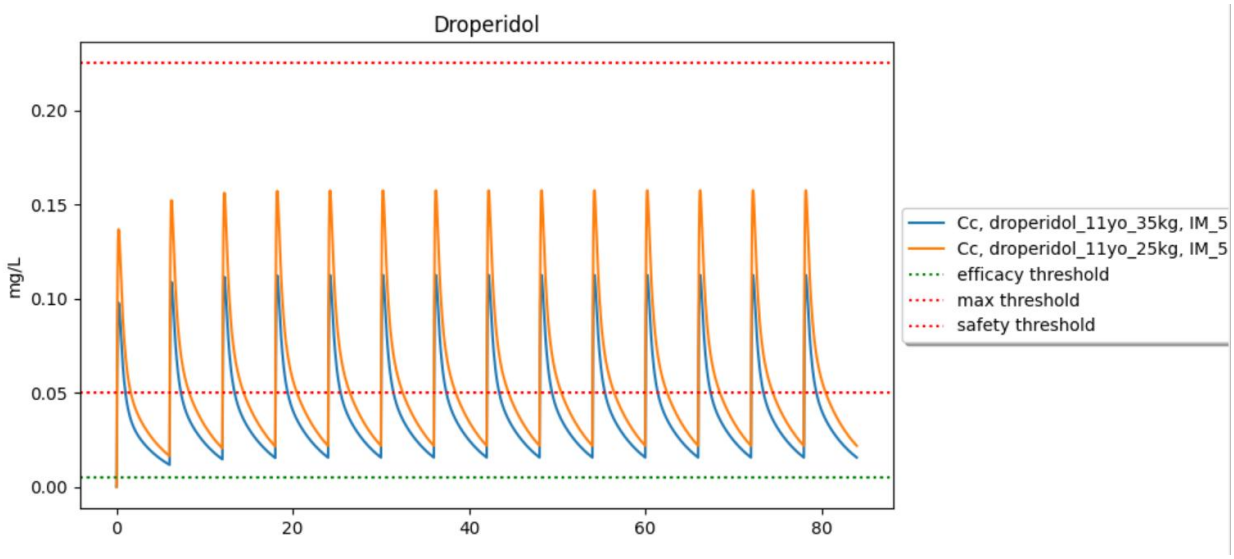

Figure 96. Test 3: 5 mg/6h for standard patients weighing 35 and 25kg.

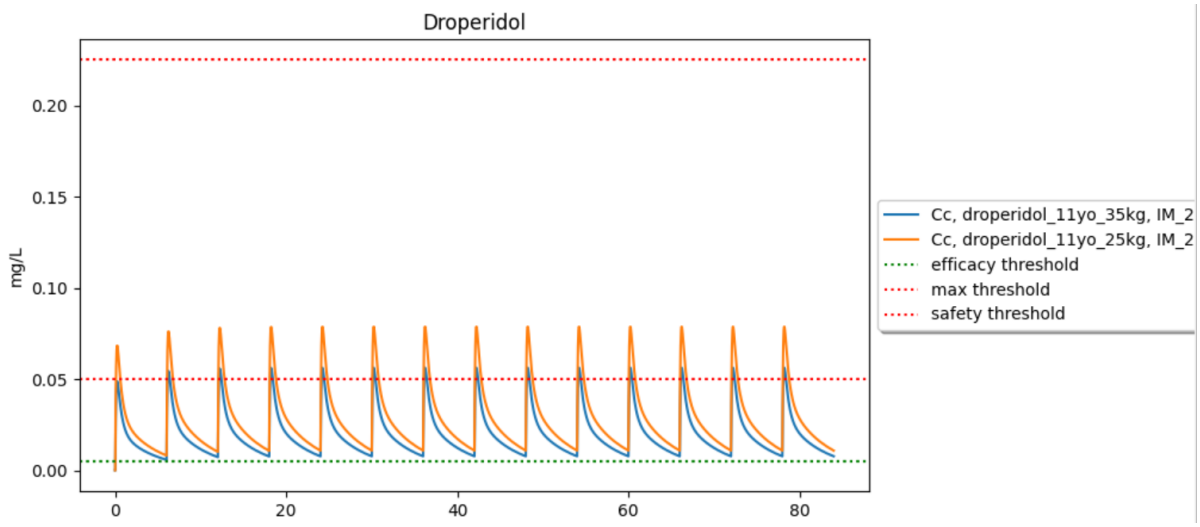

Figure 97. Test 4: 2.5 mg/6h for standard patients weighing 35 and 25kg.

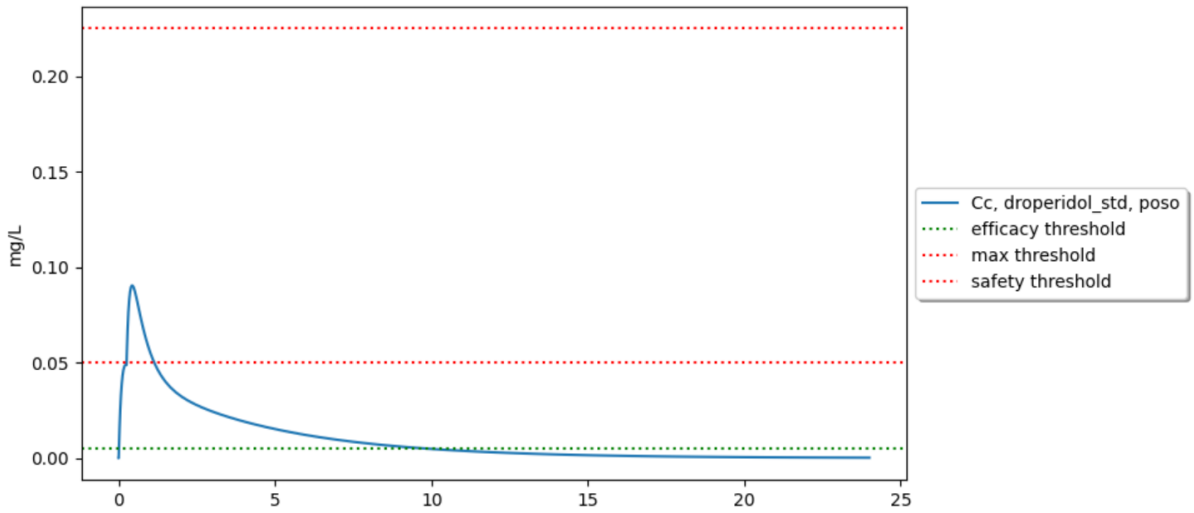

Figure 98. Test 5: 5 mg once then 5mg after 15 minutes for standard patients weighing 70 kg.

4.14 Flecainide (New)

Table *31*. Summary of flecainide validation.

Summary		
Levels	**Notations**	**Comments**
Model form level	2/5	One-compartment model built from NC data
Model inputs sources level	2/4	Parameters comes from NC data
Test samples level	2/3	Therapeutic thresholds
Tests conditions level	4/5	-
Equivalency of input parameters level	4/4	all doses and sub-populations concerned by the medication are covered by the simulations. PK is linear in the dose range.
Output comparison level	3/5	Model outputs were within therapeutic thresholds.

Conclusion: The model is validated since all criteria meet the minimum score required. Model inputs sources level can't be increased at the targeted depth level 3/4 as no popPK model was available in literature.

4.14.1 Model Form

Model form level: 2/5
Model form: Model built with NC data from regulators approved data (summary of product characteristics, regulatory agencies documents).
Model Source(s): summary of product characteristics for immediate release [31] and controlled release [32] formulations, Conard et al. [33] and Tennezé et al. [34]
Comment: The model parameters were calibrated with non-compartmental data from literature. The V, CL, kabs and F were calibrated from the sources and constitutes a one-compartment model. Absorption was calibrated for flecainide immediate release and controlled release formulations with different parameters. Then, two absorption rates (ka) were calibrated.

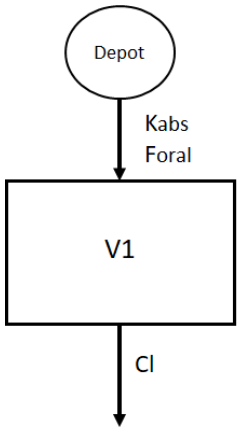

Figure 99. Model's structure, with one depot compartment, and one central compartment. Kabs, is the absorption rate, Foral the bioavailability V1 the volume of distribution, CL the clearance of elimination.

4.14.2 Model inputs sources

Model inputs sources level: 2/4
Model input: The parameters used are derived from NC data from regulatory agencies or obtained from analysis involving large numbers of patients or with low variability.
Model inputs source(s): summary of product characteristics for immediate release [31] and controlled release [32] formulations, Conard et al. [33] and Tennezé et al. [34]
Comment:
Parameters used as model inputs for calibration were:

- Immediate release bioavailability: 0.9
- Immediate release Tmax: 2.4 hours
- Controlled release Tmax: 23 hours (interval: 21 – 25 hours)
- Controlled release bioavailability: 0.72
- controlled release Tlag : 2.5 hours *(interval: 2 – 3 hours)*
- Apparent distribution volume : 8.3 L/kg
- Half-life of elimination : 14 hours

4.14.3 Quantification of sensitivities

Table 32. Analysis of the sensitivity of Cmax and AUC for flecainide by varying absorption rate constant (ka for immediate and controlled release formulations), bioavailability (F for immediate and controlled release formulations), volume of distribution (V), and clearance of elimination (CL).

Sensitivity analysis									
	ka IR			ka CR			F IR		
	-10%	ref	+10%	-10%	ref	+10%	-10%	ref	+10%
Cmax	0.1362	0.1376	0.1387	0.08509	0.08982	0.09418	0.1238	0.1376	0.1513
Expected behavior	Yes		Yes	Yes		Yes	Yes		Yes
AUC	3.129	3.129	3.129	5.006	5.006	5.006	2.816	3.129	3.442
Expected behavior	Yes		Yes	Yes		Yes	Yes		Yes
	F CR			V			CL		
	-10%	ref	-10%	ref	+10%	+10%	-10%	ref	+10%
Cmax	0.08084	0.08982	0.09881	0.1514	0.1376	0.1261	0.1388	0.1376	0.1364
Expected behavior	Yes		Yes	Yes		Yes	Yes		Yes
AUC	4.5054	5.006	5.5066	3.129	3.129	3.129	3.476	3.129	2.844
Expected behavior	Yes		Yes	Yes		Yes	Yes		Yes

Conclusion: The sensitivity analysis did not indicate any discrepancies in the expected behavior of the outputs studied, thereby confirming that there is no obstacle to the model's validation.

4.14.4 Quantification of uncertainties

Introduction

The model inputs were fixed parameters from NC literature, except for Tmax and Tlag of controlled release form which were respectively described by ranges of 21 - 25 hours and 2 to 3 hours. It has no great impact when propagating uncertainties.

Propagation in simulation results

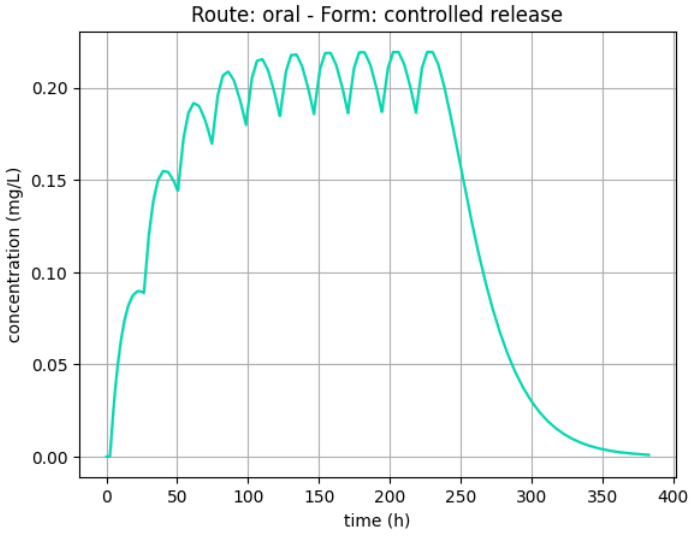

Figure 100. quantification of uncertainties for flecainide

4.14.5 Test Samples

Test sample level: 2/3
Test sample: Efficacy, overexposure, and safety thresholds used for routine therapeutic drug monitoring (TDM) in clinical settings, or thresholds reflecting specific expected events (such as efficacy or toxicity) that may occur at these levels of exposure.

- Efficacy threshold was: 0.14 mg/L
- Overexposure threshold was: 0.8 mg/L
- Safety threshold was: 1 mg/L

Test samples source(s): Schulz et al. [4] and Canadian "base de données sur les produits pharmaceutiques" [35]
Comment: /

Tests conditions
Tests conditions level: 4/5
Tests condition: Test conditions were defined with sufficient data to run simulations for each patient concerned by the drug, with complete coverage of dosage ranges, and of all sub-populations concerned by the drug.
Tests conditions source(s): summary of product characteristics for immediate release [31] and controlled release [32] formulations.
Comment: /
Test conditions were:
Test 1:

- Dosage: 50mg/12h, oral immediate release
- Groups: patient of 50, 70, 90, 100, 120 kg.

Test 2:

- Dosage: 100mg/12h, oral immediate release
- Groups: patient of 50, 70, 90, 100, 120 kg.

Test 3:

- Dosage: 150mg/12h, oral immediate release
- Groups: patient of 50, 70, 90, 100, 120 kg.

Test 4:

- Dosage: 100mg/24h, oral controlled release
- Groups: patient of 50, 70, 90, 100, 120 kg.

Test 5:

- Dosage: 200mg/24h, oral controlled release
- Groups: patient of 50, 70, 90, 100, 120 kg.

Test 6:

- Dosage: 300mg/24h, oral controlled release
- Groups: patient of 50, 70, 90, 100, 120 kg.

Test 7:

- Dosage: 1.5 mg/kg/24h intravenous (bolus), two times
- Groups: patient of 70kg

Test 8:

- Dosage: 0.003mg/kg/min, Intravenous (continuous perfusion)
- Groups: patient of 50kg

Test 9:

- Dosage: 5mg/kg/24h intravenous (bolus), two times
- Groups: patient of 70kg

4.14.6 Equivalency of Input Parameters

Equivalency of input parameters level: 4/4
Equivalency of input parameters: The model's training dataset does cover all doses or PK is linear over the dose range used in the test conditions and sub-populations concerned by the medication, or an external validation is carried out and meets validation criteria. (i.e., MDPE ≤ ± 20%, MDAPE ≤ 30%)
Equivalency of input parameters source(s): summary of product characteristics for immediate release [31] and controlled release [32] formulations.
Comment: Flecainide simulation outputs were tested with summary of products dosing regimen covering all indications.

4.14.7 Output Comparison

Output comparison level: 3/5
Output comparison: Correspondence of model outputs with the therapeutic thresholds used in routine clinical therapeutic drug monitoring or thresholds reflecting specific expected events (such as efficacy or toxicity) that may occur at these levels of exposure.
Output comparison source(s): Schulz et al. [4] and Canadian "base de données sur les produits pharmaceutiques" [35]
Comment: summary of product was used to extract dosing regimen data, and simulation outputs were compared to therapeutic thresholds.

The simulation results were consistent with the expected behaviour: patients with low body weight exhibit higher concentrations, reaching the efficacy threshold at lower doses compared to patients with higher body weight, while they surpass the safety threshold more quickly. Conversely, patients with higher body weight require higher doses to reach therapeutic concentrations.

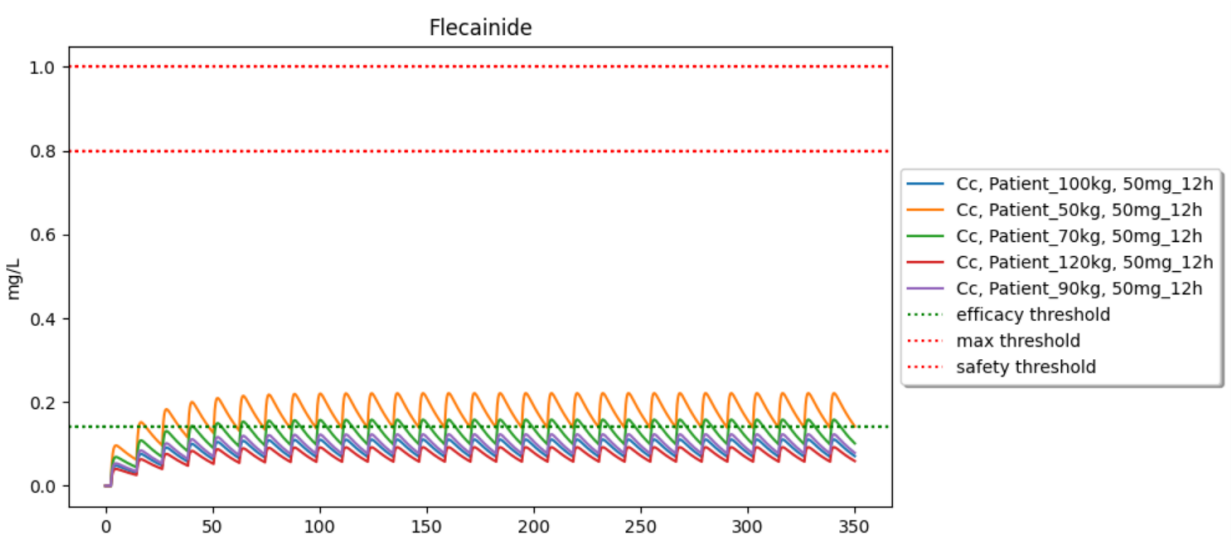

Figure 101. Test 1: 50mg/12h, oral immediate release patients of 50, 70, 90, 100, 120 kg.

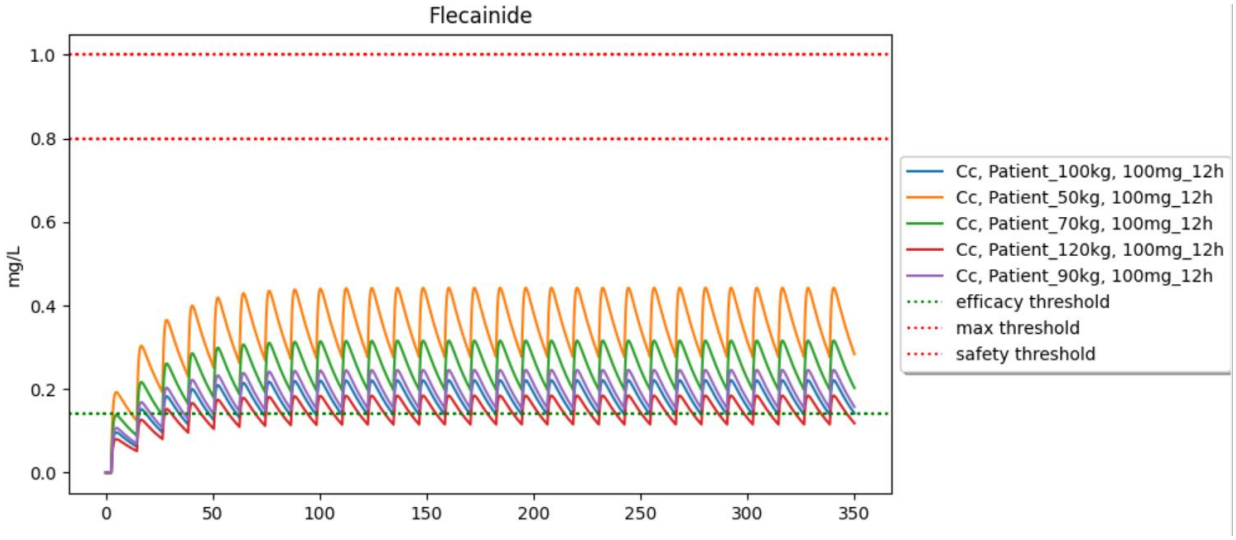

Figure 102. Test 2: 100mg/12h, oral immediate release patients of 50, 70, 90, 100, 120 kg.

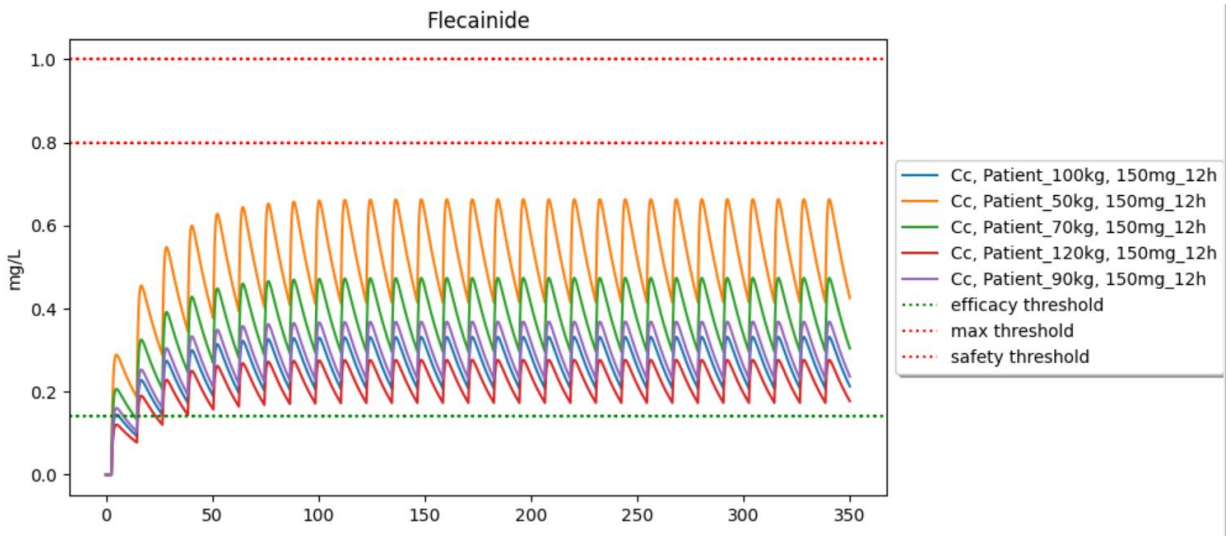

Figure 103. Test 3: 150mg/12h, oral immediate release patients of 50, 70, 90, 100, 120 kg.

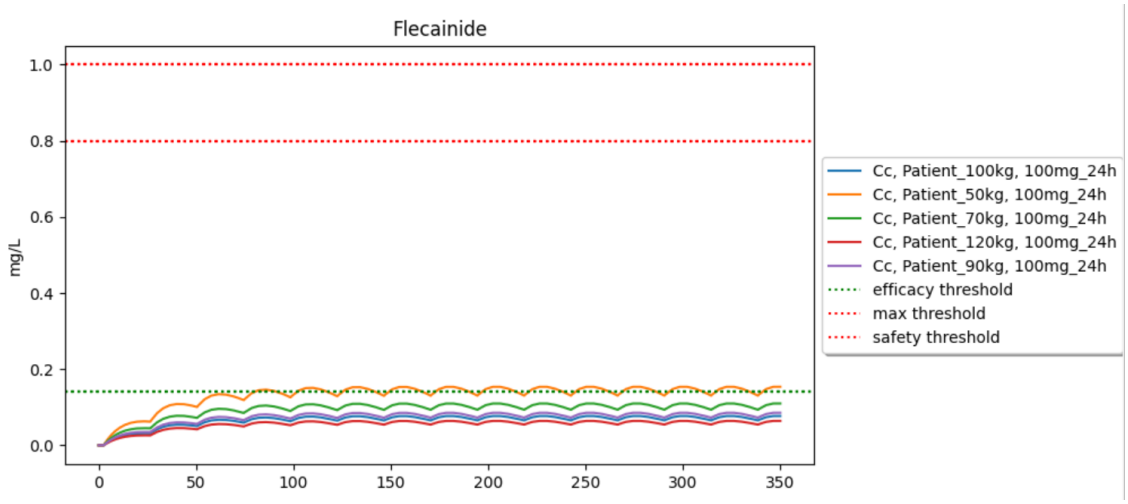

Figure 104. Test 4: 100mg/24h, oral controlled release patients of 50, 70, 90, 100, 120 kg.

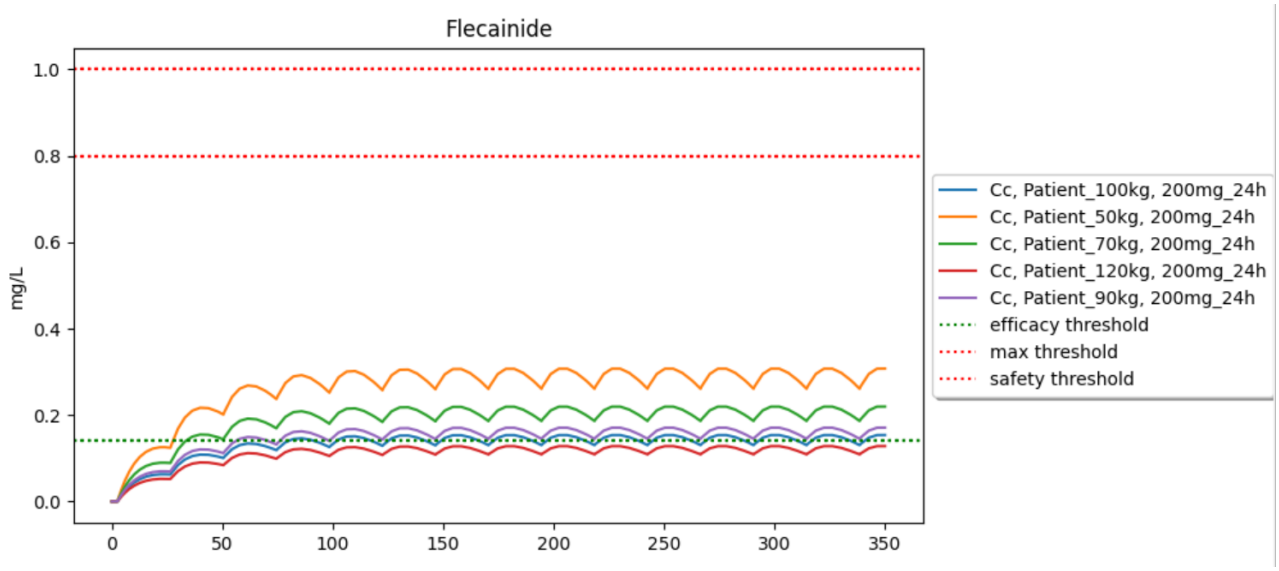

Figure 105. Test 5: 200mg/24h, oral immediate release patients of 50, 70, 90, 100, 120 kg.

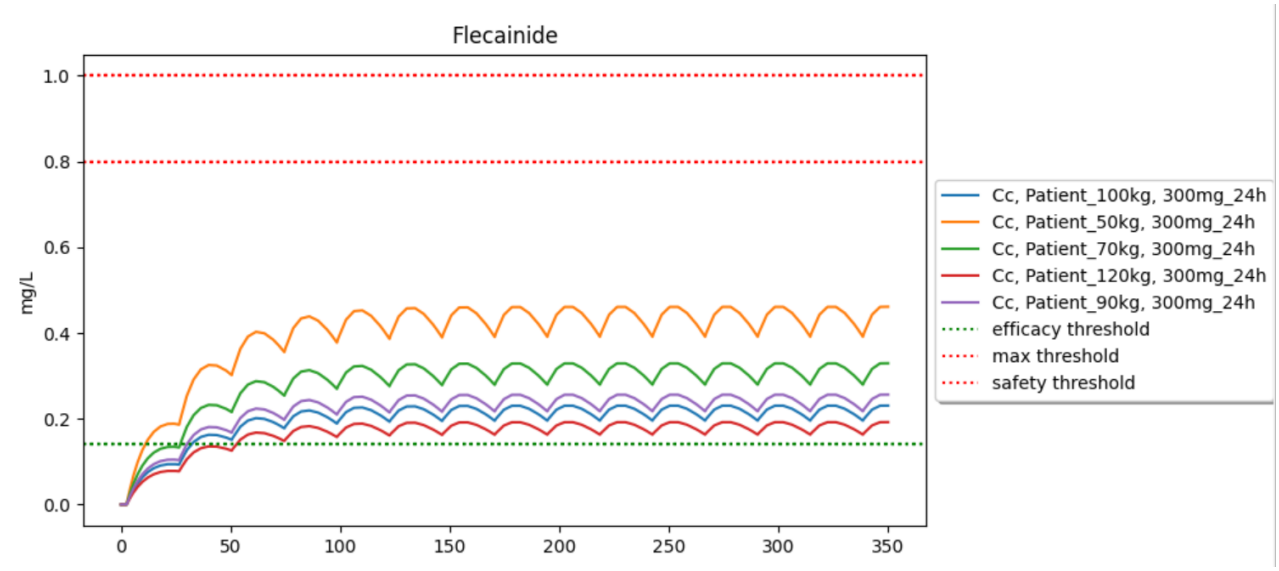

Figure 106. Test 6: 300mg/24h, oral immediate release patients of 50, 70, 90, 100, 120 kg.

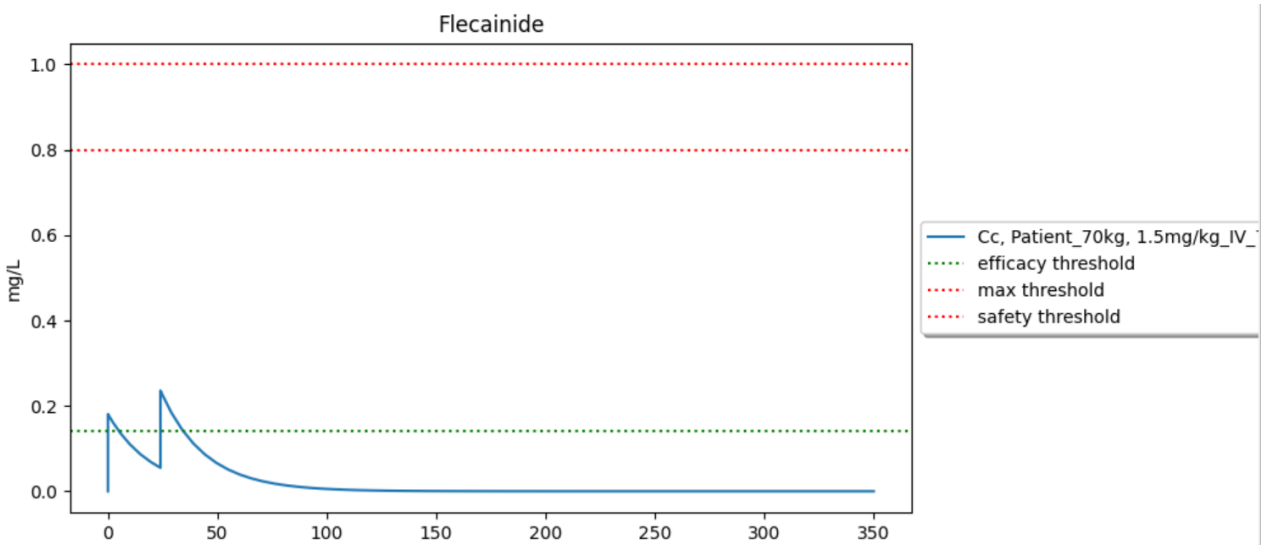

Figure 107. Test 7: 1.5 mg/kg/24h intravenous (bolus), two times for *patients of 70kg.*

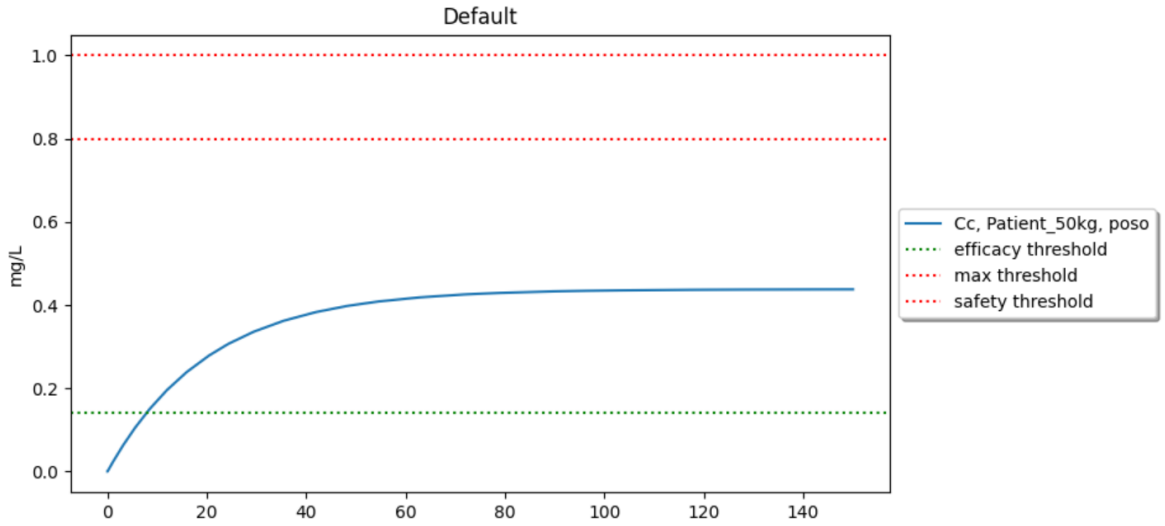

Figure 108. Test 8: 0.003mg/kg/min intravenous (continuous perfusion) patients *of 50 kg.*

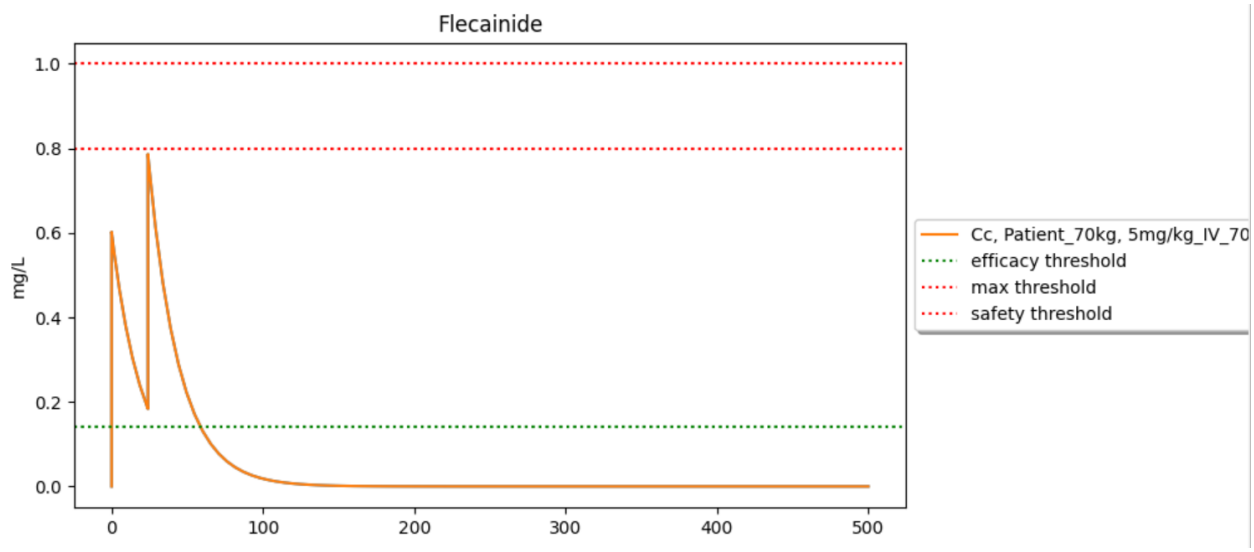

Figure 109. Test 9: 5mg/kg/24h intravenous (bolus), two times for *patients of 70kg.*

4.15 Metronidazole (New)

Table 33. Summary of metronidazole validation.

Summary		
Levels	**Notations**	**Comments**
Model form level	2/5	One-compartment model built from NC data
Model inputs sources level	2/4	Parameters comes from NC data
Test samples level	2/3	Therapeutic thresholds
Tests conditions level	4/5	-
Equivalency of input parameters level	4/4	all doses and sub-populations concerned by the medication are covered by the simulations. PK is linear in the dose range.
Output comparison level	3/5	Model outputs were within therapeutic thresholds.
Conclusion: The model is validated since all criteria meet the minimum score required. Model inputs sources level can't be increased at the targeted depth level 3/4 as no popPK model was available in literature.		

4.15.1 Model Form

Model form level: 2/5
Model form: Model built with NC data from regulators approved data (summary of product characteristics, regulatory agencies documents).
Model Source(s): summary of product characteristics for tablet [36] and oral solution [37] formulations, Turgut et al.[38], Freeman et al. [39]
Comment: The model parameters were calibrated with non-compartmental data from literature. The V, CL, kabs and F were calibrated from the sources and constitutes a one-compartment model. Absorption was calibrated for metronidazole suspension and tablet with different parameters from the same source. Then, two absorption rates (ka) were calibrated.

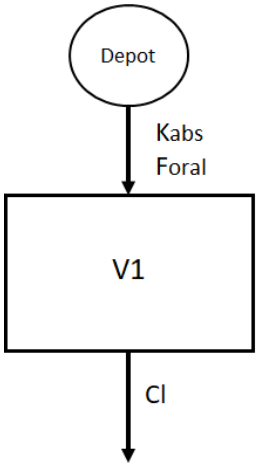

Figure 110. Model's structure, with one depot compartment, and one central compartment. Kabs, is the absorption rate, Foral the bioavailability V1 the volume of distribution, CL the clearance of elimination.

4.15.2 Model inputs sources

Model inputs sources level: 2/4
Model input: The parameters used are derived from NC data from regulatory agencies or obtained from analysis involving large numbers of patients or with low variability.
Model inputs source(s): summary of product characteristics for tablet [36] and oral solution [37] formulations, Turgut et al.[38], Freeman et al. [39]

Comment:
Parameters used as model inputs for calibration were:

- Tablet bioavailability: 1
- Tablet Tmax: 1 hours
- Oral solution Tmax: 4 hours
- Oral solution bioavailability: 0.7
- distribution volume : 0.65 L/kg
- Half-life of elimination : 9 hours (8 – 10 hours)

4.15.3 Quantification of sensitivities

Table 34. Analysis of the sensitivity of Cmax and AUC for metronidazole by varying absorption rate constant (ka tablet and solution), bioavailability (F tablet and solution), volume of distribution (V), and clearance of elimination (CL).

Sensitivity analysis									
	ka tablet			ka solution			F tablet		
	-10%	ref	+10%	-10%	ref	+10%	-10%	ref	+10%
Cmax	10.11	10.17	10.23	5.53	5.653	5.76	9.16	10.17	11.19
Expected behavior	Yes		Yes	Yes		Yes	Yes		Yes
AUC	142.7	142.7	142.7	99.88	99.88	99.88	128.4	142.7	157.0
Expected behavior	Yes		Yes	Yes		Yes	Yes		Yes
	V			CL			F solution		
	-10%	ref	-10%	ref	+10%	+10%	-10%	ref	+10%
Cmax	5.088	5.653	6.218	11.23	10.17	9.3	10.24	10.17	10.12
Expected behavior	Yes		Yes	Yes		Yes	Yes		Yes
AUC	89.89	99.88	109.87	142.7	142.7	142.7	158.5	142.7	129.7
Expected behavior	Yes		Yes	Yes		Yes	Yes		Yes

Conclusion: The sensitivity analysis did not indicate any discrepancies in the expected behavior of the outputs studied, thereby confirming that there is no obstacle to the model's validation.

4.15.4 Quantification of uncertainties

Introduction
The model inputs were parameters from NC literature with ranges used to propagate uncertainties. Uncertainties were propagated using ranges of values.
Propagation in simulation results

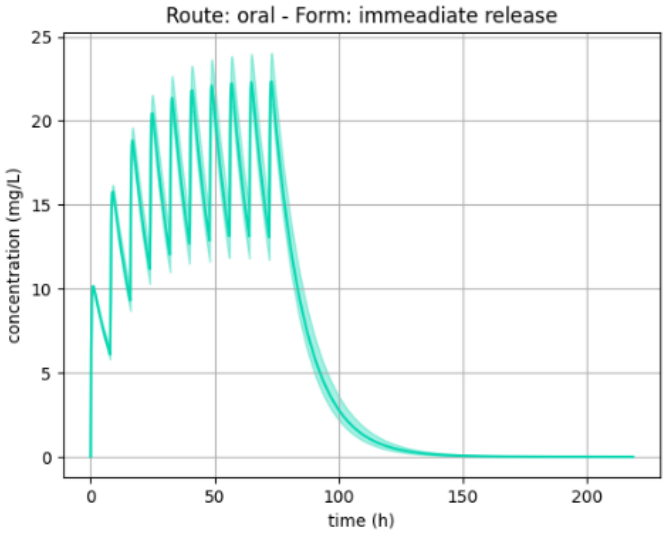

Figure 111. quantification of uncertainties for metronidazole

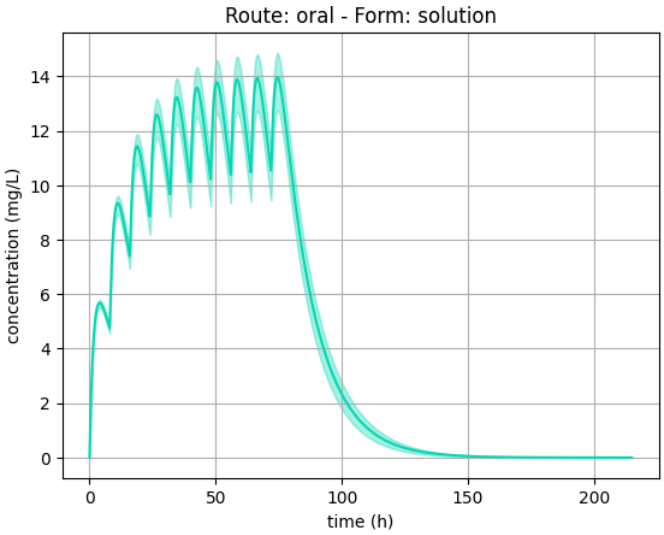

Figure 112. quantification of uncertainties for metronidazole

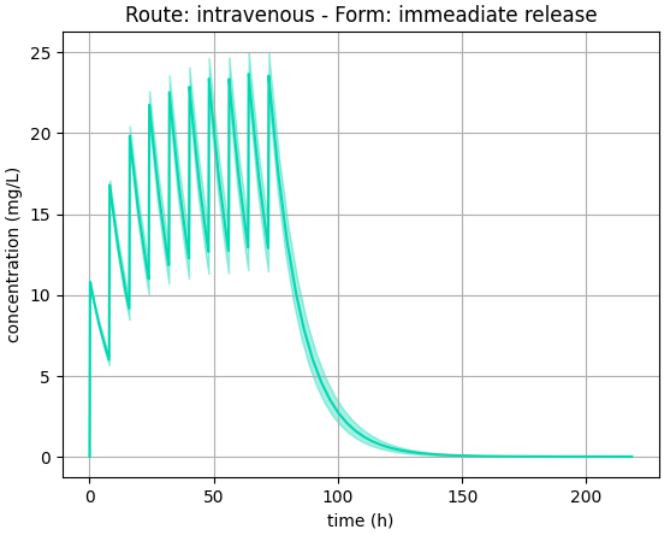

Figure 113. quantification of uncertainties for metronidazole

4.15.5 Test Samples

Test sample level: 2/3
Test sample: Efficacy, overexposure, and safety thresholds used for routine therapeutic drug monitoring (TDM) in clinical settings, or thresholds reflecting specific expected events (such as efficacy or toxicity) that may occur at these levels of exposure.

- Efficacy threshold was: 3 mg/L
- Overexposure threshold was: 30 mg/L

Test samples source(s): Schulz et al. [4]
Comment: /

4.15.6 Tests conditions

Tests conditions level: 4/5
Tests condition: Test conditions were defined with sufficient data to run simulations for each patient concerned by the drug, with complete coverage of dosage ranges, and of all sub-populations concerned by the drug.
Tests conditions source(s): summary of product characteristics for tablet [36] and oral solution [37] formulations.
Comment: /
Test conditions were:
Test 1:

- Dosage: 500mg/8h, oral tablet
- Groups: patient of 50, 70, 100 kg.

Test 2:

- Dosage: 500mg/8h, oral solution
- Groups: patient of 50, 70, 100 kg.

Test 3:

- Dosage: 750mg/24h, 1000mg/24h and 500mg/12h, oral tablet
- Groups: patient of 50, 70, 100 kg.

Test 4:

- Dosage: 750mg/24h, 1000mg/24h and 500mg/12h, oral solution
- Groups: patient of 50, 70, 100 kg.

Test 5:

- Dosage: 2000mg once, oral tablet
- Groups: patient of 50, 70, 100 kg.

Test 6:

- Dosage: 20,30,40 mg/kg/8h, oral solution
- Groups: Children of 15kg.

Test 7:

- Dosage: 250mg/24h oral solution
- Groups: Children of 8kg.

Test 8:

- Dosage : 375mg/24h, oral solution
- Groups: Children of 25kg.

Test 9:

- Dosage : 500mg/24h, oral solution

- Groups: Children of 40kg.

Test 10:

- Dosage: 500mg/8h intravenous.
- Groups: patient of 50, 70, 100 kg.

Test 11:

- Dosage: 750mg/24h, 1000mg/24h, 500mg/12h intravenous.
- Groups: patient of 50, 70, 100 kg.

Test 12:

- Dosage: 20, 30, 40mg/kg/8h intravenous.
- Groups: children of 15kg.

4.15.7 Equivalency of Input Parameters

Equivalency of input parameters level: 4/4
Equivalency of input parameters: The model's training dataset does cover all doses or PK is linear over the dose range used in the test conditions and sub-populations concerned by the medication, or an external validation is carried out and meets validation criteria. (i.e., MDPE ≤ ± 20%, MDAPE ≤ 30%)
Equivalency of input parameters source(s): summary of product characteristics for tablet [36] and oral solution [37] formulations.
Comment: Metronidazole simulation outputs were tested with summary of products dosing regimen covering all indications.

4.15.8 Output Comparison

Output comparison level: 3/5
Output comparison: Correspondence of model outputs with the therapeutic thresholds used in routine clinical therapeutic drug monitoring or thresholds reflecting specific expected events (such as efficacy or toxicity) that may occur at these levels of exposure.
Output comparison source(s): Schulz et al. [4]
Comment: summary of product was used to extract dosing regimen data, and simulation outputs were compared to therapeutic thresholds.
The simulation results were consistent with the expected behaviour: patients with low body weight exhibit higher concentrations, sometimes reaching the overexposure threshold (which is not a synonym of toxicity). For metronidazole, different dosing regimen are available and should be adapted to the patient's weight. According to our simulation, children with a very low weight (8kg) should not receive tablet: the total exposure is increased compared to oral solution. Also, 50kg patients shouldn't receive the maximal dose with tablet formulation (1000mg/24h). These simulations are concordant with the weight-adaptation dose strategy for metronidazole.

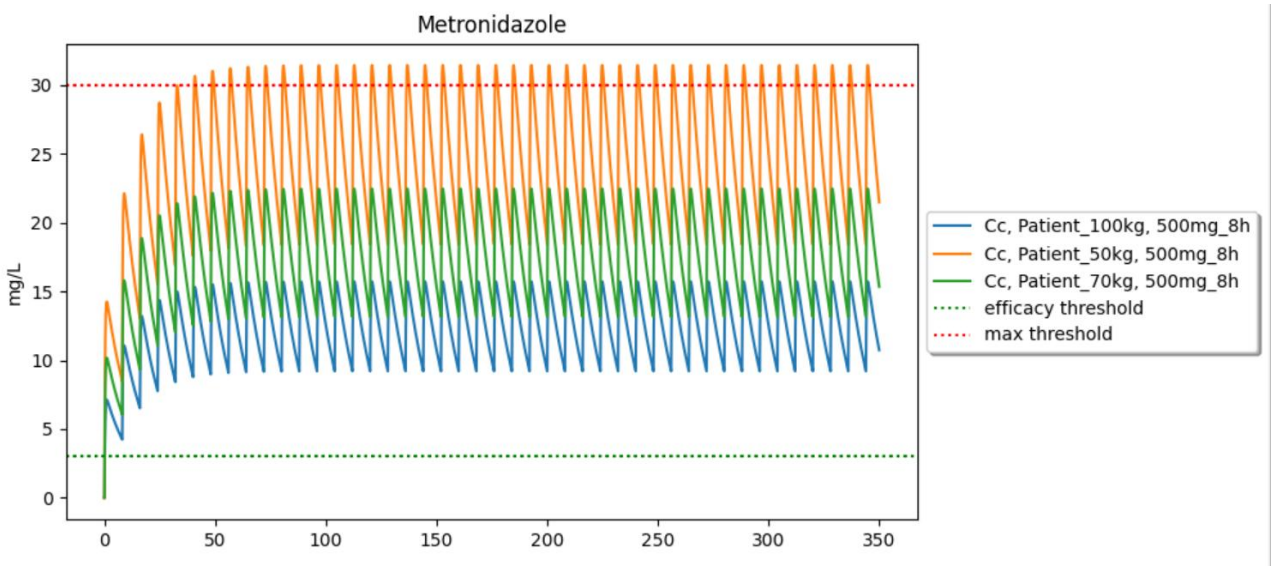

Figure 114. Test 1: 500mg/8h, oral tablet for patients of 50, 70, 100kg

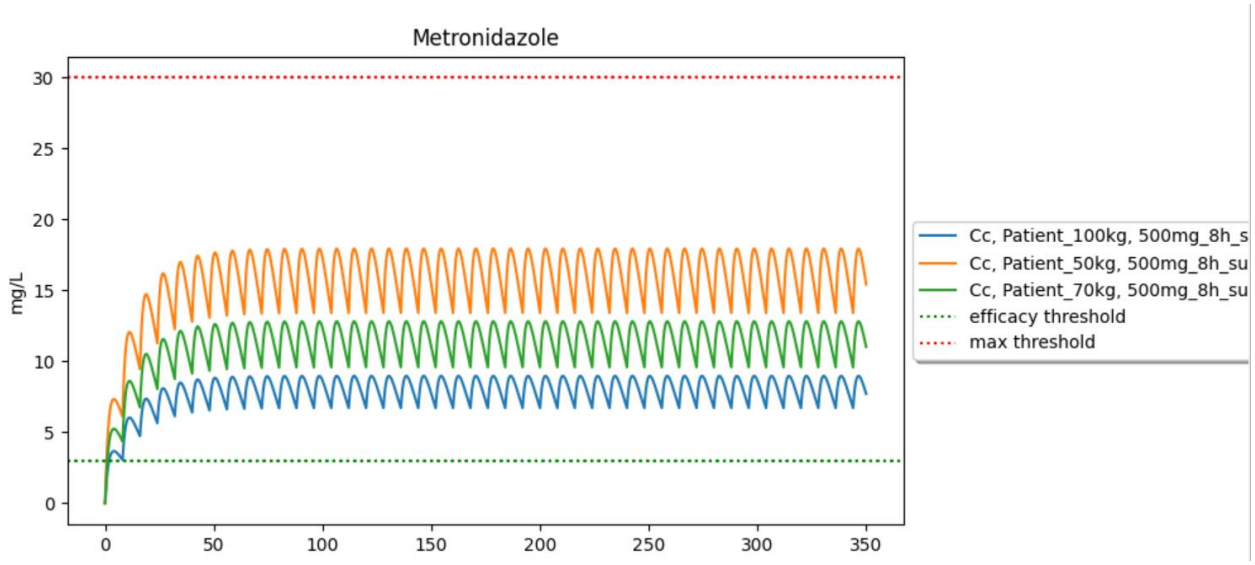

Figure 115. Test 2: 500mg/8h, oral solution for patients of 50, 70, 100kg

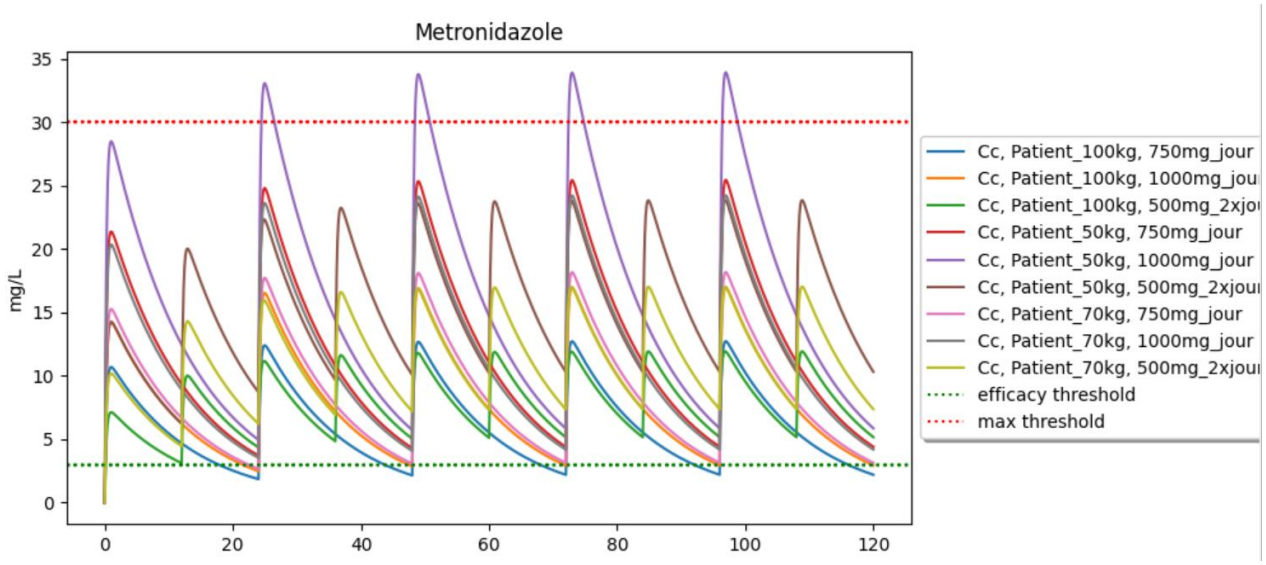

Figure 116. Test 3: 750mg/24h, 1000mg/24h and 500mg/12h, oral tablet for patients of 50, 70, 100kg

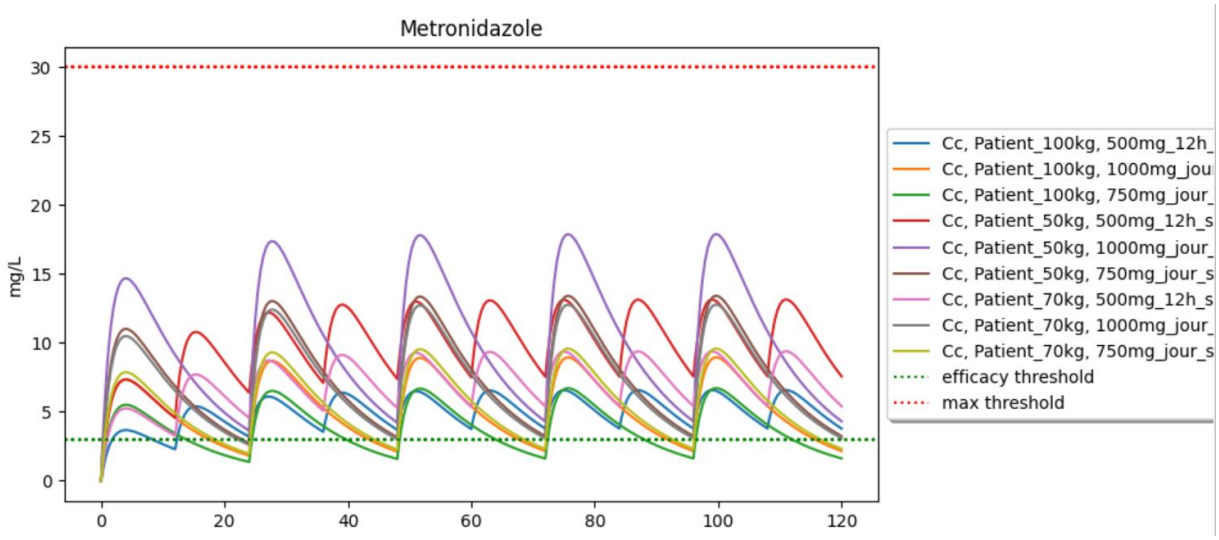

Figure 117. Test 4: 750mg/24h, 1000mg/24h and 500mg/12h, oral solution for patients of 50, 70, 100kg

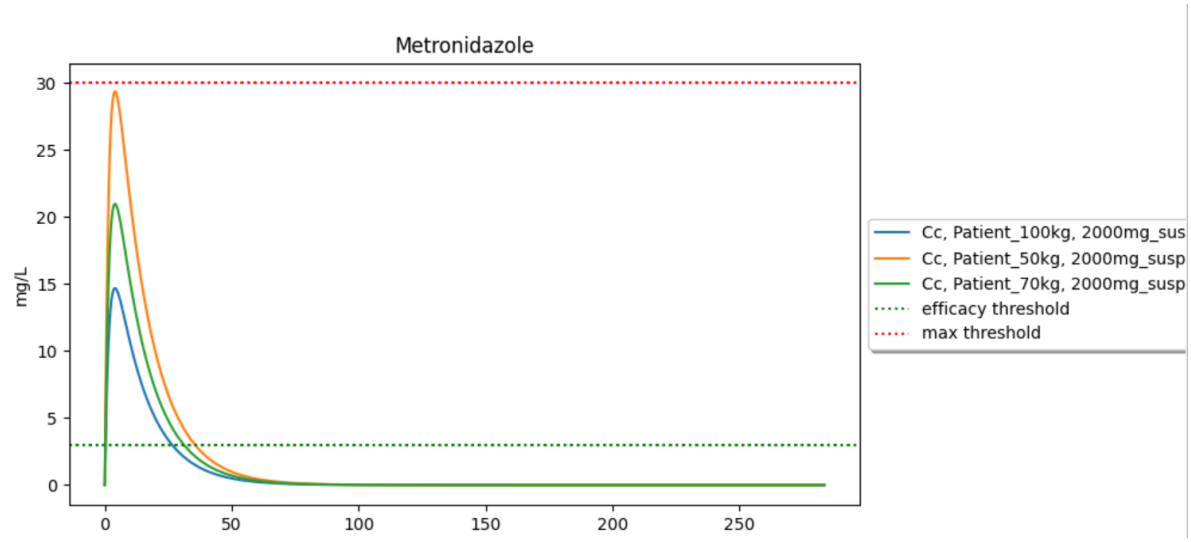

Figure 118. Test 5: 2000mg, oral tablet for patients of 50, 70, 100kg

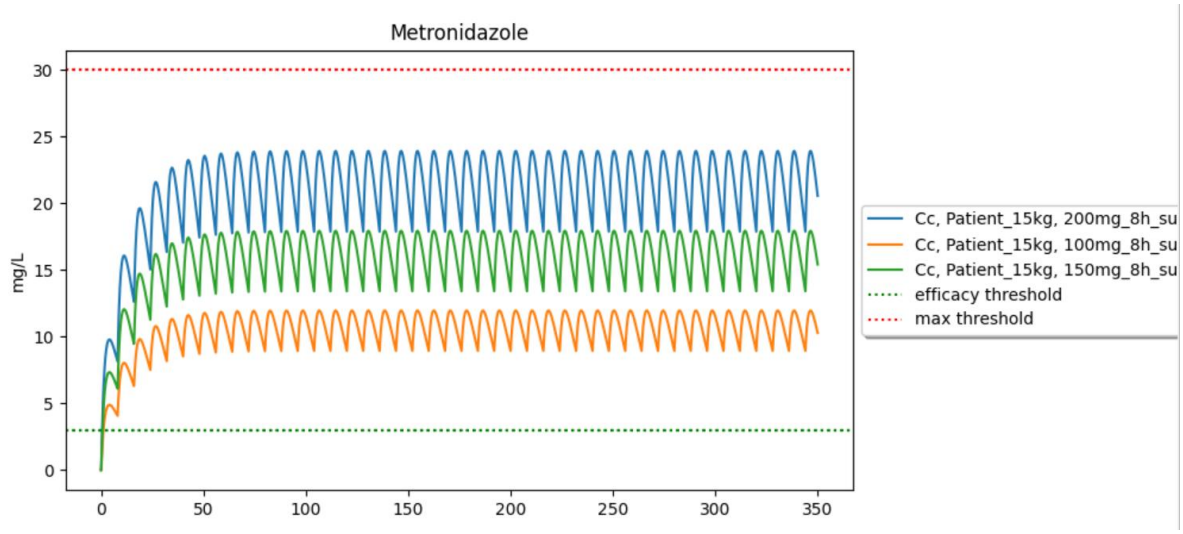

Figure 119. Test 6: 20,30,40 mg/kg/8h, oral solution for children of 15kg

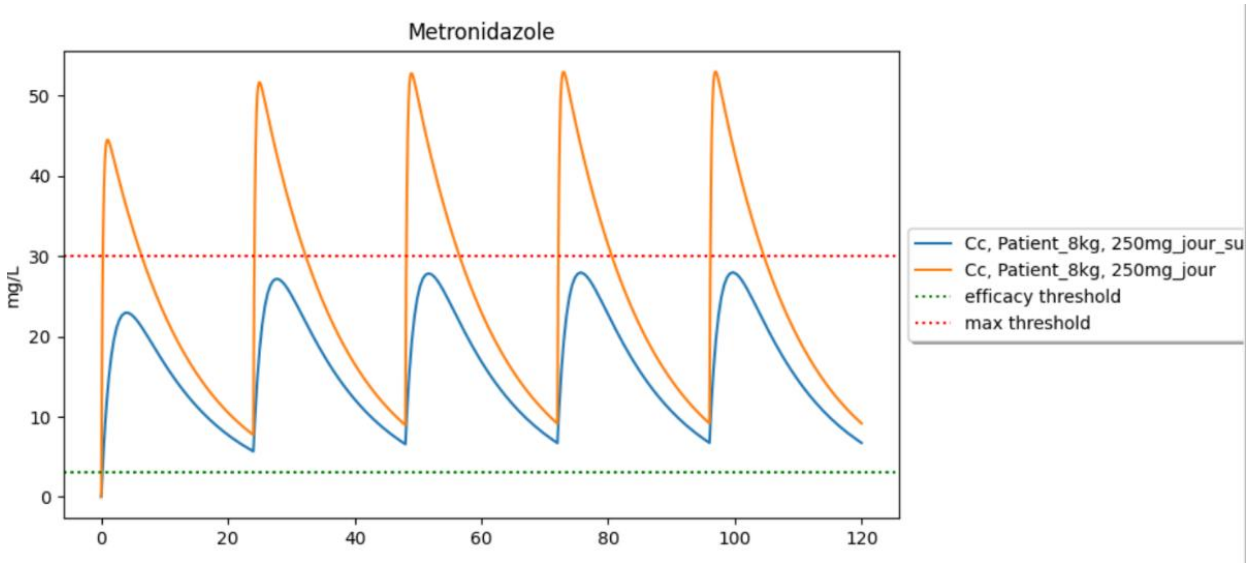

Figure 120. Test 7: 250mg/24h oral solution and tablet for children of 8kg

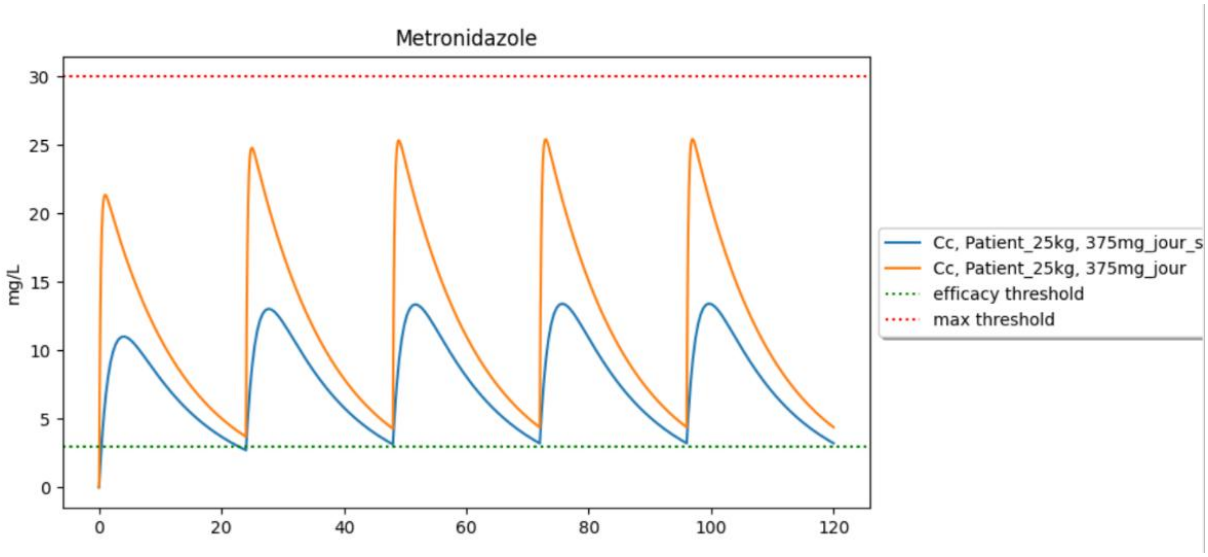

Figure 121. Test 8: 375mg/24h oral solution and tablet for children of 25kg

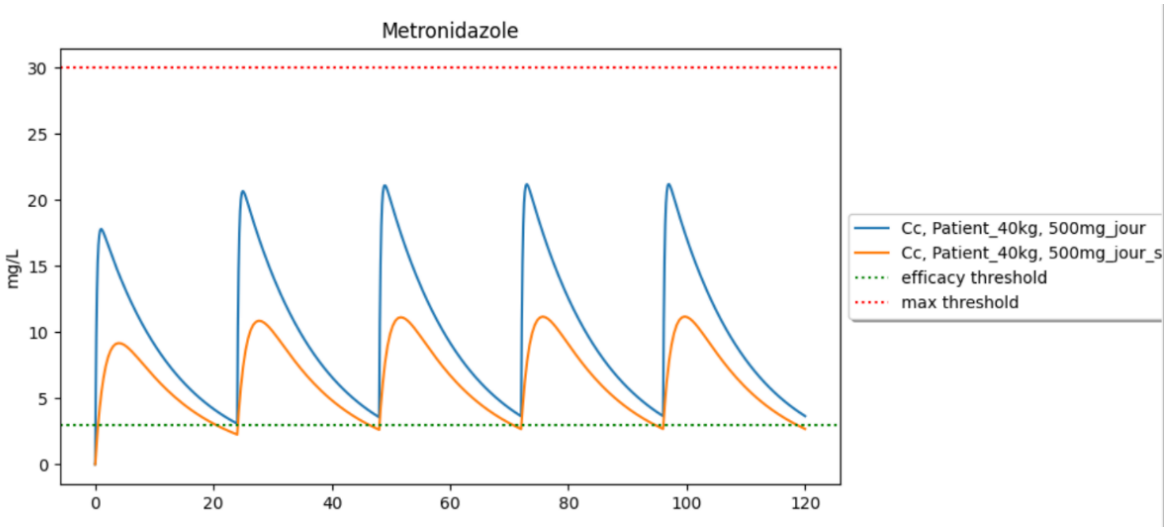

Figure 122. Test 9: 500mg/24h oral solution and tablet *for children of 40kg*

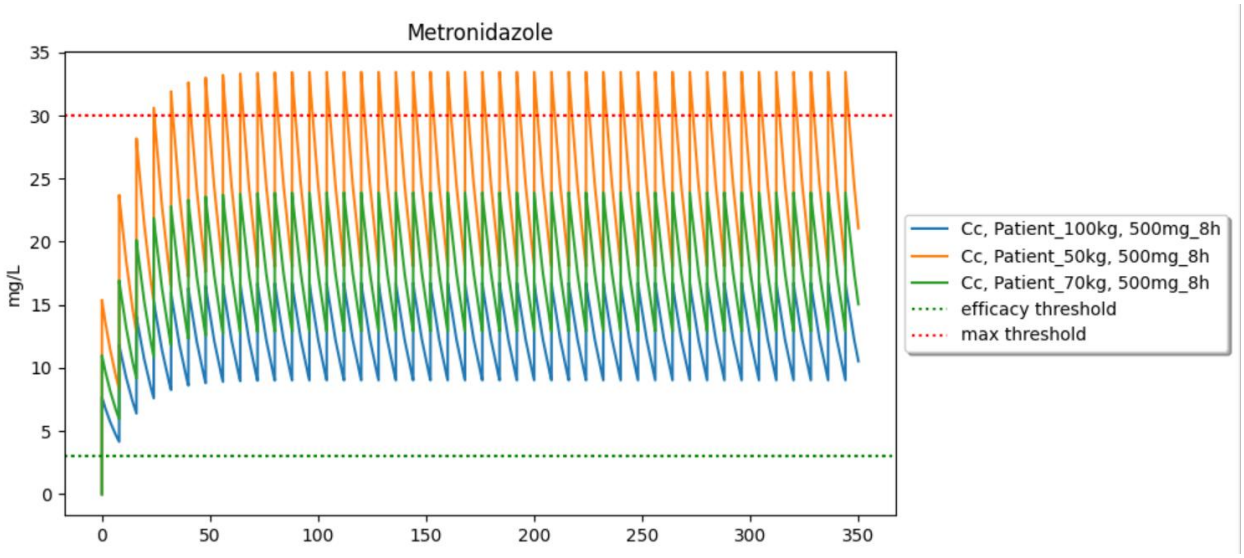

Figure 123. Test 10: 500mg/8h, intravenous for patients of 50, 70, 100kg

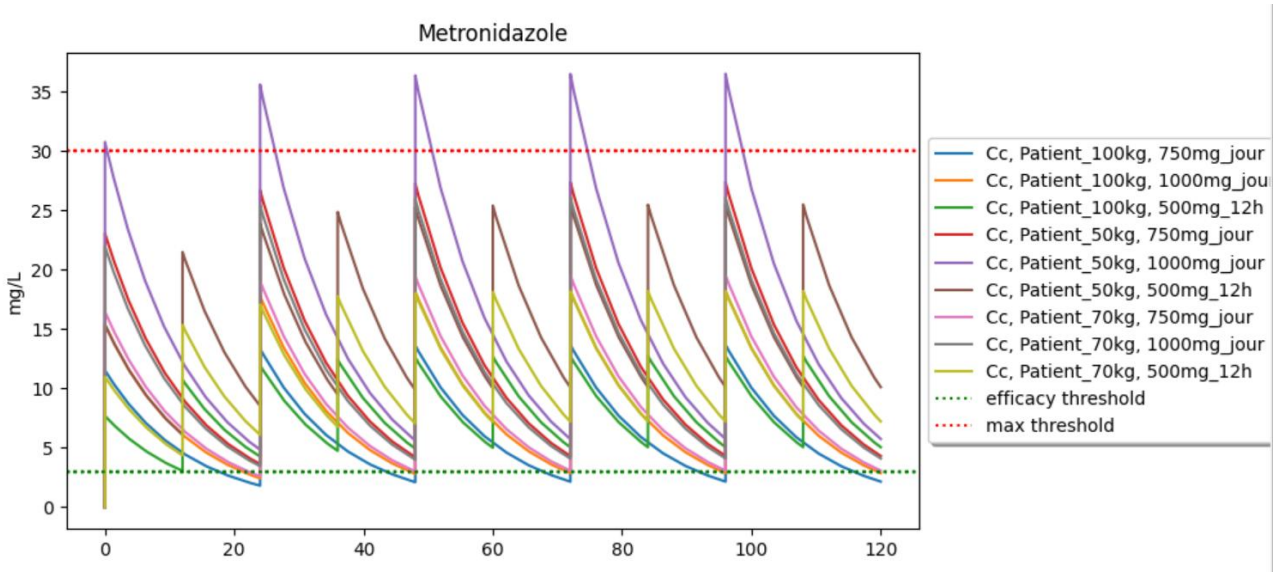

Figure 124. Test 11: 500mg/12h, 750mg/24h, 1000mg/24h intravenous for patients of 50, 70, 100kg

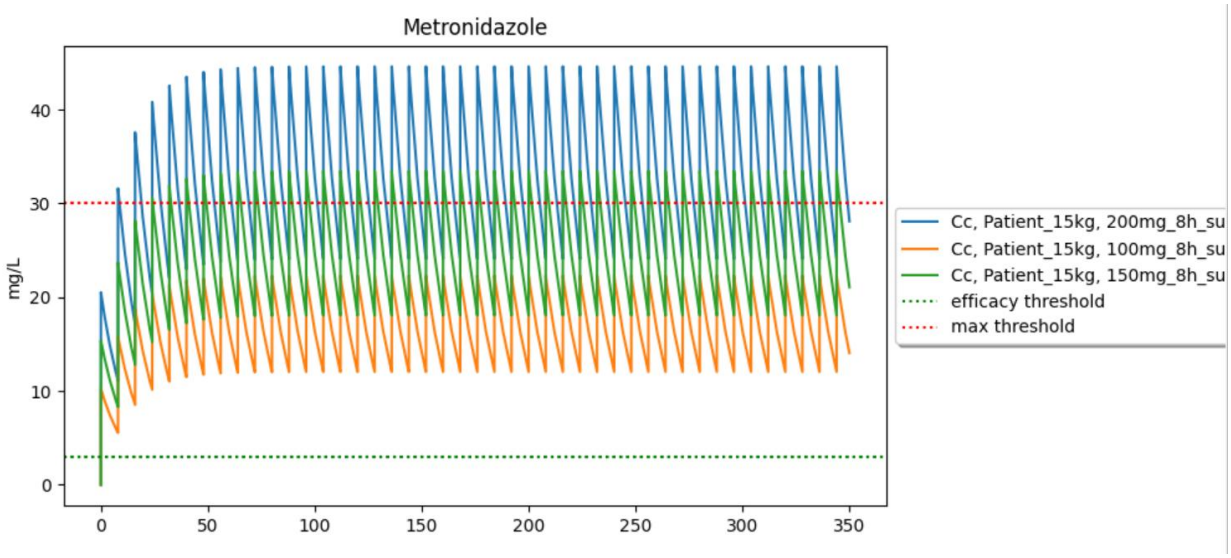

Figure 125. Test 12: 20,30,40 mg/kg/8h, intravenous for children of 15kg

4.16 Mexiletine (New)

Table 35. Summary of mexiletine validation.

Summary		
Levels	**Notations**	**Comments**
Model form level	3/5	Model built from popPK analysis
Model inputs sources level	3/4	RSE% on parameters are >30%
Test samples level	2/3	Therapeutic thresholds
Tests conditions level	4/5	-
Equivalency of input parameters level	4/4	all doses and sub-populations concerned by the medication are covered by the simulations. PK is linear in the dose range.
Output comparison level	3/5	Model outputs were within therapeutic thresholds.
Conclusion: The model is validated since all applicable criteria meet the minimum score required.		

4.16.1 Model Form

Model form level: 3/5
Model form: Model built from popPK analysis.
Model Source(s): Vozeh et al. [40]

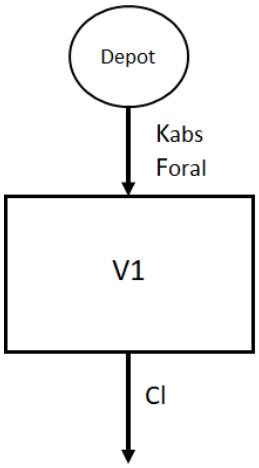

Figure 126. Model's structure, with one depot compartment, and one central compartment. Kabs, is the absorption rate, Foral the bioavailability V1 the volume of distribution, CL the clearance of elimination.

Comment: The implemented PK model is based on a popPK analysis conducted by Vozeh et al. [40]. It is a one-compartment model with first order absorption and elimination.

4.16.2 Model inputs sources

Model inputs sources level: 3/4
Model input: Parameters are obtained from popPK analysis with a relative standard error (RSE) > 30% or taken from the summary of product characteristics or from analysis conducted on many patients with little variability.
Model inputs source(s): Vozeh et al. [40]
Comment:

Parameter	Population mean		Interindividual variability	
	Estimate	SE	Estimate [σ_η][a]	SE[b]
Cl [l/h/kg]	0.38	0.017	42%	11%
Vd [l/kg]	5.3	0.23	40%	16%
ka [h^{-1}]	3.1	0.54	205%	9%
to [h]	0.3	0.03	–	–
σ_ε[c]	23%[a]	9%[b]		

Figure 127. Parameters value from Vozeh et al. [40].. Picture from Vozeh et al. [40]

4.16.3 Quantification of sensitivities

Table 36. Analysis of the sensitivity of Cmax and AUC for Mexiletine by varying absorption rate constant (ka), bioavailability (F), volume of distribution (V), and clearance of elimination (CL).

Sensitivity analysis												
	ka			F			V			CL		
	-10%	ref	+10%	-10%	ref	+10%	-10%	ref	+10%	-10%	ref	+10%
Cmax	0.5003	0.5038	0.5067	0.4534	0.5038	0.5541	0.535	0.5038	0.4787	0.5291	0.5038	0.4835
Expected behavior	Yes		Yes	Yes		Yes	Yes		Yes	Yes		Yes
AUC	37.65	37.65	37.65	33.88	37.65	41.41	37.65	37.65	37.65	41.83	37.65	34.22
Expected behavior	Yes		Yes	Yes		Yes	Yes		Yes	Yes		Yes

Conclusion: The sensitivity analysis did not indicate any discrepancies in the expected behavior of the outputs studied, thereby confirming that there is no obstacle to the model's validation.

4.16.4 Quantification of uncertainties

Introduction

The model has been built with popPK data : uncertainties were quantified as interindividual variability (IIV) and residual variability (RV).

Propagation in simulation results

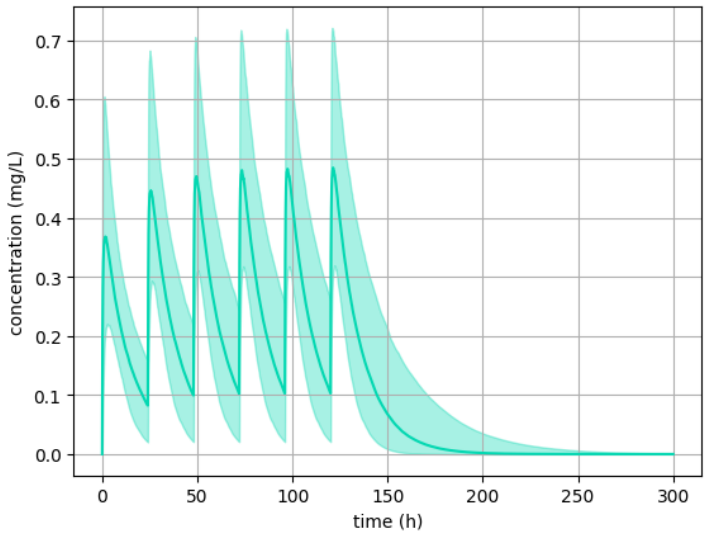

Figure 128. quantification of uncertainties for mexiletine

4.16.5 Test Samples

Test sample level: 2/3

Test sample: Efficacy, overexposure, and safety thresholds used for routine therapeutic drug monitoring (TDM) in clinical settings, or thresholds reflecting specific expected events (such as efficacy or toxicity) that may occur at these levels of exposure.

- Efficacy threshold was: 0.12 mg/L
- Toxic threshold was: 2 mg/L

Test samples source(s): Schulz et al. [4], summary of product characteristics of [41]

Comment: Schulz was used to define safety threshold, summary of product characteristics for efficacy threshold.

4.16.6 Tests conditions

Tests conditions level: 4/5

Tests condition: Test conditions were defined with sufficient data to run simulations for each patient concerned by the drug, with complete coverage of dosage ranges, and of all sub-populations concerned by the drug.

Tests conditions source(s): summary of product characteristics of [41]

Comment: /

Test conditions were:

Test 1:

- Dosage: 166 mg/24h
- Groups: Standard patients weighing 50 kg, 70 kg, 100 kg.

Test 2:

- Dosage: 166 mg/12h

- Groups: Standard patients weighing 50 kg, 70 kg, 100 kg.

Test 3:

- Dosage: 166 mg/8h
- Groups: Standard patients weighing 50 kg, 70 kg, 100 kg.

4.16.7 Equivalency of Input Parameters

Equivalency of input parameters level: 4/4
Equivalency of input parameters: The model's training dataset does cover all doses or PK is linear over the dose range used in the test conditions and sub-populations concerned by the medication, or an external validation is carried out and meets validation criteria. (i.e., MDPE ≤ ± 20%, MDAPE ≤ 30%)
Equivalency of input parameters source(s): summary of product characteristics of [41]
Comment: Mexiletine simulation outputs were tested with summary of products dosing regimen covering all indications.

4.16.8 Output Comparison

Output comparison level: 3/5
Output comparison: Correspondence of model outputs with the therapeutic thresholds used in routine clinical therapeutic drug monitoring or thresholds reflecting specific expected events (such as efficacy or toxicity) that may occur at these levels of exposure.
Output comparison source(s): Schulz et al. [4], summary of product characteristics of [41]
Comment: All patients are within therapeutic – safety threshold, even if patients reach overexposure thresholds with standard posologies.

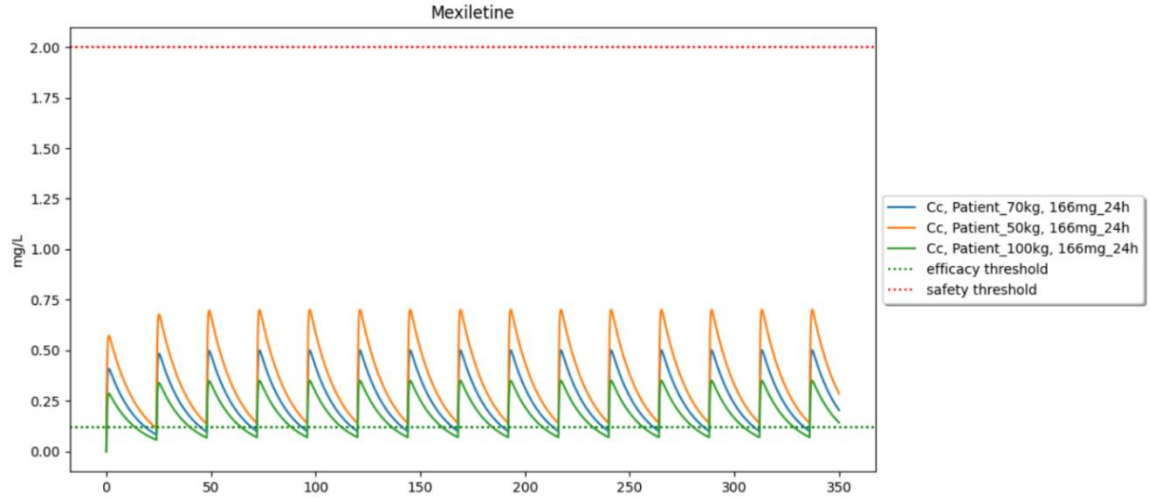

Figure 129. Test 1: 166mg/12h for standard patients weighing 50 kg, 70 kg, 100 kg.

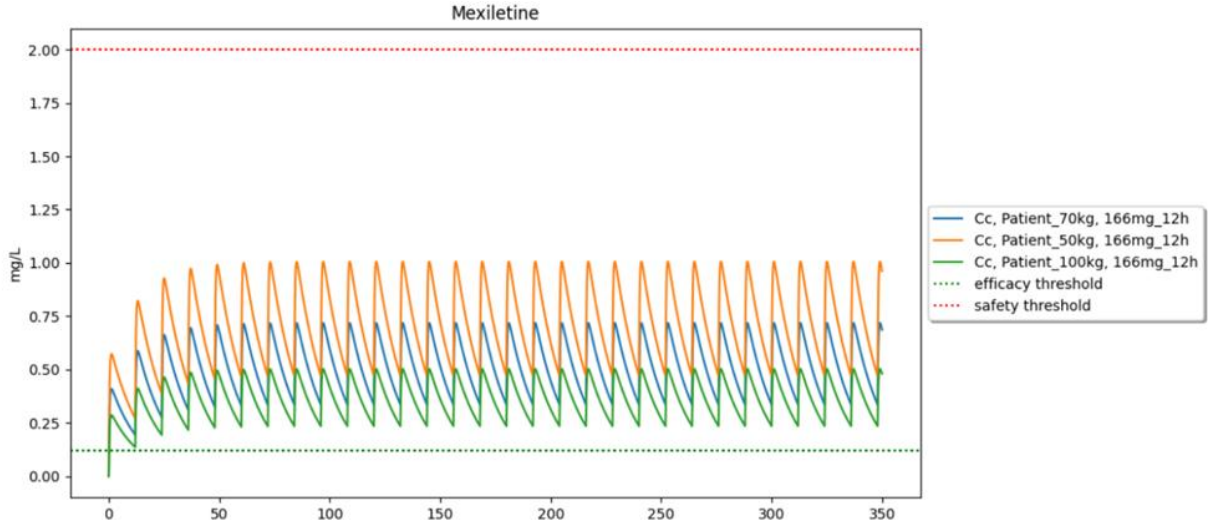

Figure 130. Test 1: 166mg/8h for standard patients weighing 50 kg, 70 kg, 100 kg.

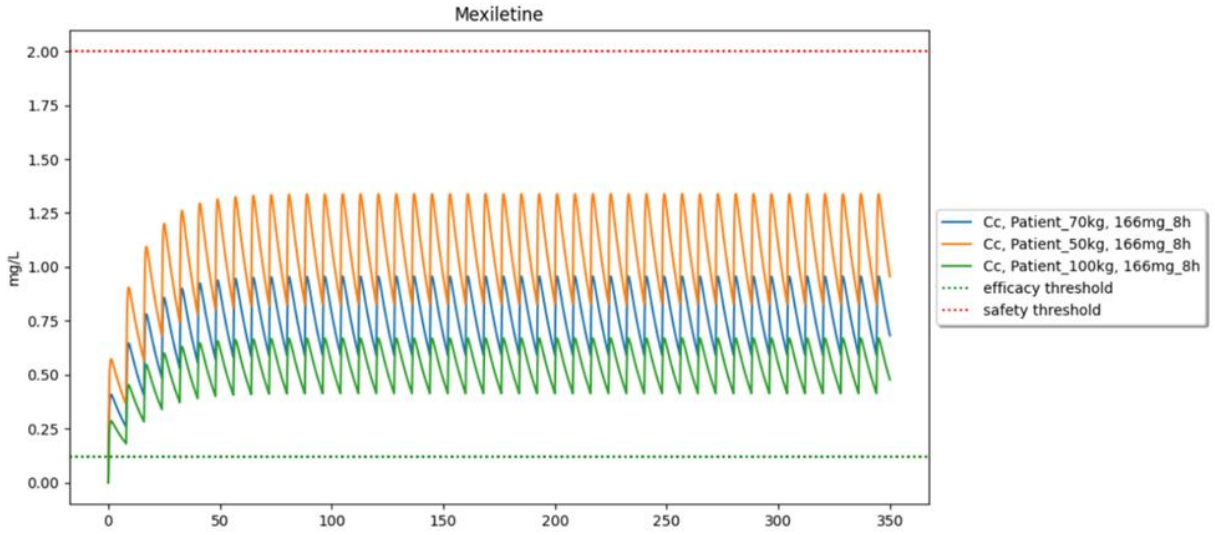

Figure 131. Test 1: 166mg/24h for standard patients weighing 50 kg, 70 kg, 100 kg.

4.17 Nicorandil (New)

Table 37. Summary of nicorandil validation.

Summary		
Levels	**Notations**	**Comments**
Model form level	3/5	Model built from popPK analysis
Model inputs sources level	3/4	RSE% on parameters are >30%
Test samples level	2/3	Therapeutic thresholds
Tests conditions level	4/5	-
Equivalency of input parameters level	4/4	all doses and sub-populations concerned by the medication are covered by the simulations. PK is linear in the dose range.
Output comparison level	3/5	Model outputs were within therapeutic thresholds.
Conclusion: The model is validated since all applicable criteria meet the minimum score required.		

4.17.1 Model Form

Model form level: 3/5
Model form: Model built from popPK analysis.
Model Source(s): Lida et al. [42]
Comment: The implemented PK model is based on a popPK analysis conducted by Lida et al. [42]. It is a one-compartment model with first order absorption and elimination.

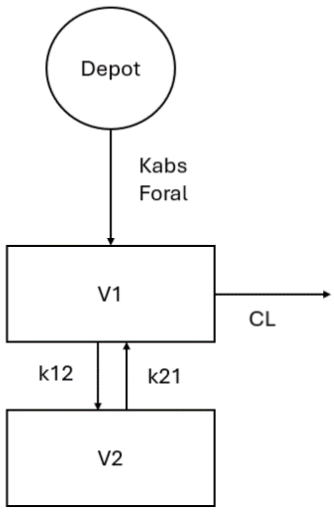

Figure 132. Model's structure, with one depot compartment, and one central compartment. Kabs, is the absorption rate, Foral the bioavailability V1 the volume of central compartment, V2 the volume of peripheral compartment and CL the clearance of elimination. K21 et K12 are transfer compartment between central and peripheral compartment.

4.17.2 Model inputs sources

Model inputs sources level: 3/4
Model input: Parameters are obtained from popPK analysis with a relative standard error (RSE) > 30% or taken from the summary of product characteristics or from analysis conducted on many patients with little variability.
Model inputs source(s): Lida et al. [42]
Comment:

Statistic	Description	Median	Units	CV %	Confidence interval 5%	95%
POP_S0	Baseline PAWP	25.6	mmHg	2.7	24.6	26.8
POP_S_{ss}	Steady state PAWP	19.5	mmHg	10.0	16.5	22.7
POP_TPROG	Progress half-life	5.83	h	69.4	0.920	11.9
POP_E_{max}	Maximum effect of nicorandil on PAWP	−11.7	mmHg	58.7	−30.0	−7.48
POP_EC_{50}	Nicorandil concentration at 50% of E_{max}	423	µg l^{-1}	107.1	165	1552
POP_CL	Nicorandil clearance	26.3	l h^{-1} 70 kg^{-1}	13.5	21.9	31.5
POP_*V1*	Central volume of distribution	18.1	l 70 kg^{-1}	14.8	14.9	23.3
POP_Q	Intercompartmental clearance	71.6	l h^{-1} 70 kg^{-1}	76.9	54.5	203
POP_*V2*	Peripheral volume of distribution	24.1	l 70 kg^{-1}	6.6	21.1	25.4
FCL	Fractional CL change in heart failure	1.94		25.0	1.03	2.63
F*V1*	Fractional *V1* change in heart failure	1.39		17.0	1.05	1.81
FQ	Fractional Q change in heart failure	0.519		42.8	0.192	0.891
F*V2*	Fractional *V2* change in heart failure	4.06		219.1	1.83	25.3

Figure 133. Parameters value from Lida et al. [42]. Picture from Lida et al. [42]

4.17.3 Quantification of sensitivities

Table 38. Analysis of the sensitivity of Cmax and AUC for nicorandil by varying absorption rate constant (ka), bioavailability (F), volume of distribution (V), and clearance of elimination (CL).

Sensitivity analysis												
	ka			F			V			CL		
	-10%	ref	+10%	-10%	ref	+10%	-10%	ref	+10%	-10%	ref	+10%
Cmax	0.06335	0.06744	0.07155	0.06070	0.06744	0.07419	0.06997	0.06744	0.06548	0.0707	0.06744	0.06471
Expected behavior	Yes		Yes	Yes		Yes	Yes		Yes	Yes		Yes
AUC	0.8798	0.8796	0.8794	0.7916	0.8796	0.9676	0.8794	0.8796	0.8798	0.9775	0.8796	0.7995
Expected behavior	Yes		Yes	Yes		Yes	Yes		Yes	Yes		Yes

Conclusion: The sensitivity analysis did not indicate any discrepancies in the expected behavior of the outputs studied, thereby confirming that there is no obstacle to the model's validation.

4.17.4 Quantification of uncertainties

The model has been built with popPK data : uncertainties were quantified as interindividual variability (IIV) and residual variability (RV).

Propagation in simulation results

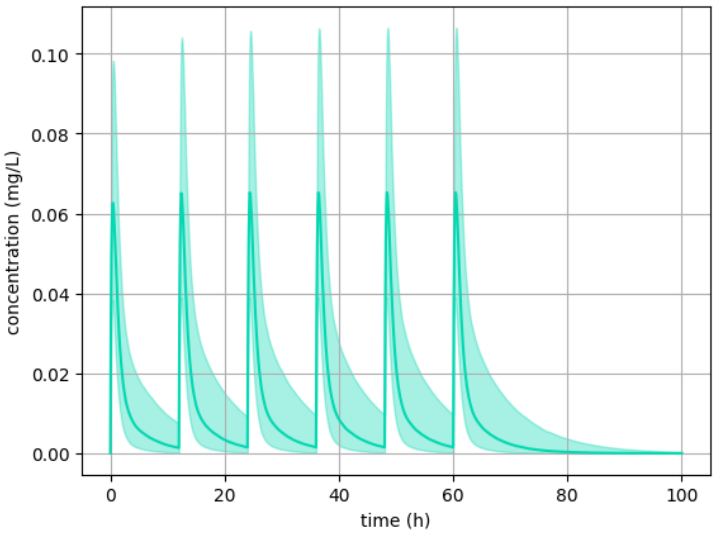

Figure 134. quantification of uncertainties for nicorandil

4.17.5 Test Samples

Test sample level: 2/3

Test sample: efficacy, overexposure, and safety thresholds used for routine therapeutic drug monitoring (TDM) in clinical settings, or thresholds reflecting specific expected events (such as efficacy or toxicity) that may occur at these levels of exposure.

- Efficacy threshold was: 0.0035 mg/L
- Overexposure threshold was: 0.246 mg/L

Test samples source(s): Frydman et al. [43]

Comment: /

4.17.6 Tests conditions

Tests conditions level: 4/5

Tests condition: test conditions were defined with sufficient data to run simulations for each patient concerned by the drug, with complete coverage of dosage ranges, and of all sub-populations concerned by the drug.

Tests conditions source(s): summary of product characteristics [44]

Comment: /

Test conditions were:

Test 1:

- Dosage: 5 mg/12h
- Groups: Standard patients weighing 50 kg, 70 kg, 100 kg.

Test 2:

- Dosage: 10 mg/12h
- Groups: Standard patients weighing 50 kg, 70 kg, 100 kg.

Test 3:

- Dosage: 20 mg/12h
- Groups: Standard patients weighing 50 kg, 70 kg, 100 kg.

Test 4:

- Dosage: 40 mg/12h
- Groups: Standard patients weighing 50 kg, 70 kg, 100 kg.

4.17.7 Equivalency of Input Parameters

Equivalency of input parameters level: 4/4
Equivalency of input parameters: the model's training dataset does cover all doses or PK is linear over the dose range used in the test conditions and sub-populations concerned by the medication, or an external validation is carried out and meets validation criteria. (i.e., MDPE ≤ ± 20%, MDAPE ≤ 30%)
Equivalency of input parameters source(s): summary of product characteristics [44]

Comment: nicorandil simulation outputs were tested with summary of products dosing regimen covering all indications.

4.17.8 Output Comparison

Output comparison level: 3/5
Output comparison: correspondence of model outputs with the therapeutic thresholds used in routine clinical therapeutic drug monitoring or thresholds reflecting specific expected events (such as efficacy or toxicity) that may occur at these levels of exposure.
Output comparison source(s): Frydman et al. [43]

Comment: all patients are within therapeutic – overexposure threshold, except patients receiving 40mg/12h which is a very high posology and not current. However, the overexposure threshold is not a safety threshold and does not correspond to high probability of safety event.

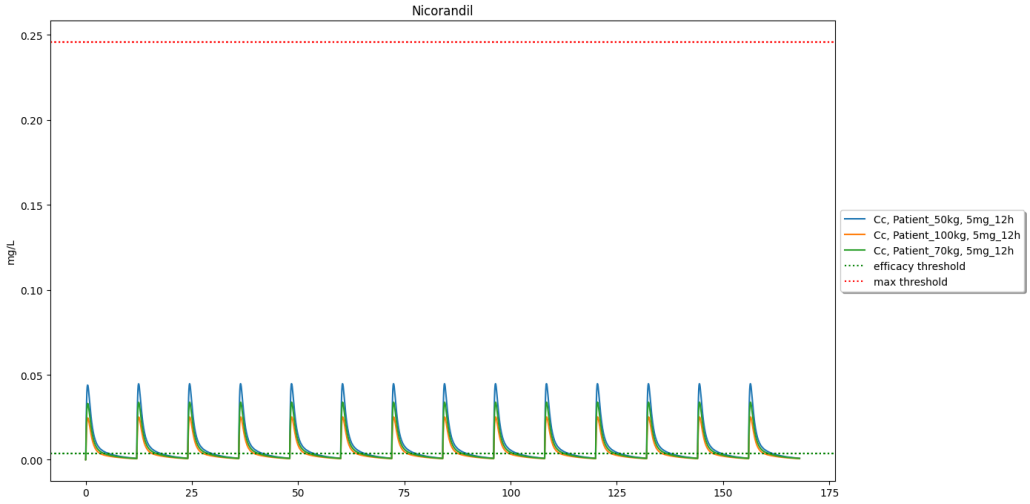

Figure 135. Test 1: 5 mg/12h for standard patients weighing 50 kg, 70 kg, 100 kg.

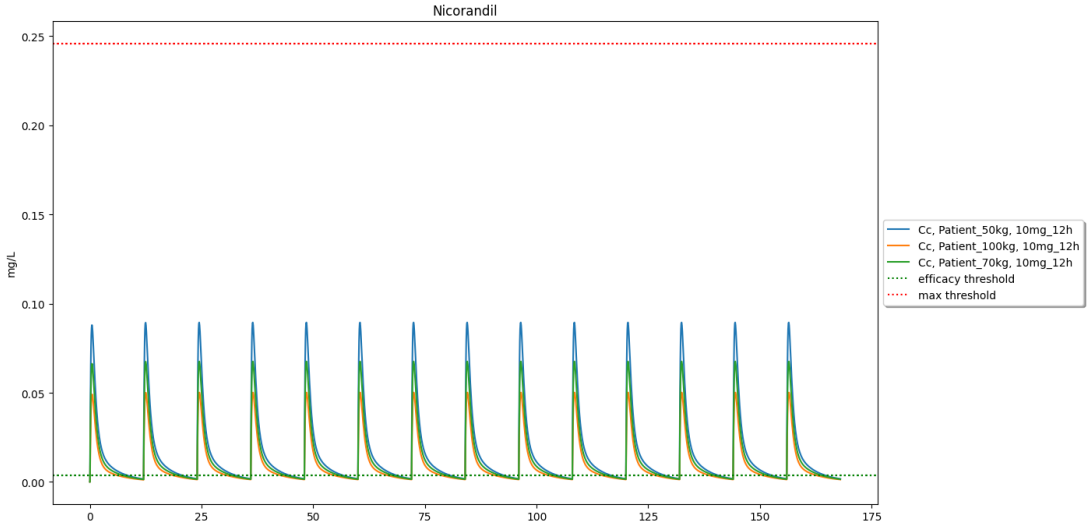

Figure 136. Test 2: 10 mg/12h for standard patients weighing 50 kg, 70 kg, 100 kg.

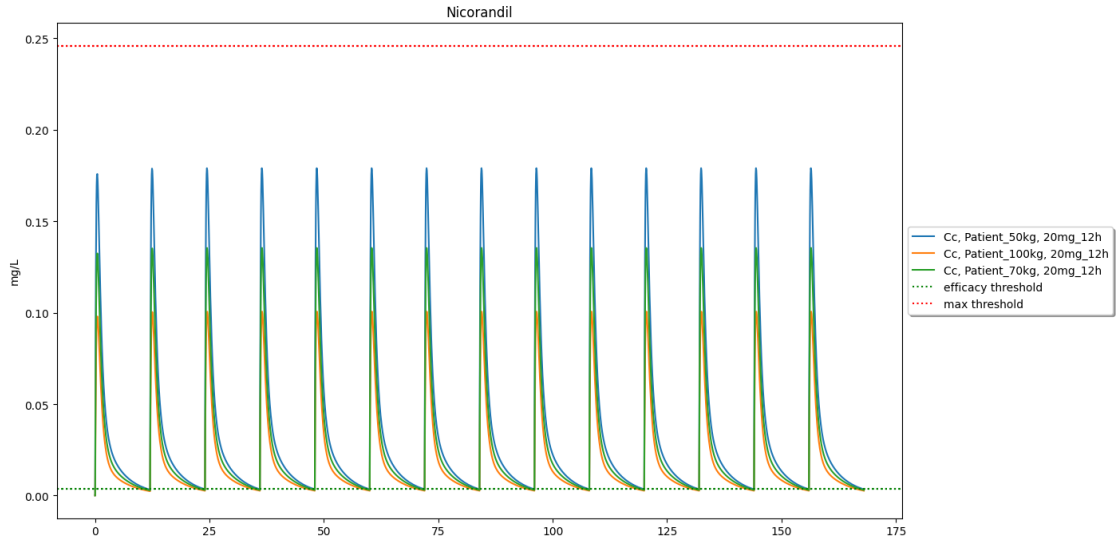

Figure 137. Test 3: 20 mg/12h for standard patients weighing 50 kg, 70 kg, 100 kg.

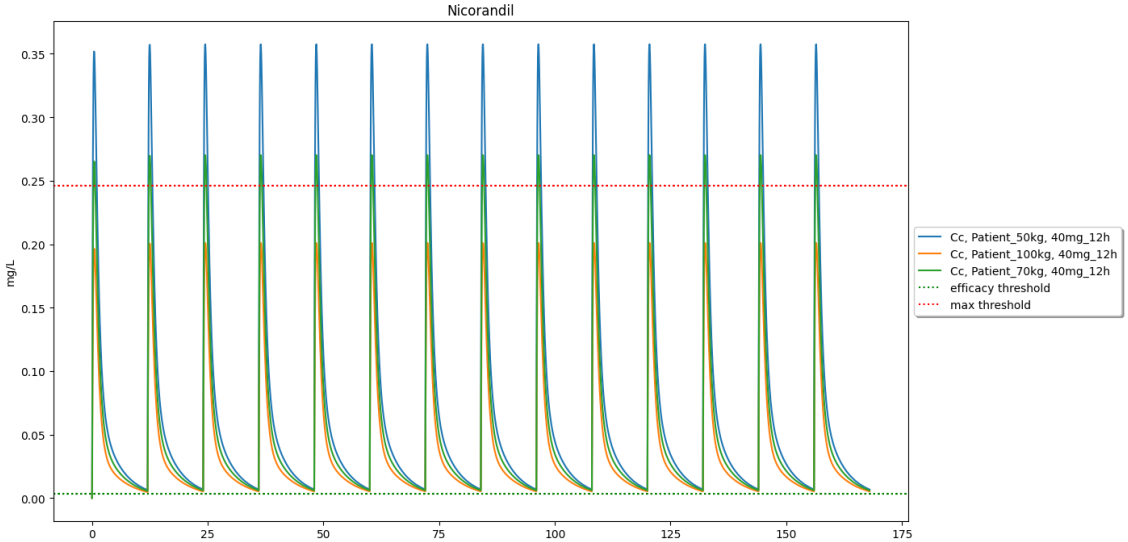

Figure 138. Test 4: 40 mg/12h for standard patients weighing 50 kg, 70 kg, 100 kg.

4.18 Ondansetron (New)

Table 39. Summary of ondansetron validation.

Summary		
Levels	**Notations**	**Comments**
Model form level	2/5	One-compartment model built from NC data
Model inputs sources level	2/4	Parameters comes from NC data
Test samples level	2/3	Therapeutic thresholds
Tests conditions level	4/5	-
Equivalency of input parameters level	4/4	all doses and sub-populations concerned by the medication are covered by the simulations. PK is linear in the dose range.
Output comparison level	3/5	Model outputs were within therapeutic thresholds.
Conclusion: The model is validated since all criteria meet the minimum score required. Model inputs sources level can't be increased at the targeted depth level 3/4 as no popPK model was available in literature.		

4.18.1 Model Form

Model form level: 2/5
Model form: Model built with NC data from regulators approved data (summary of product characteristics, regulatory agencies documents).
Model Source(s): summary of product characteristics of oral form [45], Hsyu et al. [46], Roila et al. [47].
Comment: The model parameters (F, ka, CL, V) were calibrated with non-compartmental data from literature (see sources above). Parameters calibrated constitutes a one-compartment model.

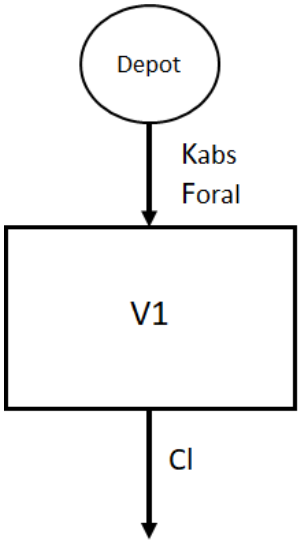

Figure 139. Model's structure, with one depot compartment, and one central compartment. Kabs, is the absorption rate, Foral the bioavailability V1 the volume of distribution, CL the clearance of elimination.

4.18.2 Model inputs sources

Model inputs sources level: 2/4
Model input: The parameters used are derived from NC data from regulatory agencies or obtained from analysis involving large numbers of patients or with low variability.
Model inputs source(s): summary of product characteristics of oral form [45], Hsyu et al. [46], Roila et al. [47].

Comment:
Parameters used as model inputs were:
F: 0.55 (interval: 0.5 – 0.6), Tlag: 0 hour, Tmax: 1.9 hours (standard deviation: 1.4 hours), V was 140 liters, T1/2 was 3 hours.
For women, a recalibration of F by +109% was used, as well as a recalibration of T1/2 for patients between 61 and 74 years old by a factor 1.36 and for patients between 75 and 82 by a factor 1.63.

4.18.3 Quantification of sensitivities

Table 40. Analysis of the sensitivity of Cmax and AUC for ondansetron by varying absorption rate constant (ka), bioavailability (F), volume of distribution (V), and clearance of elimination (CL).

Sensitivity analysis												
	ka			F			V			CL		
	-10%	ref	+10%	-10%	ref	+10%	-10%	ref	+10%	-10%	ref	+10%
Cmax	0.01968	0.02026	0.02078	0.01824	0.02026	0.02229	0.1514	0.1376	0.1261	0.1388	0.1376	0.1364
Expected behavior	Yes		Yes	Yes		Yes	Yes		Yes	Yes		Yes
AUC	0.1360	0.1360	0.1360	0.1224	0.1360	0.1496	3.129	3.129	3.129	3.476	3.129	2.844
Expected behavior	Yes		Yes	Yes		Yes	Yes		Yes	Yes		Yes

Conclusion: The sensitivity analysis did not indicate any discrepancies in the expected behavior of the outputs studied, thereby confirming that there is no obstacle to the model's validation.

4.18.4 Quantification of uncertainties

Introduction
The model inputs were parameters from NC literature with ranges used to propagate uncertainties. Uncertainties were propagated using ranges of values and standard deviations.
Propagation in simulation results

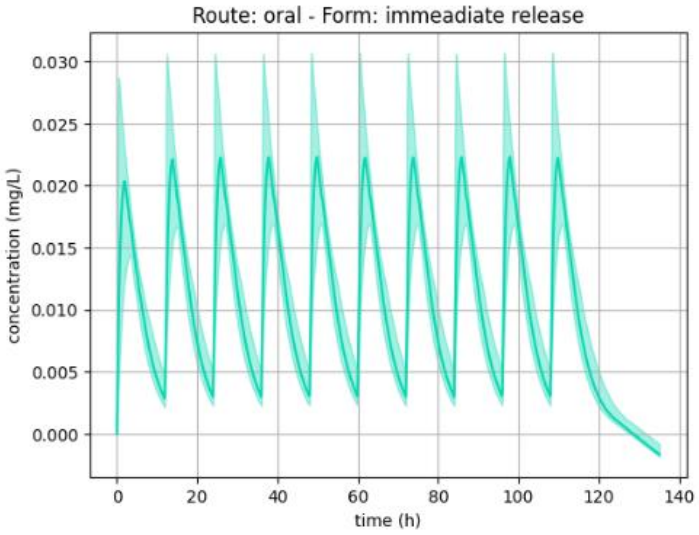

Figure 140. quantification of uncertainties for ondansetron

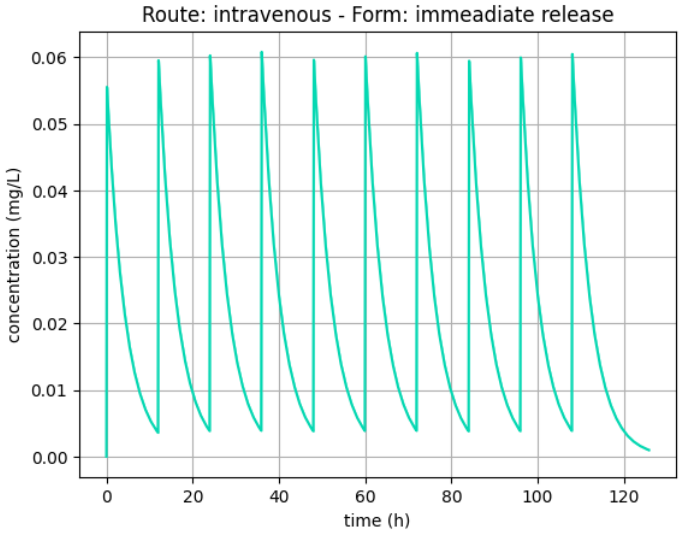

Figure 141. quantification of uncertainties for ondansetron

4.18.5 Test Samples

Test sample level: 2/3
Test sample: Efficacy, overexposure, and safety thresholds used for routine therapeutic drug monitoring (TDM) in clinical settings, or thresholds reflecting specific expected events (such as efficacy or toxicity) that may occur at these levels of exposure.

- Efficacy threshold was: 0.005 mg/L
- Overexposure threshold was: 0.3 mg/L

Test samples source(s): Pritchard [48], Schulz [4].
Comment: /

4.18.6 Tests conditions

Tests conditions level: 4/5
Tests condition: Test conditions were defined with sufficient data to run simulations for each patient concerned by the drug, with complete coverage of dosage ranges, and of all sub-populations concerned by the drug.

Tests conditions source(s): summary of product characteristics [45]
Comment: /
Test conditions were:
Test 1:
- Dosage: 8mg/12h, oral tablet
- Groups: patient male and female of 50, 70 and 100kg, older patients of 65 and 80 years old.

Test 2:
- Dosage: 8mg/12h, 16mg/12h, intravenous injection
- Groups: patient male and female of 50, 70 and 100kg, older patients of 65 and 80 years old.

Test 3:
- Dosage: 0.75mg/4h oral and intravenous
- Groups: Children of 5 kg male and female

Test 4:
- Dosage: 2mg/12h oral
- Groups: Children of 5 kg male and female

Test 5:
- Dosage: 4mg/12h oral
- Groups: Children of 5 kg male and female

Test 6:
- Dosage: 3mg/4h oral
- Groups: Children of 20 kg male and female

4.18.7 Equivalency of Input Parameters

Equivalency of input parameters level: 4/4
Equivalency of input parameters: The model's training dataset does cover all doses or PK is linear over the dose range used in the test conditions and sub-populations concerned by the medication, or an external validation is carried out and meets validation criteria. (i.e., MDPE ≤ ± 20%, MDAPE ≤ 30%)
Equivalency of input parameters source(s): summary of product characteristics [45]
Comment: Ondansetron simulation outputs were tested with summary of products dosing regimen covering all indications.

4.18.8 Output Comparison

Output comparison level: 3/5
Output comparison: Correspondence of model outputs with the therapeutic thresholds used in routine clinical therapeutic drug monitoring or thresholds reflecting specific expected events (such as efficacy or toxicity) that may occur at these levels of exposure.
Output comparison source(s): Pritchard [48], Schulz [4].
Comment: summary of product was used to extract dosing regimen data, and simulation outputs were compared to therapeutic thresholds. The simulation results were all within therapeutic thresholds.

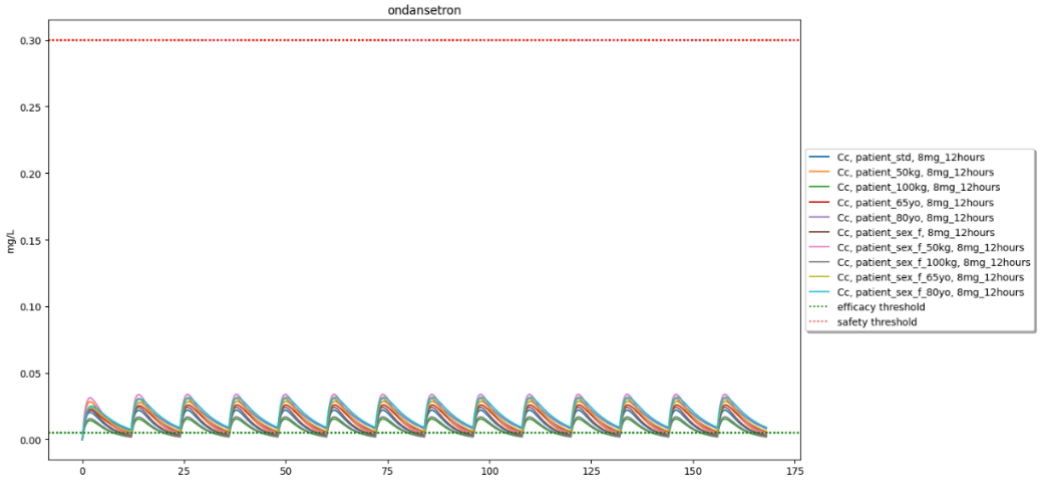

Figure 142. Test 1: 8mg per 12 hours oral for patient male and female of 50, 70100kg, older patients of 65 and 80 years old.

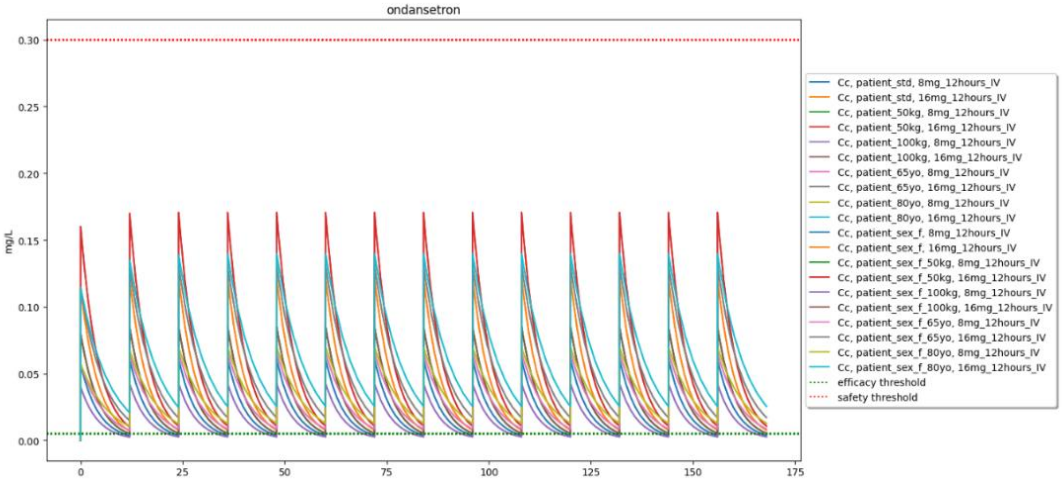

Figure 143. Test 2: 8mg per 12 hours and 16mg per 12 hours intravenous for patient male and female of 50, 70, 100kg, older patients of 65 and 80 years old.

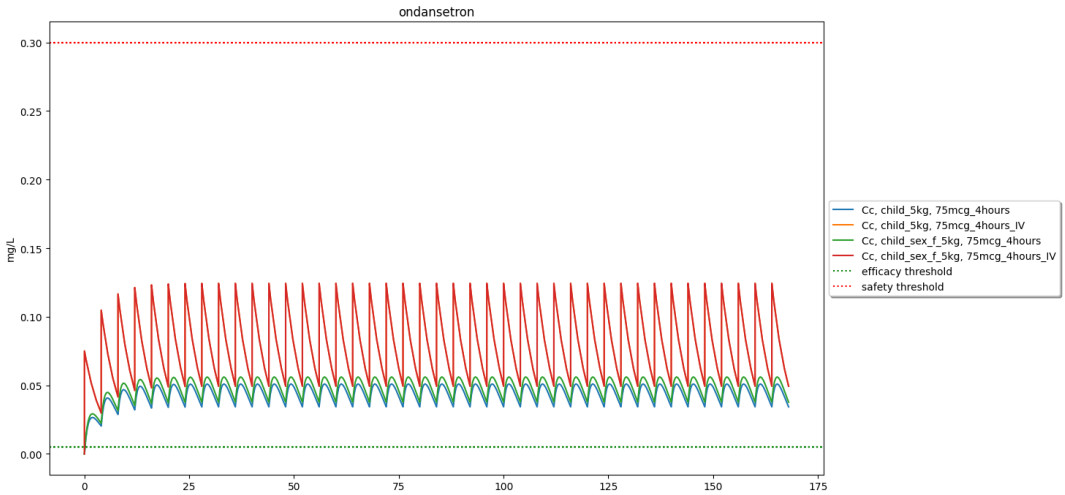

Figure 144. Test 3: 0.75mg per 4 hours oral and intravenous for children male and female of 5kg.

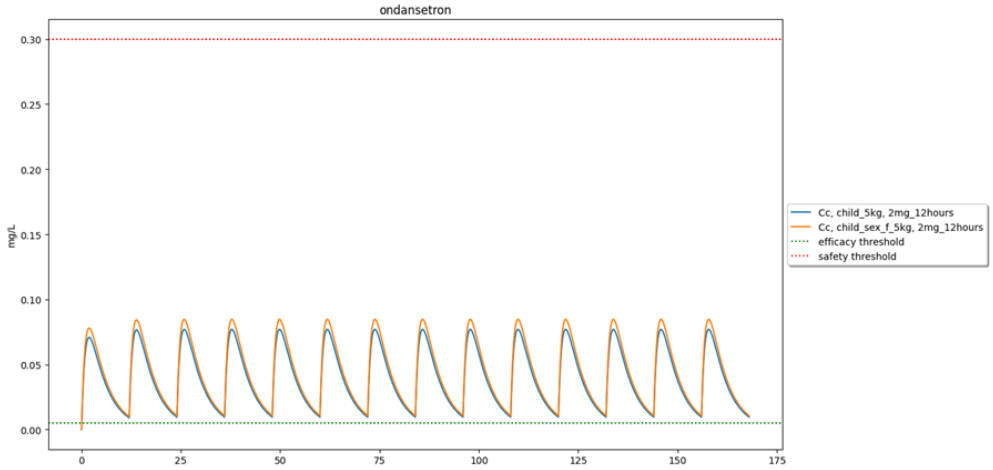

Figure 145. Test 4: 2mg per 12 hours oral for children male and female of 5kg.

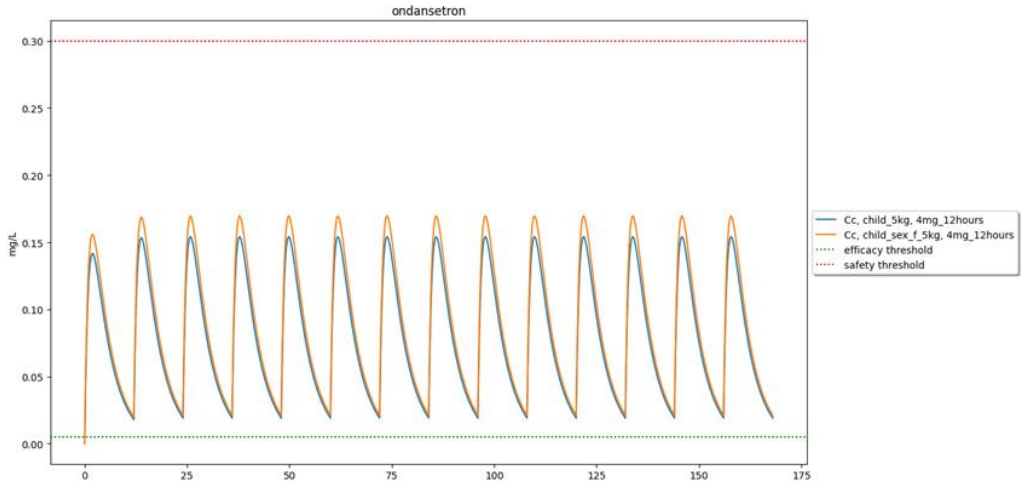

Figure 146. Test 5: 4mg per 12 hours oral for children male and female of 5kg.

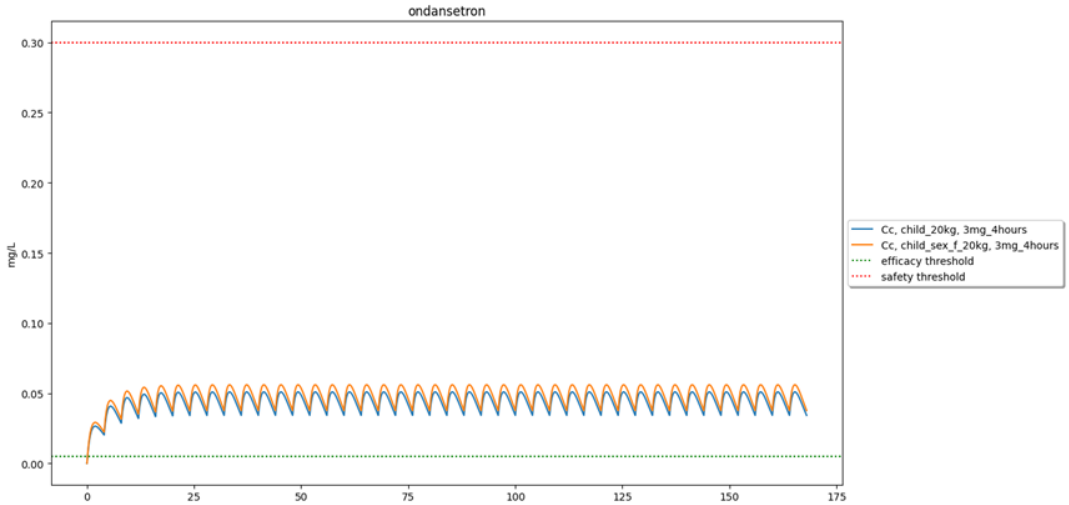

Figure 147. Test 6: 3mg per 4 hours oral and for children male and female of 20kg.

4.19 Pimozide (New)

Table 41. Summary of pimozide validation.

Summary		
Levels	**Notations**	**Comments**
Model form level	3/5	Model built from popPK analysis
Model inputs sources level	3/4	RSE% were >30% for structural parameters
Test samples level	2/3	Therapeutic thresholds
Tests conditions level	4/5	-
Equivalency of input parameters level	3/4	The model's training dataset does cover doses tested or PK is linear over the dose range use in the test conditions, but not all the sub-populations concerned by the medication.
Output comparison level	3/5	Model outputs were within therapeutic thresholds.
Conclusion: The model is validated since all applicable criteria meet the minimum score required.		

4.19.1 Model Form

Model form level: 3/5
Model form: Model built from popPK analysis.
Model Source(s): Nucci et al. [49]
Comment: The implemented PK model is based on a popPK analysis conducted by Nucci et al. [49] and published in a poster for Population Approach Group Europe (PAGE) conference in 2007. The model is a two-compartment model with first order absorption and elimination.

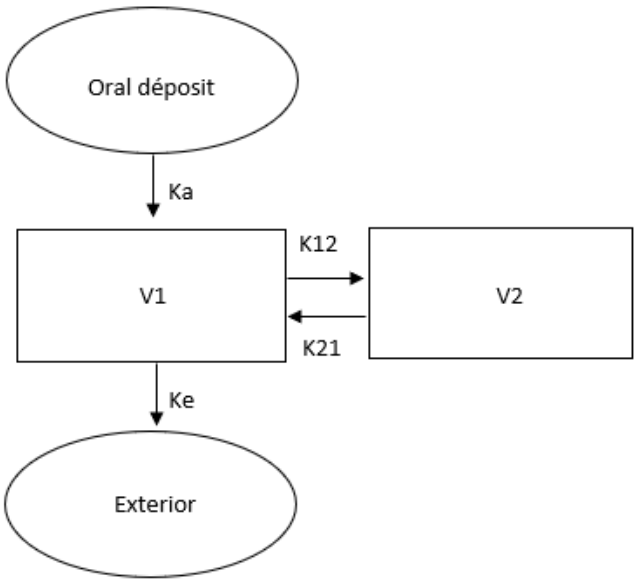

Figure 148. *Model's structure, with depot compartment, central compartment, peripheral compartment, and exterior fictive compartment. Ka is the absorption rate, V1 the volume of the central compartment, V2 the volume of the peripheral compartment, K12 and K21 transfer constant between the 2 compartments, and Ke the elimination rate.*

4.19.2 Model inputs sources

Model inputs sources level: 3/4
Model input: parameters are obtained from popPK analysis with a relative standard error (RSE) > 30%.
Model inputs source(s): Nucci et al. [49]
Comment:

Final Model Parameters

Parameter	Final Estimate	η (%)
CL/F (L/h)	14.7 $_{PM}$ 35.8 $_{IM}$ 54.9 $_{EM}$	35%
V1/F (L)	1240*(WT/70)	32%
V2/F (L)	1040*(WT/70)	21%
CLD/F (L/h)	69.2	20%
Ka (1/h)	0.68	62%
Lag (h)	1.14	18%

Figure 149. Model parameters from Nucci et al. [49] Picture from Nucci et al. [49]

4.19.3 Quantification of sensitivities

Table 42. Analysis of the sensitivity of Cmax and AUC for pimozide by varying absorption rate constant (ka), bioavailability (F), volume of distribution (V), and clearance of elimination (CL).

Sensitivity analysis												
	ka			F			V			CL		
	-10%	ref	+10%	-10%	ref	+10%	-10%	ref	+10%	-10%	ref	+10%
Cmax	0.008333	0.008440	0.008534	0.007596	0.008440	0.009284	0.008728	0.008440	0.008203	0.009082	0.008440	0.00791
Expected behavior	Yes		Yes	Yes		Yes	Yes		Yes	Yes		Yes
AUC	1.600	1.600	1.600	1.440	1.600	1.760	1.600	1.600	1.600	1.776	1.600	1.455
Expected behavior	Yes		Yes	Yes		Yes	Yes		Yes	Yes		Yes

Conclusion: The sensitivity analysis did not indicate any discrepancies in the expected behavior of the outputs studied, thereby confirming that there is no obstacle to the model's validation.

4.19.4 Quantification of uncertainties

Introduction
The model has been built with popPK data : uncertainties were quantified as interindividual variability (IIV) and residual variability (RV).
Propagation in simulation results

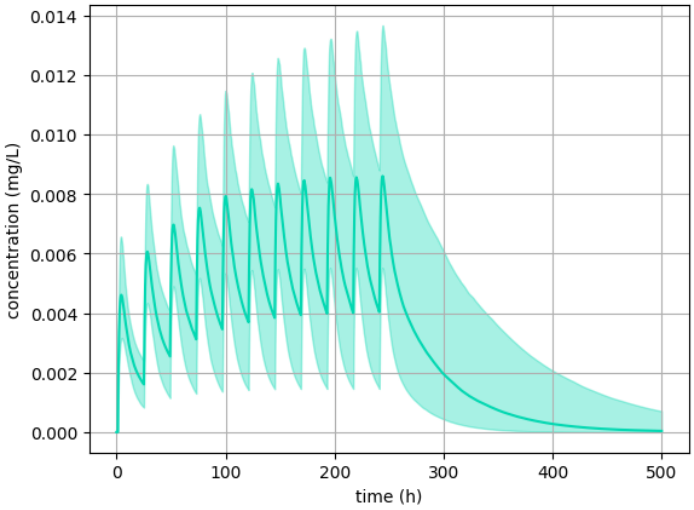

Figure 150. quantification of uncertainties for pimozide

4.19.5 Test Samples

Test sample level: 2/3
Test sample: efficacy, overexposure, and safety thresholds used for routine therapeutic drug monitoring (TDM) in clinical settings, or thresholds reflecting specific expected events (such as efficacy or toxicity) that may occur at these levels of exposure.

- Efficacy threshold was: 0.003 mg/L
- Overexposure threshold was: 0.02 mg/L

Test samples source(s): Schulz et al. [4]
Comment: /

4.19.6 Tests conditions

Tests conditions level: 4/5
Tests condition: test conditions were defined with sufficient data to run simulations for each patient concerned by the drug, with complete coverage of dosage ranges, and of all sub-populations concerned by the drug.
Tests conditions source(s): summary of product characteristics [50]
Comment: /
Test conditions were:
Test 1:

- Dosage: 6mg/24h
- Groups: patients weighing 50 kg, 70 kg, 100 kg.

Test 2:

- Dosage: 16mg/24h
- Groups: patients weighing 50 kg, 70 kg, 100 kg.

Test 3:

- Dosage: 4mg/24h
- Groups: patients weighing 50 kg, 70 kg, 100 kg.

Test 4:

- Dosage: 6mg/24h
- Groups: poor and intermediate CYP2D6 metabolizer profile.

Test 5:

- Dosage: 4mg/24h
- Groups: Children weighing 35kg.

Test 6:

- Dosage: 0.7mg/24h
- Groups: Children weighing 35kg.

Test 7:

- Dosage: 0.7mg/24h
- Groups: Children weighing 35kg and CYPD6 poor metabolizer profile.

4.19.7 Equivalency of input parameters

Equivalency of input parameters level: 3/4

1. **Equivalency of input parameters:** the model's training dataset does cover doses tested or PK is linear over the dose range use in the test conditions, but not all the sub-populations concerned by the medication.

Equivalency of input parameters source(s): summary of product characteristics [50], Nucci et al. [49].

Comment: children were not covered by the training dataset of the model. However, the behaviour of the model for children's posology is as expected regarding therapeutic threshold (see below).

4.19.8 Output Comparison

Output comparison level: 3/5

Output comparison: correspondence of model outputs with the therapeutic thresholds used in routine clinical therapeutic drug monitoring or thresholds reflecting specific expected events (such as efficacy or toxicity) that may occur at these levels of exposure.

Output comparison source(s): Schulz et al. [4]

Comment: the dosing regimen data were extracted from the summary of product characteristics, and the simulation outputs were compared to therapeutic ranges from Schulz et al. [4]. The simulation results were consistent with the expected behaviour: patients with low body weight and young children exhibit higher concentrations, reaching the efficacy threshold at lower doses compared to patients with higher body weight, while they surpass the safety threshold more quickly. Conversely, patients with higher body weight require higher doses to reach therapeutic concentrations. Patients weighing 50 kg should not receive the maximum dose of 16 mg/24h, and patients weighing 100 kg should have an increased dose compared to 4 mg/24h. Additionally, children weighing 35 kg should not receive the low dose of 0.7 mg/kg, except if the metabolizer profile is not known: for patients with a CYP2D6 poor metabolizer profile, this dose is sufficient to reach the therapeutic threshold. Since the drug should be started at the lowest dose to ensure good tolerance, it is necessary to test this dose first, unless the CYP2D6 metabolizer profile is already known.

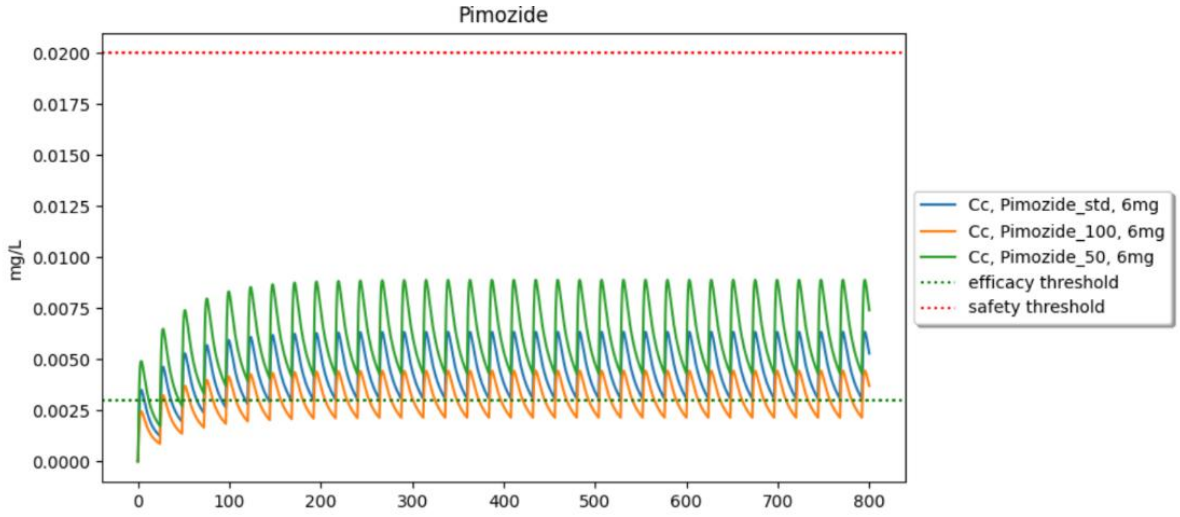

Figure 151. Test 1: 6mg per 24 hours for patients weighing 50 kg, 70 kg, 100 kg

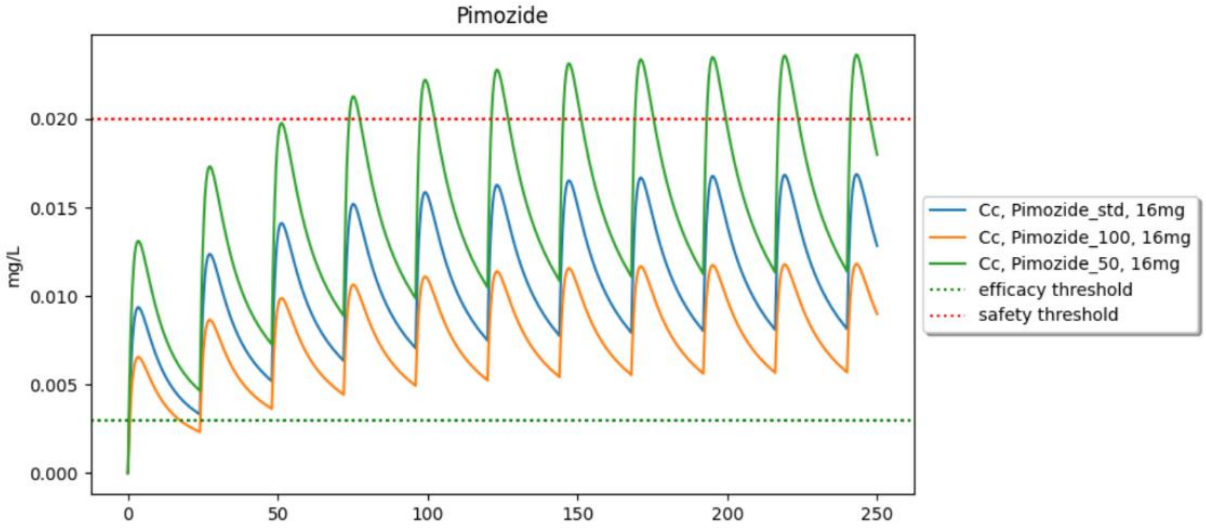

Figure 152. Test 2: 16mg per 24 hours for patients weighing 50 kg, 70 kg, 100 kg

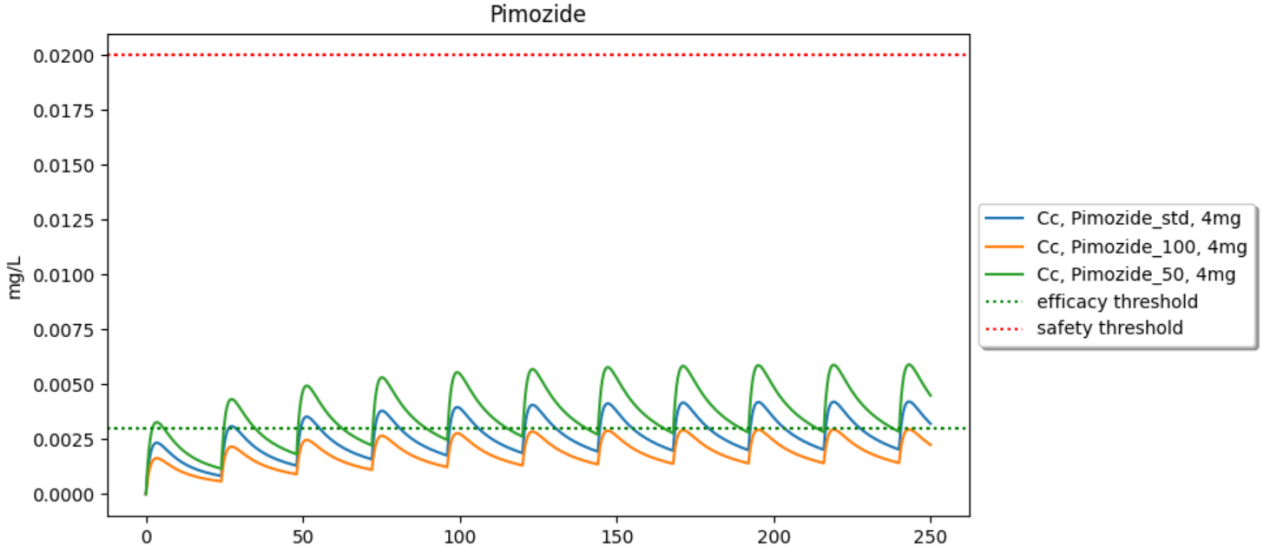

Figure 153. Test 3: 4mg per 24 hours for patients weighing 50 kg, 70 kg, 100 kg

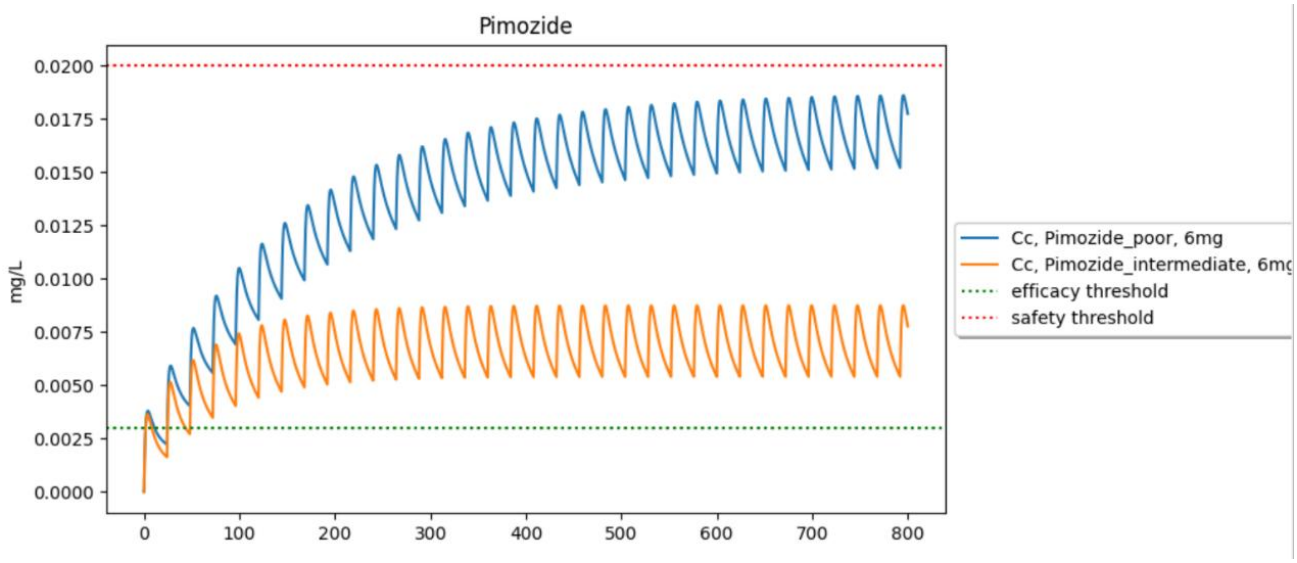

Figure 154. Test 4: 6 mg per 24 hours for poor and intermediate CYP2D6 metabolizer profile

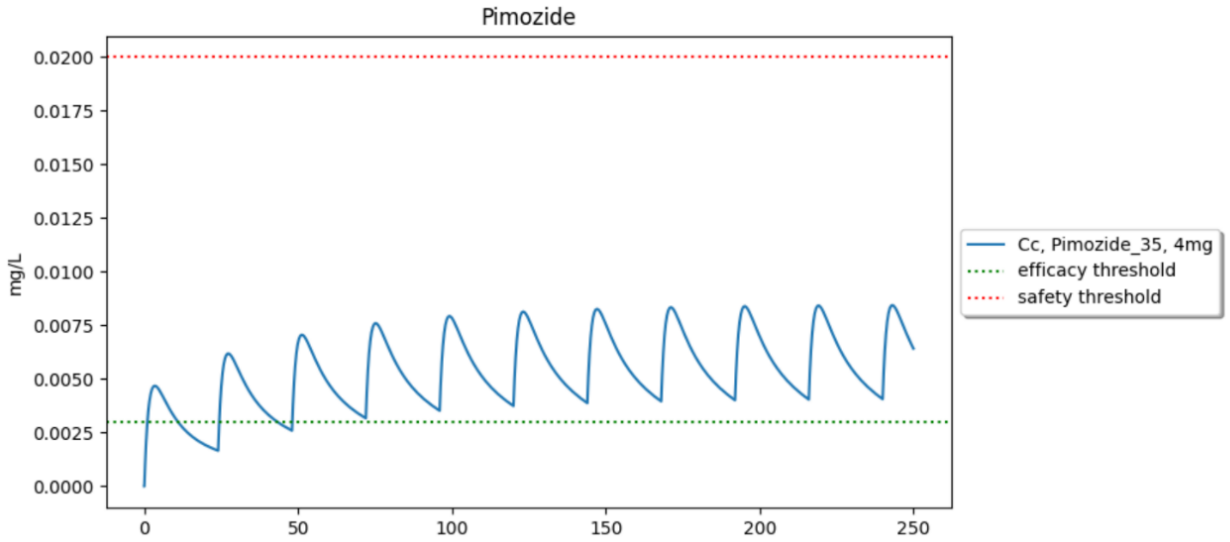

Figure 155. Test 5: 4 mg per 24 hours for children weighing 35kg

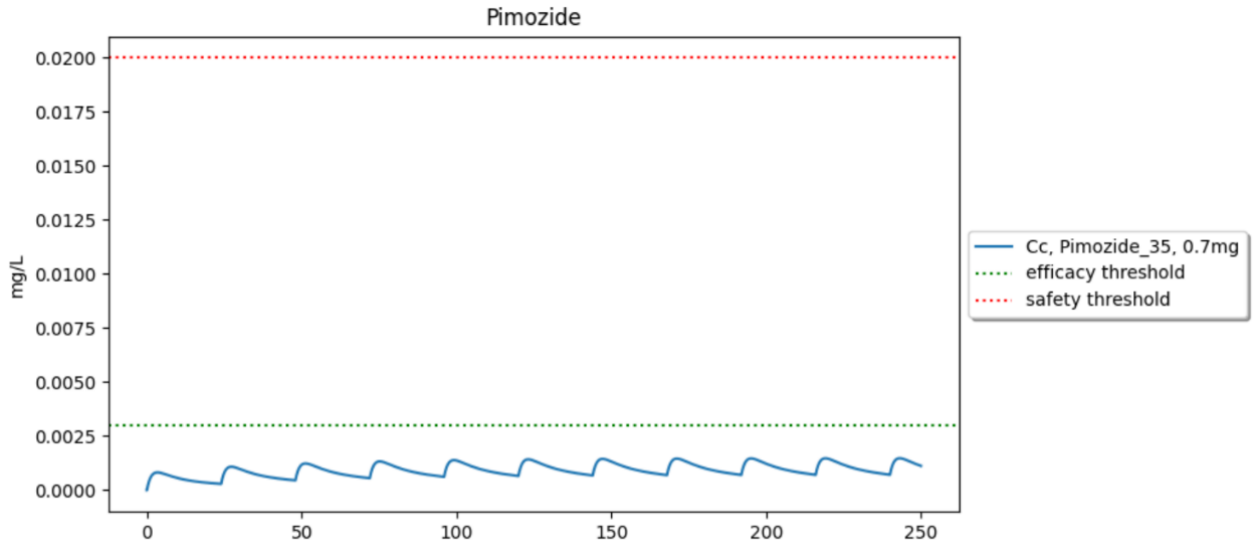

Figure 156. Test 6: 0.7 mg per 24 hours for children weighing 35kg

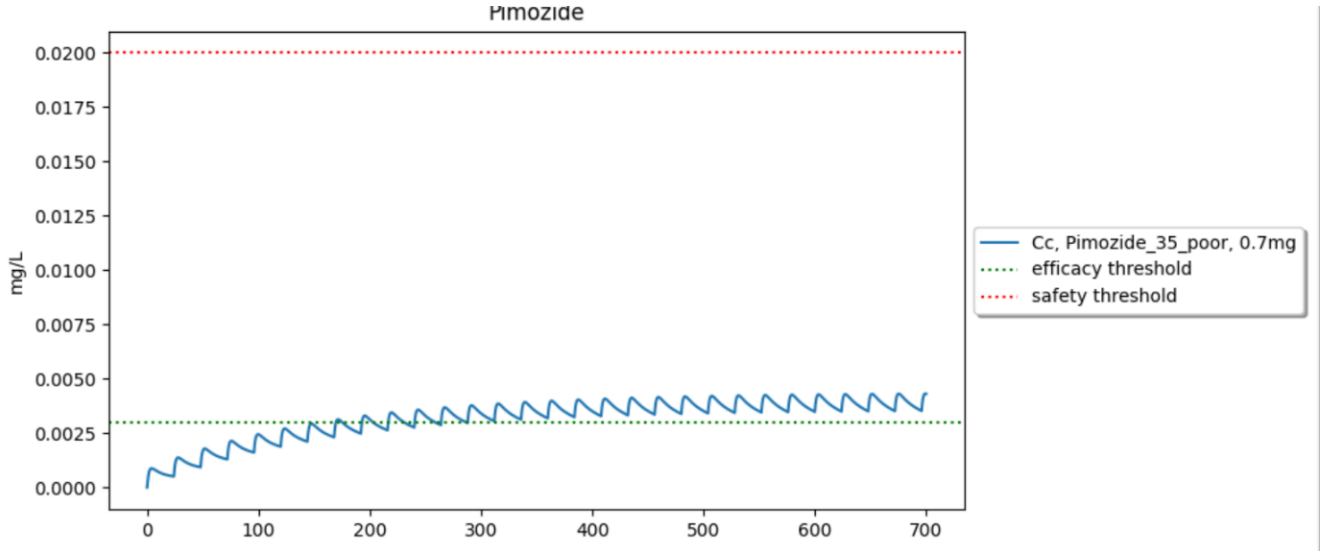

Figure 157. Test 7: 0.7 mg per 24 hours for children weighing 35kg and CYPD6 poor metabolizer profile

4.20 Quinidine (New)

Table 43. Summary of quinidine validation.

Summary		
Levels	**Notations**	**Comments**
Model form level	3/5	Model built from popPK analysis
Model inputs sources level	3/4	RSE% on parameters are >30%
Test samples level	2/3	Therapeutic thresholds
Tests conditions level	4/5	-
Equivalency of input parameters level	4/4	all doses and sub-populations concerned by the medication are covered by the simulations. PK is linear in the dose range.
Output comparison level	3/5	Model outputs were within therapeutic thresholds.
Conclusion: The model is validated since all criteria meet the minimum score required.		

4.20.1 Model Form

Model form level: 3/5
Model form: model built from popPK analysis.
Model Source(s): Verme et al. [51]
Comment: the implemented PK model is based on a popPK analysis conducted by Verme et al. [51] It is a one-compartment model with first order absorption and elimination.

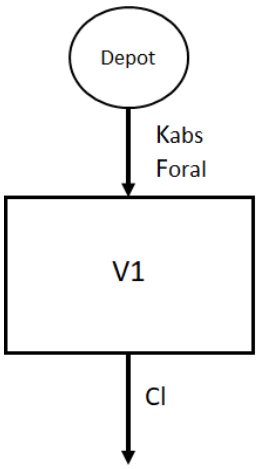

Figure 158. Model's structure, with one depot compartment, and one central compartment. Kabs, is the absorption rate, Foral the bioavailability V1 the volume of distribution, CL the clearance of elimination.

4.20.2 Model inputs sources

Model inputs sources level: 3/4
Model input: parameters are obtained from popPK analysis with a relative standard error (RSE) > 30% or taken from the summary of product characteristics or from analysis conducted on many patients with little variability.
Model inputs source(s): Verme et al. [51]
Comment:

Table IV. Parameter values for final regression model based on Data Set A

Parameter	Value	Standard error	CV(%)
P_1	18.0	2.96	16.4
P_2	230.0	10.6	4.6
P_5	−0.101	0.0432	42.8
P_6	0.156	0.0824	52.8
P_7	−0.115	0.0693	60.3
P_{10}	0.230	0.104	45.2
P_{12}	−0.178	0.0679	38.1

Abbreviation: CV = coefficient of variation.

Figure 159. Parameters of the model. P1 is the CL, P2 the Vd, P5 the effect of age on CL, P6 the effect of age, P7 the effect of heart failure, P10 the effect of alcohol and P12 the effect of glomerular filtration rate < 50 mL/min/1.73m² on CL.

4.20.3 Quantification of sensitivities

Table 44. Analysis of the sensitivity of Cmax and AUC for quinidine by varying absorption rate constant (ka), bioavailability (F), volume of distribution (V), and clearance of elimination (CL).

Sensitivity analysis												
	ka			F			V			CL		
	-10%	ref	+10%	-10%	ref	+10%	-10%	ref	+10%	-10%	ref	+10%
Cmax	4.430	4.460	4.487	4.014	4.460	4.905	4.521	4.460	4.403	4.886	4.460	4.105
Expected behavior	Yes		Yes	Yes		Yes	Yes		Yes	Yes		Yes
AUC	353.6	353.6	353.6	318.2	353.6	388.9	353.6	353.6	353.5	392.8	353.6	321.5
Expected behavior	Yes		Yes	Yes		Yes	Yes		Yes	Yes		Yes

Conclusion: The sensitivity analysis did not indicate any discrepancies in the expected behavior of the outputs studied, thereby confirming that there is no obstacle to the model's validation.

4.20.4 Quantification of uncertainties

Introduction

Uncertainties were propagated with interindividual variability and residual variability from the popPK analysis.

Propagation in simulation results

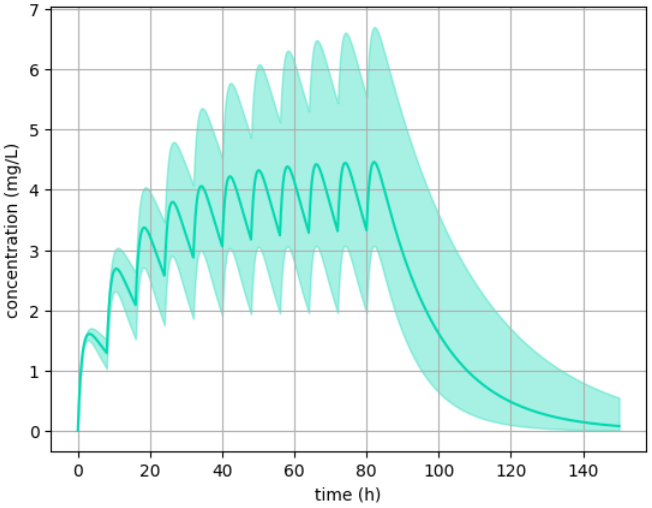

Figure 160. quantification of uncertainties for quinidine

4.20.5 Test Samples

Test sample level: 2/3

Test sample: efficacy, overexposure, and safety thresholds used for routine therapeutic drug monitoring (TDM) in clinical settings, or thresholds reflecting specific expected events (such as efficacy or toxicity) that may occur at these levels of exposure.

- Efficacy threshold was: 2 mg/L
- Overexposure threshold was: 5 mg/L
- Safety threshold was: 8 mg/L

Test samples source(s): Schulz et al. [4]
Comment: /

4.20.6 Tests conditions

Tests conditions level: 4/5
Tests condition: test conditions were defined with sufficient data to run simulations for each patient concerned by the drug, with complete coverage of dosage ranges, and of all sub-populations concerned by the drug.
Tests conditions source(s): dosing regimen published by drugs.com [52]
Comment: quinidine is no longer on the market for arrhythmias, only for malaria treatment. Thus, no summary of product characteristics is available for this indication.
Tests were:
Test 1:
- Dosage: 200mg/6hours
- Groups: patients of 30, 40, 70 years old.

Test 2:
- Dosage: 200mg/6h
- Groups: patients with height < 175cm, patients with heart failure, patients with GFR < 50mL/min/1.73m², patients alcoholic, patients with heart and renal failure, patient's alcoholic with renal failure.

Test 3:
- Dosage: 200mg/8hours
- Groups: patients of 30, 40, 70 years old.

Test 4:
- Dosage: 600mg/6h
- Groups: patients with height < 175cm, patients with heart failure, patients with GFR < 50mL/min/1.73m², patients alcoholic.

Test 5:
- Dosage: 600mg/8h
- Groups: patients with heart and renal failure, patient's alcoholic with renal failure.

Test 6:
- Dosage: 450mg/8h
- Groups: patients of 40, 30, 70 years old, patients with height < 175cm, patients with heart failure, patients with GFR < 50mL/min/1.73m², patients alcoholic, patients with heart and renal failure, patient's alcoholic with renal failure.

4.20.7 Equivalency of Input Parameters

Equivalency of input parameters level: 4/4
Equivalency of input parameters: the model's training dataset does cover all doses or PK is linear over the dose range used in the test conditions and sub-populations concerned by the medication, or an external validation is carried out and meets validation criteria. (i.e., MDPE ≤ ± 20%, MDAPE ≤ 30%).
Equivalency of input parameters source(s):
- Dosing regimen published by drugs.com [52]

Comment: /

4.20.8 Output Comparison

Output comparison level: 3/5
Output comparison: correspondence of model outputs with the therapeutic thresholds used in routine clinical therapeutic drug monitoring or thresholds reflecting specific expected events (such as efficacy or toxicity) that may occur at these levels of exposure.
Output comparison source(s): Schulz et al. [4]
Comment: all patients evaluated were in accordance with thresholds of Schulz et al. [4] Patients were within therapeutic thresholds except patients with heart failure and renal failure which is above safety thresholds : these patients should not receive the maximum dose of 600mg per 8 hours.

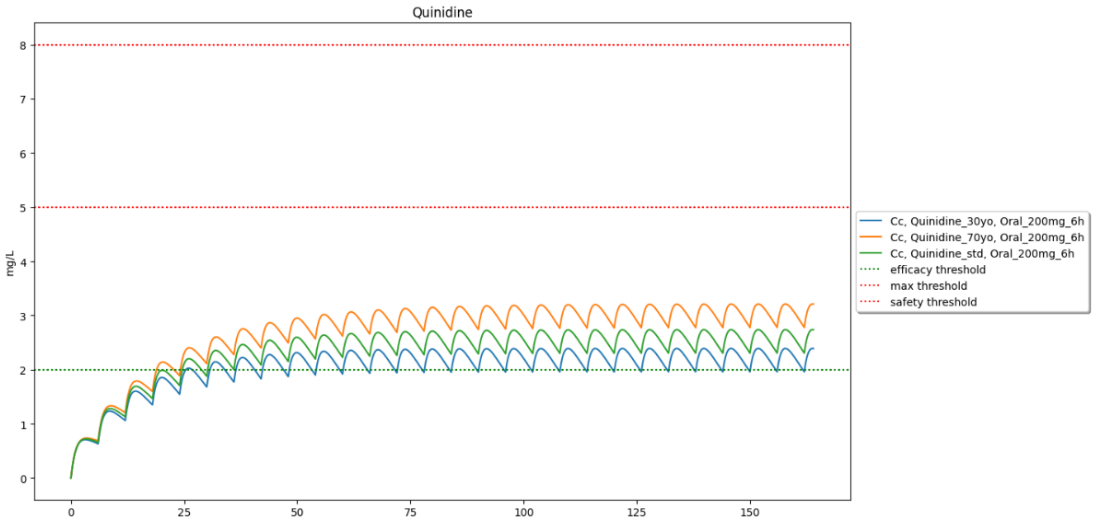

Figure 161. Test 1: 200mg/6h for patients of 30, 40 (std), 70 years old.

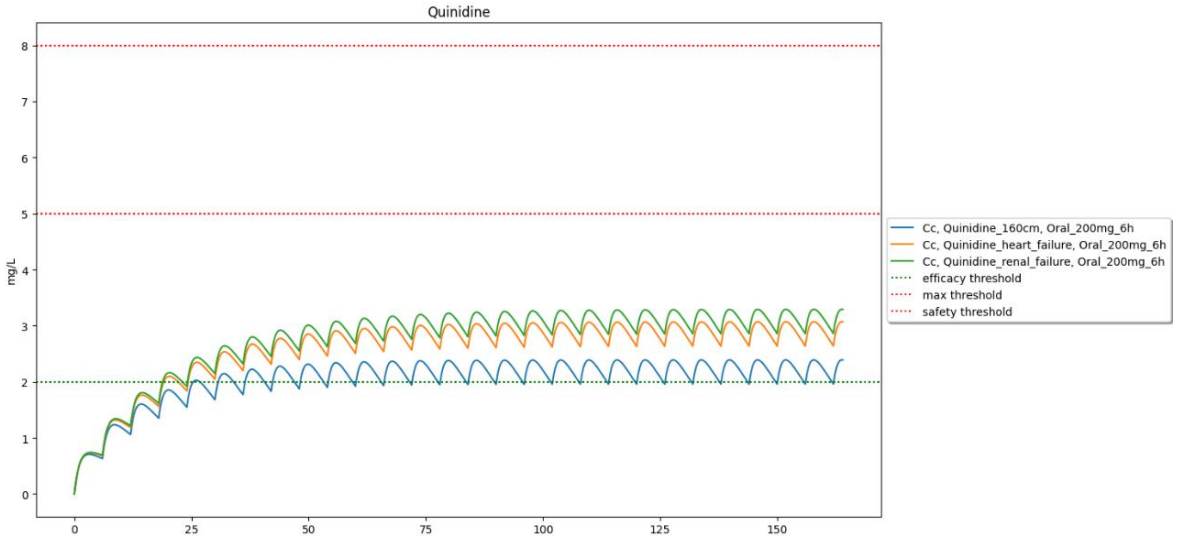

Figure 162. Test 2: 200mg/6h for patients with height < 175cm, patients with heart failure, patients with GFR < 50mL/min/1.73m², patients alcoholic, patients with heart and renal failure, patient's alcoholic with renal failure.

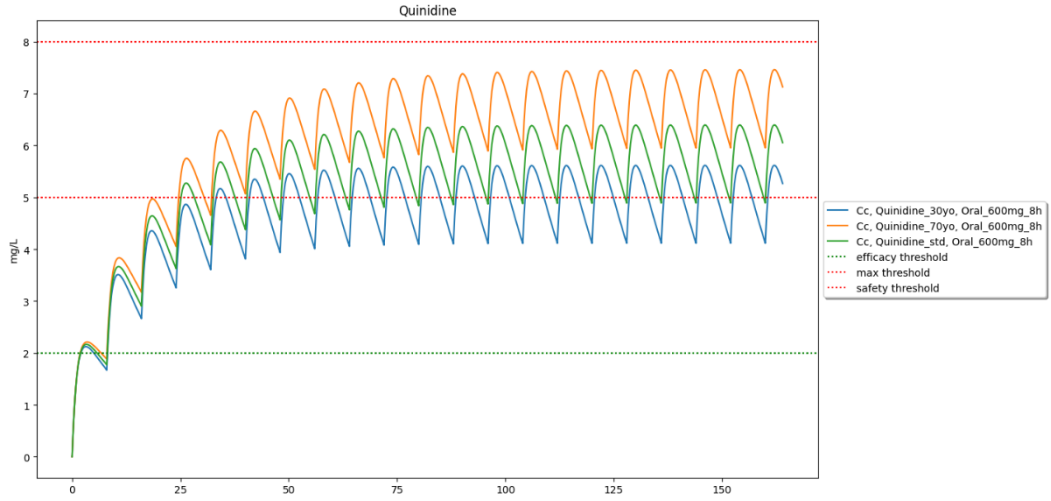

Figure 163. Test 3: 600mg/8h for patients of 30, 40, 70 years old.

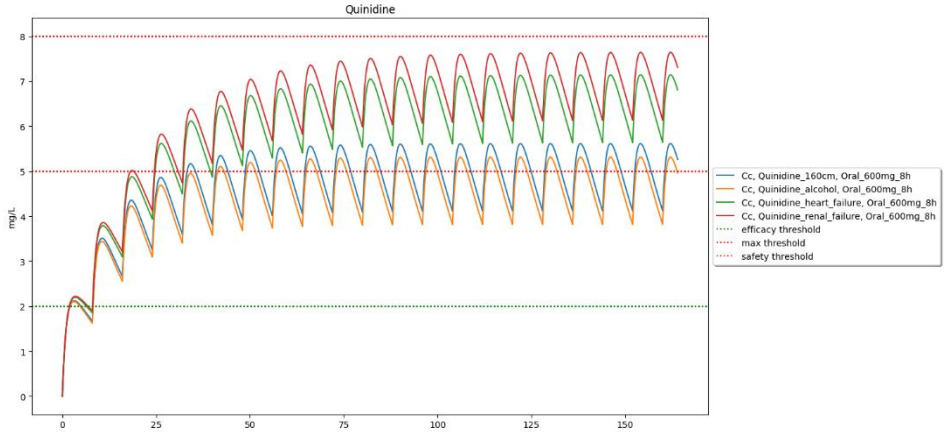

Figure 164. Test 4: 600mg/8h for patients with height < 175cm, patients with heart failure, patients with GFR < 50mL/min/1.73m², patients alcoholic.

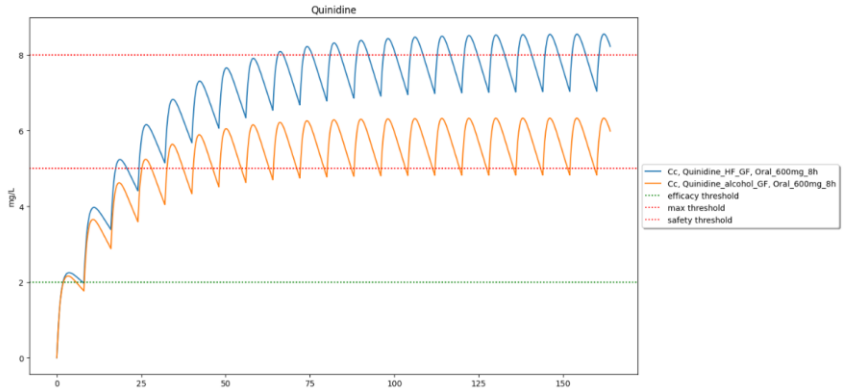

Figure 165. Test 5: 600mg/8h for patients with heart and renal failure, patient's alcoholic with renal failure

.

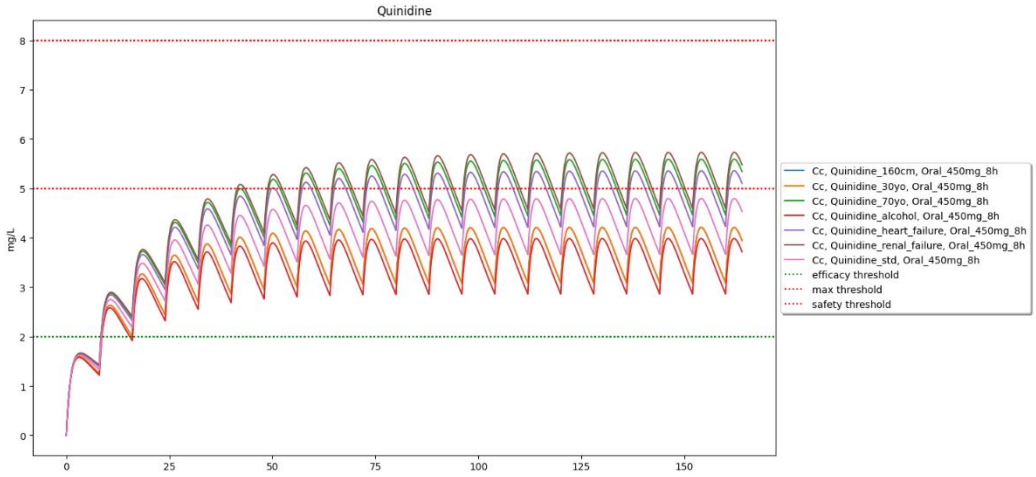

Figure 166. Test 6: 450mg/8h for patients of 40, 30, 70 years old, patients with height < 175cm, patients with heart failure, patients with GFR < 50mL/min/1.73m², patients alcoholic, patients with heart and renal failure, patient's alcoholic with renal failure.

4.21 Vandetanib (New)

Table 45. Summary of vandetanib validation.

Summary		
Levels	**Notations**	**Comments**
Model form level	2/5	Model built from NC data from regulators approved data
Model inputs sources level	2/4	Parameters comes from NC analysis from regulators data
Test samples level	2/3	Therapeutic thresholds
Tests conditions level	4/5	-
Equivalency of input parameters level	4/4	all doses and sub-populations concerned by the medication are covered by the simulations. PK is linear in the dose range.
Output comparison level	3/5	Model outputs were within therapeutic thresholds.
Conclusion: The model is validated since all criteria meet the minimum score required. Model inputs sources level can't be increased at the targeted depth level 3/4 as no popPK model was available in literature.		

4.21.1 Model Form

Model form level: 2/5
Model form: model built with NC data from regulators approved data (summary of product characteristics, regulatory agencies documents).
Model Source(s): summary of product characteristics [53], Martin et al. [54]

Comment: the model parameters were calibrated with non-compartmental data. The V, CL, kabs and F were calibrated or directly taken from the sources and constitutes a one-compartment model.

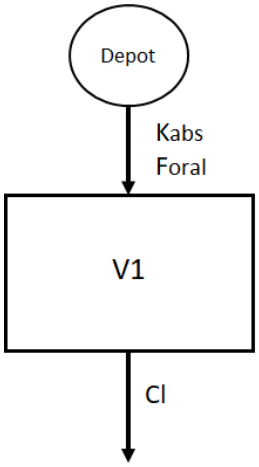

Figure 167. Model's structure, with one depot compartment, and one central compartment. Kabs, is the absorption rate, Foral the bioavailability V1 the volume of distribution, CL the clearance of elimination.

4.21.2 Model inputs sources

Model inputs sources level: 2/4
Model input: the parameters used are derived from NC data from regulatory agencies or obtained from analysis involving large numbers of patients or with low variability.
Model inputs source(s): Summary of product characteristics [53], Martin et al. [54]
Comment:
parameters were F: 1, V: 3876 liters (standard deviation: 25.1L), T1/2 of elimination: 195.4 hours (standard deviation: 67.1 hours), Tmax: 6 hours (interval: 4 – 8 hours). Recalibration of volume (V) based on weight was implemented using the formula (V * weight / 80.7 kg). Additionally, clearance (CL) was adjusted according to renal status, with factors of 1.5, 1.6, and 2 applied to the area under the curve (AUC) for mild, moderate, and severe renal impairment, respectively.

4.21.3 Quantification of sensitivities

Table 46. Analysis of the sensitivity of Cmax and AUC for vandetanib by varying absorption rate constant (ka), bioavailability (F), volume of distribution (V), and clearance of elimination (CL).

Sensitivity analysis												
	ka			F			V			CL		
	-10%	ref	+10%	-10%	ref	+10%	-10%	ref	+10%	-10%	ref	+10%
Cmax	0.08718	0.08735	0.08749	0.07862	0.08735	0.09609	0.09687	0.08735	0.07954	0.08751	0.08735	0.08720
Expected behavior	Yes		Yes	Yes		Yes	Yes		Yes	Yes		Yes
AUC	25.15	25.15	25.15	22.64	25.15	27.67	25.15	25.15	25.15	27.95	25.15	22.87
Expected behavior	Yes		Yes	Yes		Yes	Yes		Yes	Yes		Yes

Conclusion: The sensitivity analysis did not indicate any discrepancies in the expected behavior of the outputs studied, thereby confirming that there is no obstacle to the model's validation.

4.21.4 Quantification of uncertainties

Introduction

The model inputs were parameters from NC literature with ranges used to propagate uncertainties. Uncertainties were propagated using ranges of values and standard deviations.

Propagation in simulation results

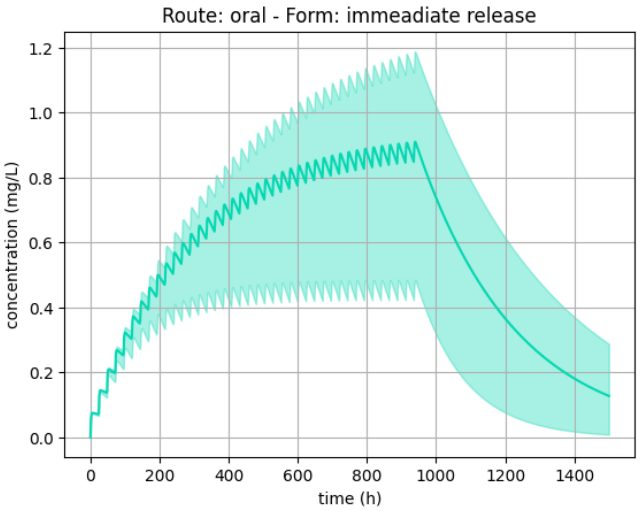

Figure 168. quantification of uncertainties for vandetanib

4.21.5 Test Samples

Test sample level: 2/3

Test sample: efficacy, overexposure, and safety thresholds used for routine therapeutic drug monitoring (TDM) in clinical settings, or thresholds reflecting specific expected events (such as efficacy or toxicity) that may occur at these levels of exposure.

- Efficacy threshold was: 0.4 mg/L
- Overexposure threshold was: 2 mg/L

Test samples source(s): Ter Heine et al. [55]

Comment: /

4.21.6 Tests conditions

Tests conditions level: 4/5

Tests condition: test conditions were defined with sufficient data to run simulations for each patient concerned by the drug, with complete coverage of dosage ranges, and of all sub-populations concerned by the drug.

Tests conditions source(s): summary of product characteristics [53]

Comment: /

Test conditions were:

Test 1:

- Dosage: 300 mg/24h
- Groups: patients with normal / mild / moderate / severe renal impairment.

Test 2:

- Dosage: 100 mg/24h
- Groups: patients with mild / moderate / severe renal impairment.

Test 3:

- Dosage: 300 mg/24h
- Groups: patients weighing 50, 80, 120kg

Test 4:

- Dosage: 100 mg/48h
- Groups: Children weighing 20kg

Test 5:

- Dosage: 100 mg/24h
- Groups: Children weighing 20kg

4.21.7 Equivalency of Input Parameters

Equivalency of input parameters level: 4/4
Equivalency of input parameters: the model's training dataset does cover all doses or PK is linear over the dose range used in the test conditions and sub-populations concerned by the medication, or an external validation is carried out and meets validation criteria. (i.e., MDPE ≤ ± 20%, MDAPE ≤ 30%)
Equivalency of input parameters source(s): Summary of product characteristics [53]
Comment: vandetanib simulation outputs were tested with summary of products dosing regimen covering all patients.

4.21.8 Output Comparison

Output comparison level: 3/5
Output comparison: correspondence of model outputs with the therapeutic thresholds used in routine clinical therapeutic drug monitoring or thresholds reflecting specific expected events (such as efficacy or toxicity) that may occur at these levels of exposure.
Output comparison source(s): Ter Heine et al. [55]
Comment: summary of product was used to extract dosing regimen data, and simulation outputs were compared to therapeutic ranges from Ter Heine et al. [55]. The simulation results were consistent with the expected behaviour. Patients were all within therapeutic thresholds.

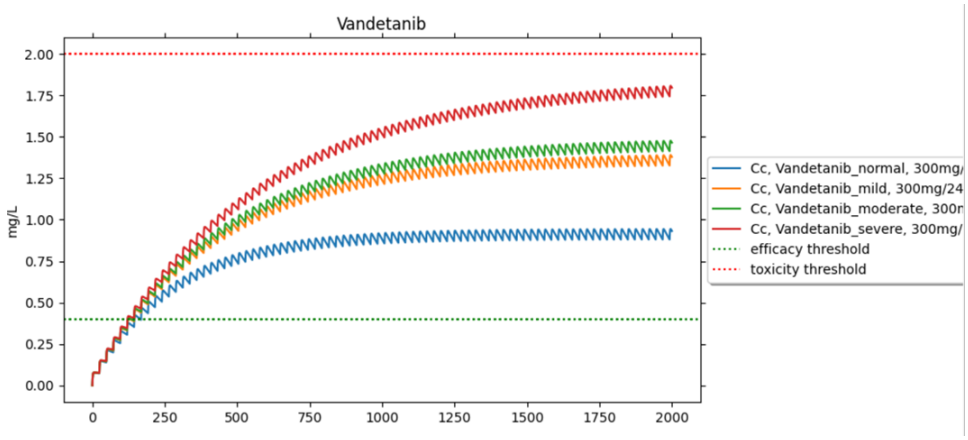

Figure 169. Test 1: 300mg/24 hours for patients with normal / mild / moderate / severe renal impairment

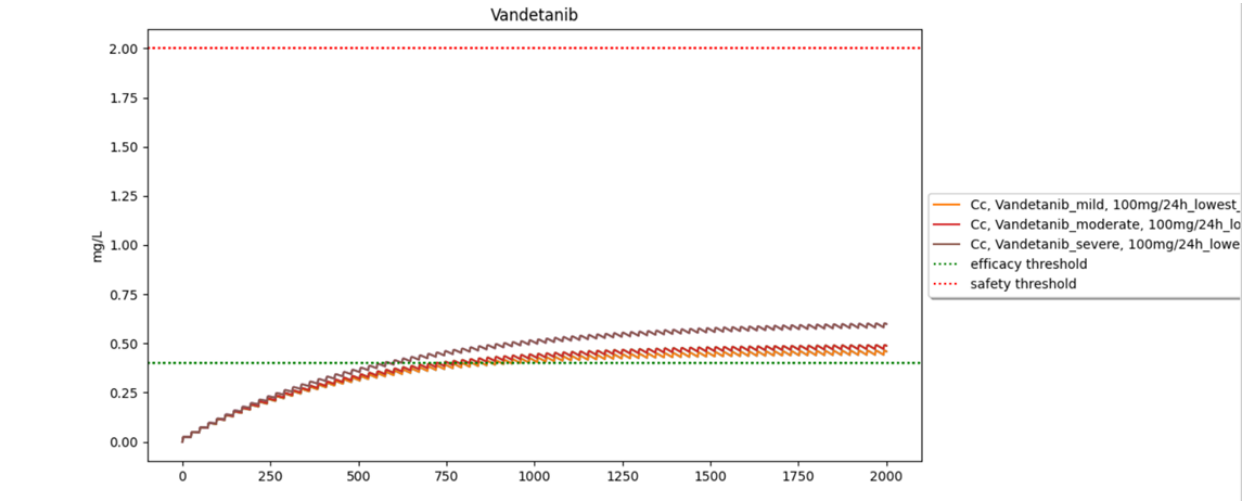

.

Figure 170. Test 2: 100mg/24 hours for patients with normal / mild / moderate / severe renal impairment.

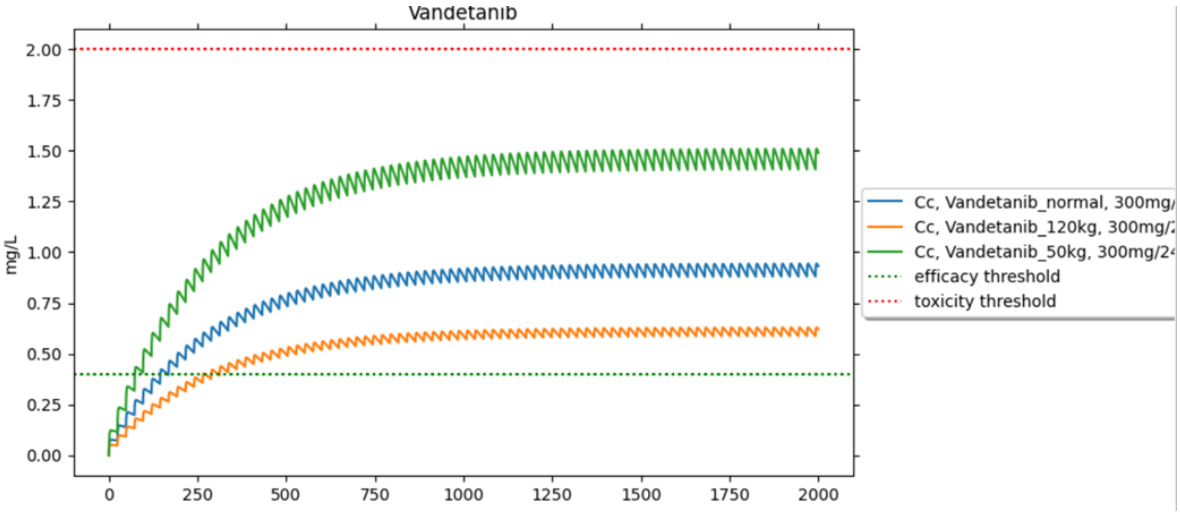

Figure 171. Test 3: 300mg/24 hours for patients of 50, 80, 120kg.

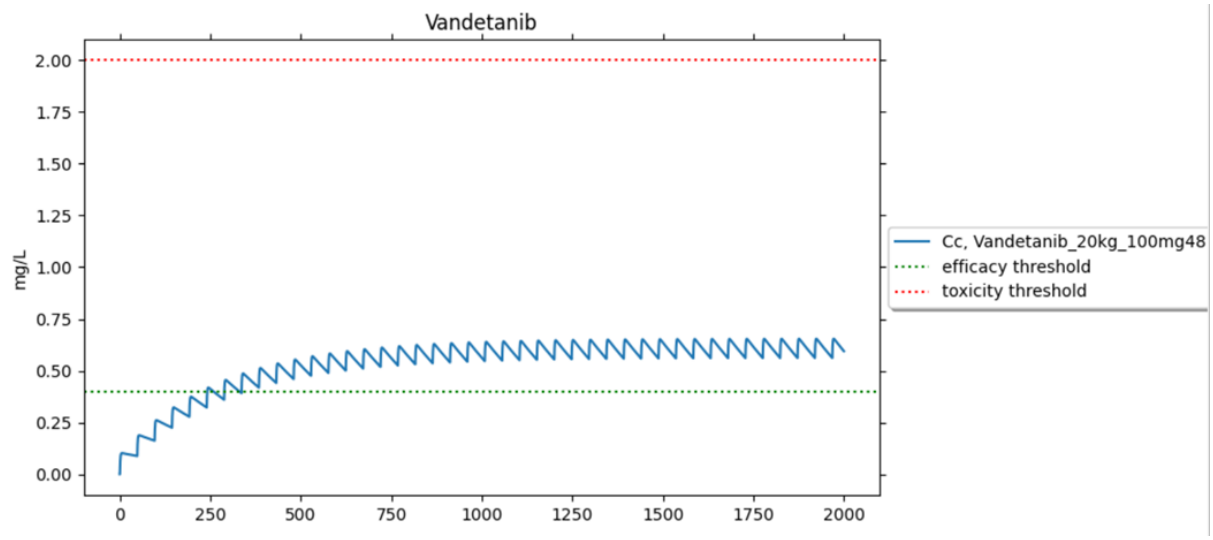

Figure 172. Test 4: 100mg/48 hours for children of 20kg.

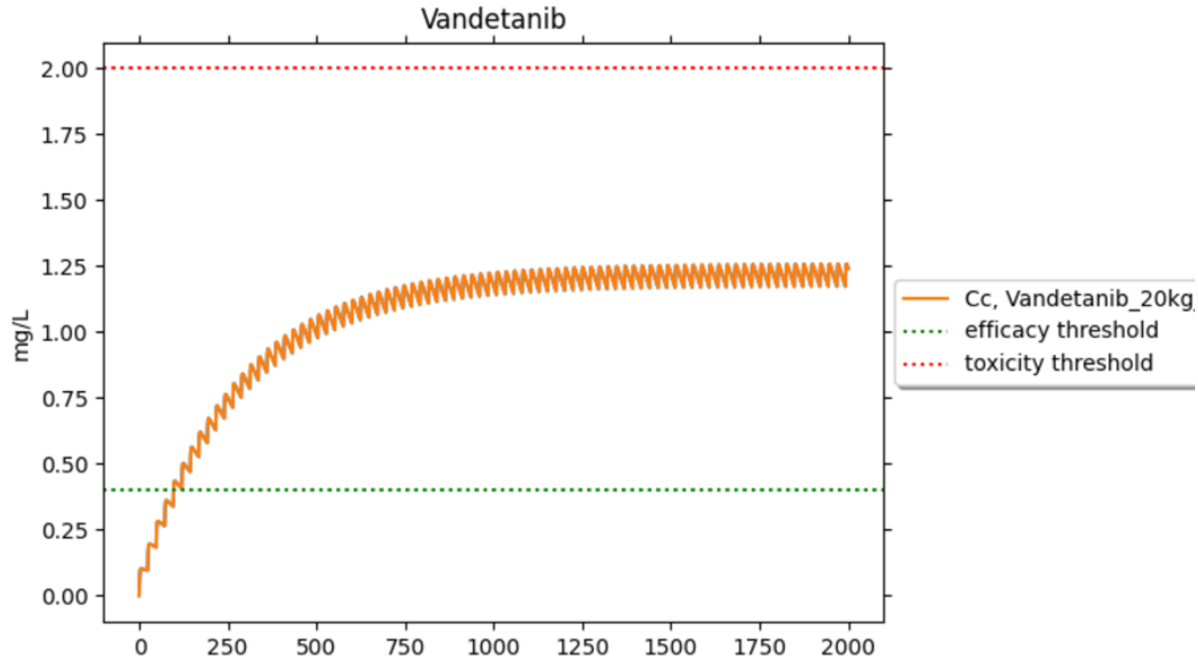

Figure 173. Test 5: 100mg/24 hours for children of 20kg.

5. Conclusion

This technical annex expands on Annex A6.2-UC3-PK which was initially included in the SimCardioTest deliverable D6.2, and reports technical details relative to the validation of the PK numerical model developed for Use Case 3 including activities performed after M30 till the end of the UC3 PK validation work. General conclusions relative to the validation of UC3 numerical model are reported in Annex A of the SimCardioTest Final Report.

6. Bibliography

[1] Jerling M, Merlé Y, Mentré F, Mallet A. Population pharmacokinetics of clozapine evaluated with the nonparametric maximum likelihood method. Br J Clin Pharmacol 1997;44:447–53. https://doi.org/10.1046/j.1365-2125.1997.t01-1-00606.x.

[2] Lereclus A, Korchia T, Riff C, Dayan F, Blin O, Benito S, et al. Towards Precision Dosing of Clozapine in Schizophrenia: External Evaluation of Population Pharmacokinetic Models and Bayesian Forecasting. Ther Drug Monit 2022;44:674–82. https://doi.org/10.1097/FTD.0000000000000987.

[3] Jin Y, Pollock BG, Frank E, Cassano GB, Rucci P, Müller DJ, et al. Effect of age, weight, and CYP2C19 genotype on escitalopram exposure. J Clin Pharmacol 2010;50:62–72. https://doi.org/10.1177/0091270009337946.

[4] Schulz M, Schmoldt A, Andresen-Streichert H, Iwersen-Bergmann S. Revisited: Therapeutic and toxic blood concentrations of more than 1100 drugs and other xenobiotics. Crit Care 2020;24:195. https://doi.org/10.1186/s13054-020-02915-5.

[5] Résumé des caractéristiques du produit - ESCITALOPRAM VIATRIS 20 mg, comprimé pelliculé sécable - Base de données publique des médicaments n.d. https://base-donnees-publique.medicaments.gouv.fr/affichageDoc.php?specid=68082865&typedoc=R#RcpPropPharmacodynamiques (accessed July 23, 2024).

[6] Thyssen A, Vermeulen A, Fuseau E, Fabre M-A, Mannaert E. Population pharmacokinetics of oral risperidone in children, adolescents and adults with psychiatric disorders. Clin Pharmacokinet 2010;49:465–78. https://doi.org/10.2165/11531730-000000000-00000.

[7] Résumé des caractéristiques du produit - RISPERDAL 1 mg, comprimé pelliculé - Base de données publique des médicaments n.d. https://base-donnees-publique.medicaments.gouv.fr/affichageDoc.php?specid=63605525&typedoc=R#RcpProp%20Pharmacocinetiques (accessed July 23, 2024).

[8] Nikolic VN, Jankovic SM, Velickovic-Radovanović R, Apostolović S, Stanojevic D, Zivanovic S, et al. Population pharmacokinetics of carvedilol in patients with congestive heart failure. J Pharm Sci 2013;102:2851–8. https://doi.org/10.1002/jps.23626.

[9] Takekuma Y, Takenaka T, Kiyokawa M, Yamazaki K, Okamoto H, Kitabatake A, et al. Evaluation of effects of polymorphism for metabolic enzymes on pharmacokinetics of carvedilol by population pharmacokinetic analysis. Biol Pharm Bull 2007;30:537–42. https://doi.org/10.1248/bpb.30.537.

[10] Résumé des caractéristiques du produit - CARVEDILOL ARROW 12,5 mg, comprimé pelliculé sécable - Base de données publique des médicaments n.d. https://base-donnees-publique.medicaments.gouv.fr/affichageDoc.php?specid=61639048&typedoc=R#RcpPropPharmacocinetiques (accessed July 23, 2024).

[11] Phillips L, Grasela TH, Agnew JR, Ludwig EA, Thompson GA. A population pharmacokinetic-pharmacodynamic analysis and model validation of azimilide. Clin Pharmacol Ther 2001;70:370–83.

[12] Corey A, Al-Khalidi H, Brezovic C, Marcello S, Parekh N, Taylor K, et al. Azimilide pharmacokinetics and pharmacodynamics upon multiple oral dosing. Biopharm Drug Dispos

1999;20:59–68. https://doi.org/10.1002/(sici)1099-081x(199903)20:2<59::aid-bdd155>3.0.co;2-6.
[13] Goodman & Gilman : Les bases pharmacologiques de la thérapeutique, 13e édition | AccessMedicine. McGraw Hill Medical n.d. https://accessmedicine.mhmedical.com/content.aspx?sectionid=165936845&bookid=2189 (accessed July 23, 2024).
[14] Résumé des caractéristiques du produit - LARGACTIL 100 mg, comprimé pelliculé sécable - Base de données publique des médicaments n.d. https://base-donnees-publique.medicaments.gouv.fr/affichageDoc.php?specid=62816804&typedoc=R#RcpPosoAdmin (accessed July 23, 2024).
[15] Preechagoon Y, Charles B, Piotrovskij V, Donovan T, Van Peer A. Population pharmacokinetics of enterally administered cisapride in young infants with gastro-oesophageal reflux disease. Br J Clin Pharmacol 1999;48:688–93. https://doi.org/10.1046/j.1365-2125.1999.00068.x.
[16] Arora V, Spino M. Cisapride: A Novel Gastroprokinetic Drug. Canadian Journal of Hospital Pharmacy 1991;44. https://doi.org/10.4212/cjhp.v44i4.2754.
[17] Résumé des Caractéristiques du Produit n.d. http://agence-prd.ansm.sante.fr/php/ecodex/rcp/R0122266.htm (accessed July 23, 2024).
[18] Benatar A, Feenstra A, Decraene T, Vandenplas Y. Cisapride plasma levels and corrected QT interval in infants undergoing routine polysomnography. J Pediatr Gastroenterol Nutr 2001;33:41–6. https://doi.org/10.1097/00005176-200107000-00007.
[19] Fiche info - ZECLAR 0,5 g, poudre pour solution à diluer pour perfusion - Base de données publique des médicaments n.d. https://base-donnees-publique.medicaments.gouv.fr/extrait.php?specid=61433564 (accessed July 23, 2024).
[20] Résumé des caractéristiques du produit - SOTALOL SANDOZ 160 mg, comprimé sécable - Base de données publique des médicaments n.d. https://base-donnees-publique.medicaments.gouv.fr/affichageDoc.php?specid=62193524&typedoc=R#RcpPropPharmacocinetiques (accessed July 24, 2024).
[21] Thorazine (chlorpromazine) : dosage, indications, interactions, effets indésirables et plus n.d. https://reference.medscape.com/drug/chlorpromazine-342970#10 (accessed July 23, 2024).
[22] Résumé des caractéristiques du produit - RYTHMODAN 100 mg, gélule - Base de données publique des médicaments n.d. https://base-donnees-publique.medicaments.gouv.fr/affichageDoc.php?specid=63063487&typedoc=R#RcpPosoAdmin (accessed July 24, 2024).
[23] Résumé des caractéristiques du produit - RYTHMODAN 250 mg A LIBERATION PROLONGEE, comprimé enrobé - Base de données publique des médicaments n.d. https://base-donnees-publique.medicaments.gouv.fr/affichageDoc.php?specid=69235837&typedoc=R#RcpPosoAdmin (accessed July 24, 2024).
[24] 020931s007lbl.pdf n.d.
[25] Tikosyn, (dofetilide) dosing, indications, interactions, adverse effects, and more n.d. https://reference.medscape.com/drug/tikosyn-dofetilide-342298#10 (accessed July 25, 2024).
[26] Résumé des caractéristiques du produit - DOMPERIDONE ARROW 10 mg, comprimé pelliculé - Base de données publique des médicaments n.d. https://base-donnees-publique.medicaments.gouv.fr/affichageDoc.php?specid=68427304&typedoc=R (accessed July 25, 2024).
[27] Helmy SA, El Bedaiwy HM. Pharmacokinetics and comparative bioavailability of domperidone suspension and tablet formulations in healthy adult subjects. Clin Pharmacol Drug Dev 2014;3:126–31. https://doi.org/10.1002/cpdd.43.
[28] Foo L-K, Duffull SB, Calver L, Schneider J, Isbister GK. Population pharmacokinetics of intramuscular droperidol in acutely agitated patients. Br J Clin Pharmacol 2016;82:1550–6. https://doi.org/10.1111/bcp.13093.

[29] Fischler M, Bonnet F, Trang H, Jacob L, Levron JC, Flaisler B, et al. The pharmacokinetics of droperidol in anesthetized patients. Anesthesiology 1986;64:486–9. https://doi.org/10.1097/00000542-198604000-00012.
[30] Fiche info - DROPERIDOL AGUETTANT 5 mg/2 ml, solution injectable (I.M.) - Base de données publique des médicaments n.d. https://base-donnees-publique.medicaments.gouv.fr/extrait.php?specid=68810459 (accessed July 25, 2024).
[31] Résumé des caractéristiques du produit - FLECAINIDE ARROW LAB 100 mg, comprimé sécable - Base de données publique des médicaments n.d. https://base-donnees-publique.medicaments.gouv.fr/affichageDoc.php?specid=69087107&typedoc=R (accessed July 26, 2024).
[32] Résumé des caractéristiques du produit - FLECAÏNE L.P. 100 mg, gélule à libération prolongée - Base de données publique des médicaments n.d. https://base-donnees-publique.medicaments.gouv.fr/affichageDoc.php?specid=64645960&typedoc=R (accessed July 26, 2024).
[33] Conard GJ, Ober RE. Metabolism of flecainide. Am J Cardiol 1984;53:41B-51B. https://doi.org/10.1016/0002-9149(84)90501-0.
[34] Tennezé L, Tarral E, Ducloux N, Funck-Brentano C. Pharmacokinetics and electrocardiographic effects of a new controlled-release form of flecainide acetate: comparison with the standard form and influence of the CYP2D6 polymorphism. Clin Pharmacol Ther 2002;72:112–22. https://doi.org/10.1067/mcp.2002.125946.
[35] 00067085.pdf n.d.
[36] Résumé des caractéristiques du produit - FLAGYL 500 mg, comprimé pelliculé - Base de données publique des médicaments n.d. https://base-donnees-publique.medicaments.gouv.fr/affichageDoc.php?specid=61659061&typedoc=R (accessed July 26, 2024).
[37] Résumé des caractéristiques du produit - FLAGYL 125 mg/5 ml, suspension buvable - Base de données publique des médicaments n.d. https://base-donnees-publique.medicaments.gouv.fr/affichageDoc.php?specid=65020253&typedoc=R (accessed July 26, 2024).
[38] Turgut EH, Özyazici M. Bioavailability File: Metronidazole 2004.
[39] Metronidazole | Drugs n.d. https://link.springer.com/article/10.2165/00003495-199754050-00003 (accessed July 26, 2024).
[40] Population pharmacokinetic parameters in patients treated with oral mexiletine - PubMed n.d. https://pubmed.ncbi.nlm.nih.gov/7151850/ (accessed July 26, 2024).
[41] namuscla-epar-product-information_fr.pdf n.d.
[42] Iida S, Kinoshita H, Holford NHG. Population pharmacokinetic and pharmacodynamic modelling of the effects of nicorandil in the treatment of acute heart failure. Br J Clin Pharmacol 2008;66:352–65. https://doi.org/10.1111/j.1365-2125.2008.03257.x.
[43] Frydman A. Pharmacokinetic Profile of Nicorandil in Humans: An Overview. Journal of Cardiovascular Pharmacology 1992;20:S34.
[44] Résumé des caractéristiques du produit - NICORANDIL ALMUS 10 mg, comprimé sécable - Base de données publique des médicaments n.d. https://base-donnees-publique.medicaments.gouv.fr/affichageDoc.php?specid=66925249&typedoc=R (accessed July 26, 2024).
[45] Résumé des caractéristiques du produit - ONDANSETRON ARROW 8 mg, comprimé pelliculé - Base de données publique des médicaments n.d. https://base-donnees-publique.medicaments.gouv.fr/affichageDoc.php?specid=63782187&typedoc=R#RcpPropPharmacocinetiques (accessed July 28, 2024).
[46] Hsyu PH, Pritchard JF, Bozigian HP, Gooding AE, Griffin RH, Mitchell R, et al. Oral ondansetron pharmacokinetics: the effect of chemotherapy. J Clin Pharmacol 1994;34:767–73. https://doi.org/10.1002/j.1552-4604.1994.tb02038.x.

[47] Roila F, Del Favero A. Ondansetron clinical pharmacokinetics. Clin Pharmacokinet 1995;29:95–109. https://doi.org/10.2165/00003088-199529020-00004.
[48] Pritchard JF, Bryson JC, Kernodle AE, Benedetti TL, Powell JR. Age and gender effects on ondansetron pharmacokinetics: evaluation of healthy aged volunteers. Clin Pharmacol Ther 1992;51:51–5. https://doi.org/10.1038/clpt.1992.7.
[49] 2013-pimozide_poppk.pdf n.d.
[50] Résumé des caractéristiques du produit - ORAP 1 mg, comprimé - Base de données publique des médicaments n.d. https://base-donnees-publique.medicaments.gouv.fr/affichageDoc.php?specid=62495939&typedoc=R (accessed July 29, 2024).
[51] Verme CN, Ludden TM, Clementi WA, Harris SC. Pharmacokinetics of quinidine in male patients. A population analysis. Clin Pharmacokinet 1992;22:468–80. https://doi.org/10.2165/00003088-199222060-00005.
[52] Quinidine Dosage Guide + Max Dose, Adjustments. Drugs.com n.d. https://www.drugs.com/dosage/quinidine.html (accessed July 29, 2024).
[53] caprelsa-epar-product-information_fr.pdf n.d.
[54] Martin P, Oliver S, Kennedy S-J, Partridge E, Hutchison M, Clarke D, et al. Pharmacokinetics of vandetanib: three phase I studies in healthy subjects. Clin Ther 2012;34:221–37. https://doi.org/10.1016/j.clinthera.2011.11.011.
[55] ter Heine R, Huitema ADR, Mathijssen RHJ, van Maarseveen EM, Malingré MM, de Wit D, et al. "Therapeutic drug monitoring" van tyrosinekinaseremmers: precisiegeneeskunde nog doeltreffender. Nederlands Tijdschrift Voor Oncologie 2015.

This project received funding from the European Union's Horizon 2020 research and innovation program under grant agreement No 101016496